2011

Yeast as a Model for Studying Aβ Aggregation, Toxicity and Clearance

Prashant R. Bharadwaj
Edith Cowan University

Edith Cowan University

Copyright Warning

YEAST AS A MODEL FOR STUDYING Aβ AGGREGATION, TOXICITY AND CLEARANCE

By

Prashant R. Bharadwaj

MS (Biotechnology)

Supervisors: Professor Ralph Martins[1]

Dr. Giuseppe Verdile[1]

Professor Ian Macreadie[2]

[1] School of Exercise, Biomedical and Health Sciences, Edith Cowan University

[2] Royal Melbourne Institute of Technology

This thesis is presented for the degree of Doctor of Philosophy of

Edith Cowan University

Faculty of Computing, Health and Science

School of Exercise, Biomedical and Health Sciences

June 2011

USE OF THESIS

The Use of Thesis statement is not included in this version of the thesis.

Abstract

Alzheimer's disease (AD) is a progressive neurodegenerative disorder of the central nervous system, characterised by acute memory loss and behavioural symptoms. The AD brain is characterized by the presence of senile amyloid plaques associated with degenerating neurites and inflammatory processes. The major protein component of these amyloid deposits is the amyloid beta (Aβ) protein. The Aβ protein is a 40 or 42 amino acid cleavage product of APP (Amyloid Precursor Protein) which is produced in low levels in the normal ageing brain. Although senile amyloid plaques is the major pathological hallmark of AD brains, accumulating evidence has been presented to show that increased levels of soluble forms of Aβ42 correlate with the clinical manifestations and severity of the disease. Increased accumulation (both intracellular and extracellular) and toxicity of Aβ42 peptide in the brain play pivotal roles in neurodegeneration and loss of memory functions in the AD brain. Therefore reducing the toxicity of Aβ42 and increasing its clearance from the brain has been considered to be main targets for AD therapeutics.

The search for a disease modifying therapy for AD has been very difficult with the majority of agents failing in later stages of clinical trials. The incomplete understanding of drug-target mechanisms and the lack of high-throughput screening systems for identifying selective target based drugs have been some of the main issues expressed for the failure of AD drugs. Yeast offer a simple eukaryotic model for studying pathological mechanisms and compared to other models there is availability of various experimental tools applicable for high throughput analysis of protein-protein, gene-gene and gene-protein interactions and associated cellular functions. It can also offer a versatile model for initial screening in drug development for various human diseases, including AD. Yeast models have been utilised for studying AD related proteins including APP and its processing enzymes (secretases) and tau phosphorylation.

The broad aims of this work were to develop yeast models for studying toxicity of oligomeric Aβ42 peptide and investigate intracellular accumulation of aggregated Aβ42. Furthermore, these models were utilized for examining

compounds which modulate Aβ42 structure/toxicity or promote its clearance from cells.

Extracellular treatment of oligomeric Aβ42 was used for studying toxicity in yeast. The uptake of extracellularly added Aβ42 peptide by yeast and its localisation indicated that oligomeric Aβ42 mediated cell death was associated with binding to the plasma membrane. It was shown that oligomeric Aβ42 inhibited the plasma membrane H^+ATPase activity which may be one important mechanism of oligomer Aβ42 mediated cell death in yeast. Further, this yeast model was utilized for investigating the effects of dairy peptides on Aβ42 oligomerization and toxicity. It was shown that suppression of Aβ42 oligomerization lead to concomitant reduction in the toxic effects of Aβ42 in both yeast and neuronal cells. In addition, studies in yeast showed that the recombinant oligomer forming MBP-Aβ42 fusion protein (representing a more stable form of oligomeric Aβ42) was toxic which was further validated in neuronal cells. Overall, these studies established the use of yeast as a model for studying oligomer Aβ42 toxicity.

Cells expressing green fluorescent protein tagged Aβ42 (GFP-Aβ42) as a fusion protein was used for investigating intracellular accumulation of Aβ. Yeast cells expressing GFP-Aβ42 showed punctate fluorescence and reduced levels of expression suggesting that it is sequestered into vesicles which are targeted for degradation. Further investigation revealed a key role for intracellular degradation pathways such as the autophagy in this process and enhancing this pathway was shown to reduce levels of GFP-Aβ42 aggregates. Further, findings presented in this thesis also provided a novel mechanism of action for a drug latrepirdine that has shown promise in AD trials. In yeast, latrepirdine was shown to enhance autophagy and promote the clearance of GFP-Aβ42. Further, preliminary data from an *in vivo* mouse model showed that latrepirdine reduced peripheral levels of injected Aβ42 and promoted uptake into liver, providing further evidence for a role of latrepirdine in enhancing Aβ clearance.

Overall, the findings presented in this thesis have highlighted the application of yeast models for investigating drug mechanisms and developing

high-throughput methods for screening. Reducing oligomer Aβ toxicity and enhancing its clearance in the brain are much sought after targets for therapeutic interventions in AD. The use of the yeast models presented in this work can therefore provide a greater scope for the search of novel AD drugs.

Declaration

I certify that this thesis does not, to the best of my knowledge and belief:

(i) incorporate without acknowledgement any material previously submitted for a degree or diploma in any institution of higher education;
(ii) contain any material previously published or written by another person except where due reference is made in the text; or
(iii) contain any defamatory material.

Signed **(Prashant R. Bharadwaj)**

Date 01/11/2011

Acknowledgements

First and foremost I would like to extend my sincere gratitude and appreciation to my supervisor Professor Ralph Martins, who has been a great source of inspiration. Thank you Ralph for supporting me through the journey of PhD. I whole heartedly thank my co-supervisor Dr Giuseppe Verdile for his boundless guidance, discussions and constantly encouraging me, which made me to realise my abilities and show my talents to the best. It was such an amazing experience working with you Giuseppe, thank you so much for all your guidance and patience. I sincerely thank my second co-supervisor Professor Ian Macreadie, who has been much more than a mentor to me for the past years. Thank you Ian, it was a great experience to have worked under you.

I would also like to acknowledge the support I received from Edith Cowan University, Centre of Excellence for Alzheimer's disease research and care for offering me the Postgraduate Scholarship and CSIRO preventive health flagship for the top-up scholarship.

I extend my heartfelt gratitude to Jo Caine, Sonia Sankovich, Jose Varghese, Richard Head, Giuseppe Ciccotosto, Victor Strelsov, Lindsay Sparrow, Louise Bennet, Jacinta White, Lynne Waddington, Lance Macaulay and Judy Callaghan for all the intellectual contributions, and technical assistance for my experiments and PhD project.

To all my friends and laboratory buddies, I extend my love and sincere appreciation for all your help and affection. Thank you so much folks for keeping me sane. My sincere thanks go to my land lord who has been very supportive and kind.

I have always felt very fortunate for having such a wonderful and understanding family. I would like to thank them for all their support and guidance throughout. Thank you, Mom, Dad, Shri and Charan. I dedicate my thesis to my dear "wife to be", for all her patience and love. Mini, I feel so lucky to have you in my life.

Publications and Conference Abstracts

Published articles

Macreadie I, **Bharadwaj P**, Martins R, “Biodiscovery of chemo preventatives of Alzheimer’s disease using yeast”, Microbiology Australia, May 2010, 31(2)

Bharadwaj P, Martins R, Macreadie I, “Yeast as a model for studying Alzheimer's disease”, FEMS Yeast Res. Jun 2010 10(8):961-9

Dubey AK, **Bharadwaj PR**, Varghese JN, Macreadie IG, “Alzheimer's amyloid-beta rescues yeast from hydroxide toxicity”, J Alzheimer’s Dis. 2009;18(1):31-3.

Bharadwaj PR, Dubey AK, Masters CL, Martins RN, Macreadie IG, “Aβ aggregation and possible implications in Alzheimer's disease pathogenesis”, J Cell Mol Med. 2009 Mar;13(3):412-21.

Bharadwaj P, Waddington L, Varghese J, Macreadie IG, “A new method to measure cellular toxicity of non-fibrillar and fibrillar Alzheimer's Aβ using yeast”, J Alzheimer’s Dis. 2008 Mar;13(2):147-50.

Caine JM, **Bharadwaj PR**, Sankovich SE, Ciccotosto GD, Streltsov VA, Varghese J. “Oligomerization and toxicity of Aβ fusion proteins”, Biochem Biophys Res Commun. 2011 May 12. [Epub ahead of print]

Manuscripts in preparation

Bharadwaj PR, Verdile G, Barr RK, Gupta V, Steele JW, Lachenmayer LM, Yue Z, Ehrlich ME, Petsko G, Ju S, Ringe D, Sankovich SE, Caine JM, Macreadie IG, Gandy S, Martins RN. “Enhancing autophagy by rapamycin or latrepirdine (DimebonTM) reduces the levels of GFP-Aβ42 in Yeast”, manuscript currently under preparation

Bharadwaj PR, Head, R, Martins RN, Raussens, V, Sarroukh, R, Sudharmarajan, S, Waddington, L, Xu, X, Bennett, L,"Modulation of amyloid beta structure and toxicity by dairy-derived peptides", manuscript currently under preparation

Conference Abstracts

Bharadwaj, P, Barr, R, Lachenmayer L, Steele J, Ehrlich M, Yue Z, Gandy S, Verdile G, Martins R, "Latrepirdine enhances Aβ degradation via an autophagic pathway", International Conference on Alzheimer's Disease, Hawaii, 2010. Alzheimer's & Dementia: The Journal of the Alzheimer's Association July 2011

Gupta V, **Bharadwaj P**, Steele J, Taddei K, Morici M, Gandy S, Verdile G, Martins R, "Latrepirdine modulates Aβ oligomer formation and attenuates oligomer-associated toxicity" International Conference on Alzheimer's Disease, Hawaii, 2010. Alzheimer's & Dementia: The Journal of the Alzheimer's Association July 2011

Bennett L, **Bharadwaj P**, Waddington L, Sudharmarajan S, Xu X, Szoeke C, Martins R, Head R, "Modulation of amyloid beta (Aβ) structure and toxicity by a dairy-derived peptide product" International Conference on Alzheimer's disease, Hawaii, 2010. Alzheimer's & Dementia: The Journal of the Alzheimer's Association July 2011

Bharadwaj P, "Modelling Alzheimer's Disease in Yeast and approaches to new Chemo Preventatives", Genetics of Industrial Microorganisms, Melbourne, Australia 2010

Bharadwaj P, "Yeast Model for Studying Drug mechanisms in Alzheimer's Disease", Australian Society for Medical Research Conference, Perth, Australia, 2010

Bharadwaj P, "A new method to measure cellular toxicity of fibrillar and non fibrillar Aβ using yeast". Alzheimer's Australia Conference, Adelaide 2009

Bharadwaj P, Caine J, Macreadie I, “Alzheimer's Beta Amyloid Fusion Protein Kills *Saccharomyces cerevisiae*” Australian Society for Microbiology Conference, Melbourne, 2008

Table of Contents

List of Figures

List of Tables

List of Abbreviations

Å	Angstrom
$^{\circ}$C	Degree Celsius
AChI	Acetyl cholinesterase inhibitors
AD	Alzheimer's disease
ADAM10/17	A disintegrin and metalloprotease 10 or 17
AICD	Amyloid beta precursor protein intracellular domain
APH-1	Anterior pharynx defective homolog 1(gene)
APLP1/2	Amyloid beta precursor protein like protein 1 or 2
APOE	Apolipoprotein E gene
ApoE	Apoliprotein E protein
APP	Amyloid beta precursor protein
Aβ	Beta amyloid
Aβ42	42 amino acid length beta amyloid peptide
Aβ42 (19:34)	42 amino acid length beta amyloid peptide with modifications at F19S and L34P
ATG8	Autophagic related gene 8
atg8Δ	Atg8 gene deletion
ATG5	Autophagic related gene 5
atg5Δ	Atg5 gene deletion
BACE	Beta site of APP cleaving enzyme
bp	base pair
BSA	Bovine serum albumin
C99	APP C-terminal fragment – direct precursor of Aβ
Ca^{2+}	Calcium
CD	Circular Dichroism

CNS	Central nervous system
CSF	Cerebrospinal fluid
CTF	Carboxy terminal fragment
CVT1	cvt1 gene
Cvt1Δ	cvt1 gene deletion
ddH_20	double-distilled water
DMSO	Dimethyl sulfoxide
DNA	Deoxy-ribonucleic acid
dNTP	Deoxyribonucleotide triphosphates
E.coli	*Escherichia coli*
ECL	Enhanced chemiluminescence
EDTA	Ethylene diamine tetra acetate disodium salt
EOAD	Early onset Alzheimer's disease
ER	Endoplasmic reticulum
FTIR	Fourier Transform Infrared
g	Gram
GFP	green fluorescent protein
GFP-Aβ fusion)	green fluorescent protein tagged to Aβ42 peptide (N-terminal
H_2O	Water
HDL	High density lipoprotein
HRP	Horseradish peroxidase
IPTG	Isopropyl β-D-1-thiogalactopyranoside
Kb	Kilo base pairs
KCl	Potassium chloride
kDa	Kilo dalton
L	Litre

LDL	Low density lipoprotein
LDS	Lithium dodecyl sulfate
LOAD	Late onset Alzheimer’s disease
LRP	Lipoprotein receptor related protein
M	Molar
MBP	Maltose binding protein
MBP-Aβ42 fusion)	Maltose binding protein tagged to Aβ42 peptide (N-terminal
MBP-Aβ16 fusion)	Maltose binding protein tagged to Aβ16 peptide (N-terminal
MES	3–(N–Morpholino)propanesulfonic acidmg Milligram
Mg^{2+}	Magnesium ion
$MgCl_2$	Magnesium chloride
$MgSO_4$	Magnesium sulphate
ml	Millilitre
mM	Millimolar
mRNA	Messenger ribonucleic acid
N Starvation	Nitrogen starvation
NaCl	Sodium Chloride
NCT	Nicastrin (gene)
NEB	New England Biolabs, Inc.
NFT(s)	Neurofibrillary tangle(s)
ng	Nanogram
NICD	Notch intracellular domain
nm	Nanometer
NMDA	N-methyl-D-aspartate
NMR	Nuclear magnetic resonance
NSAID(s)	Non-steroidal anti-inflammatory drug(s)

NTF	Amino terminal fragment
OD_{600}	Optical density at 600nm wavelength
PBS	Phosphate buffered saline
PBST	1X Phosphate buffered saline with 0.05% (v/v) Tween
PCR	Polymerase chain reaction
PEN-2	Presenilin enhancer 2 (gene)
PEP4	pep4 gene
pep4Δ	pep4 gene deletion
PET	Positron emission tomography
PIB	[11C]-Pittsburgh Compound-B
PS1/PS2	Presenilin 1 or 2 protein
ROS	Reactive oxygen species
rpm	Revolutions per minute
SDS-PAGE	Sodium dodecyl sulfate polyacrylamide gel electrophoresis
SPE	Solid phase extract
SPE40	Solid phase extract (40% acetonitrile)
SPE100	Solid phase extract (100% acetonitrile)
TAE	Tris-acetate EDTA
TBS	Tris buffered saline
TBST	1X Tris buffered saline with 0.05% (v/v) Tween
TGN	Trans Golgi Network
U	Unit
V	Volt
v/v	Volume per volume ratio
w/v	Weight per volume ratio
wt	Wild type
xg	acceleration

α-APPs	α -secreted amyloid beta precursor protein
β-APPs	β -secreted amyloid beta precursor protein
ε	epsilon
γ	gamma
µg	Microgram
µL	Microliter
µM	Micromolar

Chapter 1

Introduction

1.1 Alzheimer's disease – Background

Alzheimer's disease (AD) is a progressive neurodegenerative disease of the central nervous system and comprises approximately 80% of all dementia cases in the elderly (Terry, 2006). Dementia is posing escalating societal and financial burdens especially with the ageing generation. In 2007, 29.8 million people worldwide had dementia, with this number expected to exceed 100 million by 2050 unless a cure or prevention is found. In 2005, the total worldwide societal cost of dementia was estimated to be US$315.4 billion including US$105 billion for care for a dementia population of 29.3 million in that year. In Australia, AD is the second major cause of disability burden which exerts an immense toll on the sufferers and care givers. It is currently estimated that approximately 250,000 people are suffering from dementia in Australia and the figure is predicted to almost quadruple by 2050 (Brookmeyer et al., 2007; Ziegler-Graham et al., 2008). The cost of AD is predicted to increase from about 1% of GDP (gross domestic product) to more than 3% of GDP in the coming decades (Access Economics 2003) representing a major burden to the health care system.

1.2 Prevalence of AD

AD is the major cause of dementia worldwide with vascular dementia and other neurodegenerative diseases such as Pick's disease, Parkinson's disease, Frontotemporal dementia and diffuse Lewy-body dementia making up the majority of the remaining cases (Aronson et al., 1991; Brookmeyer et al., 2007; Ferri et al., 2005). The incidence of AD differs depending on the diagnostic criteria used, the age of the population surveyed, and other factors, including geography and ethnicity. Although AD is recognized as a major health crisis in developed countries, its impact in developing countries is expected to be much more severe (Brookmeyer et al., 2007; Ferri et al., 2005). Age is the major risk factor for sporadic AD cases with a prevalence of approximately 5% among those 65-69 years of age and increases with age to 40-50% among persons 95 years of age and over. Early-onset and genetic predisposition factors leading to

AD (mutations in APP, PS1, PS2) are comparatively less prevalent and contribute to approximately 5% of the total AD cases (Hy and Keller, 2000; Koedam et al., 2010; Koedam et al., 2008).

1.3 Clinical Manifestations and Diagnosis of the Disease

AD leads to a progressive deterioration of cognitive function starting with loss of memory and judgement and eventually resulting in complete inability to independently function in basic daily activities. The preclinical stage of AD is inconspicuous and there are no reliable and valid symptomatic markers which would allow an early diagnosis before the manifestation of irreversible loss of memory. Clinical diagnosis of AD is more likely to be accurate only in the late stages of severe cognitive impairment as other dementias have common overlapping features. In the mild dementia stage, difficulties with declarative memory are usually prominent, with less profound effects on daily activities. In the moderate dementia stage, other cognitive domains are noticeably affected including disturbances of thought, perception and behaviour. The patient is completely dependent on the care-giver during the late stage of illness. However, following clinical diagnosis of AD, life expectancy of the patient is significantly reduced (Forstl and Kurz, 1999; Reisberg et al., 1987).

Identifying the disease at a clinical stage when the pathological damage is not too severe to prevent functional recovery, or stabilization, is a major issue of current research. Strategies for clinical diagnosis of AD include evaluation of a detailed history of the type and course of symptoms combined with a battery of neuropsychological assessments. In addition, imaging techniques such as magnetic resonance imaging (MRI), computed tomography (CT) scans and positron emission tomography (PET) are also currently being used in the differentiation of the various forms of dementia (Karow et al., 2010). Since the advent of these techniques, significant cognitive deficits may be detectable before the typical cognitive, behavioral, and social criteria of AD caused dementia are met (Howieson et al., 1997; Jacobs et al., 1995; Linn et al., 1995; Masur et al., 1994; Storandt et al., 2006; Tierney et al., 2005). However, there is

still a high degree of variability between these studies, and analytical techniques need to be standardised. One major challenge for AD diagnosis and specific biomarker discovery is the substantial overlap of major brain pathologies. The indefinite relation between the amount of Aβ and tau pathology, the large overlap of AD, synucleinopathies, and cerebrovascular pathologies are problematic when interpreting a biomarker profile in individual patients. Exact methods and thresholds for specific biomarkers in AD diagnosis are currently not well defined. Establishing a model with characterized definitions of diagnostic thresholds for specific biomarkers need to be incorporated. Additionally, the model needs to be validated and calibrated (Dubois et al., 2007).

1.4 Structural changes in the AD brain

Structural changes in the brain during aging are complex and not well understood. Neurons maintain homeostatic control of essential brain functions, including gene expression, synaptic transmission, and metabolic regulation. During aging, there is a reduction in the complexity of dendrites and a host of other subtle changes within the cortex that includes alterations in receptors, loss of spines and myelin dystrophy, as well as alterations in synaptic transmission which are observed in the neurons. It is suggested that these multiple alterations in the brain may correspond to the age-related neuronal dysfunction and decline in cognitive function. However in AD, where age is the major risk factor, studies have demonstrated that neuronal losses in cortical and hippocampal regions are more severe and possibly caused by distinct pathological processes (Hof et al., 1997; Morrison and Hof, 2002; West et al., 1994; West et al., 2004).

The post-mortem AD brain is considerably atrophied with enlarged ventricles and extensive neuronal loss in the cortex and hippocampus compared to a normal aged brain (Figure 1). Significant neuron and synapse loss in specific brain regions is observed in the AD brain (Hof and Morrison, 2004; Hof et al., 1997; West et al., 1994; West et al., 2004). Unlike in the normal aging brain,

neuronal loss is extensive in the neocortical and entorhinal regions of the AD brain, accompanied by an approximate 45% decline in neocortical synapses (Terry et al., 1991; Terry et al., 1981). An average neuronal cell loss of 68% in the CA1 region of the hippocampus region of AD patients is observed compared to age matched controls (West et al., 1994). Also, a significant reduction in spine density and decrease in overall dendritic area in AD patients was observed (Einstein et al., 1994; Ferrer and Gullotta, 1990; Moolman et al., 2004)..

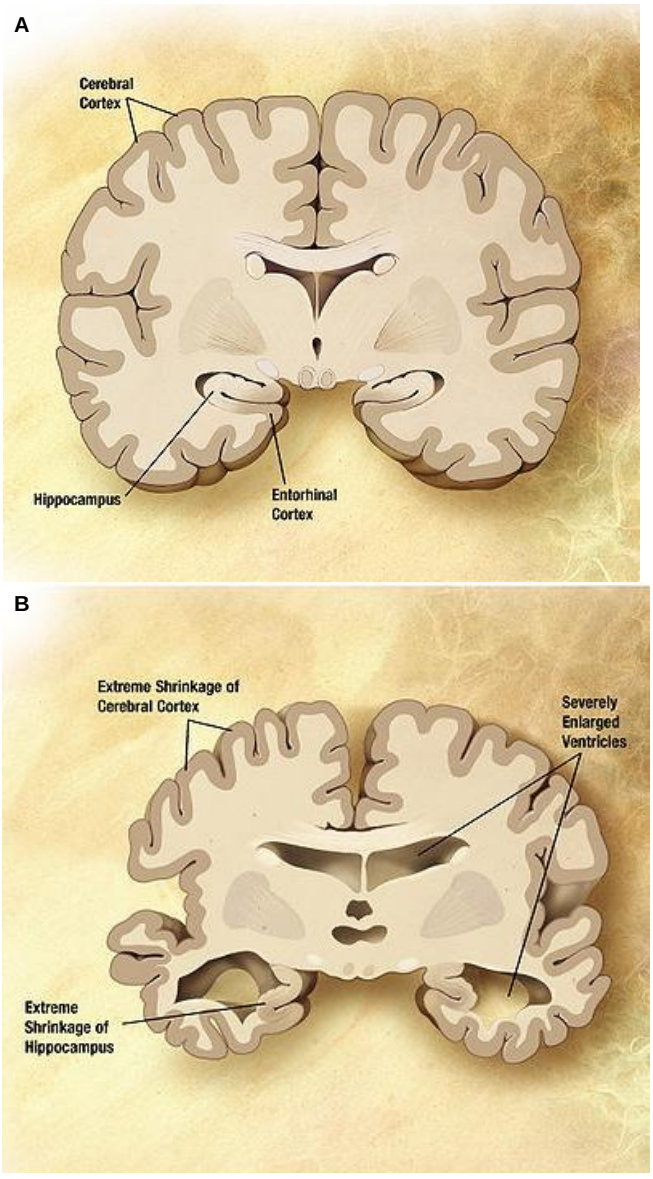

Figure 1: Representation of post mortem brain cross-section of (A) healthy control and (B) AD patient. Differential characteristics are shown in the image. The AD brain is featured by severely enlarged ventricles and shrinkage of the

cerebral cortical and hippocampal regions, which are responsible for memory and cognitive functions.

1.5 Pathological lesions in the AD brain

Accompanying the selective damage in brain regions, distinguished abnormal fibrous protein deposits are observed within the brains of AD patients which include the extracellular senile amyloid plaques, intraneuronal neurofibrillary tangles (NFTs) and amyloid deposits in the walls of cerebral blood vessels (cerebral amyloid angiopathy) (Figure 2). Amyloid deposition and NFTs are also found in the neocortical, hippocampal, and entorhinal regions of cognitively normal elderly people, although in fewer numbers and considered to be largely non-pathogenic (Arriagada et al., 1992; Goldman et al., 2001; Kazee and Johnson, 1998; Price et al., 1991) although it could be argued that these individuals have the pre-clinical form of the disease and had they lived longer would have exhibited clinical symptoms. In AD, however, the robust number of plaques and NFTs is associated with dystrophic neurites and synaptic loss and show increased distribution in specific regions of the brain (Braak and Braak, 1991; Price et al., 1991).

1.5.1 Senile amyloid plaques

The senile plaques in the AD brain consist of a central core of amyloid deposits surrounded by dystrophic neurites together with reactive microglia and astrocytes (Ma et al., 2010a; McGeer et al., 1994; Yasuhara et al., 1994). The amyloid core is composed of straight, unbranching fibrils of 8-10nm diameter, and display strong affinity to Congo red staining and resistance to proteolysis. These properties are representative of a predominant cross-β sheet structure of the polypeptide constituents of the plaque (Goedert and Spillantini, 2006).

The amyloid-β-protein (Aβ) has been found to be the main protein component in the nucleating core of the senile plaques which is also the same protein originally isolated from cerebral blood vessels (Glenner and Wong,

1984a; Glenner and Wong, 1984b; Masters et al., 1985a; Masters et al., 1985b). In addition to Aβ, other proteins accumulate within senile plaques, including apolipoprotein E (ApoE), α2-macroglobulin, interleukins, components of the complement system, α2-macroglobulin receptor, low-density lipoprotein receptor-related protein, collagenous Alzheimer amyloid component (Griffin et al., 1989; McGeer et al., 1989; McGeer et al., 1994; Namba et al., 1991; Strauss et al., 1992; Thal et al., 1997). In addition to the insoluble senile plaques, plaques of a more diffuse nature are also observed in the brain. In contrast, the diffuse plaques show no association with abnormal neurites or reactive glial cells and have few or no amyloid fibrils content. It is suggested that diffuse plaques are an early stage of plaque formation (Goedert and Spillantini, 2006). In AD, diffuse plaques are usually more abundant and widespread throughout the CNS than typical senile plaques. However, substantial amounts of these diffuse types of Aβ deposits are found in the limbic and associated cortices in many healthy older humans (Dickson, 1997).

1.5.2 Neurofibrillary tangles

The dystrophic neurites surrounding the amyloid core of the senile plaques contain paired helical filaments (PHFs) which are pairs of filaments (10nm in diameter) strung into a left-handed helical structure (~80nm in diameter). These PHFs constitute the main structural element of the neurofibrillary tangles (NFTs). The NFTs comprise of hyperphosphorylated tau, a protein involved in microtubule assembly and stabilization (Brion et al., 1985; Delacourte and Defossez, 1986; Ihara et al., 1986; Iqbal et al., 1986). In the human brain, six tau isoforms are produced from a single gene via alternative mRNA splicing (Goedert et al., 1989). Based on the number of microtubule-binding repeats, the isoforms are classified into two groups (three and four repeats: 3R, 4R respectively). The nature of N-terminal inserts distinguishes the three isoforms in each group. In tau filaments isolated from AD brains, similar levels of 3R and 4R isoforms are expressed which are present in similar proportions to those in normal brains. Filamentous tau deposits are also found in a number of other neurodegenerative diseases, including progressive supranuclear palsy (PSP),

corticobasal degeneration (CBD), Pick's disease, argyrophilic grain disease (AGD), and Guam Parkinson dementia (GPD) [reviewed in (Lee et al., 2001)]. Hyperphosphorylation of tau leading to the disintegration of microtubules and abnormal accumulation of tau proteins is common to these diseases and is thought to be associated with toxicity (Avila, 2006). However the absence of beta amyloid pathology distinguishes a majority of these diseases from AD.

The comparative relevance of these lesions in the pathogenesis of AD is controversial. It has been widely acknowledged that senile plaques are a better representative of AD pathology compared to NFTs (Terry et al., 1987). Therefore, quantification of senile plaques, rather than of NFTs, forms the basis of current post-mortem diagnostic criteria for AD (Khachaturian, 1985; Mirra et al., 1991). Although senile plaques are widespread in the AD brain, they are a poor indicator of cognitive decline and disease severity. Growing evidence has indicated that the soluble oligomeric forms of Aβ are responsible for the loss of memory functions in AD and a better correlate than plaques, of cognitive decline and disease severity (Fonte et al., 2001; Lue et al., 1999; McLean et al., 1999). The role of Aβ in neurodegeneration and cellular dysfunction in the AD brain is discussed further.

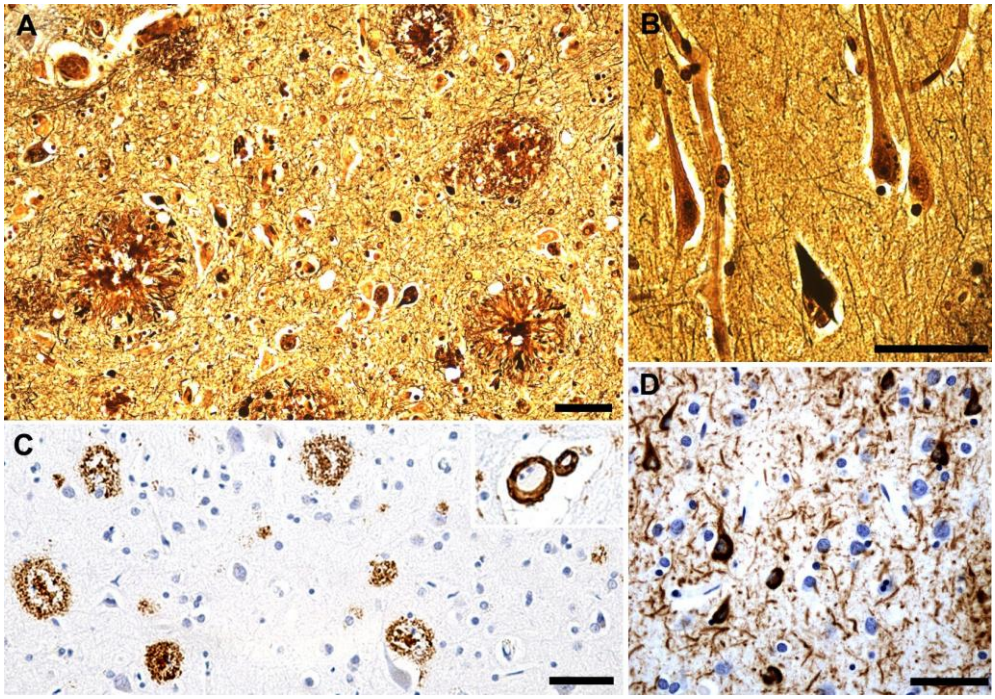

Figure 2: AD pathological hallmarks **(A)** Senile plaques (SPs) indicated by dense cores and radially oriented dystrophic neurites in entorhinal cortex. **(B)** A typical neurofibrillary tangle in CA3. **(C)** Aβ protein immunohistochemistry demonstrates frequent plaques in posterior cingulate cortex, accompanied by cerebral amyloid angiopathy. **(D)** Immunohistochemical stains for hyperphosphorylated tau show aggregation in NFTs and cortical dystrophic neurites. Scale bars indicate 50µm. (Image courtesy: http://knol.google.com/k/lara/alzheimer-s-disease/Ing3X-NE/g1JpHQ).

1.6 Role of Aβ in Neurodegeneration

Although Aβ containing senile plaques are seen associated with dystrophic neurites and reactive microglia, they are poorly correlated with the clinical manifestations of the disease. Moreover, the quantitative correlations between manual microscopic counts of amyloid plaques in post-mortem brain sections and the severity of cognitive decline measured by neuropsychological tests are fraught with methodological challenges. Counting plaques in two-dimensional brain sections provides an inaccurate measure of Aβ load in the brain and is likely to miss other small and heterogeneous Aβ-assembly forms. Specific Aβ enzyme-linked-immunosorbent assays (ELISAs) coupled with western blotting and mass spectrometry analysis has enabled a more sensitive and comprehensive qualitative and quantitative assessment of Aβ forms in the brain. Using these techniques, studies have identified that levels of soluble Aβ correlate much better with the degree of cognitive deficits than plaque counts (Fonte et al., 2001; Lue et al., 1999; McLean et al., 1999). Also the fact that fibrillar amyloid plaques (~20–120-µm diameter) present much less Aβ surface area to neuronal membranes compared to small diffusible forms of Aβ, indicates that soluble assembly forms are better candidates for inducing neuronal dysfunction than plaques containing amyloid fibrils (Haass and Selkoe, 2007). Furthermore, ‘amyloid’ structuring of proteins is thought to be a detoxification strategy to mask the promiscuous surface of the toxic oligomeric building blocks

(Carrell et al., 2008). Studies have also identified novel biological functions for amyloidogenic protein fibrils in bacteria, fungi and even mammals (Kelly and Balch, 2003).Supporting evidence from a range of studies in several neurodegenerative diseases including AD, Huntington's disease, Parkinson's disease, prion diseases and many other amyloidosis point to soluble protein oligomers in the brain as an indicator of cognitive decline rather than the insoluble fibrillar deposits (Ferreira et al., 2007; Glabe and Kayed, 2006; Popik et al., 1999). It is also indicated that oligomeric and fibrillar assemblies maybe formed via distinct mechanisms, possibly mediated by external factors (binding ligands including other proteins, metals, lipids etc) [reviewed in (Bharadwaj et al., 2009)].

1.6.1 Oligomeric forms of natural and synthetic derived Aβ

Amyloid β-protein (Aβ) is a proteolytic product of its larger parent protein, the Amyloid precursor protein and is found in the brains and cerebrospinal fluid (CSF) of both healthy normal individuals and those with AD (Citron et al., 1992; Haass et al., 1992 ; Ida et al., 1996; Vigo-Pelfrey et al., 1993; Walsh et al., 2000). Numerous isoforms of Aβ (Aβ1-42, Aβ4-42, Aβ1-40 and the 3-pyroglutamate derivate of Aβ3-42 (pGluAβ3-42) constituting ~80% of total species) have been detected in the brains of healthy, sporadic and familial AD subjects. However the AD brain (both sporadic and familial cases) exhibit markedly increased levels of the Aβ42 isoform. Distinct regional specific differences are observed with the hippocampus exhibiting heavy Aβ deposition compared to the cerebellum which results in memory impairment (Portelius et al., 2010; Portelius et al., 2009; Tekirian, 2001). Neurodegeneration in AD is believed to be caused by self association of the Aβ42 molecules into toxic isoforms due to its increased accumulation in the brain (Busciglio et al., 1992; Geula et al., 1998; Pike et al., 1991a, b), and studies have clearly demonstrated that aggregation of Aβ42 is essential for toxicity.

Reports indicate soluble oligomeric Aβ as an indicator of the scale of cognitive deficits in AD (Cleary et al., 2005). In general, soluble oligomers are

defined as Aβ assemblies that are not pelleted from physiological fluids by high speed (>100,000g) centrifugation (Lue et al., 1999; McLean et al., 1999). Oligomeric assemblies have been isolated from post-mortem AD brains, and their presence correlated with memory loss (Cleary et al., 2005; Gong et al., 2003). Intracellular and secreted soluble dimeric and trimeric oligomers have been described in cultured cells (Podlisny et al., 1995; Walsh et al., 2000). SDS-stable oligomers of varying sizes have also been detected in APP transgenic mouse brain and human brain (Enya et al., 1999; Funato et al., 1999; Kawarabayashi et al., 2004; Lesne et al., 2006; Roher et al., 1996). Such natural Aβ oligomers can be resistant not only to SDS but also to the Aβ-degrading enzymes like insulin degrading enzyme (IDE), which can only digest monomeric Aβ (Walsh et al., 2002a). The presence of similar SDS-stable dimers and trimers in the soluble fraction of human brain and in extracts of amyloid plaques suggest that these SDS stable low n-oligomers (dimers and trimers) of Aβ are the basic building blocks of insoluble amyloid deposits and could be the earliest mediators of neuronal dysfunction.(Lesne et al., 2006)) reported that a unique and novel Aβ isoform (Aβ*56: 56-kD soluble Aβ42 assembly, dodecamer) as the key neurotoxic Aβ42 isoform responsible for cognitive decline in APP overexpressing Tg2576 mice, based on its stability, abundance and occurrence during memory decline. However, a more recent study (Shankar et al., 2008) identified Aβ dimers from the soluble extract of AD cerebral cortex tissues. This report specifically attributed Aβ dimers to the loss of long-term potentiation (LTP), enhanced long-term depression, reduced dendritic spine density in normal rodent hippocampus and memory disruption of a learned behaviour in normal rats. Importantly this study showed that insoluble amyloid plaque isolated from AD cortex did not impair LTP. However Aβ dimers released from the plaques following solubilisation (TBS, SDS, formic acid) showed neurotoxic properties similar to the soluble Aβ extracts, suggesting that plaque cores are largely inactive but can sequester toxic Aβ forms. Both the Lesne et al and Shankar et al studies identify different toxic Aβ species (dimer or Aβ*56), which might reflect the species differences (mouse and human respectively) and also the Aβ detection techniques employed. It is also suggested that an array of soluble oligomeric Aβ species (ranging from dimers

to dodecamers) may have similar neurotoxic properties associated with memory impairment in AD.

A substantial amount of structural and functional information of Aβ comes from studies using Aβ produced by solid phase peptide synthesis (SPPS). Similar to naturally derived forms, Aβ42 solutions prepared from synthetic lyophilized peptides have shown to form multiple forms ranging from monomeric, oligomeric, fibrillar and many more other multimeric structures and show neurotoxic properties. A large body of literature describes many types of assembly forms of synthetic Aβ, including protofibrils (PFs), annular structures, paranuclei, Aβ-derived diffusible ligands (ADDLs), globulomers and amyloid fibrils [reviewed in (Bharadwaj et al., 2009)].

Although synthetic Aβ has been widely used for variety of experimental purposes, the preparation and handling of the peptide solutions have not been very straightforward. In addition to the heterogeneous and variable nature of Aβ42 peptide, substantial compositional variation in Aβ produced by SPPS resulting in experimental irreproducibility has been reported (Howlett et al., 1995; Simmons et al., 1994; Soto et al., 1995a; Soto et al., 1995b). Most lyophilized peptides contain salts which can complicate the initial solvation and preparation of peptide stock solutions. In addition, these non-peptide substances can alter the biophysical and biological behaviour of the peptide. Preparation of a homogenous Aβ solution is quintessential; but Aβ can form many different forms in aqueous state and the equilibrium and stability among these assemblies are not entirely understood. Some controversy exists as to the actual state of aggregate-free starting preparations. Chaotropic agents ([DMSO]), organic acids (TFA), organic solvents (trifluoroethanol [TFE] and hexafluoroisopropanol [HFIP]), and sodium hydroxide (NaOH) all have been used to solubilise and disaggregate lyophilized Aβ peptide (Teplow, 2006). Causes of irreproducibility may include the aggregation state of the peptide in the solid state (Fezoui et al., 2000) and immediately after reconstitution. There are also some early studies regarding the variable behaviour of different peptide stocks (Brining, 1997; May et al., 1992). Currently, a range of carefully

optimized protocols for preparation of Aβ42 oligomers from synthetic lyophilized stocks are available (Stine et al., 2010; Teplow, 2006).

1.6.2 Potential mechanisms of Aβ mediated toxicity

Over the past two decades extensive work on understanding the mechanism of Aβ toxicity has been undertaken. Although Aβ is largely secreted from the cell surface, it can be present in many cellular compartments. Consequently Aβ has been found to be associated with disruption of several cellular functions including mitochondrial activity (Butterfield et al., 2001 ; Dyrks et al., 1992; Lustbader et al., 2004a; Palmblad et al., 2002), oxidative stress (Butterfield et al., 2001 ; Martins et al., 1986), receptor mediated functions (Bhaskar et al., 2009; Fuentealba et al., 2004; Pereira et al., 2004; Wei et al., 2002 ; Yaar et al., 1997), disruption of Ca^{2+} homeostasis (Hartmann et al., 1994; Mattson et al., 1993), membrane depolarization and disorder (Müller et al., 2001; Verdier et al., 2004) and microglial activation (Giulian et al., 1996). Some of the well known mechanisms of Aβ induced toxicity will be discussed here.

1.6.2.1 Mitochondrial dysfunction

The central nervous system (CNS) has a high metabolic rate, as it consumes about 20% of oxygen inspired, even though it accounts for only 2% of the body weight (Silver and Erecinska, 1998). This large metabolic demand is because neurons are highly differentiated cells that need huge amounts of adenosine tri-phosphate (ATP) for maintenance of ionic gradients across the cell membranes and for neurotransmission. Since most neuronal ATP is generated by oxidative metabolism, neurons critically depend on mitochondrial function and oxygen supply (Ames, 2000; Erecinska et al., 2004). Conversely, neuronal function and survival are very sensitive to mitochondrial dysfunction (Fiskum et al., 1999; Nicholls and Budd, 2000).

Growing evidence indicates that mitochondrial dysfunction may be an important factor in AD pathogenesis. The AD brain is featured by altered glucose metabolism, mitochondrial activity and morphology (Baloyannis et al., 2004; Bubber et al., 2005; Duara et al., 1986; Haxby et al., 1986), and an overall decrease in the number of mitochondria within vulnerable neurons (Hirai et al., 2001). Studies have reported an intracellular interaction between Aβ and ABAD (Aβ binding alcohol dehydrogenase). It was shown that Aβ accumulated in the mitochondria of AD brain and altered the enzyme's active site and prevented native dehydrogenase activity (Caspersen et al., 2005; Lustbader et al., 2004b). These studies therefore provided evidence for the presence of a mitochondrial pool of Aβ within the AD brain that also had the capacity to disrupt normal mitochondrial functionality. Other groups also provide evidence for Aβ accumulation in mitochondria within the brains of AD patients, rodent models, and neuronal cells over expressing APP (Caspersen et al., 2005; Crouch et al., 2005; Manczak et al., 2006). There is evidence that APP and γ-secretase components are present in the mitochondria, indicating that Aβ could be generated within mitochondria (Anandatheerthavarada et al., 2003; Devi et al., 2006; Hansson et al., 2004). Alternatively, Aβ may accumulate in the mitochondria due to decreased capacity to regulate Aβ levels. It has been shown that the human mitochondrial metallo-protease PreP (presequence protease) is capable of degrading Aβ (Falkevall et al., 2006; Stahl et al., 2002). Whether a decline in the PreP activity is related to intracellular Aβ accumulation or toxicity remains to be determined.

Several studies have shown that direct exposure of isolated mitochondria to Aβ significantly impairs functionality of the mitochondrial electron transport chain which is essential for the cell's energy requirement (Casley et al., 2002; Crouch et al., 2005). Aβ has been shown to inhibit the COX (cyclooxygenase) activity *in vitro* supported by reports that COX activity was decreased in the AD brain (Chagnon et al., 1995; Mutisya et al., 1994). Aβ treatment has also been shown to decrease mitochondrial membrane potential and respiration rates, induce mitochondrial swelling, cytochrome c release, transition pore opening, and mitochondrial ROS output [reviewed in (Crouch et al., 2008)]. Most of the

Aβ related effects on mitochondria can contribute to neuronal dysfunction and pathology in the AD brain. Aβ induced mitochondrial dysfunction is closely associated with oxidative stress, which is considered a key feature in the pathogenesis of AD.

1.6.2.2 Oxidative stress

Oxidative stress has been implicated as a major cause of neurotoxicity in a number of neurodegenerative disorders including AD, and there is strong evidence linking oxidative stress to Aβ. Oxidative stress occurs when free radical production exceeds antioxidant defence systems, thereby leading to oxidative damage to cellular components. Most free radicals within a cell originate from reactive oxygen species (ROS) produced via the oxidative phosphorylation within the mitochondria. As described above the CNS consumes 20% of the total oxygen and therefore generates high levels of ROS. The brain is rich in unsaturated fatty acids and comprised mostly of post-mitotic tissue with limited regenerative capacity and a relatively poor antioxidant system (Cooper and Kristal, 1997) which makes it particularly vulnerable to oxidative stress. An initial report by Martins et al (Martins et al., 1986) described an increase in activity of enzymes from the hexose monophosphate pathways in post-mortem AD brain samples compared to age-matched controls, reflecting the increased oxidative stress in the AD brain. Several reports following have shown extensive oxidative damage in AD, including lipid peroxidation (Butterfield et al., 2002; Sayre et al., 1997), oxidized proteins (Bissette et al., 1991; Smith et al., 1991) nucleic acid damage (Gabbita et al., 1998; Lovell et al., 1999) and advanced glycation end products (AGE) (Markesbery and Lovell, 1998; Perry et al., 2003).

Oxidative damage in AD may be a direct result of Aβ peptide accumulation. The senile amyloid plaques in the AD brain are associated with oxidative markers, mainly lipid peroxidation (Lovell et al., 1995; Mecocci et al., 1994). As discussed above, Aβ mediated oxidative stress could be a result of the inhibition of mitochondrial function. Alternatively, oxidative stress may involve direct

production of ROS by Aβ. Aβ can cause neurotoxicity by production of ROS (Behl et al., 1994). One of the widely known mechanisms of Aβ induced ROS is via interaction with metals, mainly copper (Cu) (Curtain et al., 2001; Dong et al., 2003). Aβ-Cu generated H_2O_2 can result in oxidative damage of lipids and intracellular proteins. Aβ-metal interactions are also known to exacerbate aggregation and potentiate toxicity in neuronal cells, which can be rescued by catalase (Atwood et al., 2004; Barnham et al., 2004). Furthermore, neurons depleted of essential antioxidants such as glutathione are more susceptible to Aβ-Cu mediated toxicity (White et al., 1999). Overall, these studies indicate that Aβ mediated generation of free radicals is possibly involved in the neuronal cell death in AD. However reactive oxygen species (ROS) generation could also be a result of tissue injury, and it is unclear whether this is a primary or secondary event of Aβ mediated toxicity to cells in AD.

In addition to oxidative stress and mitochondrial stress many other mechanisms of toxicity have been identified [review in (Harkany et al., 2000)]. Since Aβ has been shown to induce a variety of toxic effects in cells, it is unclear whether the neurodegeneration and cognitive deficits observed in AD are caused by disruption/loss of a particular cellular function or a collective contribution of several toxic outcomes. Also different isoforms of Aβ (predominantly fibrillar and oligomeric forms) have been shown to be toxic in distinct pathways (Dahlgren et al., 2002). While Aβ42 may have been shown to induce a variety of pathological events in the cell, it is possible that some of them are not associated with the disease symptoms. Also, it is argued that the high concentrations of Aβ peptide used in some studies may not represent the actual levels that may be present at any point of time in the AD brain. And most importantly, increased levels of soluble protein oligomers and synaptic loss in the AD brain have been established as the main indicators of cognitive decline rather than the insoluble fibrillar deposits. Therefore the role of Aβ in disrupting synaptic function and promoting dendrite loss has gained much interest in recent years.

1.6.2.3 Synaptic toxicity

Memory impairment in AD is categorized by the loss of ability to form and retain new episodic memories. Cognitive impairment is often attributed to synaptic dysfunction and neuronal cell loss particularly in the cells interconnecting the hippocampal formation with the associating structures crucial for memory (Davies et al., 1987 ; Hyman et al., 1984). Depleted neurotransmitters (Hyman et al., 1984), synaptic connections (Small et al., 2001; Whitehouse et al., 1982) and quantitative correlations of postmortem cytopathology with cognitive deficits indicate that synaptic loss is more robustly correlated than the extent of cortical gliosis (Davies et al., 1987). An intensively studied electrophysiological correlate of learning and memory is long-term potentiation (LTP). LTP is a long-lasting enhancement in signal transmission between neurons using repetitive and synchronous high frequency electrical stimulation. It is an important phenomena underlying synaptic plasticity. As memories are thought to be determined by modification of synaptic strength, LTP is considered as one of the major cellular mechanisms that underlies learning and memory (Bliss and Collingridge, 1993; Cooke and Bliss, 2006).

Several reports provide evidence that naturally secreted low-n Aβ oligomers (Walsh et al., 2002a) and synthetically derived oligomeric Aβ42 (Lambert et al., 1998) can inhibit the maintenance of hippocampal LTP. This effect has been shown by treatment of hippocampal slices (Townsend et al., 2006) or by *in vivo* microinjections in living rats (Walsh et al., 2002a), and can be specifically neutralized by anti-Aβ antibodies *in vivo* (Klyubin et al., 2005). Reports indicate that the induction of long term synaptic depression (LTD) affects hippocampal plasticity and results in decreased dendritic spine volume (Nagerl et al., 2004; Zhou et al., 2004). Although it is established that soluble Aβ oligomers can inhibit LTP in the hippocampus, the effects of Aβ on the induction of LTD are not well understood. Some reports show Aβ42 peptides to induce LTD in CA1 *in vivo* (Cheng et al., 2009; Kim et al., 2001b; Li et al., 2009), whereas other studies show no effect on LTD (Raymond et al., 2003; Wang et al., 2004).

The biochemical mechanism by which soluble oligomers bind to synaptic plasma membranes and interfere with signalling molecules that are required for synaptic plasticity is unclear. Aβ oligomers can interact with membranes to induce structural changes (Kremer et al., 2000), create ion pores (Demuro et al., 2005; Kremer et al., 2000), enhance membrane permeability or ion conductance (Kayed et al., 2004), modulate a wide array of ion channels (Demuro et al., 2010), and osmotic flux (Demuro et al., 2010; Mattson and Chan, 2003). Several studies have implicated disrupted cellular homeostasis to neuritic dystrophia and blockage of intra neuronal signalling essential for cognitive functions (De Fusco et al., 2003; Lingrel et al., 2007; Moseley et al., 2007). The role of cation transporters has been previously reported in AD. Decreased Na+/K+ ATPase activity was observed in APP (Amyloid precursor protein) +PS1 (Presenilin 1) double transgenic mice (Dickey et al., 2005) and Aβ causes inhibition of Cl-, Na+/K+ ATPase in neuronal cell cultures (Bores et al., 1998; Mark et al., 1995; Yagyu et al., 2001). Interestingly, a recent study showed that neuronal electrical activity stimulated BACE (β-secretase) and therefore increased Aβ production, and the resulting increased levels of Aβ depressed synaptic transmission (Kamenetz et al., 2003). Moreover, synaptic activity in APP transgenic mice was correlated with the interstitial fluid Aβ concentrations (Cirrito et al., 2005).

It is suggested that soluble Aβ oligomers may interfere with signalling pathways downstream of certain NMDA (N-methyl-d-aspartate), metabotropic glutamate (mGluR) or AMPA (α-amino-3-hydroxy-5-methyl-4-isoxazole) receptors at synaptic plasma membranes (Snyder et al., 2005). It has also been shown that oligomeric Aβ can interfere indirectly with LTP through an inhibition of ubiquitin C-terminal hydrolase (UCH) (Gong et al., 2006). In addition to extracellular Aβ, studies indicate that aberrant accumulation of Aβ within neurons could also be involved in synaptic dysfunction. Aβ accumulation is most prominent in distal neurites and synapses in the brains of AD transgenic mice (Takahashi et al., 2002). Since accumulating Aβ42 in endosomes are known to reside near synapses (Cooney et al., 2002), altered function of these

organelles (Nixon et al, 2007) might lead to disruption of axonal transport and synaptic dysfunction.

It has been shown that intracellular accumulation of Aβ and soluble Aβ oligomers can induce synaptic dysfunction and dendrite loss (Figure 3). However, the molecular mechanisms that underlie the loss of synapses and ensuing decline in memory related functions caused by Aβ are complex. Neurodegeneration in AD is specific to particular regions of the brain, but it is still not clear what makes the particular subset of neurons and their processes more vulnerable to the effects of Aβ toxicity.

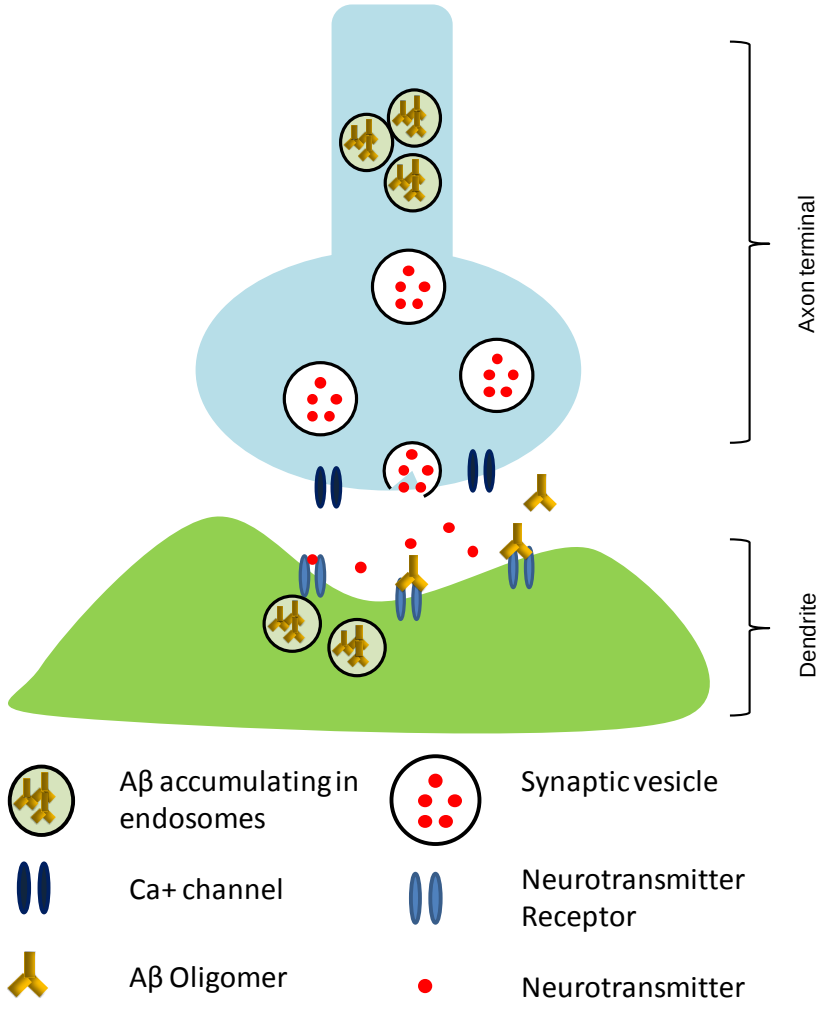

Figure 3: Aβ causes synaptic dysfunction

Extracellular Aβ oligomers can mediate synaptic dysfunction via the neurotransmitter receptors (NMDA, mGluR, AMPA) on the synaptic plasma

membranes. Intracellular accumulation of Aβ in endosomes may disrupt axonal transport or affect dendrites can also be a cause of synaptic loss in AD.

1.6.3 Neurotrophic effects of Aβ

Although the toxic effects of Aβ peptide in mature neurons is well established, some early reports have demonstrated its neurotrophic effects in neurons. C-terminal truncated Aβ [Aβ (1-28)] peptide was shown to enhance survival in embryonic hippocampal cells (Whitson et al., 1989). In the same year, (Yankner et al., 1990) showed that the Aβ (1-40) was neurotrophic to undifferentiated hippocampal neurons at low concentrations and neurotoxic to mature neurons at higher concentrations. However, in differentiated neurons, Aβ (1-40) protein caused cell loss and shrinkage of dendritic processes, which is a widely observed phenomenon with Aβ induced neurotoxicity. Low concentrations of Aβ have also shown to promote neurite outgrowth (Koo et al., 1993) and stimulate tyrosine phosphorylation /phosphatidylinositol-3-kinase activity (Luo et al., 1996a; Luo et al., 1996b) in neuronal cells under low serum conditions. Aβ also exhibits anti-apoptotic properties in serum deprived conditions and anti-oxidant properties [reviewed in (Atwood et al., 2003)]. Although largely neglected and poorly characterized, the trophic actions of Aβ reported in these studies may be related to the physiological role of the APP in neuronal development process and even AD pathology. It is even suggested that Aβ production may be linked to a regenerative response of the brain elicited in an attempt to ameliorate the degeneration and neuronal injury associated with AD.

Along similar lines, recent evidences support the notion that abnormal activation of cell cycle events in regions susceptible to neurodegeneration in the AD brain (Husseman et al., 2000; Yang et al., 2003). Increased levels of cell cycle proteins (Cdc2, cyclin B, activated cdc25A) (Ding et al., 2000; Vincent et al., 2001) and mitotic signalling phosphoepitopes (p-eIF4E, p-mTOR and p-4E-BP1. p-PKR and p-eIF2α) (Chang et al., 2002; Li et al., 2005; Li et al., 2004)

have been observed in the AD brain. A number of studies also show that Aβ42 treatment (both fibrillar and oligomer) can induce neuronal cell cycle events via mTOR/MAP kinase cell proliferation pathways in neurons (Bhaskar et al., 2009; Frasca et al., 2004; Malik et al., 2008; Varvel et al., 2008; Wu et al., 2000). In contrast to Aβ's neurotrophic effects shown in previous reports, these studies suggest that cell cycle events induced by Aβ are associated with neurodegeneration and cell death. It is possible that neurons have different response patterns to Aβ treatment depending on their cell cycle and availability of neurotrophic factors, which also may explain the selective susceptibility of a particular subset of neuronal population to Aβ mediated toxicity in late onset AD.

The studies on Aβ clearly indicate its pivotal role in neurodegeneration in the AD brain, although the exact role of Aβ in AD pathology and loss of cognitive functions are not completely understood. Besides the physical evidence, the critical role of Aβ in AD is strongly supported by the genetic risk factors associated with the onset of the disease.

1.7 Genetic risk factors of AD

There is a large amount of data about potential risk factors for AD. The major risk factors include age, genetics, and head injury. Many other risk factors have also been identified including hormonal levels, cognitive reserve (education and occupation), physical activity and exercise, midlife obesity, alcohol intake and medical conditions like stroke, diabetes, hypertension, and hypercholesterolaemia. However, there is insufficient overall evidence from epidemiological studies to support any association of lifestyle factors or medical conditions to the risk of AD caused dementia (Verghese et al., 2011). Age represents the major risk factor for AD with ε4 allele of the apolipoprotein E gene also playing a key role (60-80% of attributed risk) (Lambert and Amouyel, 2011) which are discussed below.

1.7.1 Early Onset (Familial) AD

AD incidence increases exponentially with every 5 years of age, such that about 5% of people aged 65 have AD, whereas greater than 20% of people over 80 have AD (Brookmeyer et al., 2007). Based on the age at onset, the major types of AD are differentiated into the early-onset forms (less than age65), and late-onset forms (greater than age of 65). The early-onset AD (EOAD) have a clear family history of AD and are caused by autosomal dominant mutations in the genes encoding APP, presenilin-1(PSEN1), and presenilin-2 (PSEN2) (Levy-Lahad et al., 1995; Rogaev et al., 1995; Sherrington et al., 1995). A common feature of these EOAD mutations is change in APP metabolism leading to increased production or stability of the Aβ peptide secreted. While EOAD accounts for only a small fraction (~5%) of the total AD cases, it has presented a useful model for studying the fundamental aspects of the disorder.

1.7.2 Late onset (Sporadic) AD

The more common sporadic cases (late onset AD: LOAD) usually start manifesting symptoms after the age of 65. The ε4 allele of the Apolipoprotein E (APOE) gene is long known to be a major genetic risk factor for the late onset AD cases and many studies have reported and confirmed the association of this allele with the disease (Farrer et al., 1997; Laws et al., 2003). In the past two decades several candidate genes apart from APOE have been idenified as risk factors for LOAD (~ 660), although with poor correlations in significantly larger cohorts (the Alzgene database) (Bertram et al., 2007).

The major function of the apoE is to mediate the clearance of lipoproteins by interacting with the low-density lipoprotein (LDL) family of receptors in liver cell (Beisiegel et al., 1989). ApoE-containing lipoproteins initially bind to cell surface heparin-sulphate proteoglycans, and are subsequently transferred to the LDL receptor-like protein (LRP) or LDL receptor for endocytosis via clathrin coated

vesicles (Havel, 1998; Ji et al., 1993). Studies also suggest an important role for apoE in the uptake and redistribution of cholesterol within the CNS (Holtzman et al., 1995; Pitas et al., 1987; Roheim et al., 1979).

1.7.3 The role of APOE in AD

ApoE is comprised of 299 amino acids, and exists as three major isoforms namely: apoE ε2, apoE ε3 and apoE ε4 (Rall et al., 1982; Zannis and Breslow, 1982). The APOE ε3 allele is present in 50–90% of people in all populations, whereas APOE ε4 is present in 5–35% and APOE ε2 in 1–5% of people (Verghese et al., 2011). Risk of AD is associated with APOE ε4. The APOE ε4 allele is present in about 50% of patients who have late-onset disease, compared with 20–25% of controls (Saunders, 2000; Saunders et al., 1993). The presence of one copy of the APOE ε4 allele increases risk of AD by about 3 times and two copies increases risk about 12 times. Furthermore, in patients with late-onset disease, the presence of APOE ε4 leads to an earlier age of onset compared with non-carriers (Corder et al., 1993). The APOE ε4 allele steadily increases risk with age, exerting its greatest effect on AD between the ages of 60 and 79 years, and decreasing thereafter (Farrer et al., 1997). Additionally, the APOE ε4 allele is associated with more rapid memory decline in non-demented individuals and preclinical memory impairment in asymptomatic middle aged individuals (Caselli et al., 2001; Deary et al., 2002; Flory et al., 2000). Epidemiological studies from various populations have confirmed the increased frequency of APOE ε4 in patients with late-onset AD compared with non-carriers, however the frequency varies between different ethnic groups (Roses, 1996). Although APOE alleles alter the onset of the disease, controversy exists about whether they are associated with the rate of progression of cognitive decline in AD after its onset (Corder et al., 1995a; Corder et al., 1995b). The role of APOE in the predisposition to AD is well established, but the association of APOE with rate of disease progression is not completely understood (Hone et al., 2003; Laws et al., 2003). Evidence strongly supports the notion that apoE plays a key role with the regulation of both

extracellular and intracellular Aβ clearance in the brain (Kim et al., 2009). The important role of apoE in Aβ clearance is discussed in a later section of this review (Section 1.9.1).

1.7.4 Newly identified genetic risk factors

Genome wide association studies (GWAS) is a high throughput genotyping technique for screening the whole genome for single nucleotide polymorphisms (SNPs). In contrast to candidate gene studies, GWAS is based on a non-hypothesis driven genome wide analysis. Studies indicate that the GWAS approach can be problematic and the significance of its findings may require further validation (Manolio, 2010; Pearson and Manolio, 2008). Nevertheless, recent studies performed on GWAS of ~53000 autosomal SNPs in large european cohorts have reported association of CR1 gene (complement component 3b/4b receptor1), clusterin gene (CLU), phophatidylinositol-binding clathrin assembly gene (PICLAM) and bridging integrator 1 (BIN1) loci in the risk of AD (Corneveaux et al., 2010; Harold et al., 2009; Lambert et al., 2009; Seshadri et al., 2010). A more recent GWAS study has shown variants at ABCA7, MS4A6A/MS4A4E, EPHA1, CD33 and CD2AP to be associated with AD (Hollingworth et al.). Although the newly identified genes do not represent a major risk factor for incidence of AD, some of them have been attributed to roles in lipid transport and Aβ clearance (including CLU, CR1). However, no distinct causative roles for these genes in AD pathology have been identified so far.

Mechanisms underlying AD pathogenesis are unclear. There are several hypotheses, but much attention has been given to the amyloid pathway of neurodegeneration. The amyloid hypothesis proposes that accumulation of Aβ42 and subsequent toxicity as the key events responsible for neurodegeneration in AD (see Figure 4). Mutations in APP, PS1 and PS2 genes causing overproduction of Aβ leading to its accumulation in the brain is an important feature in the early onset AD cases. Although the causative roles of genes associated with sporadic AD are still unclear, APOE and the identification

of these new AD genetic determinants suggest that the common and late-onset forms of the disease are associated with a defect in Aβ peptide clearance. In addition, impaired degradation of Aβ by cellular pathways (autophagy, proteasome), by enzymes neprilysin and insulin-degrading enzyme (Iwata et al., 2000; Miller et al., 2003) and reduced perivascular drainage (Weller et al., 1998) have been suggested as possible causes of Aβ accumulation in sporadic AD brains. Also, a recent study has shown direct evidence of decreased clearance of Aβ, but no increased production in the brains of sporadic AD patients (Mawuenyega et al., 2010). The mechanisms involved in the production and clearance of Aβ in the brain and their contribution to AD pathogenesis will be discussed further.

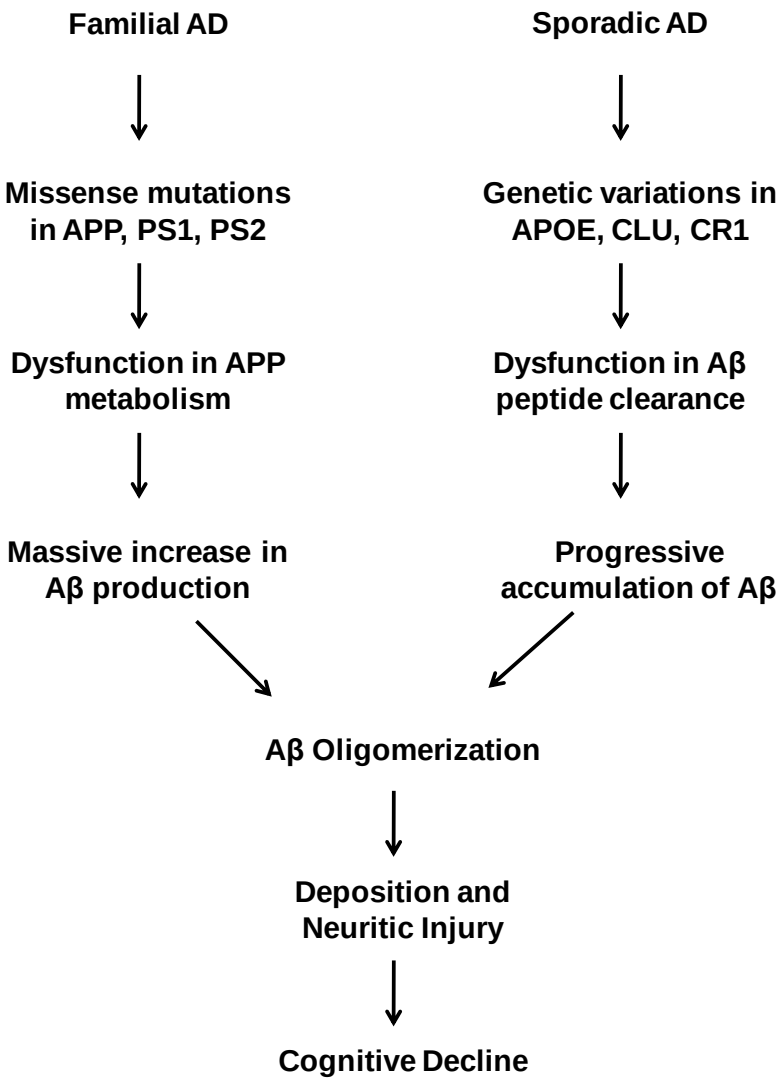

Figure 4: The sequence of genetic risk factors associated with the pathogenic events leading to cognitive decline and dementia in familial and sporadic cases of AD.

1.8 Production of Amyloid-β protein (Aβ)

Aβ is a 38-43 amino acid length peptide, formed by intramembrane proteolysis of the amyloid precursor protein (APP) by successive action of the β and γ secretases. APP metabolism and regulation of its processing are crucial factors involved in the pathogenesis of AD.

1.8.1 APP Biology

The APP molecule is an integral transmembrane glycoprotein ubiquitously expressed in many tissues and concentrated in the synapses of neurons. The APP gene is located on chromosome 21 in humans with three major isoforms arising from alternative splicing known as APP695, APP751, and APP770. APP751 and APP770 are expressed in most tissues and contain a 56 amino acid Kunitz Protease Inhibitor (KPI) domain within their extracellular regions. The major form in neurons is the APP695 which lacks the KPI domain. Its primary functions are not clear, although it has been implicated as a regulator of synaptic function (Priller et al., 2006), neural plasticity (Turner et al., 2003) and iron export (Duce et al., 2010). Aβ is produced by cleavage of the APP protein by enzymes termed β- and γ-secretases. Three enzymes (ADAM9, ADAM10 and ADAM17) belonging to the ADAM family (a disintegrin- and metalloproteinase-family enzyme) with α-secretase activity have been identified (Allinson et al., 2003). The β-secretase enzyme has been identified as β-site APP-cleaving enzyme 1 (BACE1), and is a type I integral membrane protein belonging to the pepsin family of aspartyl proteases (Hussain et al., 1999; Sinha et al., 1999; Vassar et al., 1999). The γ-secretase enzyme has been identified as a complex of proteins composed of presenilin 1 or 2, (PS1 or PS2), nicastrin, anterior pharynx defective homolog 1 and presenilin enhancer 2 (Edbauer et al., 2002; Francis et al., 2002; Steiner et al., 2002; Wolfe et al., 1999a; Wolfe et al., 1999b). In addition to the four critical components, several other factors have been proposed as additional modulators of γ-secretase (CD147, TMP21/p23). Although not core components, these factors have a role in modulating γ-secretase activity (Krishnaswamy et al., 2009; Zhang et al., 2011).

1.8.2 APP processing pathways

The processing of APP involves two competing pathways: the non-amyloidogenic and amyloidogenic pathways (Figure 5). In the non-amyloidogenic pathway, APP is cleaved by the α-secretase at a position located 83 amino acids from the carboxyl (C) terminal, producing an amino (N) terminal

ectodomain (sAPPα) which is secreted into the extracellular medium (Kojro and Fahrenholz, 2005). sAPPa has an important role in neuronal plasticity/survival and regulates neural stem cell proliferation which is important for early CNS development (Furukawa et al., 1996; Ohsawa et al., 1999). The resulting C-terminal fragment (C83) is retained in the membrane and subsequently cleaved by the γ-secretase, producing a short fragment termed p3 (Haass et al., 1993). Cleavage by the α-secretase occurs within the Aβ region, thereby precluding formation of Aβ.

The amyloidogenic pathway is a competitive cleavage pathway for APP which leads to secretion of Aβ. The initial proteolysis is mediated by the β-secretase at a position located 99 amino acids from the C terminus, resulting in the release of sAPPβ into the extracellular space. The 99-amino-acid C-terminal fragment (C99) within the membrane is subsequently cleaved (between residues 38 and 43) by the γ-secretase liberating the Aβ peptide, although the exact site can vary. Cleavage of C99 by γ-secretase can yield Aβ40, the majority species, and Aβ42 (approximately 10%), the more amyloidogenic species, as well as releasing the intracellular domain of APP (AICD). The Aβ42 variant is more hydrophobic and has an increased tendency to aggregate than Aβ40 (Jarrett et al., 1993) and is the predominant isoform found in cerebral plaques observed in AD brains (Younkin, 1998). Recent data has shown that PS/γ-secretase also mediates ζ-site cleavage (Aβ46) (Zhao et al., 2004) and ε-site cleavage (Aβ49) (Sastre et al., 2001), suggesting a sequential cleavage model where cleavage at the ε-site is followed by the ζ-site and γ-site. The processing of APP by secretase activity in the generation of Aβ and other APP metabolites is expertly reviewed in (Zhang et al., 2011).

1.8.3 APP/Presenilin mutations in EOAD

Mutations in APP and components of PS1 and PS2 have been reported in EOAD cases. A common feature of these EOAD mutations is change in APP metabolism leading to increased production or stability of the Aβ peptide secreted. All APP mutations have profound effects on APP processing, resulting

in increased levels of the Aβ peptide (Citron et al., 1992; Eckman et al., 1997; Hendriks et al., 1992; Jonghe et al., 2001). The APP mutations that cluster near the APP γ-secretase cleavage site have been shown to shift the balance of γ-secretase cleavage products towards the Aβ42 over Aβ40 species. One common mutation in the APP gene is the Swedish mutation which leads to increased cleavage of APP by the β-secretase (Haass et al., 1995). Some APP mutations, such as the Arctic (E22G), Italian (E22K), and Iowa (D23N) have shown to increase the aggregation of the secreted Aβ (Grabowski et al., 2001; Murakami et al., 2002 ; Nilsberth et al., 2001; Tagliavini et al., 1999). Reports have also shown loss of APP synpatotrophic functions and decreased interaction with PS1 as a result of EOAD APP mutations (Herl et al., 2009; Seeger et al., 2009). The vast majority of EOAD cases are associated with mutations in the PS1 gene (>180). A large number of these mutations are missense mutations involving substitution of a single amino acid. Others include small deletions, insertions or splice mutations (De Strooper, 2007). Mutations in the presenilins have been shown to affect APP metabolism causing increased production of Aβ42 (Guo et al., 1999; Jankowsky et al., 2004). Recently, a study has also shown that EOAD mutations in PS1 may result in impaired autophagy-lysosomal function (Lee et al., 2010). Overall, these studies indicate that in addition to increased production of Aβ, EOAD mutations can also be associated with loss of functions of the protein which may contribute to the pathology of the disease.

In addition to the intramembrane cleavage of APP at the cell surface by secretase complexes leading to secretion of Aβ, many studies also provide evidence for the occurrence of intracellular Aβ in the AD brains. Growing evidence also indicate that Aβ can accumulate intracellularly which precedes plaque formation and may contribute to cognitive decline in AD. The possible sources of intracellular Aβ have been discussed further.

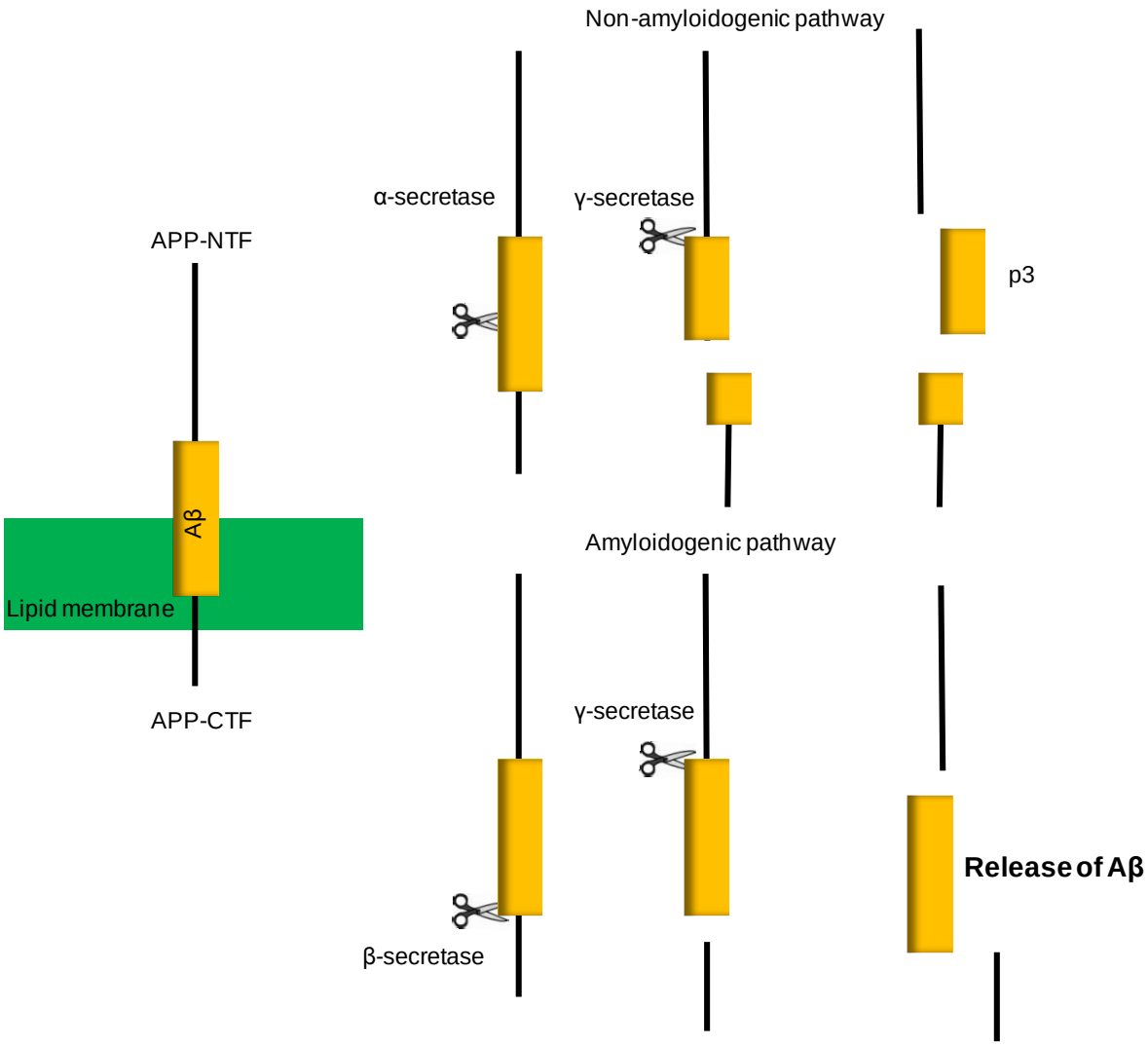

Figure 5: Processing of APP by α-, β-, γ-secretases by non-amyloidogenic pathway and by amyloidogenic pathway leading to generation of Aβ peptide.

1.8.4 Intracellular sites of Aβ production

The occurrence of APP/Aβ products in intracellular compartments has been reported. APP has been found localized in the endoplasmic reticulum (ER), trans-Golgi network (Xu et al., 1995), endosomal, lysosomal (Kinoshita et al., 2003) and mitochondrial membrane (Mizuguchi et al., 1992). Intracellular accumulation of Aβ has been observed in cells expressing APPSwe (familial APP Swedish mutation) but not wild-type APP (Martin et al., 1995). Similarly, duplication in the APP gene has also been associated with higher levels of

intracellular Aβ formation (Cabrejo et al., 2006; Rovelet-Lecrux et al., 2006). Sortilin-related receptor 1 (SORL1) has been found to regulate trafficking of APP from the plasma membrane into retromer recycling endosomes (Golde et al., 1992). APP and BACE1 interactions have been observed within the endosomes and is indicated as a possible site of Aβ generation (Kinoshita et al., 2003). Importantly, genetic variants in SORL1 lead to increased APP trafficking into these Aβ-producing endosomes, which has been linked to an increased risk for late-onset AD (Lee et al., 2007). Also, blocking APP internalization significantly reduced Aβ levels, demonstrating that the internalization of APP by endocytosis is an important pathway for the generation of Aβ (Koo and Squazzo, 1994; Perez et al., 1999). Furthermore, low-density lipoprotein (LDL) receptor-related protein 1B (LRP1B), an LDL family member has been shown to bind APP holoprotein at the plasma membrane thereby preventing Aβ internalization and leading to decreased Aβ production and increased sAPPα secretion (Cam et al., 2004). In addition to the endosome system, evidence has been provided in support of the notion that Aβ is generated intracellularly along the ER-Golgi secretory pathway (Busciglio et al., 1993). It has been shown that retention of APP in the ER blocks production of Aβ40 but not Aβ42, suggesting that Aβ42 can be produced in the ER (Lee et al., 1998; Skovronsky et al., 1998; Wild-Bode et al., 1997). It was further shown that Aβ40 could be produced in the trans-Golgi network (Lee et al., 1998; Skovronsky et al., 1998; Wild-Bode et al., 1997). It is notable that intracellular Aβ42 and Aβ40 can be generated at different sites. A number of studies also indicate that amyloidogenic processing of APP occurs in cholesterol- and sphingolipid-enriched membrane raft microdomains of intracellular organelles (Ehehalt et al., 2003; Riddell et al., 2001; Vetrivel et al., 2005). Although intracellular synthesis of Aβ is evident, the organelles/transport vesicles where Aβ is generated are not fully characterized. A recent study showed evidence of PS1 and PS2 enriched in a compartment of the endoplasmic reticulum associated with mitochondria known as mitochondrial associated membranes (MAM) (Area-Gomez et al., 2009). This study indicates that presenilin components in the mitochondria may contribute to generation of intracellular Aβ.

In addition to being generated intracellularly, secreted Aβ in the extracellular media can be taken up by cells and internalized into intracellular pools. Binding to the cell surface and subsequent internalization via receptor proteins into the cell is thought to be an important pathway for clearance of Aβ in the brain. Different isoforms of Aβ have been shown to internalize via a variety of cell surface receptors in neurons and also in inflammatory cells (astrocytes and microglia). These receptors include , α7 nicotinic acetylcholine receptor (α7nAChR) (Nagele et al., 2002), apolipoprotein E (APOE) receptors (Zerbinatti et al., 2006), members of the low-density lipoprotein receptor (LDLR) family (Jaeger and Pietrzik, 2008), scavenger receptor for advanced glycation end products (RAGE) (Yan, 1996), formyl peptide receptor-like 1 (FPRL1) (Yazawa, 2001) and NMDA (N-methyl- D-aspartate) receptors (Snyder et al., 2005). As Aβ can be generated intracellularly, secreted into the extracellular lumen and also re-internalised (Figure 6), it is not surprising that the clearance of Aβ can be associated with a range of mechanisms. This is discussed further below.

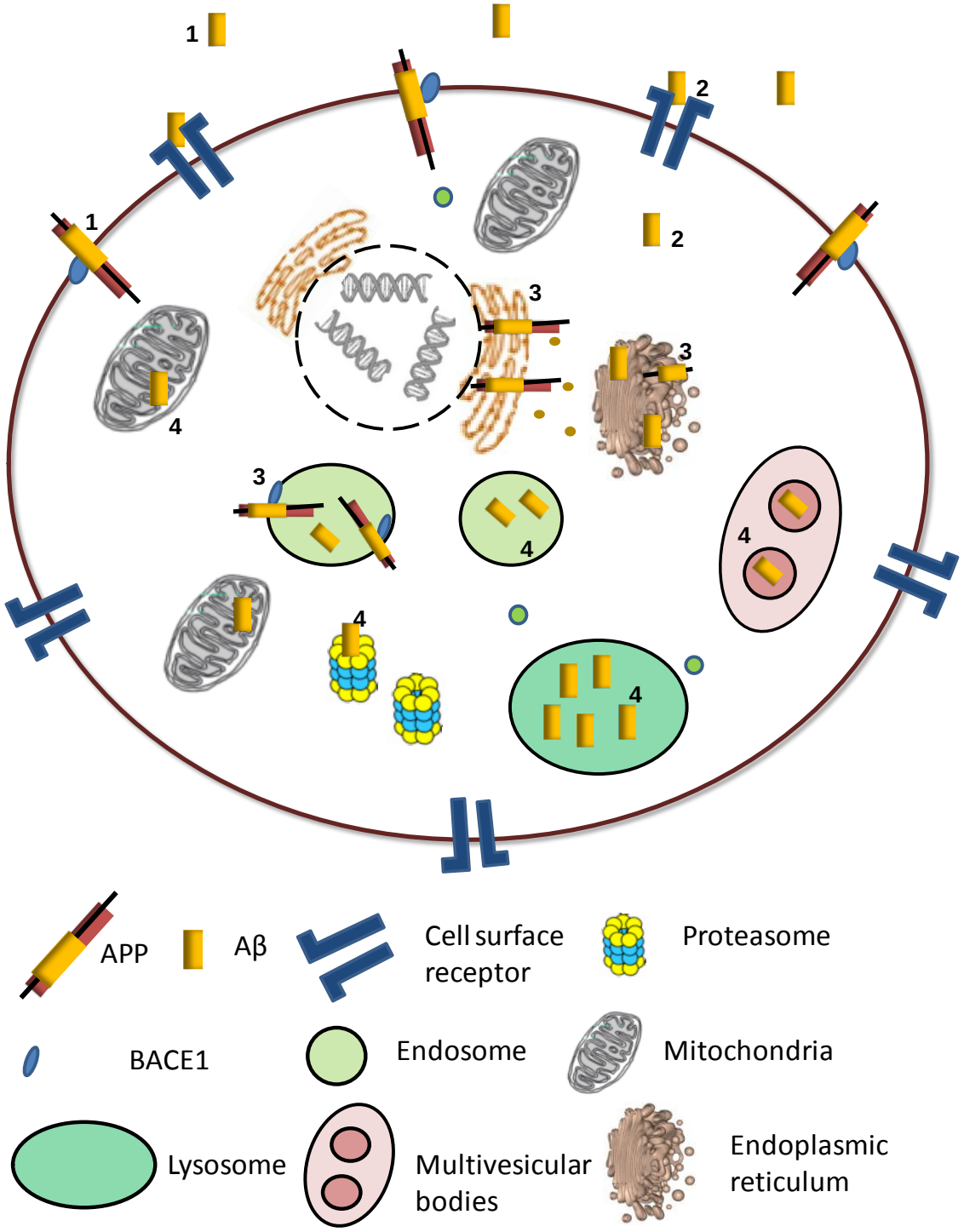

Figure 6: Intracellular accumulation of Aβ

Aβ is secreted into extracellular media by secretase activity of APP localized in the plasma membrane **(1)**. Secreted Aβ can bind to cell surface receptors (for example, LRP, RAGE, FPRL1, NMDA receptors and α7nAChR), and can be internalized **(2)**. Aβ can be produced from APP processing within the

endoplasmic reticulum (ER) and Golgi system and in early endosomes **(3)**. Intracellular accumulation of Aβ is seen predominantly in the multivesicular body and lysosomes, but also in the mitochondria, ER, Golgi and the cytosol, where it is known to affect proteasome function **(4)**.

1.9 Clearance mechanisms of Amyloid-β protein

Defective clearance of Aβ in the brain is implicated as one of the primary causes of its increased accumulation and associated pathology in sporadic AD brains. Gene polymorphisms in APOE and some of the newly identified risk factors (CLU and CR1) suggest impaired Aβ clearance in sporadic AD cases. Direct evidence for decreased clearance of Aβ from the CNS in the brains of AD patients has also been provided (Mawuenyega et al., 2010). The various clearance mechanisms and their roles in the accumulation of Aβ in the brain will be discussed here.

1.9.1 Effect of ApoE on Aβ clearance

One of the major risk factors associated with LOAD is APOE. It is thought that the isoform specific effects of ApoE may contribute to decreased clearance of Aβ in the AD brain. Evidences show that ApoE alters both the transport and metabolism of Aβ in the brain. There is no clear evidence for isoform-specific effects on APP processing or production of Aβ (Biere et al., 1995; Cedazo-Minguez and Cowburn, 2001; Cedazo-Minguez et al., 2001; Irizarry et al., 2004). Regardless, ApoE is known to play an important role in the clearance of Aβ. ApoE-containing lipoprotein particles can modulate the cellular uptake and degradation of Aβ by receptor-mediated endocytosis (Beffert et al., 1998, 1999a; Beffert et al., 1999b; Cole and Ard, 2000; Yamauchi et al., 2002; Yamauchi et al., 2000). Studies have reported that lipid-associated ApoE2 and ApoE3 formed SDS-stable complexes with Aβ to a much greater extent than ApoE4 (Aleshkov et al., 1997; LaDu et al., 1994; Yang et al., 1997). It has been shown that the efficiency of complex formation between lipidated ApoE and Aβ

follows the order of ApoE2 > ApoE3 ≫ ApoE4 (Tokuda et al., 2000). Since the binding efficiency of ApoE isoforms to Aβ correlates inversely with the risk of developing AD, it has been thought that ApoE2 and ApoE3 may enhance the clearance of Aβ, compared to ApoE4.

Alternatively, ApoE may modulate Aβ removal from the brain to the systemic circulation by transport across the blood-brain-barrier. ApoE is known to play a very important role in mediating Aβ clearance in the periphery. Previous *in vivo* data from Prof. Martins laboratory has demonstrated that Aβ is rapidly removed from the plasma by the liver and kidney and the rate of its clearance is affected by ApoE in C57BL/6J and APOE knockout mice (Hone et al., 2003). More recently it was shown that APOE influences the rate at Aβ42 clearance in the bloodstream. Both APOε4 mice and APOE knockout mice treated with lipidated ApoE4 demonstrated increased retention of plasma Aβ42 compared to APOε2/APOE knockout rE2 and APOε3/APOE knockout rE3 mice (Sharman et al., 2010). ApoE3-Aβ and ApoE4-Aβ complexes were shown to be cleared out of the brain at a significantly faster rate than ApoE4-Aβ (Bell et al., 2007; Deane et al., 2008; Ito et al., 2007). However a study using mice expressing human ApoE3 or ApoE4 did not show any differences in the clearance of Aβ from the brain (Ji et al., 2001).

In addition to its isoform-specific difference in the clearance of Aβ, ApoE can affect Aβ aggregation *in vitro*. One study demonstrated that all three ApoE isoforms promoted Aβ42 fibrillization, with the effect being more enhanced with the ApoE4 isoform and least with ApoE2 (Ma et al., 1994). Subsequently, others also found that ApoE4 was more efficient than ApoE3 at increasing Aβ40 aggregation (Castano et al., 1995; Wisniewski et al., 1994). Overall these findings provide evidence for the pathogenic role of ApoE4 in the decreased clearance and also enhanced accumulation of Aβ in AD brain.

1.9.2 Aβ degrading enzymes

Multiple enzymes within the central nervous system (CNS) also play important roles in Aβ clearance. Such enzymes are produced by neurons or microglia, and also expressed in the cerebral vasculature. Studies show that the reduced Aβ-degrading activity may contribute to Aβ deposition in the brain and in vascular system. Insulin-degrading enzyme (IDE) and neprilysin (NEP) are identified as the main Aβ degrading enzymes expressed in neurons and in the cerebral vasculature. Other enzymes which can degrade Aβ include endothelin converting enzymes (ECE-1,2), plasmin, matrix metalloproteinase (MMP-2, -3 and -9) and angiotensin-converting enzyme (ACE). Reduced levels of IDE, NEP, plasmin, plasminogen activators (uPA and tPA) and ECE-2 enzymes in AD have been demonstrated, although the correlation of Aβ accumulation with the activities of these enzymes are still not entirely clear. Reductions in neprilysin, IDE and plasmin in AD have also been associated with occurrence of APOE e4 alleles. The roles of Aβ degrading enzymes in the development of AD pathology and their potential therapeutic benefits have been extensively studied (reviewed in (Miners et al., 2008)), however this is not of major focus in this review.

In addition to extracellular accumulation of Aβ, numerous reports show evidence for intraneuronal deposition of Aβ in brains of AD patients and transgenic animal models (LaFerla et al., 2007). A study has shown that increased Aβ levels in membrane-associated and intracellular fractions isolated from the temporal neocortex of AD patients to be more closely related to AD symptoms than other measured Aβ species (extracellular soluble and extracellular insoluble) (Steinerman et al., 2008). A recent study also shows correlation of the presence of the APOE ε4 allele with an increased accumulation of intraneuronal Aβ peptides in sporadic AD brains (Christensen et al., 2010). Intraneuronal Aβ accumulation is thought to be an early event in AD pathogenesis and has been reported to be critical in the synaptic dysfunction, cognitive decline and the formation of plaques in AD (Gouras et al., 2000; Oddo et al., 2006). The autophagy-lysosome pathway and ubiquitin-

proteasome system are the main intracellular degradation pathways in cells. Disruption of these pathways has been observed in AD brains and believed to play important roles in Aβ mediated neurodegeneration.

1.9.3 Autophagy-Lysosome Pathway

Autophagy is a vital cellular degradation pathway involved in degradation of long-lived, aggregated proteins and even whole organelles inside the cells. Based on the nature and delivery of substrates for degradation autophagy can be classified into three types: macroautophagy, microautophagy and chaperone mediated autophagy (CMA) (Figure 7). Macroautophagy is considered to be the main contributor to the overall autophagy in cells. It is mostly a non-specific process conserved from yeast to mammals, which is up-regulated during stress and nutrient starvation conditions. This process mediated through the mammalian target of rapamycin (mTOR) kinase and regulated through signalling cascades AMPactivated protein kinase (AMPK) or the class I phosphatidylinositol 3-kinase (PI3K)/Akt pathways (Hay and Sonenberg, 2004; He and Klionsky, 2009). The inhibition of mTOR initiates the formation of the autophagosome which sequesters the cytoplasmic material for delivery into the lysosome for degradation by acidic hydrolases (Klionsky and Emr, 2000).

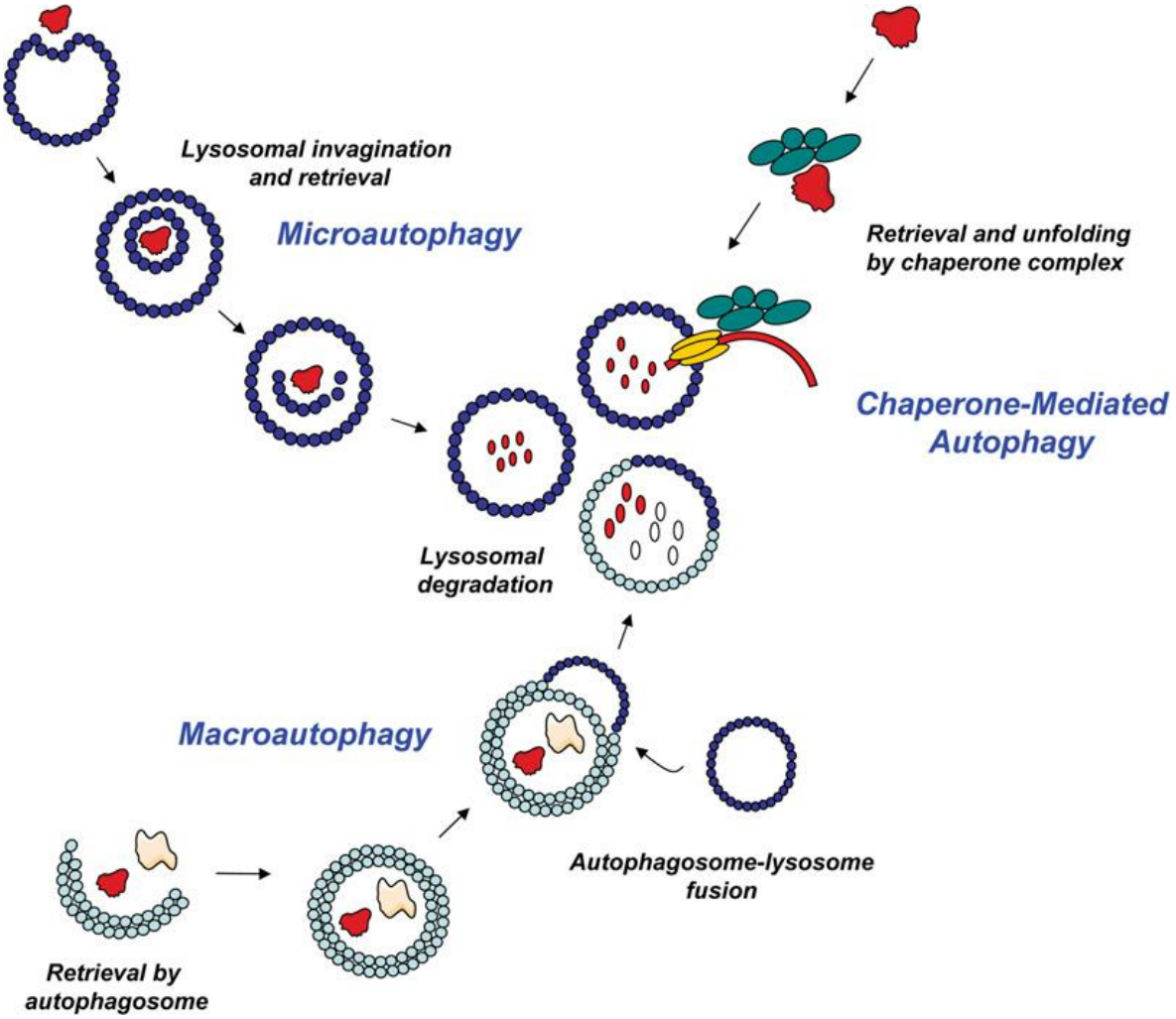

Figure 7: The different types of autophagy in eukaryotes
Macroautophagy featured by bulk degradation of cytosolic material in the lysosome after delivery by autophagosomes. Microautophagy is a process where bulk degradation by lysosome does not require intermediate vacuoles for delivery. Chaperone mediated autophagy is selective degradation of a cytosolic protein target in the lysososme by a dedicated chaperone complex.
(Adapted from Martinet et al, 2009)

1.9.3.1 Extensive accumulation of autophagic vacuoles in AD

A number of reports indicate that autophagy is minimal but constitutively active in neurons and is essential for protein turnover and survival (Hara et al., 2006; Komatsu et al., 2006). Autophagic vacuoles are less abundant in neurons of the healthy brain (Cota et al., 2006; Mizushima et al., 2008; Nixon et al.,

2005). However in the AD brain, severe abnormalities in endocytic and autophagic pathway including extensive accumulation of autophagic vacuoles (AVs) containing APP/Aβ products and dystrophic neurites containing these AVs is observed (Nixon, 2007; Nixon et al., 2005). Autophagy-related pathology has also been increasingly documented in several other neurodegenerative diseases such as Parkinson's disease, Frontotemporal dementia and transmissible spongiform encephalopathy (Anglade et al., 1997; Liberski et al., 2008; Rudnicki et al., 2008; Yue et al., 2002; Zhou et al., 1998).

Severe autophagic pathology develops in mouse models of AD expressing familial AD forms of APP and PS1 mutations (Cataldo et al., 2004; Chishti et al., 2001; Yang et al., 2011; Yu et al., 2005). Accumulation of autophagy substrates and AVs are also observed in PS1-null blastocysts and neurons of mice conditionally depleted of PS1 (Esselens et al., 2004; Wilson et al., 2004). A recent study has shown that the critical component of the Aβ-generating, γ-secretase enzyme presenilin-1 (PS1) is required for autophagy and familial AD causing PS1 mutations are associated with impairments in the autophagy-lysosome pathway. This study has identified a specific role of PS1 in the acidification of autolysosomes/lysosomes (Lee et al., 2010). It is suggested that loss of PS1 function can induce autophagy impairment alongside Aβ accumulation which could account for the cell death and dysfunction observed in AD.

1.9.3.2 Defective lysosomal proteolysis in AD

Many lines of evidence indicate that disruption of the lysosomal proteolytic clearance forms the basis for the neuronal accumulation of AVs in the AD brain. The AD brain is featured by AVs filled with undigested or partially digested substrates (Nixon et al., 2005). A similar pattern of AV accumulation and neuritic dystrophy is observed when lysosomal degradation is inhibited by deletion of cathepsins (Felbor et al., 2002; Koike et al., 2000; Koike et al., 2005) or by lysosomal enzyme inhibitors (Bednarski et al., 1997; Boland et al., 2008; Ivy et al., 1989; Takeuchi and Takeuchi, 2001; Yang et al., 2008). The abnormal autophagic-lysosomal pathology is comparable to that seen in particular

lysosomal storage disorders (LSDs), which are also associated with accumulation of autophagic and endosomal substrates (Nixon et al., 2008). Importantly, some LSDs, such as GM1 and GM2 gangliosidoses, Niemann Pick type C disease (NPC) and neuronal ceroid-lipofuscinosis (NCL) are associated with prominent nervous system degeneration (Jeyakumar et al., 2005; Walkley, 1998, 2009). Furthermore, other similarities are also being identified between the cellular pathologies of AD and of certain LSDs (Chevrier et al., 2010; Eckhardt, 2010; Fukuda et al., 2006; Settembre et al., 2008). Some notably include NFTs, increased levels of the BACE-1, Aβ deposition. A recent study has shown that stimulating lysosomal proteolysis by deletion of an endogenous inhibitor of lysosomal cysteine proteases (cystatin B) in AD transgenic mice, diminishes accumulation of autophagy substrates, extracellular amyloid deposition and ameliorates learning and memory deficits (Yang et al., 2011). These studies establish the pathogenic significance of autophagic-lysosomal dysfunction in AD and specifically the importance of deficient lysosomal proteolysis. But, the exact contribution of autophagy to the clearance of intracellular Aβ is unclear.

1.9.3.3 Enhancing Autophagy promotes Aβ clearance

Modulation of autophagy to enhance clearance of protein aggregates is gaining interest as a therapeutic strategy in many neurodegenerative diseases (Rubinsztein et al., 2007). Enhancing autophagy has been suggested as a treatment strategy for HD (Ravikumar et al., 2004; Sarkar et al., 2007b; Williams et al., 2008) and α-synucleinopathies such as Dementia with Lewy Bodies (DLB; (Crews et al., 2010)). In mammalian AD models, activators of autophagy have been shown to be neuroprotective and confer cognitive benefits (Hung et al., 2009; Spilman et al., 2010). The best-characterised drug that enhances autophagy is rapamycin. Inhibition of mTOR by rapamycin has been widely reported to enhance clearance of aggregate-prone proteins by macro-autophagy (Berger et al., 2006; Ravikumar et al., 2004; Sarkar and Rubinsztein, 2008). Small molecules which activate autophagy by 1) mTOR inhibition (Berger et al., 2006; Ravikumar et al., 2003; Webb et al., 2003), 2) reducing

inositol levels (Fornai et al., 2008; Sarkar et al., 2005) or by 3) Ca2+ channel modulation (Zhang et al., 2007) have also shown to reduce aggregation in cellular models of neurodegeneration, reduce amyloid deposition and abolish cognitive deficits in mice models (Sarkar and Rubinsztein, 2008). Further, derivatives of known agents shown to have benefits in AD models, such as resveratrol, have been developed and shown to modulate mTOR signalling and facilitate autophagy and Aβ degradation (Vingtdeux et al., 2010). A recent study has also shown that small molecule enhancer of rapamycin (SMER28) decreases levels of Aβ and APP-CTF via *Atg5* dependent autophagy in neuronal cells (Tian et al., 2011). Autophagy can also be regulated in an mTOR-independent manner by drugs that reduce intracellular inositol levels, such as lithium, valproate and carbamazepine (Sarkar and Rubinsztein, 2008). In addition to autophagy, the proteasome is an important pathway for maintenance of protein homeostasis in cells. It also has an important role in AD pathology.

1.9.4 Ubiquitin-Proteasome System

The proteasome is a large protein complex that is located in the nucleus and the cytoplasm and is essential for the degradation of ubiquitin tagged proteins. The ubiquitin-proteasome system (UPS) is essential for maintaining a constant balance of protein synthesis and degradation in cells and is conserved from archaebacteria to mammals. The UPS functions constitutively and is essential for the normal functioning of the cell. Protein clearance by the UPS occurs in two sequential steps, an ubiquitin tagging reaction catalysed by the ubiquitin ligase and a subsequent degradation of the tagged proteins by the proteasome system. Unlike autophagy the UPS substrates mostly includes proteins with short half-life and signalling functions inside the cell.

1.9.4.1 Altered proteasomal activity in the AD brain

Increasing evidence indicates that alterations in the UPS function may be involved in AD pathogenesis. Accumulation of an ubiquitin-B mutant protein (UBB+1) in both plaques and tangles has been observed (Mori et al., 1987;

Morishima-Kawashima et al., 1993; Perry et al., 1987). UBB+1 is a frameshift mutant of ubiquitin B gene and has been shown to block ubiquitin-dependent proteolysis (Lindsten et al., 2002) and mediate Aβ-induced neurotoxicity in neuronal cells (Song et al., 2003). Also the ubiquitin carboxy-terminal hydrolase L1 (UCH-L1), a deubiqutinating enzyme, is oxidized and down-regulated in the specific brain regions of AD cases (Castegna et al., 2002; Pasinetti, 2001). Recent evidence provided a positive association for genetic polymorphisms in an ubiquitin-like protein UBQLN1, in sporadic AD (Bertram et al., 2005). Direct evidence of altered proteasome activity showing a selective decrease in activity in specific regions of AD brain like the hippocampus has also been reported (Keller et al., 2000). Together, these reports suggest a possible role for dysfunctional UPS function in AD pathogenesis.

1.9.4.2 Aβ interacts with the proteasome

Numerous studies have reported interactions between Aβ and the proteasome system. Both Aβ40 and Aβ42 have shown to selectively inhibit the chymotrypsin-like activity of the 20S proteasome (Gregori et al., 1995; Gregori et al., 1997; Oh et al., 2005). Using a cell-free proteasome activity assay, oligomeric forms of Aβ were found to significantly decrease proteasomal activity in a dose-dependent manner (Tseng et al., 2008). Elevated levels of an ubiquitin-conjugating enzyme, E2-25K/Hip2 have been identified as a mediator of Aβ neurotoxicity in primary cortical neurons (Song et al., 2003). In addition, it has also been shown that the Aβ induced synaptic dysfunction and cognitive deficits can be rescued via restoring proteasomal enzymatic activity by increasing expression of UCH-L1 (Gong et al., 2006). Intraneuronal Aβ accumulation due to decreased proteasome function has been reported in the brains of AD transgenic models, primary neurons isolated from APP transgenic mice and in N2A cells treated with a proteasome inhibitor (Almeida et al., 2006; Oddo et al., 2006; Oh et al., 2005; Tseng et al., 2008).

Evidence shows that tau can be degraded by the proteasome as inhibition using lactacystin in cell culture inhibits tau degradation (David et al., 2002;

Tseng et al., 2008). Injection of anti-Aβ antibodies into the brains of AD transgenic mice showed that Aβ clearance led to a significant reduction in early tau pathology but not late aggregated tau deposits. However concomitant injection of the anti-Aβ antibody with a proteasome inhibitor led to a reduction of Aβ deposits but no changes in tau pathology were detected (Oddo et al., 2004). These data indicate that the accumulation of Aβ may impair proteasome function thus facilitating tau accumulation.

It is evident that disruption of proteasomal and autophagy-lysosomal functions corresponds to intracellular Aβ deposition and ensuing pathology including tau aggregation and memory impairments in AD. It is widely accepted that functions of the proteasomal and autophagic systems become compromised during the normal aging process contributing to benign protein deposition in the brain. But the exact causes of the failure of these functions in AD are unclear. Whether loss of specific functions in the cellular degradation systems leading to pathological amyloid deposition can contribute to AD is yet to be determined.

The literature reviewed above has presented evidence of the pathogenic nature of Aβ in AD. The accumulation/ aggregation of Aβ and associated toxicity have been considered as a target for therapeutic intervention for AD and there is a number of therapeutics that have been developed. There has been considerable progress in the development of anti-amyloid therapeutics for clinical trials. The current strategies for drug designing and treatments underway in AD clinical trials for targeting Aβ production, aggregation and clearance in the brain are discussed further.

1.10 AD therapeutics

With an increasing ageing population, the need for preventative and disease modifying treatments for AD caused dementia is critical for the future. Current AD treatments target cognitive decline or failure and provide only minor benefits

across the array of clinical symptoms (Omerovic et al., 2007; Tariot, 2006). Approved AD drugs such as acetylcholine esterase (ACE) inhibitors (Aricept, Namenda, Exelon, etc.) and N-methyl-D-aspartate (NMDA) receptor antagonists (Memantine) are generally prescribed in monotherapy or in combination. However they are expensive and most importantly, do not prevent disease progression are of limited benefit to most patients (Jelic et al., 2006; Raschetti et al., 2007). Other drugs are used to manage mood disorder, anxiety and neurosis in later stages of the disease, but no treatment with a strong disease-modifying effect is currently available.

1.10.1 Anti-amyloid therapies

The main strategies that target Aβ include 1) reducing its production by modulating APP processing by α-, β- and γ-secretases, 2) reducing aggregation of Aβ and 3) enhancing clearance of Aβ by immunotherapy.

1.10.1.1 Drugs to reduce Aβ production

Therapeutic strategies to reduce production of Aβ include BACE1 inhibitors, γ-secretase inhibitors and α-secretase activators. PPAR (peroxisome proliferator activator receptor) agonists like rosiglitazone and pioglitazone and BACE1 inhibitors like CTS-21166 (Landreth et al., 2008) which reduce Aβ levels are currently under investigation (Mangialasche et al., 2010). A range of γ-secretase inhibitors (semagacestat, MK-0752, BMS-708163, PF-3084014, begacestat), E-2012 and a subset of non-steroidal anti-inflammatory drugs (NSAIDs) which act as γ-secretase modulators have shown to decrease Aβ production (Tomita, 2009). Up-regulation of α-secretase activity and non-amyloidogenic cleavage of APP to decrease production of Aβ and increase sAPPα have been shown to be neuroprotective. Many compounds have been shown to activate α-secretase activity (Marcade et al., 2008) and some of them are also currently being tested in patients with mild-to-moderate AD

(Mangialasche et al., 2010). Despite showing positive results in animal models, most drugs targeting Aβ production have failed in AD clinical trials. Development of drugs targeting secretases is particularly challenging because of the fact that these enzymes have a wide array of neuronal substrates and may have undesirable long term side-effects. Of these the type I transmembrane protein receptor, Notch is the most pharmacologically relevant as it has been difficult to develop specific inhibitors/modulators of Aβ42 without affecting Notch signalling. Indeed, a phase 3 trial of Eli Lilly's γ-secretase inhibitor, Semagacestat in 2,600 patients, with mild-to-moderate AD, recently failed. In addition, cognition and the ability to complete activities of daily living worsened with drug treatment and increased the risk of skin cancer for the patients on the drug compared to those on placebo. These side effects were most likely related to inhibition of Notch processing. A suitable therapeutic window needs to be defined, through which γ-secretase activity is selectively modulated, thereby allowing Notch and other substrates to be normally processed while simultaneously reducing Aβ generation. Although results from the Lily's recent trial has placed doubts on inhibiting γ-secretase as an effective approach to treating AD, it does not rule out other approaches to modulating this target. Indeed, there is a push by major pharmaceutical companies such as Pfizer to develop Notch-sparing inhibitors (BioCentury; Bernstein Report on Biobusiness, 23/8/10).

1.10.1.2 Drugs preventing Aβ aggregation

Evidence for the neurotoxic activity of Aβ oligomers constitutes the scientific basis for the development of compounds that inhibit Aβ aggregation or destabilise Aβ oligomeric species. A range of compounds targeting Aβ aggregation have been investigated including Tramiprosate (homotaurine, Alzhemed; a small compound that binds preferentially to soluble Aβ and prevents fibrillisation) (Aisen et al., 2007; Gauthier et al., 2009), Clioquinol (metal chelators which reduces Aβ-metal association: PBT1 and PBT2) (Adlard et al., 2008; Biran et al., 2009), Scyllo-inositol (promotes dissociation of Aβ

aggregates) (McLaurin et al., 2006) and Epigallocatechin-3-gallate (EGCG, anti-aggregation properties including a range of other neuroprotective functions) (Mandel et al., 2008). Compounds targeting Aβ aggregation have shown mixed results in AD clinical trials. Although promising, a major challenge in designing such compounds is to specifically target the toxic form of Aβ. Although soluble oligomers have been identified as the main toxic species, structural information is significantly lacking to engage target specific inhibitors. A fair amount of risk in modulating Aβ aggregation leading to increased toxic species in the brain may also be involved.

Inhibitors of Aβ aggregation from natural food products or dietary intake have been of interest in AD therapeutics. Peptides with capacity for amyloid inhibition, derived from bovine dairy sources including whey, casein and lactoferrin, have also been reported (Bennett et al., 2009). The Colostrinin peptide complex (proline-rich polypeptides derived from colostrums) was shown to inhibit and disrupt β-sheets of amyloid proteins (Schuster et al., 2005) and exert several other bioactive properties (Boldogh and Kruzel, 2008; Zimecki, 2008) that translated to proven neuroprotective bioactivity against AD (Bilikiewicz and Gaus, 2004). Successful *in vivo* neuroprotective studies with Colostrinin (Bilikiewicz and Gaus, 2004) suggest that other exogenous peptides, perhaps dietary sources, with amyloid inhibition capacity might be also be protective against AD.

1.10.1.3 Immunotherapy to promote Aβ clearance

Active and passive immunisations have been developed to remove soluble and aggregated Aβ from the CNS. In a phase 2 clinical trial of AN-1972 (anti-Aβ vaccine) in mild-to-moderate AD, some patients developed aseptic meningoencephalitis, which was attributed to cytotoxic T cells and/or autoimmune reactions to AN-1972 (Gilman et al., 2005). To avoid neuroinflammation, new vaccines that selectively target B-cell epitopes without stimulating T cells have been developed like CAD-106, ACI-24, UB-311, ACC-001 and V-950 which are currently in clinical trials (Muhs et al., 2007; Wang et

al., 2007). Another active immunisation strategy is AFFITOPE which is based on short peptides mimicking parts of native Aβ42 (Schneeberger et al., 2009). Passive immunisation using monoclonal/polyclonal antibodies targeting Aβ have been shown to reduce brain amyloid load with improvement in cognitive functions in AD models (Wilcock and Colton, 2008). Monoclonal antibodies currently being tested in clinical trials include bapineuzumab (humanised anti-Aβ monoclonal antibody), solanezumab (specific monoclonal antibody for soluble Aβ), PF-04360365 (humanised, modified IgG2 antibody that binds to the C terminus of Aβ40), GSK-933776, R-1450, and MABT-5102A (Salloway et al., 2009). Passive immunisation may be more effective in the elderly than active immunotherapy, due to reduced responsiveness to vaccines. But administration of antibodies is time consuming and costly. Active immunotherapy is cost effective and may guarantee constant high antibody titres. However the risk of inflammation and possible adverse effects are of concern.

1.10.2 Latrepirdine (Dimebon^{TM})

Several neuroprotective compounds which can enhance neurogenesis and reduce amyloid deposition are of current interest in many neurodegenerative diseases (Pieper et al., 2010). However their mode of action is largely uncharacterized and poorly understood. One of them is latrepirdine (2,3,4,5-tetrahydro-2,8-dimethyl-5-[2-(6-methyl 3-pyridinyl)ethyl]-1H-pyrido[4,3-b]indole), which is an orally-available, small molecule previously approved in Russia as a non-selective antihistamine (Bachurin et al., 2001). Latrepirdine was shown to weakly inhibit butyrylcholinesterase and acetyl cholinesterase, block the N-methyl-D-aspartate receptor signalling pathway, and inhibit mitochondrial permeability transition pore opening (Bachurin et al., 2001; Grigorev et al., 2003; Lermontova et al., 2001). Latrepirdine has also shown neuroprotective effects in models for AD (Bachurin et al., 2001) and Huntington's disease. In the initial clinical study in a Russian cohort, latrepirdine showed great promise for improving cognition in mild-moderate AD (Doody et al., 2008). However, a subsequent 6 month, US-Based replication (CONNECTION) trial showed no

benefits of the drug for AD. The exact causes for the mixed results in the AD clinical trials were unclear. The lack of understanding of a specific mechanism of action for latrepirdine was one of the main issues expressed for its mixed outcomes in two different phase II AD clinical trials (Bezprozvanny, 2010; Editorial, 2010a, b; Jones, 2010).

Interest in latrepirdine rebounded recently with the Steve McKnight paper in Cell pointing out the similarity of the latrepirdine scaffold to that of a new, neuroprotective class of drugs (Pieper et al., 2010). Subsequent studies have identified more neuroprotective functions for latrepirdine including enhanced neuronal survival (Zhang et al., 2010b), modulated Aβ secretion and metabolism (Steele et al., 2009) and clearance of α-synuclein protein aggregates (Wu et al., 2008; Yamashita et al., 2009). Some recent studies have also reported latrepirdine's cognitive enhancing properties, although the mechanism of action responsible for improving memory functions is still unclear (Giorgetti et al., 2010; Vignisse et al., 2011). Currently, a longer 12 month (CONCERT) trial for AD is still in progress and Phase 3 trial for Huntington's disease is also underway.

1.10.3 Current challenges in AD therapeutics

The search for a disease modifying therapy for AD has been very difficult. Some of the challenges that need to be addressed are 1) the heterogeneous nature of the disease (both pathology and epidemiology), 2) lack of a reliable diagnostic test for early detection and intervention, 3) drug delivery and ageing factors which may influence response to treatment, 4) linear and target driven reductionist approach in drug discovery 5) lack of high-throughput drug screening systems, 6) incomplete understanding of the drug-target mechanism and 7) AD drugs are targeted at a stage when brain is irreparably damaged and therefore effective treatment is unlikely.

The use of disease models ranging from *in vitro* non-cell based systems to transgenic animals form the basis for drug discovery and evaluation and elucidating disease mechanisms in AD. The use of animal models and the significance of alternative model systems in studying disease mechanisms and drug targets have been discussed further.

1.10.4 Disease models for AD

The majority of transgenic AD animal models represent overexpression of an EOAD associated mutation or particular fragments of human APP, to develop AD like pathology. Hence they are of immense value to gain knowledge about the mechanisms underlying AD pathology. AD animal models that provide information on Aβ deposition and memory impairment are most popular in drug testing as these attributes are considered relevant to AD pathogenesis. Apart from single, double and triple transgenic mice (Duyckaerts et al., 2008), other animal models used in AD research are hamsters (Hartig et al., 2007), rabbits (Woodruff-Pak et al., 2007), guinea pigs (Arjona et al., 2002), non-human primates (Kulstad et al., 2005), fruit flies (Ganguly et al., 2008), zebrafish (Newman et al., 2010) and worms (Link, 1995). A difficulty with any model is its relevance to AD and therefore extrapolation is indispensable, even in animal models (Duff and Suleman, 2004; Duyckaerts et al., 2008). Animal models are also very expensive, require rigorous maintenance and time-consuming, with years being required to reproduce an ageing process. In addition, animal models are unsuitable for high throughput screening techniques. Therefore, use of simpler model systems like yeast, worms, flies and zebrafish for studying disease mechanisms and map drug targets are more attractive. Yeasts are simple eukaryotic cells and provide a greater advantage comparing other model systems mainly due to its powerful genomic and proteomic screening methods and availability of a range of tools for molecular level analysis. The potential applications of yeast cell systems and models in AD research will be discussed further.

1.11 Yeast Models

Yeast is a unicellular eukaryotic organism and is widely known for its applications in molecular and cellular biology studies. Yeast growth and division can be controlled efficiently by adjusting environmental conditions. Moreover yeast species including baker's yeast *Saccharomyces cerevisiae* and fission yeast *Schizosaccharomyces pombe* are genetically tractable and greatly amenable to modifications such as gene disruption, mutations or gene-dosage effects. Because of these advantageous features, yeast cells have been the model organism of choice in both fundamental and applied medical research. For example, cell division cycle proteins (CDKs) were first identified in yeast cells (Nurse et al., 1998). Molecular pathways and essential proteins involved in autophagy were first identified and modelled in yeast cells (Klionsky, 2010). Also the cellular target of rapamycin (mTOR pathway inhibitor) was first discovered in yeast (Heitman et al., 1991).

1.11.1 Yeast genes and human disease

Yeast has been successfully used as a model for human diseases and particularly neurodegenerative disorders characterized by protein misfolding and aggregation (Braun et al., 2010; Winderickx et al., 2008). Comparison of the yeast and human genomes has revealed that 31% of genes involved in human disease have functional homologs in yeast and nearly 50% of human genes implicated in heritable diseases have yeast homologs (Foury, 1997; Hartwell, 2004a; Hartwell, 2004b; Koutnikova et al., 1997). In addition to similarity in gene sequences, yeast cells demonstrate similarity in various cell signalling and metabolic pathways. Studies have shown evidence of morphological markers of apoptotic and necrotic cell death in yeast (Madeo et al., 1997; Madeo et al., 1999). Yeast cells have also shown to demonstrate pathological markers associated with human neurodegenerative diseases such as oxidative stress, mitochondrial dysfunction and endoplasmic reticulum (ER) stress with expression of human proteins or exogenous treatment with toxic

agents (Eisenberg et al., 2007; Haynes et al., 2004). Intriguingly, ageing (both chronological and replicative ageing) also show similar markers in yeast cells.

Despite the evolutionary distance, the molecular pathways involved in cell death are highly conserved in yeast and humans (Braun et al., 2010). For example, regulators of cell death in yeast may include apoptosis-inducing factor (Aif1p), metacaspase (Yca1p), Ndi1p (homolog of AIF homologous mitochondrion-associated inducer of death; AMID), Bir1p (homolog of the inhibitor of apoptosis (IAP) family), Nuc1p (homolog of endonuclease G, EndoG), Bax inhibitor (BI-1), Nma111p (homolog of HtrA2/Omi), and Cpr3p (homolog of cyclophilin D) (Aerts et al., 2009; Buttner et al., 2007; Eisenberg et al., 2007; Madeo et al., 2009). It is to be noted that even though these cell death pathways are similar between yeast and humans, replication in mammalian cell models is essential for validation.

1.11.2 Yeast as an experimental tool for AD research

One of the most attractive advantages of yeast compared to other models is the availability of various experimental tools applicable for high throughput analysis of protein-protein, gene-gene and gene-protein interactions and associated cellular functions. Such tools offer an unbiased approach for studying the pathological functions of human disease proteins and establish models for drug screening. Some of the notable tools may include the classical yeast two/three-hybrid system for studying protein-protein interactions for a range of eukaryotic proteins (Ito et al., 2001), the Saccharomyces Genome Deletion Project (SGD) (Winzeler, 1999) which is a unique collection of knock-out strains covering 96% of the yeast genome and provides a unique tool for the functional analysis of the yeast genome (Giaever, 2002), Synthetic Genetic Array analysis (SGA) which is a high-throughput technique for exploring lethal or growth inhibitory genetic interactions (Tong et al., 2001) and large-scale protein localization analysis using green fluorescent protein (GFP) tags inserted individually at the C terminus of 6029 yeast ORFs covering 75% of the total proteome (Huh et al., 2003). These tools present a variety of applications in AD

research including studying drug targets/mechanisms and functional analysis of pathological AD related proteins.

A range of yeast models for studying AD related proteins have been developed to date (Table 1). Yeast models have been utilized for exploring APP processing, secretase activities, Aβ oligomerization/toxicity and tau phosphorylation (Figure 8). Yeast offers numerous advantages compared to mammalian models with its relatively less complex and well characterized biology. But, yeast also has natural limitations: they are unicellular and not functionally linked to other cells. Although they are primitive compared to neurons as they lack structures like synapses, axons and dendrites and related functions, yeast models continue to be a very valuable initial tool for investigating cellular mechanisms involved in AD (Bharadwaj et al., 2010) which can then be further validated in model systems.

Alzheimer's Disease Pathology	**Yeast Model**
Amyloid Precursor Protein (APP) processing	Expression of human APP (Le Brocque et al., 1998; Zhang et al., 1994; Zhang et al., 1997)
γ-secretase	Functional expression of human APP with engineered γ-secretase complex (Edbauer et al., 2004; Edbauer et al., 2003; Futai et al., 2009; Yagishita et al., 2008)
β-secretase	Expression of human β-secretase in yeast (Luthi et al., 2003; Middendorp et al., 2004)
C99	Processing of C99 Fragment (Sparvero et al., 2007)
In vivo Aβ Oligomerization	Two hybrid system (Aβ linked to LexA DNA binding domain and B42 transactivation domain (Hughes et al., 1996)
	Expression of Aβ/GFP fusion protein (Caine et al., 2007a)
	Expression of Aβ/Sup35p fusion protein (Bagriantsev and Liebman, 2006; von der Haar et al., 2007)
Extracellular Aβ Toxicity	Toxicity of oligomeric and fibrillar Aβ (Bharadwaj et al., 2008)
tau phosphorylation	Expression of human tau-3R and tau-4R isoforms, clinical mutant tau-P301L (Vandebroek et al., 2006; Vandebroek et al., 2005)

Table 1: Yeast models developed for studying AD pathology

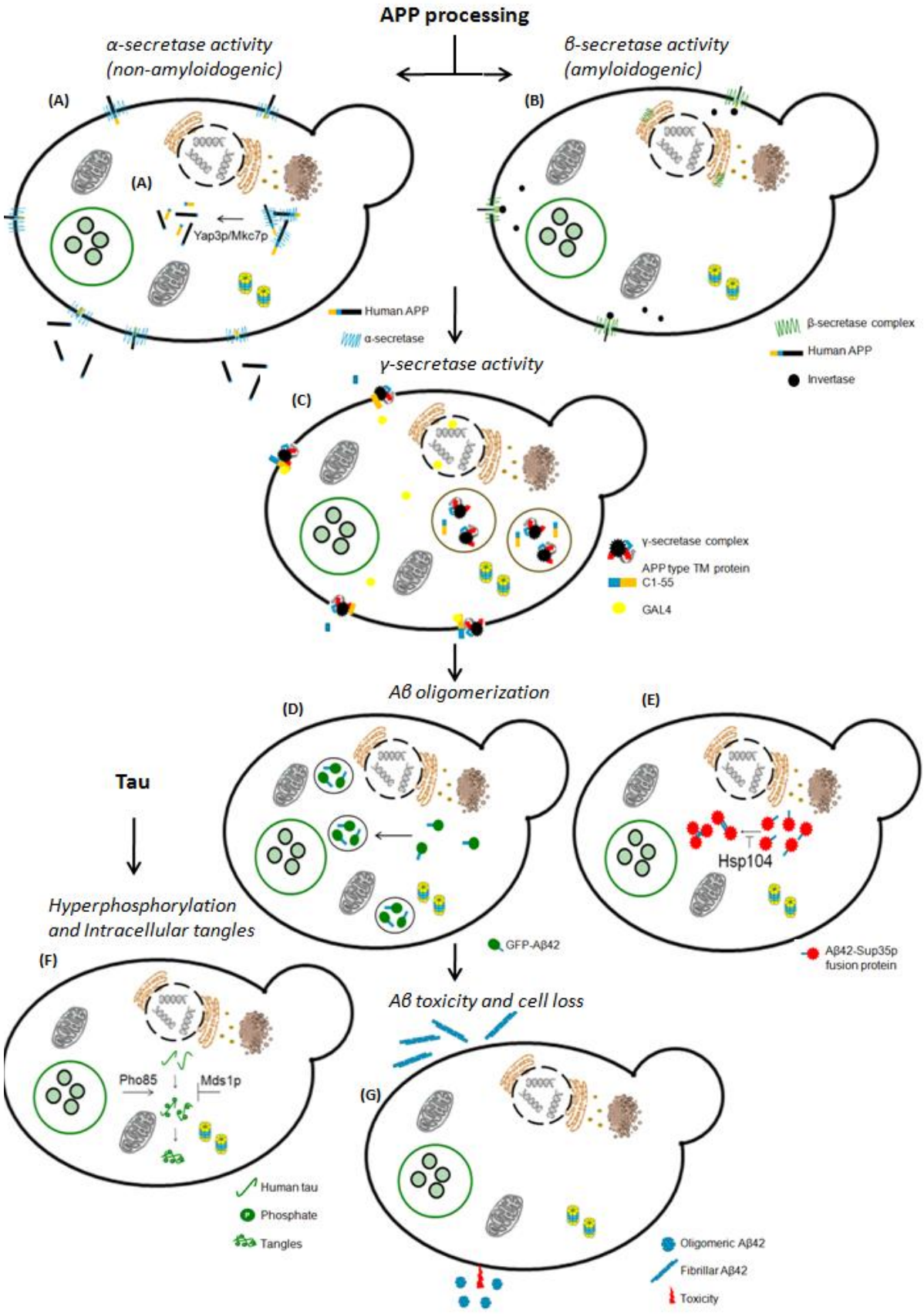
APP processing
α-secretase activity
(non-amyloidogenic)
β-secretase activity
(amyloidogenic)
(A)
(A)
Yap3p/Mkc7p
(B)
Human APP
α-secretase
β-secretase complex
Human APP
Invertase
γ-secretase activity
(C)
γ-secretase complex
APP type TM protein
C1-55
GAL4
Aβ oligomerization
(D)
(E)
Tau
Hsp104
Hyperphosphorylation
and Intracellular tangles
GFP-Aβ42
Aβ42-Sup35p
fusion protein
(F)
Aβ toxicity and cell loss
Pho85
Mds1p
(G)
Human tau
Phosphate
Tangles
Oligomeric Aβ42
Fibrillar Aβ42
Toxicity

Figure 8: Diagrammatic representation of engineered yeast models developed for studying downstream pathological events in AD

(A) Cells transfected with human APP to study endogenous α-secretase activity **(B)** Growth assay developed to monitor human β-secretase activity and screen for inhibitors, **(C)** Reconstitution of γ-secretase components using β-gal assay, **(D)** Aβ tagged to GFP to monitor localization and oligomerization, **(E)** Aβ42 tagged to Sup35p protein to study oligomerization, **(F)** Endogenous phosphorylation of human tau, **(G)** Extracellular toxicity of oligomeric and fibrillar Aβ42. (Adapted from Bharadwaj et al., 2009)

1.12 Hypothesis and Objectives:

AD is a very heterogeneous and a multifactorial ageing disorder of the nervous system. Accumulation and toxicity of the Aβ protein are key mediators of neurodegeneration in AD and a major target of interest in developing effective treatments. As described above yeast have a number of characteristics that allows investigation of AD related proteins that have key roles in AD pathogenesis and can enable the development of cell based screening techniques for novel drug discovery and identification of essential gene functions for Aβ clearance and protection against toxicity. This project mainly focuses on establishing and validating a yeast model of Aβ oligomer mediated toxicity and intracellular accumulation. Using these yeast models the project will address the following hypotheses:

- Oligomeric Aβ42 alters viability and proliferation of yeast cells.
- Whey derived peptides inhibit Aβ oligomer formation and associated toxicity.
- Recombinant MBP-Aβ42 fusion protein forms oligomers and is toxic
- The ubiquitin-proteasome and autophagy-lysosome intracellular degradation pathways have a role in reducing intracellular Aβ aggregates in yeast
- Enhancing autophagy in yeast reduces levels of intracellular Aβ aggregates
- Latrepirdine enhances autophagy and reduces the levels of intracellular Aβ aggregates in yeast.
- Latrepirdine promotes Aβ42 clearance *in vivo*.

The aims of the project are as follows:

1.) Study Aβ42 toxicity and growth effects

a.) Determine toxicity and uptake of Aβ42 and a modified Aβ42 (19:34) peptide in yeast cells.

b.) Investigate the effect of dairy derived peptides on Aβ42 oligomerization and toxicity

c.) Determine structural characteristics and toxicity of MBP-Aβ fusion proteins

d.) Determine if Aβ42 can promote proliferation of yeast within the stationary phase of cell growth and whether this can be blocked by inhibition of mTOR by rapamycin.

2.) Study intracellular accumulation and degradation of Aβ42

a.) Establish a yeast model for intracellular Aβ accumulation using GFP-Aβ42 and GFP-Aβ42 (19:34) expressing yeast.

b.) Study cellular degradation pathways involved in clearance of GFP-Aβ42 inside the yeast cell using autophagy and proteasomal activity deficient mutants.

c.) Determine if activation of autophagy by rapamycin promotes clearance of intracellular GFP-Aβ42 in yeast.

d.) Determine if latrepirdine can stimulate autophagy and promote GFP-Aβ42 clearance

e.) Determine if latrepirdine influences Aβ clearance *in vivo*

Chapter 2

Materials and Methods

2.1 Materials:

2.1.1 Yeast strains:

Strain	Genotype	Source
Candida glabrata	*Candida glabrata* ATCC 90030	Ass. Prof. Ian Macreadie, RMIT University
Saccharomyces cerevisiae (Kvy55)	*MAT*α *leu2 ura3 trp1 lys2 his3 suc2-* Δ*9*	Dr. Kuninori Suzuki, Tokyo Institute of Technology (Kirisako et al., 2000)
Saccharomyces cerevisiae (Kvy55:atg8Δ)	*MAT*α *leu2 ura3 trp1 lys2 his3 suc2-* Δ*9* Δ*apg8::HIS3*	Dr. Kuninori Suzuki, Tokyo Institute of Technology (Kirisako et al., 2000)
Saccharomyces cerevisiae (BY4743)	*MATa/MAT*α *his3*Δ*1/his3*Δ*1 leu2*Δ*0/leu2*Δ*0 LYS2/lys2*Δ*0 met15*Δ*0/MET15 ura3*Δ*0/*ura3Δ0	Dr. Gabriel Perrone University of New South Wales
Saccharomyces cerevisiae (BY4743:pep4Δ)	*MAT*α *his3*Δ*1/his3*Δ*1 leu2*Δ*0/leu2*Δ*0 LYS2/lys2*Δ*0 met15*Δ*0/MET15 ura3*Δ*0/*ura3Δ0 pep4Δ/pep4Δ	Dr. Gabriel Perrone University of New South Wales
Saccharomyces cerevisiae (BY4743:cvt1Δ)	*MAT*α *his3*Δ*1/his3*Δ*1 leu2*Δ*0/leu2*Δ*0 LYS2/lys2*Δ*0 met15*Δ*0/MET15 ura3*Δ*0/*ura3Δ0 cvt1Δ/cvt1Δ	Dr. Gabriel Perrone University of New South Wales
Saccharomyces cerevisiae (Wcg4a)	*MATa ura3 his3-11,15 leu2-3,112*	Dr. Ben Distel, University of Amsterdam (Heinemeyer et al., 1993)
Saccharomyces cerevisiae (Wcg4a:pre1Δ)	*MATa ura3 his3-11,15 leu2-3,112 pre1-1*	Dr. Ben Distel, University of Amsterdam (Heinemeyer et al., 1993)

Saccharomyces cerevisiae (Wcg4a:pre1-2Δ)	*MATa ura3 his3-11,15 leu2-3,112 pre1-1pre2-1*	Dr. Ben Distel, University of Amsterdam (Heinemeyer et al., 1993)

2.1.2 Yeast media:

1) Rich media (YEPD) contains 1% yeast extract, 2% peptone and 2% glucose in distilled water

2) Minimal media (YNB+2% glucose) contains 0.67% yeast nitrogen base (YNB) with 0.5% ammonium sulphate and 2% glucose in distilled water

3) Synthetic complete media (YNB complete) contains minimal media (YNB+2% glucose) supplemented with 20mg/L each of uracil, tryptophan, adenine, histidine and 30mg/L of leucine in distilled water.

4) Selective media (YNB+2% glucose, -selective amino acid) contains synthetic complete media with the selected amino acid omitted from the mixture for selective growth.

5.) Starvation media (YNB+ different carbon sources) contains 0.67% yeast nitrogen base with 0.5% ammonium sulphate and 2% maltose or 2% glycerol or 2% ethanol or 0.1% glucose in distilled water.

6.) Nitrogen starvation media (YNB -N) contains 0.67% yeast nitrogen base without ammonium sulphate, and 2% glucose in distilled water

For solid media, 1.7% bacto-agar was added to the liquid media composition.

2.1.3 Bacterial strains and media:

For plasmid amplification, *E. coli DH5α* strain (*fhuA2* Δ *(argF-lacZ) U169 phoA glnV44 Φ80* Δ*(lacZ)M15 gyrA96 recA1 relA1 endA1 thi-1 hsdR17)* was used. For production of MBP-Aβ fusion proteins, *BL21 (DE3) F- ompT hsdSB (rB-, mB-) gal dcm (DE3)* strain was used. Bacterial strains were grown in YT

media [0.8% bacto-tryptone, 0.5% yeast extract, 0.5% sodium chloride] plus 50µg/ml ampicillin.

For solid media, 1.7% agar was added to the liquid media composition.

Yeast extract, peptone, yeast nitrogen base (YNB), bacto-tryptone and bacto-agar were purchased from Difco or MP Biomedical. Amino acids were obtained from Sigma-Aldrich.

2.1.4 Plasmids:

Expression	**Plasmid vector**	**Selective marker**	**Reference**
GFP	p416	*URA3*	(Caine et al., 2007a)
GFP-N terminal fusion Aβ42	p416	*URA3*	(Caine et al., 2007a)
GFP-N terminal fusion Aβ42 (F19S:L34P)	p416	*URA3*	Constructed by Sonia Sankovich, CSIRO
GFP-N terminal fusion Atg8p with endogenous *Atg8* promoter	pRS306	*URA3*	Prof. Daniel Klionsky, University of Michigan (Suzuki et al., 2001)
MBP-5ala	pMALc2	*AmpR*	(Caine et al., 2007b)
MBP-N terminal fusion Aβ42	pMALc2	*AmpR*	(Caine et al., 2007b)
MBP-N terminal fusion Aβ16	pMALc2	*AmpR*	(Caine et al., 2011)

2.1.5 Mammalian cell culture reagents:

The human M17 neuroblastoma cell line was kindly provided by Dr. Kim Wark (CSIRO, Material Sciences and Engineering, VIC, Australia). SH-SY5Y human neuroblastoma cells and other cell culture reagents including Opti-MEM (minimum Eagle's medium), Dulbecco's MEM, neurobasal media, FCS (Foetal calf serum), horse serum, non-essential amino acids, penicillin, streptomycin, sodium pyruvate, trypsin were purchased from Gibco, Life Technologies (USA). Primary mouse cortical neuronal cultures were kindly provided by Dr. Giuseppe Ciccotosto (University of Melbourne). Primary cultures were prepared under sterile conditions as described previously (Barnham et al., 2003; Ciccotosto et al., 2004) and approved by the local institutional animal ethics committee. Briefly, embryonic, day 14, BL6J mouse cortices were removed, dissected free of meninges, and dissociated in 0.025% (w/v) trypsin in phosphate buffer. The dissociated cells were triturated using a filter-plugged fine pipette tip, pelleted, resuspended in plating medium (DMEM, 10% FCS, 5% horse serum).

2.1.6 Reagents:

Synthetic human Aβ42 was purchased from the W. M. Keck Laboratory (Yale University, New Haven, CT). Aβ42 with substitutions at positions [F19S] and [L34P] [Aβ42 (19:34)] was purchased from Biomatik Corporation (Wilmington, USA).

Mouse monoclonal antibody WO2, raised against amino acid residues 5-8 of N-terminal Aβ sequence (Cherny et al., 1999) was kindly provided by Prof. Colin Masters (University of Melbourne, VIC, Australia). Rabbit polyclonal antibody raised against GFP was purchased from Abcam. Horseradish peroxidase (HRP) conjugated anti-mouse and anti-rabbit antibodies were purchased from Abcam. Gold-conjugated anti-mouse antibody (Ultrasmall Gold) was purchased from Aurion (ProSciTech).

QuikChange II Site Directed Mutagenesis Kit was purchased from Stratagene. All restriction enzymes and T4 ligase were purchased from New England Biolabs (Beverley, MA). All were used according to the manufacturer's

instructions. DNA fragment purification was by QIAquick Gel Extraction Kit and DNA preparations by QIAprep Spin Miniprep Kit, both from Qiagen (Germany). DNA sequencing was carried out by Micromon Sequencing Facility (Monash University).

Oligonucleotide primers (for GFP cDNA), GFP-L (5' - 3') (TCACTGGTGTTGTCCCAATTT) and GFP-R (5' - 3') (CGT AAGTAGCATCACCTTCACCT) were purchased from GeneWorks, Australia. CellSure cDNA kit was purchased from Bioline, Australia. KAPA SYBR® FAST universal qPCR 2X mix was kindly supplied by Dr. Mark Brown (Edith Cowan University, WA, Australia).

FM 4-64 stain [N-(3-triethylammoniumpropyl)-4-(6-(4-(diethylamino) phenyl) hexatrienyl) pyridinium dibromide, (Cat no. T-3166)] and Fluorescein 5-isothiocyanate (FITC, Cat no. F1907) were purchased from Molecular Probes, Invitrogen. α-naphthyl phosphate disodium salt (Cat no. N7255) and D-sorbitol (S1876) were purchased from Sigma. Rapamycin (MW: 914.17, Sigma, Cat no. R0395) was a generous gift from Mr. Jay Steer (University of Western Australia, WA, Australia). Latrepirdine (Dimebolin dihydrochloride MW: 392.37) was purchased from Biotrend AG, Zurich. MTT reagent [3-(4,5-dimethylthiazol-2-yl)-2,5-diphenyltetrazolium bromide] was purchased from Sigma (M5655). CytoTox 96® Cytotoxicity assay kit (G1780) and CellTiter 96® AQueous Cell Proliferation assay (G3582) kits were purchased from Promega (NSW, Australia).

2.1.7 Miscellaneous consumables:

Nupage Novex 4-12% Bis-Tris gels, lithium dodecyl sulfate (LDS) sample buffer (40% glycerol 4% LDS, 0.025% phenol red, 0.025% serva blue G250, 2mM EDTA disodium, pH 7.6), MES running buffer (50mM Tris base, 50mM 3–(N–Morpholino)propanesulfonic acid, 1mM EDTA, 0.01% SDS at pH 7.3), iBlot western transfer kit were purchased from Invitrogen. Micro BCA protein assay kit and 0.2µm filters dialysis cassette with a 2kDa cut-off were purchased from Thermo scientific. 96 well microtitre plates were purchased from NuncBrand products. 10 kDa MWCO spin column and 0.2µm filters were purchased from

Pall Corporation (Australia). Gas permeable membrane was purchased from Diversified Biotech Inc. Uranyl acetate, LR Whiteresin and nickel grids (200 mesh) were purchased from ProSciTech. HRP-reactive Enhanced Chemiluminiscence reagent (ECL), Pharmacia S200 columns was purchased from GE Healthcare. Complete protease inhibitor cocktail was purchased from Roche. 1,1,1,3,3,3-hexafluoro-2-propanol (HFIP), dimethyl sulfoxide (DMSO), polyoxyethylene (20) sorbitan monolaurate (Tween-20), ampicillin, glutaraldehyde, formaldehyde, adenosine triphosphate (ATP), ammonium sulphate, glucose, maltose, ethanol, 1,4-piperazinediethanesulfonic acid (PIPES), Magnesium chloride ($MgCl_2$), Calcium chloride ($CaCl_2$), potassium chloride (KCl), ovalbumin, disodium hydrogen phosphate (Na_2HPO_4), potassium dihydrogen phosphate (KH_2PO_4). sulphuric acid (H_2S04), hydrochloric acid (HCl), methanol, isopropanol, ethylene diamine tetraacetic acid (EDTA), acetic acid (Ch_3COOH), magnesium sulphate ($MgSO_4$), 2-(N-morpholino)ethanesulfonic acid (MES). isopropyl b-D-thiogalactopyranoside (IPTG), ammonium molybdate ($(NH_4)_6Mo_7O_{24}$), sodum Nitrate (NaN_3), tris-(hydroxyl methyl)-methyamine (Tris), bovine serum albumin (BSA), sodium chloride (NaCl), phenylmethylsulfonyl fluoride (PMSF), sodium orthovanadate (Na_3VO_4), ascorbate were purchased from Sigma. Sodium Dodecyl sulphate (SDS) and Coomassie G-250 were purchased from Bio-Rad (Irvine, USA). Glycerol was purchased from ICN biomedicals. Cholesterol, triolein, oleate cholesterol, egg yolk phosphatidylcholine were purchased from Sigma. Human recombinant ApoE4 was purchased from Invitrogen.

2.2 Methods:

2.2.1 Protein detection and analysis:

2.2.1.1 Coomassie staining

Proteins samples containing LDS sample buffer were loaded and electrophoretically resolved on 4-12% Bis-Tris gels at 100V in MES buffer. The gels were then stained with Coomassie staining solution (0.2% Coomassie G-250, 7.5% Acetic Acid and 50% methanol) for 2-3h. Following the staining solution was removed and the gels were immersed in destaining solution (20%

methanol, 10% acetic acid) till clear bands appeared. The gels were scanned on a VersaDoc 4000MP imaging system.

2.2.1.2 Western Immunoblotting Analysis

Proteins samples containing LDS sample buffer were loaded and electrophoretically resolved on 4-12% Bis-Tris gels at 100V in MES buffer. The proteins were transferred from the polyacrylamide gel to a nitrocellulose membrane using iBlot dry transfer method. Membranes were blocked in 5% skim milk in TBS solution (50mM Tris, 150mM NaCl, pH 7.4) for 1h. Primary antibody was diluted in TBST solution (0.5% skim milk, 0.05% Tween in TBS) at concentrations of (1/3000 for WO2 and 1/5000 for anti-GFP). Incubation (2h at RT) was followed by three washes with TBST. HRP conjugated secondary antibody (anti-mouse or anti-rabbit) was diluted by 1/5000 in TBST solution and incubated with membranes for 1h. After washing with TBST followed by TBS, membranes were incubated for 2 min with ECL reagent. The membranes were then developed on films which were scanned using a Bio-Rad GS800^{TM} calibrated densitometer. The immunoreactive bands were later quantified using Quantity One 1-D analysis software (version 4.6.8).

2.2.1.3 Determination of protein concentration:

The Micro BCA Pierce protein assay kit was used to estimate the total protein concentration in all samples indicated. 100µl of blanks (respective lysis or suspension buffer) including standards and diluted samples (1/500) were added to a 96 well microtitre plate. Freshly prepared colorimetric reagents were added (100µl) to each sample and incubated for 30 min at 60°C. Following incubation the absorption at 595nm was measured using the FLUOstar OPTIMA multi-detection microplate reader. The protein concentrations in the samples were determined by reference to the bovine serum albumin (BSA) standard curve.

2.2.2 Preparation and characterisation of dairy SPE products

The dairy peptide products were kindly provided by Louise Bennet (CSIRO, Food Sciences Australia, Victoria, Australia). Dairy protein hydrolysate was prepared from bovine whey protein isolate (Murray Goulburn, Natrapro WPI, MG Nutritionals, Brunswick, Australia) by dispersing at 10% total protein (w/w) in 10mM tri-ethanolamine (Sigma, USA), 10% EtOH, and maintaining at pH 7.4 throughout processing. The enzymes: Glutaminase (Daiwa Kasei K.K., Shiga, Japan), Corolase PN-L (AB Enzymes GmbH, Darmstadt, Germany), Alcalase (2.4L, Novozymes, Bagsvaerd, Denmark) and Flavourzyme (1000L, Novozymes), were introduced in sequence, each at a final concentration of 0.5% (w/w) and incubated sequentially at 50°C for 1h. Finally, Trypsin (Novozymes, 0.5%, w/w) was added and incubated at 37°C for 17h before heating at 90°C for 30 min to inactivate all enzymes. The molecular size fraction <8 kDa was recovered by dialysis using regenerated cellulose membrane (6-8 kDa molecular weight cut-off, Spectrum Laboratories, Inc., Dominguez, CA) before further processing by ion exchange (IEX) chromatography, using 2 columns (4.6 x 10 cm) connected in series. Column 1 was packed with cation exchange resin (SP Sepharose Big Beads, GE Healthcare, Uppsala, Sweden) and Column 2 was packed with anion exchange resin (Q Sepharose Big Beads, GE Healthcare). Batches of dialysate (400ml) were loaded onto the pair of IEX columns with 400ml of eluant containing non-binding peptides recovered. In this case, the IEX-binding fractions were not recovered. Eluates were freeze dried and stored at -20°C. A single batch of the total hydrolysate was used for the reported studies.

The product (containing 12.2% nitrogen) was sub-fractionated using C18 solid phase cartridges (Strata-X 33µm Polymeric Reverse Phase cartridges (500mg/6ml, Phenomenex, California, USA). After washing with methanol and re-equilibrating with water, sample (100mg/ml total solids in water, 5.0ml) was loaded and non-binding solids eluted in a further 5.0ml of water (designated Load+Void sample). Bound fractions were sequentially eluted with 5.0ml of 40%

and 100% acetonitrile respectively (Ajax Fine Chem, NSW, Australia) and designated SPE40, and SPE100 respectively. In some cases the bound fraction was eluted entirely into 100% acetonitrile (SPE-total product). The ratio of solid eluted by 40% to 100% acetonitrile was approximately 19:1. Products were dried by evaporation under vacuum and stored at -20°C.

Amino acid analysis of the SPE-total product was conducted in duplicate using the High Sensitivity Waters AccQTag Ultra (Milford, MA, USA) chemistry. Results were expressed in mole percent of detectable amino acids. Tryptophan was not detectable by this method. SPE products were analysed (5mg/ml, 20µl injection) by reverse phase HPLC (Jupiter 5µ C18 300Å, 250 x 4.6 - Phenomenex, USA) under gradient elution (mobile phase A (0.1% TFA in water, Sigma) and B (0.1% TFA in 95% acetonitrile), using a Waters Alliance HPLC with a flow rate of 1.0 ml/min and photo-diode array detector set at 220nm. The gradient was programmed for 2 to 50% B over 54 mins, then 100% B for 4 mins before re-equilibration to starting conditions. The equivalence of batches of SPE40, SPE100 and SPE-total prepared for these studies, was routinely verified by HPLC profiling.

2.2.3 Expression and purification of MBP-Aβ fusion proteins

The cloning, expression and purification of recombinant MBP-Aβ fusion proteins was done as previously described (Caine et al., 2007b). Bacterial transformants were grown in 2X YT + 50 mg/ml ampicillin + 0.2% glucose at 37°C until the OD600 reached 0.8. For induction of recombinant protein expression, IPTG was added to a level of 0.3mM. Following overnight growth at 30^{o}C, the cells were harvested by centrifugation, weighed and resuspended in cold lysis buffer (50mM Tris pH 7.5, lysozyme 0.05mg/ml, Complete Protease Inhibitor) for 30 min. This solution was then sonicated and the crude protein extract was collected by centrifugation and purified by affinity chromatography using an amylose column (10mm X 10mm). All chromatography procedures were performed at 4°C. The MBP fusion proteins were eluted in 50mM Tris pH 7.5 buffer containing 10mM maltose. After elution, the eluted peak was

concentrated using 10 kDa MWCO spin column, sterile filtered using 0.2µM filters and stored at 4°C. The eluted protein was checked for purity and stability by SDS-PAGE and Western blotting using 4-12% NuPage gels in a MES buffering system and coomassie staining as described in Section 2.2.1. Gel filtration was performed on a superdex S200 (Pharmacia S200) column in 50mM Tris pH 8.0 at 0.5ml/min. Absorbance was monitored at 280nm.

2.2.4 Aβ peptide preparations and treatment in cells

2.2.4.1 Preparation of Aβ peptides:

Solutions of Aβ peptides were prepared according to the method of (Bharadwaj et al., 2008) with some modifications. 0.5mg Aβ peptide was dissolved in 500µl HFIP solution and incubated overnight at RT. The Aβ dissolved HFIP solution was aliquoted into 5 tubes each containing 0.1mg Aβ peptide. The HFIP was then evaporated by vacuum and the tubes containing the peptide films were stored in the -80 freezer. Aβ peptide solutions were prepared fresh prior to use. The 0.1mg peptide film in the tube was dissolved in 200µl sterile double-distilled water. The solution was vortexed and sonicated on ice for 5 min followed by centrifugation for 10 min at 14000xg. The supernatant was incubated at RT overnight which was used for the toxicity experiments. The concentration of the Aβ solution was approximately 0.5mg/ml (~110µM). The exact concentration was determined by measuring absorbance at 214nm. The final concentration was calculated using the formula Aβ (M) = Abs214 x dilution factor (DF) / 75887. All solvents used for the preparation of Aβ solutions were filtered using 0.2µm filters and the entire procedure was performed in laminar air flow hoods. Both Aβ42 and Aβ42 (19:34) peptide solutions were prepared as described above.

2.2.4.2 Fluorescein isothiocyanate (FITC) labelling of Aβ peptides:

FITC labelling of Aβ peptide was done as described by manufacturer's (Invitrogen, Molecular probes) instructions with slight modifications. FITC

dissolved in DMSO (10mg/ml) was mixed with premade Aβ solution [0.5mg/ml (~110µM)] at 1:10 (wt/wt) dye: protein ratio. The mixture was incubated at 4˚C on a rotator for 2h. The labelled peptide solution was dialyzed in sterile double-distilled water at 4˚C for 2h using a dialysis cassette with a 2kDa cut-off to remove unlabelled FITC molecules. Following dialysis, the solution was centrifuged for 10 min at 14000g and the supernatant was used for experiments. Aβ42 and Aβ42 (19:34) were FITC labelled as described above.

2.2.4.3 Aβ treatment in Yeast cells: colony count viability assay:

Yeast cells (*Candida glabrata*) were stored on YEPD agar plates at 4ºC. A single yeast colony from stock agar plates was inoculated in 5ml YNB+2%glucose and incubated with shaking at 30ºC overnight. The overnight culture was resuspended in fresh YNB+2%glucose to an initial cell density (OD at 600nm) of 0.2. The culture was then incubated at 30ºC with shaking and grown up to exponential phase (OD 1.5-2). These cultures were diluted to ~5X10^3 yeast cells/ml in sterile, pure water. Cells were then aliquoted into 96-well microtitre plates for peptide treatments. Vehicle or peptide preparations were added to the diluted cell suspension to required concentrations. The final volume in each well was made up to 125µl. The microtitre plate was then sealed with a gas permeable membrane and incubated at 30°C constantly shaken at 150rpm for time periods as indicated. Cell survival was determined by plating aliquots of the cell suspensions onto YEPD agar plates to measure the number of colony-forming units (CFU) after incubation at 30°C for 2 days. Cell viability following Aβ treatment was calculated from the CFU count and represented as percent change from vehicle treated.

2.2.4.4 Aβ treatment in M17 Neuroblastoma cells: MTT viability assay:

The human M17 neuroblastoma cell line was maintained in Opti-MEM medium supplemented with 10% FCS (Foetal calf serum), 0.1mM non-essential

amino acids, 50 IU/ml penicillin, 50mg/ml streptomycin, and 1mM sodium pyruvate, in 5% CO2 at 37˚C. Cells were seeded in 96-well tissue culture plates at 10^4 cells per well and incubated for 20h. Cells maintained in serum free Opti-MEM media were incubated with freshly prepared Aβ solutions for 48h at 37˚C. Cell viability was determined using MTT toxicity assays (Robert et al., 2009). Following Aβ treatment, cells were re-suspended in 100µl fresh Opti-MEM media containing 5mg/ml MTT [3-(4,5-dimethylthiazol-2-yl)-2,5-diphenyltetrazolium bromide] for a 24h incubation at 37˚C. Plates were centrifuged, the supernatant was removed and 100µl of 0.1M HCl in isopropanol was added to each well to dissolve the MTT crystals. The absorbance was measured at 560nm using the FLUOstar OPTIMA multi-detection microplate reader. Cell viability following Aβ treatment was calculated from the absorption values at 560nm and represented as percent change from vehicle treated.

2.2.4.5 Aβ treatment in SH-SY5Y human neuroblastoma cells: LDH and MTS viability assays

The SH-SY5Y human neuroblastoma cell line was maintained in DMEM medium supplemented with 10% FCS (Foetal calf serum), 50 IU/ml penicillin, 50mg/ml streptomycin in 5% CO2 at 37˚C as described in (Zhang et al., 2009). For Aβ42 toxicity experiments, cells were plated in 96-well tissue culture plates at a density of 10^4 cells/well in DMEM media containing 1% FCS for 20h. Oligomeric Aβ42 (10µM) co-incubated for 20h with SPE products (0.001-0.1 mg/ml) was added to the cells and incubated for 72h at 37°C. Lactate dehydrogenase (LDH) released into the media as a result of Aβ42 toxicity, was measured in cell supernatants using the CytoTox 96R Cytotoxicity assay as per manufacturer's (Promega) instructions. The cells were then incubated (4h at 37°C) with fresh DMEM medium containing 1% (v/v) MTS reagent and viability was measured as per manufacturer's (Promega) instructions. The fluorescence (LDH) or colorimetric (MTS) measurements were determined using a Fluostar Optima plate reader (BMG Labtech, Victoria, Australia), and results corrected

for reagent controls. The data were reported as the percentage standardized change compared with sample-free controls, after correction for reagent blanks.

2.2.4.6 MBP-Aβ fusion protein treatment in primary cortical neurons: CCK-8 assay

The mouse primary cortical cell cultures were prepared and maintained in an incubator set at 37 °C with 5% CO_2 as described before in Section 2.1.5. The cells were allowed to mature for 6 days in culture before commencing treatment using freshly prepared neurobasal medium plus B27 supplements minus antioxidants. For the treatment of neuronal cultures, freshly prepared soluble MBP-Aβ and MBP stock solutions were diluted to 30µM in neurobasal medium and added to neuronal cells for up to 4 days *in vitro*. Cell viability was quantitated using the CCK-8 assay kit according to the manufacturer's instructions (Dojindo, Maryland, USA). Briefly, the medium was replaced with fresh neurobasal medium supplemented with B27 lacking antioxidants, and 10 % v/v CCK-8 was added to each well and incubated for 3h at 37°C in a 5% CO_2 incubator. Plates were gently shaken, and a 150µl aliquot from each well was transferred to separate wells of a 96-well plate. The colour change of each well was determined by measuring the absorbance at 450nm using a FLUOstar Omega (BMG LABTECH, Germany) microplate reader and background readings of CCK-8 incubated in cell-free medium were subtracted from each value before calculations. The data were normalized and calculated as a percentage of untreated vehicle control values.

2.2.5 Localization analysis of Aβ peptide treated yeast cells:

2.2.5.1 Preparation of cell extracts from Aβ treated yeast cells

Uptake of Aβ was determined by Aβ immunoblotting analysis of soluble and insoluble membrane protein extracts of yeast cells treated with Aβ peptides. Exponentially-growing yeast cells (*Candida glabrata*) in YNB+2%glucose were treated with Aβ peptide (5µM) for 3, 6, or 20h. Following treatment, the cells

were washed in 1XPBST (1XPBS+0.05% tween) and resuspended in 1XPBS containing 1Xcomplete protease inhibitor cocktail (PI). For cell lysis, the mixture was vortexed with 0.5-0.6mm diameter glass beads for 4 min with intermittent cooling on ice and centrifuged at 14000g for 15 min. The supernatant contained the soluble cytosolic protein fraction. The pellet was washed in 1XPBST and resuspended in lysis buffer (1% SDS/2M urea/200mM Na_2CO_3) + 1XPI. The mixture was incubated at 50°C for 20-30 min followed by centrifugation at 14000xg for 15 min. The supernatant contained the insoluble membrane associated protein fraction (Caine et al., 2007a). The protein extracts were analysed by Aβ western immunoblotting as described above.

2.2.5.2 Fluorescent Light Microscopy:

For studying the localization of Aβ, yeast cells were treated with FITC labelled Aβ peptides (5μM) for 6h, washed in 1XPBST (1XPBS+0.05% tween) and resuspended in 1XPBS. A total of 4-5μl of the suspension was loaded on a microscopic slide for imaging using oil immersion at 100X magnification. Cells were analysed by fluorescent microscopy using wide field optics in Olympus BX51 Upright Microscope. Fluorescent and bright field images were taken using Olympus DP71 digital camera. For a better resolution and co-localization analysis, yeast cells treated with FITC-Aβ42 peptide were observed using Leica TCS NT upright confocal microscope (Dr. Judy Callaghan, Monash Micro Imaging). Yeast cells were treated with FITC labelled Aβ42 (5μM) for 6h, washed in 1XPBST (1XPBS+0.05% tween) and resuspended in 1XPBS. The cells were then incubated with lipophilic membrane stain FM4-64 (1μM) for 20min at RT, followed by further washing in 1x PBST and resuspended in 1X PBS. A total of 4-5μL of the suspension was loaded on microscopic slide for imaging using oil immersion at 100X magnification. Images were taken with different fluorescent filters (red and green channels) using Olympus DP71 digital camera. Image and overlay analysis was done using Leica LASAF imaging software.

2.2.5.3 Transmission electron microscopy of yeast cells:

Aβ42 peptide treated yeast cells (6h) were prepared for imaging by transmission electron microscopy according to the protocol described by (Wright, 2000). The method involved fixation, cell wall permeabilization, ethanol dehydration, embedding in LR White resin, sectioning, labelling and imaging.

Pre-fixation: The cells were incubated in 1X fixative (0.2M PIPES, pH 6.8, 0.2M sorbitol, 2mM $MgCl_2$, 2mM $CaCl_2$, 0.5% glutaraldehyde, 4% formaldehyde) at RT for 5 min. The cells were washed in water and resuspended in 1X fixative and incubated for 30 min at 4°C. The fixative was removed by centrifugation and cells were resuspended in water and incubated for 10 min. To permeabilize the cell wall, the yeast cell suspension was incubated in 1% sodium metaperiodate for 15 min at RT. The cells were then washed in water and resuspended in 50 mM ammonium chloride for 15 min at room temperature for quenching of free aldehydes. Dehydration was done by incubating the cells in a graded ethanol series (25, 50, 75, 95, and 100% ethanol).

Embedding: The dehydrated yeast cell suspensions were embedded in LR White resin. The ethanol dehydrated yeast pellet was suspended in 2:1 ethanol:resin and incubated in a glass vial for 1h. The resin was replaced twice with 1:1 ethanol:resin and incubated overnight. Following incubation the ethanol:resin mixture was removed and replaced twice with 100% resin and incubated for 1h. The resin was then filled into a gelatine capsule.

Thin-Sectioning: The capsules were incubated in a temperature block at 45°C for hardening. Thin sections of 80-120nm were prepared using an ultra-microtome with diamond knife (Jacinta White, CSIRO, Material Sciences Engineering, Clayton, Australia). The thin sections were then overlayed onto nickel grids.

Aβ Immunolabeling: The nickel grids were blocked in $TBSTO_{em}$ (140mM NaCl, 3mM KCl, 0.05% Tween-20, 2% ovalbumin, 8mM Na_2HPO_4 and1.5mM KH_2PO_4) for 15-30 min. The grids were removed from blocking buffer and

excess liquid was removed using a piece of torn filter paper. Following the grids were then incubated with the primary antibody (WO2, 1/1000 dilution in $TBSTO_{em}$) for 2h. Following three washes with $TBST_{em}$ (140mM NaCl, 3mM KCl, 0.05% Tween-20, 8mM Na_2HPO_4 and1.5mM KH_2PO_4) the grids were blocked in $TBSTO_{em}$ for 15-30 min. Later the grids were incubated for 1h with gold conjugated secondary antiserum (anti-mouse, 1/2000 dilution in $TBSTO_{em}$). The grids are washed in $TBST_{em}$ three times. Following the grids were submerged in 2% glutaraldehyde in TBS and incubated for 1h. The grids are then washed in three times in $TBST_{em}$, two times in TBS and in distilled water. The grids are then air dried and stored in a grid box.

Imaging of yeast sections using transmission electron microscope: The grids were stained with 2% uranyl acetate for 5–15 min and washed in water. The grids were then stained with reynolds' lead citrate for 5 min at RT following another wash step. Grids were examined in a Tecnai 12 transmission electron microscope operating at 120 keV, and images were obtained using a Soft Imaging Systems MegaView III CCD camera.

2.2.6 Preparation of crude yeast plasma membrane fractions:

The isolation of yeast plasma membrane fractions was performed as described by (Monk et al., 1991). Untreated cells were washed twice with distilled water and resuspended in homogenization medium (2.5mM EDTA, 1mM phenylmethylsulfonyl fluoride (PMSF), and 50mM Tris, pH 7.5) with 0.5-0.6µm diameter glass beads. The mixture was then vortexed for 4 min with intermittent cooling on ice and centrifuged. Immediately after cell disruption, the homogenate was adjusted to pH 7.25 with 2M Tris. After two centrifugations at 5000g for 10 min to remove cellular debris and unbroken cells, a crude membrane fraction was pelleted from the supernatant by centrifugation at 30000g for 1h. The crude plasma membrane fraction was pelleted from the supernatant by centrifugation at 76000g for 1 h. The crude membranes were washed and suspended in plasma membrane suspension buffer (20% glycerol, 1mM EDTA, 1mM PMSF and 10mM Tris, pH 7.0). The crude plasma

membranes were snap-frozen in liquid nitrogen and transferred to -70˚C for storage.

2.2.7 Delipidation of yeast plasma membrane fractions and sample preparation for mass spectrometric analysis:

Crude plasma membrane fractions from cells treated with 5μM Aβ42 and Aβ42 (19:34) were prepared as described above. Delipidation of Aβ-treated yeast membrane fractions was done according to (Mirza et al., 2007). The crude plasma membrane fractions were incubated in 0.75ml of chloroform on a shaker at room temperature for 1h. To this, 0.75ml of methanol water (1:1 vol/vol) was added, and the mixture was vortexed for 10 min. The mixture was centrifuged at 2000g for 1 min, and the chloroform layer was discarded. Another 1ml of chloroform was added to the mixture and sonicated in a bath sonicator for 30 min. The mixture was then centrifuged at 14000g for 5 min. The chloroform layer was discarded. To the aqueous layer 1ml acetone was added and incubated at 4°C for 1h. The protein was recovered by centrifugation at 10000g for 15 min. The protein precipitate was dissolved in 70% acetonitrile, 0.1% TFA and analysed in an Agilent Q-TOF 6510 mass spectrometer (Bio21, University of Melbourne, VIC, Australia).

2.2.8 Plasma membrane ATPase assays:

Yeast plasma membrane ATPase assays were performed by the colorimetric measurement of free phosphate released by ATP hydrolysis in microtiter plates (Monk et al., 1991). The basic ATPase assay medium contained 15mM MgSO4 and 15mM ATP in 50mM MES-Tris buffer at pH 6.0 but also included 0.2mM ammonium molybdate, and 5mM NaN_3 to eliminate nonspecific phosphatase, and mitochondrial ATPase activities. The crude plasma membrane fractions were incubated with different concentrations of freshly prepared Aβ peptide solutions for 15-20 min, prior to addition of ATPase assay medium. The final reaction mixture was incubated for 1h at RT, and the

reaction was stopped by addition of 100µl of a stop developing reagent containing 1% SDS, 100mM ammonium molybdate, 0.6M H_2S04, and 0.8% ascorbate. After a 10 min of incubation at RT, the absorbance at 630nm was determined. Activity was measured by subtracting the absorbance at 630nm of the same set of sample treated with ATPase inhibitor vanadate (Na_3VO_4). The amount of phosphate (Pi) liberated was estimated by reference to a linear standard curve containing 0-100nM of H_3PO_4 in the reaction mixture. The values were represented as percent activity of the vehicle treated.

2.2.9 Protein structure analysis

2.2.9.1 Dynamic light scattering of MBP and MBP-Aβ fusion proteins

Dynamic light scattering (DLS) analysis of MBP and MBP-Aβ solutions was done by Dr. Jo Caine (CSIRO, Parkville, Australia) as described in (Caine et al., 2011). DLS was completed using Dyna Pro Nano Star plate reader at laser wavelength 830nm. Both MBP and MBP-Aβ42 (~0.8mg/ml) was set up in triplicates in a Greiner 384-well low volume glass bottom plate (approx 20 µl working volume). Forty individual 5 second DLS collections per well were taken at 25ºC. The hydrodynamic radius, R_h, was estimated from translation diffusion coefficient by the Stokes–Einstein relationship. For comparison the radius of gyration, R_g, was calculated as follows. For MBP protein the MOLREP program (Vagin and Teplyakov, 1997) was used with the crystal structure [PDB: 4MBP] (Quiocho et al., 1997)) and R_g was adjusted by a scaling factor of $\rho=R_g/R_h=0.77$ (Wilkins et al., 1999) for globular protein structures like MBP. For MBP-Aβ fusion proteins with unknown structures the empirical relationships established by (Wilkins et al., 1999) $R_h=0.475\ N^{0.29}$ nm for native proteins and $R_h=0.221\ N^{0.57}$ nm for highly denatured proteins, where N is a number of protein residues, were used. The average radii, R_{av}, of the MBP-Aβ fusion proteins were also estimated from volumes occupied by the protein molecules: $V = D\ M\ 10^{-3}$, where D=1.43 (nm^3/Da) is the mean density of proteins (Quillin and Matthews, 2000), M, the molecular weight in Dalton and V, the volume of the protein in nm^3.

2.2.9.2 Circular Dichroism Spectroscopy

Aβ42 peptide solutions were prepared as described in Section 2.2.4.1. Aβ42 peptide solutions (0.05mg/ml; 11µM), pre-incubated with different concentrations of SPE40 and SPE100 preparations (Section 2.2.2) (final concentrations: 005, 0.05 & 0.25 mg/ml in de-ionised water) were analysed by Jasco J-810 CD Spectropolarimeter (JASCO Inc., Easton, MD, USA). The mean residue ellipticities of samples were recorded across the far UV range (190-260 nm), using a 0.1cm path-length quartz cuvette, at room temperature, monitoring at 0.1 nm intervals. The acquisition parameters were 100 nm/min with 1 sec response times, 1.0 nm bandwidth, and 0.1 nm data pitch, and data sets were averaged over 3 scans. Spectra of SPE products alone at appropriate concentrations were subtracted from respective profiles of Aβ42+SPE product, but were otherwise unsmoothed. The instrument was calibrated with de-ionised water. The spectra were analysed and generated using the Jasco's Spectra Manager ^{TM}.

2.2.9.3 Fourier Transform Infra-Red Spectroscopy

Fourier transform infrared (FTIR) spectroscopic analysis of Aβ42+SPE fractions were done by Rabia Sarroukh (Université Libre de Bruxelles, Belgium). Aβ42 peptide solutions were prepared as described in Section 2.2.4.1. Aβ42 peptide solutions (0.05mg/ml; 11µM) were pre-incubated with different concentrations of SPE40 and SPE100 preparations (Section 2.2.2) (final concentrations: .001, 0.005, 0.01, 0.05 & 0.1 mg/ml mg/ml in de-ionised water). Following, IR spectra of the solutions were recorded using a Equinox 55 infrared spectrophotometer (Bruker Optics, Ettlingen, Germany) placed in a thermoregulated room (21°C) and equipped with a liquid N_2-refrigerated mercury-cadmium-telluride detector. Fourier self-deconvolution was applied to increase the resolution of spectra in the amide I region, which is that most sensitive to protein secondary structure. The FTIR data were preprocessed as described in (Goormaghtigh et al., 1999). Briefly, the water vapor contribution was subtracted with $1956^{-1}935$ cm^{-1} as the reference peak, and then the spectra were baseline-corrected and normalized for equal area between 1700-1500

cm^{-1}. The spectra were finally smoothed at a final resolution of 4 cm^{-1} by apodization of their Fourier transform using a Gaussian peak shape (full width at half height of 13.33 cm^{-1}) and self-deconvolution was carried out using a Lorentzian peak shape (full width at half height of 20 cm^{-1}). The resolution enhancement factor was therefore 1.5. Extraction of spectral data was conducted using in-house software generated with Matlab (Mathworks Inc. Natick, MA, USA).

2.2.9.4 Transmission Electron Microscopy

Aβ42 peptide pre-incubated with SPE fractions (Section 2.2.2) and MBP/MBP-Aβ fusion protein were analysed by transmission electron microscopy (TEM). The samples were diluted to a final concentration of 0.01mg/ml with de-ionised, filtered (0.2 µm) water before applying to carbon-coated 400-mesh copper grids, which had been glow discharged in nitrogen. After 1 min adsorption time excess sample was wicked off with filter paper and the sample stained with 2–3 drops of 2% aqueous uranyl acetate. The grids were air-dried and examined in a Tecnai 12 Transmission Electron Microscope (FEI, Eindhoven, The Netherlands) operating at 120 KV. Micrographs are recorded using a Megaview III CCD camera running under AnalySiS imaging software (Olympus Australia, Mt Waverley, Australia).

2.2.10 Inducing stationary phase in yeast

Yeast cells were stored on YEPD agar plates at 4ºC. A single yeast colony from stock agar plates (*Candida glabrata* or *Saccharomyces cerevisiae* BY4743) was inoculated in 5ml YNB+2%glucose or YNB+2%glucose (-trp) respectively and incubated with shaking at 30ºC overnight. For inducing stationary phase, the overnight culture was washed in sterile water and resuspended in YNB+ different carbon sources including 2% maltose or 2% glycerol or 2% ethanol or 0.1% glucose media at a starting dilution of 0.2 optical density (OD) at 600nm and incubated for 7h at 30°C. For normal growth the

overnight culture was incubated in YNB+2%glucose or YNB+2%glucose (-trp) for *Candida glabrata* or *Saccharomyces cerevisiae* BY4743 respectively. The growth was determined every hour for 7h by measuring the OD at 600nm.

Flow cytometric analysis of yeast cells (*Candida glabrata*) was done in Beckman Coulter EPIC flow cytometer. The size distribution of actively growing cells (exponential phase) in YNB+2%glucose and starved cells (stationary phase) in YNB+2%maltose were studied by forward scatter (FSC) analysis (Tzur et al., 2011). Data was analysed using CellQuest analysis software. To determine budding, the cells were analysed by light microscopy.

2.2.11 Aβ treatment of stationary phase yeast cells

The stationary phase yeast cells were treated with Aβ42 peptide similar to treatment in exponential phase cells described above (Section 2.2.2.3). Cell proliferation was determined by plating aliquots of the cell suspensions onto YEPD agar plates to measure the number of colony-forming units (CFU) after incubation at 30°C for 2 days. Cell proliferation following Aβ treatment was calculated from the CFU count and represented as percent change from vehicle treated.

2.2.12 Construction of GFP-Aβ42 (19:34) mutant in p416 plasmid

The yeast shuttle plasmid, p416.GPD (Mumberg et al., 1995) was used to express GFP, GFP-Aβ42 and the mutant GFP-Aβ42 (19:34) in yeast. It is a centromeric plasmid stably maintained at one or two copies per cell, and has the strong constitutive GPD promoter to direct heterologous gene expression throughout the yeast life cycle. Standard molecular biology techniques were used for the construction of recombinant plasmids. Briefly, a GFP coding fragment was isolated from pAS1N (Prescott et al., 1997) and inserted into p416.GPD. The GFP-Aβ42 fragment was obtained from pAS1N.GFP-Aβ42 from the previous work (Caine et al., 2007a).

The GFP-Aβ42 (19:34) mutant was constructed in p416 (Figure 1) by Sonia Sankovich, CSIRO. To create the GFP-Aβ42 (19:34) mutant, site-directed mutagenesis was carried out on a sub-fragment cloned into pBluescript to avoid spurious changes in coding sequences. The changes effected were F19S, L34P, with numbering referring to Aβ amino acid residue number. Sequencing was carried out to confirm that the required changes had been effected and that no additional mutations were introduced into the Aβ coding sequence. Mutated fragments were subsequently cloned back into p416.GPD.

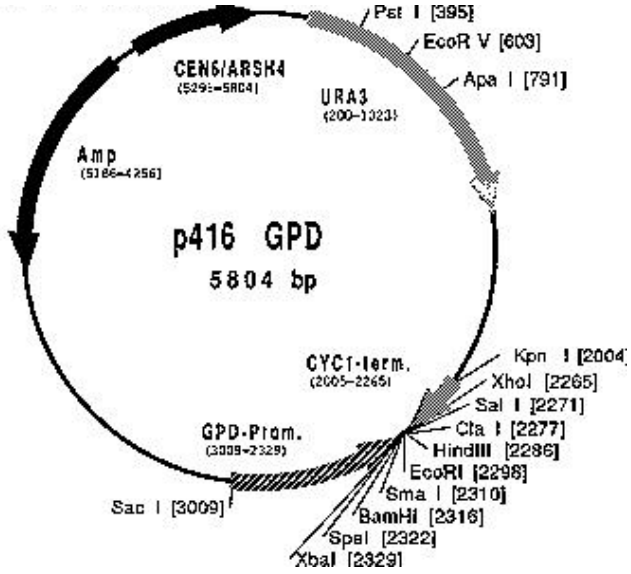

Figure 1: The p416 is a shuttle vector with low copy number. It has the ampicillin resistance selectable marker (*AmpR*) and uracil synthesis selectable marker (*URA3*) genes. (Adapted from www.atcc.org)

2.2.13 Yeast Transformation:

Yeast cells were transformed with p416 (GFP/GFP-Aβ expressing) and pRS306 (GFP-Atg8p expressing) using electroporation. A single colony of the untransformed yeast strain was inoculated in 5ml YEPD media and incubated at 30ºC overnight with shaking. The overnight culture was transferred into fresh YEPD media and grown until mid-exponential phase (OD at 600nm, 1). Cells were washed in ice-cold sterile water two times and then in 1M sorbitol. The cells were then resuspended in 1M sorbitol. A 50µl aliquot of the yeast

suspension was mixed with ~5µg plasmid DNA in a pre-chilled electroporation cuvette (0.2cm) and pulsed once at V=1.5kV, 25µF, 200Ohms. A 1M sorbitol (500µL) was added to the yeast suspension and plated out on selective media agar plates (YNB+2%glucose –ura for p416 and pRS306 expression). The plates were then incubated at 30ºC for 5-6 days. Yeast colonies from the transformant plates were then re-streaked onto fresh selective media agar plates (YNB+2%glucose –ura) and stored at 4ºC after formation of yeast colonies.

2.2.14 cDNA synthesis and Real Time PCR:

Starting culture (OD 0.2) of GFP, GFP-Aβ42 and GFP-Aβ42 (19:34) expressing yeast cells (KVY55) were grown in selective YNB+2%glucose (-ura) media till exponential phase (OD 0.6). Untransformed cells (KVY55) grown in YEPD media were also collected (OD 0.6). Total cell number and viability was measured by Vi-CELL XR cell counter. The cDNA from the frozen pellets (~1-3 X 10^6 cells) was synthesized using CellSure cDNA kit (Bioline). A 1uL aliquot of the cDNA template was mixed with KAPA SYBR® FAST universal qPCR 2X mix, primers for GFP (L, R: 5µM final) and DNase free water to a final volume of 15µl. The samples were run on the iQ5 real-time PCR detection system. Using the LinRegPCR (version 2009) software the threshold C_t values and the mean PCR efficiencies were calculated. GFP transcript levels/10^6 cells was calculated by using the comparative C_t method with slight modifications, The transcript levels were expressed as levels/10^6 cell = 10^6 * (relative $2^{-(\Delta Ct)}$ value/total number of cells) (Schmittgen and Livak, 2008).

2.2.15 Agarose gel electrophoresis:

The PCR products (from rtPCR reaction described above, Section 2.2.14) were analysed by agarose gel electrophoresis and observed under UV transillumination. Agarose (1.5%) was prepared in 1 x TAE (0.04M Tris-acetate, 0.001M EDTA, pH 8.3) by boiling in a microwave. The dissolved agarose was cooled to ~60°C and then poured into a gel tray to set, with combs positioned to

produce sample wells. Set gels were placed in tanks (Bio-Rad), which were then filled with 1XTAE buffer. Ethidium bromide (stock solution 10mg/ml) was added to give a final concentration of 1 µg/mL in the cooled gel before pouring. Sample loading dye was added to samples and loaded into the wells. Gels were run at 70 Volts for 45 minutes to an hour, then visualised under UV light in the Bio-Rad Gel Doc™ UV transilluminator system.

2.2.16 Analysis of GFP fluorescence by microscopic imaging:

GFP/GFPAβ expressing yeast cells were stored on YNB+2%glucose (-ura) agar plates at 4ºC. A single yeast colony from stock agar plates was inoculated in 5ml YNB+2%glucose (-ura) and incubated with shaking at 30ºC overnight. The overnight culture was resuspended in fresh YNB+2%glucose (-ura) to an initial cell density (OD at 600nm) of 0.2 and incubated at 30°C with shaking. Yeast cell suspensions were collected at different points of growth from early exponential phase till late log phase for microscopic analysis and GFP fluorescence quantification. Following washing in distilled water, a total of 4-5µL of the suspension was loaded on microscopic slide for imaging using oil immersion at 100X magnification. Images were taken using similar fluorescence and bright field exposure levels using Olympus DP71 digital camera. GFP fluorescing cells were counted relative to the total number of cells in the frame to determine the levels of the GFP/GFP-Aβ protein in the cell population. A number of 10 image frames each containing approximately 50 cells were quantified for each sample.

2.2.17 Preparation of cell extracts from GFP/GFPAβ expressing yeast

Yeast cell suspensions of GFP/GFPAβ expressing yeast were collected at different points of growth from early exponential phase till late log phase as described above. Total cell protein extracts from yeast were used for immunoblotting. Frozen cell pellets were resuspended in 150µl cold lysis buffer (50mM Tris pH 8, 1mM EDTA, 150mM NaCl, 1mM DTT, 2% SDS) with freshly

added 1XPI and then incubated at 70ºC for 15-20min. Following centrifugation at 18000g for 10min, the supernatant was collected and protein concentration of each sample was measured using the Micro BCA protein assay kit as described above (Section 2.2.1.3). A total of 50µg protein of each sample was studied by SDS-PAGE and western blot analysis as described previously as described above (Section 2.2.1.2).

2.2.18 Assessing autophagy in yeast

Autophagy was assessed by FM 4-64 staining, vacuolar alkaline phosphatase activity: Pho8 assay and by GFP-Atg8p transport assay as described below.

2.2.18.1 FM 4-64 staining:

Vacuolar membrane specific lipophilic dye, FM 4-64 staining in yeast was performed as described in (Journo et al., 2008). *Saccharomyces cerevisiae* (KVY55, and atg8Δ) yeast cells were cultured to mid exponential phase in YEPD media. The cells were later washed in 50mM HEPES (pH 7) twice and resuspended in YNB+2%glucose (complete) or YNB (-N) media containing 1mM PMSF. Latrepirdine or rapamycin treatment was done in YNB+2%glucose (-trp) media. Following 6h incubation at 30ºC, the cells are washed and resuspended in YNB (-trp) media containing 10mM sodium citrate (pH 4.3). FM 4-64 stain was added to the cells to a final concentration of 1µM. The solutions were incubated for 30min at RT. The cells were washed and resuspended in YNB+2%glucose (-trp) media containing 10mM sodium citrate (pH 4.3) and observed under the fluorescence microscope. A total of 4-5µL of the suspension was loaded on microscopic slide for imaging using oil immersion at 100X magnification. Images were taken using similar fluorescence and bright field exposure levels for all samples using Olympus DP71 digital camera

2.2.18.2 Vacuolar Alkaline phosphatase activity: Pho8 assay

Vacuolar alkaline phosphatase activity in yeast cell lysates were measured as described in (Noda and Klionsky, 2008). *Saccharomyces cerevisiae* (KVY55, atg8Δ) yeast cells were cultured to mid exponential phase in YEPD media. The cells were later washed in sterile water twice and resuspended in YNB+2%glucose (complete) media or YNB (-N) media. Latrepirdine or rapamycin treatment were done in YNB complete) media. Following 6h incubation at 30ºC, the cells are washed and re-suspended in ice-cold assay buffer (250mM; Tris-HCl, pH 9.0; 10mM MgSO4, and 10mM ZnSO4). The cells were lysed using glass beads vortexing for 3 X 2min on ice. The samples were centrifuged at 14000g for 5min. The supernatant was used for the assay. Protein concentration of each sample was measured using Micro BCA protein assay kit as described before (Section 2.2.1.3). A total of 100µg of cell lysate was incubated with 55mM α-naphthyl phosphate disodium salt for 20min at 30ºC and diluted in the lysis buffer to a final volume of 0.5ml. The reaction was stopped by adding 0.5mL stop buffer (2M glycine-NaOH, pH 11). The fluorescence was measured at 345nm excitation and 470nm emission wavelengths. After correcting for blank, the activity was calculated as Units/µg of sample.

2.2.18.3 GFP-Atg8p transport assay:

The atg8Δ cells were transformed with pRS306 (GFP-Atg8p expressing) plasmid as described in section 2.2.9.2). For the GFP-Atg8p processing assay (Yen et al., 2007), yeast strains harbouring the GFP-Atg8 plasmid were grown to mid exponential phase in YNB+2%glucose (-ura). Cells were then treated with latrepirdine, rapamycin or nitrogen starved for 6h at 30ºC. Following incubation the samples were collected for fluorescence microscopy. Following washing in distilled water, a total of 4-5µl of the suspension was loaded on microscopic slide for imaging using oil immersion at 100X magnification. Images were taken using similar fluorescence and bright field exposure levels using Olympus DP71 digital camera. Intravacuolar GFP fluorescence in cells relative to the total number of cells in the frame was determined as an indicator of

activation of autophagy in the cell population. The intravacuolar green fluorescence indicates GFP-Atg8p transport to vacuole and cleavage of GFP into vacuole. A number of 10 image frames each containing approximately 50 cells were quantified for each sample.

2.2.19 Aβ clearance in APOE knockout mice:

The Aβ peripheral clearance experiment in mice were performed by Dr Ian Martins, Kevin Taddei, Mike Morici and Linda Wijaya from our laboratory. APOE knockout mice (B6.129P2 ApoE−/−), were originally obtained from the Jackson Laboratory, Bar Harbor, Maine. All mice were bred and maintained at the Animal Resources Centre (ARC, Perth,Western Australia). Mice were housed 5–6 per cage in a controlled environment at 22°C on a 12h day/night cycle (light from 0700 to 1900 h). A standard laboratory chow diet (Rat and Mouse Cubes, Specialty Feeds Glen Forrest,WA, Australia) and water were consumed ad libitum. This study was conducted in accordance with the Australian code of practice for the care and use of animals for scientific purposes as specified by the National Health and Medical Research Council (NHMRC). The experimental protocols were approved by the University of Western Australia Animal Ethics Committee.

Stock Aβ42 was prepared by dissolving the Aβ42 peptide in DMSO to a concentration of 1mg/ml. The stock was diluted in sterile isotonic saline solution (0.9% w/v NaCl) immediately before experimentation to a concentration of 20μg in 50μL. The ApoE4 lipid emulsions were prepared as described in (Sharman et al., 2010). The composition of the remnant like emulsions was triolein 45.8%±3.2%, total cholesterol and cholesterol oleate 21.5% ± 3.2% and egg yolk phosphatidylcholine 32.7% ± 2.5%. The remnant like emulsion particles had a mean diameter of 133nm ± 17.6nm as measured by laser light scattering using the Malvern Instruments particle Zetasizer (Malvern Instruments, Worcestershire, United Kingdom). Partially lipidated human recombinant ApoE4 (Invitrogen, Madison, WI, USA) was freeze dried, resuspended in isotonic saline and then lipidated by incorporation into lipid emulsion particles that were

prepared by sonication and purified by ultracentrifugation as described previously (Hone et al., 2003; Yang et al., 1999b).

To determine the role of latrepirdine in the peripheral clearance of Aβ42 12monthold APOE knockout mice were anaesthetized with an intraperitoneal injection of Ketamine/Xylazine (75/10 mg/kg). APOE knockout mice were injected with lipidated recombinant ApoE4 (75µg) plus Aβ42 (20µg/50µl) pre-incubated with latrepirdine (3.5mg/kg) or vehicle (saline). Blood samples were taken from the retroorbital sinus using 1.0mm diameter heparinised haematocrit tubes at 2.5, 5 and 15 min postinjection for Aβ analysis by immunoblotting (3µl of plasma) as described in Section 2.2.19. Injected mice were sacrificed by decapitation and liver tissues were collected at similar time points (2, 5 and 15min). Tissue samples were homogenised in TBS (pH 7.4) containing 5µg/ml aprotinin, 0.1mMPMSF and 5µg/ml leupeptin followed by Aβ immunoblotting analysis (100µg of total protein of total homogenate) as described in Section 2.2.1.2.

2.2.20 Statistical Analysis:

Student t-tests and one-way ANOVA tests were used for statistical analysis and *p*-value analysis. All graphs were made in Microsoft Excel™. All data were represented as Data±SEM (Standard error of mean).

Chapter 3

Toxicity and Cellular localization of Oligomeric Aβ42 in Yeast

3.1 Introduction:

Soluble oligomer Aβ42 is a key mediator of neuronal dysfunction and toxicity in the AD brain. As described in Chapter 1, Aβ can affect a wide array of neuronal functions and thereby may lead to neurodegeneration [reviewed in (Bharadwaj et al., 2009)]. Aβ42 mediated toxicity has been found to be associated with disruption of mitochondrial activity (Butterfield et al., 2001 ; Dyrks et al., 1992; Lustbader et al., 2004a; Palmblad et al., 2002), receptor-mediated functions (Bhaskar et al., 2009; Fuentealba et al., 2004; Pereira et al., 2004; Wei et al., 2002 ; Yaar et al., 1997), disruption of Ca^{2+} homeostasis (Hartmann et al., 1994; Mattson et al., 1993) and oxidative damage of membranes (Butterfield et al., 2002; Müller et al., 2001; Verdier et al., 2004).

The natural occurrence of multiple structural entities of Aβ42 in the brain and the complexity of detecting specific isoforms in cellular compartments have confounded the study of oligomer Aβ-mediated toxicity in neuronal cell models. Although, the toxicity of exogenously-added oligomeric Aβ42 peptide compared to other forms has been well established in neurons, the cellular localization and target of oligomeric Aβ42 by which it mediates the cascade of events leading to cell death are unclear. A growing body of evidence indicates that membrane mediated cytotoxicity is an inherent property of protein oligomers including Aβ (Glabe, 2006; Glabe and Kayed, 2006). Since the majority of Aβ42 produced is secreted into the extracellular lumen, it is thought that it can have a major impact on neuronal functions and viability by interacting with the cell surface membranes (Talaga and Quere, 2002; Verdier and Penke, 2004; Verdier et al., 2004). A recent study has also shown that increased Aβ levels in membrane-associated and intracellular fractions isolated from the temporal neocortex of AD patients to be more closely related to AD symptoms than other measured Aβ species (extracellular soluble and extracellular insoluble) (Steinerman et al., 2008).

Aβ-mediated toxicity has been studied in other non-mammalian models including *Caenorhabditis elegans* (worm) (Link, 1995) and *Drosophila*

melanogaster (fly) (Finelli et al., 2004). However these models are largely based on transgenic overexpression of Aβ/APP and are complex systems compared to yeast cells. Moreover, yeast is a well established model organism for studying toxic proteins involved in neurodegenerative diseases (Bharadwaj et al., 2010; Braun et al., 2010; Winderickx et al., 2008). Yeast cells combine a high level of conservation in cellular processes with mammalian cells with added advantages of fast cell division, simple growth requirements and an abundance of experimental tools (Hughes, 2002; Mager and Winderickx, 2005; Simon and Bedalov, 2004).

Recently, I developed a novel method for determining toxicity of different Aβ isoforms in yeast (Bharadwaj et al., 2008). In this study, oligomeric Aβ treatment was shown to be more toxic compared to fibrillar Aβ, consistent with previous observations in neuronal cells (Dahlgren et al., 2002; Stine et al., 2003). The yeast model of oligomeric Aβ toxicity (Bharadwaj et al., 2008) therefore represents a simple cellular model for studying Aβ toxicity and uptake. In this chapter, I have extended the work to compare the toxicity of oligomeric Aβ42 and a non-oligomeric Aβ42 (19:34) peptide in yeast and neuronal cells. Further I have investigated the cellular localization and binding of Aβ peptide to the yeast plasma membrane to provide potential mechanisms of oligomer Aβ42 mediated toxicity in yeast cells.

3.2 Aims:

1.) Compare the toxicity of oligomeric Aβ42 and non-oligomeric Aβ42 (19:34) peptides in yeast and in M17 neuroblastoma cells.
2.) Determine the uptake and cellular localization of oligomeric Aβ42 and non-oligomeric Aβ42 (19:34) peptide in yeast.

3.3 Materials and Methods:

Aβ42 and Aβ42 (19:34) peptide solutions were prepared as described in Section 2.2.4.1. The peptide solutions were characterized by SDS-PAGE

followed by western blotting analysis. The toxicity of the peptides were tested in yeast (*Candida glabrata*) and M17 neuroblastoma cells by colony count and MTT assays respectively as described in Section 2.2.4.3 and Section 2.2.4.4. Uptake of exogenously added Aβ42 in yeast was studied by immunoblotting analysis (with WO2, an anti Aβ antibody) of cell extracts (soluble and membrane-associated) as described in Section 2.2.5.1. Sub-cellular localization was analysed using Leica TCS NT (upright confocal microscope) by 2 channel fluorescence imaging of yeast cells treated with FITC-labelled Aβ42 (green channel) for 6h followed by staining with lipophilic membrane stain (FM4-64, red channel). Yeast cells treated with Aβ42 (6h) were also analysed by immunoelectron microscopic analysis as described in Section 2.2.5.3. Plasma membrane fractions of Aβ42-treated yeast cells were delipidated and analysed by electrospray ionization-mass spectrometry (ESI-MS) as described in Section 2.2.7. Aβ42 peptides were co-incubated with crude plasma membrane fractions and assayed for vanadate sensitive H^+ATPase (ATP hydrolysing) activity as described in Section 2.2.8.

3.4 Results:

3.4.1 Toxicity of oligomeric and fibrillar Aβ42 peptides in yeast:

In neuronal cells, fibrillar Aβ42 is less toxic compared to oligomeric Aβ42 peptide (Dahlgren et al., 2002). In the previous work, I showed that similar to neuronal cells, fibrillar Aβ42 was less toxic to yeast cells (Figure 1A), whereas oligomeric Aβ42 treatment caused a dose-dependent loss of cell viability in yeast (Figure 1B). Significant cell death was observed from concentrations of 1μM with complete loss of cell viability at higher concentrations of 30μM (Bharadwaj et al., 2008).

Due to its heterogeneous nature and advanced aggregation state, fibrillar Aβ42 would be an inappropriate control to compare cellular uptake and localization. Instead a non-aggregating, monomeric form of Aβ would be better suited. Aβ42 is difficult to be maintained in a monomeric form due to its hydrophobic nature and tendency to aggregate under physiological conditions.

Besides, a control would need to be prepared under the same conditions. Therefore, an Aβ42 peptide modified at positions F19S and L34P [Aβ42 (19:34)] with reduced tendency to aggregate was chosen for this work (Ahmed et al., 2010; Hughes et al., 1996; Luhrs et al., 2005; Wurth et al., 2002).

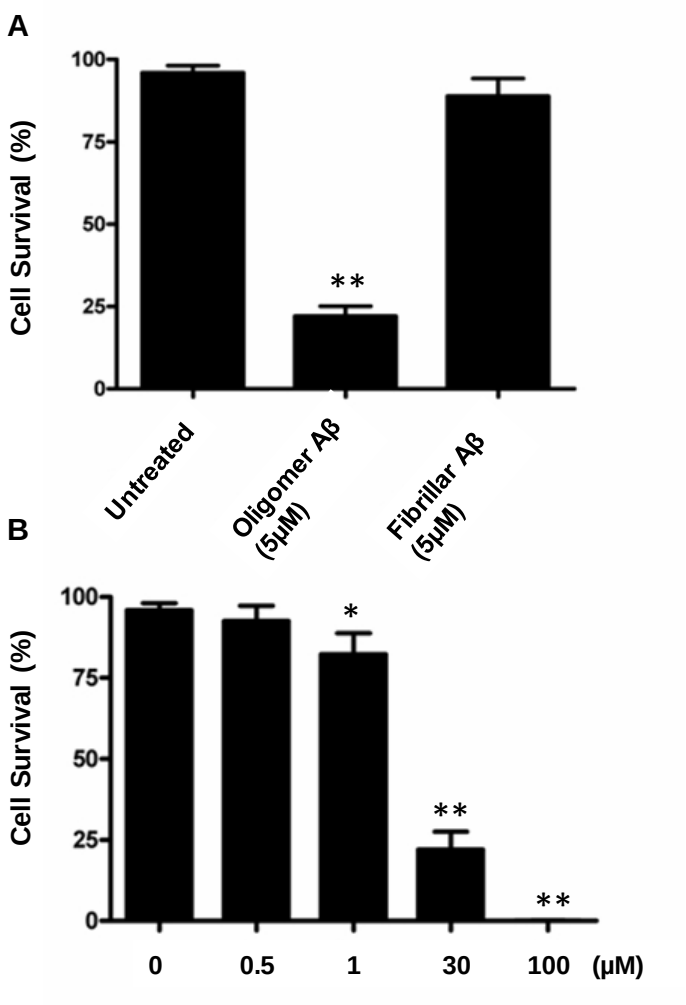

Figure 1: Toxicity of oligomeric and fibrillar Aβ42 peptides in yeast (Bharadwaj et al, 2008)

Toxicity of oligomeric and fibrillar Aβ peptide preparations were tested in yeast cells. Exponentially growing yeast cells (*Candida glabrata*) were treated with 5μM oligomeric, fibrillar Aβ42 peptide or vehicle buffer alone for 20h at 30ºC **(A)**. Cell viability was determined by counting the number of colonies formed and expressed as a percentage of vehicle treated control. Compared to vehicle treated cells, cell viability was significantly reduced (** $p<0.01$) in cells treated with oligomeric Aβ42. No significant loss of viability was observed with fibrillar

Aβ42 treatment. Dose response of oligomeric Aβ42 (0.5, 1, 5. 30 and 100μM) peptide in yeast **(B)** Compared to vehicle treated cells, cell viability was significantly reduced with oligomeric Aβ42 peptide in a dose dependent manner (* $p<0.05$, ** $p<0.01$). All data are expressed as mean ± SEM (n=4).

3.4.2 Oligomerization and toxicity of Aβ42 and Aβ42 (19:34) peptides:

Firstly, oligomer Aβ42 and non-aggregating Aβ42 (19:34) peptide were characterized by SDS-PAGE electrophoresis followed by coomassie staining and western immunoblotting analysis (Figure 2A). Aβ42 peptide was observed as monomers (4.5kDa) and SDS stable oligomers in the 7-17kDa range, indicative of low-n oligomers (dimers, trimers, tetramers) by both coomassie staining and Aβ immunoblotting using WO2 (Figure 2A, lanes 1, 3). However in Aβ42 (19:34) peptide, only monomeric species (4.5kDa) was detectable by both methods (Figure 2A, lanes 2, 4). Supporting the (Wurth et al., 2002) study, this result shows that Aβ42 (19:34) had reduced tendency to form oligomers compared to Aβ42.

Further the toxicity of oligomeric Aβ42 and non-oligomeric Aβ42 were tested in yeast and M17 neuroblastoma cells. Oligomeric Aβ42 treatment caused a 75-90% cell death at concentrations of 5-10μM as measured by viable counts. However Aβ42 (19:34) treatment showed less than 5% cell death at similar concentrations (Figure 2B). The toxicity of Aβ peptides at similar concentrations was also tested in human M17 neuroblastoma cell lines by determining the ability of cells to reduce MTT to purple formazan after treatment (Mosmann, 1983) (Figure 2C). 5-10μM of oligomeric Aβ42 treatment caused ~75-95% decrease in cell viability, whereas Aβ42 (19:34) caused only ~5% decline in MTT reduction (Figure 2C). Overall the results showed that Aβ42 (19:34) had reduced tendency to form oligomers and was less toxic in yeast and neuronal cells compared to oligomeric Aβ42. This result supports previous studies indicating that oligomerization is essential for Aβ mediated toxicity in

cells [reviewed in (Bharadwaj et al., 2009)]. Further, the uptake and localization of Aβ42 and Aβ42 (19:34) peptides in yeast cells was studied.

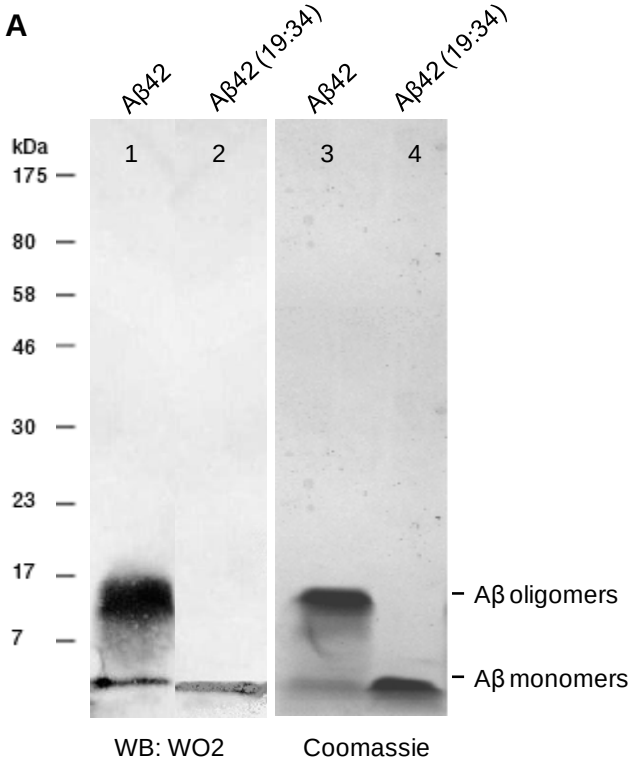

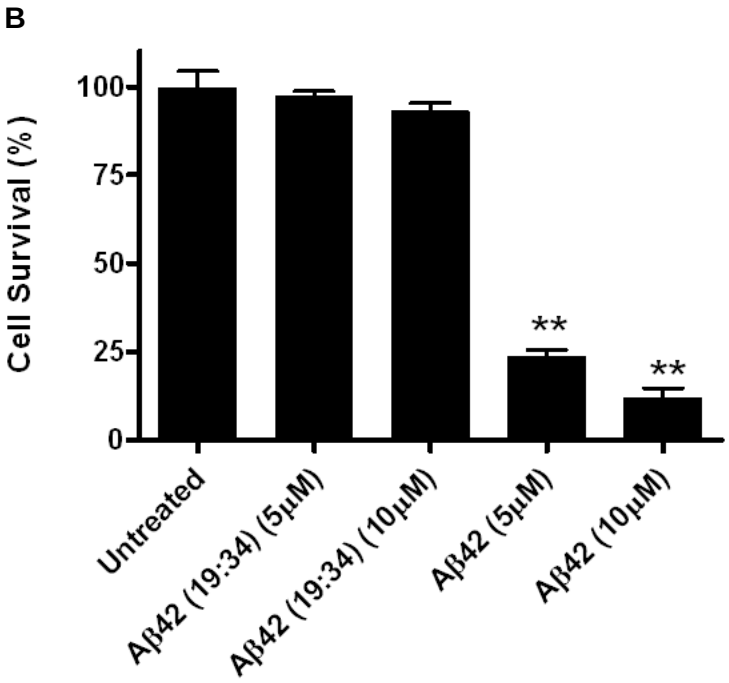

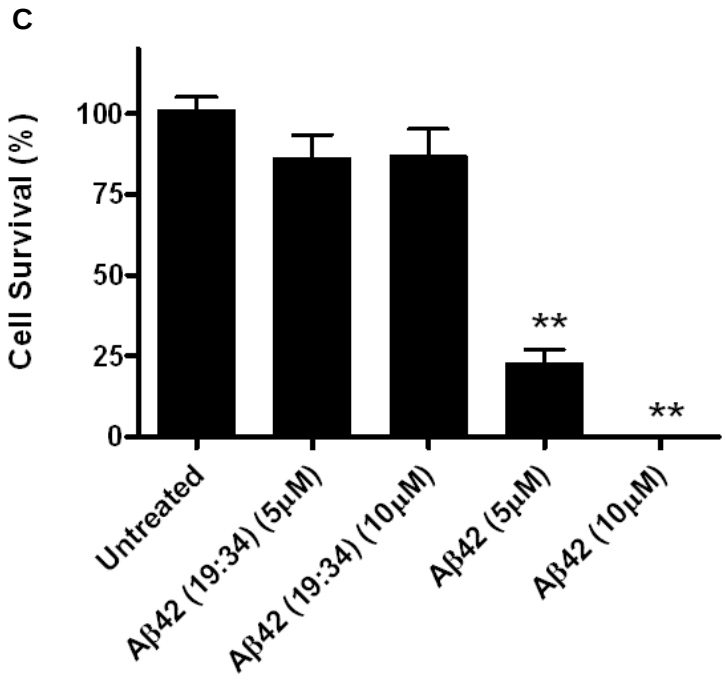

Figure 2: Toxicity of Aβ42 and Aβ42 (19:34) in yeast and M17 neuroblastoma cells

The Aβ42 and Aβ42 (19:34) peptides were prepared as described Section 2.2.4.1. The peptide solutions were size fractionated by SDS-PAGE electrophoresis (4-12% Bis-Tris gels) **(A).** 100ng of Aβ42 (lane 1) and Aβ42 (19:34) (lane 2) were analysed by immunoblotting (anti-Aβ, WO2). 5μg of Aβ42 (lane 3) and Aβ42 (19:34) (lane 4) of the same peptide stock were analysed by coomassie staining. Exponentially growing yeast cells (*Candida glabrata*) were treated with Aβ42 or Aβ42 (19:34) peptide (5μM and 10μM) for 20h at 30ºC. Cell viability was determined by counting the number of colonies formed and expressed as a percentage of untreated control **(B)**. Compared to untreated cells, cell viability was significantly reduced (**, $p<0.01$) in cells treated with 5 or 10μM Aβ42. Treatment with Aβ42 (19:34) did not significantly alter cell viability. M17 neuroblastoma cells plated in Opti-MEM were treated with Aβ42 or Aβ42 (19:34) peptide (5μM and 10μM) for 48h at 37°C. Cell viability was measured by MTT assay as described in Section 2.2.4.4 and expressed as a percentage of untreated control **(C)**. Similar to yeast cells, Aβ42 treatment caused significant loss of viability at concentrations 5 and 10μM (**$p<0.01$), whereas treatment with Aβ42 (19:34) did not significantly alter cell viability in M17 neuroblastoma cells. All data are expressed as mean ± SEM (n=4).

3.4.3 Uptake and toxicity of Aβ42 and Aβ42 (19:34) peptides in yeast:

The uptake of exogenously added Aβ peptides in yeast was first determined by fluorescent microscopy of cells treated with fluorescein isothiocyanate (FITC)-labelled Aβ peptides. FITC labelling of Aβ42 and Aβ42 (19:34) peptides was performed as described in Section 2.2.4.2. Exponentially growing yeast cells were treated with FITC-labelled Aβ peptides for 6h at 30°C and observed under the microscope. Cells treated with FITC-Aβ42 showed a strong intense green fluorescence around the cell surface (Figure 3A). Cells treated with FITC-Aβ42 (19:34) also showed a similar pattern but lower intensity of fluorescence around the cell surface (Figure 3C). No internalization of Aβ peptide (both Aβ42 and Aβ42 (19:34)) was observed at 6h incubation. To determine if Aβ internalizes with longer incubation, yeast cells were treated with FITC labelled Aβ for 20h. However, even with longer incubation times no intracellular fluorescence could be observed. This suggested that Aβ42 was largely associated with the cell surface.

Aβ peptide uptake was also studied by western immunoblotting analysis in yeast cells. Soluble (cytosolic) and insoluble (membrane associated, 1% SDS solubilised) extracts of yeast cells treated with Aβ42 and Aβ42 (19:34) peptides for 3, 7 and 20h were analysed by Aβ immunoblotting (WO2). Both Aβ42 and Aβ42 (19:34) were detected in the insoluble extracts (lanes 5, 6, 10 and 11) and undetectable in the soluble extract (lanes 7, 8, 12 and 13) (Figure 3G, H and I). Also, cells treated with Aβ42 showed increased uptake with longer incubation times (7, 20h) compared to Aβ42 (19:34) treatment. At 3h, only monomeric Aβ42 (4.5kDa) was detectable, but with 7 and 20h incubation, Aβ42 oligomers (7-17kDa range and 50-200kDa range) were evident in the insoluble extract (Figure 3G, H, I: lanes 5 and 6). However with Aβ42 (19:34) peptide treatment, only monomeric forms were detectable and no significant increase in levels of uptake was observed (Figure 3G, H, I: lanes 10 and 11). These results indicated that Aβ42 had increased affinity to cell surface membrane compared to Aβ42 (19:34). It was notable that both the Aβ peptides were undetectable in

the soluble cytosolic lumen of the cell, even with longer incubation times. The increased uptake of Aβ with longer incubation times was evident in Aβ42 but not in Aβ42 (19:34) treatment. One explanation is that Aβ42 is more hydrophobic and prone to self-aggregation than Aβ42 (19:34) and as a result shows increased association with the cell surface membrane.

To determine if there is a correlation of Aβ42 uptake with toxicity, cell viability of yeast cells treated with oligomer Aβ42 (5μM) was determined at different incubation times (0, 3, 7 and 20h) (Figure 3J). Compared to vehicle treated cells, cell viability was significantly reduced with increasing incubation time with 5μM Aβ42. Cell death was significant from 3h incubation with Aβ42 (~20%) and was found to increase to ~60% at 7h and ~75% at 20h. This indicated that toxicity of oligomer Aβ42 was dependent on the incubation period. Together with the immunoblotting analysis, the result suggested a correlation of detection of Aβ42 oligomers with toxicity in yeast cells. With Aβ42 treatment at 3h, only monomeric forms were detectable with a cell death of ~20%. Whereas at 7h and 20h, Aβ42 oligomers (7-17kDa range and 50-200kDa range) were detected comparing to increased cell death of up to ~60-75% (compare Figure 3G, H, I with J).

Figure 3: Analysis of the uptake and toxicity of Aβ42 and Aβ42 (19:34) peptides in yeast cells

Uptake of Aβ42 in yeast cells was analysed by microscopic analysis of FITC labelled Aβ treated yeast. Fluorescent and bright-field images of exponentially growing yeast cells (*Candida glabrata*) treated with FITC-Aβ42 **(A, B)** and FITC-Aβ42 (19:34) **(C, D)** for 6h and 20h at 30°C are shown here. Cells treated with FITC-Aβ42 showed a strong intense fluorescence around the cell surface. Cells treated with FITC-Aβ42 (19:34) exhibited a similar pattern but lower intensity of fluorescence. Vehicle buffer treatment showed no fluorescence at similar exposure levels **(E, F).** Yeast cells incubated with unlabelled Aβ42 or Aβ42 (19:34) peptides were collected for western immunoblotting analysis (WO2) at 3h **(G)**, 7h **(H)** and 20h **(I)**. Soluble (cytosolic) proteins were isolated by glass bead lysis in lysis buffer and insoluble (membrane) proteins were extracted using 1% SDS/200mM Na_2CO_3/2M urea in lysis buffer. Samples (in duplicates) were size fractionated by SDS-PAGE electrophoresis (4-12% Bis-Tris gels) and analysed by Aβ immunoblotting (anti Aβ-WO2) (G, H). Lanes are- vehicle treated: insoluble (1, 2), soluble (3, 4), Aβ42 treated: insoluble (5, 6), soluble (7, 8) and Aβ42 (19:34) treated insoluble (10, 11), soluble (12, 13) including 100ng loading standards of Aβ42 (9) and Aβ42 (19:34) (14). Both Aβ42 and Aβ42 (19:34) were detected in the insoluble extracts and undetectable in the soluble extracts. Cell viability of yeast cells treated with oligomer Aβ42 (5μM) was determined at different incubation times (0, 3, 7 and 20h) and expressed as a percentage of vehicle treated control **(J)**. Compared to vehicle treated cells, cell viability is significantly reduced (*, $p<0.05$, **, $p<0.01$) with increasing incubation time (from 3h) with 5μM Aβ42. Data are expressed as mean ± SEM (n=4).

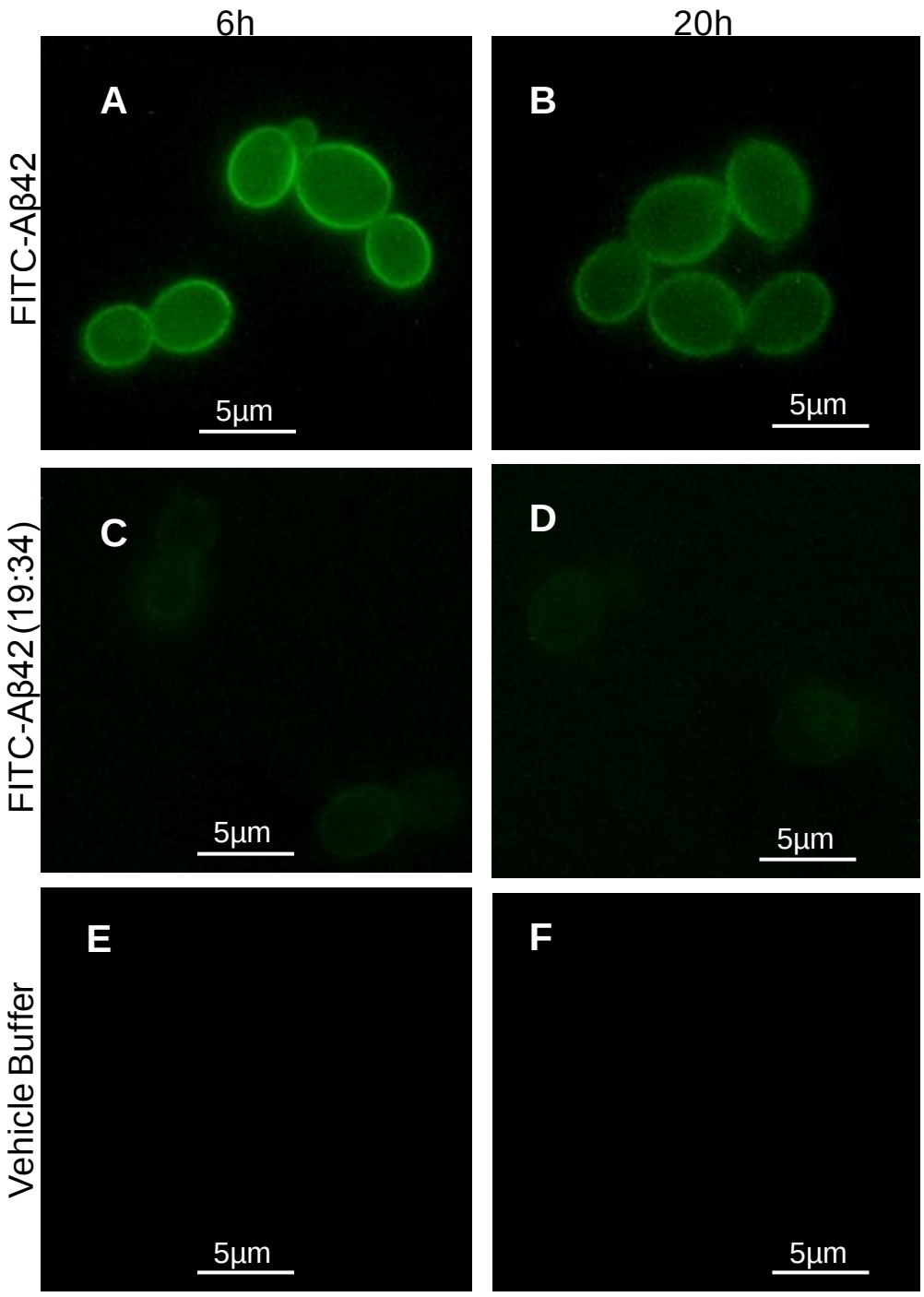
6h
20h
FITC-Aβ42
FITC-Aβ42(19:34)
Vehicle Buffer
A
B
C
D
E
F
5µm
5µm
5µm
5µm
5µm
5µm

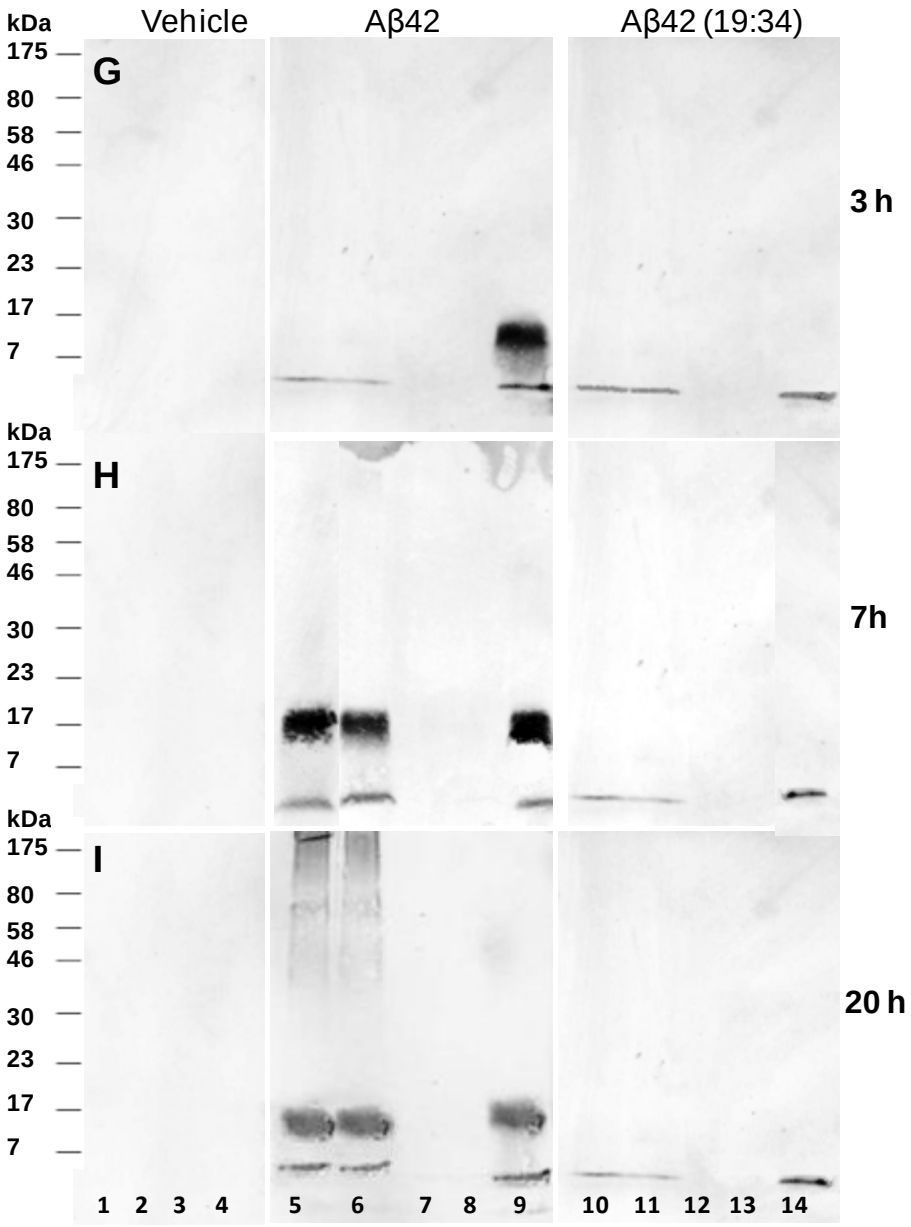

Cell extracts of Aβ42 peptide treated cells

J

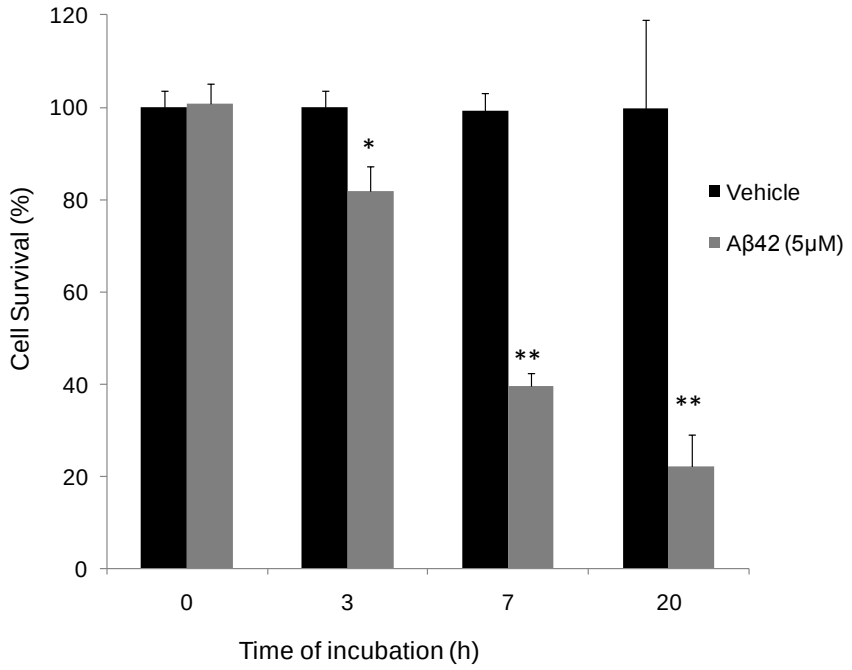

3.4.4 Cellular localization of Aβ42 in yeast

FITC-Aβ and western blot analysis in yeast showed that Aβ42 bound to the cell surface membrane and was undetectable in the soluble cytosolic lumen of the cell. The data suggested that Aβ42 was associated with the cell surface and not internalized into the cells. To further study the sub-cellular localization of Aβ42, cells were analysed by fluorescent imaging confocal microscopy. To determine whether Aβ42 associated with the plasma membrane, cells were treated with FITC-Aβ42 for 6h followed by staining with FM4-64 stain for 15 min at 30°C (Figure 4A-C). FM4-64 stain is a lipophilic styryl dye which binds to cellular membranes. The fluorescence of FM4-64 dye is quenched in aqueous state, but when inserted into membranes it fluoresces. It is ideally used for analysis of endocytosis and as a plasma membrane marker (Fischer-Parton et al., 2000). Co-localization analysis of FITC (green channel) and FM4-64 fluorescence (red channel) showed association of FITC-Aβ42 with FM4-64 staining (Figure 4D). To determine the levels of co-localization, a region of interest (ROI) across the diameter of the cell was chosen and fluorescence intensities was measured across the red (FM4-64) and the green (FITC-Aβ42)

channels (Figure 4D). Significant overlap of the red and green channels indicated the association of FITC-Aβ42 with FM4-64 fluorescence. Although FITC-Aβ42 and FM4-64 fluorescence were not completely overlapping, the result indicated a strong association of Aβ42 with the yeast plasma membrane.

For enhanced image resolution and sensitivity of Aβ detection, yeast cells treated with oligomeric Aβ42 were analysed by immunoelectron microscopy (Mulholland and Botstein, 2002; Wright, 2000) as described in Section 2.2.5.3. Aβ localization was detected by WO2 (anti-Aβ) probing followed by incubation with gold conjugated secondary antibody. The yeast sections were then stained with uranyl acetate and Reynolds's citrate solution for imaging by electron microscopy. Aβ immunoreactivity was indicated by the appearance of distinct dark spots. Cells treated with Aβ42 showed dark spots associated with the cell surface, whereas no such spots were observed within the cell. The dark spots were mainly found populated on the cell wall and also in the outer leaflet of the yeast plasma membrane (Figure 4F). Vehicle treated cells showed no dark spots associated with the cell (Figure 4E). Overall the data from co-localization analysis (with plasma membrane marker FM4-64) and immunoelectron microscopy showed that Aβ42 binds to the yeast cell surface and supported the previous data where intracellular uptake of Aβ was absent in yeast (Section 3.4.3).

To provide insight into specific Aβ oligomeric forms associated with the yeast plasma membrane, crude fractions of yeast plasma membranes were isolated from cells treated with Aβ42 and Aβ42 (19:34) peptide (5μM, 6h) and analysed by electrospray ionization mass spectrometric analysis (ESI-MS) (Figure 5). Distinct species with mass/charge ratio of 4514.09, 9027.61 and 13539.88, indicating Aβ42 monomer, dimer and trimer respectively were detected in the crude membrane fractions of cells treated with Aβ42 (Figure 5A). Crude membrane fractions isolated from cells treated with Aβ42 (19:34) (5μM) for 6h showed no detectable levels of Aβ (Figure 5B). The peaks observed in the Figure 5B represent the yeast plasma membrane proteins. This was absent in the crude membranes isolated from Aβ42 treated cells (Figure

5A) because the levels of Aβ42 detected was ~10 fold higher than the yeast membrane proteins. Due to this, the graphs are represented in different Y-axis range [(relative abundance): highest point of $2X10^4$ in figure 5B and $9.5X10^5$ in figure 5A]. Overall, the result supported the earlier observations showing that Aβ42 has increased affinity to the plasma membrane compared to Aβ42 (19:34).

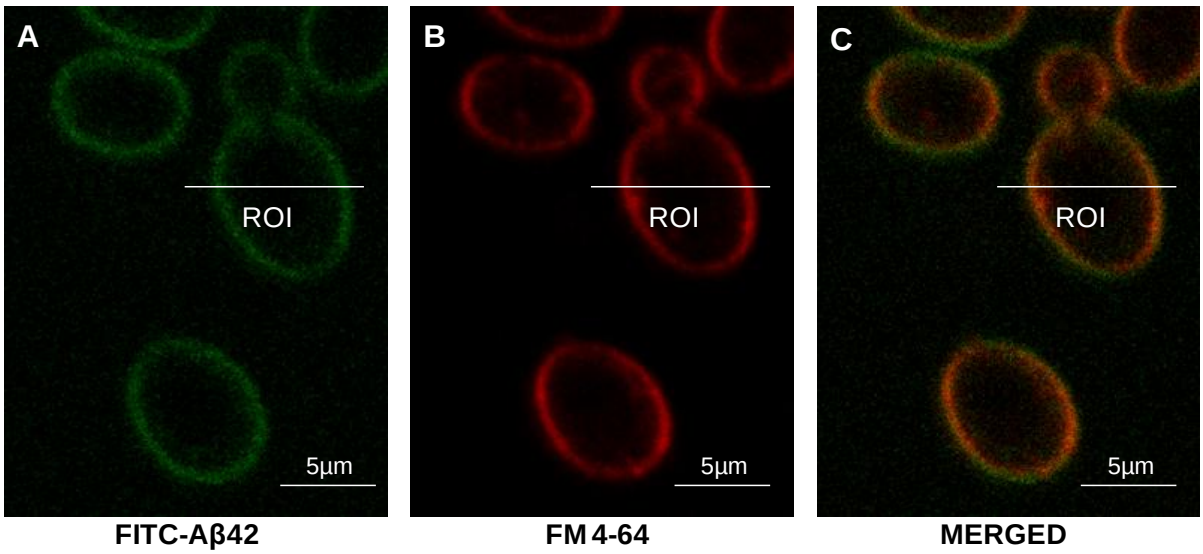

FITC-Aβ42 **FM 4-64** **MERGED**

D

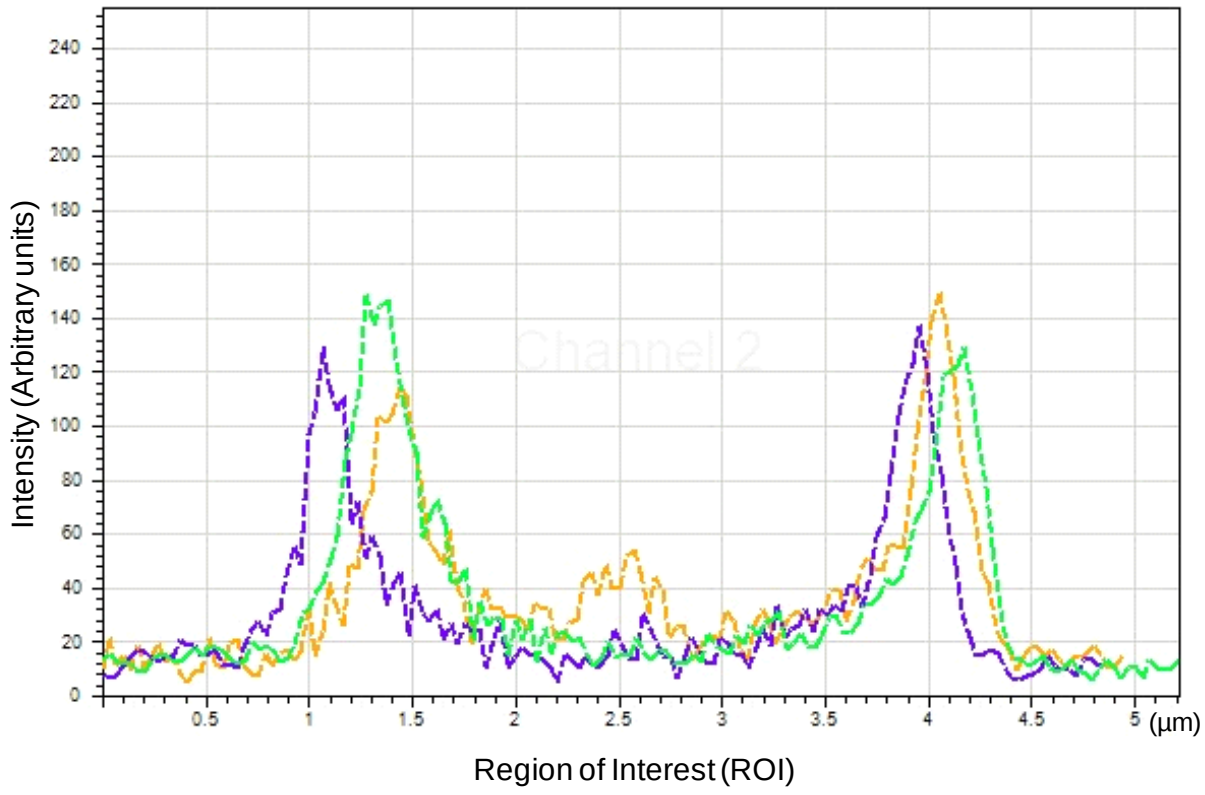

Region of Interest (ROI)

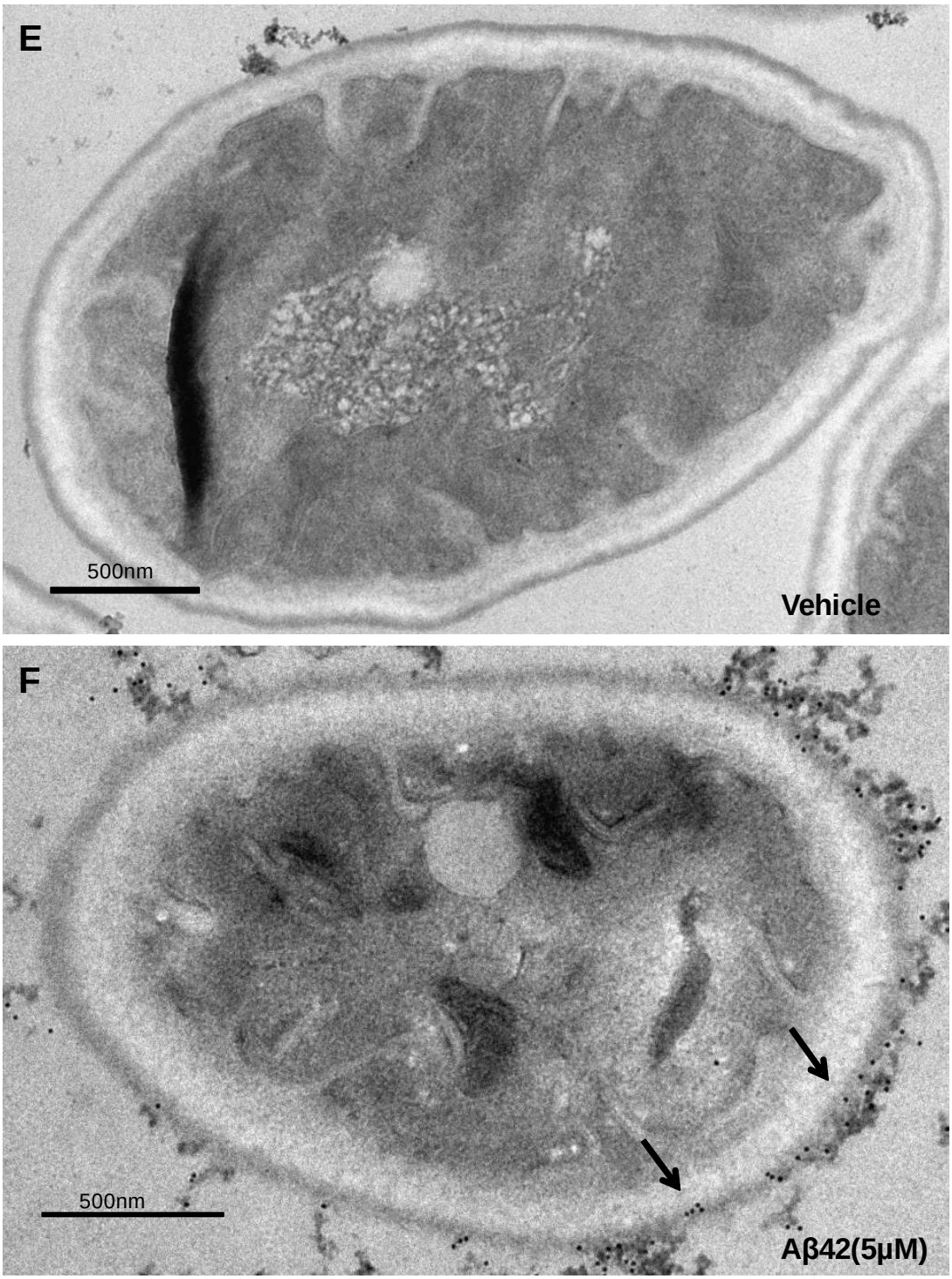

Figure 4: Aβ42 associates with the yeast plasma membrane

Cellular localization of Aβ42 in yeast was analysed by confocal and immunoelectron microscopic analysis of *Candida glabrata* cells treated with Aβ42. Cells were analysed by dual channel fluorescence imaging (Leica TCS

NT confocal microscope) after treatment with FITC labelled Aβ42 (**A**, green channel) for 6h and staining with FM4-64 stain for 15 min (**B**, red channel) at 30°C. Images were recorded using Olympus DP70 camera. Image overlay **(C)** and co-localization of FITC-Aβ42 and FM4-64 staining across the region of interest (ROI) was done using Leica LASAF software image analysis. Fluorescence intensities (arbitrary units) of FITC-Aβ42 (green), FM4-64 (red) and overlay (orange) across the ROI is represented by the green, purple and orange dotted lines respectively **(D)**. A significant association of FITC-Aβ42 with FM4-64 staining was observed. Cells treated with vehicle **(E)** or unlabelled Aβ42 (6h) **(F)** were fixed, permeabilized and prepared on gold grids for electron microscopic imaging. The grids were probed with WO2 (anti-Aβ) followed by incubation with gold conjugated anti-mouse secondary antibody. The samples were observed by negative staining using 2% aqueous uranyl acetate and Reynold's lead citrate and micrographs were recorded using a Megaview III CCD camera. Cells treated with Aβ42 showed dark circular spots around the cell surface, indicative of Aβ42 associating with the yeast plasma membrane **(F)** (indicated by black arrows). No distinct dark spots were observed with the untreated sample. Overall, the data suggested that Aβ42 localized on the yeast plasma membrane. However, Aβ42 was not detected in the intracellular lumen of yeast.

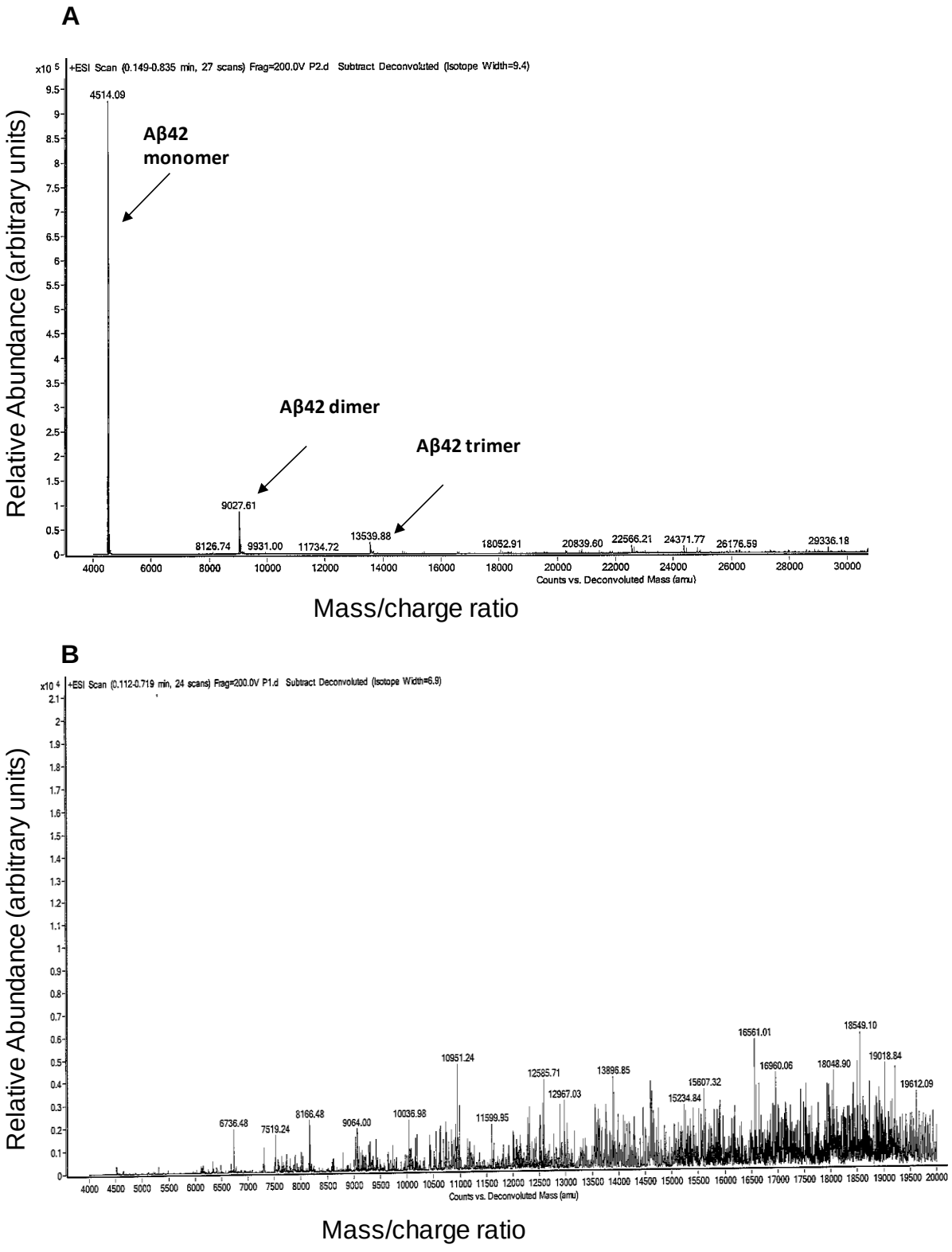

Figure 5: Mass spectrometric (ESI-MS) analysis of plasma membrane fractions of Aβ42 treated yeast cells

Mass spectrometric (ESI-MS) analysis of plasma membrane fractions of Aβ42 treated yeast cells: Plasma membrane fractions of yeast cells treated with Aβ42 (5μM) **(A)** and Aβ42 (19:34) **(B)** were isolated and analysed by mass spectrometry (ESI-MS). The crude plasma membrane (CPM) fractions from the cells were delipidated using chloroform/methanol/water extraction. The protein from the aqueous layer was recovered using acetone precipitation and air dried. The protein pellet was dissolved in 70% acetonitrile, 0.1% TFA and analysed in an Agilent QTOF 6510 mass spectrometer (mass range of 4-100kDa). Distinct species with mass/charge ratio of 4514.09, 9027.61 and 13539.88, indicating Aβ42 monomer, dimer and trimer respectively were detected in cells treated with oligomer Aβ42 as shown in the ESI-MS spectra here. However, no species representative of Aβ was identified in cells treated with Aβ42 (19:34). The graphs are represented in different Y-axis range (relative abundance: highest point of $2X10^4$ in figure 5B and $9.5X10^5$ in figure 5A).

3.4.5 Effects of Aβ42 and Aβ42 (19:42) peptides on plasma membrane H^+ATPase activity

Cellular localization analysis of Aβ42 and Aβ42 (19:34) uptake in yeast clearly showed that exogenously added Aβ42 is localized to the cell surface, strongly associated with the plasma membrane. It was suggested that Aβ42 caused cell death in yeast is possibly mediated by plasma membrane associated toxicity. In neuronal cells, Aβ42 is known to disrupt membrane associated proteins and related functions contributing to its ability to induce cell death. One of these targets for Aβ42 that has been suggested is the Na+/K+ ATPase, which is critically important for osmotic balance and cell volume maintenance. Decreased overall Na+/K+ ATPase enzyme activity is observed in the hippocampus of the APP+PS1 mice (Dickey et al., 2005). Reports have shown that Aβ42 can mediate disruption of cellular homeostasis via inhibition of Na+/K+ ATPase activity in neurons (Dickey et al., 2005; Mattson et al., 1993).

In yeast, the proton (H^+)-transporting plasma membrane protein (H^+-ATPase) is mainly responsible for maintenance of cellular homeostasis and viability (Ambesi et al., 2000). It is also a member of the P2-ATPase family in eukaryotes and a functional homolog of the Na+/K+ ATPase. The H^+-ATPase is the most abundant plasma membrane protein in yeast cells (Ambesi et al., 2000) and also an important target for anti-fungal drugs implying its essential role in cell survival (Billack et al., 2010; Manavathu et al., 1999).

To determine if oligomeric Aβ42 can damage the yeast H^+-ATPase, *in vitro* plasma membrane H^+-ATPase (vanadate sensitive ATP hydrolysis) activity was determined in crude membrane fractions incubated with Aβ peptides (Figure 6). ATPase activity measurement was performed as described in Section 2.2.8. Following Aβ pre-incubation for 15-20min, the crude membranes were tested for plasma membrane ATPase activity. The assay was done in presence of ammonium molybdate and sodium nitrate to prevent residual effects of nonspecific phosphatase, and mitochondrial ATPase activities. Pre incubation with oligomeric Aβ42 was found to cause a dose-dependent inhibition of H^+-ATPase activity of yeast plasma membranes. A ~70% and ~95% loss of ATPase activity was observed when 15µg of total yeast membrane suspension was incubated with 1 and 1.5µM of Aβ42, respectively. However, treatment with similar amounts of Aβ42 (19:34) did not alter the ATP hydrolysing activity. The result suggested that inhibition of H^+-ATPase activity was mediated by oligomeric Aβ42 and not by non-oligomeric Aβ42 (19:34).

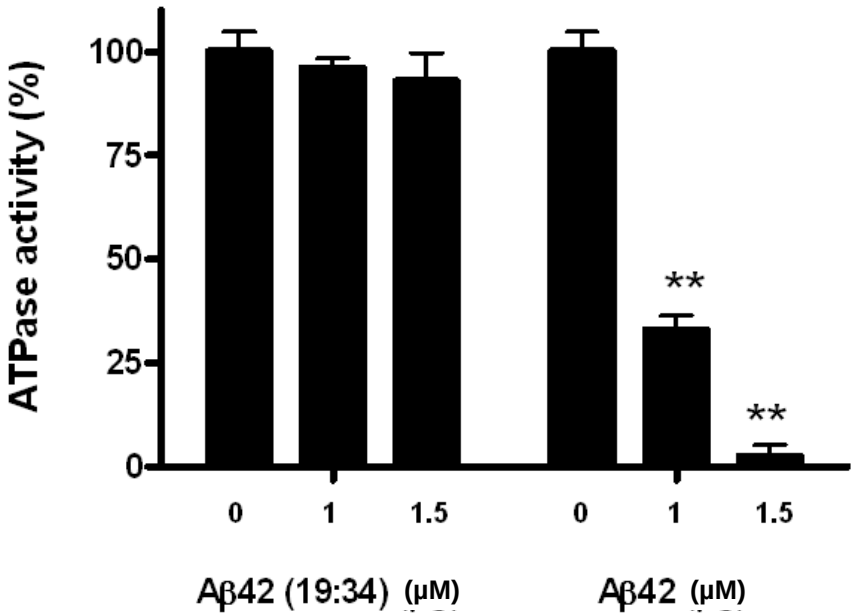

Figure 6: Oligomeric Aβ42 inhibits H^+-ATPase activity in yeast plasma membrane fractions

Crude plasma membranes (CPM) were prepared from exponentially growing yeast. The CPM fractions (15μg) was pre-incubated with different concentrations (0-1.5μM) of oligomeric Aβ42 or the non-aggregating Aβ42 (19:34) peptide for 15-20 min followed by addition of ATP assay buffer containing 10mM ATP and reaction at RT for 45-60 min. The ATP hydrolysing property of the plasma membrane H^+-ATPase was determined from the phosphate released, which was measured colorimetrically at (630nm) using ammonium molybdate stop buffer. Activity (%) was measured by subtracting the Abs (630nm) of vanadate-treated CPM fractions and normalized using phosphate standard curve. A significant inhibition of H^+-ATPase activity was observed with Aβ42 pre-incubation (**, $p<0.01$), but not with Aβ42 (19:34). Data are expressed as mean ± SEM (n=4).

3.5 Discussion:

3.5.1 Modified Aβ42 (19:34) exhibited reduced aggregation and toxicity

It is well established that the toxicity of Aβ is associated with its ability to oligomerize and aggregate. A number of mammalian models have been used to study mechanisms of Aβ mediated toxicity. A major advantage of using yeast cells for Aβ toxicity is the ability to perform the assay in water. Unlike mammalian cells which require osmotic and nutrient support, yeast cells can survive in water for several days with minimal loss of viability (Bharadwaj et al., 2008). Since Aβ42 has an increased tendency to form heterogeneous aggregates in the presence of salts under physiological conditions (Stine et al., 2003), studies of oligomer Aβ specific toxicity in mammalian cell models can be problematic. Using yeast cells for oligomer Aβ42 toxicity in water therefore can overrule the influence of the salts on Aβ aggregation. In this chapter, I have extended my previous finding where I showed that oligomeric Aβ was more toxic than fibrillar Aβ (Figure 1). The major aim of this study was to investigate the uptake and localization of oligomeric Aβ42 in yeast cells.

Due to the heterogeneous nature of Aβ fibrillar preparations, an Aβ42 peptide modified at positions F19S and L34P [Aβ42 (19:34)] (Wurth et al., 2002) with reduced tendency to aggregate was chosen as a control for oligomeric Aβ42 in this study. *In vitro* structural modelling and yeast two hybrid analysis indicate that positions 19 (phenylalanine) and 34 (leucine) in Aβ42 sequence play an important role in self interaction of the peptide monomers (Ahmed et al., 2010; Hughes et al., 1996; Luhrs et al., 2005). Size fractionation analysis by SDS-PAGE showed that Aβ42 (19:34) peptide was completely monomeric, compared to the stable low-n oligomers (7-17kDa range) observed with oligomeric Aβ42 preparations (Figure 2A). In both yeast and M17 neuroblastoma cells, oligomeric Aβ42 caused significant loss in cell viability (Figure 2B, C). Approximately 75% cell death was observed at concentrations of 5μM of Aβ42 in both yeast and M17 neuroblastoma cells, compared to less than 5% cell death at similar concentrations of Aβ42 (19:34). As expected,

these results showed that oligomeric Aβ42 was more toxic than the non-oligomerizing Aβ42 (19:34). This data supports the previous studies in mammalian cells indicating that soluble oligomeric form of Aβ42 is the main toxic species responsible for cell death (Dahlgren et al., 2002; McLean et al., 1999; Shankar et al., 2007; Shankar et al., 2008).

3.5.2 Accumulation of Aβ42 in the yeast plasma membrane

Due to its hydrophobic nature, Aβ has an inherent nature to associate with biological membranes. The ability to interact with membranes is therefore an important feature of oligomer Aβ mediated toxicity to cells. The cellular localization of the oligomeric Aβ42 and the non-oligomeric Aβ42 (19:34) was determined by fluorescence microscopy (Figure 3A-F) and Aβ immunoblotting of cell extracts (Figure 3G-H) showed that both Aβ peptides bound the cell surface. However, oligomeric Aβ42 displayed an increased binding affinity compared to the modified Aβ42 (19:34) (Figure 3). Also, an increased level of Aβ42 oligomers (7-17kDa range and 50-200kDa range) in the insoluble membrane fraction was evident with longer incubation periods (Figure 3G, H and I: lanes 5 and 6). However no increase in levels of the modified Aβ42 (19:34) was observed with longer incubation times (Figure 3G, H and I: lanes 10 and 11). The hydrophobic nature of Aβ42 and its ability to oligomerize may explain its accumulation in the insoluble membrane fraction, which was clearly reduced with Aβ42 (19:34) treatment. It is likely that the decreased ability of the Aβ42 (19:34) peptide to self associate (Hughes et al., 1996; Wurth et al., 2002) may contribute to its low affinity and accumulation in the cell compared to oligomeric Aβ42.

Importantly, the progressive accumulation of Aβ and the appearance of Aβ oligomers (7-17kDa range and 50-200kDa range) in the insoluble membrane fraction showed correlation with increased loss of viability in yeast with longer incubation times (compare lanes 5, 6 Figure 3G-I with 3J). This observation supports previous reports indicating that increased binding to the plasma membrane can enhance the neurotoxic property of Aβ (Ciccotosto et al., 2004;

Crouch et al., 2008). Further, confocal microscopic analysis and immunoelectron microscopy clearly showed that oligomeric Aβ42 was largely populated on the cell surface, strongly associated with the cell wall and the outer leaflet of the plasma membrane of the yeast cell. The crude plasma membranes of Aβ42 and modified Aβ42 (19:34) peptide treated cells were analysed by ESI-MS (Figure 5A). Aβ42 treated cells revealed monomer and oligomeric forms (dimer and trimer). However, the membrane fractions isolated from cells treated with modified Aβ42 (19:34) showed no detectable levels of Aβ (Figure 5B). It is likely that Aβ42 (19:34) was stripped during the delipidation process of sample preparation for ESI-MS, due to its weak binding to the yeast cell surface membranes (cell wall and plasma membrane). This suggests that the modification at residues 19 and 34 of the Aβ sequence affects not only the self interaction of the Aβ42 (19:34) peptides, but its nature of membrane interaction. Furthermore the results suggested that the reduced affinity of Aβ42 (19:34) peptide to the cell surface could be one of the reasons for its decreased cytotoxicity. However, it could be argued that the lack of detection of the modified Aβ42 (19:34) peptide in the crude plasma membrane fractions may be due to its vulnerability to degradation compared to Aβ42 because of its inability to form oligomers.

The binding dynamics of Aβ42 to membranes is complex. Aβ42 has a long hydrophobic C-terminus which can insert into the lipid bilayer membranes of cell surfaces. Studies suggest that these cell surfaces can catalyse amyloid aggregate nucleation, perhaps in a different mechanism from that observed in solution state (Sethuraman and Belfort, 2005; Stefani, 2007). Cellular surfaces can also accelerate amyloidogeneis and possibly impact the structural integrity and functions of membranes (Porat et al., 2003). Aβ can bind a variety of cofactors on the plasma membrane including ion channels proteins, receptor complexes, lipid and sterol molecules which can impact its binding and also contribute to cellular dysfunction and death. The results presented in this chapter provide evidence in support of the idea that binding to the plasma membrane plays an important role in oligomer Aβ mediated cell death.

3.5.3 Inhibition of H^+-ATPase *in vitro* activity by oligomeric Aβ42

Ion motive ATPases are vital plasma membrane protein complexes responsible for the active transport of ions across the plasma membrane and maintenance of cellular homeostasis (Skou, 1982). Decreased Na^+/K^+ ATPase, Cl^--ATPase activity and protein levels has been observed in APP +PS1 double transgenic mice (Dickey et al., 2005) and also in the AD brains (Hattori et al., 1998). Reduced activity of the Na^+/K^+-ATPase and Cl^--ATPase has been associated with elevated intracellular Ca^+, Na^+, swelling of neurons, increased vulnerability to excitotoxic stress, accumulation of reactive oxygen species (ROS) and apoptotic cell death in AD (Dickey et al., 2005; Mark et al., 1995). Moreover decreased activity of Na^+/K^+-ATPase proteins has been observed to be associated with amyloid deposition in the hippocampus of APP+PS1 mice (Dickey et al., 2005). In addition, reports suggest that disruption of Na^+/K^+ ATPase and Cl^- ATPase activity by Aβ can result in neuronal cell death in AD (Bores et al., 1998; Mark et al., 1995; Yagyu et al., 2001).

Aβ42 toxicity in yeast was found to be mediated by its binding to the plasma membrane. Oligomeric Aβ42 was toxic to cells and showed increased affinity to the plasma membrane compared to the modified Aβ42 (19:34) which had reduced binding to the plasma membrane (Section 3.4.3). Furthermore oligomer Aβ42 was found to inhibit the H^+ATPase activity in isolated yeast plasma membranes whereas the modified non-oligomerizing Aβ42 (19:34) did not affect the activity. Approximately a 70-95% decrease in activity with 1-1.5μM of oligomeric Aβ42 treatment was observed compared to only a 5% decrease with Aβ42 (19:34) at similar concentrations (Figure 6). Collectively the data indicated that inhibition of the plasma membrane H^+-ATPase as one of the possible mechanisms of oligomer Aβ42 mediated cell death. This finding was consistent with the data obtained from neuronal cells.

Previous studies report decreased Na^+/K^+ ATPase and Cl^--ATPase activity in plasma membranes isolated from Aβ42 peptide treated hippocampal cells

(Bores et al., 1998; Mark et al., 1995; Xiao et al., 2002). It is however difficult to distinctly associate the effect of Aβ42 peptide to the inhibition of the ion-motive ATPase activity. Aβ42 induced disruption of membrane integrity, lipid peroxidation and other affected cellular functions may also contribute to the decreased activity. It has also been shown that mRNA for the Na+/K+ ATPase αIII subunit is consistently down-regulated in the hippocampus ridden with amyloid deposition (Dickey et al., 2003). Alternative pathways involving interactions of Aβ with membrane proteins leading to modulation of signal transduction cascades can also contribute to the decreased expression of Na+/K+ ATPase. A study showing that Lyn, a tyrosine kinase can phosphorylate Na+/K+ ATPase leading to its reduced expression levels (Bozulic et al., 2004) further supports this idea. However, Aβ peptide treatment [both oligomer Aβ42 and non-oligomeric Aβ42 (19:34)] was performed in isolated wild type yeast plasma membranes. Moreover, the assay was done in the presence of ammonium molybdate and sodium nitrate to prevent residual effects of nonspecific phosphatase, and mitochondrial ATPase activities. This suggested that oligomer Aβ42 specifically inhibited the ATP hydrolysing property of the yeast plasma membrane H^+-ATPase. Overall the data from the toxicity, cellular localization of Aβ peptides and the isoform specific effects on the H^+-ATPase activity suggested that inhibition of plasma membrane H^+-ATPase activity can be one of the main causes of cell death mediated by oligomeric Aβ42 in yeast.

3.6 Summary:

The results presented in this chapter have confirmed the toxicity of oligomeric Aβ42 to yeast cells. In addition I have shown that oligomeric Aβ42 binds the yeast plasma membrane where it can alter the activity of the plasma membrane proton pump H^+ATPase. This may be one mechanism by which oligomeric Aβ can impact cellular homeostasis and cause cell death. Preventing the formation or disrupting oligomeric structures of Aβ has shown to inhibit toxicity (Yang et al., 1999a; Yang et al., 2005). In the next chapter, I determine the effects of dairy derived peptides in modulating Aβ structure and toxicity in yeast and neuronal cells.

Chapter 4

Suppression of Aβ42 Oligomerization prevents Toxicity in Yeast and Neuronal cells

4.1 Introduction

Preventing the formation or disrupting the specific Aβ toxic oligomer structures that cause neuronal dysfunction in the brain has been proposed as a therapeutic strategy for AD (Klein, 2007; Zimecki, 2008). A wide range of inhibitors and modulators of Aβ42 aggregation, including peptide, protein and small molecular classes of natural and synthetic origin (Estrada and Soto, 2007; Gordon et al., 2002; Kokkoni et al., 2006) have been shown to regulate toxicity of Aβ42 both *in vitro* and *in vivo* (Amijee et al., 2009; Bastianetto et al., 2008; Dumery et al., 2001; Findeis, 2002; Nerelius et al., 2009). A major challenge in designing such Aβ inhibitors is to specifically target the toxic form of Aβ and identify potent compounds with low cytotoxicity.

Inhibitors of Aβ aggregation from natural food products or dietary intake has been of interest in AD therapeutics. Milk proteins are well known for chaperone activity. The micellar structure of the bovine milk caseins represents a thermodynamically stable architecture that accommodates the amphiphillic casein proteins and colloidal calcium phosphate components of milk (Ferrandini et al., 2005). Two of the four proteins of the casein micelle, κ-casein (κCn) and αS2 casein on isolation readily form fibrils under either reducing or non-reducing conditions, respectively (Thorn et al., 2008; Thorn et al., 2005a) but this behaviour is suppressed by αS1-casein and β-casein, present in stoichiometric excess, in fresh milk (Thorn et al., 2008; Thorn et al., 2005a). Anti-fibril properties have been previously demonstrated in milk protein hydrolysates (Bennett et al., 2009). Anti-fibril and other bioactivities have also been extensively characterised in a peptide extract from ovine colostrum (Schuster et al., 2005) and also shown to improve learning and memory in rats (Popik et al., 1999). The chaperoning activity of milk proteins implicates them as interesting candidates for targeting Aβ oligomerization and associated toxicity.

Toxicity of oligomeric Aβ42 has been recently established in a yeast cell model [(Bharadwaj et al., 2008), (Chapter 3)]. In addition to its high level of

conservation in cellular processes with mammalian cells, yeast cells present added advantages of simple growth requirements, fast cell division, and a robust nature making it a very attractive cellular model for drug screening (Hughes, 2002; Mager and Winderickx, 2005; Simon and Bedalov, 2004). The yeast model for oligomer Aβ toxicity is therefore well suited for characterizing the effects of Aβ structure modifying compounds. In this chapter, the dose-dependence effects of a whey protein-derived peptide hydrolysate (SPE product series) on Aβ42 structure were characterized using circular dichroism, fourier transform infrared spectroscopy (FTIR), transmission electron microscopy (TEM) and by size fractionation (SDS-PAGE). To determine the effects of SPE mediated modulation of Aβ42 structure, the toxicity of pre-incubated SPE-Aβ42 mixtures were studied in yeast and further validated in neuronal cell models.

4.2 Aims:

1.) Preparation and amino acid analysis of SPE hydrolysate fractions from bovine whey protein isolate
2.) Study the effects of SPE fractions on Aβ42 secondary structure and oligomerization
3.) Investigate the effects of SPE fractions on Aβ42 toxicity

4.3 Materials and Methods:

Preparation and amino acid analysis of SPE fractions recovered from dairy whey protein hydrolysate was done as described in Section 2.2.2 (Louise Bennett, CSIRO). Aβ42 solutions were prepared and incubated with different concentrations of SPE fractions. The SPE-Aβ42 mixtures were then analysed by circular dichroism (CD), Fourier transform infrared spectroscopy (FTIR, Rabia Sarroukh, Université Libre de Bruxelles, Belgium) for determining the secondary structure constitution as described in Section 2.2.9.2 and Section 2.2.9.3. The mixtures were also studied by transmission electron microscopy

(TEM) and size fractionation (SDS-PAGE, Aβ immunoblotting) for analysis of Aβ oligomerization. Cellular toxicity of the pre-incubated SPE-Aβ42 solutions were studied in yeast by CFU (colony forming units) count and in SH-SY5Y human neuroblastoma cells by LDH and MTS assays as described in Section 2.2.4.5.

4.4 Results:

4.4.1 Characterization of Whey Peptide SPE Product

The dairy whey protein hydrolysate was fractionated by preparative SPE and fractions recovered in either 40% acetonitrile (SPE40) followed by 100% acetonitrile (SPE100) elution, or a 'total' fraction recovered in 100% acetonitrile (SPE) were studied. HPLC profiles indicated significant retention of peptides by the C18 SPE media and overlap between SPE40 and SPE100 peptide assemblages (Figure 1A). However, the SPE40 contained a relatively higher proportion of species eluting in the 15 to 22 min range (Figure 1A).

The amino acid composition of the SPE product was compared with Colostrinin, which is a proline rich peptide complex derived from ovine colostrums, reported to exhibit many functional properties of relevance to bioactivity of the bovine whey SPE product (Boldogh and Kruzel, 2008; Kruzel et al., 2001; Zimecki, 2008). Colostrinin has also shown to inhibit Aβ oligomer mediated toxicity (Schuster et al., 2005), regulate levels of reactive oxygen species (ROS) and immunomodulatory functions (Boldogh et al., 2008; Boldogh and Kruzel, 2008). A significant correlation was observed between the amino acid contents of the two products (Pearson Product Moment correlation coefficient was 0.604 and P=0.013, Figure 1B). Colostrinin was significantly richer in mole percentage of Glu+Gln and Proline whereas SPE was relatively richer in the non-polar amino acids: Alanine and Leucine.

Dairy derived peptides have previously shown to have anti-fibril and protein chaperoning properties (Bennett et al., 2009; Thorn et al., 2005b), however its

effects on Aβ42 structure and aggregation has not been studied before. To study the effects of SPE fractions on Aβ42 secondary structure and oligomerization, pre-incubated mixtures of Aβ42 with different concentrations of SPE were studied by circular dichroism, Fourier transform infrared spectroscopy (FTIR), transmission electron microscopy (TEM) and by size fractionation (SDS-PAGE).

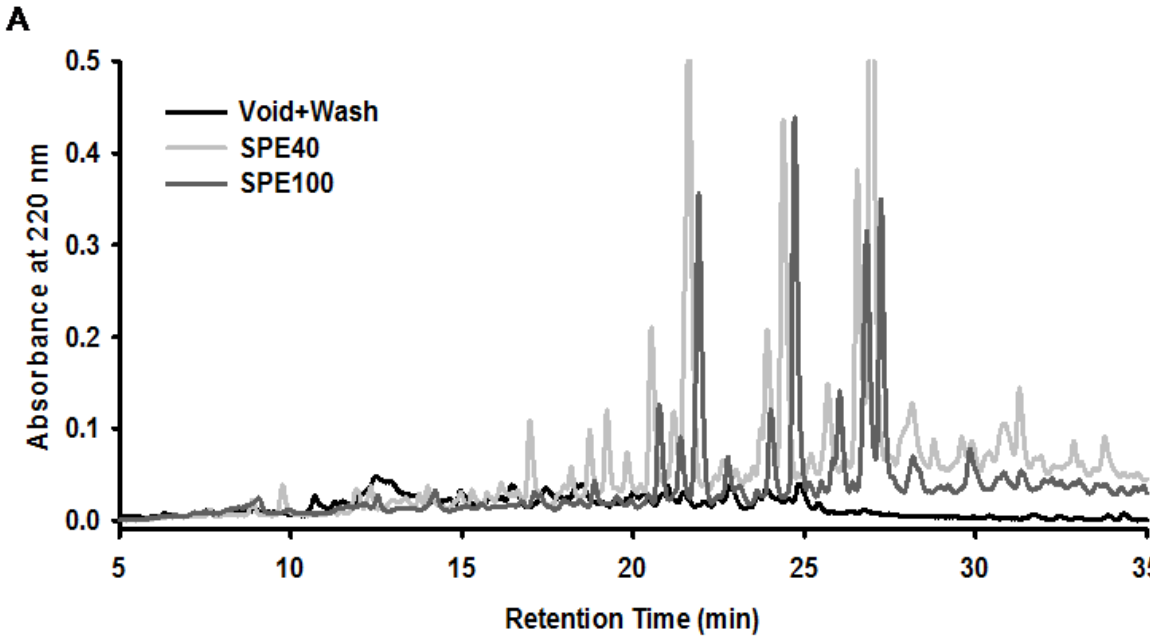

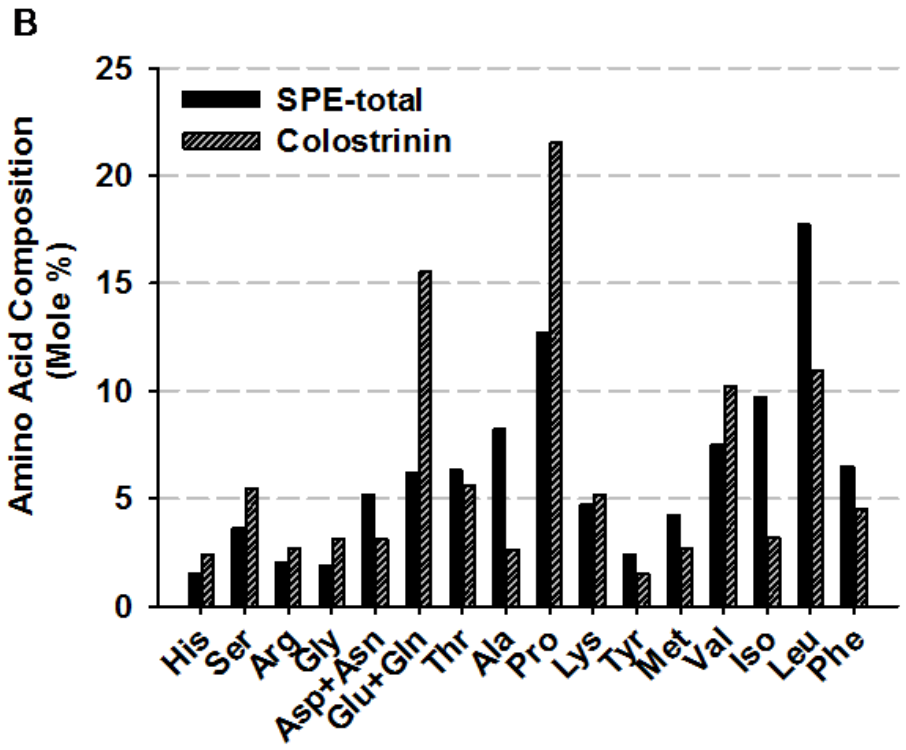

Figure 1: Preparation and characterization of SPE fractions from dairy whey protein hydrolysate

Reverse phase HPLC profiles of sub-fractions of dairy peptide hydrolysate showing solid phase extraction (SPE) cartridge non-binding void plus wash fraction (pooled) and products eluted with 40% and 100 % acetonitrile, designated SPE40 and SPE100, respectively. The ratio of SPE40 to SPE100 present in SPE-total was approximately 19:1 and profiles have been standardised for mass of solids analysed. **(A)**. Amino acid analysis of total SPE retentate of dairy hydrolysate was compared with ovine colostral 'Colostrinin' (Georgiades, 2004). The Pearson Product Moment correlation coefficient for colostrinin with the SPE total was 0.604 and P=0.013 **(B)**.

4.4.2 Effect of SPE on Aβ42 secondary structure

Aβ42 peptide solutions (0.05 mg/ml; 11μM), pre-incubated with different concentrations of SPE40 and SPE100 (final concentrations: 0.005, 0.05 & 0.25 mg/ml in de-ionised water) were analysed by CD spectrometer. The mean residue ellipticities of samples were recorded across the far UV range (190-260 nm). Spectra of SPE products alone at appropriate concentrations were subtracted from respective profiles of Aβ42+SPE product, but were otherwise unsmoothed. The beta sheet content of Aβ42 in the presence of increasing concentrations of SPE40 and SPE100 was analysed using the CD spectra generated (Figure 2). The ratio of Aβ42 molarity per mg of SPE product was 2200 down to 44, from 0.005 to 0.25 mg/ml, respectively. Inhibition of β-sheet development of Aβ42 (peak at 215 nm) was evident at a ratio of 44 (0.25 mg/ml) and not above 220 (0.05 or 0.005 mg/ml). The suppression of β-sheet was also accompanied by progressive apparent loss of alpha helix (190-200 nm, Figure 2). The results showed that the SPE product was able to interfere with assembly of β-sheet structures in Aβ42.

Modulation of Aβ42 secondary structure in the presence of increasing concentrations of SPE product was further studied using FTIR spectroscopy. FTIR characteristics of SPE product indicated that SPE did not absorb in designated β-sheet regions at either 1695 or 1629 cm^{-1}. FTIR analysis also showed no change in SPE peptide secondary structure over the concentration range studied. After incubation for 20h at 30°C in the absence of the SPE product, Aβ42 exhibited anti-parallel β-sheet structure associated with the presence of oligomers as previously shown (Cerf et al., 2009). Similar to CD data (Figure 2), modulation of Aβ42 secondary structure by the SPE product was evident by FTIR spectroscopy. The SPE product induced FTIR spectral changes in the Amide I region (1700-1600 cm^{-1}) reflecting its effects on the extent of Aβ42 self-assembly (Figure 3). Specifically, curve fitting indicated that SPE-concentration-dependent structural changes occurred in the β-sheet (1613-1629 and 1695 cm-1) and to a lesser extent, in the α-helix and/or random

coil structure regions, clustering between 1620 and 1705 cm^{-1}. Difference spectra produced after subtraction of SPE product at each concentration permitted evaluation of 'pure' Aβ42 FTIR spectra (Figure 3A). The ratio of 1695/1630 cm^{-1} allowed the ratio of anti-parallel to total β-sheet to be quantified, and detect the effect of SPE product specifically on formation of oligomeric Aβ42. By this method, the oligomer content of Aβ42 was found to be significantly lowered by the SPE product in a concentration-dependent manner (Figure 3B). Overall, these results suggested that the SPE product progressively inhibited the self-assembly of Aβ42 into oligomers and reversed existing β-sheet structures. To further study the effect of SPE mediated β-sheet inhibition of Aβ, pre-incubated Aβ42+SPE mixtures were examined by TEM and SDS-PAGE analysis.

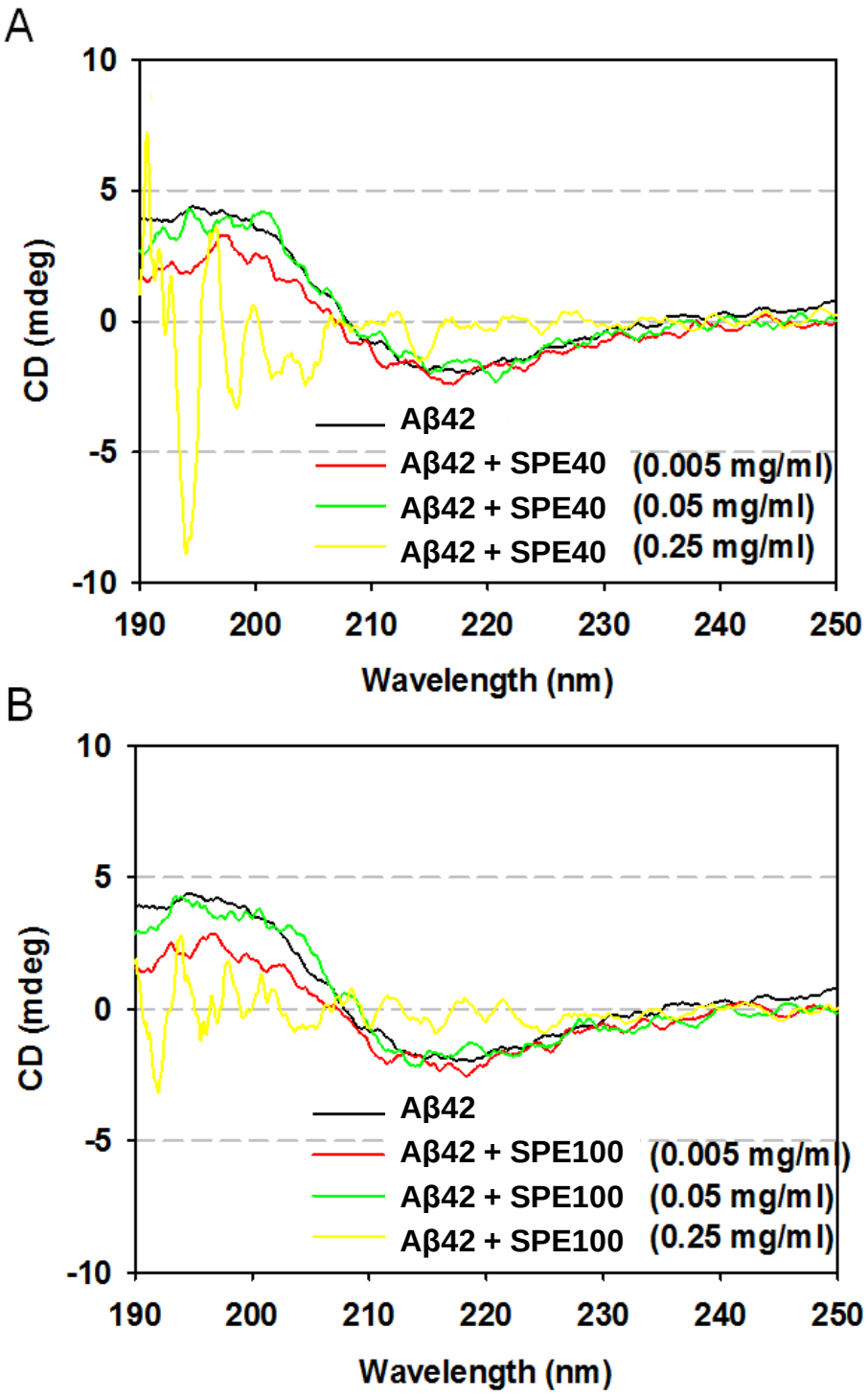

Figure 2: CD spectroscopy of Aβ42+SPE mixtures

The absorption bands of Aβ42 peptide solutions (11 μM), pre-incubated with different concentrations of SPE40 and SPE100 were analysed by Jasco J-810 CD Spectropolarimeter. The mean residue ellipticities of samples were recorded across the far UV range (190-260 nm), using a 0.1 cm path-length quartz cuvette, at room temperature, monitoring at 0.1 nm intervals. Concentration-

dependent effects of SPE40 (A) and SPE100 (B) on Aβ42 peptide (11 μM), following 24 hr incubation at 22ºC was determined. Spectra of SPE products alone at appropriate concentrations were subtracted from respective profiles of Aβ42+SPE product. Individual data sets (n=3) acquired were averaged over 3 scans. At higher concentrations (0.25mg/ml) SPE fractions (40 and 100) reduced total beta sheet content in Aβ42 solutions, as indicated by the changes in the 210-230nm band region.

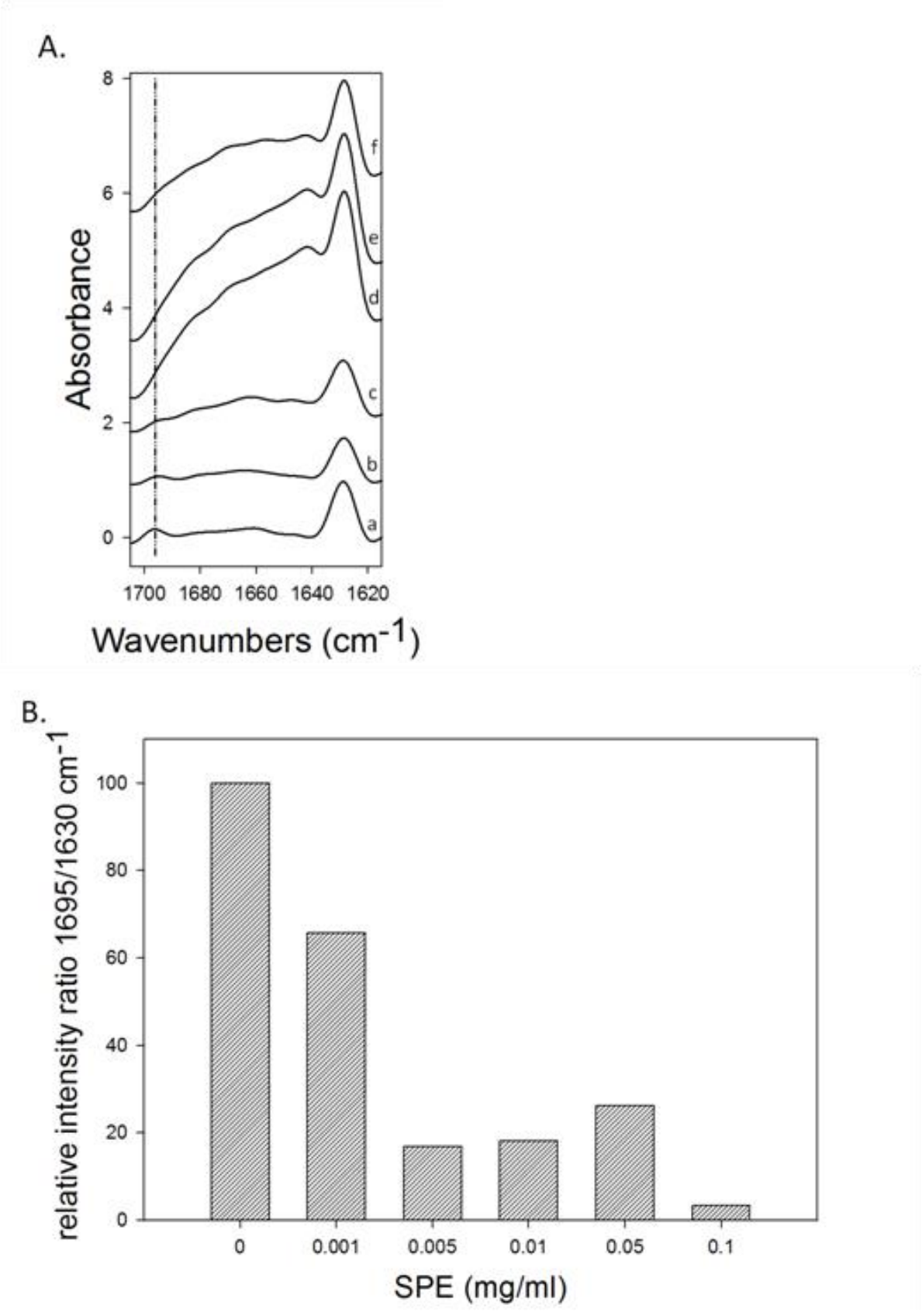
A.
Absorbance
8
6
4
2
0
f
e
d
c
b
a
1700 1680 1660 1640 1620
Wavenumbers (cm-1)
B.
relative intensity ratio 1695/1630 cm-1
100
80
60
40
20
0
0
0.001
0.005
0.01
0.05
0.1
SPE (mg/ml)

Figure 3: FTIR spectroscopy of Aβ42+SPE mixtures

Infra red (IR) spectra of Aβ42 solution pre-incubated with different concentrations of SPE fraction (total) were measured using an Equinox 55 infrared spectrophotometer. Spectral subtraction was applied between 4000 and 800 cm^{-1} and changes mainly reflected effects of SPE-total on Aβ42 secondary structure in the Amide I band region (1700-1600 cm^{-1}). Fourier self-deconvolution was applied to increase the resolution of spectra in the amide I region, which is that most sensitive to protein secondary structure. The FTIR data was preprocessed, baseline corrected and normalized for equal area between 1700-1500 cm^{-1}as described in (Goormaghtigh et al., 1999). ATR-FTIR spectra of Aβ42 incubated at 30°C for 20h in the presence of (a) 0, (b) 0.001, (c) 0.005, (d) 0.01, (e) 0.05, (f) 0.1 mg/ml of SPE-total, after subtraction of SPE-total controls **(A)**. Ratio of 1695/1630 cm^{-1} intensities normalized to control Aβ42 (100%) is plotted as a function of the concentration of SPE-total **(B)**. Each spectrum represents the mean of 128 repetitions recorded at a resolution of 2 cm^{-1} and further averaged across triplicate independent sample preparations. Increasing concentrations of SPE reduced the relative absorbance intensity at 1695/1630 cm^{-1} band region, indicating decrease of anti-parallel β-sheet structures

4.4.3 Effect of SPE on Aβ42 oligomerization

The oligomerization of Aβ42 is initiated by a conformational change from random coil or α-helix into a β- sheet maximized by cross linking hydrophobic interactions, quite similar to prion and other amyloidogenic proteins (Lansbury Jr, 1996; Tycko, 2003). Previously it was shown that increasing concentrations of SPE showed significant inhibition of β-sheet structures in Aβ42 (Figure 2, 3). To study the effects of SPE induced β-sheet inhibition on Aβ42 structure and oligomerization, pre-incubated Aβ42-SPE100 mixtures (11μM Aβ42+0.1 mg/ml SPE100) were observed by transmission electron microscopy or analysed by Aβ immunoblotting.

Aβ42 alone exhibited globular oligomeric (50-60nm in diameter) and proto-fibrillar structures (100-150nm in length, Figure 4A) as observed by TEM analysis. However, Aβ42 co-incubated with SPE also comprised small globular structures (10-20nm in diameter, Figure 4B) similar to the SPE100 control, and was devoid of larger oligomeric and fibrillar structures. The SPE product alone was characterised by small globular particles of approximately 10 nm diameter (Figure 4C). It is notable, that TEM analysis showed visible aggregates (10nm diameter) in SPE100 fraction, whereas CD and FTIR analysis of pure SPE fractions contained less hydrophobic peptides and showed no detectable aggregation. The TEM images of Aβ42 incubated with the SPE100 reflected strong suppression of oligomer/protofibril development (Figure 4B) compared to Aβ42 only (Figure 4A).

Freshly prepared Aβ42 was incubated with increasing concentrations of SPE100 and aliquots were collected for SDS-PAGE/Aβ immunoblotting analysis at 0h, 24h and 48h time points. Aβ42 showed increasing levels of higher-order oligomers (~50-110 kDa) with increasing incubation time (0, 24 and 48h), with no noticeable change in lower-order oligomers (dimer, trimer, tetramer) (Figure 5). Higher mass oligomeric Aβ42 (~50-110 kDa range) products were suppressed with increasing concentrations of SPE product (Figure 5). However, no change was observed with the levels of low mass Aβ42 oligomer (~7-20 kDa range) and monomer bands.

Overall, the data from secondary structure analysis (CD, FTIR), showed clear evidence for suppression of total β-sheet content and anti-parallel β-sheets associated with Aβ42 oligomerization by SPE products. TEM and western blotting analysis further supported the data from CD and FTIR showing that SPE inhibited formation of Aβ oligomers. Further the toxicity of the Aβ42-SPE mixtures were determined in yeast and validated in neuronal cells.

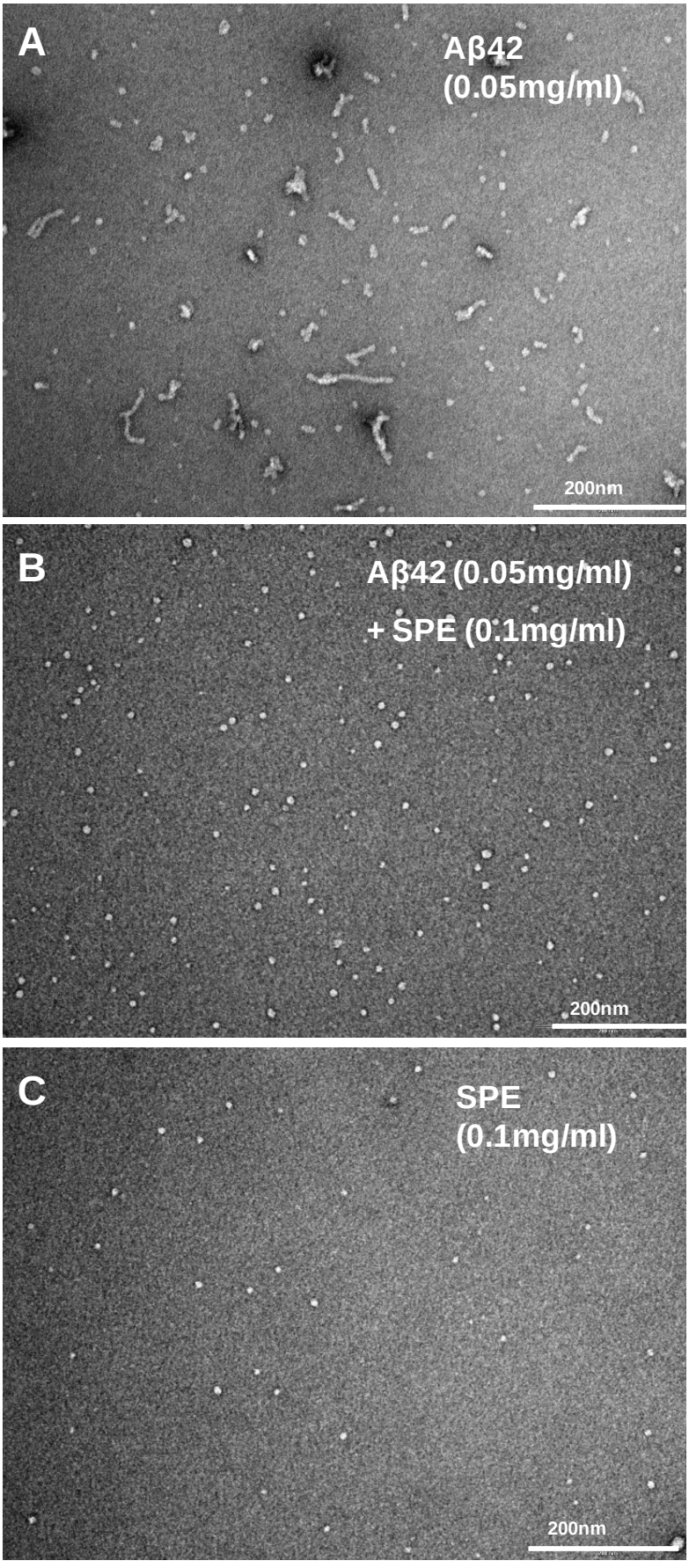
A
Aβ42
(0.05mg/ml)
200nm
B
Aβ42 (0.05mg/ml)
+ SPE (0.1mg/ml)
200nm
C
SPE
(0.1mg/ml)
200nm

Figure 4: Electron micrographs of Aβ42+SPE mixtures

Aβ42 solutions (11μM) pre-incubated with SPE100 (0.1 mg/ml in 10% ethanol) or vehicle (10% ethanol) for 20 h at 22°C were applied to glow discharged carbon-coated 400-mesh copper grids. The excess sample is removed and the grids are stained with 2–3 drops of 2% aqueous uranyl acetate (Sigma). The grids were air-dried and examined by Tecnai 12 Transmission Electron Microscope operating at 120 KV. Micrographs of Aβ42 alone **(A)**, Aβ42 pre-incubated with SPE100 **(B)** and SPE100 alone **(C)** were recorded using a Megaview III CCD camera. Oligomer Aβ42 preparations showed oligomeric structures (50-60 nm in diameter) and proto-fibrillar structures (100-150 nm in length), which were undetectable in pre-incubated SPE100-Aβ42 samples and SPE100 samples.

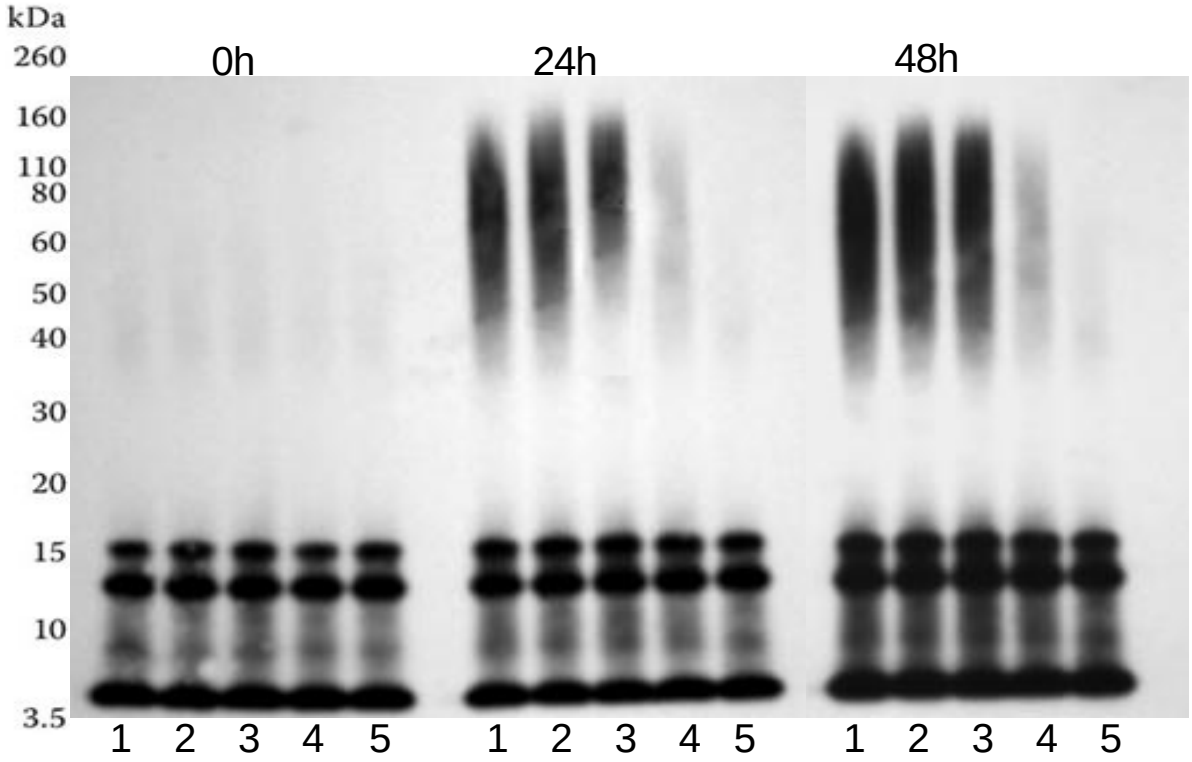

Figure 5: SDS-PAGE western blotting analysis of Aβ42+SPE mixtures

Aliquots from pre-incubated Aβ42 (10μM) with increasing concentrations of SPE100 (lanes 1-5 are 0, 0.005, 0.01, 0.05, 0.1 mg/ml) at different time points (0h, 24h and 48h) were analysed by western blot analysis. The samples were separated by electrophoresis using a 4-12% Bis-Tris gel with MES buffering system. The protein was transferred to nitrocellulose membrane and probed with WO2 antibody (anti-Aβ) and developed on films using enhanced chemiluminiscence (ECL). SPE100 inhibited the formation of higher Aβ oligomers (50-110kDa) in a dose dependent manner.

4.4.4 Modulation of Aβ42 toxicity

Aβ42 oligomerization is strongly associated with toxicity to both yeast and neuronal cells [Chapter 3, (Bharadwaj et al., 2008)]. Compounds which inhibit Aβ oligomerization have shown to protect cells from toxicity (Amijee et al., 2009; Findeis, 2002). The previous data showed suppression of Aβ42 oligomerization by SPE (Figure 2-5). To correlate the reduced oligomer content with toxicity to cells, SPE products were tested in Aβ42 toxicity assays with both yeast and neuronal cells. Oligomeric Aβ42 peptide was toxic to both yeast and neuronal cells in a dose-dependent manner (Figure 6A) with the concentration of 10μM chosen for subsequent experiments.

Pre-incubated Aβ42 (10μM) +SPE (0.001-0.1mg/ml) mixtures were treated with yeast cells for 20h followed by viability analysis using colony forming unit (CFU) count. A dose-dependent increase in yeast cell viability was observed with increasing concentrations of SPE in the Aβ42+SPE mixtures (Figure 6B). Protection against Aβ toxicity was evident at higher concentrations of 0.05 and 0.1mg/ml concentrations. Aβ42 only (10μM) caused ~50% cell death compared to ~40% with 0.05mg/ml SPE100 and complete reversal of toxicity at 0.1mg/ml SPE100. Interestingly, at lower concentrations of SPE (0.001-0.01mg/ml), cell death was increased compared to Aβ42 only (by 10%). Yeast toxicity experiments indicated that SPE100 was more protective than SPE40 at 0.05 and 0.1 mg/ml (Figure 6B) and subsequent studies with neuronal cells focussed on effects of SPE100.

SHSY5Y cells were treated with pre-incubated Aβ42 (10μM) +SPE100 (0.01-0.1mg/ml) mixtures for 3days followed by viability analysis by LDH and MTS assays as described in Section 2.2.4.5. Similar to yeast, the SPE100 product exhibited concentration-dependent rescue of Aβ toxicity, measured by either decreased release of LDH or enhanced reduction of MTS reagent in cells (Figure 6C). A 50% loss of viability as measured by MTS assay was seen with Aβ42 treatment (10μM). Increased viability of ~65% with SPE concentrations of

0.01mg/ml was observed which further improved to ~80% with 0.1mg/ml of SPE100. A similar pattern of rescue was observed with LDH release in cells. Aβ42 only treatment induced ~35% cell death whereas the cell death decreased to 20-15% with SPE100 concentrations of 0.01-0.1mg/ml. Overall, the data from the toxicity analysis of Aβ42+SPE mixtures in yeast and neuronal cells showed that SPE inhibited Aβ42 induced toxicity at higher concentrations. Together with the effects of SPE on Aβ42 structure and oligomerization, the results indicated that suppression of Aβ42 oligomerization inhibited its toxicity in both yeast and neuronal cells.

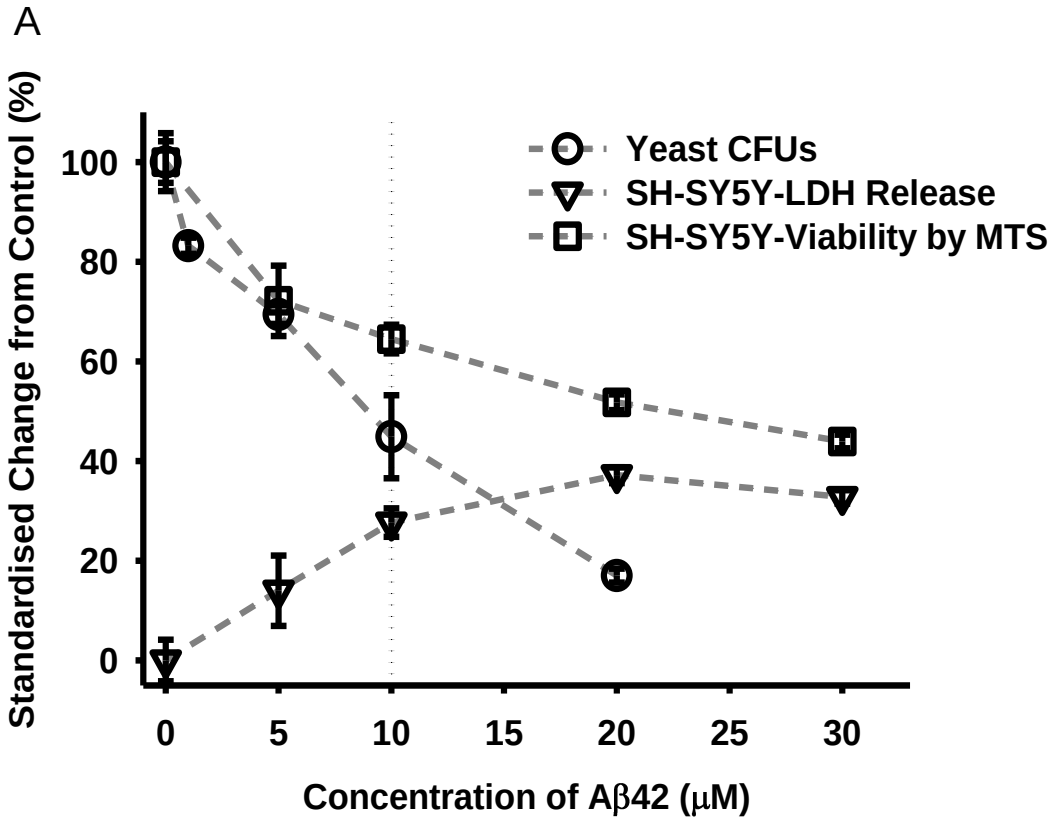

B

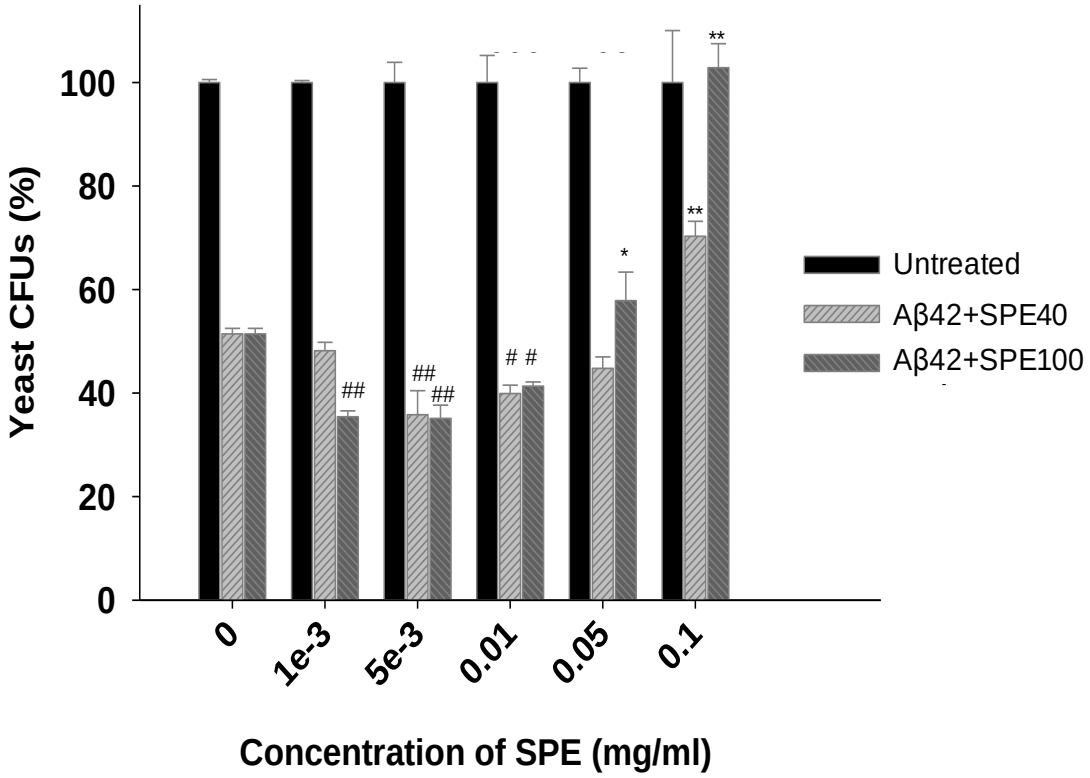
Yeast CFUs (%)
100
80
60
40
20
0
0
1e-3
5e-3
0.01
0.05
0.1
Concentration of SPE (mg/ml)
Untreated
Aβ42+SPE40
Aβ42+SPE100
##
##
##
# #
*
**
**

C

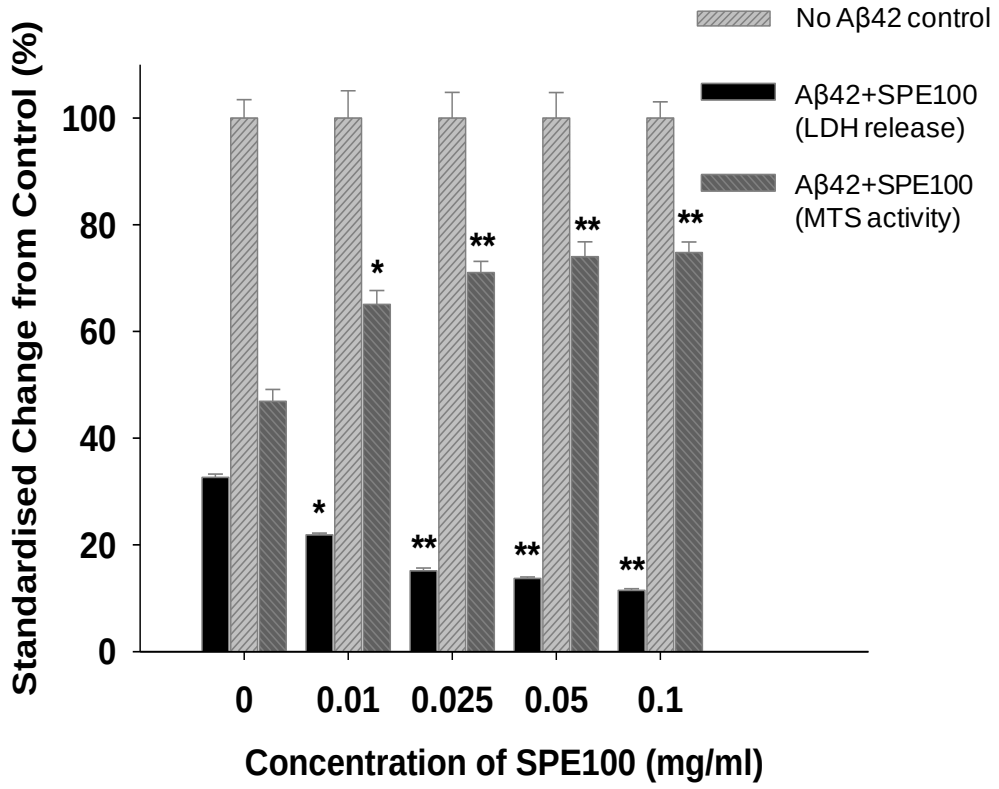
Standardised Change from Control (%)
100
80
60
40
20
0
0
0.01
0.025
0.05
0.1
Concentration of SPE100 (mg/ml)
No Aβ42 control
Aβ42+SPE100
(LDH release)
Aβ42+SPE100
(MTS activity)
*
*
**
**
**
**
**

Figure 6: Toxicity of Aβ42+SPE mixtures in yeast and neuronal cells Dose response of Aβ42 treatment on viability in yeast (by colony forming units count, CFU) and SHSY5Y cells (by LDH and MTS methods) **(A)**. Dose response effects of Aβ42 pre-incubated with SPE100 (0.01 to 0.1 mg/ml) on viability of exponentially growing yeast cells incubated at 30˚C for 20h **(B)**. Dose response effects of Aβ42 pre-incubated with SPE100 (0.01 to 0.1 mg/ml) on viability of SHSY5Y cells **(C)**. Cell viability was determined by the ratio of colony numbers in the absence and presence of SPE samples, and reported by LDH and MTS assay methods. At higher concentrations, SPE fractions significantly reduced Aβ42 toxicity in yeast and SHSY-5Y cells. However, at lower concentrations, SPE40 and SPE100 enhanced Aβ42 toxicity in yeast but not in SHSY-5Y cells. Results represent the mean and SEM of triplicate determinations at each concentration with significance of differences to control (*, P<0.05; **, P<0.01; #, P<0.05; ##, P<0.01) determined by Students t test.

4.5 Discussion:

The self-assembly of proteins into fibrillar structures based on cross β-sheet 'laminae' of amyloidogenic polypeptides represents a common folding pathway of many proteins (Krebs et al., 2008). Furthermore, 'amyloid' structuring of proteins has been described as a detoxification strategy to mask the promiscuous surface of the oligomeric building block (Carrell et al., 2008). Studies have also identified novel biological functions for amyloidogenic protein fibrils in bacteria, fungi and even mammals (Kelly and Balch, 2003). Supporting evidence from a range of studies in several neurodegenerative disease including AD correlate soluble protein oligomers in the brain as the indicator of cognitive decline rather than insoluble fibrillar deposits (Ferreira et al., 2007; Glabe and Kayed, 2006; Popik et al., 1999).

Aβ42 fibrils are assembled from a planar 'laminate' of up to six parallel β-sheets, stacking and elongating the fibril perpendicular to the laminate plane (Burkoth et al., 2000). However, formation of meta-stable oligomeric Aβ42 represents an early competing folding pathway (Necula et al., 2007) characterised by anti-parallel β-sheet structure (Sarroukh et al., 2010). Widely differentiated behaviour in propensities for self-aggregation into oligomers and fibrils is observed in naturally-secreted forms of Aβ (e.g., Aβ37-42, Aβ40) and also in forms of Aβ generated by mutations of APP in the brain (Tomiyama et al., 2008) (Bharadwaj et al., 2009; Peralvarez-Marin et al., 2009). Underlying these effects is the key role of primary Aβ sequence in permitting β-sheet organisation. Studies have also identified key amino acids involved in Aβ structural morphology. For example, deletion of E22-glutamate from Aβ42 permitted assembly of dimers and trimers but not ThT-binding fibrils (Tomiyama et al., 2008) whereas substitution of Phe19 to Pro19 in Aβ42, prevented ability to form oligomers and fibrils (Bernstein et al., 2005). Also, modification of Phe19 to Ser19 and Leu34 to Pro34 in Aβ42 showed decreased aggregation (Wurth et al., 2002) and was less toxic compared to oligomeric Aβ42 in yeast and neuronal cells (Chapter 3). Apart from its natural tendency to self-associate via multiple folding pathways sequence, several environmental factors and binding partners can alter Aβ aggregation in the brain. Studies implicate that Aβ structures in the brain can be heterogeneous (Bibl et al., 2006), and associate with chaperone like species that may affect its morphology and regulate proteostasis (Voisine et al., 2010). Actually, increased chaperone levels have shown to be associated with longer lifespan (Tatar et al., 1997) and also protect cells from the toxic proteins (Balch et al., 2008; Zhou et al., 2001).

Chaperones that facilitate or prevent assembly of either the β-sheet laminate or the intra-laminate assembly are likely to catalyse or inhibit, respectively, the self-assembly of Aβ42. The development of peptide-based inhibitors of Aβ42 aggregation has focussed significantly on active domains of chaperone proteins. For example, transgenically-expressed human Aβ42 in *C. elegans* elicited the expression of known heat shock 'chaperone' proteins that were subsequently immunoprecipitated with Aβ42 (Fonte et al., 2002) (Fonte et al.,

2008), and which regulated the folding of Aβ42 towards less toxic pathways. Similarly, α1-anti-chymotrypsin (ACT), which is present in AD brain plaque, drives Aβ42 along either amorphous aggregation or fibril pathways, depending on the molar ratio (Janciauskiene et al., 1998). A peptide fragment of the chaperone protein α-crystallin also inhibited aggregation of Aβ42 (Raman et al., 2005) and its toxicity to PC12 cells (Santhoshkumar and Sharma, 2004). By analogy, mixture studies with different ratios of Aβ42 in the presence of Aβ40, show that the presence of Aβ40 can inhibit mature fibril development when Aβ40 approaches equimolar ratios to Aβ42, with corresponding attenuation of cell toxicity (Jan et al., 2008). Also, compounds which dissociate intact cross β-sheet structures (β-sheet 'breakers') have been successfully designed from peptoid and retro-peptoid analogues of an amyloidogenic peptide such as amylin (Elgersma et al., 2007). Chaperone-mediated interactions can alter the morphology and toxicity of amyloid proteins (Fonte et al., 2002) and supports that aggregation pathways can be strategically manipulated by exogeneous 'chaperone' agents.

In this study, the chaperoning like effects of whey derived peptide hydrolysate (SPE) on beta-amyloid protein (Aβ42) folding pathways and cellular toxicity was demonstrated. The SPE product bioactivity described follows the precedent reported for proline-rich complex 'Colostrinin' (Kruzel et al., 2001) and other mammalian sources of colostrum (Sokolowska et al., 2008). Peptides with capacity for fibril regulation, derived from bovine dairy sources including whey, casein and lactoferrin, have also been reported (Bennett et al., 2009). The colostrinin peptide complex was shown to inhibit and disrupt β-sheets of amyloid aggregates (Schuster et al., 2005) and exert several other bioactive properties including neuroprotection in AD (Bilikiewicz and Gaus, 2004). It is suggested that other exogenous peptides, perhaps dietary sources, with aggregate inhibition capacity might be also be protective against AD and other amyloidogenic diseases (Balch et al., 2008; Powers et al., 2009). The SPE product prepared from bovine whey proteins described in this study appears to be of very similar but not identical composition to Colostrinin (Figure 1B),

probably reflecting differences in respective host materials and the processing method used to produce the SPE product.

4.5.1 Inhibition of Aβ42 oligomerization and toxicity by SPE

CD and FTIR spectroscopy were used for studying the modulation of secondary structure of Aβ42, with FTIR results permitting evaluation of the ratio of anti-parallel (oligomer) to parallel (fibril) β-sheet content (Cerf et al., 2009) (Sarroukh et al., 2010). FTIR monitoring of Aβ42 self-assembly in the presence of SPE product indicated that the Aβ42-SPE mixtures contained structures of net lower β-sheet content and specifically lower anti-parallel β-sheet (Figure 3). Analysis by TEM (Figure 4) and Western blot analysis (Figure 5) clearly showed that SPE inhibited Aβ42 oligomerization, supporting previous data from CD and FTIR studies. The concomitantly protective effects against Aβ42 toxicity in yeast and neuronal cells (Figure 6B, C), were clearly evident. The pattern of loss of high mass oligomers of Aβ42 and associated toxicity was very similar to that seen in the presence of curcumin (Yang et al., 2005). Low mass ratio of SPE to Aβ42 showed enhanced toxicity in yeast (Figure 6B). However, the 'promotion of toxicity' was not present for neuronal cell studies or detected by CD or FTIR studies. This observation reflects the sensitivity of the methods and the possibility that different Aβ isoforms might possess differentiated toxicity profiles in yeast compared with neuronal cells. There is a possibility that the 'enhanced' toxicity observed (Figure 6B), is a result of SPE (at lower concentrations) induced formation of 'off pathway' toxic soluble complexes with Aβ42.

Overall, a positive correlation between suppression of β-sheet content and oligomerization by SPE fractions (Figures 2-5) and protection against Aβ42-mediated toxicity to both yeast and neuronal cells (Figure 6) was observed. Collectively, these results provide important evidence that suppression of anti-parallel β-sheet structures can prevent formation of oligomeric structures linked with toxicity. The lack of toxicity of a mutant form of Aβ12-28 (Peralvarez-Marin

et al., 2009), in contrast to Aβ25-35 and related variants (Pike et al., 1995) , in spite of the presence of aggregates characterised by having β-sheet secondary structure, further supports these observations.

The Aβ structure modulating properties of the dairy derived peptides (SPE fractions) demonstrated in this study implicate them as interesting candidates for identifying novel inhibitors of Aβ oligomerization and toxicity. Further characterization of the SPE product mixture aided by cleaner and better resolved preparations is necessary to isolate specific peptides which are responsible for anti-Aβ activity. However for future therapeutic application, it will be essential to determine whether these dietary peptide preparations can survive gut enzymatic degradation and if they will be able to cross the blood brain barrier.

4.6 Summary:

A number of molecular species have been shown to act as chaperones and thereby regulate the folding pathway of Aβ42. In many cases, the toxicity of products is differentiated from unchaperoned Aβ42, usually attenuated. Thus, 'chaperones' of Aβ42 represent obvious molecules for development into disease-modifying therapeutics, if *in vitro* bioactivities can translate to protective effects *in vivo*. These results demonstrate the important finding that suppression of *anti*-parallel β-sheet structures is specifically required for regulation of oligomer toxicity to cells. In addition to inhibition and disruption of Aβ42 oligomers, the SPE dairy peptide product may display other useful neuroprotective properties as shown for Colostrinin. It is unknown the extent to which dietary factors already play a role in chaperone-mediated modulation of Aβ42 toxicity *in vivo*, if at all, however, based on *in vitro* properties, it is possible that a wide range of adequately bio-available dietary peptides and phytochemicals might contribute to neuroprotection by chaperone-mediated activity.

Chapter 5

Oligomerization and Toxicity of MBP-Aβ fusion proteins

5.1 Introduction:

A substantial amount of structural and functional information of Aβ comes from studies using synthetically derived Aβ produced by solid phase peptide synthesis (SPPS). Although synthetic Aβ has been widely used for variety of experimental purposes, the preparation and handling of the peptide solutions have not been very straightforward. In addition to its intrinsic heterogeneous and variable nature, substantial compositional differences and intrinsic impurities in Aβ produced by SPPS resulting in experimental irreproducibility has been reported (Dobeli et al., 1995; Howlett et al., 1995; Simmons et al., 1994; Soto et al., 1995a; Soto et al., 1995b; Zagorski et al., 1999). In addition, aggregation kinetics and toxicity of synthetic Aβ have been reported to fluctuate between different batches and also with storage and solubilisation conditions (Soto et al., 1995b).

The *in-vitro* solubility and aggregation properties of the Aβ peptide are found to be dependent on the pH environment, temperature, peptide concentration, incubation times (Burdick et al., 1992; Stine et al., 2003), hydrostatic pressure (Foguel et al., 1999) and other local interacting factors including metals, lipids and other proteins [reviewed in (Bharadwaj et al., 2009)]. However, the precise molecular interaction leading to the formation of the toxic Aβ oligomers have not been completely understood. Several papers report methods to produce Aβ oligomers from synthetic Aβ (Barghorn et al., 2005; Lambert et al., 1998; Lambert et al., 2001; Stine et al., 2003) but the preparations differ in the sizes of oligomers, and stability and even reproducibility can be an issue (Brining, 1997).

In addition to synthetic Aβ (SPSS derived), recombinantly produced Aβ proteins have also been reported. Recombinantly–derived Aβ present significant advantages comparing SPSS synthesized Aβ mainly for the reason that primary structure changes are rare because of the high fidelity of the cellular expression systems and the physiological conditions under which these

operate. Moreover recombinant production is more cost effective than SPSS synthesis for large scale manufacture. There are several studies reporting methods for recombinant production of Aβ in different cellular systems (Dobeli et al., 1995; Hortschansky et al., 2005; Lee et al., 2005; Li et al., 2009; Luhrs et al., 2005; Sharpe et al., 2005; Subramanian and Shree, 2007; Walsh et al., 2009; Wiesehan et al., 2007). However, most of the existing methods either yield low amounts or require enormous efforts for purification. More importantly, a majority of these studies have not established the toxic properties of the recombinantly derived Aβ. Caine *et al* 2007 described a novel method for producing Aβ as an N-terminal fusion to maltose binding protein (MBP). In this methods, the maltose binding protein tagged Aβ42 (MBP-Aβ42) fusion protein could be stably produced in large quantities, purified easily using affinity columns and showed properties (binding to Cu and Zn) similar to Aβ peptide (Caine et al., 2007b). However, the toxic properties of these MBP-Aβ fusions have not been determined.

Toxicity of synthetically derived Aβ oligomers has been established in yeast cells (Bharadwaj et al., 2008). In chapter 3 it was shown that oligomeric Aβ was more toxic than the non-oligomerizing Aβ peptide in yeast and neuronal cells. In chapter 4, it was shown that inhibition of Aβ oligomerization using dairy derived peptides (SPE fraction) suppressed its toxicity both in yeast and neuronal cells. In this chapter, the MBP-Aβ fusion proteins were studied in the yeast model where their toxicity was demonstrated. Furthermore the toxicity of the MBP-Aβ fusion proteins was also observed in neuronal cells.

5.2 Aims:

1.) Purification and characterization of MBP-Aβ fusion proteins
2.) Determine the toxicity of MBP-Aβ fusion proteins in yeast and neuronal cells.

5.3 Materials and Methods:

Purification of MBP, MBP-Aβ16 and MBP-Aβ42 fusion proteins were done as described in Section 2.2.3. The MBP fusion proteins were harvested in bacteria followed by purification via affinity chromatography using an amylose column and analysis by size exclusion chromatography (superdex-200 gel filtration column) as described in Section 2.2.3. The purified fusion proteins were characterized using SDS-PAGE followed by western blotting analysis and coomassie staining. Volume analysis of the protein gel bands was done using the Quantity-1D analysis software. The fusion proteins were studied using Transmission electron microscopy (TEM) and Dynamic light scattering (DLS) (Jo Caine, CSIRO) as described in Section 2.2.9. Toxicity of purified MBP, MBP-Aβ16 and MBP-Aβ42 fusion proteins were tested in yeast cells and primary mouse cortical cells by colony count and CCK-8 assays respectively as described in Section 2.2.4.3 and Section 2.2.4.6 respectively.

5.4 Results:

5.4.1 Purification and characterisation of MBP-Aβ42 fusion protein

MBP fusion variants were expressed and purified from *E. coli* and analysed by SDS-PAGE followed by coomassie staining (Figure 1A) and western blot analysis using anti-Aβ (WO2) (Figure 1B) and anti-MBP (Figure 1C). The molecular mass estimated from the SDS PAGE analysis were found to be to be 39.6 kDa for MBP, 42.6 kDa for MBP-Aβ16, and 45.7 kDa for MBP-Aβ42. In addition, the proteins exhibited no breakdown products. The MBP-Aβ42, under non-reducing conditions, demonstrated additional higher molecular weight bands, corresponding to sizes ~97 kDa (dimer), ~135 kDa (trimer), ~160 kDa (tetramer), and ~235kDA (hexamer) (Figure 1B, C). Volume analysis of these bands showed the monomeric band to be the major species on the gel (~71% of the total protein) followed by tetramers, hexamers, dimers and trimers (~19%, 6%, 3% and 1% of total protein respectively). The shorter MBP-Aβ16 fusion shows ~94% of the total protein in the lane made up of a monomeric

band at 42 kDa and a faint dimer band (~6%) (Figure 1B, C).

The MBP-Aβ fusion proteins were further studied by size exclusion chromatography using a superdex-200 gel filtration column (performed by Jo Caine). The gel filtration profile of the concentrated peaks eluted from the amylose affinity column showed two major peaks plus a small peak for MBP-Aβ42 (Figure 1D). The S200 profile of MBP-Aβ16 protein showed one main peak and a small peak (Figure 1E). Interestingly, purified peaks collected and left at 4^{o}C for 1 week or more reproduced the original profile of three peaks when re-run on the S200 column. The results from the SDS-PAGE western blotting and size exclusion chromatograph showed that MBP-Aβ42 formed higher oligomeric structures compared to MBP-Aβ16. To further analyse their structure, the MBP-Aβ proteins were observed by transmission electron microscopy (TEM).

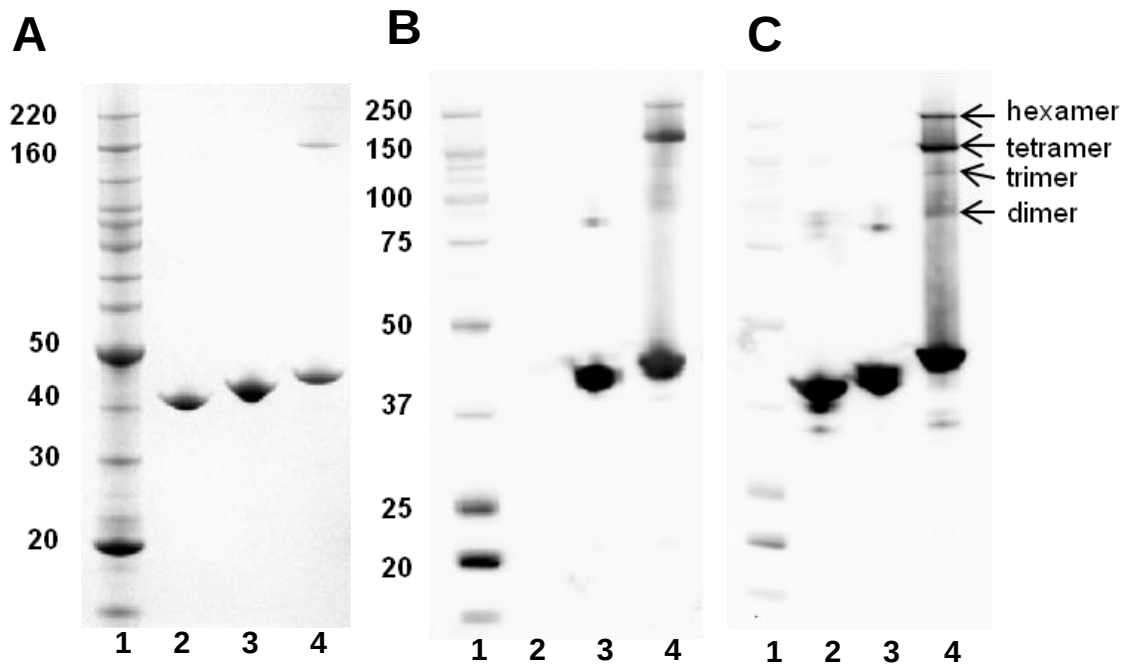

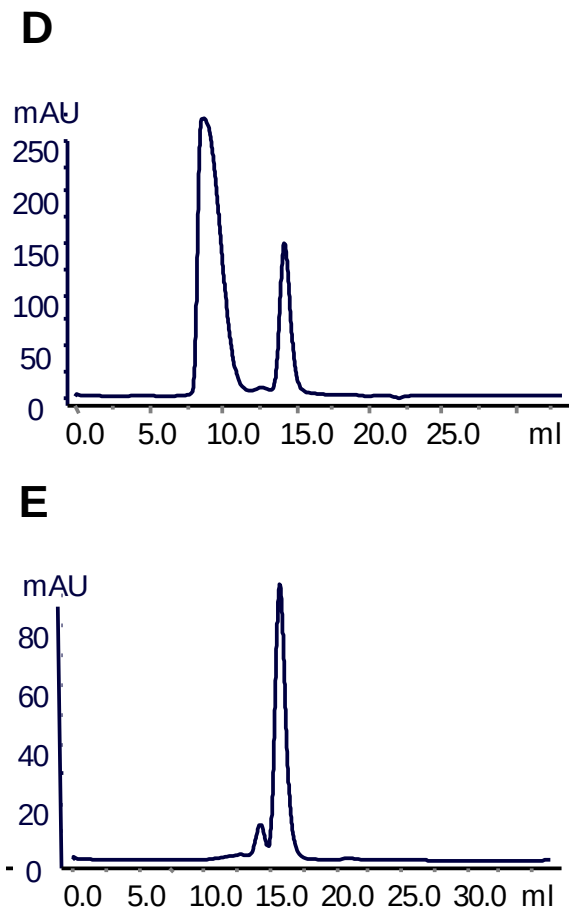

Figure 1: SDS-PAGE Western blotting and gel filtration profiles of MBP-Aβ42 and MBP-Aβ16.

MBP-Aβ samples (5µg) were run on a 4-12% Bis-Tris gel in a MES buffering system and coomassie stained **(A)**. For immunoblotting, MBP-Aβ samples (0.5µg) were run on identical gels, transferred to nitrocellulose membranes and probed with anti-Aβ (WO2) **(B)** and anti-MBP **(C)** antibodies and visualised using chemiluminescence. Lane loadings as follows: Lane 1 = molecular weight markers, Benchmark (A) and Precision Western C (B and C); Lane 2 = MBP; Lane 3 = MBP-Aβ16 and Lane 4 = MBP-Aβ42. Samples from the amylose affinity column were concentrated on a spin concentrator (10kDa MWCO) and fractionated using Superdex-200 gel filtration column equilibrated in 50mM Tris pH8.0 at 0.5ml/min. Absorbance was monitored at 280nm. The plots of the S200 gel filtration profile show profiles of MBP-Aβ42 **(D)** and MBP-Aβ16 **(E)**.

5.4.2 Transmission electron microscopy of MBP-Aβ fusion proteins

Samples from the MBP-Aβ fusion proteins (MBP, MBP-Aβ16 and MBP-Aβ42) were analysed by TEM (Figure 2). The electron micrographs showed that the MBP control and MBP-Aβ16 proteins had small globular structures of 5-9nm in diameter (Figure 2A and 2B respectively). However, MBP-Aβ42 showed large amorphous globular structures ranging from 11-16 nm in diameter in addition to globular structures of 5-9nm in the TEM (Figure 2C). However no fibrillar structures were seen in any of the fusion protein preparations. TEM analysis of the MBP-Aβ fusion proteins showed that MBP-Aβ42 formed larger amorphous structures compared to smaller globular structures found in MBP-Aβ16 and MBP solutions. The results supported the previous observations from SDS-PAGE immunoblotting and size exclusion chromatography analysis indicating that MBP-Aβ42 can form higher oligomeric structures (Figure 1). To determine the size distributions of these oligomeric structures, the MBP-Aβ fusion proteins were analysed by dynamic light scattering (DLS).

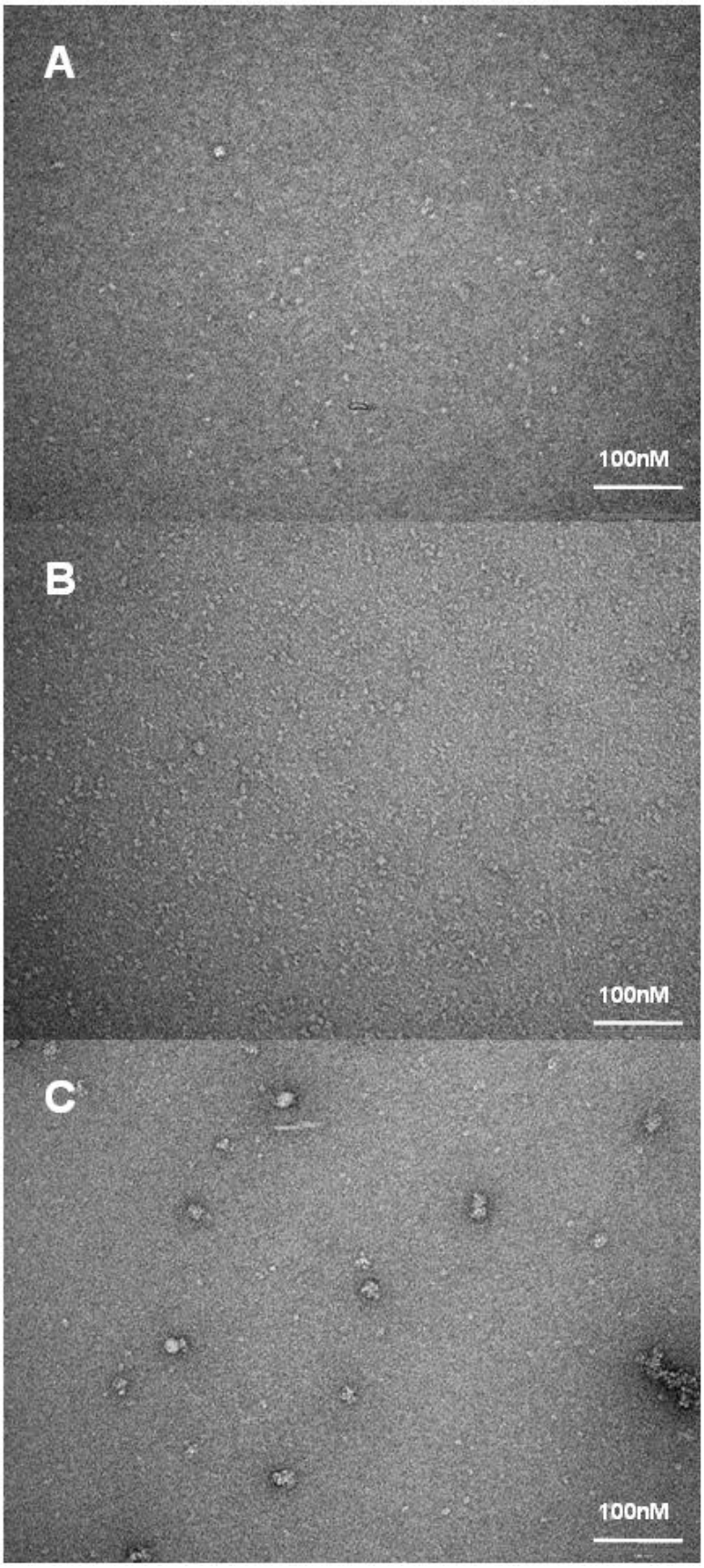
A
100nM
B
100nM
C
100nM

Figure 2: Electron micrographs of MBP-Aβ solutions.

The MBP-Aβ fusion proteins (MBP, MBP-Aβ16 and MBP-Aβ42) were applied to carbon coated copper grids which were glow-discharged in nitrogen. After the application of uranyl acetate, the grids were examined by TEM. MBP **(A)** and MBP-Aβ16 **(B)** contain species mainly 5-9nm in size; whereas MBP-Aβ42 **(C)** contains species 11-16 nm in size and 5-9nm range.

5.4.3 Dynamic light scattering analysis of MBP-Aβ fusion proteins

The size distribution of MBP-Aβ fusion proteins (MBP and MBP-Aβ42) in solution were analysed by Dynamic light scattering (DLS) (performed by Jo Caine). DLS of MBP and MBP-Aβ42 (~0.8mg/ml) proteins were performed using the DynaPro^{TM} NanoStar plate reader at laser wavelength 830nm. The particle size of MBP and MBP-Aβ42 fusion proteins in solution were represented as hydrodynamic radii (R_h) and radius of gyration (R_g) which were calculated as described in Section 2.2.9.1. The size distributions of the particles were determined on the basis of modality and dispersity. Modality refers to the number of 'peaks' in the size distribution and dispersity is a measure of heterogeneity or homogeneity of the species comprising the population.

MBP was found to be a monomodal monodispersed species with an average hydrodynamic radius (R_h) of 2.8 ± 0.3 nm (Figure 3A). The radius of gyration for MBP calculated from the available crystal structure was found to be R_g = 2.07 nm. This would be converted to an $R_h = R_g/0.77 = 2.69$ nm which was very close to the experimental R_h value for MBP. The DLS data collected for MBP-Aβ42 showed that the sample was monomodal polydispersed, indicating the presence of different forms of MBP-Aβ42. The R_h for the most abundant species of MBP-Aβ42 was determined to be 8.8 ± 0.5 nm (Figure 3B) with a range of radii between 3-100 nm. The polydiversity of the MBP-Aβ42 peaks indicated that there is a range of oligomeric species present. This result supported the previous data from SDS-PAGE, size exclusion chromatography (Figure 1) and TEM analysis (Figure 2) indicating that MBP-Aβ42 forms

oligomers whereas the MBP alone remained largely monomeric in physiological aqueous solutions.

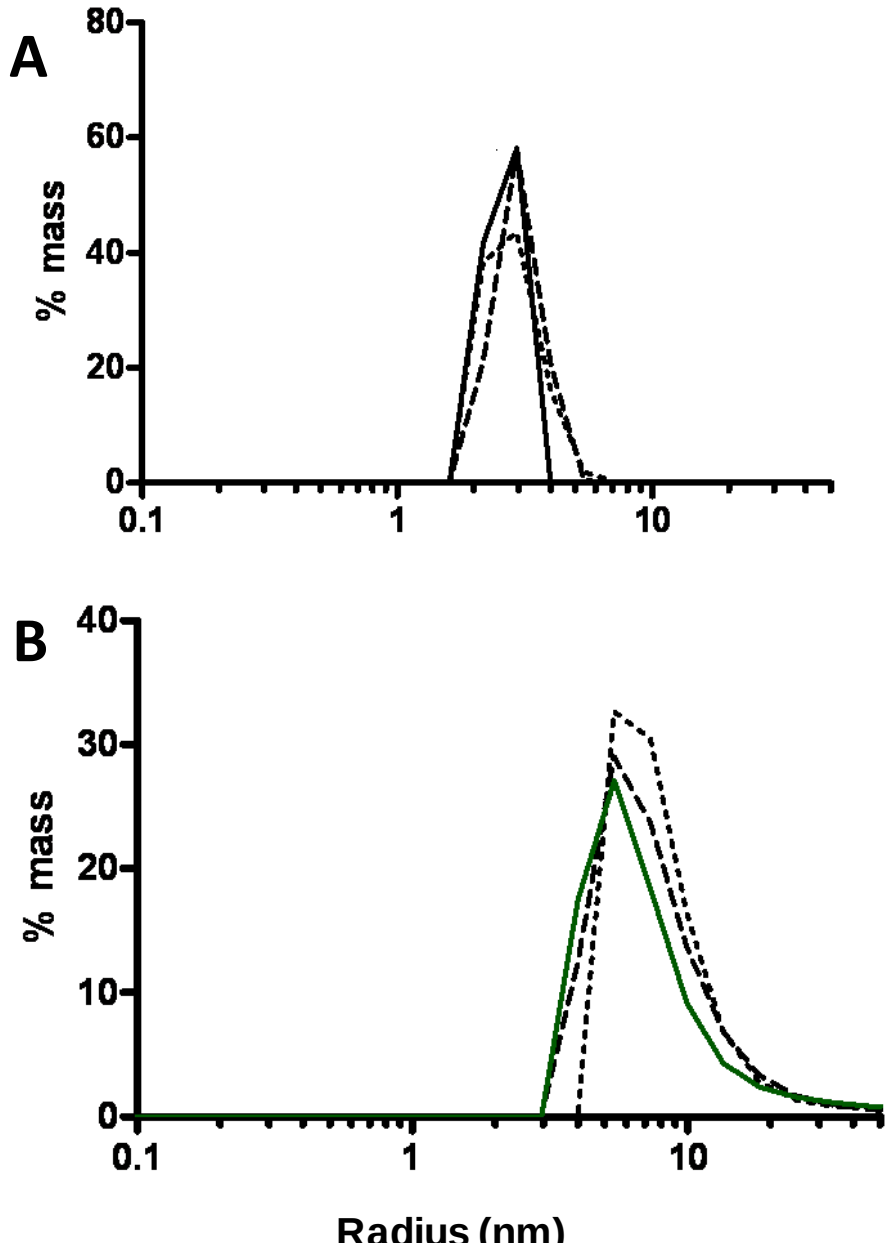

Figure 3: DLS measurements of MBP & MBP-Aβ42

The dynamic light scattering plot is representative of the average of 40 individual 5 sec DLS collections for 3 separate dilutions of the MBP **(A)** and MBP-Aβ42 **(B)**. The results indicate a monomodal monodisperse species in MBP with hydrodynamic radii of 2.8 ± 0.3 and monomodal polydisperse in MBP-Aβ42 (B) with a hydrodynamic radii range 3–100 nm with a peak at 8.8 ± 0.5.

5.4.4 Toxicity of MBP-Aβ fusion proteins in yeast and neuronal cells:

The previous data showed that MBP-Aβ42 formed oligomers whereas MBP alone and MBP-Aβ16 remained largely monomeric. Further, the toxicity of these fusion proteins were determined in yeast and subsequently validated in mouse primary cortical neuronal cultures. The toxic effects of the MBP-Aβ fusion proteins was determined using a colony forming unit (CFU) count assay after treatment in yeast (Bharadwaj et al., 2008). The full length MBP-Aβ42 was significantly toxic while MBP-Aβ16 and MBP alone were not. At a concentration of 22μM, MBP-Aβ42 caused 50% loss of yeast cell viability, compared to less than 5% cell death with MBP-Aβ16 treatment, while MBP alone was not toxic (Figure 4A). Untreated yeast cells were exposed to 10mM maltose/20mM Tris/HCl vehicle buffer alone. In addition, the MBP-Aβ42 protein mediated toxicity was dose dependent with 25% cell death seen at 10μM and a 3-fold higher 75% cell death measured at concentration of 44μM (Figure 4B).

Having confirmed that the MBP-Aβ42 fusion protein was toxic in yeast, the toxicity of the MBP-Aβ fusion proteins was determined in mouse primary cortical neuronal cultures treated with 30μM of different isoforms of MBP-Aβ for 4 days. Cell viability was determined by CCK-8 assay. The CCK-8 assay uses a tetrazolium dye (WST-8, 2-(2-methoxy-4-nitrophenyl)-3- (4-nitrophenyl)-5-(2,4-disulfophenyl)-2H-tetrazolium, monosodium salt) which is reduced to a yellow colored product (formazan) by dehydrogenases in cells. The amount of the formazan dye generated was determined to measure viability following treatment (Zhang et al., 2010a). Vehicle treated cells were exposed to 10mM maltose/20mM Tris/HCl buffer alone. Treating the cortical cultures with MBP-Aβ42 caused a significant reduction (25% loss) in cell viability (Figure 4C). In contrast, the MBP-Aβ16 fusion and MBP control proteins did not display any neurotoxicity at the same concentration tested (Figure 4C). Overall the data showed that MBP-Aβ42 was more toxic than MBP and MBP-Aβ16 proteins in both yeast and neuronal cells.

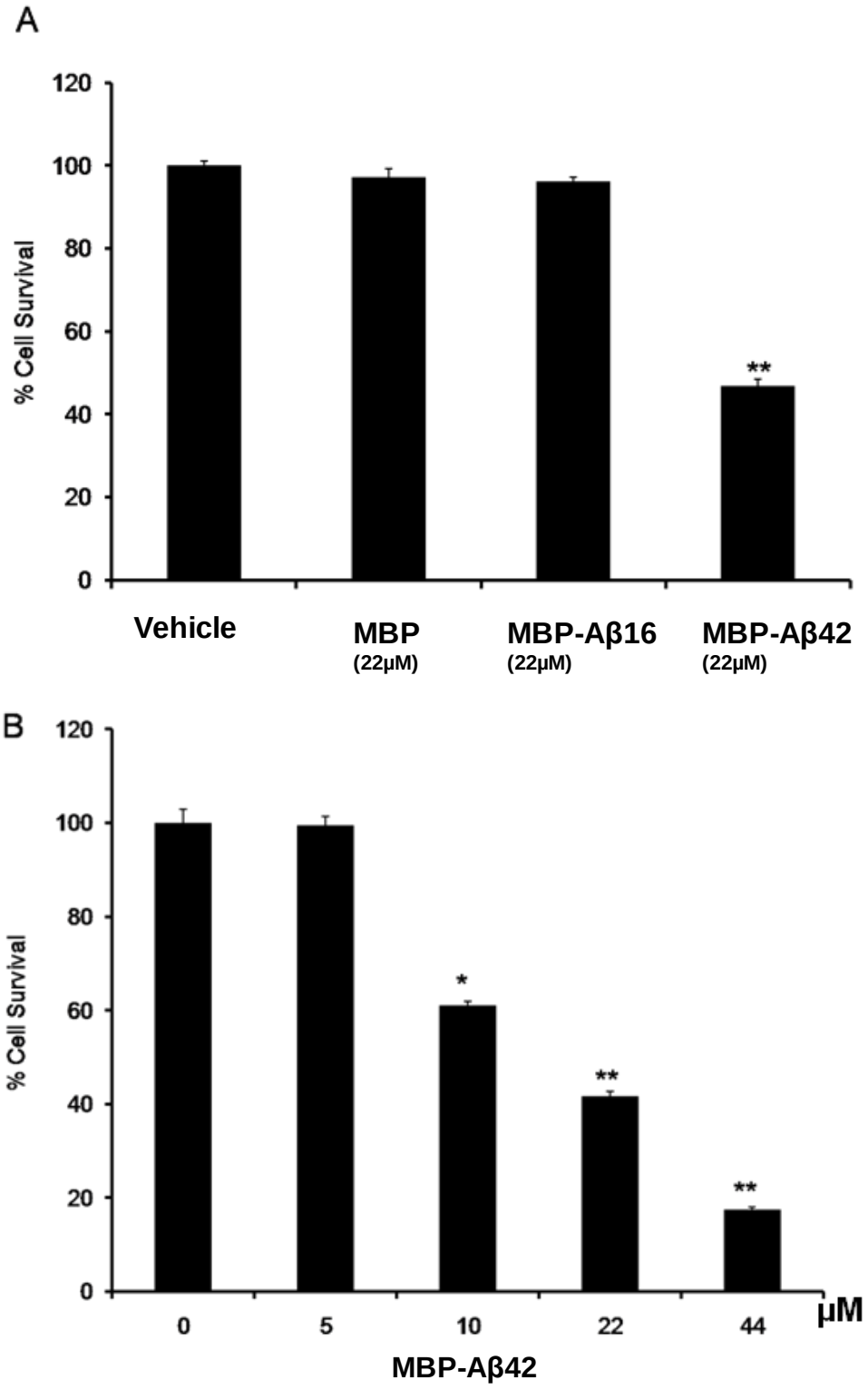
A
120
100
80
60
40
20
0
% Cell Survival
**
Vehicle
MBP
(22μM)
MBP-Aβ16
(22μM)
MBP-Aβ42
(22μM)
B
120
100
80
60
40
20
0
% Cell Survival
*
**
**
0
5
10
22
44
μM
MBP-Aβ42

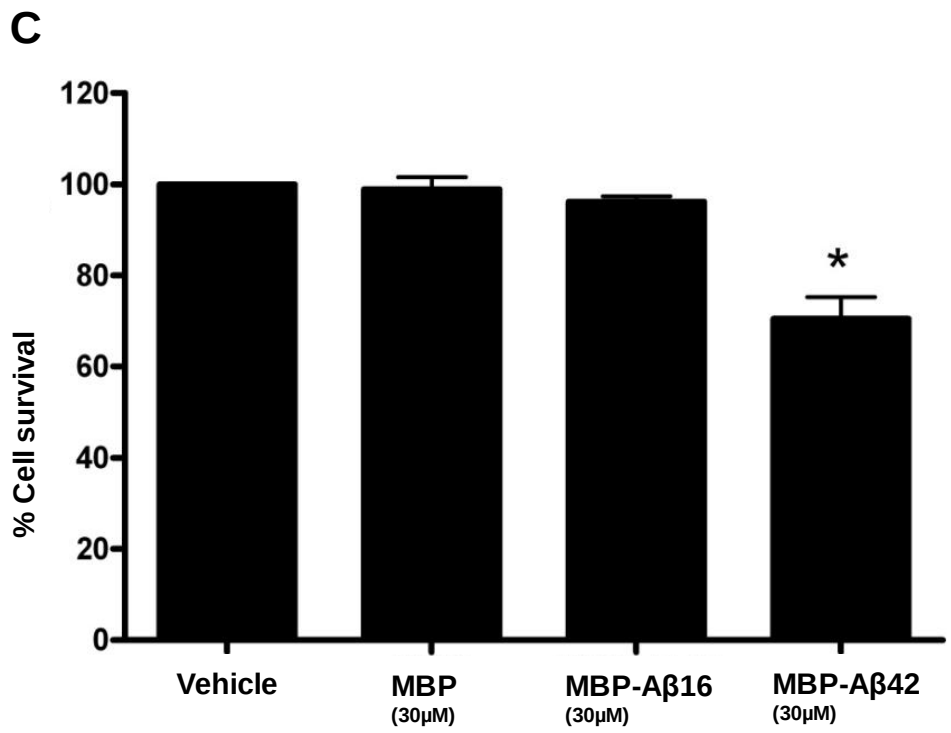

Figure 4: Toxicity of MBP-Aβ proteins in yeast and neuronal cells

Yeast cells were treated with 22µM MBP, MBP-Aβ16 and MBP-Aβ42 proteins. Untreated cells were exposed to 10mM maltose/20mM Tris/HCl vehicle buffer alone. Following treatment, cell viability was determined by counting the number of colonies formed **(A)**. 22µM MBP-Aβ42 caused significant loss of yeast cell viability (50%, **p<0.0001) compared to less than 5% cell death with MBP-Aβ16 treatment, while MBP alone was not toxic. Yeast cells were treated with increasing concentrations of MBP-Aβ42 fusion protein (5-44µM) **(B)**. A dose dependent increase in cell death was seen with MBP-Aβ42 treatment (**p<0.0001, *p<0.01). Primary cortical neurons were treated with 30µM MBP, MBP-Aβ16 and MBP-Aβ42 proteins for 4 days **(C)**. Vehicle treated cells were exposed to 10mM maltose/20mM Tris/HCl buffer alone. Following treatment, cell viability was determined by CCK-8 assay. 30µM MBP-Aβ42 caused significant loss of cell viability (25%, *p<0.01) while MBP-Aβ16 and MBP were not toxic. Data is presented as mean +/- SEM, n=4 per treatment group.

5.5 Discussion:

Similar to naturally derived forms, Aβ42 prepared from synthetic lyophilized peptides have shown to form multiple forms ranging from monomeric, oligomeric, fibrillar and many more other multimeric structures and show neurotoxic properties. Various methods are also available to prepare oligomeric Aβ from synthetic Aβ peptides including filtration using low molecular weight cut-off filters (Bitan and Teplow, 2005), treatment of lyophilized Aβ with strong acids and bases to disrupt pre-formed aggregates (Stine et al., 2010; Zagorski et al., 1999), photo-induced crosslinking (Bitan et al., 2003), density gradient centrifugation (Ward et al., 2000) and size exclusion chromatography (SEC) (Lambert et al., 1998; Walsh et al., 1997).

However, the above methods for preparing Aβ oligomers involve tedious purification work and high costs for pure lyophilized peptides stocks. Although well suited for studies involving physiological level analysis (requiring nanomolar concentrations), such methods for Aβ oligomer preparations are not suitable for larger scale purposes required for physicochemical and structural analysis. Therefore recombinantly produced Aβ can be beneficial for such high throughput screening methods. It is however essential to characterize the structural and functional properties of such recombinantly derived Aβ. Previously, (Caine et al., 2007b) described a method for producing large quantities of soluble MBP tagged Aβ fusion protein using a bacterial expression system. In this chapter, the oligomerization and the toxicity of these recombinantly produced MBP-Aβ fusion proteins were studied to enable further characterization of these fusion proteins. The structural characteristics of the MBP-Aβ fusion proteins were studied using a variety of techniques. Further, the toxicity of the MBP-Aβ fusion proteins was determined in yeast and neuronal cells.

5.5.1 Oligomerization of MBP-Aβ42

The structural characteristics of MBP-Aβ fusions were studied using SDS-PAGE, size exclusion, TEM and DLS analysis. The MBP-Aβ42 fusion protein was shown to form SDS stable higher molecular weight oligomeric structures corresponding to dimers (~97 kDa), trimers (~135 kDa) tetramers (~160 kDa), and hexamers (~ 235 kDa) (Figure 1). MBP-Aβ16 solutions were found to contain a faint band at ~97kDa which also corresponded to the small peak found by size exclusion (gel filtration analysis) (Figure 1). This indicated the presence of a possible dimer species, which formed ~6% of the total protein, as measured by band volume analysis (Figure 1). However, no higher molecular weight structures (trimers, tetramers and hexamers) could be found in MBP-Aβ16 solutions similar to that present in MBP-Aβ42. TEM and DLS analysis further showed that the particle sizes present in the MBP-Aβ42 solutions were bigger and morphologically different compared to those in MBP and MBP-Aβ16 proteins (Figure 2, 3). DLS analysis also showed that the size ranges of the particles in MBP-Aβ42 solutions are monomodal polydispersed. This showed that MBP-Aβ42 contained a mixture of particles derived from a single monomeric form, which suggested that the solutions contained a mixture of monomeric and oligomeric forms (Figure 3). However MBP had a monomodal monodispersed population indicating that the majority of the solution contained monomers. Overall the data indicated the presence of oligomeric forms in MBP-Aβ42 solutions.

In addition to its nature of forming oligomers, the MBP-Aβ42 fusion was stable. Size exclusion, TEM and DLS results indicated that this fusion protein does not form fibrils but small oligomers which maintain species equilibrium on the removal of higher oligomers. The major SDS stable oligomeric species from the gel electrophoresis and DLS measurements appear to be multimeric species up to hexamers. In the literature, the toxic state of the Aβ peptide has been variously ascribed to multimers ranging from dimers to dodecamers (Barghorn et al., 2005; Singh et al., 2002; Walsh et al., 2002a). The absence of

higher molecular weight (greater than hexamers) or fibrillar forms in MBP-Aβ42 may be due to lower self-association propensity of MBP-Aβ42 compared to Aβ42 due the attached MBP fusion protein. Higher oligomers of the MBP-Aβ42 are prevented from forming most likely due to steric clashes from the much larger globular part of the fusion protein. This has been clearly shown in the crystallographic study of MBP fusion with a T-cell leukemia virus type 1 gp21 ectodomain (Kobe et al., 1999) where the 31 amino acid gp21 fusion peptide forms a trimer while possible higher oligomers were prevented from forming due to the close proximity of the globular MBP protein.

5.5.2 Toxicity of MBP-Aβ42

The toxicity of these different fusions was determined in yeast and also in neuronal cells to establish their functional nature. MBP-Aβ42 was found to be significantly more toxic than MBP-Aβ16 and MBP in both yeast and neuronal cells. Moreover MBP-Aβ42 showed a dose-dependent response on yeast viability (Figure 4). However, MBP-Aβ42 was found to be less toxic compared to Aβ42 peptide in mammalian cell lines (Hung et al., 2008) and also in yeast [Chapter 3, (Bharadwaj et al., 2008)]. It is likely that the steric hindrance from the much larger globular part of the fusion protein (MBP) may contribute to reduced toxicity. The inability to form higher molecular weight structures (greater than hexamer) may also contribute to its reduced toxicity compared to Aβ42 in cells.

Although it is widely accepted that soluble oligomeric forms of Aβ42 are the main toxic species in the AD brain, no particular Aβ species has been identified as the main cause of neuronal dysfunction and death. (Lesne et al., 2006) study implicated a unique and a novel Aβ isoform (Aβ*56: 56-kD soluble Aβ42 assembly, dodecamer) as the key neurotoxic Aβ42 species responsible for cognitive decline. However, a more recent study (Shankar et al., 2008) has identified Aβ dimers from the soluble extract of AD cerebral cortex tissues as the main toxic isoform. Both Lesne et al and Shankar et al studies identify

different toxic Aβ species (dimer or Aβ*56), which might reflect differences in the Aβ detection techniques employed. Alternatively, it is also suggested that an array of soluble oligomeric Aβ species (ranging from dimers to dodecamers) may have neurotoxic properties associated with memory impairment in AD. The MBP-Aβ42 toxicity data shown here supports the notion that oligomer Aβ42 mediated cell death can be a collective contribution of a variety of toxic isoforms and not mediated by a single isoform. Compared to Aβ42, MBP-Aβ42 solutions lacked higher oligomeric forms (greater than hexamers) which only reduced its toxicity and did not rescue it completely. The reduced toxicity of MBP-Aβ42 solutions could therefore represent the absence of the toxic higher oligomeric forms. In addition, due to its MBP fusion partner, it is also quite likely that the oligomers formed by MBP-Aβ42 are structurally different compared to the natural Aβ42 oligomers which further suggests that different oligomeric structures of Aβ42 can be toxic. Due to its nature of maintaining species equilibrium, it was difficult to unequivocally attribute the toxicity to the oligomeric MBP-Aβ42 isoforms. Further investigation using stable cross-linking analysis of the MBP-Aβ42 oligomeric species can provide a better idea of the contribution of different isoforms to toxicity and cell death.

5.6 Summary

Overall the data presented here shows that MBP-Aβ42 forms oligomers and is a stable protein. The oligomer forming MBP-Aβ42 protein was also found to be toxic in yeast and neuronal cells. It is therefore a well suited model for structural elucidation and physicochemical studies of smaller Aβ oligomers (Caine et al., 2011). The MBP-Aβ42 fusion protein could also be a potential tool for analysing the toxicity of Aβ42. In addition, it provides the opportunity of developing assays for screening potential inhibitors of Aβ oligomer induced toxicity.

Chapter 6

Effect of Aβ42 Induced Cell Division in Yeast is Restricted to Stationary Phase

6.1 Introduction:

There is now strong evidence to show abnormal activation of cell cycle events in the regions of the brain that are susceptible to neurodegeneration in AD (Husseman et al., 2000; Yang et al., 2003). Increased levels of cell cycle proteins (Ding et al., 2000; Vincent et al., 2001) and mitotic signalling phosphoepitopes (Chang et al., 2002; Li et al., 2005; Li et al., 2004) have also been observed in degenerating hippocampal neurons of AD brains.

A number of studies have shown that Aβ42 treatment (both fibrillar and oligomer) can induce neuronal cell cycle events *via* mTOR/MAP kinase pathways in neurons (Bhaskar et al., 2009; Frasca et al., 2004; Malik et al., 2008; Varvel et al., 2008; Wu et al., 2000) and associated toxicity *via* activation of protein kinase R (PKR) through calcium signalling and caspase 8 activation (Suen et al., 2003). A recent study also showed that long-term inhibition of mTOR by rapamycin prevented AD-like cognitive deficits and lowered levels of Aβ42 in the PDAPP transgenic mouse model (Spilman et al., 2010).

In contrast, other studies show a significant decrease in p-mTOR and p-p70S6K (serine/threonine kinase) levels in differentiated neuroblastoma cells (N2a. SH-SY5Y cells) treated with Aβ42 (Lafay-Chebassier et al., 2005; Lafay-Chebassier et al., 2006). A recent study also showed correlation between the inhibition of mTOR signalling and impairment in synaptic plasticity in hippocampal slices from an AD mouse model and also with Aβ42 treatment (Ma et al., 2010b). One possible explanation for the conflicting findings observed with modulating mTOR signalling by Aβ42, is that neurons have different response patterns to Aβ42 treatment depending on their cell cycle and availability of neurotrophic factors. However it is unclear whether Aβ induced growth or toxic effects in neurons are dependent on the cell cycle.

Investigating Aβ42 induced cell cycle events in neurons can be problematic and unreliable. One problem is that neurons of the adult brain are terminally

differentiated and lack the capacity to divide *in vivo* and *in vitro*, (McShea et al., 1999). Also, re-activation of cell cycle machinery in post-mitotic neurons can lead to cell loss (Feddersen et al., 1992; Park et al., 2007). Moreover Aβ42 is a known neurotoxic protein. Therefore this poses a challenge to dissect the toxic and trophic properties of Aβ42 in neurons. A particular advantage of studying cell cycle in yeast cells compared to neurons is their robust nature. Cell cycle can be physiologically modulated effectively by nutrient limitations without loss of viability and they can survive prolonged periods in starvation, which makes it a very useful model for studying Aβ induced effects (Lillie and Pringle, 1980). Moreover, Aβ42 has been shown to be toxic in yeast cells [Chapter 3, (Bharadwaj et al., 2008)] which will enable differentiating the biphasic properties of Aβ42.

In the studies presented in this chapter, I determined whether Aβ42 can induce cell division in yeast cells within the stationary phase of the cell cycle and assessed the role of mTOR signalling in this process.

6.2 Aims:

1) Induce entry of yeast cells into the stationary phase of cell growth by nutrient starvation
2) Determine if Aβ42 can promote proliferation of cells within the stationary phase of cell growth and whether this can be blocked by inhibition of mTOR by rapamycin.

6.3 Materials and Methods:

Candida glabrata cells and *Saccharomyces cerevisiae* (BY4743) grown in YNB+2% glucose (no amino acids) and YNB+2%glucose (-Trp) respectively were used for this study. For inducing stationary phase, cell division was inhibited via starvation in media lacking essential nutrients (non-fermentable carbon source) as described in Section 2.2.10. Aβ42 peptide was prepared as

described in Section 2.2.4.1 and used to treat yeast cells as described in Section 2.2.11. Stationary phase cells were treated with Aβ42 (in the presence or absence of 0.2µM rapamycin).

6.4 Results:

6.4.1 Starvation induced entry of yeast cells into a stationary growth phase:

To induce starvation, yeast cells (*Candida glabrata*) were incubated in YNB+2% or 0.1% glucose or starved in non growing media (YNB+ non-fermentable carbon source i.e. 2% ethanol, 2% maltose, 2% Glycerol) for 6-7h at 30°C. Following incubation, the cell density (OD at 600nm) at different time points was measured. In addition, the morphology of the cells was studied by flow cytometry using forward scatter (FSC) analysis (Tzur et al., 2011) and light microscopy. These results are shown in Figure 1. An increase in cell density was observed in cells incubated in YNB+2%glucose compared to YNB+ other non-fermentable carbon sources (Figure 1A). Forward scatter analysis for cell volume showed that cells incubated in YNB+2% glucose showed increased cell volume (Figure 1B) indicative of active metabolism. Also the actively growing cells were distributed across a size range of 3-8µm (Figure 1C). Whereas cells incubated in YNB+2% maltose showed no increase in cell volume (Figure 1D) and were distributed over a size range of 2-4µm (Figure 1E). Microscopic analysis of cells incubated in YNB+2% glucose showed active budding [(Figure 1F), indicative of cell division in yeast] (Mortimer and Johnston, 1959) whereas cells incubated in YNB+2% maltose showed no budding (Figure 1G). Overall the data showed that starvation in non-growing media induces entry into stationary phase in yeast. Cells in exponentially and stationary phase were used for subsequent experiments

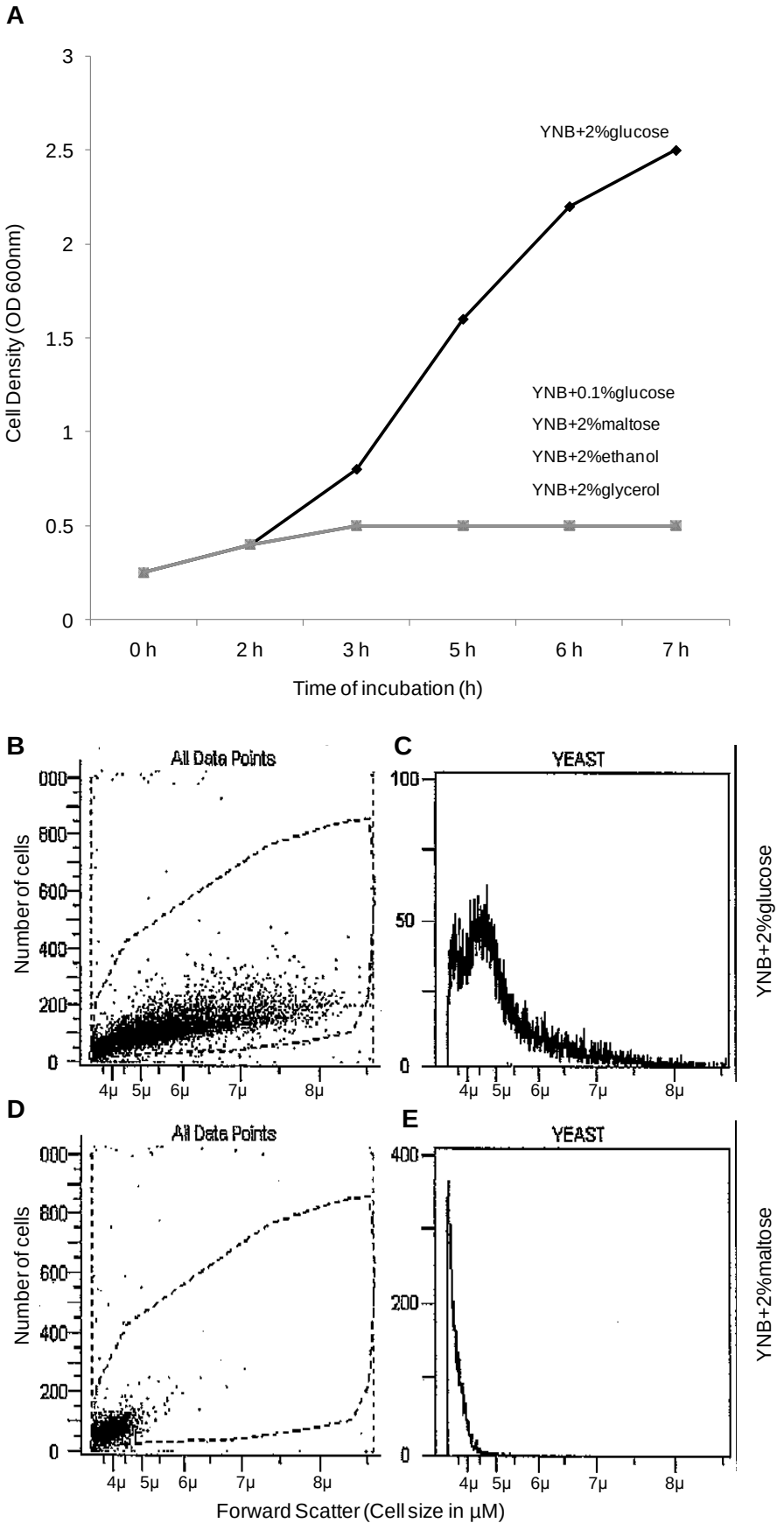
A
Cell Density (OD 600nm)
3
2.5
2
1.5
1
0.5
0
YNB+2%glucose
YNB+0.1%glucose
YNB+2%maltose
YNB+2%ethanol
YNB+2%glycerol
0 h
2 h
3 h
5 h
6 h
7 h
Time of incubation (h)
B
All Data Points
Number of cells
C
YEAST
YNB+2%glucose
D
All Data Points
Number of cells
E
YEAST
YNB+2%maltose
4µ 5µ 6µ 7µ 8µ
Forward Scatter (Cell size in µM)

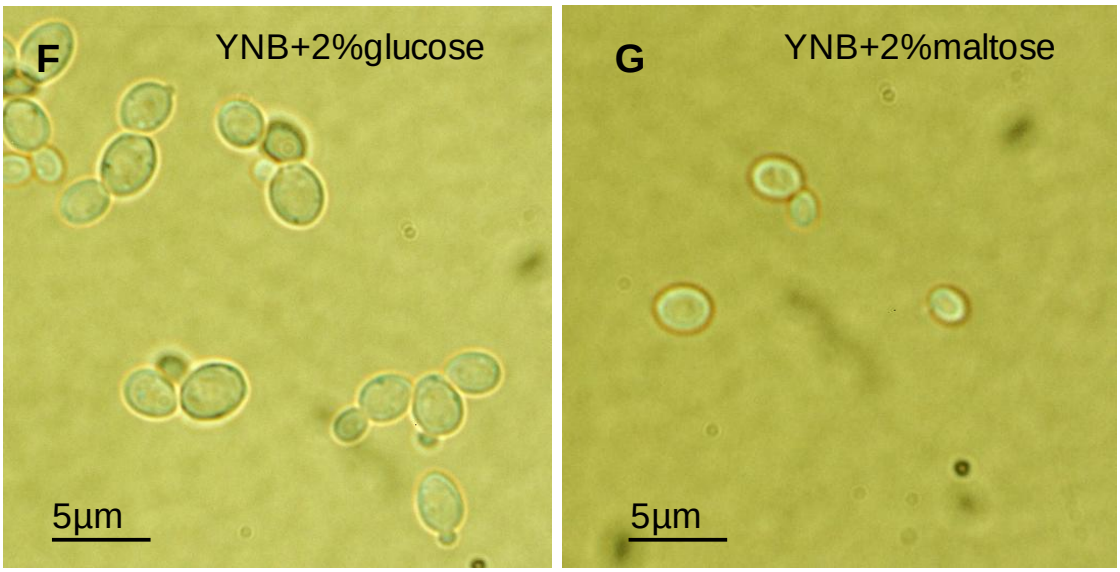

Figure 1: Nutrient starvation inhibits cell division and induces stationary phase in Candida glabrata cells. Exponentially growing *Candida glabrata* cells in YNB+ 2% glucose were washed and incubated in YNB containing different carbon sources (2% glucose, 0.1% glucose, 2% ethanol, 2% maltose or 2% glycerol). Cell density at 600 nm was measured at different time points (0-7 h) **(A)**. Cells incubated in YNB+2% glucose and YNB+2% maltose were analysed by forward scatter analysis **(B, D)** and size distributed **(C, E)** using flow cytometry (FACS). The cells were also analysed by bright field microscopy **(F, G)**. Cells incubated in YNB+2% glucose showed increasing cell density and active budding indicating growth, however, cells incubated in other carbon sources showed no increase in cell density, no budding and reduced cell size indicating entry into stationary phase.

6.4.2 Aβ42 induced cell division in starved cells:

To determine the effects of Aβ42 on cell growth, *Candida glabrata* cells in stationary phase and exponential phase were treated with Aβ42. *Candida glabrata* cells incubated in YNB+ 2% glucose and YNB+ 2% maltose for 7h were treated with vehicle or 5µM Aβ42 for 20h at 30°C. Following treatment the cells were spread on YEPD media plates. Images of media plates from the

viable count assay are showed in Figure 2A-D. Aβ42 induced cell death in exponential phase cells (grown in YNB+2% glucose) is indicated by the decrease in the number of colonies compared the untreated (Figure 2A, B). In contrast, Aβ42 induced growth in stationary phase cells (incubated in YNB+2% maltose) is indicated by the increase in the number of colonies compared to the vehicle treated (Figure 2C, D).

Quantitative analysis of Aβ42 induced cell division in stationary phase cells was determined by colony forming unit (CFU) count. *Candida glabrata* cells incubated in YNB+ different carbon sources (2% glucose, or 0.1% glucose, 2% maltose or 2% glycerol) for 7h were treated with vehicle or 5μM Aβ42 for 20h at 30°C. Exponential phase cells (YNB+2% glucose) showed marked loss of viability (25-30% viable) with Aβ42 treatment, compared to vehicle (Figure 2E). This level of reduction is similar to that shown in Chapter 3 and as previously reported (Bharadwaj et al., 2008). However, treating cells in stationary phase (YNB+0.1% glucose, 2% maltose or 2% glycerol) with Aβ42 caused a significant increase in the number of colonies (200-250%) indicating an increase in cell division (Figure 2E).

To determine if lower doses of Aβ42 could significantly increase cell division, cells in stationary or exponential growth phases were treated with vehicle or 0.1-5μM of Aβ42. Cells were also treated with 20 and 50μM of Aβ42 to determine if higher levels were toxic. The results are shown in Figure 2F. A dose-dependent decrease in the number of colonies with Aβ42 treatment was observed in exponential phase cells indicating loss of viability. In stationary cells, a significant increase in the number of colonies was observed from concentrations of 100nM (~150%) up to a maximum of ~200-250% increase at 2-5μM. However at, higher concentrations of Aβ42 (≥20μM), cell viability decreased in both exponential growing and stationary phase cells (Figure 2F). These results indicate that Aβ42 can promote proliferation only in cells that are in the stationary phase at doses that are otherwise toxic to exponentially growing cells. Overall the data above indicates that Aβ42 may induce mitotic cell division in *Candida glabrata* promoting cell proliferation. An essential

pathway for cell cycle progression and proliferation in eukaryotes is the mTOR signalling pathway (Hay and Sonenberg, 2004). To determine if this signalling pathway has a role in Aβ42 induced cell division stationary phase growing cells were treated with Aβ42 in the absence or presence of mTOR inhibitor, rapamycin.

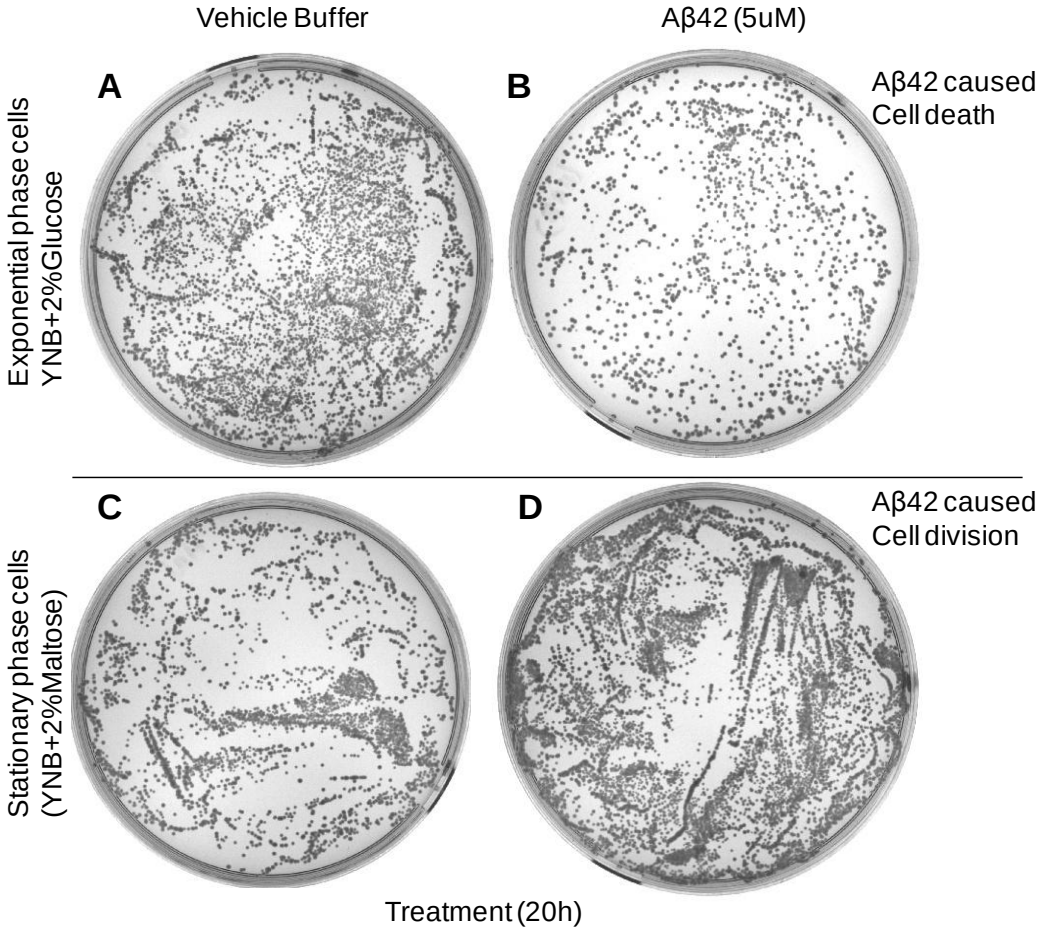

E

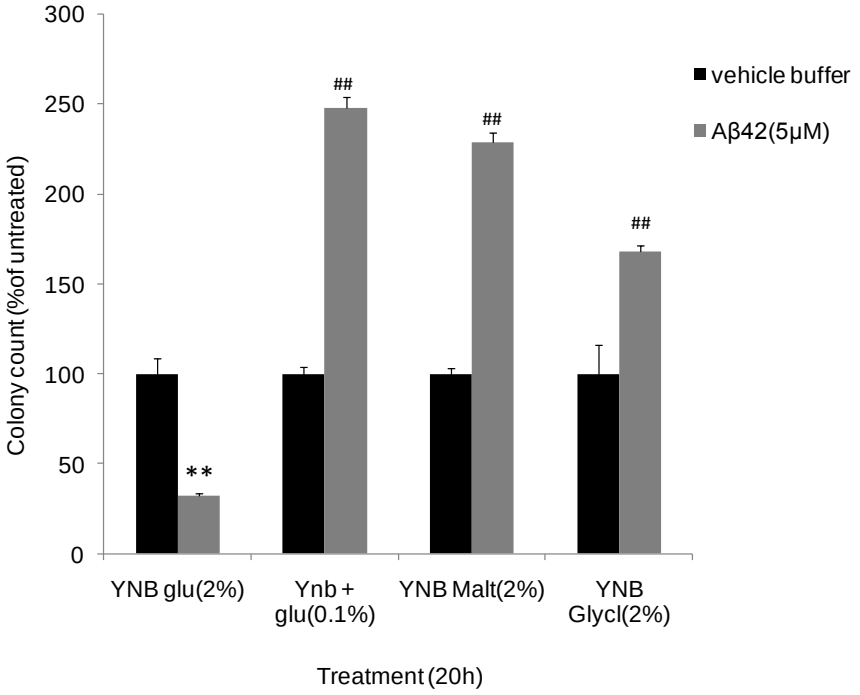
300
250
200
150
100
50
0
Colony count (%of untreated)
vehicle buffer
Aβ42(5μM)
##
##
##
**
YNB glu(2%)
Ynb + glu(0.1%)
YNB Malt(2%)
YNB Glycl(2%)
Treatment (20h)

F

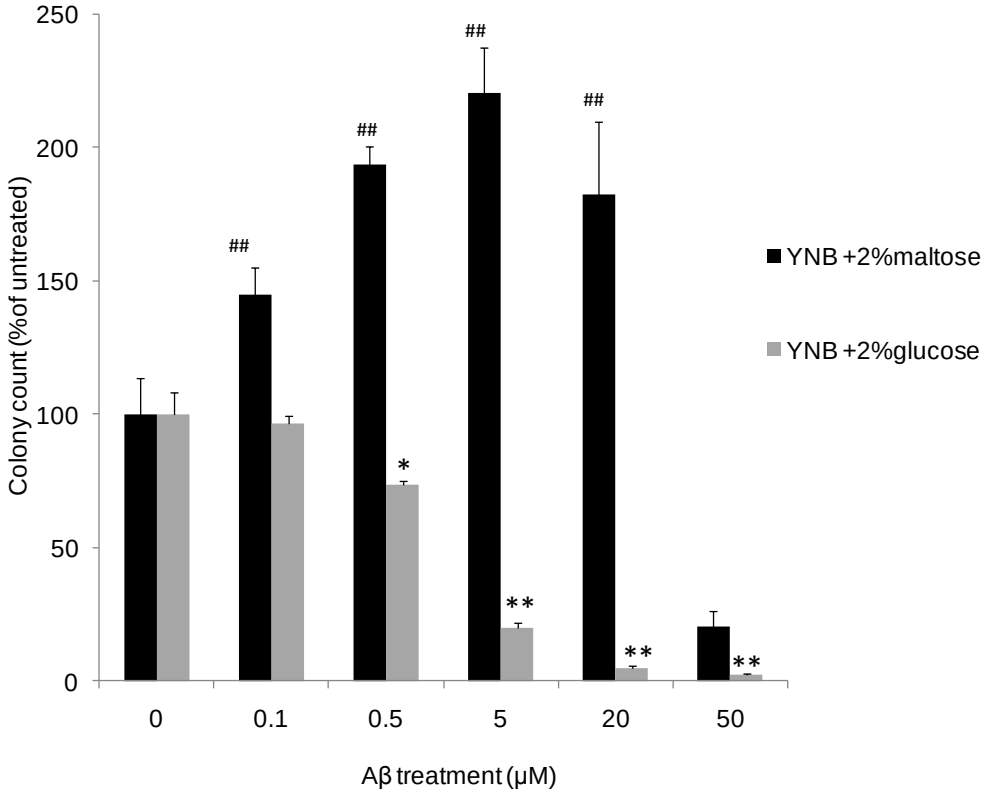
250
200
150
100
50
0
Colony count (%of untreated)
YNB +2%maltose
YNB +2%glucose
##
##
##
##
*
**
**
**
0
0.1
0.5
5
20
50
Aβ treatment (μM)

Figure 2: Aβ42 induces cell division in stationary phase yeast cells

Candida glabrata cells incubated in YNB+ 2% glucose and YNB+ 2% maltose for 7h were treated with vehicle or 5μM Aβ42 for 20h at 30°C. Following treatment the cells were spread on YEPD media plates. Images of yeast media plates showing Aβ42 caused cell death (decrease in number of colonies) in exponentially growing cells (YNB+2% glucose) **(A, B)** and cell division (increase in number of colonies) in stationary phase cells (YNB+2% maltose) **(C, D)** after a 20h treatment at 30°C are shown. Quantitative analysis of Aβ42 induced cell division in stationary phase cells was determined by colony forming unit (CFU) count. Exponentially growing *Candida glabrata* cells were incubated in YNB+ different carbon sources (2% glucose, or 0.1% glucose, 2% maltose or 2% glycerol) for 7h followed by Aβ42 (5μM) treatment for 20h. Cell viability was measured by the number of colonies (CFU) and expressed as percent change compared to untreated control **(E)**. Aβ42 caused significant cell death in yeast grown in YNB+2% glucose (**p<0.001). However, a significant increase in cell division with Aβ42 treatment was observed in cells grown in other carbon sources (0.1% glucose, 2% maltose or 2% glycerol, ##p<0.001). To determine effects of low concentrations of Aβ42, cells incubated for 7h in YNB+2% glucose and YNB+2% maltose were treated with increasing concentrations of Aβ42 (0.05-5μM). A dose-dependent effect of Aβ42 induced loss of viability in cells grown in YNB+2% glucose and increased cell division in cells grown in YNB+2% maltose was observed **(F)** (*p<0.05, **p<0.001, ##p<0.001). However, at very high concentrations, Aβ42 was toxic in cells grown in YNB+2% maltose (**p<0.001). All data are represented as mean ± SEM (n=4).

6.4.3 Rapamycin suppressed Aβ42 induced cell division in yeast:

Rapamycin is a macrolide which binds to FK-binding protein 12 (FKBP12) and inhibits the complex formation with mTORC1 thereby suppressing the downstream growth signalling pathway (Brown et al., 1994). It has been shown to inhibit G1 cell cycle progression *via* mTOR pathway in a variety of cell types including yeast at concentrations from 0.1-0.2μM (Heitman et al., 1991). To determine whether inhibition of mTOR signalling affects Aβ42 induced cell division, stationary phase yeast (*Candida glabrata)* cells were treated with increasing doses of Aβ42 (0.1-5μM) in the absence or presence of rapamycin (0.2μM) for 20h at 30°C followed by colony count.

Compared to vehicle treated cells, treating cells with Aβ42 in the absence of rapamycin induced a dose-dependent increase in the number of colonies in stationary phase *Candida glabrata* cells (Figure 3). The number of colonies increased by ~125-150% on treatment with 0.1-0.5μM Aβ reaching a maximum of ~200-250% increase at 2-5μM. However, in cells treated with Aβ42 in the presence of rapamycin, a significant decrease in the number of colonies compared to Aβ42 *per se* was observed (Figure 3). The inhibition of Aβ42 induced cell division by rapamycin was significant at all concentrations of Aβ42 tested (0.1-5μM). At lower concentrations of Aβ42 (0.1-0.5 μM) co-incubated with rapamycin, the number of colonies decreased to 80-90% compared to ~125-150% with Aβ42 *per se*. However this decrease in cell number [Aβ42 (0.1-0.5μM) +0.2μM rapamycin] was not significant compared to the untreated control (Figure 3). Overall rapamycin suppressed Aβ42 induced cell division in stationary phase yeast cells. To gain a better insight into the Aβ42 induced growth effect, Aβ42 peptide treatment was assessed in genetically diverse species *Saccharomyces cerevisiae* and *Candida glabrata*.

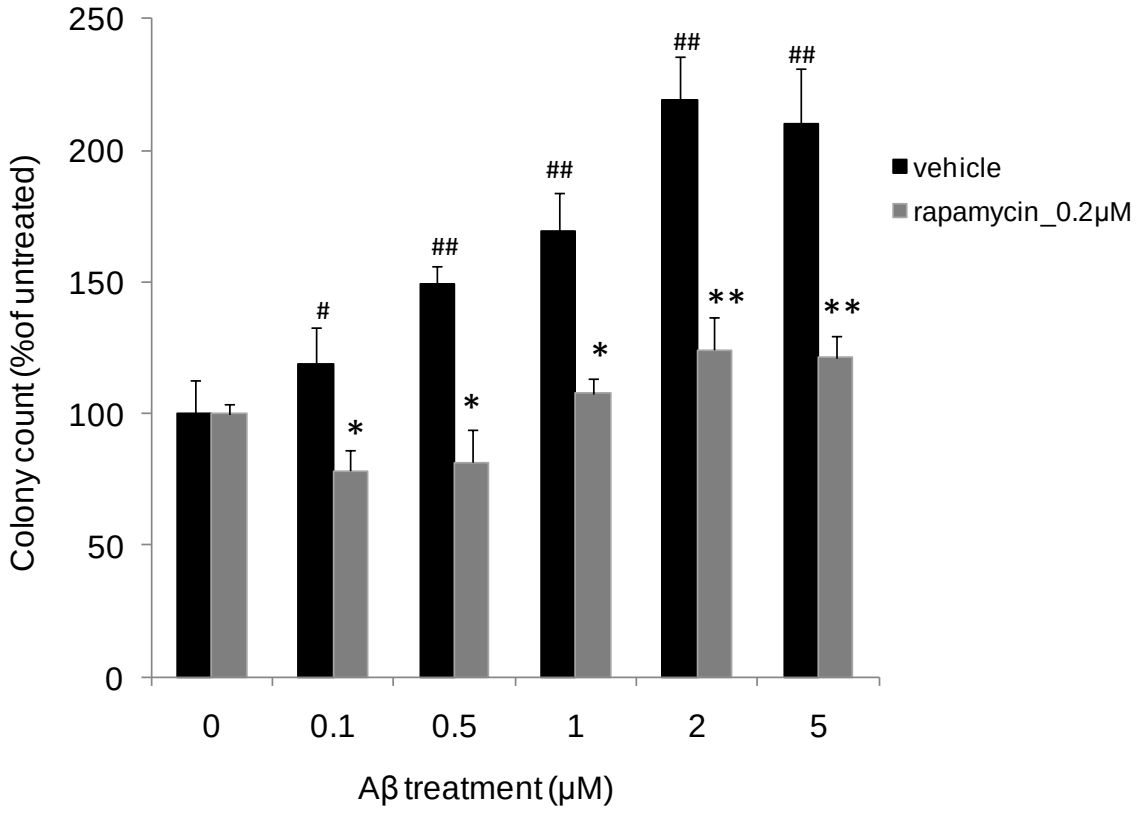

Figure 3: Rapamycin treatment inhibited Aβ42-induced cell division in yeast Exponentially growing *Candida glabrata* cells were incubated in YNB+ 2% maltose for 7h to inhibit cell division and induce stationary phase. The stationary cells are co-incubated with rapamycin (0.2μM) and different concentrations of Aβ42 (0-5μM) for 20h at 30°C. Aβ42 induced cell division was determined by colony forming unit (CFU) count and expressed as percent change compared to untreated control. A dose-dependent increase in number of colonies was observed with Aβ42 treatment without rapamycin (##$p<0.01$, #$p<0.05$). However in the presence of rapamycin, a significant decrease in the number of colonies compared to Aβ42 alone was observed (*$p<0.05$, **$p<0.01$). All data are represented as mean ± SEM (n=4).

6.4.4 Aβ42 does not induce cell division in *Saccharomyces cerevisiae* cells

Candida glabrata and *Saccharomyces cerevisiae* cells represent the main models in evolutionary yeast biology. *Candida glabrata* cells shows considerable genomic diversity in growth signalling pathways compared to *Saccharomyces cerevisiae* (Bowman et al., 1992; Walsh et al., 2002b). Although the gene expression patterns in *Candida glabrata* and *Saccharomyces cerevisiae* are highly conserved, significant diversity is observed in the signalling and regulatory networks (Lelandais et al., 2008). Therefore, to gain insight into the mechanism of Aβ42 induced cell division, stationary phase *Candida glabrata* and *Saccharomyces cerevisiae* cells were treated with Aβ42 peptide.

Candida glabrata cells were initially used for studying Aβ42 induced growth effects mainly for its faster growth rates compared to *Saccharomyces cerevisiae* (Lelandais et al., 2008). Aβ42 induced growth effects were studied in stationary phase *Saccharomyces cerevisiae* and *Candida glabrata* cells. Similar to *Candida glabrata*, *Saccharomyces cerevisiae* cells (BY4743) were subjected to starvation in YNB+2% maltose (Figure 4A) to induce stationary phase. *Saccharomyces cerevisiae* cells (BY4743) showed increased cell density with time in YNB+2% glucose (-Trp), however no increase was seen in YNB+2% maltose for both cell types indicating entry into stationary phase. As expected, *Saccharomyces cerevisiae* cells (BY4743) showed a slower growth rate compared to *Candida glabrata* in normal media (Figure 4A).

Next, Aβ42 induced growth effect was also tested in *Saccharomyces cerevisiae* yeast cells alongside *Candida glabrata* (Figure 4B). Stationary phase induced *Candida glabrata* and *Saccharomyces cerevisiae* (BY4743) cells were treated with increasing concentrations of Aβ42 (0.5-5μM) (Figure 4B) for 20h at 30°C. As seen before in Section 6.4.2 and 6.4.3, a dose dependent increase in the number of colonies was observed with Aβ42 treatment in *Candida glabrata* cells. A maximum of ~150-200% increase in colonies at 2-5μM Aβ42 was

observed. No increase in the number of colonies was seen at lower Aβ42 concentrations (0.5 and 1μM) in *Saccharomyces cerevisiae* cells. Interestingly, at higher Aβ42 concentrations (2-5μM), a significant decrease in the number of colonies in *Saccharomyces cerevisiae* cells was observed indicating cell death (by ~20-25%, Figure 4B). The results showed that stationary phase *Saccharomyces cerevisiae* cells were unresponsive to Aβ42 induced growth effects. The effect of Aβ42 to induce cell division with longer incubation times was then assessed considering the slower growth rate of *Saccharomyces cerevisiae* compared to *Candida glabrata* cells.

To determine growth effects at longer incubation times, Aβ42 (2μM) was incubated with stationary phase *Candida glabrata* and *Saccharomyces cerevisiae* cells for 12, 24 and 36h followed by colony count analysis (Figure 5A, B). Aβ42 treatment induced a significant increase in the number of colonies (~200%) at 12-24h incubation in *Candida glabrata*. However, the number of colonies started to decline (~150%) with longer incubations (36h) (Figure 5A). No change in number of colonies was observed in *Saccharomyces cerevisiae* cells treated with Aβ42 for 12h. Indeed, at 24 and 36h incubation times Aβ42 treatment caused a significant decrease in the number of colonies (~20-25%), indicating cell death (Figure 5B).

Overall the results showed that Aβ42-induced growth effects were absent in *Saccharomyces cerevisiae* cells. As previously discussed, *Candida glabrata* and *Saccharomyces cerevisiae* have considerable differences in genomic structure and cellular make-up (Bowman et al., 1992; Walsh et al., 2002b), which is the most likely factor responsible for the differential effects of Aβ42.

A

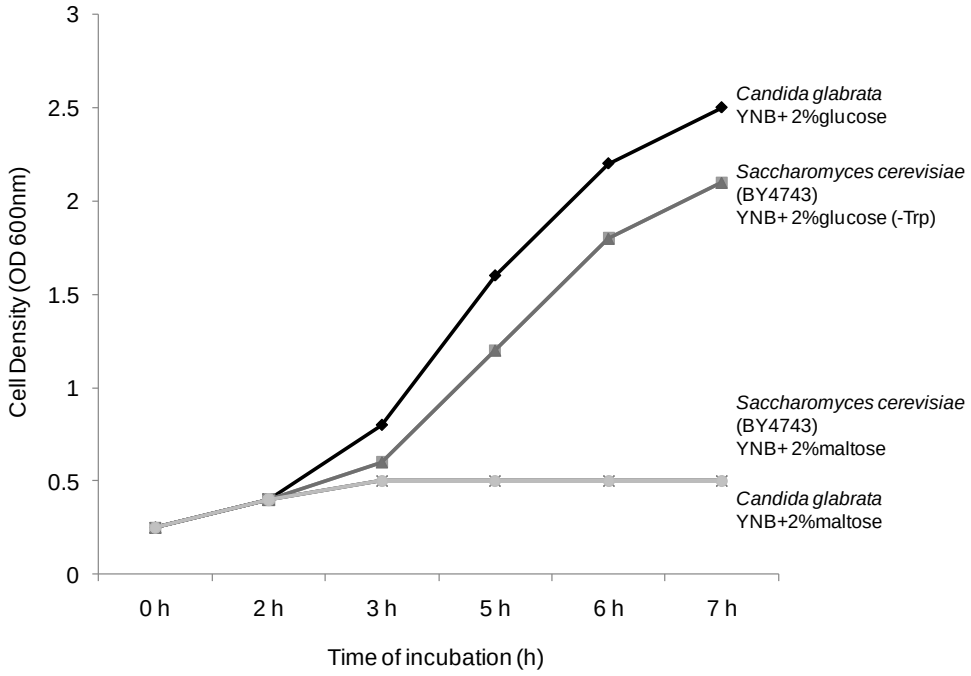
3
2.5
2
1.5
1
0.5
0
Cell Density (OD 600nm)
0 h
2 h
3 h
5 h
6 h
7 h
Time of incubation (h)
Candida glabrata
YNB+ 2%glucose
Saccharomyces cerevisiae
(BY4743)
YNB+ 2%glucose (-Trp)
Saccharomyces cerevisiae
(BY4743)
YNB+ 2%maltose
Candida glabrata
YNB+2%maltose

B

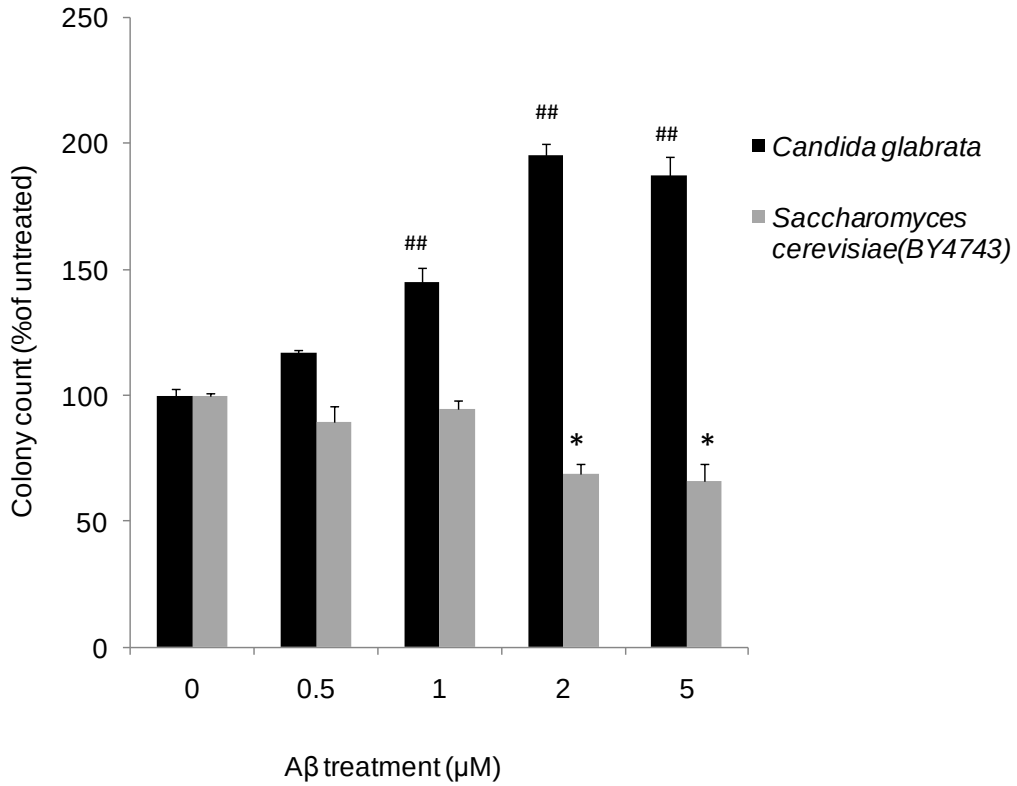
250
200
150
100
50
0
Colony count (%of untreated)
##
##
##
*
*
0
0.5
1
2
5
Aβ treatment (μM)
Candida glabrata
Saccharomyces cerevisiae(BY4743)

Figure 4: Concentration dependent Aβ42 growth effects in *Candida glabrata* and *Saccharomyces cerevisiae.*

Candida glabrata and *Saccharomyces cerevisiae* (BY4743) cells grown in YNB+ 2% glucose and YNB+ 2% glucose (-Trp) respectively were washed and incubated in fresh growth media [YNB+ 2% glucose or YNB+ 2% glucose (-Trp)] or in YNB+ 2% maltose to induce stationary phase. Cell density at 600 nm was measured at different time points (0-7h) **(A)**. Similar to Figure 1, *Candida glabrata* cells showed increased cell density in YNB+ 2% glucose and no growth in YNB+ 2% maltose. Similarly, *Saccharomyces cerevisiae* (BY4743) cells showed growth in YNB+ 2% glucose (-Trp), but absent in YNB+ 2% maltose. Wild type *Candida glabrata* cells and *Saccharomyces cerevisiae* (BY4743) were grown in YNB+2% glucose and YNB+2% glucose (-Trp) respectively followed by starvation in YNB+2% maltose for 7 h. The starved cells were then treated with different concentrations of Aβ42 (0-5μM) for 20h at 30°C. Colony forming units (CFU) were counted and expressed as percent change compared to untreated control **(B)**. A dose-dependent increase in number of colonies was observed in *Candida glabrata* with Aβ42 treatment (##$p<0.01$). No change in number of colonies was seen in *Saccharomyces cerevisiae* cells (BY4743) at lower Aβ42 concentrations (0.5-1μM). At higher concentrations (2-5μM), Aβ42 showed a significant decrease in number of colonies in *Saccharomyces cerevisiae* cells (BY4743) (*$p<0.05$).

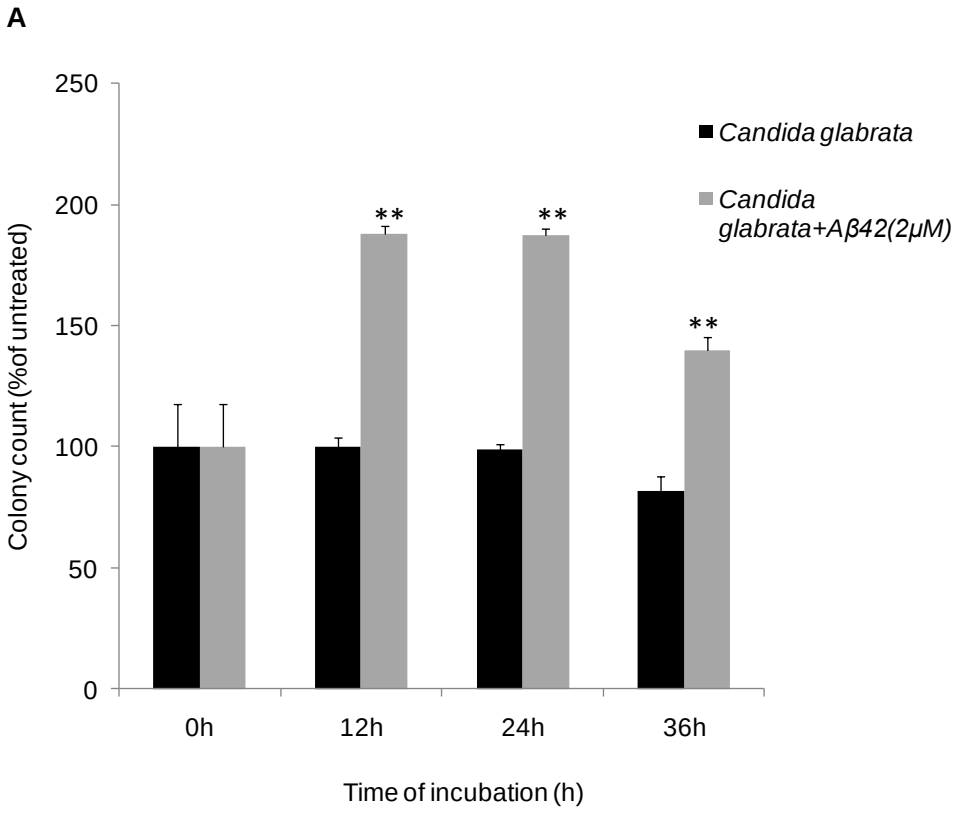
A
250
200
150
100
50
0
Colony count (%of untreated)
**
**
**
Candida glabrata
Candida glabrata+Aβ42(2μM)
0h
12h
24h
36h
Time of incubation (h)

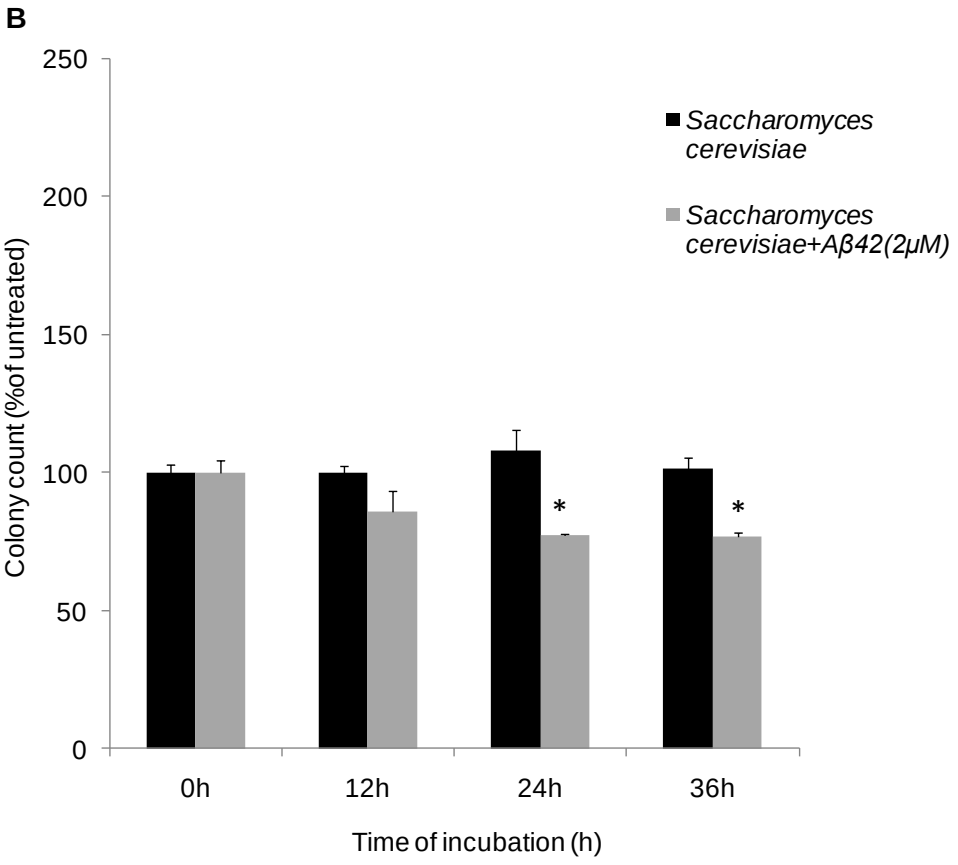
B
250
200
150
100
50
0
Colony count (%of untreated)
*
*
Saccharomyces cerevisiae
Saccharomyces cerevisiae+Aβ42(2μM)
0h
12h
24h
36h
Time of incubation (h)

Figure 5: Time dependent Aβ42 growth effects in *Candida glabrata* and *Saccharomyces cerevisiae.*

Candida glabrata and *Saccharomyces cerevisiae* (BY4743) cells grown in YNB+ 2% glucose and YNB+ 2% glucose (-Trp) respectively were washed and incubated in fresh growth media [YNB+ 2% glucose or YNB+ 2% glucose (-Trp)] or in YNB+ 2% maltose to induce stationary phase. Aβ42 (2μM)-induced growth effect at different incubation time points (12h, 36h and 48h) was also measured in starved *Candida glabrata* cells **(A)** and *Saccharomyces cerevisiae* (BY4743) cells **(B)**. Aβ42 treatment induced a significant increase in the number of colonies from 12h incubation in *Candida glabrata* (**p<0.01). But, no change in the number of colonies was observed in *Saccharomyces cerevisiae* cells (BY4743) at 12h incubation with Aβ42. However, at 24h and 36h incubation times, Aβ42 showed significant decrease in the number of colonies in *Saccharomyces cerevisiae* cells (BY4743) (*p<0.05). All data are represented as mean ± SEM (n=4).

6.5 Discussion

6.5.1 Aβ42 mediated growth or toxicity is dependent on cell cycle stage

The neurotoxic property of Aβ42 is thought to play a key role in mediating neurodegeneration in AD. In contrast to its toxic nature, Aβ42 can also possess mitogenic properties and has shown to enhance cell survival in neurons (Luo et al., 1996a; Whitson et al., 1989). However, the relationship between the mitogenic properties of Aβ and AD pathology is poorly understood. It is hypothesized that the biphasic nature of Aβ-induced toxic or proliferative effects may depend on the cell cycle.

In this chapter, the effects of Aβ42 within different cell cycles (exponential and stationary phase) of yeast growth were determined. Yeast cells were starved in non-growth media to induce stationary phase (G0) or incubated in

normal media to maintain exponential growth phase (Figure 1) prior to Aβ42 treatment. In exponentially growing yeast cells, Aβ42 caused a dose-dependent loss of viability as previously observed [Chapter 3, (Bharadwaj et al., 2008). However in the stationary phase cells, low concentrations of Aβ42 (0.1-5μM) induced cell division up to a maximum of ~250%, but at higher concentrations (≥20μM) the cell viability decreased, indicating toxicity (Figure 2). The results showed that Aβ42 can promote proliferation only in cells that are in the stationary phase and induce cell death in exponentially growing cells (Figure 2). The Aβ-induced growth and toxic effects within different cell cycles in yeast is comparable to the initial report showing that Aβ can enhance survival in freshly plated undifferentiated hippocampal cells (Yankner et al., 1990), but toxic in aged differentiated cultures. Studies showing Aβ42 mediated cell death in neurons expressing particular cell cycle-related elements (cyclin dependent kinases, Cdk4/6, Cdk5) (Giovanni et al., 1999; Liu et al., 2004), and in G1 cell cycle stage (Simakova and Arispe, 2007) further supported the notion that Aβ42 mediated toxicity or growth is dependent on the cell cycle. The data presented here also indicated that Aβ42 induced growth effect happens at a much lower concentration range (0.1-5μM) compared to its toxicity which is significant only at higher concentrations (>5μM).

It was also evident from the data that induction of stationary phase in yeast increased resistance to Aβ42 toxicity. At concentrations of 5-20μM, Aβ42 treatment caused 50-75% cell death in exponential phase cells whereas at the same concentrations Aβ42 induced cell proliferation in stationary phase cells (~200%). Toxicity of Aβ42 in stationary phase cells was observed only at concentrations as high as 50μM. Induction of stationary phase in yeast is featured by enormous cellular transformation including development of a thick cell wall, sharp decline in metabolic rates, increased lipid, glycogen and trehalose storage, resistance to a variety of toxic insults, stimulated catabolic pathways like autophagy and repression of high energy consumers like ion channel proteins and proton pumps (Herman, 2002; Werner-Washburne et al., 1993). The rate of protein synthesis falls ~300 fold in stationary phase cells and only a low level of protein synthesis (less than 10%) essential for stationary

phase survival is maintained (Paz and Choder, 2001; Werner-Washburne et al., 1996). It is therefore possible that one or many of these featured changes in the cell may contribute to the increased resistance to Aβ42 toxicity. Of particular interest are the ion channel proteins and cell surface receptors expressed or repressed during the stationary phase, since Aβ42 was found to be largely localized in the yeast plasma membrane and inhibited the activity of the proton pump H^+ATPase (Chapter 3). Whether repression of H^+ATPase expression during stationary phase is directly associated with decreased Aβ42 toxicity remains to be determined.

Collectively the data raises a wide range of possibilities on the nature of Aβ42 interaction with the cell and the potential receptor coupled pathways that maybe associated with the distinct effects observed in this chapter. The Aβ42-induced growth effect is observed within a physiological concentration range (starting from 100nM) compared to its toxicity (>5μM), suggesting that Aβ42-mediated cell division involves a high-affinity receptor. Since Aβ42-induced effects are dependent on the cell cycle stage, a broad array of proteins and receptors associated with metabolism, stress, transcription factors and intracellular growth signalling pathways are potential candidates involved with the response to Aβ treatment.

6.5.2 Inhibition of mTOR signalling suppressed Aβ42 induced growth effects

The cell cycle is a tightly regulated process with several checkpoints that ensure normal development when appropriate nutritional and trophic signals are present. Neurons of the adult brain are terminally differentiated and do not show mitotic cell division. Also, differentiated neurons lack the capacity to divide *in vivo* and *in vitro*, possibly due to lack of components necessary to complete the cell division process (McShea et al., 1999). However in AD, studies show increased levels of cell cycle related proteins and abnormal entry into mitosis in areas vulnerable to neurodegeneration in AD (reviewed in (Bonda et al., 2010;

Lee et al., 2009). It is suggested that in AD, the neurons may be attempting to initiate the early phases of mitosis (Zhu et al., 2008). Studies have shown that re-activation of cell cycle machinery in post mitotic neurons can lead to cell loss and degeneration (Feddersen et al., 1992; Park et al., 2007). It is believed that in AD, the incomplete transition of the neuronal cells into M phase makes them vulnerable to reactive oxygen species, excitotoxic stress and apoptosis (Park et al., 2000).

mTOR is an eukaryotic cell signalling pathway essential for cell cycle progression, and proliferation. Reports show increased levels of mTOR pathway components (p-eIF4E, p-mTOR and p-4E-BP1) in AD brains (Li et al., 2005; Li et al., 2004) and it is believed that Aβ42 induced cell cycle events in neurons are closely associated with mTOR signalling. However studies in neuronal cell cultures and animal models have yielded contradictory results as previously discussed (Ma et al., 2010b; Pei and Hugon, 2008; Spilman et al., 2010). In this Chapter, the role of mTOR signalling in Aβ42 mediated growth effects was determined. Aβ42 treatment induced a dose-dependent increase in cell division in stationary yeast cells (Figure 3). But when co-incubated with rapamycin, an mTOR inhibitor, the increase in cell division was significantly repressed (Figure 3). Overall the result showed that rapamycin suppressed Aβ42-induced cell division in stationary phase yeast cells. It suggested that mTOR is one pathway by which Aβ42 can stimulate growth effects in the yeast cell. mTOR signalling can be initiated by extracellular membrane bound sensors and transporters of growth factors and nutrients in eukaryotic cells. Yeast cells possess several nutrient-sensing systems localized in the plasma membrane that are associated with growth signalling. Importantly, some of the plasma membrane sensors include the amino acid permease Ssy1p-Ptr3p-Ssy5p family (SPS) and the glucose transporters Gpa2p, Snf3p and Rgt2p which are also members of highly conserved nutrient-transport protein families involved with TOR signalling (Cardenas et al., 1999; Cutler et al., 1999; Forsberg et al., 2001; Forsberg and Ljungdahl, 2001a, b). Immunoelectron and confocal microscopy analysis showed that Aβ42 was localized in the yeast plasma membrane (Chapter 3). It is therefore likely that Aβ42 may induce growth *via* interaction

with one or more of these transmembrane receptors involved with mTOR pathway.

6.5.3 Aβ42 induced growth effect was absent in *Saccharomyces cerevisiae*

Aβ42 induced growth effect was evident in stationary phase *Candida glabrata* cells and was suppressed by mTOR inhibitor, rapamycin (Figure 2, 3). Interestingly, the increased cell division with Aβ42 treatment was absent in *Saccharomyces cerevisiae* cells (Figure 4). No evidence of cell division was seen at lower Aβ42 concentrations (0.5-1μM) or even with extended periods of treatment (Figure 4). In fact at concentrations of 2-5μM, Aβ42 caused cell death (20-25%) in *Saccharomyces cerevisiae* cells compared to increased cell division (~200%) in *Candida glabrata* (Figure 4). It is well accepted that *Candida glabrata* cells have considerable genomic diversity compared to *Saccharomyces cerevisiae*, which is probably the most likely explanation for this phenomenon. It is notable that *Saccharomyces cerevisiae* cells showed a slower growth rate compared to *Candida glabrata*, which is a widely accepted phenomenon among yeast biologists.

One important difference between the species is the supplements required for growth. *Candida glabrata* is a prototrophic strain, which indicates that it has wild-type characteristics of a naturally-occurring fungal cell capable of growth in media depleted of amino acids (YNB+2% glucose media without amino acids for *Candida glabrata*). However, *Saccharomyces cerevisiae* is an auxotrophic laboratory strain which needs amino acid supplements for growth (YNB +2% glucose+ histidine+ alanine+ uracil+ leucine for *Saccharomyces cerevisiae* BY4743). It is therefore a possibility that *Candida glabrata* expresses high affinity amino acid transporters (amino acid permeases) compared to *Saccharomyces cerevisiae* which enables it to survive in amino acid depleted conditions (Yadav and Bachhawat). It is likely that Aβ42 could bind to such high affinity amino acid transporters to induce growth in *Candida glabrata*. It also explains the absence of the Aβ42 induced growth effect in *Saccharomyces*

cerevisiae, which could be attributed to the lack or repressed expression of such receptors. However further investigation of other fungal species using mutational analysis is required to confirm this interesting notion.

6.6 Summary:

Aβ42 was found to induce cell division in stationary phase yeast cells, but was toxic in exponential phase cells at similar concentrations. The effect of mTOR inhibition by rapamycin in blocking Aβ42-growth effects was also studied. Rapamycin suppressed the Aβ growth effect, indicating that Aβ-induced cell division is possibly mediated via mTOR signalling. Interestingly, the Aβ42-induced growth effect was observed only in *Candida glabrata* cells and not in *Saccharomyces cerevisiae* cells. Overall, the data has provided a greater understanding of the interplaying roles of the cell cycle and mTOR signalling in the Aβ42-induced growth in yeast cells.

Chapter 7

Yeast Model for Intracellular Aβ42 Expression and Accumulation

7.1 Introduction:

In the previous chapters, the effects of exogenously added Aβ (as a peptide and fusion protein) were studied in yeast. Oligomerizing Aβ42 peptide was significantly more toxic compared to the non-aggregating isoform Aβ42 (19:34) in yeast and also in neuronal cells. Localization analysis in yeast showed that both Aβ peptides bound the cell surface but were undetectable in the intracellular lumen. Oligomer Aβ42 showed increased affinity to the plasma membrane compared to non-aggregating Aβ42 (19:34) peptide and data suggested the plasma membrane H^+ATPase as a possible target of oligomeric Aβ42 mediated cell death in yeast (Chapter 3).

Although extracellular Aβ deposition and neuronal cell death are key pathological events in AD, growing evidence indicate that the clinical manifestations of the disease could be a collective contribution of numerous other pathological events associated with intraneuronal Aβ accumulation; reviewed in (LaFerla et al., 2007). Apart from uptake of secreted Aβ from the extracellular media, several reports indicate that Aβ can be generated intracellularly by APP processing in the trans-Golgi network (Xu et al., 1995), endoplasmic reticulum (ER), endosomal, lysosomal compartments (Kinoshita et al., 2003; Nixon et al., 2005; Yu et al., 2005) and mitochondrial membranes (Mizuguchi et al., 1992). Studies have reported accumulation of Aβ within neurons in post-mortem AD and transgenic mouse brains (Gouras et al., 2000; Nagele et al., 2002). Studies also indicate that the build-up of intracellular Aβ may be an early event in the pathogenesis of AD, preceding the formation of extracellular Aβ deposits (Gouras et al., 2000; Mori, 2002). It is thought that neurodegeneration and synaptic loss in AD could be the direct result of defective clearance mechanisms leading to intracellular Aβ accumulation and toxicity (Boland et al., 2008; Lee et al., 2010; Nixon, 2007). However, the contribution of various intracellular clearance pathways in the degradation of Aβ aggregates is not completely understood. In the following chapters, I have used yeast as a model to investigate the intracellular clearance of Aβ42 aggregates.

In chapter 3, I showed that Aβ42 was largely localised to the plasma membrane and was undetectable in the cytosolic lumen. Thus a model where, Aβ42 is expressed intracellularly would be more amenable for investigating clearance pathways. Yeast models expressing pathogenic proteins as green fluorescent protein (GFP) tagged fusion partners including α-synuclein (Cooper et al., 2006; Soper et al., 2008; Zabrocki et al., 2008; Zabrocki et al., 2005) have been engineered to reduce targeting for proteolysis in yeast cells and therefore enable real time monitoring of the protein of interest. Recently, a yeast model expressing GFP-Aβ42 was developed in Prof Macreadie's laboratory (Caine et al., 2007a). The expression of GFP-Aβ42 expression in yeast was shown to induce growth stress and heat shock response (Caine et al., 2007a). Also, GFP-Aβ42 was found to localize into inclusion like structures compared to diffuse cytosolic expression of GFP in yeast. Overall, these findings suggest that GFP-Aβ42 was misfolded and subsequently gets accumulated into amorphous inclusions inside the cell.

In the following chapters, I have employed the GFP-Aβ42 expressing yeast model for investigating intracellular Aβ accumulation and degradation and evaluated the efficacy of agents that enhance clearance of intracellular Aβ aggregates. In the current chapter, a GFP-fusion Aβ42 (19:34) expression vector was generated and used to express the non-aggregating Aβ42 mutant in yeast. This chapter characterises intracellular expression and localisation of the mutant Aβ42 and native Aβ42 within yeast cells, prior to utilising these cells to investigate clearance pathways in subsequent chapters.

7.2 Aim:

Characterise localization and expression of GFP, GFP-Aβ42 and GFP-Aβ42 (19:34) fusion proteins in yeast cells.

7.3 Materials and Methods:

Wild type yeast cells (*Saccharomyces cerevisiae*, KVY55) transformed with p416 plasmids harbouring GFP/GFPAβ fusion protein construct and a URA selectable marker for growth in selective media (YNB+2% glucose –ura) was used in this work. GFP-Aβ42 (19:34) mutant was constructed from GFP-Aβ42:p416 by site directed mutagenesis as described in Section 2.2.12 (the construct was made by Sonia Sankovich, CSIRO, Parkville). GFP levels and localization in GFP/GFPAβ expressing yeast grown in YNB+2% glucose (–ura) was analysed throughout the growth phase (early exponential till late log phase) by fluorescent microscopy as described in Section 2.2.16. Also the levels of GFP/GFPAβ protein in yeast cell lysates were analysed using immunoblotting with anti-GFP or anti-Aβ (WO2) as described in Section 2.2.17. The mRNA levels of GFP transcript were quantified in the GFP/GFPAβ expressing cells by real time q-PCR and comparative C_t analysis as described in Section 2.2.14. Cell viability of GFP/GFPAβ yeast transformants at different stages of growth was also determined using the Vi-Cell Cell viability analyser (Beckman Coulter).

7.4 Results:

7.4.1 Intracellular expression of GFP tagged Aβ42 fusion protein in yeast:

Yeast is a widely used model for expression of neurotoxic proteins (Braun et al., 2010; Winderickx et al., 2008). Wild type yeast cells (*Saccharomyces cerevisiae*) constitutively expressing GFP-Aβ42 protein (Caine et al., 2007a) were utilized as a model for intracellular Aβ expression. Cells were transformed with a plasmid construct harbouring either the GFP or GFP-Aβ42 sequence with a uracil synthesis gene (URA3) (Figure 1A, B) for selective growth in media lacking uracil [YNB+2%glucose (-ura)], thus allowing for only stable transformants to be selected. To determine the localization of the fusion proteins within the cells, GFP and GFP-Aβ42 expressing yeast were studied by

fluorescent and immunoelectron microscopy. GFP expressing cells showed a diffuse green pattern of fluorescence compared to a punctate form of fluorescence in GFP-Aβ42 expressing cells (Figure 1C, D). The levels of fluorescence in GFP-Aβ42 expressing cells were also low compared to GFP alone. Immunoelectron microscopy using anti-GFP and anti-Aβ antibodies showed that GFP had a cytosolic distribution, whereas GFP-Aβ42 seemed to be localized into amorphous bodies (Figure 1E, F).

This punctate fluorescence pattern and localization within inclusion like structures in yeast was reminiscent of an unfolded protein response in the cell (UPR) (Mori, 2009). GFP-Aβ42 expression also induced a heat shock response and growth stress (~5%) in the cell compared to GFP only (Caine et al., 2007a). Overall the data suggested that Aβ42 evoked a stress response in the cell, however it was unclear whether it was specific to the aggregating and toxic nature of Aβ42. To address this, a GFP tagged modified Aβ42 (19:34) isoform was generated for expression in yeast cells.

A

```
........10........20........30........40..
          .         .         .         .
DAEFRHDSGYEVHHQKLVFFAEDVGSNKGAIIGLMVGGVVIA   Aβ
```

B

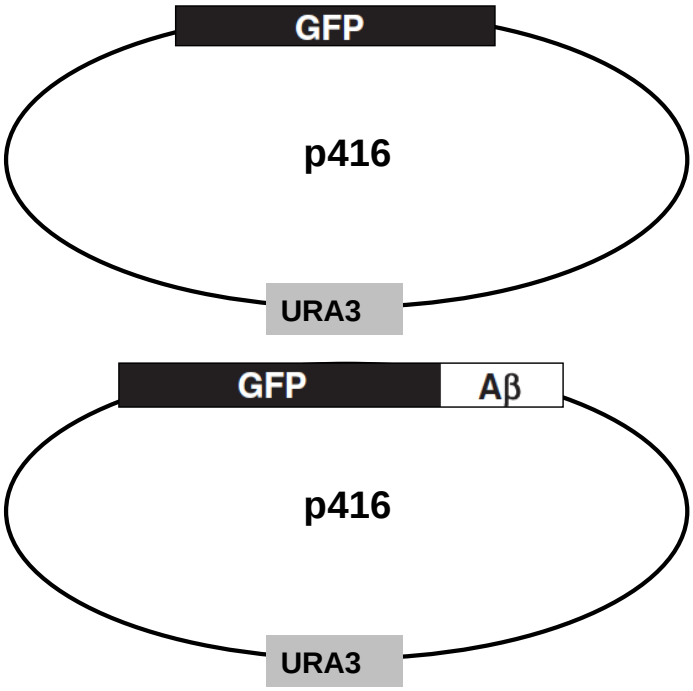

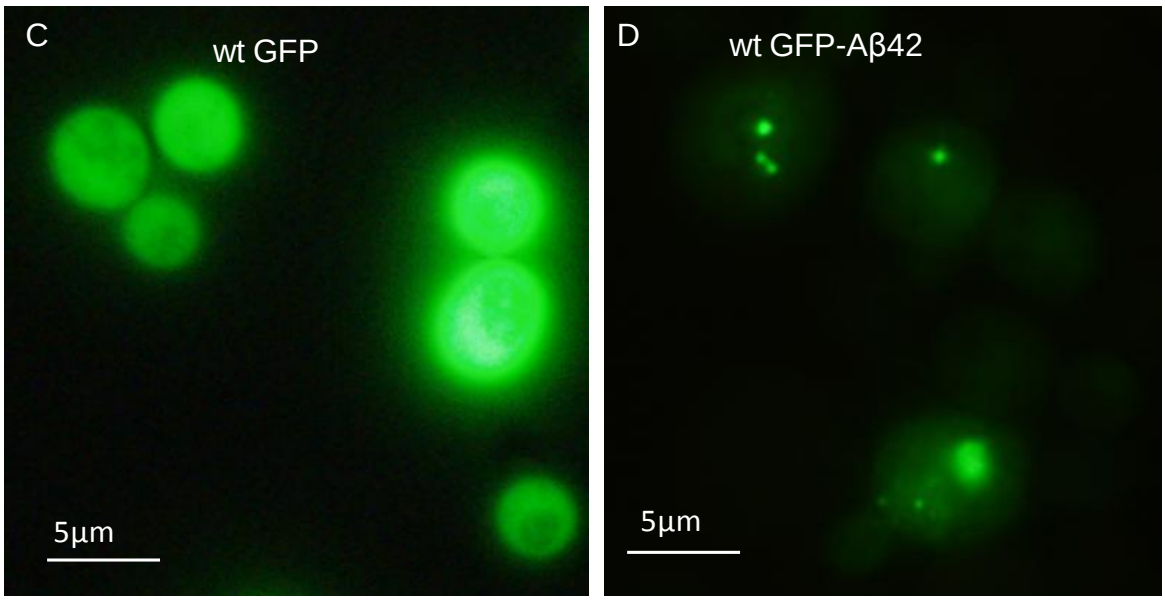

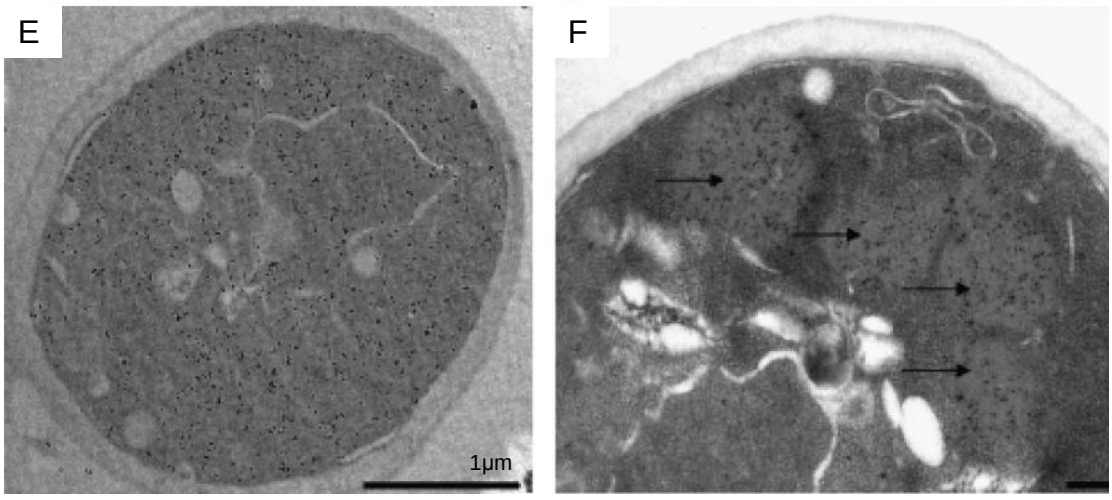

Figure 1: Expression of GFP-Aβ42 in yeast cells

Sequence of the full length Aβ42 **(A)**, Schematic diagram of the yeast centromere plasmid p416 harbouring the GFP–Aβ fusion protein gene **(B)**. Fluorescent images of mid log phase yeast (w303-1a) cells grown in YNB+2%glucose (-ura) expressing GFP **(C)** or GFP-Aβ42 **(D)**. GFP expressing cells show bright diffuse green fluorescence compared to punctate staining observed in GFP-Aβ42. Immunoelectron micrographs of yeast transformants expressing GFP **(E)** and GFP-Aβ42 **(F)** are shown here. Antibody to GFP was gold-labelled and probed against cells expressing GFP or GFP-Aβ42. Cells expressing GFP showed cytosolic localization as indicated by the black dots. However cells expressing GFP-Aβ42 showed localization in inclusion like structures. Note the labelling (black arrows) of amorphous structures (adapted from (Caine et al., 2007a).

7.4.2 Generation of yeast cells expressing GFP-Aβ42 (19:34):

Aβ42 peptide modified at positions F19S and L34P [Aβ42 (19:34)] has been shown to have reduced tendency to aggregate (Ahmed et al., 2010; Hughes et al., 1996; Luhrs et al., 2005; Wurth et al., 2002). In chapter 3, I showed that compared to native Aβ42 the Aβ42 (19:34) mutant remained largely monomeric,

and did not form SDS stable oligomers (dimers, trimers and tetramers). Extracellular treatment in yeast and neuronal cells further showed that the non-aggregating Aβ42 (19:34) mutant did not induce cell death compared to oligomeric Aβ42 (Section 3.4.2).

Yeast cells expressing the GFP tagged non-aggregating Aβ42 (19:34) fusion protein was generated and its expression and localization pattern was compared to cells expressing GFP only or GFP-Aβ42. As described above, GFP-Aβ42 was found to localize into punctate like patterns (Figure. 2A) within the cell compared to the diffuse cytosolic localisation in cells expressing GFP only (Figure. 2C). Cells expressing GFP-Aβ42 (19:34) showed a similar diffuse pattern of expression to those expressing GFP only (compare Figure. 2B with 2C). The GFP fluorescence patterns in the cells expressing the GFP/GFPAβ fusions suggested that GFP-Aβ42 was packaged and compartmentalized into inclusion bodies, whereas, GFP, GFP-Aβ42 (19:34) was mainly localized in the cytoplasm.

From the qualitative analysis of localisation it was noted that the fluorescence intensity was markedly less throughout the growth phase in cells expressing GFP-Aβ42 compared to those expressing GFP-Aβ42 (19:34) or GFP. To provide a more quantitative measure of expression and if it was altered through cell growth, the expression pattern and levels at early, intermediate and late stages of cell growth were assessed.

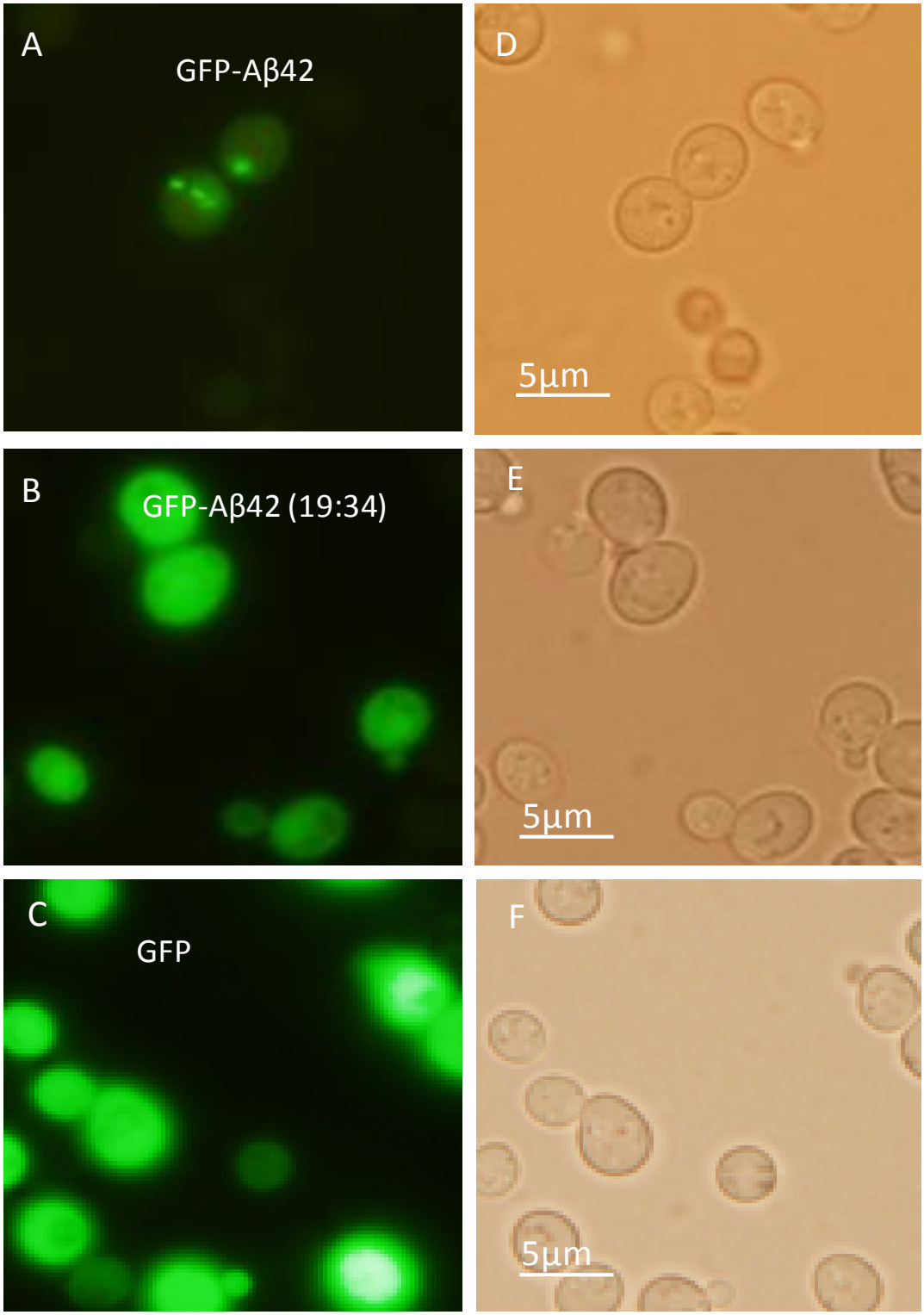

Figure 2: Localization of GFP, GFP-Aβ42 and GFP-Aβ42 (19:34) in yeast. GFP/GFP-Aβ yeast (*Saccharomyces cerevisiae*, KVY55) transformants were stored on selective minimal YNB+2%glucose (-ura) agar plates at 4ºC. A single

yeast colony from stock agar plates was inoculated in 5ml YNB+2%glucose (-ura) and incubated with shaking at 30ºC overnight. The overnight culture was resuspended in fresh YNB+2%glucose (-ura) media to an initial cell density (OD at 600nm) of 0.2. The culture was then incubated at 30ºC with shaking. Aliquots at mid-late log phase (OD of 1-1.6) in selective minimal media (YNB+2%glucose, -ura) were collected and observed under the fluorescent and bright field microscope. Localization of GFPAβ42 **(A, D)**, GFPAβ42 (19:34) **(B, E)** and GFP **(C, F)**, expressed in wild-type yeast was investigated.

7.4.3 Assessment of expression levels of GFP, GFP-Aβ42 and GFP-Aβ42 (19:34) over the yeast growth phase

The expression levels of GFP/GFPAβ fusions in the cells were monitored throughout different growth phases. A single yeast colony of GFP/GFP-Aβ expressing yeast transformants from stock agar plates was inoculated in 5ml YNB+2%glucose (-ura) and incubated with shaking at 30ºC overnight. The overnight culture was resuspended in fresh YNB+2%glucose (-ura) media to an initial cell density (OD at 600nm) of 0.2 and incubated at 30°C. Following, sample aliquots throughout different growth phases starting from early exponential till mid-late log phase (cell density OD 600nm, 0.4-1.6) were collected for microscopy and immunoblotting analysis

The percentage of green fluorescing cells was estimated in all cells from the starting point (initiation at cell density 0.2), through the early exponential phase (6-9 hours after initiation of the culture- cell density 0.4 and 0.7) till mid-late log growth phase of cells (10-12 hours after initiation; cell density 1 and 1.6) (Figure 3). In the cells expressing GFP only, the percentage of fluorescent cells (~95%) remained stable throughout the growth phase. However, in cells expressing the GFP-Aβ42, only a maximum of ~15-20% of cells were fluorescent at the exponential phase and mid-late log phase (OD=1) of growth. In cells expressing

GFP-Aβ42 (19:34), ~70% cells were fluorescent in the exponential phase and mid-late log phase. A comparison of the percentage fluorescing cells between those cells expressing GFP-Aβ42 and those expressing GFP-Aβ42 (19:34), showed almost 50% less cells expressing GFP-Aβ42 (Figure 3). The percentage of fluorescing cells in GFP-Aβ42 expressing cells declined sharply during the mid-late log phase and was almost undetectable (less than 5%) at OD>1.6. However the percentage of GFP fluorescing cells were unchanged in GFP and GFP-Aβ42 (19:34) and remained at ~95% and ~70% respectively (Figure 3).

As a more quantitative measure of the levels of these fusion proteins in the cells, extracts of the yeast transformants at different stages of the cell growth phase [early exponential phase (0.4) till mid-late log growth phase of cells (1.6)] was analysed by western immunoblotting with anti-Aβ and anti-GFP (Figure 4). Samples at the initiation point (0.2) were not collected for immunoblotting, due to lack of cell growth for protein extraction and analysis. Similar to the fluorescence quantification, the levels of GFP-Aβ42 (Figure 4A) was significantly lower than GFP-Aβ42 (19:34) (Figure 4B) and GFP (Figure 4C) throughout the growth phase (Figure D). Also GFP-Aβ42 protein levels sharply reduced and became undetectable at OD>1.6, compared to GFP and GFP-Aβ42 (19:34) levels which were unchanged. Viability at different points of the growth phase was determined in all the transformants. No significant change in viability of the yeast GFP/Aβ transformants was observed throughout the cell cycle indicating that decreased levels of GFP-Aβ42 compared to GFP and GFP-Aβ42 (19:34) was not due to cell death (Figure 4E).

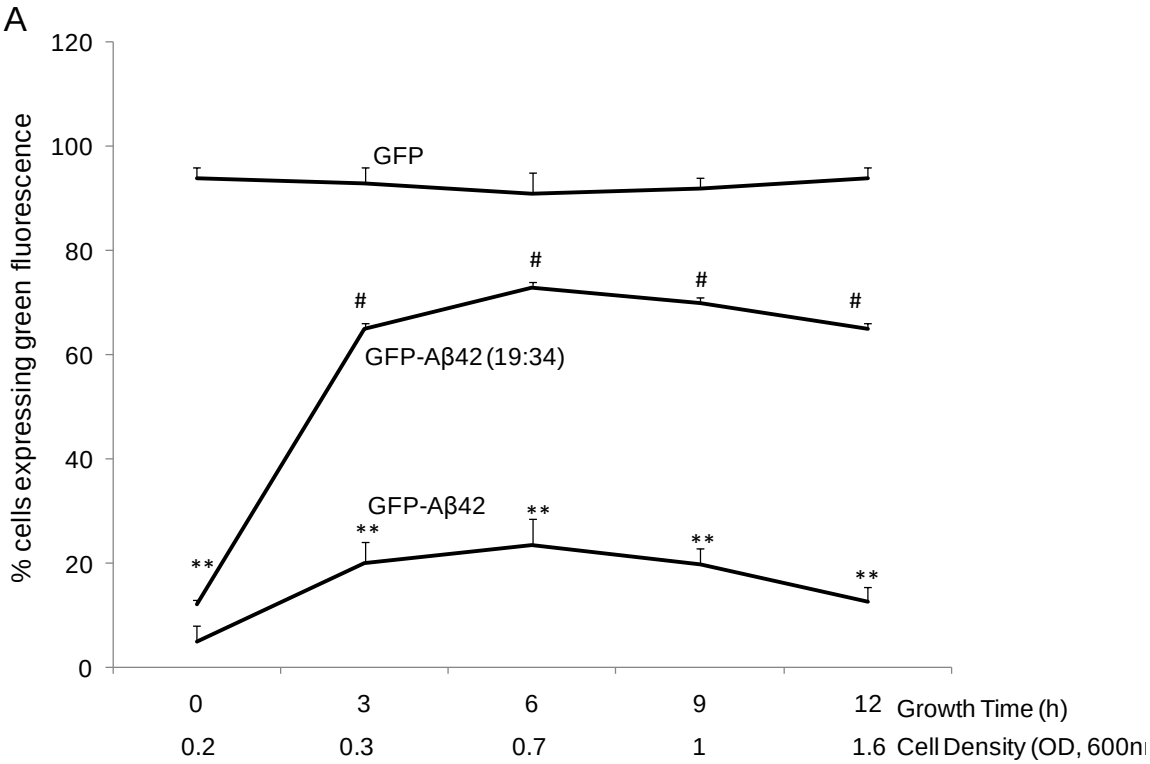

Figure 3: GFP fluorescence levels in cells expressing GFP, GFP-Aβ42 and GFP-Aβ42 (19:34).

GFP/GFP-Aβ yeast (*Saccharomyces cerevisiae*, KVY55) transformants were stored on selective minimal YNB+2%glucose (-ura) agar plates at 4ºC. A single yeast colony from stock agar plates was inoculated in 5mL YNB+2%glucose (-ura) and incubated with shaking at 30ºC overnight. The overnight culture was resuspended in fresh YNB+2%glucose (-ura) media to an initial cell density (OD at 600nm) of 0.2. The culture was then incubated at 30ºC with shaking. The percentage of cells expressing green fluorescence in cells expressing GFP, GFPAβ42 and GFPAβ42 (19:34) fusion proteins were quantified at different phases of growth starting from early exponential phase (OD: 0.4) till late-log phase (OD: 1-1.6) as described in Section 2.2.16 **(A)**. The percentage of fluorescing cells was significantly reduced in cell expressing GFP-Aβ42 (**, $p<0.001$), compared to those expressing GFP and GFP-Aβ42 (19:34) throughout the growth phase. The percentage of GFP fluorescence was significantly reduced in cell expressing GFP-Aβ42 (19:34) (**, $p<0.001$#, $p<0.05$), compared to those expressing GFP throughout the growth phase Data is expressed as mean ± SEM (n=4).

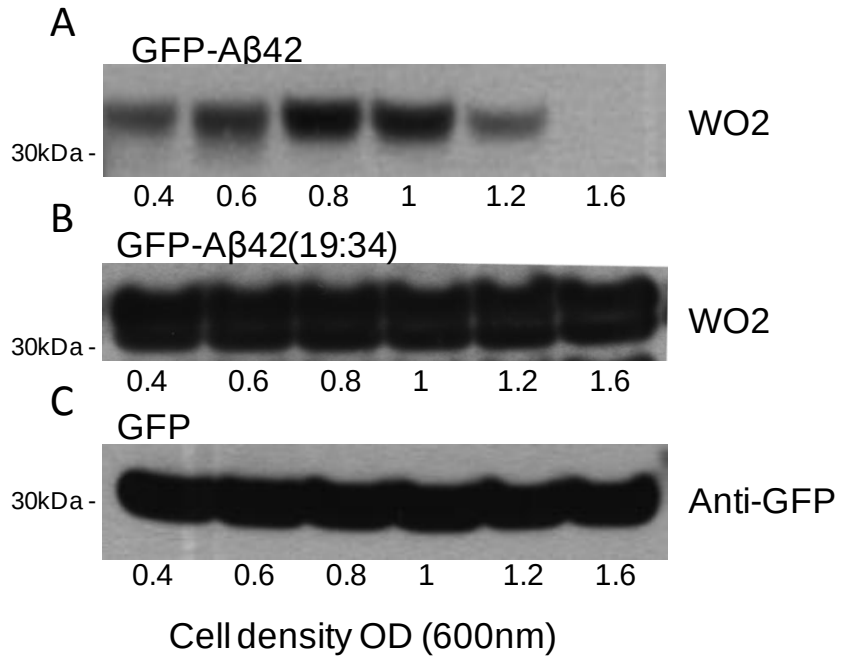
A
GFP-Aβ42
30kDa -
WO2
0.4 0.6 0.8 1 1.2 1.6
B
GFP-Aβ42(19:34)
30kDa -
WO2
0.4 0.6 0.8 1 1.2 1.6
C
GFP
30kDa -
Anti-GFP
0.4 0.6 0.8 1 1.2 1.6
Cell density OD (600nm)

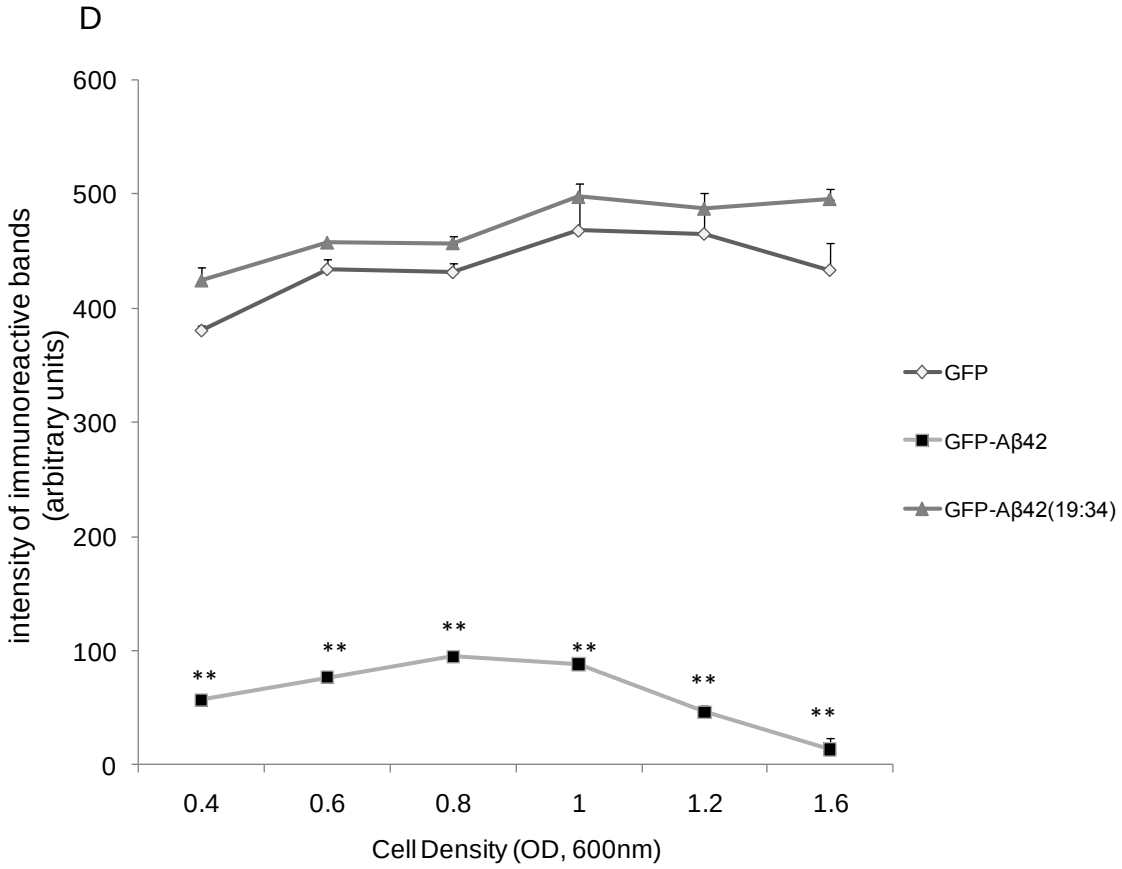
D
intensity of immunoreactive bands (arbitrary units)
600
500
400
300
200
100
0
**
**
**
**
**
**
0.4 0.6 0.8 1 1.2 1.6
Cell Density (OD, 600nm)
GFP
GFP-Aβ42
GFP-Aβ42(19:34)

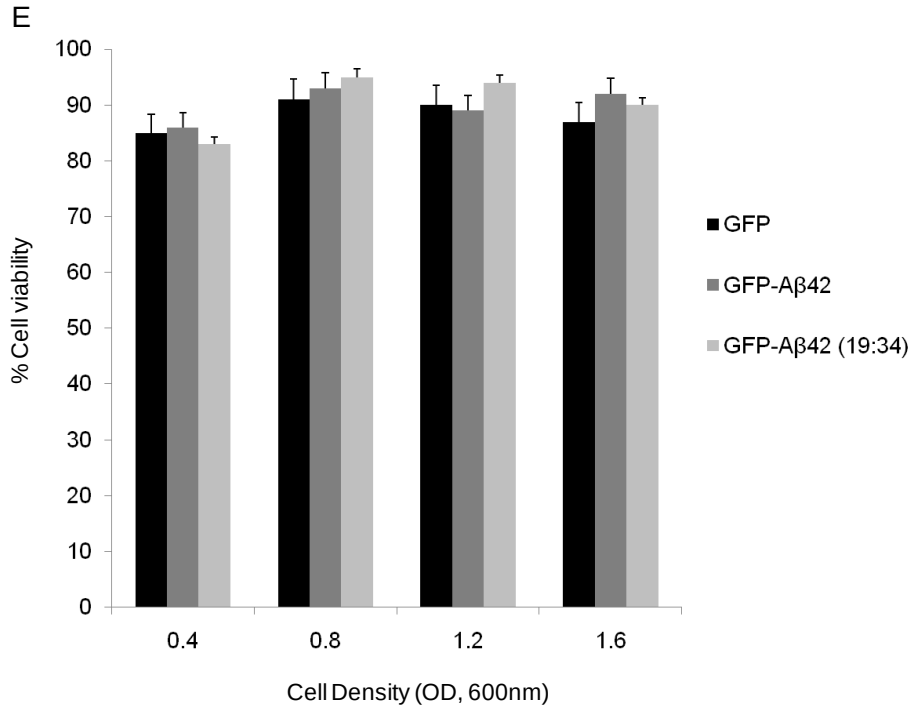

Figure 4: Expression levels of GFP-Aβ42, GFP-Aβ42 (19:34) and GFP proteins in yeast

GFP/GFP-Aβ yeast (*Saccharomyces cerevisiae*, KVY55) transformants were stored on selective minimal YNB+2%glucose (-ura) agar plates at 4ºC. A single yeast colony from stock agar plates was inoculated in 5mL YNB+2%glucose (-ura) and incubated with shaking at 30ºC overnight. The overnight culture was resuspended in fresh YNB+2%glucose (-ura) media to an initial cell density (OD at 600nm) of 0.2. The culture was then incubated at 30ºC with shaking. Aliquots at different cell densities were collected for western blot analysis. Total protein extracts (50µg) from wild-type cells expressing GFPAβ42 **(A)**, GFPAβ42 (19:34) **(B)** and GFP **(C)** throughout the growth phase (early exponential phase till mid log phase) were probed with anti-Aβ (WO2) or anti-GFP. Immunoreactive bands were quantified by densitometric analysis and expressed as arbitrary units **(D)**. The protein levels of GFP-Aβ42 was significantly lower compared to GFP and GFP-Aβ42 (19:34) throughout the growth phase (**p<0.001). Cell viability of yeast transformants (GFP, GFP-Aβ42 and GFP-Aβ42 (19:34)) at different stages of growth in YNB+2%glucose (-ura) media at 30ºC was also measured **(E)**. Data represented as mean ± SEM, n=3. No significant change in cell viability was observed among the different clones.

7.4.4 GFP transcription analysis using real time RT-PCR:

To rule out the possibility that transcription levels of GFP-tagged Aβ genes were altered, GFP transcription was quantified by real time RT-PCR using comparative C_t method (Schmittgen and Livak, 2008). Equal number of yeast cells (~1-3 X 10^6 cells) expressing GFP, GFP-Aβ42 and GFP-Aβ42 (19:34) were collected at exponential growth phase (OD of 0.6). cDNA was synthesized from the frozen pellets and used for the real time PCR amplification targeting the GFP transcript. The PCR products were analysed by 1.5% agarose gel electrophoresis and observed by UV transillumination. A ~90bp size band, representing GFP, was observed in all the transformants, but absent in untransformed and no-cell control (Figure 5A). This indicated the presence of the GFP mRNA transcripts in the yeast transformants. The levels of the transcripts were quantified from the C_t (threshold cycle) values. The C_t value represents the number of cycles required for the amplified PCR product (GFP) to reach the saturation threshold. The GFP mRNA levels were measured from the C_t values as described in Section 2.2.14 and were found to be similar in cells expressing GFP, GFP-Aβ42 and GFP-Aβ42 (19:34) (Figure 5B).

In summary, I have characterised the localisation and expression of GFP, GFP-Aβ42 and Aβ42 (19:34) fusion proteins expressed in yeast. Compared to cells expressing GFP, or the non-aggregating GFP-Aβ42 (19:34), cells expressing GFP-Aβ42 showed punctate fluorescence staining. The expression levels of GFP-Aβ42 were markedly reduced, despite equal levels of transcript generated, indicating that transcription of the different GFP fusion proteins were not altered.

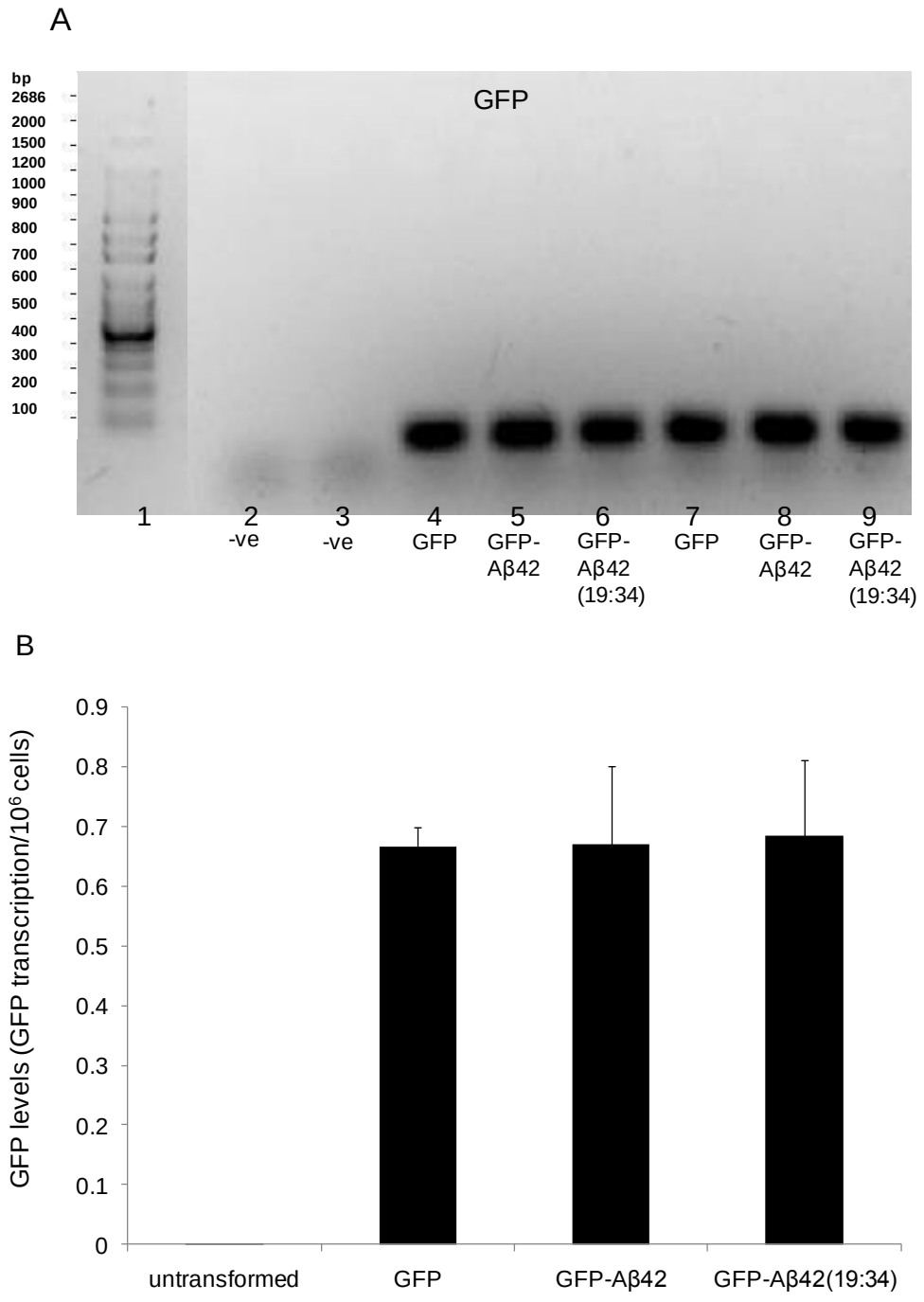

Figure 5: Transcription of GFP is not altered in yeast expressing GFP, GFP-Aβ42 or GFP-Aβ42 (19:34).

GFP, GFP-Aβ42 and GFP-Aβ42 (19:34) expressing yeast cells (KVY55) were grown in selective YNB+2%glucose (-ura) media till exponential phase (OD 0.6). Untransformed cells (KVY55) grown in YEPD media were also collected (OD 0.6). cDNA from the frozen pellets (~1-3 X 10^6 cells) was used for the real time PCR. The PCR products were analysed by 1.5% agarose gel

electrophoresis and observed under UV transillumination. Lanes (from left) are 1) 100bp DNA ladder, 2) no cells control, 3) Untransformed cells, 4, 7) GFP, 5, 8) GFP-Aβ42, 6, 9) GFP-Aβ42 (19:34) **(A)**. A ~90bp size band, representing GFP, was observed in all the transformants, but absent in untransformed and no-cell control. The fold change in GFP transcription/10^6 cells using the comparative C_t method was measured as described previously (Schmittgen and Livak, 2008) **(B)**. Levels of GFP transcript were similar in all cell lines. Data is expressed as mean ± SEM, n=3.

7.5 Discussion:

7.5.1 Yeast model for studying intracellular Aβ

The budding yeast *Saccharomyces cerevisiae* has proven to be a valuable model organism for studying fundamental cellular processes and pathways involved in aggregation and toxicity of pathogenic proteins in neurodegenerative diseases (Bharadwaj et al., 2010; Braun et al., 2010; Winderickx et al., 2008). Yeast models have been extensively used for expression of misfolding proteins including α-synuclein (α-synucleinopathies) (Brandis et al., 2006; Cooper et al., 2006; Flower et al., 2005; Franssens et al., 2009; Lee et al., 2008; Oien et al., 2009; Outeiro and Lindquist, 2003; Sharma et al., 2006; Willingham et al., 2003; Zabrocki et al., 2005), Huntington protein (polyglutamine disorders) (Gokhale et al., 2005; Krobitsch and Lindquist, 2000; Meriin et al., 2002; Sokolov et al., 2006), Tau (tauopathies) (Vandebroek et al., 2006; Vandebroek et al., 2005; Vanhelmont et al., 2010), TDP-43 (Frontotemporal dementia and Amyotrophic lateral sclerosis)(Armakola et al., 2010; Johnson et al., 2008; Kryndushkin et al., 2011) and Aβ42 (Alzheimer's disease) (Bagriantsev and Liebman, 2006; Caine et al., 2007a; von der Haar et al., 2007). The Aβ expression model as developed in Prof. Ian Macreadie's laboratory by Caine and colleagues (2007) was the model of choice, since it was fused to green fluorescent protein (GFP) for much easier tractability as compared to the models developed by Bagriantsev and colleagues (2006) and von der Haar and colleagues (2007) who utilized Aβ fused to Sup35p prion proteins.

Initial attempts at expressing native Aβ42 in yeast using a copper inducible system was unsuccessful (Caine et al., 2007a). This study showed that native expression of Aβ42 in yeast was undetectable, which was similar to findings from other attempts at generating yeast models of protein aggregates such as α-synuclein (Outeiro and Lindquist, 2003). It was suggested that using native expression, led to a rapid proteolysis of the protein of interest within the cell (Outeiro and Lindquist, 2003). Expression of native human proteins as GFP tagged fusions is known to reduce targeting for proteolysis in yeast cells and also enables real time monitoring of the protein of interest (Caine et al., 2007a; Outeiro and Lindquist, 2003). Thus, Caine and colleagues developed a yeast model expressing GFP-tagged fusion Aβ42 protein. The findings from this chapter have further characterised the localisation and expression of GFP-Aβ42 in this model.

The original study by Caine and colleagues showed that GFP-Aβ42 induced a heat shock response and a slight growth stress. It could be argued that this may alter cell growth or viability, or reduce expression of the labelled protein. However, the findings in Figure 4 show that cell viability is not altered by intracellular Aβ42 and that equal amount of transcript was generated in all cell lines. However, extracellular treatment of yeast cells with oligomeric Aβ42 caused significant loss of viability and cell death [Chapter 3, (Bharadwaj et al., 2008)]. It is notable that toxicity in wild type yeast cells was associated only with specific isoforms (oligomeric) and supraphysiological levels of Aβ42 treatment (micromolar). It is most likely that expression levels of GFP-Aβ42 intracellularly would therefore be too low to cause any significant toxicity. Further, the markedly reduced levels of GFP-Aβ42, compared to levels of the non-aggregating, non-toxic GFP-Aβ42 (19:34) mutant and GFP alone, indicate that the cell can deal with the intracellular over-expression of Aβ42. The expression levels coupled with the previously reported heat shock response in the cell suggests that GFP-Aβ42 may be activating intracellular degradation pathways which may account for its decreased levels detected in the yeast cell.

Immunoelectron microscopy showed that GFP-Aβ42 is localized into vesicles reminiscent of autophagic bodies or endosome like structures ((Caine et al., 2007a), Figure 1). Reports showing that Aβ accumulates in vesicular/lysosomal structures in neurons of a variety of AD mouse models (Oddo et al., 2006; Wirths, 2001), human AD brains (Gouras et al., 2000; Nixon et al., 2005) and in neuronal cells treated with extracellular Aβ42 (Hu et al., 2009) collectively supports the idea that GFP-Aβ42 may be accumulating in such vesicles in yeast.

7.5.2 Altered localization of non aggregating Aβ42 (19:34) isoform in yeast

Aβ42 is known to attain multiple isoforms in physiological conditions [reviewed in (Bharadwaj et al., 2009)]. The pathological basis of Aβ42 in AD is dependent on its ability to oligomerize and accumulate leading to cellular dysfunction. In addition to its intrinsic self associating nature, several environmental factors and binding partners can also affect Aβ aggregation and toxicity (Burdick et al., 1992; Holtzman, 2001; Stine et al., 2003). In chapter 3, synthetic derived Aβ42 was shown to form SDS stable low-n oligomers compared to monomeric Aβ42 (19:34) peptide. Although GFP-Aβ42 localized into punctate patterns within the cell indicated aggregation, oligomeric forms of GFP-Aβ42 were not observed by immunoblotting analysis. It is also suggested that identifying intracellular Aβ oligomers can be difficult due to their strong association with membranes (LaFerla et al., 2007).

Therefore, expressing the non aggregating Aβ42 (19:34) as a GFP tagged fusion protein in yeast was beneficial in addressing whether the aggregating nature of Aβ affects the localization and expression levels of the GFP-Aβ fusion proteins in yeast. The modified form of Aβ42 (19:34) did not exhibit a punctate pattern like GFP-Aβ42, but rather had a cytoplasmic distribution similar to cells expressing GFP only. Recent findings also showed that expression of GFP-Aβ42 (19:34) induced a markedly weak heat shock response compared to GFP-

Aβ42 in yeast, as measured by β-galactosidase activity (Antony, 2008). Along with the aggregation/toxic properties of synthetically derived Aβ42 and Aβ42 (19:34) peptides (Section 3.4.2), the distribution patterns of GFP-Aβ42 and GFP-Aβ42 (19:34) in yeast suggested that GFP-Aβ42 is misfolded/aggregated and is sequestered into vesicular structures (diagrammatic representation in Figure 6). The sequestering of GFP-Aβ42 into these vesicles may indicate a potential mechanism in yeast by which it could be targeted for degradation by the yeast vacuole. This is further investigated in chapters 7 and 8.

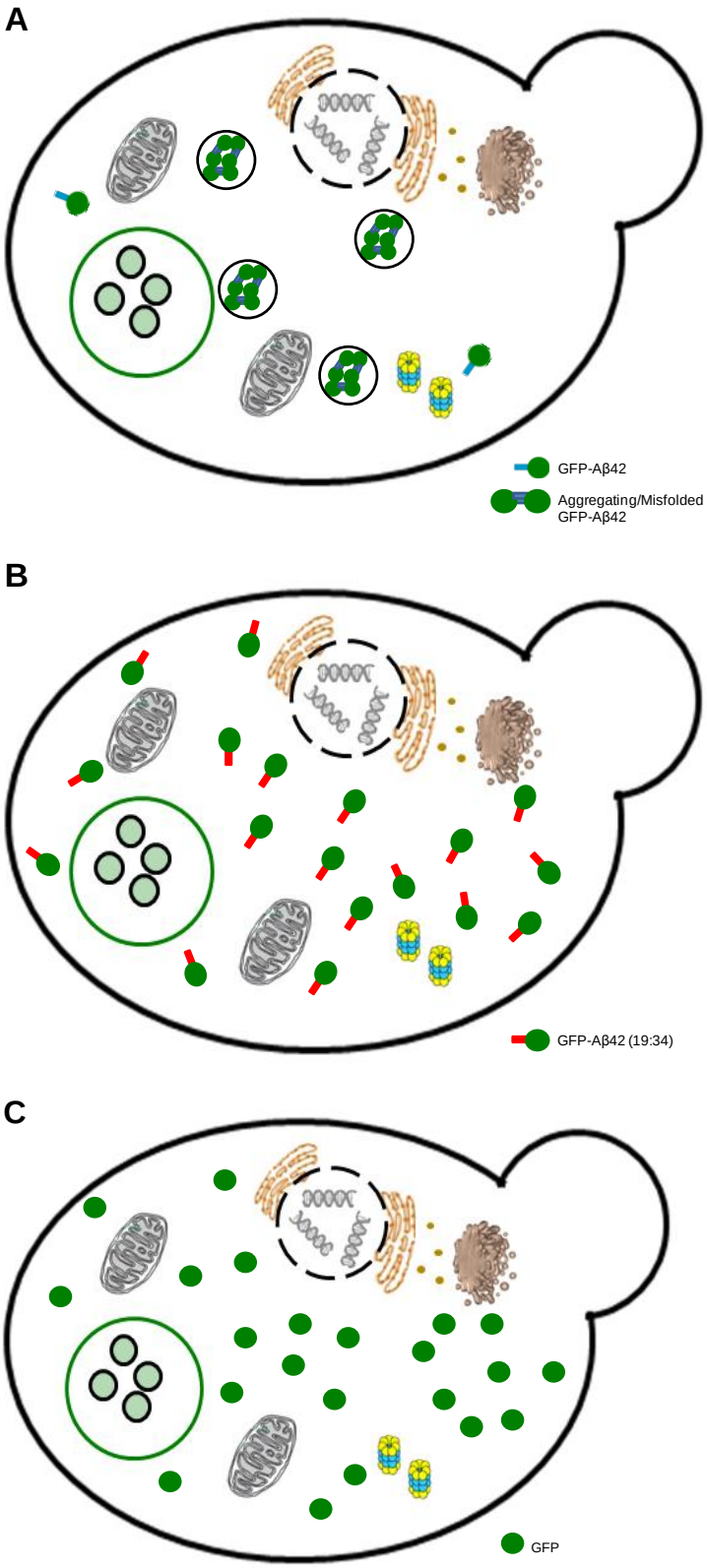

Figure 6: Schematic of GFP/GFPAβ fusion expression in yeast

A diagrammatic representation of localization of GFP-Aβ42 **(A)**, GFP- Aβ42 (19:34) **(B)** and GFP **(C)** expression in yeast, GFP-Aβ42 protein is selectively

sequestered into inclusions, whereas GFP-Aβ42 (19:34), a non aggregating Aβ42 isoform and GFP are localized in the cytosol.

7.5.3 Reduced expression levels of GFP-Aβ42 in yeast

Apart from the distinct localization patterns in the cells, the levels of GFP-Aβ42 were markedly reduced throughout different stages of cell growth compared to GFP or GFP-Aβ42 (19:34) (Figure 4). Interestingly, the levels of GFP-Aβ42 were dramatically reduced and became almost undetectable during the mid-late log phase of growth, whereas GFP and GFP-Aβ42 (19:34) levels remained unchanged. Similar levels of GFP transcript in all three cell lines indicate transcription of the GFP fusion construct was not altered and therefore could not account for the marked reduction in percentage of cells expressing GFP-Aβ42. Further, cell viability was not significantly altered by expression of GFP-Aβ42 (Figure 4E).

Overall the results from fluorescence quantification and immunoblotting analysis in GFP/GFPAβ transformants indicate that GFP-Aβ42 was degraded rapidly throughout the growth phase (exponential till late log phase) compared to GFP and GFP-Aβ42 (19:34) in yeast. The expression levels of GFP-Aβ42 were consistently low compared to GFP and GFP-Aβ42 (19:34) during the exponential growth phase (OD 0.4-1.2), and further declined sharply during the mid-late log phase (>1.2) (Figure 3, 4). One possible explanation is that Aβ42 is degraded continuously during the growth phase, but during the late-log phase, there is an additional boost to the degradation possibly by activation of catabolic pathways. Notably the late-log phase indicates point of nutrient limitation and entry into starvation, where pathways like autophagy are stimulated. The results therefore indicate that Aβ42 can be degraded via distinct pathways in the cell depending on the different phases of growth.

7.6 Summary

Overall this chapter has characterised a novel yeast model of intracellular Aβ42 accumulation, where Aβ42 was localised in a punctate pattern and expression was reduced over the growth phase of the cells. These findings provide evidence in support of Aβ42 being sequestered into cytoplasmic inclusion bodies/ vesicles which may be targeted for degradation. In the subsequent chapter, I report on the use of this model to investigate two intracellular clearance pathways, the ubiquitin-proteasome and the autophagy-lysosome pathways and their contribution to the reduction of GFP-Aβ42 expression observed in this model.

Chapter 8

Clearance mechanisms of intracellular Aβ42 aggregates in Yeast

8.1 Introduction:

Intraneuronal accumulation of beta amyloid (Aβ) protein in the brains of AD patients and transgenic mouse models has been widely reported previously (LaFerla et al., 1997; Nagele et al., 2002). Levels of Aβ rise substantially in endosomal-lysosomal compartments (Cataldo et al., 2004; Takahashi et al., 2004) and cognitive deficits have been reported in AD models in which intracellular Aβ levels are elevated in the absence of plaque deposition (Koistinaho et al., 2001; LaFerla et al., 2007). Impaired clearance of Aβ from the CNS, rather than overproduction has been suggested to be the main contributor to accumulation of this peptide in the brains of sporadic AD patients (Bates et al., 2009; Mawuenyega et al., 2010). In addition to Aβ degrading enzymes, changes in efflux of Aβ from CNS into the periphery can influence cerebral Aβ accumulation and clearance. Another Aβ clearance mechanism is via the two main intracellular degradation/recycling pathways

Firstly, the ubiquitin-proteasome system (UPS) which is responsible for the degradation of short lived peptides (Hochstrasser, 1996), and secondly, the autophagy-lysosome system which regulates longer lived proteins and organelles [reviewed in (Martinet et al., 2009)] are the two pathways which maintain protein homeostasis in cells. In AD, both autophagy-lysosome system and the UPS have been implicated to play important roles in regulating the levels of intracellular Aβ. Autophagy has been shown to be an active pathway for turning over APP and generating the Aβ peptide (Nixon, 2007) and impaired clearance of autophagic vesicles are observed in AD mice models and AD brain (Nixon et al., 2005; Yu et al., 2005; Yu et al., 2004). Suggestions have been made that in AD, deficiences in autophagy and impaired clearance of autophagic vesicles could contribute to the accumulation of Aβ-containing autophagic vesicles within affected neurons (Nixon et al., 2005; Yu et al., 2005) (Boland et al., 2008). Apart from extensive involvement of autophagic processes in the AD brain, studies have also shown selective decrease of proteasomal activity in specific regions (Keck et al., 2003; Keller et al., 2000)

and accumulation of ubiquitin in plaques and tangles of AD brains (Mori et al., 1987; Morishima-Kawashima et al., 1993; Perry et al., 1987; Tabaton et al., 1991). Reports also suggest that Aβ oligomers can inhibit proteasomal function (Oh et al., 2005; Tseng et al., 2008). Although defective clearance by autophagy-lysosome and the ubiquitin-proteasome pathways are associated with increased Aβ accumulation in the brain, their exact roles and contributions of the various components involved in the degradation of Aβ aggregates inside the cell still remain unclear.

In chapter 7, the GFP tagged Aβ expression system (Caine et al., 2007a) in yeast was utilized for studying intracellular Aβ accumulation. GFP-Aβ42 was found to be sequestered into amorphous inclusions, whereas GFP and GFP-Aβ42 (19:34) showed diffuse cytosolic localization in the cell. Also compared to cells expressing GFP or GFP-Aβ42 (19:34), the levels of GFP-Aβ42 were markedly reduced throughout different stages of cell growth. Together with differences in distribution and levels of GFP fusion proteins, the results indicated that compared to non-aggregating GFP-Aβ42 (19:34) mutant, GFP-Aβ42 aggregates are efficiently cleared from yeast. Also, the data supported the idea that GFP-Aβ42 is sequestered into cytoplasmic inclusion bodies/vesicles which may be targeted for degradation by autophagy or the proteasome in the cell.

In this chapter, I describe the use of this yeast model in an attempt to understand the roles of autophagic vesicle (AV) transport, vacuolar protease activity and proteasomal chymotrypsin activity in clearance of GFP-Aβ42 aggregates inside the cell. To achieve this objective, expression levels and distribution of GFP, GFP-Aβ42 and GFP-Aβ42 (19:34) fusion proteins were studied in mutants deficient in AV synthesis (atg8Δ), vacuolar proteases associated with autophagy (pep4Δ and cvt1Δ) and 26 proteasome subunits essential for chymotrypsin activity (pre1Δ and pre1-2Δ).

8.2 Aims:

1.) Comparative analysis of the expression levels and localization of GFP/GFPAβ fusion proteins in wild type and AV synthesis mutant (atg8Δ) transformants.
2.) Comparative analysis of the expression levels and localization of GFP/GFPAβ fusion proteins in wild type and vacuolar protease deficient mutants (pep4Δ and cvt1Δ) transformants.
3.) Comparative analysis of the expression levels and localization of GFP/GFPAβ fusion proteins in wild type and proteasomal activity deficient mutants (pre1Δ and pre1-2Δ) transformants.

8.3 Materials and Methods:

GFP/GFPAβ fusion protein constructs were transformed into wild type, AV synthesis mutant (atg8Δ), vacuolar protease deficient mutants (pep4Δ and cvt1Δ) and proteasomal activity deficient mutants (pre1Δ and pre1-2Δ) yeast mutants cells. As described in Section 2.2.16 and Section 2.2.17, expression levels and localization of GFP/GFPAβ fusion proteins were studied by fluorescent microscopy and immunoblotting in all the yeast transformants.

8.4 Results:

In chapter 7, using a GFP tagged Aβ expressing yeast model, it was shown that compared to non-aggregating GFP-Aβ42 (19:34) mutant, levels of GFP-Aβ42 were markedly reduced, suggesting clearance of Aβ aggregates. This was also supported by the punctate staining of GFP-Aβ42, compared to GFP-Aβ42 (19:34) indicating sequestration of Aβ42 aggregates into cytoplasmic inclusion bodies/ vesicles, which may be targeted for degradation. This chapter reports on the contribution of autophagy and proteasomal activity in the degradation of GFP-Aβ42 in yeast.

8.4.1 Localization and expression levels of GFP/GFPAβ in autophagic vesicle (AV) synthesis mutant (atg8Δ)

A pathway that has been implicated in clearing/ degrading intracellular aggregated proteins is autophagy. Autophagy is a catabolic process initiated by the formation of an autophagic vesicle (AV) which sequesters and transports the bulk of the cytoplasmic material for degradation in the lysosome (vacuole in yeast) by acid hydrolases. To determine the role of AV transport in GFP-Aβ42 degradation in yeast, the distribution and expression levels of GFP/GFPAβ fusion proteins were determined in yeast cells deficient of a protein Atg8p (homolog of human LC3) essential for AV synthesis (atg8Δ).

GFP, GFP-Aβ42 or the GFP-Aβ42 (19:34) transformants were generated in atg8Δ mutant cells and corresponding background wild type strain (*Saccharomyces cerevisiae*, KVY55). The distribution of GFP fluorescence in wild-type and atg8Δ cells expressing the GFP/GFPAβ fusion proteins was assessed. As described in chapter 7, in wild-type cells expressing GFP-Aβ42, fluorescence was found to localize into punctate like patterns (Figure. 1A) within the cell compared to diffuse cytosolic fluorescence in those expressing GFP only (Figure. 1C) or GFP-Aβ42 (19:34) (Figure. 1B). In atg8Δ mutant cells, the localization of GFP and GFP-Aβ42 (19:34) was diffuse and similar to that observed in wild type cells (compare Figure.1E, F with 1B, C). In atg8Δ cells expressing GFP-Aβ42, fluorescence was more diffuse and cytosolic compared to the punctate staining observed in wild-type cells expressing GFP-Aβ42 (compare Figure. 1D with 1A) during the mid-late log phase (OD>1). The diffuse fluorescence in atg8Δ cells expressing GFP-Aβ42 suggested that the mutant had reduced ability to sequester the GFP-Aβ42 aggregates, possibly due to the lack of AV synthesis. Next, the expression levels of the GFP/GFPAβ fusion proteins in wild type and atg8Δ cells were determined.

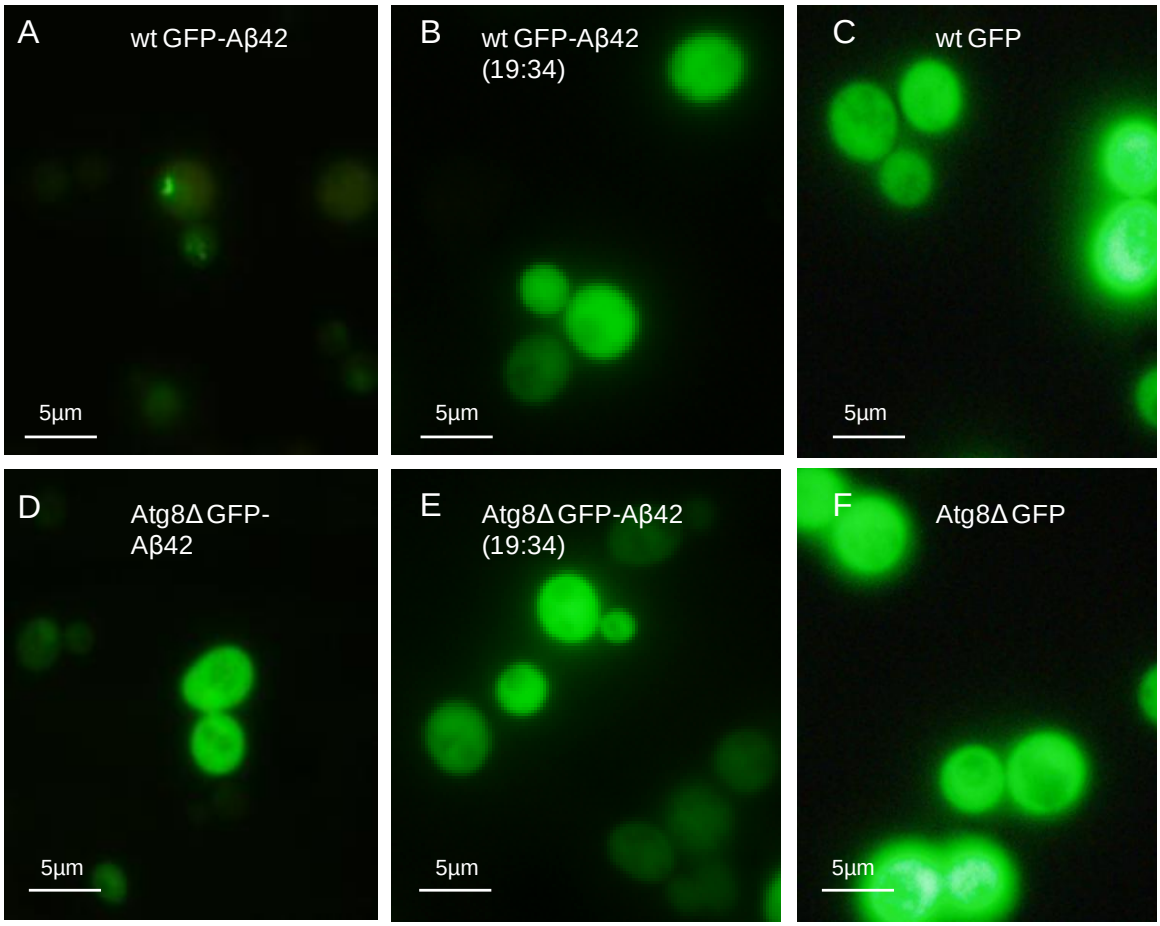

Figure 1: Localization of GFP, GFP-Aβ42 or GFP-Aβ42 (19:34) in wild type and atg8Δ yeast transformants.

GFP/GFP-Aβ transformants were generated in wild type and atg8Δ cells (*Saccharomyces cerevisiae*, KVY55), and stored on selective minimal YNB+2%glucose (-ura) agar plates at 4ºC. A single yeast colony from stock agar plates was inoculated in 5mL YNB+2%glucose (-ura) and incubated with shaking at 30ºC overnight. The overnight culture was resuspended in fresh YNB+2%glucose (-ura) media to an initial cell density (OD at 600nm) of 0.2. The culture was then incubated at 30ºC with shaking. Aliquots at mid-late log phase (OD of 1-1.6) of growth in selective minimal media (YNB+2%glucose, -ura) were observed under the fluorescent microscope. Localization of GFPAβ42 **(A, D)**, GFPAβ42 (19:34) **(B, E)** and GFP **(C, F)** in wild-type and atg8Δ cells respectively were investigated.

To determine if deficiency of AV synthesis in atg8Δ cells altered the levels of the fusion proteins, the percentage of green fluorescent cells were estimated for the transformant cell lines (Figure 2). A similar profile of percentage of GFP expressing cells to that shown in the previous chapter (Chapter 7, Figure 3) was observed for the wild-type transformant cells. Cells expressing GFP showed ~90% fluorescent cells throughout the growth phase compared to a maximum of only ~15-20% fluorescence (exponential to mid-late log phase) in cells expressing GFP-Aβ42. And, in cells expressing GFP-Aβ42 (19:34), ~70% cells were fluorescent in the exponential phase and mid-late log phase. In atg8Δ cells expressing GFP and GFP-Aβ42 (19:34), the profile was similar to that seen in wild-type cells. However, compared to wild-type cells, a two-fold increase (up to ~40%) in fluorescent cells was observed from the early exponential growth phase in atg8Δ mutant cells expressing GFP-Aβ42 (Figure 2). Also the levels were found to remain stable after mid-late log phase, even at cell density OD>1, whereas fluorescence was almost undetectable in wild-type cells at similar growth phase.

To specifically determine the levels of these fusion proteins in the cells, extracts of the wild type (i) and atg8Δ (ii) yeast transformants at different time points in the growth phase was analysed by SDS-PAGE western blotting (Figure 3). Western immunoblotting of cell extracts for Aβ showed similar results to fluorescence data. No significant changes in the levels of GFP and GFP-Aβ42 (19:34) was observed between wild type and atg8Δ cells (Figure 3B and C). It is noted that compared to cells expressing GFP-Aβ42, cells expressing GFP-Aβ42 (19:34) exhibit higher levels of the modified Aβ42. Compared to wild-type cells, GFP-Aβ42 levels were increased in atg8Δ cells during mid-late log phase of growth (OD>0.6) (Figure. 3A). Also the GFP-Aβ42 levels remained unchanged in the atg8Δ even at OD>1.6, whereas it was markedly reduced at OD=1.2 and undetectable at OD=1.6 in the wild type (Figure 3A).

The overall differences in GFP-Aβ42 levels and distribution between wild-type and atg8Δ mutant yeast cells suggested that disruption of AV synthesis lead to increased accumulation of GFP-Aβ42 in the mutant compared to the wild type.

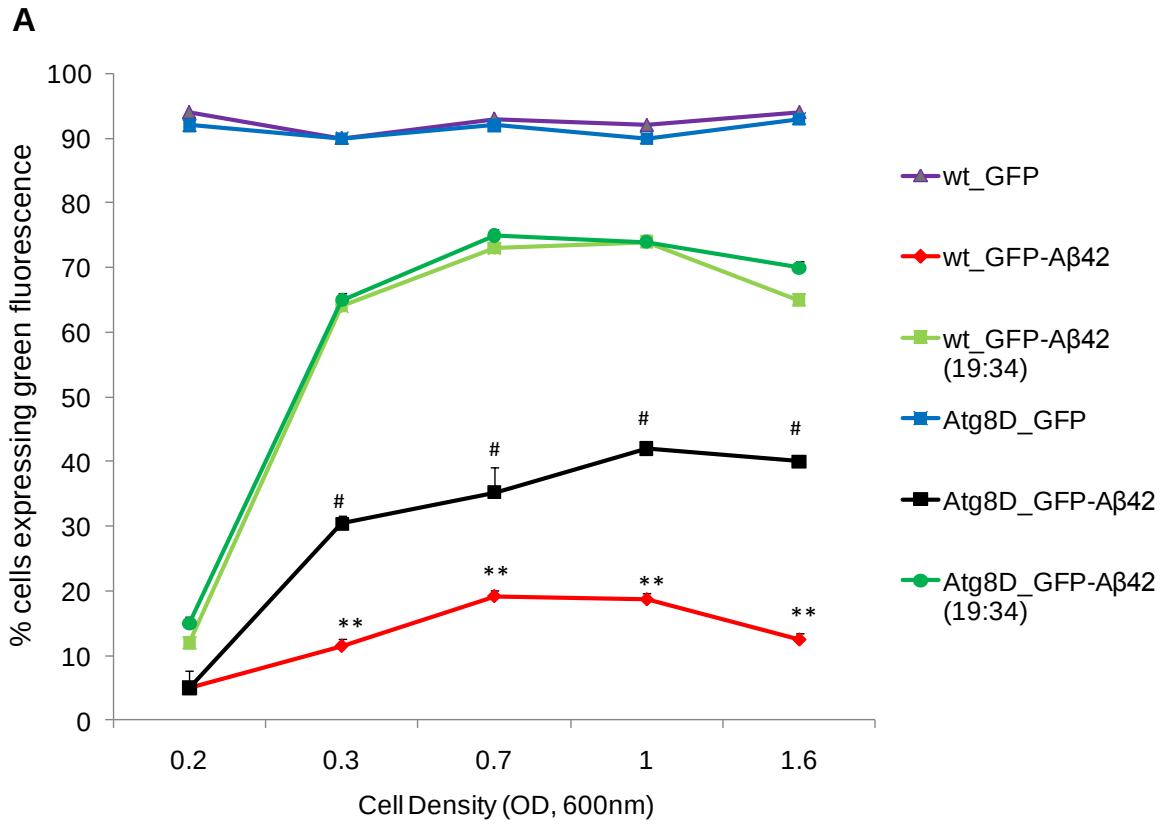

Figure 2: GFP fluorescence levels in GFP, GFP-Aβ42 or GFP-Aβ42 (19:34) expressing wild type and atg8Δ yeast transformants.

GFP/GFP-Aβ transformants were generated in wild type and atg8Δ cells (*Saccharomyces cerevisiae*, KVY55), and stored on selective minimal YNB+2%glucose (-ura) agar plates at 4ºC. A single yeast colony from stock agar plates was inoculated in 5mL YNB+2%glucose (-ura) and incubated with shaking at 30ºC overnight. The overnight culture was resuspended in fresh YNB+2%glucose (-ura) media to an initial cell density (OD at 600nm) of 0.2. The culture was then incubated at 30ºC with shaking. Aliquots at different cell

densities were collected and observed under the fluorescent microscope. The percentage of cells expressing green fluorescence in wild type and atg8Δ cells expressing GFP, GFPAβ42 and GFPAβ42 (19:34) fusion proteins were quantified at different phases of growth starting from initiation (OD: 0.2) till late-log phase (OD: 1-1.6) **(A)**. The percentage of fluorescing cells was significantly reduced in wild type cells expressing GFP-Aβ42 (**, p<0.001), compared to those expressing GFP and GFP-Aβ42 (19:34) throughout the growth phase. The percentage of fluorescing cells was significantly higher in atg8Δ cells expressing GFP-Aβ42 (#, p<0.005) compared to wild type GFP-Aβ42. Data is expressed as mean ± SEM (n=4).

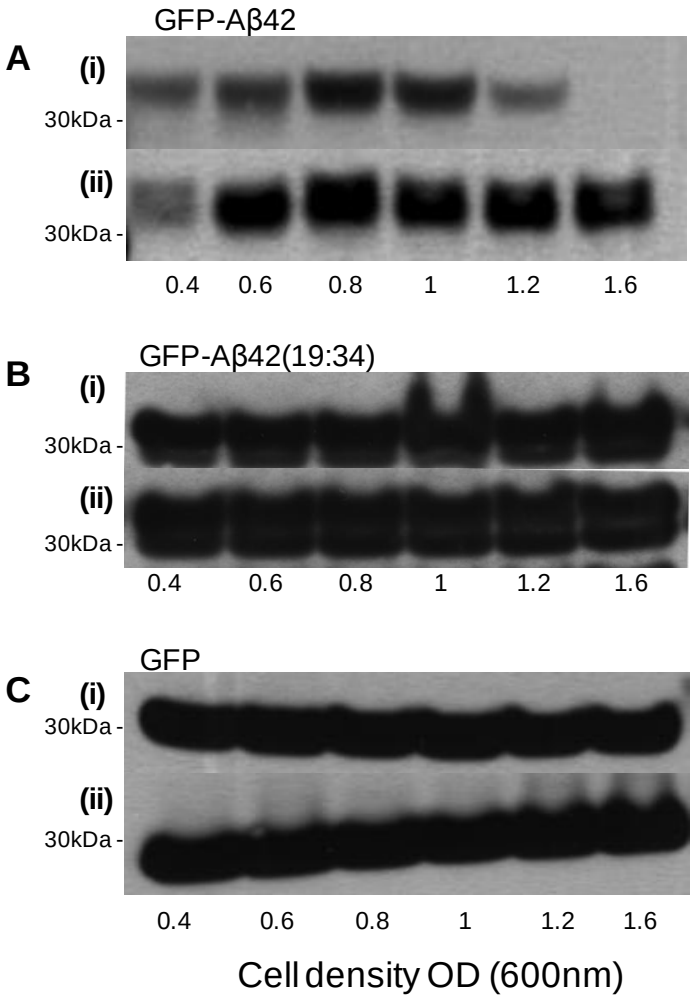

Figure 3: Expression levels of GFP, GFP-Aβ42 or GFP-Aβ42 (19:34) proteins in wild type and atg8Δ yeast transformants.

GFP/GFP-Aβ transformants were generated in wild type and atg8Δ cells (*Saccharomyces cerevisiae*, KVY55), and stored on selective minimal

YNB+2%glucose (-ura) agar plates at 4ºC. A single yeast colony from stock agar plates was inoculated in 5ml YNB+2%glucose (-ura) and incubated with shaking at 30ºC overnight. The overnight culture was resuspended in fresh YNB+2%glucose (-ura) media to an initial cell density (OD at 600nm) of 0.2. The culture was then incubated at 30ºC with shaking. Aliquots at different cell densities were collected for immunoblotting analysis. Cell extracts (50µg) from wild-type **(i)** or atg8Δ mutant **(ii)** cells expressing GFPAβ42 **(A)**, GFPAβ42 (19:34) **(B)** and GFP **(C)** were probed using anti-Aβ (WO2) and anti-GFP antibodies.

8.4.2 Localization and expression levels of GFP/GFPAβ in vacuolar protease mutants (pep4Δ and cvt1Δ)

Vacuolar proteases are a family of acid hydrolases in yeast which operate as the key enzymes essential for degradation of cytoplasmic material transported to the vacuole (Klionsky and Emr, 2000). In yeast, pep4p ([homolog of human cathepsin D (Ammerer et al., 1986; Jones et al., 1982)], yscA) and cvt1p [(member of subtilisin family), yscB] are the main vacuolar endopeptidases (Teichert et al., 1989). To determine the contribution of vacuolar proteases in the degradation of GFP-Aβ42 in yeast, the distribution and expression levels of GFP/GFPAβ fusion proteins in mutant cells deficient of enzymes pep4p (pep4Δ) and cvt1p (cvt1Δ) was determined.

GFP, GFP-Aβ42 and GFP-Aβ42 (19:34) transformants were generated in pep4Δ, cvt1Δ mutant cells and corresponding background wild type strain (*Saccharomyces cerevisiae*, BY4743). The distribution of GFP fluorescence in wild-type, pep4Δ, and cvt1Δ cells expressing GFP/GFPAβ fusion proteins was assessed (Figure 4). The distribution of GFP fluorescence in wild-type cells expressing GFP, GFP-Aβ42 and GFP-Aβ42 (19:34) were similar to previous observations as described in chapter 7. In pep4Δ and cvt1Δ cells, the localization of GFP and GFP-Aβ42 (19:34) were diffuse and was similar to that in observed in wild type cells (compare Figure 4D-F and Figure 4G-I). In pep4Δ and cvt1Δ cells expressing GFP-Aβ42 the fluorescence was punctate similar to

wild type expressing GFP-Aβ42. However both pep4Δ and cvt1Δ cells expressing GFP-Aβ42 showed increased number of punctate staining compared to the wild type during the mid-late log phase (OD>2) (compare Figure 4A with 4B, C). This result suggested an increased accumulation of GFP-Aβ42 in pep4Δ and cvt1Δ compared to the wild type during starvation periods.

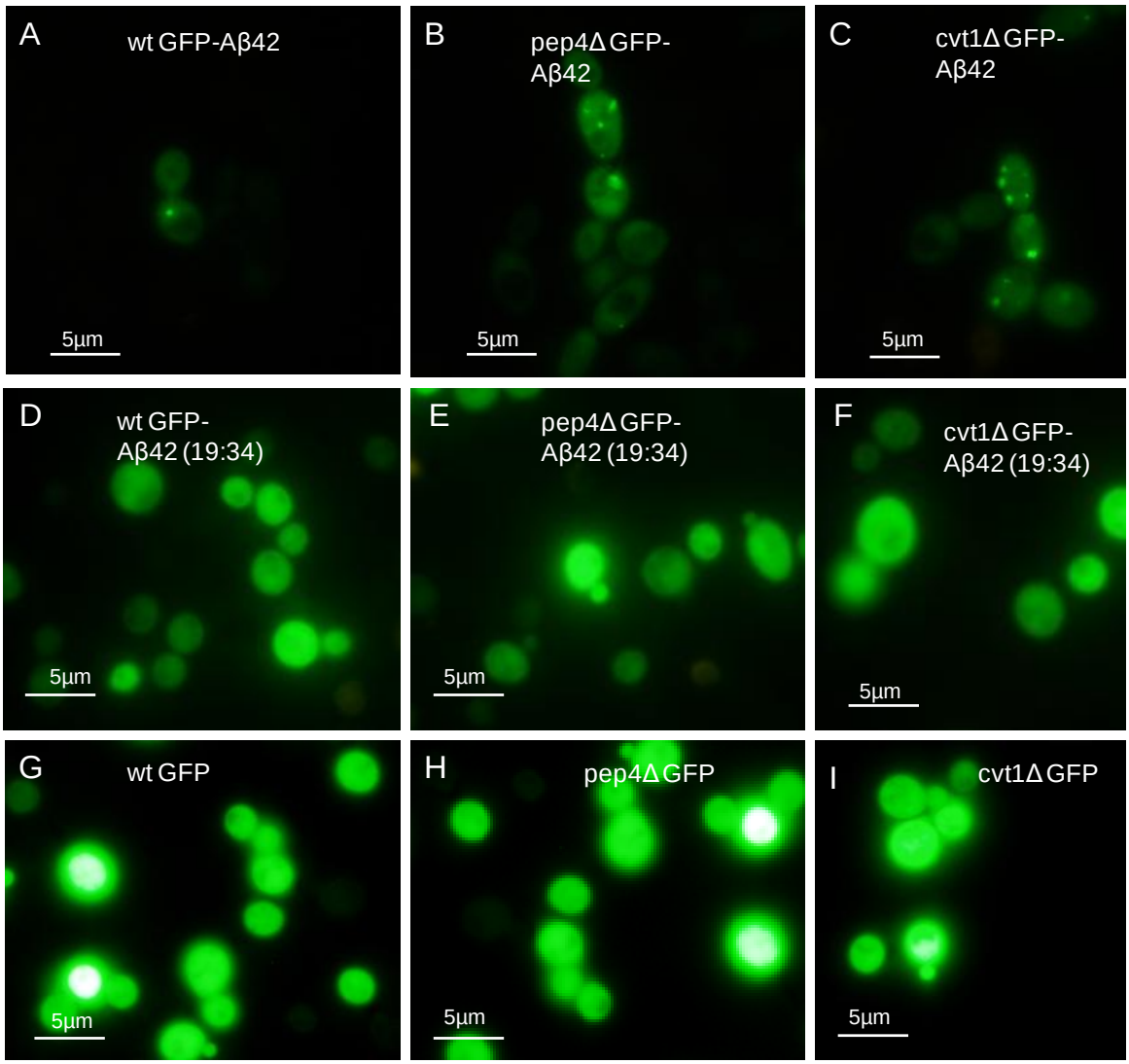

Figure 4: Localization of GFP, GFP-Aβ42 or GFP-Aβ42 (19:34) in wild type, pep4Δ and cvt1Δ yeast transformants.

GFP/GFP-Aβ transformants were generated in wild type, pep4Δ and cvt1Δ cells (*Saccharomyces cerevisiae*, BY4743), and stored on selective minimal YNB+2%glucose (-ura) agar plates at 4ºC. A single yeast colony from stock

agar plates was inoculated in 5ml YNB+2%glucose (-ura) and incubated with shaking at 30ºC overnight. The overnight culture was resuspended in fresh YNB+2%glucose (-ura) media to an initial cell density (OD at 600nm) of 0.2. The culture was then incubated at 30ºC with shaking. Aliquots at mid-late log phase (OD of 2-2.5) of growth in selective minimal media (YNB+2%glucose, -ura) were observed under the fluorescent microscope. Localization of GFPAβ42 **(A-C)**, GFPAβ42 (19:34) **(D-F)** and GFP **(G-I)**, in wild-type, pep4Δ, and cvt1Δ cells respectively were investigated.

To determine if lack of the vacuolar proteases (pep4p and cvt1p) altered the levels of the fusion proteins, the percentage of green fluorescent cells were estimated for the transformant cell lines (Figure 5). A similar profile of percentage of fluorescing cells to that shown in Chapter 7 (See Figure. 3) was observed for the wild-type transformant cells. Also, the levels of GFP fluorescence in pep4Δ, cvt1Δ cells expressing GFP and GFP-Aβ42 (19:34) were similar to that of the wild type (Figure 5A, B). Comparing the wild type, the percent of fluorescing cells were increased in GFP-Aβ42 expressing cvt1Δ and pep4Δ cells during the mid-late log phase (OD 1.5-3). In pep4Δ-GFP-Aβ42 cells, the percent of fluorescing cells were similar (~25%) to the wild type up to the mid-log phase (OD~1-1.5). However during the late log phase (>1.5), the decrease in percent fluorescing cells was significantly slow in pep4Δ cells compared to the wild type (~5% in wt compared to ~20% in pep4Δ) (Figure 5A). Interestingly, a similar trend was also observed in cvt1Δ-GFP-Aβ42 (~5% in wt compared to ~30% in cvt1Δ) (Figure 5B).

Immunoblotting analysis for all transformant cell lines was also done (Figure 6). Similar to wild-type cells, the levels of GFP and GFP-Aβ42 (19:34) were unchanged throughout the growth phase in pep4Δ, cvt1Δ cells (Figure 6B, C). The GFP-Aβ42 protein levels were reduced markedly after OD>1.6 (late log phase) in the wild type cells. However in pep4Δ and cvt1Δ cells, the GFP-Aβ42 protein levels do not reduce until OD 3.3. Unlike the atg8Δ mutant expressing GFP-Aβ42, the protein levels are not higher than the wild type during the early stages of growth (OD 0.4-1.6) (Figure 6A). Overall, the differences in GFP-Aβ42

levels and distribution between wild-type and the vacuolar protease mutants showed that, deficiency in acid hydrolases (pep4p, cvt1p) can result in increased accumulation of GFP-Aβ42, especially during the late log phase of growth (OD>1.6).

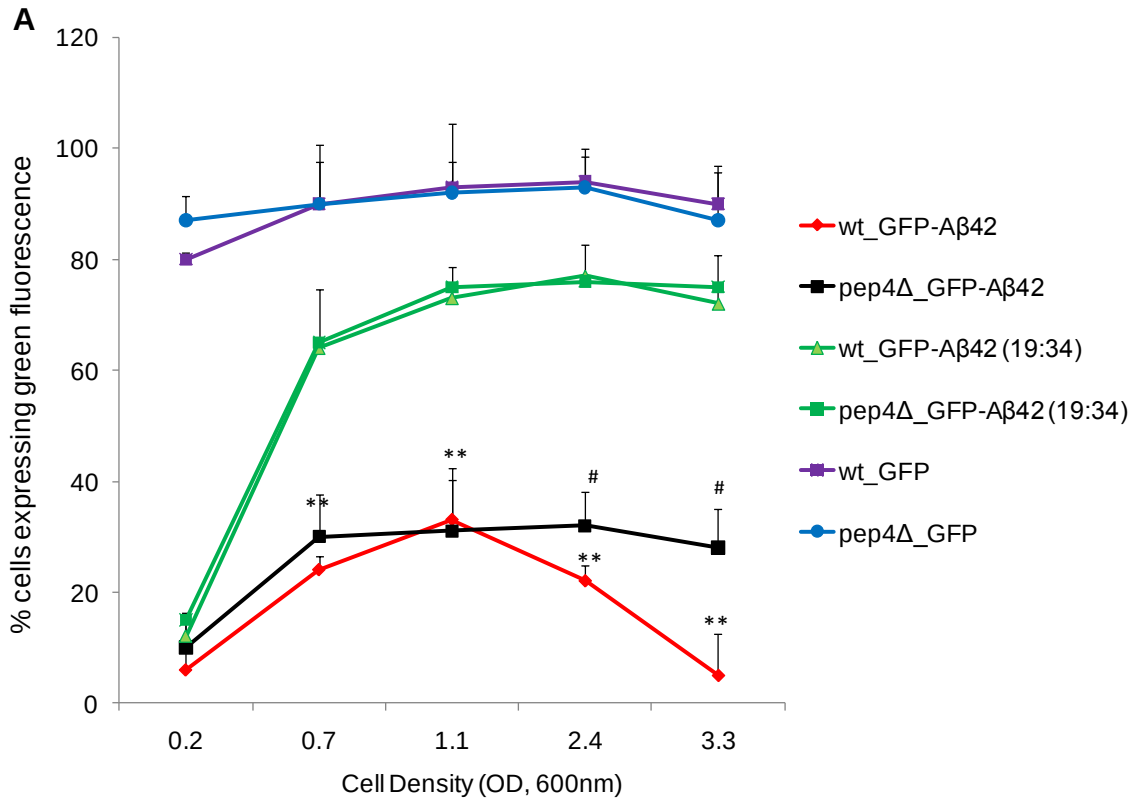

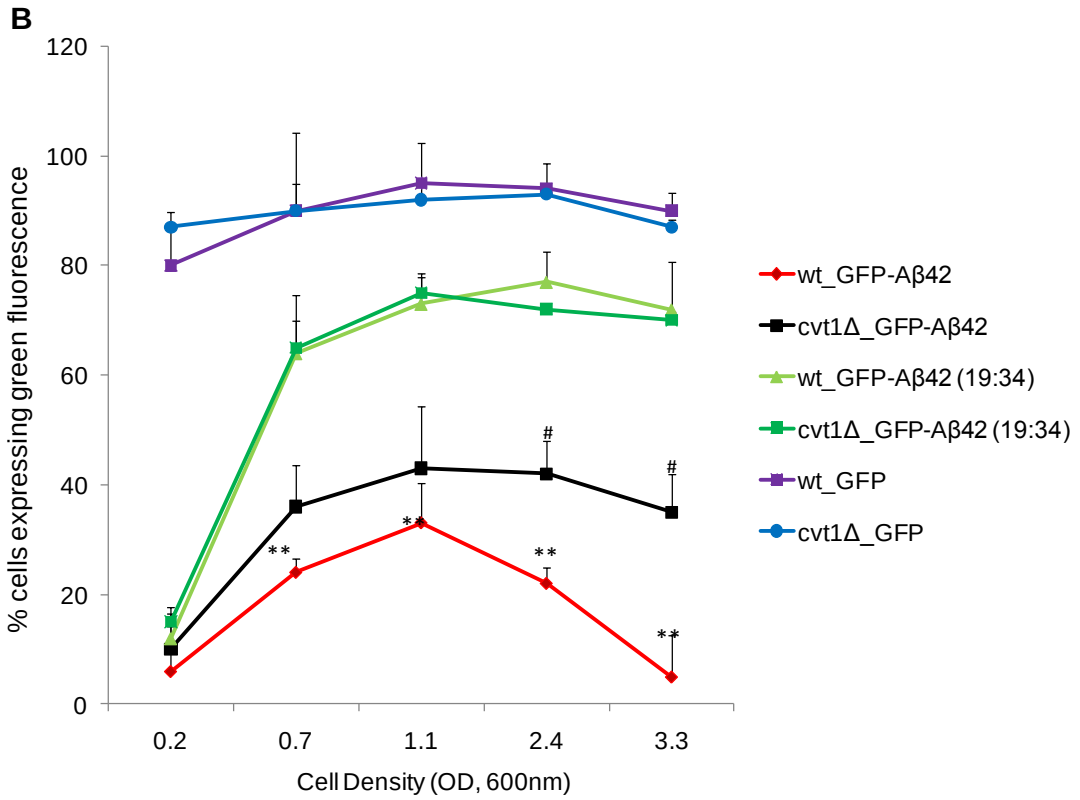

Figure 5: GFP fluorescence levels in GFP, GFP-Aβ42 or GFP-Aβ42 (19:34) expressing wild type, pep4Δ and cvt1Δ yeast transformants.

GFP/GFP-Aβ transformants were generated in wild type, pep4Δ and cvt1Δ cells (*Saccharomyces cerevisiae*, BY4743), and stored on selective minimal YNB+2%glucose (-ura) agar plates at 4ºC. A single yeast colony from stock agar plates was inoculated in 5mL YNB+2%glucose (-ura) and incubated with shaking at 30ºC overnight. The overnight culture was resuspended in fresh YNB+2%glucose (-ura) media to an initial cell density (OD at 600nm) of 0.2. The culture was then incubated at 30ºC with shaking. Aliquots at different cell densities were collected and observed under the fluorescent microscope. The percentage of cells expressing green fluorescence in wild type compared individually to pep4Δ **(A)**, cvt1Δ **(B)** cells expressing GFP, GFPAβ42 and GFPAβ42 (19:34) fusion proteins were quantified at different phases of growth starting from early exponential phase (OD: 0.2) till late-log phase (OD: 3.3) The percentage of fluorescing cells `is significantly reduced in wild type cells expressing GFP-Aβ42 (**, $p<0.001$), compared to those expressing GFP or GFP-Aβ42 (19:34) throughout the growth phase. The percentage of fluorescing

cells was similar in wild type, pep4Δ, and cvt1Δ cells expressing GFP and GFP-Aβ42 (19:34). Comparing the wild type, % fluorescing cells was increased (#, $p<0.05$) in GFP-Aβ42 expressing cvt1Δ and pep4Δ cells during the mid-late log phase (OD 1.5-3). Data is expressed as mean ± SEM (n=4).

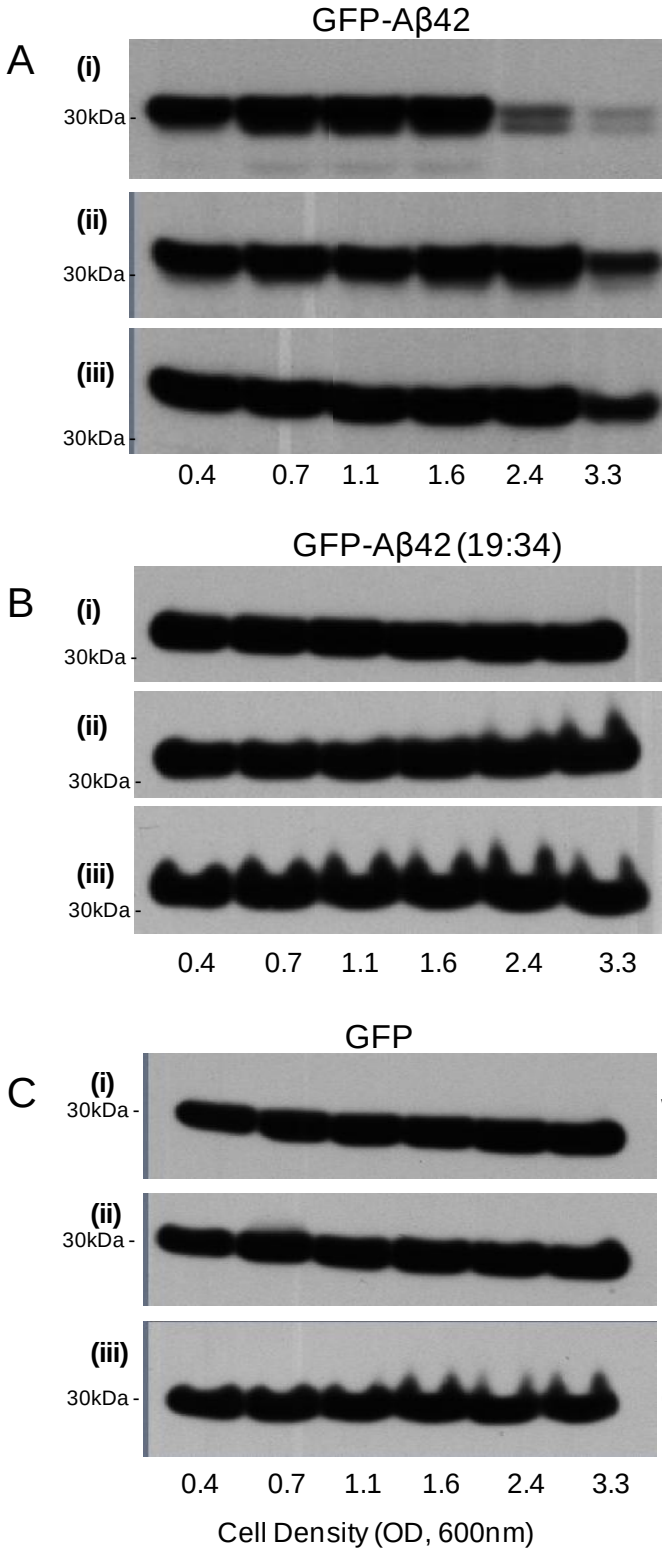

Figure 6: Expression levels of GFP, GFP-Aβ42 and GFP-Aβ42 (19:34) fusions in wild type pep4Δ, and cvt1Δ yeast transformants

GFP/GFP-Aβ transformants were generated in wild type, pep4Δ, and cvt1Δ cells (*Saccharomyces cerevisiae*, BY4743), and stored on selective minimal YNB+2%glucose (-ura) agar plates at 4ºC. A single yeast colony from stock agar plates was inoculated in 5ml YNB+2%glucose (-ura) and incubated with shaking at 30ºC overnight. The overnight culture was resuspended in fresh YNB+2%glucose (-ura) media to an initial cell density (OD at 600nm) of 0.2. The culture was then incubated at 30ºC with shaking. Aliquots at different cell densities (OD 600nm, 0.4-3.3) were collected for immunoblotting analysis. Cell extracts (50µg) from wild-type **(i)**, pep4Δ **(ii)**, and cvt1Δ **(iii)** mutant cells expressing **(A)** GFPAβ42 **(B)**, GFPAβ42 (19:34) and **(C)** GFP were probed using anti-Aβ (WO2) or anti-GFP antibodies.

8.4.3 Localization and expression levels of GFP/GFPAβ in proteasomal mutants (pre1Δ and pre1-2Δ)

The data from Chapter 7 (see Figure 3) and current chapter (Figure 2 and 5) in wild type yeast clearly shows that apart from the late log phase, GFP-Aβ42 levels are significantly low throughout the exponential phase compared to wild-type yeast expressing GFP and GFP-Aβ42 (19:34). This shows that levels of GFP-Aβ42 are tightly controlled during the entire growth phase (exponential phase till log phase). Under conditions of normal growth, the bulk of protein degradation occurs via the ubiquitin proteasomal system (UPS) (Hershko and Ciechanover, 1998). To determine the role of UPS activity in the degradation of GFP-Aβ42, the distribution and expression levels of GFP/GFPAβ fusion proteins were determined in yeast strains bearing mutations in genes coding for two proteolytic proteasome subunits responsible for chymotrypsin like activity: β4 (*PRE1*) and β5 (*PRE2*) (pre1Δ and pre1-2Δ) (Egner et al., 1995; Kragt et al., 2005).

GFP, GFP-Aβ42 and GFP-Aβ42 (19:34) transformants were generated in pre1Δ, pre1-2Δ cells and corresponding background wild type strain (*Saccharomyces cerevisiae*, Wcg4a). The distribution of GFP fluorescence in wild-type, pre1Δ and pre1-2Δ cells expressing GFP/GFPAβ fusion proteins was assessed (Figure 7). The distribution of GFP fluorescence in wild-type cells expressing GFP, GFP-Aβ42 and GFP-Aβ42 (19:34) were similar to previous observations in chapter 7. In pre1Δ and pre1-2Δ cells, the localization of GFP and GFP-Aβ42 (19:34) were diffuse and was similar to that in wild type (compare Figure 7D, E, F and Figure 7G, H, I). However, pre1Δ and pre1-2Δ cells expressing GFP-Aβ42 showed increased levels of punctate staining compared to wild type (Figure 7A-C). The increased punctuate fluorescence in pre1Δ and pre1-2Δ cells comparing wild type suggested an increased accumulation of GFP-Aβ42 within the cell.

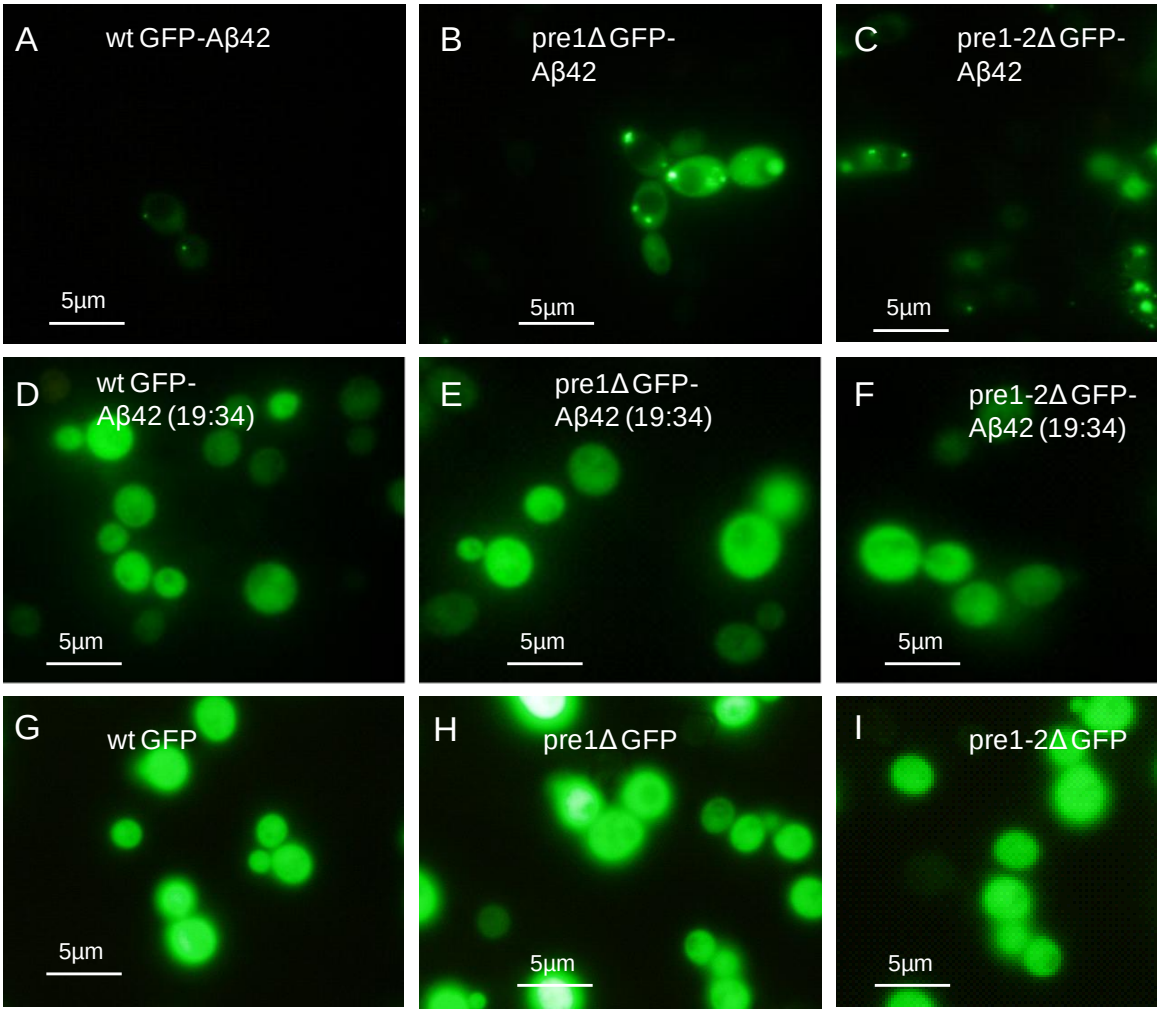

Figure 7: Localization of GFP, GFP-Aβ42 or GFP-Aβ42 (19:34) in wild type, pre1Δ and pre1-2Δ.

GFP/GFP-Aβ transformants were generated in wild type, pre1Δ and pre1-2Δ cells (*Saccharomyces cerevisiae*, Wcg4a), and stored on selective minimal YNB+2%glucose (-ura) agar plates at 4ºC. A single yeast colony from stock agar plates was inoculated in 5mL YNB+2%glucose (-ura) and incubated with shaking at 30ºC overnight. The overnight culture was resuspended in fresh YNB+2%glucose (-ura) media to an initial cell density (OD at 600nm) of 0.2. The culture was then incubated at 30ºC with shaking. Aliquots at mid-late log phase (OD of 2-2.5) of growth in selective minimal media (YNB+2%glucose, -ura) were observed under the fluorescent microscope. Localization of GFPAβ42 **(A-C)**, GFPAβ42 (19:34) **(D-F)** and GFP **(G-I)**, in wild type, pre1Δ and pre1-2Δ cells respectively were investigated.

The percentage of green fluorescent cells was estimated for the transformant cell lines (Figure 8). A similar profile of percentage of GFP expressing cells to that shown in the previous chapter (Chapter 7, Figure. 3) was observed for the wild-type transformant cells. The percent of fluorescing cells in pre1Δ and pre1-2Δ cells expressing GFP and GFP-Aβ42 (19:34) were similar to that of the wild type (Figure 8A, B). However, percent of fluorescing cells were ~2 fold higher throughout the growth phase (OD 0.7-3) in GFP-Aβ42 expressing pre1Δ and pre1-2Δ cells compared to wild type (Figure 8A, B). Also, pre1-2Δ cells showed increased percent of fluorescing cells (~40%) compared to pre1Δ cells (~30%) during late log phase (OD 3.3), which was markedly higher than the wild type (~5%) at the same growth phase.

Immunoblotting analysis for all transformant cell lines was also performed (Figure 9). Similar to wild-type cells, levels of GFP and GFP-Aβ42 (19:34) were unchanged throughout the growth phase in pre1Δ and pre1-2Δ cells (Figure 9B, C). However, GFP-Aβ42 levels in pre1Δ and pre1-2Δ were consistently high throughout the growth phase (OD 0.4-3.3) compared to the wild type (Figure 9A). At the late-log phase of cells growth (OD 3.3), levels of GFP-Aβ42 were undetectable in wild-type cells (Figure 9A). Similar to the fluorescence data, pre1-2Δ cells showed increased GFP-Aβ42 levels compared to pre1Δ cells during late log phase (OD 3.3), whereas undetectable in wild type. The data has shown that decreased chymotrypsin activity of the proteasome resulted in increased levels of GFP-Aβ42 in the cell throughout the growth phase of yeast (from exponential till the late log phase).

A

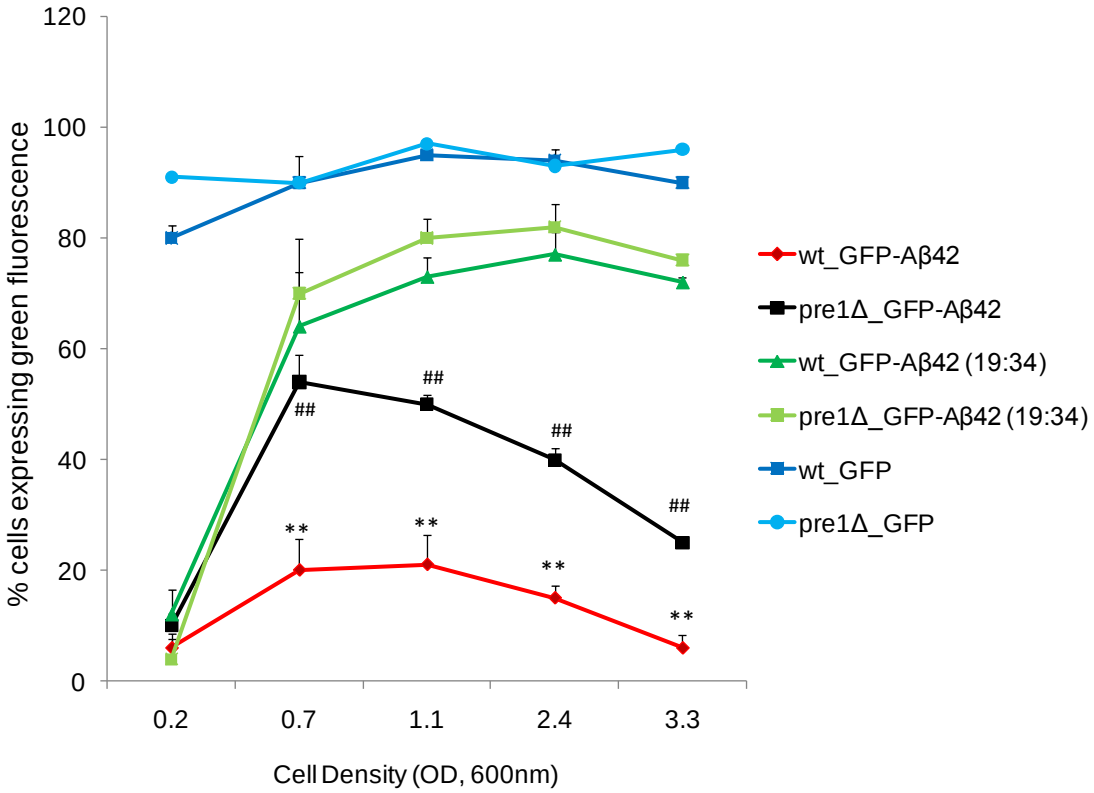
120
100
80
60
40
20
0
% cells expressing green fluorescence
0.2
0.7
1.1
2.4
3.3
Cell Density (OD, 600nm)
##
**
wt_GFP-Aβ42
pre1Δ_GFP-Aβ42
wt_GFP-Aβ42 (19:34)
pre1Δ_GFP-Aβ42 (19:34)
wt_GFP
pre1Δ_GFP

B

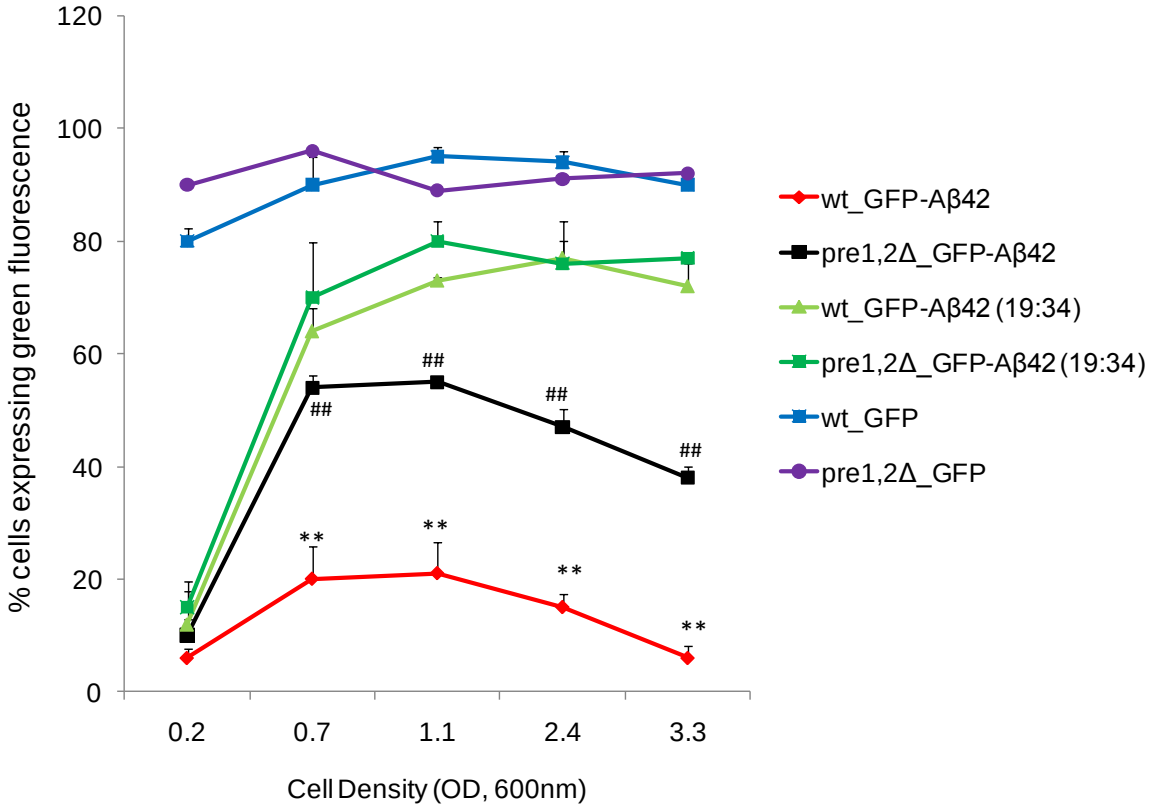
120
100
80
60
40
20
0
% cells expressing green fluorescence
0.2
0.7
1.1
2.4
3.3
Cell Density (OD, 600nm)
##
**
wt_GFP-Aβ42
pre1,2Δ_GFP-Aβ42
wt_GFP-Aβ42 (19:34)
pre1,2Δ_GFP-Aβ42 (19:34)
wt_GFP
pre1,2Δ_GFP

Figure 8: GFP fluorescence levels in GFP, GFP-Aβ42 or GFP-Aβ42 (19:34) expressing wild type, pre1Δ and pre1-2Δ yeast transformants

GFP/GFP-Aβ transformants were generated in wild type, pre1Δ and pre1-2Δ cells (*Saccharomyces cerevisiae*, Wcg4a), and stored on selective minimal YNB+2%glucose (-ura) agar plates at 4ºC. A single yeast colony from stock agar plates was inoculated in 5mL YNB+2%glucose (-ura) and incubated with shaking at 30ºC overnight. The overnight culture was resuspended in fresh YNB+2%glucose (-ura) media to an initial cell density (OD at 600nm) of 0.2. The culture was then incubated at 30ºC with shaking. Aliquots at different cell densities were collected and observed under the fluorescent microscope. The percentage of cells expressing green fluorescence in wild type compared individually to pre1Δ **(A)** and pre1-2Δ **(B)** cells expressing GFP, GFPAβ42 and GFPAβ42 (19:34) fusion proteins were quantified at different phases of growth starting from early exponential phase (OD: 0.2) till late-log phase (OD: 3.3) The percentage of GFP fluorescence is significantly reduced in wild type cells expressing GFP-Aβ42 (**, $p<0.001$), compared to those expressing GFP or GFP-Aβ42 (19:34) throughout the growth phase. The percentage of GFP fluorescence was similar in wild type, pre1Δ and pre1-2Δ cells expressing GFP and GFP-Aβ42 (19:34). Comparing the wild type GFP fluorescence was increased (##, $p<0.05$) in GFP-Aβ42 expressing pre1Δ and pre1-2Δ cells throughout the growth phase (OD 0.7-3). Data is expressed as mean ± SEM (n=4).

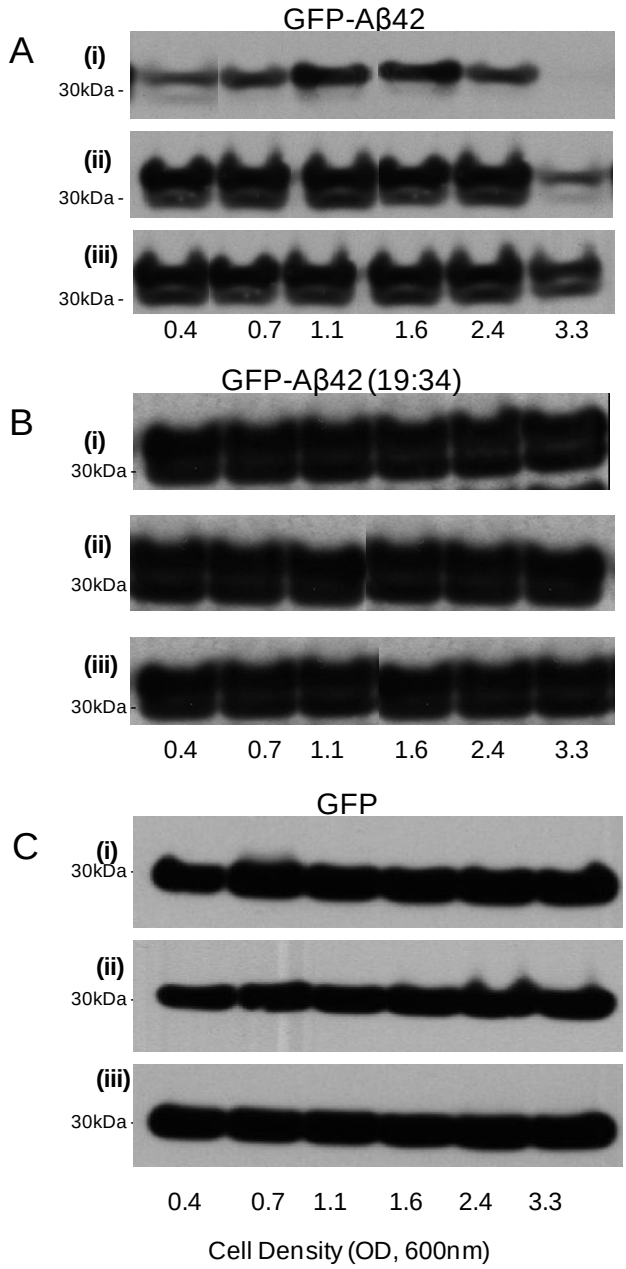

Figure 9: Expression levels of GFP, GFP-Aβ42 and GFP-Aβ42 (19:34) fusions in wild type, pre1Δ and pre1-2Δ yeast transformants

GFP/GFP-Aβ transformants were generated in vacuolar protease deficient yeast mutants (*Saccharomyces cerevisiae* Wcg4a, pre1Δ and pre1-2Δ), and stored on selective minimal YNB+2%glucose (-ura) agar plates at 4ºC. A single yeast colony from stock agar plates was inoculated in 5mL YNB+2%glucose (-

ura) and incubated with shaking at 30ºC overnight. The overnight culture was resuspended in fresh YNB+2%glucose (-ura) media to an initial cell density (OD at 600nm) of 0.2. The culture was then incubated at 30ºC with shaking. Aliquots at different cell densities (OD 600nm, 0.4-3.3) were collected for immunoblotting analysis. Cell extracts (50µg) from wild-type **(i)**, pre1Δ **(ii)** and pre1-2Δ **(iii)** cells expressing **(A)** GFPAβ42 **(B)**, GFPAβ42 (19:34) and **(C)** GFP were probed using anti-Aβ (WO2) or anti-GFP.

8.5 Discussion:

In chapter 7, the GFP tagged Aβ expressing system was utilized as a model for studying the intracellular accumulation of Aβ42. This system allowed the study of the various degradation pathways involved in the clearance of Aβ aggregates in the cell, without any loss of viability. Intracellular degradation pathways like autophagy and ubiquitin-proteasome have been comprehensively studied in yeast cells (Abeliovich and Klionsky, 2001; Hilt et al., 1996; Hilt and Wolf, 1996; Hochstrasser, 1995; Jentsch, 1992a, b; Nair and Klionsky, 2005; Yang and Klionsky, 2009). In addition, a variety of mutants deficient in specific processes of these pathways are available which can be used to dissect the mechanism and the various elements associated with Aβ42 trafficking and degradation inside the cell.

8.5.1 Disruption of autophagic vesicle (AV) synthesis reduced GFP-Aβ42 trafficking and degradation

The localization and expression of GFP-Aβ42 was determined in the mutant deficient of AV synthesis (atg8Δ). The Atg8p protein (and human homologue LC3) is essential for the formation of AV's that deliver intracellular components to the vacuole for degradation (Kabeya et al., 2000). Compared to the punctate inclusion pattern of localization in wild type GFP-Aβ42, the atg8Δ cells showed a more diffuse form of distribution. In addition the atg8Δ cells increased levels of

GFP-Aβ42 during late log phases of growth (Figure 1, 2, 3). Overall, the data suggested that the disruption of AV synthesis lead to a reduced ability to sequester the GFP-Aβ42 resulting in increased accumulation of GFP-Aβ42 in the mutant compared to the wild type.

The function of Atg8p protein in yeast autophagy is well characterized. Atg8p undergoes conjugation to phosphatidylethanolamine forming the Atg8p-PE complex. The Atg8p-PE complex plays an important role in the expansion of the autophagic membrane vesicle (phagophore) and in the formation of the autophagosome/AV (Huang et al., 2000; Xie et al., 2008). *Atg8* gene expression is induced at least 10-fold in response to starvation (Gasch et al., 2000; Kirisako et al., 1999). In wild-type cells, GFP-Aβ42 is markedly reduced during late log phases of growth (Figure 3) which is a period of starvation in yeast. However compared to the wild type cells, the levels remain unchanged in the atg8Δ mutant throughout all stages of cell growth, most likely due to the inability to generate autophagosomes (AV), despite the initial signal by cell starvation to induce an autophagic response. Indeed, the atg8Δ mutants have been shown previously to have a low resistance to starvation conditions due to inability to form AV's and undergo autophagy (Xie et al., 2008). Interestingly, in wild-type cells only GFP-Aβ42 was reduced whereas GFP and GFP-Aβ42 (19:34) levels remained relatively stable during the late log phases. As GFP-Aβ42 (19:34) is unable to aggregate, these findings suggest that autophagy has a role in clearing Aβ42 aggregates and its up-regulation during the late stages of cells growth can enhance the clearance of these aggregates.

The homolog of Atg8p in mammals belongs to a multigene family, consisting of GATE16 (GABA-A receptor-associated protein like protein), GABARAP (GABA-A receptor-associated protein), and LC3 (microtubule associated protein 1) (Amar et al., 2006; Behrends et al., 2010; Hemelaar et al., 2003). Reports show co-localization of Aβ with LC3-II indicating that internalized Aβ can associate with autophagosomes (AV) (Hung et al., 2009). Also, a recent study showed that APP over-expressing mice with beclin1 (an autophagy related

protein, Atg6p in yeast) deficiency (APP+Becn1+/–) had reduced levels of LC3 associated with intraneuronal accumulation of Aβ and AD like neurodegeneration and pathology (Pickford et al., 2008). These findings clearly showed that the disruption of neuronal autophagy can contribute to AD pathology. There are more than 30 autophagy-related (ATG) proteins identified so far in yeast. Analysis of yeast mutants deficient in ATG proteins can therefore help understanding the pathway of intracellular Aβ clearance and identify potential targets for intervention. A recent study has shown that cells deficient in Atg5p show increased levels of Aβ and altered metabolism (Tian et al., 2011). It is notable that Atg5p is a highly conserved protein which binds to Atg12p, and is involved in Atg8p lipidation and autophagosome (AV) synthesis (Mizushima et al., 1998; Mizushima et al., 2001).

8.5.2 Vacuolar proteases mediate GFP-Aβ42 degradation during late log phase:

Previous studies of AD brain revealed a marked up-regulation of lysosomal activity, including extensive involvement of various acid hydrolases and proteases such as cathepsins B and D with Aβ protein deposits (Cataldo et al., 1995; Cataldo et al., 1996; Dreyer et al., 1994; Evin et al., 1995; Nixon and Cataldo, 1993; Tagawa et al., 1991). Several lines of evidence indicate that autophagy in AD is predominantly a cause of defective lysosomal proteolysis (Nixon and Yang, 2011). In yeast, proteinases pep4p (yscA, homolog of cathepsin D) and cvt1p (yscB, member of subtilisin family) are the vital endopeptidases which are responsible for activation of most of the proteases which operate in the vacuolar (lysosomal) lumen under nutritional stress conditions and autophagy (Nair and Klionsky, 2005; Teichert et al., 1989).

Unlike the atg8Δ mutant which showed diffuse fluorescence, GFP-Aβ42 showed increased punctate fluorescence in the vacuolar protease deficient cells (pep4Δ and cvt1Δ). These findings suggest that although the GFP-Aβ42 can be

sequestered into AVs, the lack of vacuolar proteases prevent its degradation, leading to the accumulation of Aβ42 containing vesicles. This notion is supported by the findings that compared to wild-type cells, the pep4Δ and cvt1Δ mutants showed accumulation of GFP-Aβ42 levels during late log phase (Figure 4, 5, 6), suggesting that degradation by the vacuole is impaired at these stages of growth. These findings are in line with others that show vacuolar hydrolase activity of pep4p and cvt1p are required for degradation of autophagic bodies (Xie et al., 2008) and are also associated with targeted degradation of misfolded proteins in the vacuole (Hong et al., 1996). A similar pattern of AV accumulation and neuritic dystrophy is also observed in the brain when lysosomal degradation is inhibited by deletion of cathepsins (pep4p in yeast) (Felbor et al., 2002; Koike et al., 2000; Koike et al., 2005) or by lysosomal enzyme inhibitors (Bednarski et al., 1997; Boland et al., 2008; Ivy et al., 1989; Takeuchi and Takeuchi, 2001; Yang et al., 2008). Cathepsin mutations are also associated with lysosomal storage disorders coupled with severe neurodegeneration (Tyynela et al., 2000). Interestingly, compared to wild-type yeast, in the pep4Δ and cvt1Δ mutants the levels of GFP-Aβ42 expression during the active growth phase (OD 0.2-1.1, Figure 5) were unaltered. These results indicate that the proteases pep4p and cvt1p are not involved in actively degrading GFP-Aβ42 during the active growth phase of yeast. Unlike pep4Δ and cvt1Δ, the levels of GFP-Aβ42 were increased during the active growth phase in atg8Δ mutant compared to the wild type. This indicates that low levels of autophagy can operate in the cell during the active growing stage. Atg8p is also known to be involved in the formation of vesicles required for the cytoplasm to vacuole (CVT) pathway which operates constitutively under growing conditions (Kirisako et al., 2000; Nair and Klionsky, 2005). Therefore this result suggests that Aβ42 degradation maybe targeted via the CVT pathway in addition to macroautophagy as both pathways involve Atg8p.

8.5.3 Decreased proteasomal activity increases GFP-Aβ42 accumulation:

Overall data from the GFP-Aβ42 expression in autophagosome/AV synthesis deficient (atg8Δ) cells and vacuolar protease deficient (pep4Δ, cvt1Δ) cells suggests that apart from catabolic mechanisms like autophagy operating during starvation, degradation of GFP-Aβ42 can also occur constitutively during the growth phase. Another pathway that can be active during cell growth and can actively degrade proteins is the ubiquitin-proteasome pathway. Apart from short lived proteins, the 26S proteasome is also responsible for degradation of damaged, misfolded proteins (Cohen et al., 2008; Hilt and Wolf, 1996; Hochstrasser, 1996; Loayza and Michaelis, 1998; Werner et al., 1996). Studies also reveal interactions between UPS and autophagy suggesting a coordinated and complementary relationship between these degradation systems which is critical during periods of cellular stress (Nedelsky et al., 2008).

The expression of GFP/GFPAβ was studied in yeast strains (pre1Δ and pre1-2Δ) bearing mutations in genes coding for two proteolytic proteasome subunits responsible for chymotrypsin like activity: β4 (*PRE1*) and β5 (*PRE2*) (Egner et al., 1995; Kragt et al., 2005). The pre1-2Δ mutant has been shown to have lower chymotrypsin activity than pre1Δ (Heinemeyer et al., 1991). Compared to wild-type cells, GFP-Aβ42 accumulated throughout the growth phases in pre1Δ and pre1-2Δ mutant cells (Figure 7, 8 and 9). This result indicates that in yeast, these proteolytic proteasomal subunits can degrade Aβ42. At the later stages of cell growth (OD3.3) GFP-Aβ42 expression was undetectable in wild-type yeast but also reduced in pre1Δ and pre1-2Δ mutant cells. These results indicate that at later stages of cell growth, autophagy is the prominent pathway that is responsible for the reduction in Aβ42 levels. Differences in GFP-Aβ42 degradation in pre1Δ and pre1-2Δ cells were apparent only during the late log phase (OD 3.3) (Figure 8, 9). This may suggest that autophagy maybe compensating for the differences in chymotrypsin activity between pre1Δ and pre1-2Δ during the growth phase.

Herein this chapter, I showed that levels of Aβ42 can be regulated by both autophagy and the proteasome pathways in the cell. Since Aβ42 has a strong tendency to self-aggregate, it is likely that a variety of GFP-Aβ42 isoforms (low-n oligomer to aggregates) maybe be present in the cell. It is possible that different GFP-Aβ42 forms are degraded differently by autophagy and the proteasome in the cell as it is widely accepted that the proteasome and autophagy have distinct differences in substrates for degradation (Rubinsztein, 2007). It is possible that smaller misfolded oligomeric forms of GFP-Aβ42 are degraded by the proteasome and the larger aggregated forms are degraded by autophagy. This might also explain the different patterns of GFP-Aβ42 expression levels in autophagy-lysosomal pathway and ubiquitin-proteasome deficient mutants.

8.6 Summary

In this chapter the GFP-Aβ expressing yeast model was used for characterizing the role of important pathways involved in the intracellular degradation of Aβ42 aggregates. Mutants deficient in vesicular transport of autophagic vesicles (atg8Δ), acid hydrolases involved in degradation in the vacuole (pep4Δ, cvt1Δ) and proteasomal activity (pre1Δ and pre1-2Δ) have provided insight into some of the pathways involved in the clearance of Aβ42 aggregates inside the cell. Modulation of these cellular degradation pathways to enhance clearance of protein aggregates is gaining interest as a therapeutic strategy in many neurodegenerative diseases particularly AD where the majority of cases are defective in clearing Aβ. Similar to other yeast models for studying protein aggregates such as huntington poly Q aggregates (Sokolov et al., 2006) or α-synculein aggregates (Zabrocki et al., 2005) the GFP-Aβ42 yeast model can also be used to identify/screen agents that can enhance Aβ42 intracellular clearance. In the next chapter, the use of this yeast model to determine the ability of known autophagy enhancer rapamycin in GFP-Aβ clearance is presented. In addition, the molecular action of the AD drug latrepirdine in enhancing autophagy and promoting GFP-Aβ clearance has been assessed.

Chapter 9

The Role of Latrepirdine in Enhancing Aβ42 Clearance

9.1 Introduction:

In chapter 8, the role of the intracellular degradation/clearance pathways (autophagy-lysosome and ubiquitin-proteasome) on distribution and levels of GFP-Aβ42 in yeast was studied. The expression levels and distribution of GFP/GFPAβ fusion proteins were analysed in yeast cells deficient in AV synthesis (atg8Δ), vacuolar proteases (pep4Δ and cvt1Δ) or proteasomal activity (pre1Δ and pre1-2Δ). Overall, the data showed that GFP-Aβ42 accumulated in yeast mutant cells that lacked autophagy or proteasomal activity, indicating that disruption of these intracellular degradation pathways impaired the clearance of GFP-Aβ42 in the cell.

Modulating cellular degradation pathways to enhance clearance of protein aggregates is gaining interest as a therapeutic strategy in many neurodegenerative diseases (Rubinsztein et al., 2007). However, stimulating proteasomal activity as a therapeutic approach can have serious undesirable effects because many key short-lived intracellular regulators, which are essential for the normal functioning of the cell, are also degraded. Therefore up-regulating autophagy is considered to be more safer and tractable alternative as its substrates are generally long lived proteins and are not believed to be selectively degraded (Rubinsztein, 2006). Enhancing autophagy has been suggested as a treatment strategy for Huntington's Disease (HD) (Ravikumar et al., 2004; Sarkar et al., 2007b; Williams et al., 2008) and α-synucleinopathies such as Dementia with Lewy Bodies (DLB; (Crews et al., 2010)). Currently the commonly used pharmacological agent for up-regulating autophagy in neurons is rapamycin (Rubinsztein et al., 2007; Williams et al., 2008). This agent is known to activate autophagy by inhibiting mTOR and has been shown to enhance clearance of Huntington protein and α-synuclein aggregates in various cell and animal models (Crews et al., 2010; Ravikumar et al., 2004). It has also been shown to protect SH-SY5Y cells from Aβ42 toxicity (Hung et al., 2009), and recently been shown to improve cognition and reduce cerebral amyloid load in a mouse model of AD (Spilman et al., 2010). A recent study has also shown

that a small molecule enhancer of rapamycin (SMER28) decreases levels of Aβ via Atg5 dependent autophagy in neuronal cells (Tian et al., 2011).

Another agent which has received considerable attention recently as a result of successful phase II clinical trials for HD (Kieburtz et al., 2010) and AD (Doody et al., 2008) is latrepridine (Dimebon, dimebolin). Like rapamycin, latrepridine also shows neuroprotective activity (Bachurin et al., 2001; Lermontova et al., 2001; Wu et al., 2008; Zhang et al., 2010b). A study of synucleinopathy in a mouse model has found that latrepirdine reduced levels of α-synuclein protein deposits and associated neurodegeneration, suggesting enhanced clearance of protein deposits (Bachurin et al., 2009). It has also been shown to modulate Aβ secretion and metabolism in neuronal cells and promote the secretion of Aβ42 into the interstitial fluid of AD mice (Steele et al., 2009). Recent studies have also reported latrepirdine's cognitive enhancing properties in wild-type and AD transgenic mice, although the mechanism of action responsible for improving memory functions is unclear (Giorgetti et al., 2010; Vignisse et al., 2011). It is conceivable that latrepirdine may have multiple targets that may account for its neuroprotective functions; however the studies from Bachurin et al., (2009) and Steele et al., (2009) in particular, suggest a role for latrepirdine in the removal of protein aggregates or preventing the formation through enhancing clearance. This may represent an underlying mechanism for latrepirdine's benefits in neurodegenerative disease characterised by accumulation of misfolded or aggregated proteins. In this chapter, I employed the GFP-Aβ42 expressing yeast model to investigate whether enhancing autophagy can reduce levels of Aβ aggregates. I investigated whether latrepirdine (Dimebon^{TM}) upregulates autophagy similar to that observed for established activators rapamycin or nitrogen starvation. Latrepirdine's ability to alter GFP-Aβ42 levels and protect against oligomer Aβ toxicity in the yeast model was also assessed.

The clearance of Aβ42 from the periphery is thought to play an important role in preventing the accumulation of Aβ in the brain (see introduction Section

1.9.1). Our laboratory has developed an *in vivo* model in which the clearance of peripherally injected human Aβ42 is followed over a period of time (Hone et al., 2003; Sharman et al., 2010). We have used this model to show APOE genotype specific effects on the peripheral clearance of Aβ42, in which the presence of APOEε4 results in impaired clearance from the blood and the major peripheral organ to degrade Aβ, the liver (Sharman et al., 2010). Using this model, the ability of latrepirdine to enhance clearance of Aβ42, in the presence of APOE ε4 was also determined.

9.2 Aims:

1.) Assess the levels of GFP-Aβ42 in wild-type and autophagy deficient (atg8Δ) mutant yeast cells following treatment with rapamycin.
2.) (i) Determine if latrepirdine can induce autophagy by evaluating vacuolar uptake of FM4-64 dye, Pho8 activity and Atg8p localization in latrepirdine treated wild type and atg8Δ yeast cells and (ii) compare activity with those observed for the known activators of autophagy in yeast, nitrogen starvation and rapamycin treatment.
3.) Assess the cellular distribution and levels of GFP-Aβ42 in wild-type and autophagy deficient (atg8Δ) mutant yeast cells following activation of autophagy via latrepirdine.
4.) Determine if enhancing autophagy can protect yeast cells from oligomer Aβ42 induced toxicity.
5.) Determine if latrepirdine can enhance the peripheral clearance of Aβ42, *in vivo*, in the presence of APOE ε4.

9.3 Materials and Methods:

Non transformant or GFP-Aβ42/ GFP-Aβ42 (19:34) expressing (wild type and atg8Δ) yeast cells treated with rapamycin (0.1-0.2μM), latrepirdine (1-5μM) or incubated in nitrogen depleted media were analysed by anti-Aβ (WO2) immunoblotting and assays for measuring autophagy as described in Section

2.2.18. Aβ42 mediated loss of cell viability in yeast (*Candida glabrata*) cells following pre-treatment with latrepirdine, rapamycin or nitrogen starvation was measured by colony count assay as described in Section 2.2.4.3.

APOE KO mice were injected with Aβ42 (20µg) +ApoE4 lipid emulsions in the absence or presence of latrepirdine (3.5mg/kg). Following injections, the animals were sacrificed at different time points (2.5, 5 and 15 min) and the levels of Aβ42 in the blood plasma and liver tissues were determined by immunoblotting analysis as described in Section 2.2.19. The peripheral clearance experiments in mice were performed by Dr Ian Martins, Kevin Taddei, Mike Morici and Linda Wijaya from our laboratory.

9.4 Results:

9.4.1 Rapamycin treatment in GFP-Aβ expressing wild type and atg8Δ yeast cells

To determine if activation of autophagy would reduce levels of intracellular Aβ42 in yeast, actively growing (OD 0.7) wild type and autophagy deficient mutant (atg8Δ) cells expressing GFP-Aβ42 and wild type cells expressing GFP-Aβ42 (19:34) were treated with rapamycin. Rapamycin inhibits mTOR signalling and activates autophagy by binding to FK-binding protein 12 (FKBP12) and preventing the complex formation with mTORC1. It is also a widely used compound for enhancing autophagy in yeast cells (Klionsky, 2010; Nair and Klionsky, 2005). Following rapamycin treatment for 1h at 30°C, cells were collected for fluorescence quantification, Aβ immunoblotting and cell viability.

The GFP fluorescence images of untreated and rapamycin treated (0.2µM) wt-GFP-Aβ42, atg8Δ-GFP-Aβ42 and wt-GFP-Aβ42 (19:34) expressing cells are shown in Figure 1A-F.The distribution of the GFP fusion proteins in wild-type and atg8Δ cells are similar to that described in chapter 8 (Section

8.4.1). Rapamycin treatment did not appear to alter the distribution of GFP fluorescence but instead in wild-type cells expressing GFP-Aβ42, appeared to reduce the amount of punctate/ diffuse fluorescence. To provide a quantitative assessment, the percentage of green fluorescent cells was estimated following treatment (Figure 1G). Compared to vehicle, rapamycin treatment (0.1 and 0.2μM) resulted in significant reduction in the percentage of cells expressing GFP. However, wild-type cells expressing GFP-Aβ42 were more sensitive to rapamycin where treatment resulted in an 80-95% decrease in Aβ42 levels. Rapamycin treatment of atg8Δ mutant yeast, resulted in a 55-80% decrease in fluorescence levels, whilst treatment of wild type cells expressing non aggregating GFP-Aβ42 (19:34) resulted in a 40-75% decline (Figure 1G).

As a more quantitative measure of levels of the GFP-Aβ proteins after rapamycin treatment, aliquots of cells were collected for Aβ immunoblotting analysis (Figure 2). Compared to vehicle treatment, rapamycin treatment (0.1, 0.2μM) resulted in a significant reduction in Aβ42 levels in all cell lines (Figure 2A, B). In addition, to enhancing autophagy, rapamycin is a potent inhibitor of mTOR which is an important pathway for cell growth and protein synthesis. To rule out the possibility that the reduction in GFP-Aβ42 in wild-type and mutant cells was due to impaired cell growth, percentage cell viability was estimated following treatment. The results (Figure 2C) show that rapamycin treatment did not alter cell viability indicating that the decrease in Aβ levels following rapamycin treatment was not due to a reduction in the percentage of viable cells (Figure 2C). However, it cannot be ruled out that the non-specific effects of rapamycin on protein synthesis contributed to the reduction in GFP-Aβ42 levels in treated wild-type and atg8Δ cells.

The reduction of Aβ42 levels was more prominent in wild-type yeast cells expressing GFP-Aβ42, compared to mutant cells expressing GFP-Aβ42 or wild-type cells expressing GFP-Aβ42 (19:34). Wild-type cells expressing GFP-Aβ42 were more sensitive to rapamycin where treatment resulted in an 80-95% decrease in Aβ42 levels. Rapamycin treatment of atg8Δ mutant yeast, resulted in a 65-80% decrease in Aβ42 levels, whilst treatment of wild type cells

expressing non- aggregating GFP-Aβ42 (19:34) resulted in a 40-80% decline in GFP-Aβ42 levels (Figure 2B). These results indicate that although rapamycin led to non-specific background effects in yeast, its ability to induce autophagy resulted in a reduction in intracellular GFP-Aβ42. I next investigated if similar to rapamycin; latrepirdine induced autophagy and reduced the intracellular accumulation of GFP-Aβ42 aggregates.

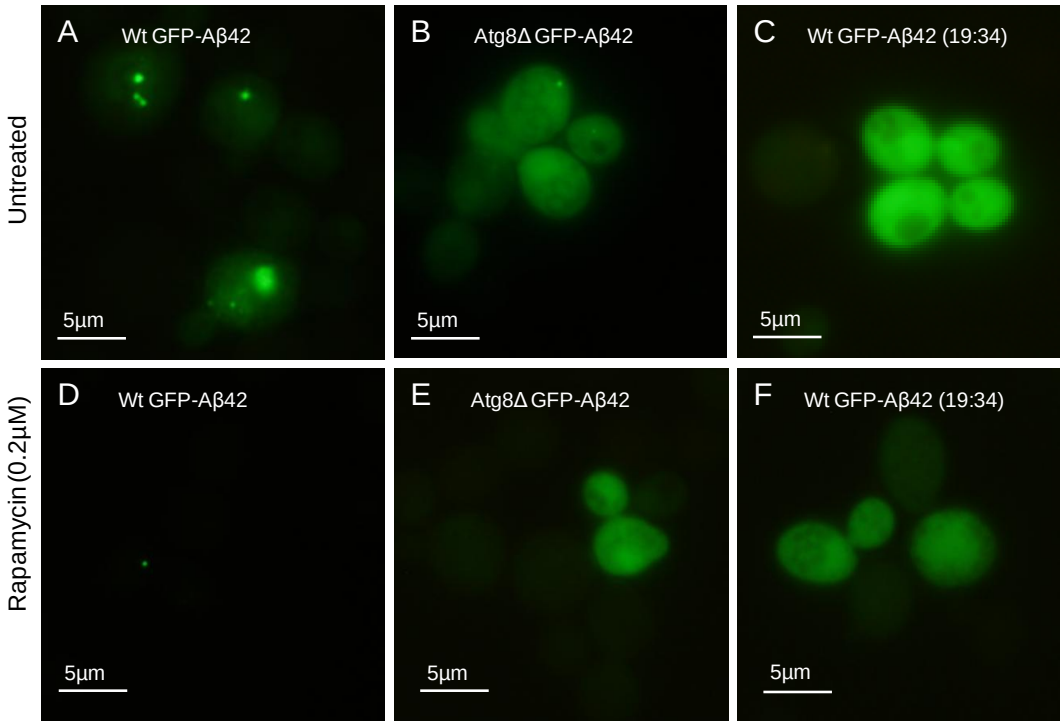

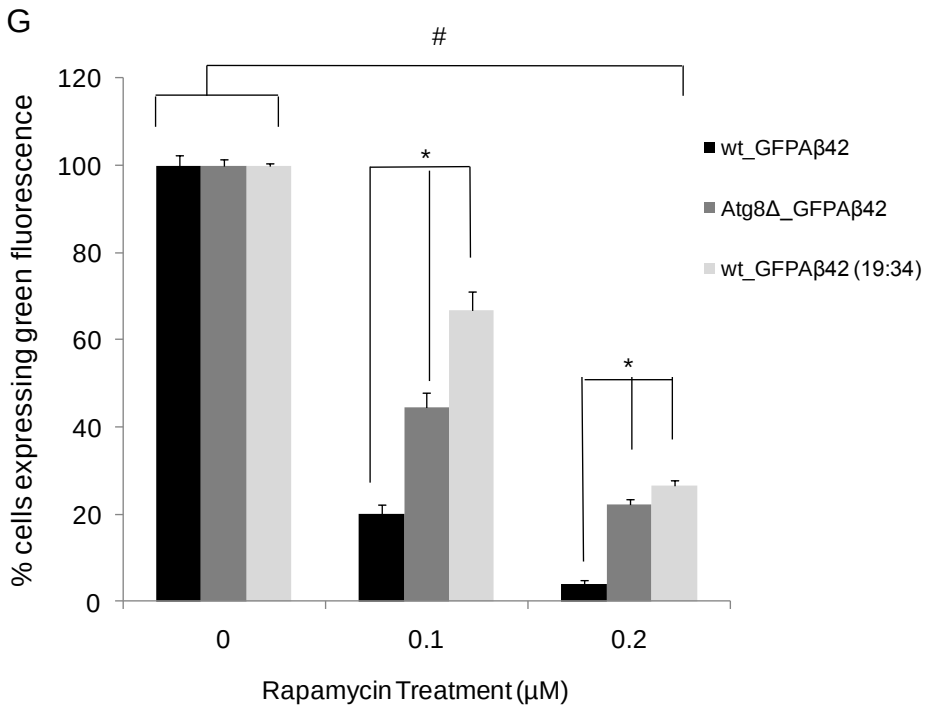

Figure 1: Rapamycin treatment in GFP-Aβ42 and GFP-Aβ42 (19:34) expressing wild type and atg8Δ cells: percentage of fluorescing cells

Wild type and atg8Δ *Saccharomyces cerevisiae* (KVY55) yeast cells were grown overnight in 5ml YNB+2%glucose (-ura) media. Cells were resuspended in fresh YNB+2%glucose (-ura) to a cell density (OD at 600nm) of 0.2-0.3. After incubation at 30ºC, at OD of 0.7, the cells were treated with rapamycin (0, 0.1 and 0.2µM) for 1h. Following treatment the cells were collected for microscopic analysis. GFP fluorescence images of untreated and rapamycin treated (0.2µM) wt-GFP-Aβ42 **(A, D)**, atg8Δ-GFP-Aβ42 **(B, E)** and wt-GFP-Aβ42 (19:34) **(C, F)** expressing cells are shown here. The percentage of cells expressing green fluorescence following treatment was estimated as described in the Section 2.2.16 **(G)**. Compared to untreated control, the percentage of cells expressing green fluorescence were significantly reduced in all cell lines treated with rapamycin (#, $p<0.01$). Compared to wild-type cells expressing GFP-Aβ42 (19:34) or atg8Δ mutant cells expressing GFP-Aβ42, the fluorescence levels were significantly reduced in wild-type cells expressing GFP-Aβ42 (*, $p<0.01$ at 0.1 and 0.2µM rapamycin treatment). Data is represented as mean ± SEM (n=3).

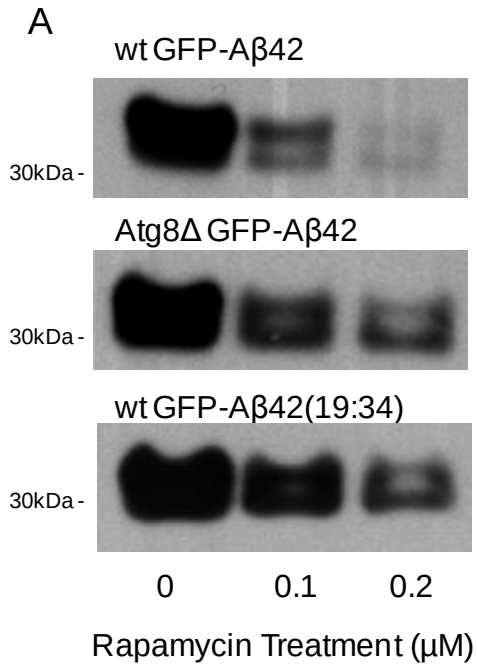
A
wt GFP-Aβ42
30kDa -
Atg8Δ GFP-Aβ42
30kDa -
wt GFP-Aβ42(19:34)
30kDa -
0
0.1
0.2
Rapamycin Treatment (μM)

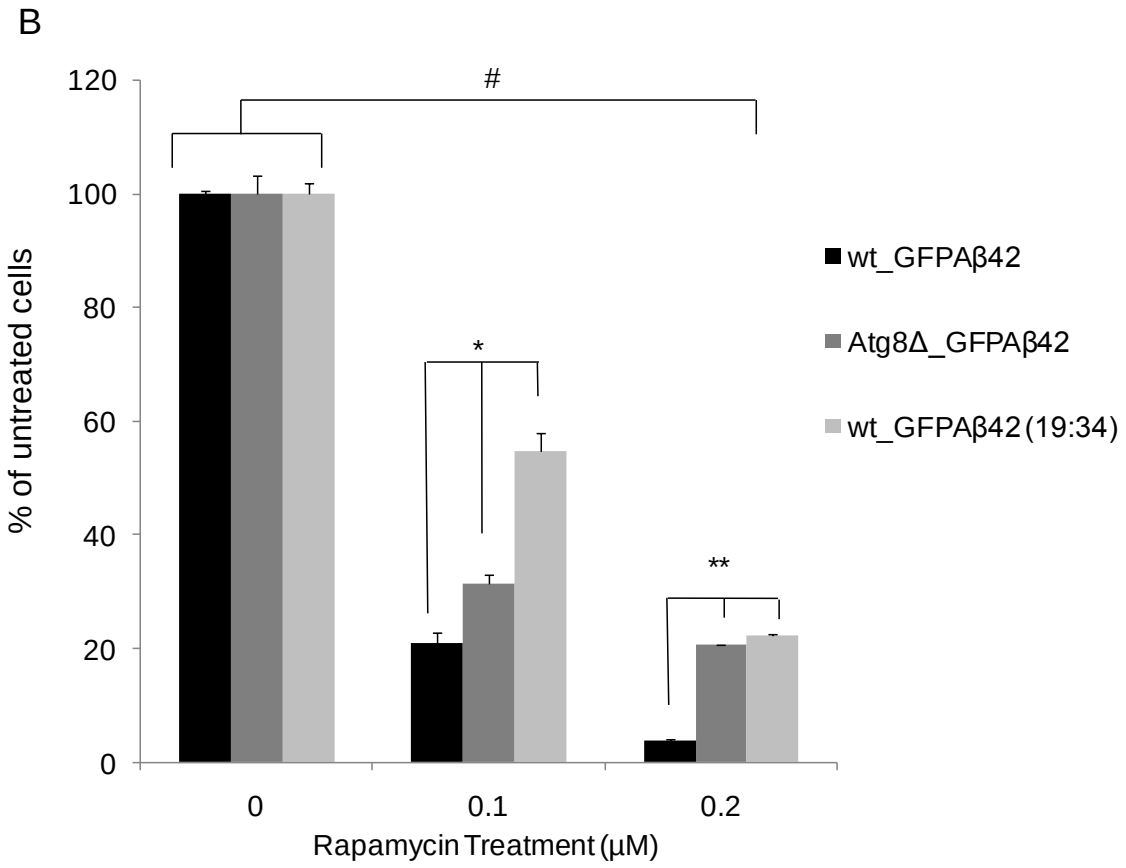
B
120
100
80
60
40
20
0
% of untreated cells
#
*
**
0
0.1
0.2
Rapamycin Treatment (μM)
wt_GFPAβ42
Atg8Δ_GFPAβ42
wt_GFPAβ42(19:34)

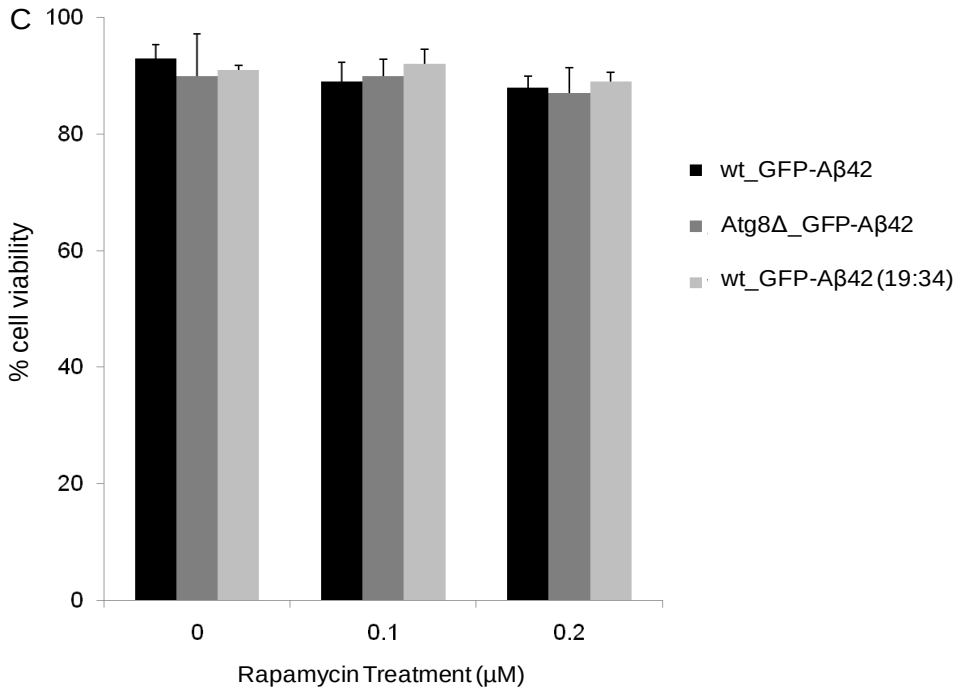

Figure 2: Rapamycin treatment in GFP-Aβ42 and GFP-Aβ42 (19:34) expressing wild type and atg8Δ cells: Levels of GFP-Aβ fusion proteins

Wild type and atg8Δ *Saccharomyces cerevisiae* (KVY55) yeast cells were grown overnight in 5mL YNB+2%glucose (-ura) media. Cells were resuspended in fresh YNB+2%glucose (-ura) to a cell density (OD at 600nm) of 0.2-0.3. After incubation at 30ºC, at OD of 0.7, the cells were treated with rapamycin (0, 0.1 and 0.2µM) for 1h. Following treatment the cells were collected for immunoblotting and viability analysis. Cell extracts (100µg) from untreated and rapamycin treated (0.1µM or 0.2µM) wild-type and atg8Δ mutant cells expressing GFP-Aβ42 or wild-type cells expressing GFP-Aβ42 (19:34) were prepared and probed with anti-Aβ (WO2) **(A)**. Expression levels of Aβ42 (immunoreactive bands) were quantified and expressed as a percentage of untreated control and data represented as mean ± SEM (n=3) **(B)**. Compared to untreated control, levels of Aβ42 were significantly reduced in all cell lines treated with rapamycin (#, $p<0.01$). Compared to wild-type cells expressing GFP-Aβ42 (19:34) or atg8Δ mutant cells expressing GFP-Aβ42, Aβ42 levels were significantly reduced in wild-type cells expressing GFP-Aβ42 (*, $p<0.05$ **, $p<0.01$ at 0.1 and 0.2µM rapamycin treatment). Cell viability was estimated in

all untreated and treated cell lines and expressed as a percentage of untreated control **(C)**. Rapamycin treatment did not significantly alter the viability of cells.

9.4.2 Autophagy in nitrogen starved, rapamycin or latrepirdine treated wild type and atg8Δ yeast cells

Latrepirdine's ability to enhance autophagy was compared to known activators of autophagy in yeast. Incubating cells in growth media depleted of any form of nitrogen source or treating with rapamycin are well known methods of inducing autophagy in yeast (Cheong and Klionsky, 2008). Exponentially growing wild-type and atg8Δ mutant cells (OD 0.7) were either nitrogen starved, treated with various doses of latrepirdine or 0.2μM rapamycin for 6h. Autophagy was then monitored by following the bulk transport of cytosolic material for degradation in the vacuole using a vacuolar specific lipophilic dye FM 4-64 (Journo et al., 2008) and by measuring increased vacuolar alkaline phosphatase (Pho8) activity in cell extracts using the fluorimetric α-naphthyl phosphate assay (Noda and Klionsky, 2008).

Cells that either underwent nitrogen starvation or treated with rapamycin (0.2μM) or latrepirdine (2.5μM) were stained with FM 4-64 (Figure 3). Activation of autophagy was indicated by intravacuolar staining and multivesicular bodies as shown in wild-type cells treated with rapamycin or nitrogen starved (Figure 3B, C) indicating transport of cytosolic material for degradation. However, in the absence of autophagy in either untreated wild-type cells or atg8Δ mutant cells, staining of the vacuole perimeter was observed (Figure. 3A, I-L). The percentage of cells showing intravacuolar staining was estimated and shown in Figure 3Q. As expected, nitrogen starvation and rapamycin treatment resulted in almost 90% of cells showing intravacuolar staining, indicating strong activation of autophagy. Although latrepirdine treatment also showed significantly increased intravacuolar staining (up to ~40% cells, Figure 3D, Q, $p<0.01$), it was ~2 fold less than nitrogen starvation and rapamycin treatment. As expected nitrogen starvation, rapamycin or latrepirdine treatment of atg8Δ

mutant cells did not result in significant intravacuolar staining, consistent with the inability of these cells to undergo autophagy.

Similar results were obtained when vacuolar alkaline phosphatase (Pho8) activity was assessed. Compared to untreated wild-type cells, nitrogen starvation and rapamycin treatment resulted in a 4-5 fold increase in alkaline phosphatase activity (Figure. 4A). Treatment of cells with latrepirdine also resulted in an increase in alkaline phosphatase activity (Figure. 4B). However, Latrepirdine was less potent than either rapamycin or nitrogen starvation (eg. activity for nitrogen starvation = 4.5 U/μg, highest activity for latrepirdine =1.7 U/μg). Treatment of atg8Δ mutant cells did not result in any increase in vacuolar phosphatase activity. To investigate a more specific autophagic marker, I studied the localization of Atg8p, an essential autophagic protein involved in autophagosome formation which is up-regulated and transported to vacuole during autophagy (Xie et al., 2008).

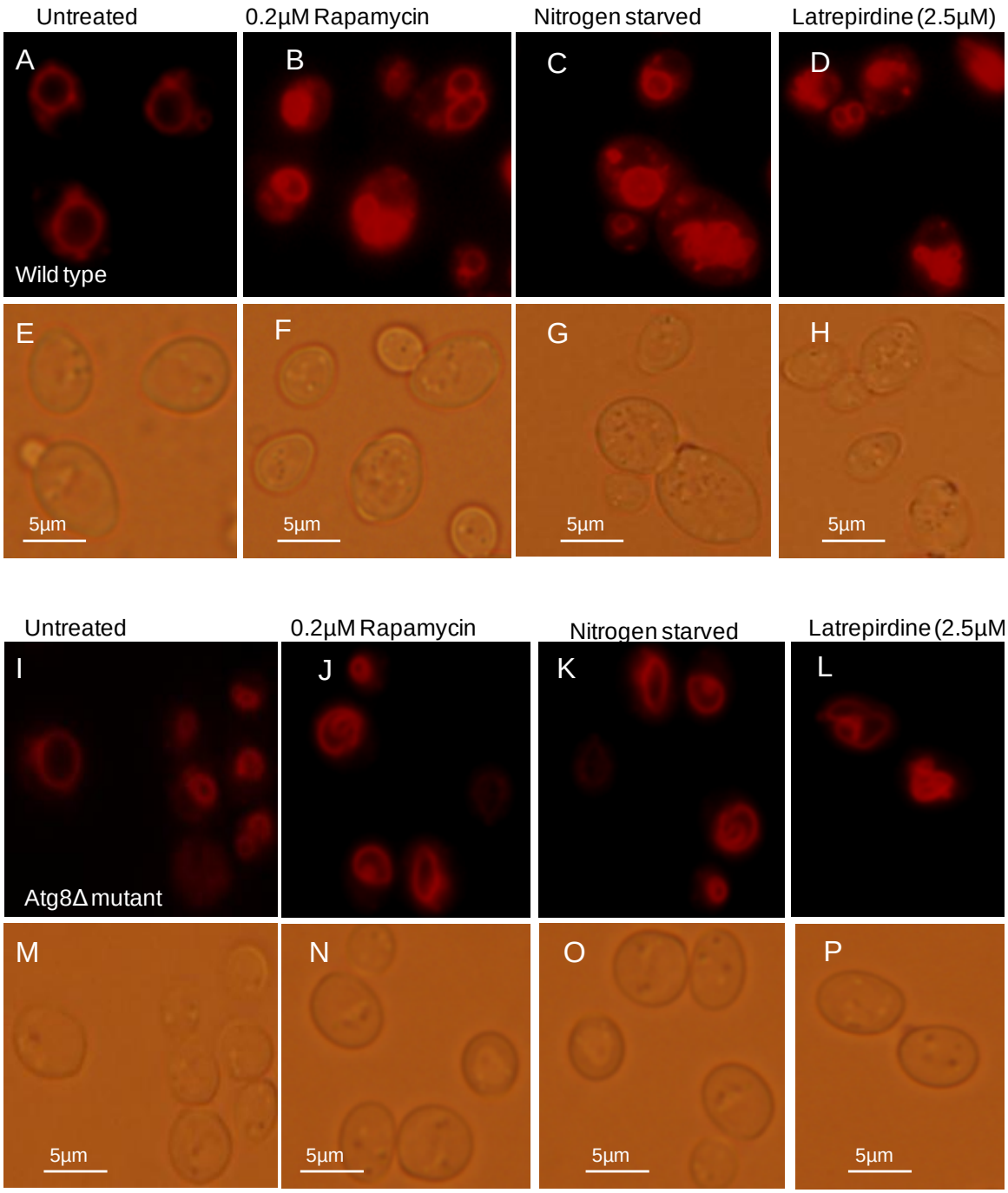
Untreated
0.2µM Rapamycin
Nitrogen starved
Latrepirdine (2.5µM)
A
B
C
D
Wild type
E
F
G
H
5µm
5µm
5µm
5µm
Untreated
0.2µM Rapamycin
Nitrogen starved
Latrepirdine (2.5µM
I
J
K
L
Atg8Δ mutant
M
N
O
P
5µm
5µm
5µm
5µm

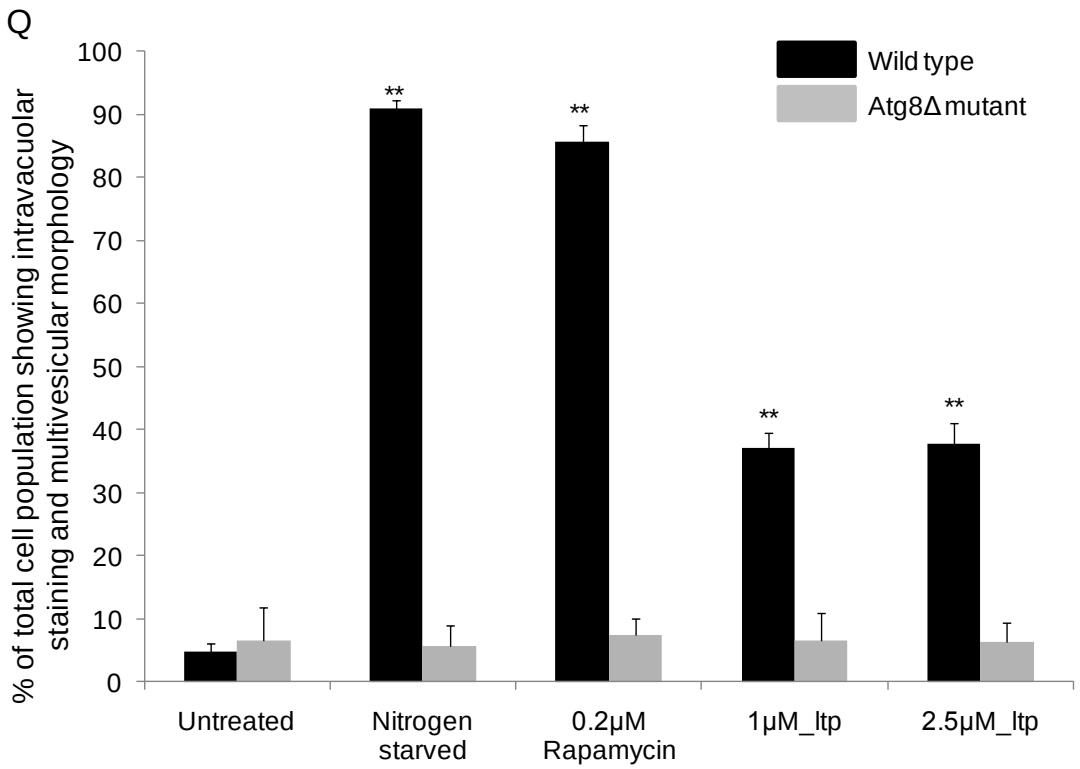

Figure 3: N-starvation, rapamycin and latrepirdine treatment induces vacuolar uptake of FM 4-64 dye.

Wild type and atg8Δ yeast were grown overnight in 5mL YEPD media. Cells were resuspended in fresh YEPD to a cell density (OD at 600nm) of 0.2-0.3. After incubation at 30ºC, at OD of 0.7, the cells were washed in sterile water and resuspended in minimal media (YNB complete) containing rapamycin (0.2μM) or latrepirdine (ltp) (1μM, 2.5μM) or in YNB (-N) media for 6h. Following treatment cells were stained with FM 4-64 as described in the material and methods. FM 4-64 staining was observed by fluorescence microscopy in wild type **(A-H)** and atg8Δ **(I-P)** cells. The number of cells showing intravacuolar staining and multivesicular morphology were counted as percentage of total cell population **(Q)**. Untreated cells showed minimal (<10%) of intravacuolar or multivesicular staining. Significant increase in intravacuolar or multivesicular staining was observed in wild-type cells compared to atg8Δ mutant cells that underwent N-starvation, rapamycin treatment (0.2μM) or latrepirdine treatment (1μM, 2.5μM) (**, $p<0.01$). Data represents mean ±SEM (n=4).

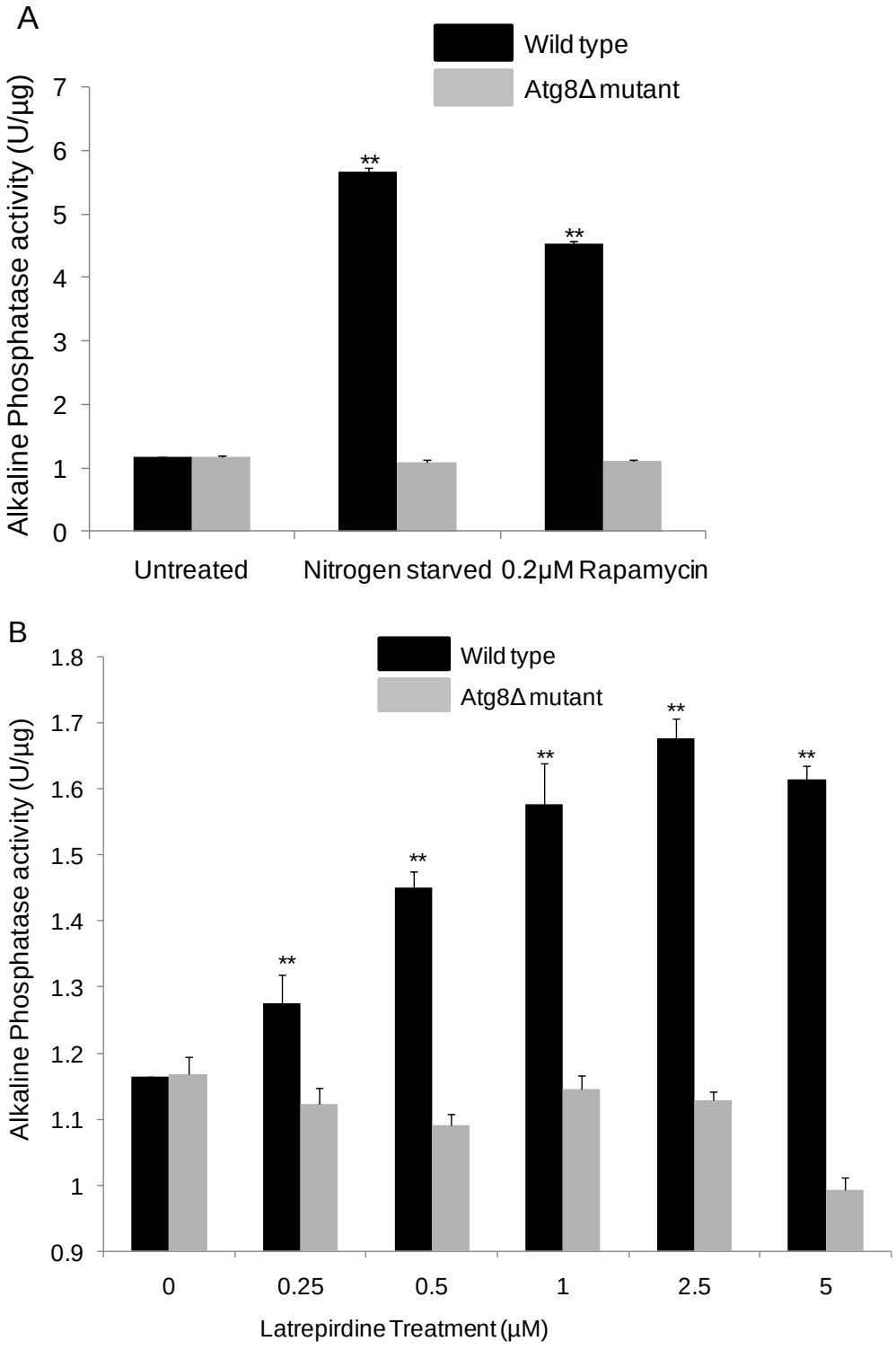

Figure 4: N-starvation, rapamycin and latrepirdine treatment increases vacuolar Alkaline Phosphate (Pho8) activity.

Wild type and atg8Δ yeast were grown overnight in 5mL YEPD media. Cells were resuspended in fresh YEPD to a cell density (OD at 600nm) of 0.2-0.3.

After incubation at 30ºC, at OD of 0.7, the cells were washed in sterile water and resuspended in minimal media (YNB complete) containing rapamycin (0.2µM) or latrepirdine (0.25µM, 0.5µM, 1µM, 2.5µM and 5µM) or in YNB (-N) media for 6h. Vacuolar alkaline phosphatase activity was measured in cell extracts and expressed as U/µg of total protein in the cell extract **(A)**. Alkaline phosphatase activity was significantly increased (**, p< 0.01, n=3) in wild type compared to atg8Δ cells that underwent N-starvation or treatment with 0.2µM rapamycin. Cells treated with latrepirdine exhibited ~4 fold lesser activity than those that underwent N-starvation or rapamycin treatment and thus activities were represented on separate graphs **(B)**. Activity was significantly increased dose dependently in wild type compared to atg8Δ cells treated with latrepirdine (**, p<0.01, n=3). atg8Δ mutant cells that underwent latrepirdine treatment showed similar levels of activity as untreated wild-type cells in accordance with the inability of this cell line to undergo autophagy. Data is represented as mean ± SEM (n=4).

A GFP-Atg8p expressing yeast was used to examine the transport of Atg8p to the vacuole (Yen et al., 2007). atg8Δ cells were transformed with GFP-Atg8p plasmid (pRS306). Starting at OD 0.2 yeast culture (wt, atg8Δ) was cultured until exponential phase (OD 0.7) and then treated with rapamycin (0.2µM) (Figure 5B, F), nitrogen starved (Figure 5C, G) or latrepirdine (2.5µM) (Figure 5D, H) for 6h. Following treatment, the cells were observed by fluorescent microscopy. With activation of autophagy, the GFP-Atg8p is transported to the vacuole for degradation. While the Atg8p is recycled, the GFP moiety remained intact in the vacuole showing diffuse green fluorescence which was used to monitor autophagic flux (Kim et al., 2001a). Compared to vehicle treated cells, rapamycin, nitrogen starvation and latrepirdine treated cells showed significant increase in cells with diffuse GFP fluorescence. With 2.5µM latrepirdine treatment ~25% of the cell population exhibited diffuse GFP fluorescence compared to ~90% with nitrogen starvation or rapamycin treatment (Figure 5I), indicating activation of autophagy. Overall, employment of three different

markers of the autophagy-vacuolar pathway indicates that although not a very strong inducer of autophagy compared to nitrogen starvation or rapamycin, latrepirdine induces autophagic like characteristics in yeast. Next I determined if similar to rapamycin, latrepirdine enhanced autophagy contributes to a reduction in GFP-Aβ42 levels.

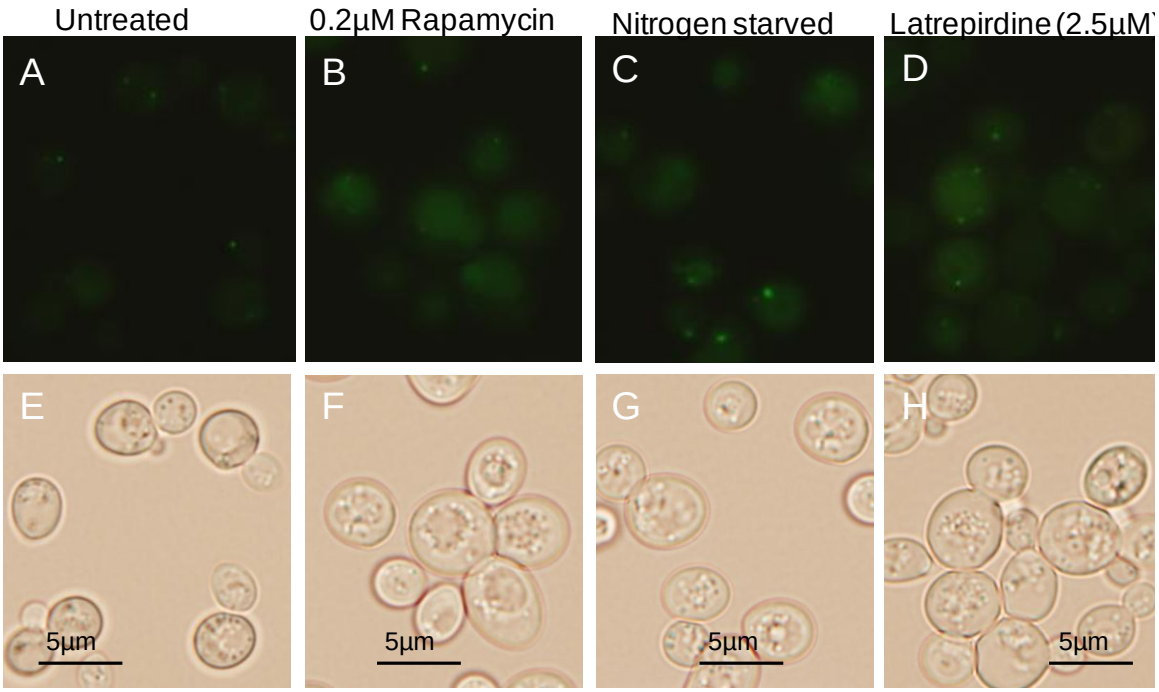

I

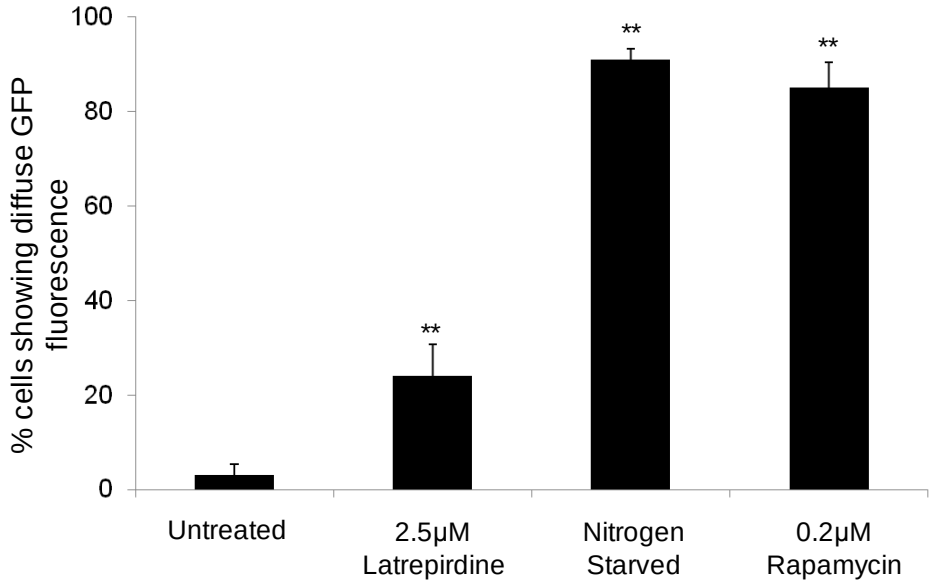

Figure 5: N-starvation, rapamycin and latrepirdine treatment enhances transport of GFP-Atg8p to the vacuole.

atg8Δ cells were transformed with GFP-Atg8p plasmid with URA selectable marker. The transformants were stored on YNB+2%glucose (-ura) agar plates at 4ºC. A single yeast colony from stock agar plates was inoculated in 5mL YNB+2%glucose (-ura) and incubated with shaking at 30ºC overnight. The overnight culture was resuspended in fresh YNB+2%glucose (-ura) media to a cell density (OD at 600nm) of 0.2. At cell density of 0.7, the cells were treated with rapamycin (0.2μM) **(B, F),** Nitrogen starved **(C, G)** or latrepirdine (2.5μM) **(D, H)** for ~6h till OD 0.8. Following treatment, the cells were observed by fluorescent microscopy. The number of cells showing diffuse green fluorescence was counted as a percentage in the total cell population **(I)** as described in the materials and methods. Data is represented as mean ± SEM (n=4). Rapamycin (0.2μM), Nitrogen starved or latrepirdine treatment (2.5μM) significantly increased the levels of diffuse GFP fluorescence (**, $p<0.01$, n=3) indicating the increased transport of GFP-Atg8p to the vacuole.

9.4.3 Latrepirdine treatment in GFP-Aβ expressing wild type and atg8Δ yeast cells

To determine if activation of autophagy by latrepirdine reduced GFP-Aβ42 levels, wild type and autophagy deficient mutant (atg8Δ) cells expressing GFP-Aβ42 and wild type yeast expressing GFP-Aβ42 (19:34) were treated with latrepirdine. Exponentially growing yeast cells (OD 0.7) were treated with different concentrations of latrepirdine ranging from 1-5μM. After incubating at 30°C till OD 0.8 for ~4-5h, aliquots were collected for fluorescence quantification, Aβ immunoblotting and cell viability.

GFP fluorescence images of untreated and latrepirdine treated (5μM) wt-GFP-Aβ42, atg8Δ-GFP-Aβ42 and wt-GFP-Aβ42 (19:34) expressing cells are shown in Figure 6A-F. The distribution of the GFP fusion proteins in wild-type and atg8Δ cells are similar to that described in chapter 8 (Section 8.4.1). Latrepirdine treatment did not appear to alter the distribution of GFP fluorescence but instead in wild-type cells expressing GFP-Aβ42, appeared to reduce the amount of punctate/ diffuse fluorescence. To provide a quantitative assessment, the percentage of green fluorescent cells were estimated following treatment (Figure 6G). Compared to vehicle, latrepirdine treatment resulted in a significant reduction in percent of green fluorescent cells in wild type expressing GFP-Aβ42 (Figure 6G). A decrease of ~10% with 1μM up to ~40-50% with 2.5-5μM was observed with latrepirdine treatment in wild type expressing GFP-Aβ42 (Figure 6G). However, latrepirdine treatment did not significantly alter the percentage of fluorescence wild-type yeast cells expressing GFP-Aβ42 (19:34) or atg8Δ mutant cells expressing GFP-Aβ42 (Figure 6G).

As a more quantitative measure of the levels of the GFP-Aβ proteins after latrepirdine treatment, aliquots of cells were collected for Aβ immunoblotting analysis (Figure 7). Compared to vehicle, latrepirdine treatment resulted in a significant reduction in GFP-Aβ42 protein levels in wild-type cells as measured by densitometric analysis of the Aβ immunoreactive bands (Figure

7A and B). A decrease of ~20% with 2.5µM up to ~40% with 5µM was observed with latrepirdine treatment in wild type expressing GFP-Aβ42 (Figure 7B). However, latrepirdine treatment did not significantly alter the Aβ levels of wild-type yeast cells expressing GFP-Aβ42 (19:34) or atg8Δ mutant cells expressing GFP-Aβ42 (Figure 7A and B). In addition, latrepirdine treatment did not alter cell viability (Figure 7C).

Overall, the data indicated that latrepirdine can reduce the levels of GFP-Aβ42 in wild type cells expressing GFP-Aβ42. Unlike rapamycin, latrepirdine treatment reduced Aβ levels only in the wild type GFP-Aβ42 expressing cells and not in atg8Δ GFP-Aβ42 and wild type -GFP-Aβ42 (19:34) cells (compare Figure 6, 7 with 1, 2). Both rapamycin and latrepirdine have shown neuroprotective functions against Aβ toxicity in neurons. I further determined whether rapamycin and latrepirdine pre-treatment enhanced survival against Aβ toxicity in wild type and atg8Δ cells.

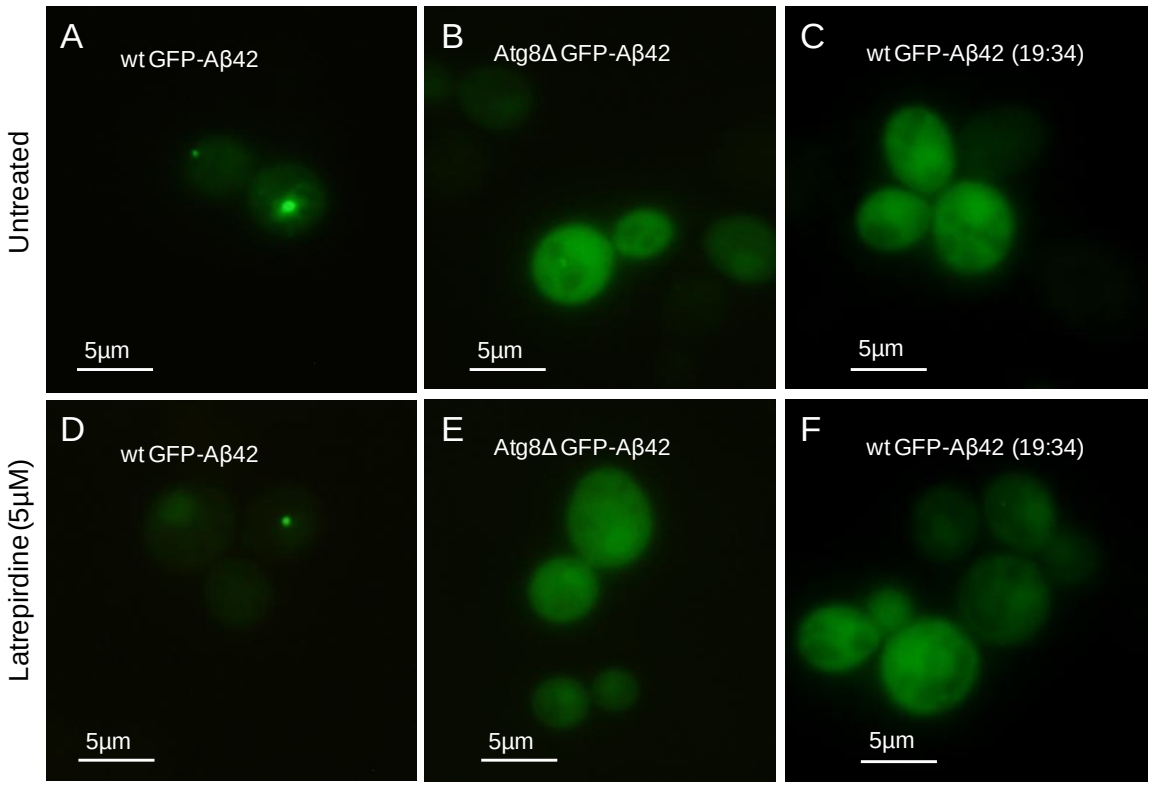
A
wt GFP-Aβ42
B
Atg8Δ GFP-Aβ42
C
wt GFP-Aβ42 (19:34)
Untreated
5µm
5µm
5µm
D
wt GFP-Aβ42
E
Atg8Δ GFP-Aβ42
F
wt GFP-Aβ42 (19:34)
Latrepirdine (5µM)
5µm
5µm
5µm

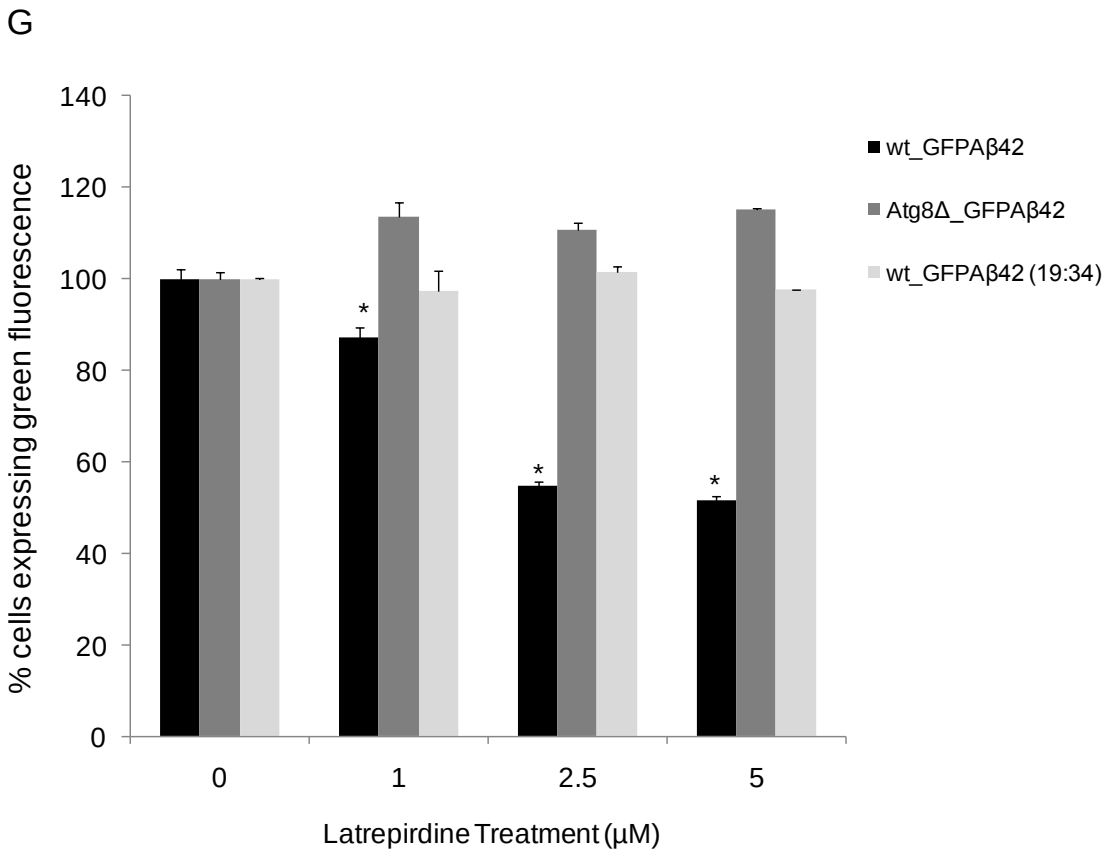
G
% cells expressing green fluorescence
140
120
100
80
60
40
20
0
0
1
2.5
5
Latrepirdine Treatment (µM)
wt_GFPAβ42
Atg8Δ_GFPAβ42
wt_GFPAβ42 (19:34)
*
*
*

Figure 6: Latrepirdine treatment in GFP-Aβ42 and GFP-Aβ42 (19:34) expressing wild type and atg8Δ cells: percentage of fluorescing cells

Wild type and atg8Δ *Saccharomyces cerevisiae* (KVY55) yeast cells were grown overnight in 5mL YNB+2%glucose (-ura) media. Cells were resuspended in fresh YNB+2%glucose (-ura) to a cell density (OD at 600nm) of 0.2-0.3. After incubation at 30ºC, at OD of 0.7, the cells were treated with latrepirdine (0, 1, 2.5, 5μM) for 6h. Following treatment the cells were collected for microscopic analysis. GFP fluorescence images of untreated and latrepirdine treated (5μM) wt-GFP-Aβ42 **(A, D)**, atg8Δ-GFP-Aβ42 **(B, E)** and wt-GFP-Aβ42 (19:34) **(C, F)** expressing cells are shown here. The percentage of cells expressing green fluorescence following treatment was quantified as described in the materials and methods **(G).** Compared to untreated cells, latrepirdine treatment resulted in significant reduction in fluorescence levels in the wild type-GFP-Aβ42 (*$p<0.05$). However no significant change in fluorescence levels was observed in wild type expressing GFP-Aβ42 (19:34) and atg8Δ expressing GFP-Aβ42. Data is represented as mean ± SEM (n=3).

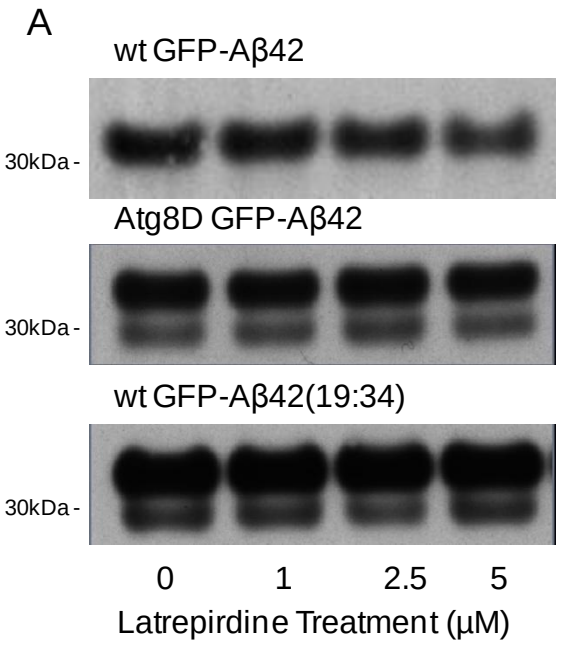
A
wt GFP-Aβ42
30kDa -
Atg8D GFP-Aβ42
30kDa -
wt GFP-Aβ42(19:34)
30kDa -
0
1
2.5
5
Latrepirdine Treatment (μM)

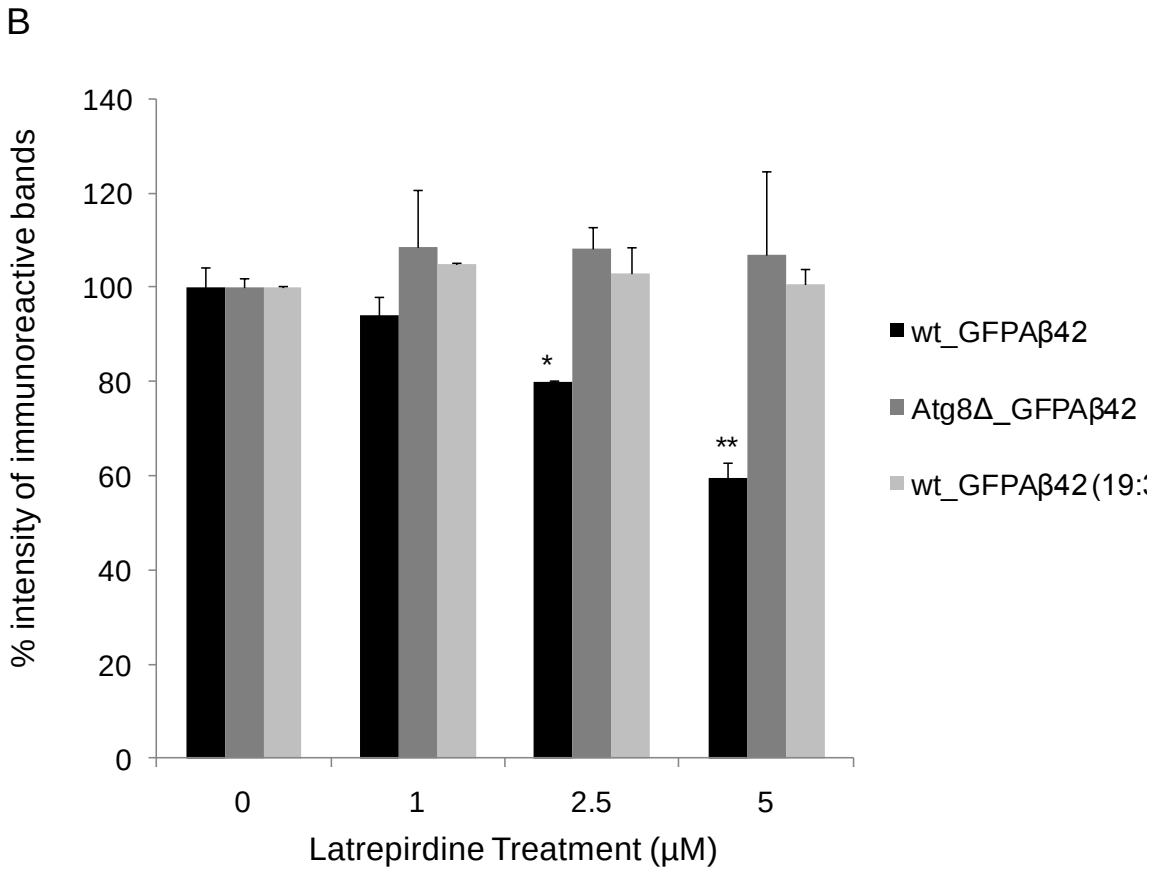
B
% intensity of immunoreactive bands
140
120
100
80
60
40
20
0
*
**
0
1
2.5
5
Latrepirdine Treatment (μM)
wt_GFPAβ42
Atg8Δ_GFPAβ42
wt_GFPAβ42 (19:

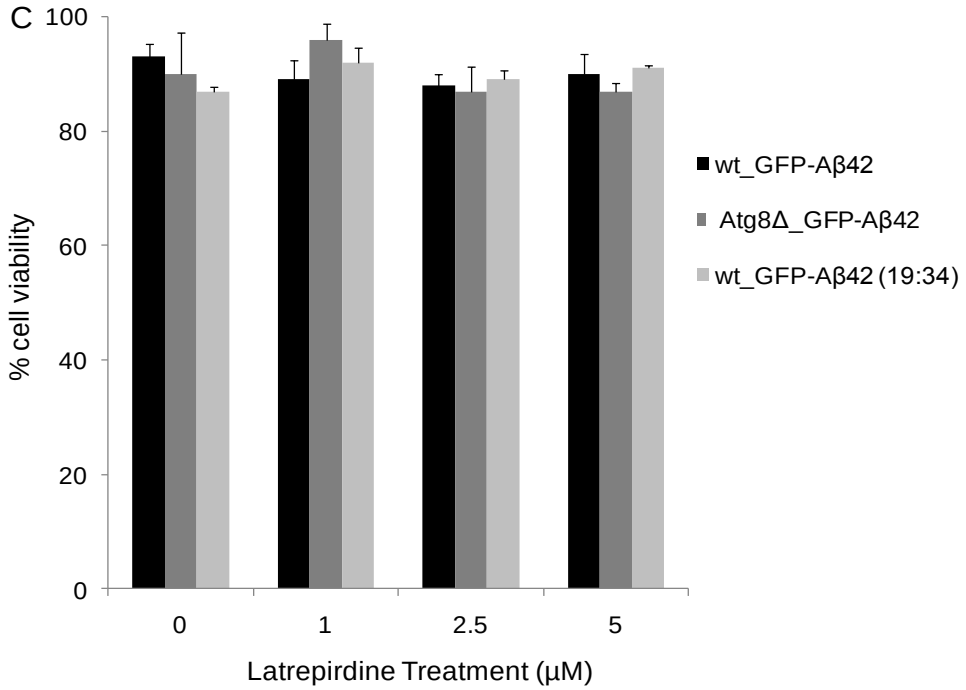

Figure 7: Latrepirdine treatment in GFP-Aβ42 and GFP-Aβ42 (19:34) expressing wild type and atg8Δ cells: Levels of GFP-Aβ fusion proteins

Wild type and atg8Δ *Saccharomyces cerevisiae* (KVY55) yeast cells were grown overnight in 5mL YNB+2%glucose (-ura) media. Cells were resuspended in fresh YNB+2%glucose (-ura) to a cell density (OD at 600nm) of 0.2-0.3. After incubation at 30ºC, at OD of 0.7, the cells were treated with latrepirdine (0, 1, 2.5, 5µM) for 6h. Following treatment the cells were collected for immunoblotting and viability analysis. Cell extracts (50µg) from untreated and latrepirdine treated (1-5µM) wild-type and atg8Δ mutant cells expressing GFP-Aβ42 or wild-type cells expressing GFP-Aβ42 (19:34) were prepared and immunoblotted with WO2 **(A)** Expression levels of Aβ42 (immunoreactive bands) were quantified and expressed as a percentage of untreated control **(C)** and data represented as mean ± SEM (n=3). Compared to untreated cells, latrepirdine treatment resulted in significant reduction in Aβ levels wild type-GFP-Aβ42 (*p<0.05, **p<0.01). However no significant change in fluorescence levels was observed in wild type expressing GFP-Aβ42 (19:34) and atg8Δ expressing GFP-Aβ42. Cell viability was estimated in all untreated and treated cell lines and expressed as a percentage of untreated control. Latrepirdine treatment did not significantly alter the viability of cells.

9.4.4 Aβ42 toxicity in yeast cells pre-treated with rapamycin, nitrogen starvation or latrepirdine

Both rapamycin and latrepirdine have been shown to protect cerebellar neuron cultures against Aβ induced toxicity, modulate Ca^{+} channels (Bachurin et al., 2001; Lermontova et al., 2001; Wu et al., 2008) and enhance mitochondrial function in the absence or presence of cell stresses (Zhang et al., 2010b). Thus, I next determined whether enhancing autophagy by rapamycin, latrepirdine or nitrogen starvation can reduce Aβ42 mediated toxicity in yeast.

Exponentially growing *Saccharomyces cerevisiae* (KVY55) wild type cells (OD 0.7) were incubated with rapamycin (0.2μM), latrepirdine (1-5μM) or nitrogen depleted media for 6h. After treatment, cells were treated with oligomer Aβ42 (2μM) for 20h. Cell viability was measured by viable colony count and represented as percent of untreated (Figure 8). Aβ42 (2μM) treatment caused significant cell death (~80%) in vehicle treated wild type cells. However in nitrogen starved or rapamycin pre-treated wild type cells, Aβ42 caused only ~30-40% cell death. Similarly with latrepirdine pre-treatment (2.5 and 5μM) of wild type cells, Aβ42 caused only 40-50% cell death. The data showed that rapamycin, latrepirdine or nitrogen starvation pre-treatment reduced Aβ42 mediated toxicity in wild type yeast (Figure 8A).

To determine whether activation of autophagy induced protection against Aβ42, autophagy deficient (atg8Δ) cells pre-treated with rapamycin (0.2μM), latrepirdine (1-5μM) or nitrogen starved were treated with Aβ42 similar to the wild type cells. Interestingly, atg8Δ cells showed increased cell viability compared to wild type cells with Aβ42 treatment (see Figure 8B, A). Treatment of cells with 2μM Aβ42 caused cell death of only ~40% (~60% survival) in the atg8Δ cells compared to ~80% (~20% survival) in the wild type. However unlike wild type, the cell survival did not increase in atg8Δ cells pre-treated with rapamycin (0.2μM), latrepirdine (1-5μM) or nitrogen starved following Aβ42 treatment. This showed that rapamycin, latrepirdine or nitrogen starvation did

not affect Aβ42 mediated toxicity in atg8Δ cells (Figure 8B).

Overall the data showed that pre-treatment with known activators of autophagy, rapamycin and nitrogen starvation enhanced survival against Aβ42 toxicity. In a similar fashion, latrepirdine pre-treatment also enhanced survival against Aβ42 toxicity. The increase in cell survival with rapamycin, nitrogen starvation or latrepirdine pre-treatment was evident only in wild type cells and was absent in the autophagy deficient mutant (atg8Δ). This result indicated that stimulation of autophagy in wild type cells increased its resistance against Aβ42 toxicity, whereas due to the lack of autophagy atg8Δ cells did not show any increase in cell survival with rapamycin, nitrogen starvation or latrepirdine. Supporting this data is the previous observations where atg8Δ cells did not show any increase in autophagy with rapamycin, nitrogen starvation or latrepirdine treatment (Figure 3, 4 and 5). Interestingly, the atg8Δ cells displayed an increased resistance to Aβ42 toxicity (Figure 8). Whether this phenomenon is associated with a deficiency in autophagy in the mutant or due to a secondary effect of *Atg8* gene deletion remains to be determined.

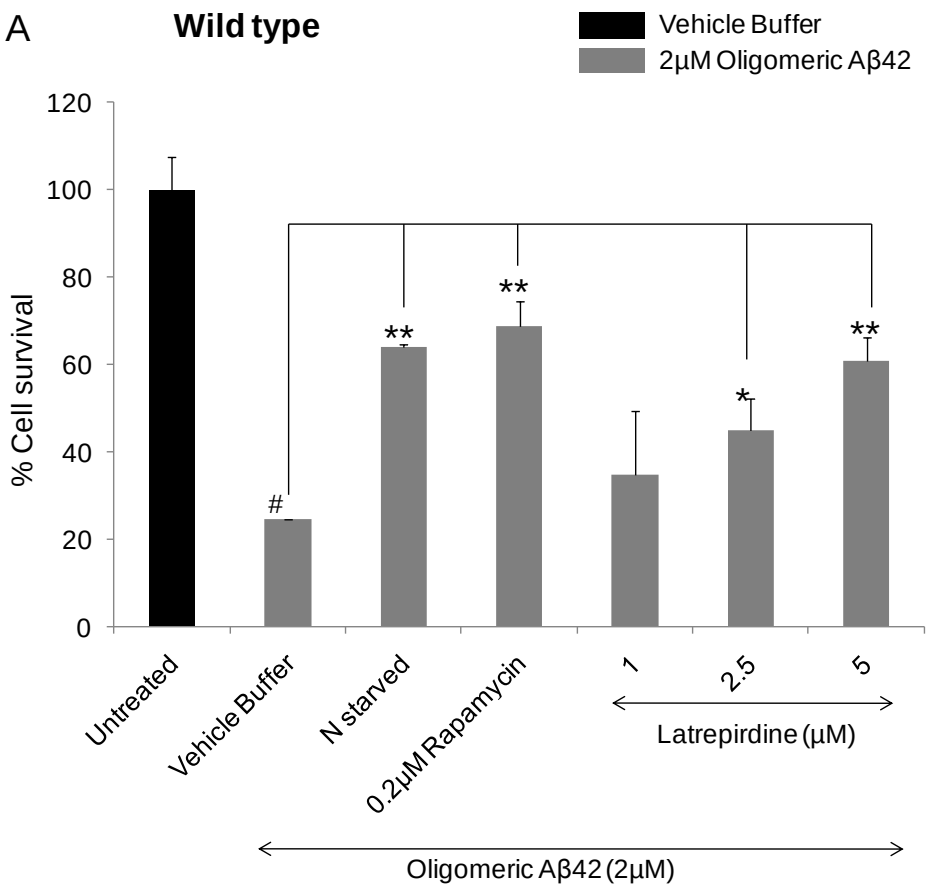
A
Wild type
Vehicle Buffer
2μM Oligomeric Aβ42
% Cell survival
120
100
80
60
40
20
0
#
**
**
**
*
Untreated
Vehicle Buffer
N starved
0.2μM Rapamycin
1
2.5
5
Latrepirdine (μM)
Oligomeric Aβ42 (2μM)

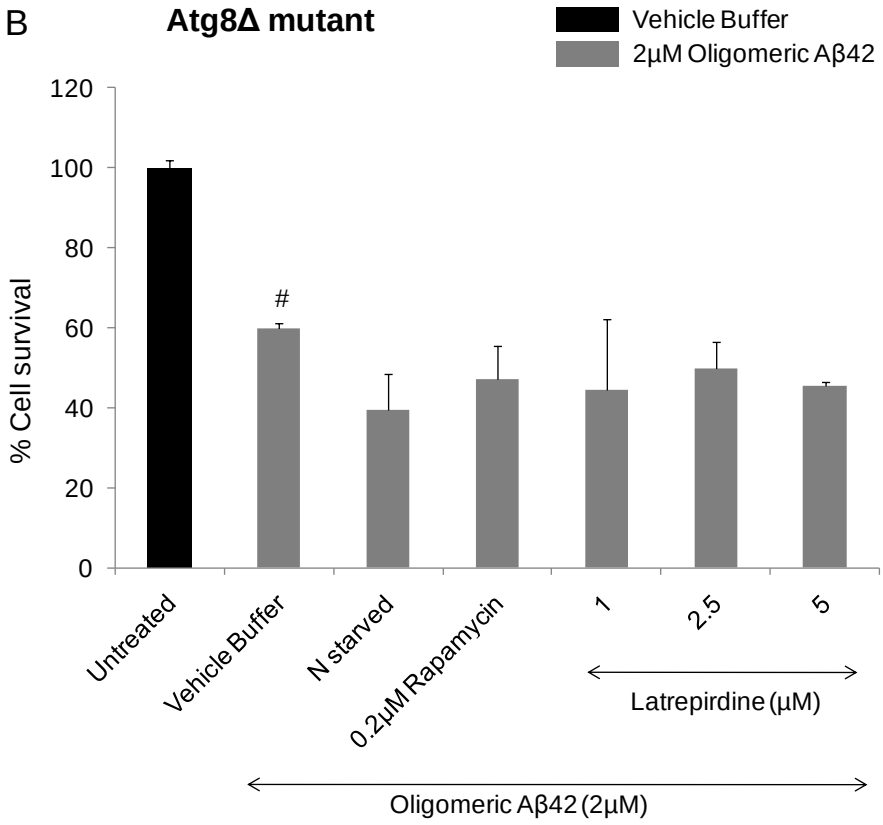
B
Atg8Δ mutant
Vehicle Buffer
2μM Oligomeric Aβ42
% Cell survival
120
100
80
60
40
20
0
#
Untreated
Vehicle Buffer
N starved
0.2μM Rapamycin
1
2.5
5
Latrepirdine (μM)
Oligomeric Aβ42 (2μM)

Figure 8: Oligomer Aβ42 toxicity in wild type and atg8Δ cells pre-treated with rapamycin, nitrogen starvation or latrepirdine

Exponentially growing *Saccharomyces cerevisiae* (KVY55) wild type were incubated with rapamycin (0.2μM), nitrogen depleted media or increasing concentrations of latrepirdine (1-5μM) for 6h. After treatment, cells were treated with oligomer Aβ42 (2μM) for 20h. Cell viability was measured by viable colony count and represented as percent of untreated **(A)**. Aβ42 treatment caused significant loss of viability in vehicle treated cells (#, $p<0.001$). However cell viability following Aβ42 treatment was significantly higher in nitrogen starved, rapamycin treated or latrepirdine (2.5 and 5μM) treated wild type cells compared to vehicle treated (*, $p<0.05$ **, $p<0.01$). Similarly, exponentially growing *Saccharomyces cerevisiae* (KVY55) atg8Δ cells were incubated with rapamycin (0.2μM), nitrogen depleted media or increasing concentrations of latrepirdine (1-5μM) for 6h. After treatment, cells were treated with oligomer Aβ42 (2μM) for 20h. Viability was represented as percent of untreated **(B)**. Aβ42 treatment caused significant loss of viability in vehicle treated cells (#, $p<0.001$). No significant change in cell viability following Aβ42 treatment was observed in nitrogen starved, rapamycin treated or latrepirdine (2.5 and 5μM) treated atg8Δ cells compared to vehicle treated. All data expressed as mean± SEM (n=5).

9.4.5 Latrepirdine enhanced the peripheral clearance of Aβ42 *in vivo*.

A recent study has shown that latrepirdine stimulates secretion of Aβ in cell culture and also into the interstitial fluid of AD mouse brains (Steele et al., 2009), suggesting that latrepirdine may promote the secretion/efflux from neuronal cells/brain. The efflux of Aβ42 from the CNS into the periphery and subsequent clearance/degradation by peripheral tissues is thought to be an important mechanism to regulate Aβ levels within the brain (basis of the peripheral sink hypothesis: see introduction section 1.9.1). Using an *in vivo* model developed by our laboratory to assess the clearance of Aβ42 in the

periphery, latrepirdine's ability to enhance clearance was evaluated.

The clearance of peripherally injected human Aβ42 in plasma and subsequent degradation by peripheral organs was assessed as described in Section 2.2.19. Our laboratory has demonstrated that Aβ is rapidly removed from the plasma by the liver and kidney and the rate of its clearance is affected by ApoE in C57BL/6J and APOE knockout mice (Hone et al., 2003). Recently our laboratory showed that peripheral clearance of Aβ42 was impaired by the presence of ApoE4 (Sharman et al., 2010). This was shown in mice expressing human APOE ε4 (APOE ε4 targeted replacement (TR) mice) and also in APOE knockout mice injected with Aβ42 and lipidated ApoE4. To determine whether latrepirdine can promote clearance of Aβ42 in the periphery in the presence of ApoE4, APOE knockout mice were injected via the lateral tail vein with Aβ42 (20μg) + lipidated ApoE4 in the absence or presence of latrepirdine. Mice were sacrificed at 2.5, 5 and 15 mins and blood plasma and liver tissues were collected. The levels of Aβ42 in blood plasma and liver were determined by immunoblotting analysis (Figure 9).

Aβ42 levels were significantly decreased in the plasma of mice injected with Aβ42+latrepirdine compared to Aβ42+saline at 2.5 and 5 minute time points (Figure 9A, B). At 2.5-5 minutes, the plasma Aβ42 levels were 50-65% less with latrepirdine injections compared to saline (Figure 9B). At 15 minutes, a trend towards a reduction in Aβ42 levels was observed between the two groups but this was not statistically significant. To further determine whether the reduced levels of Aβ42 in the plasma were associated with increased uptake in the liver, total protein extracts from the liver tissue homogenates were analysed by Aβ immunoblotting at similar time points (Figure 9A, C). A significant increase in the levels of Aβ42 was observed in the liver homogenates of Aβ42+latrepirdine injected mice compared to that of Aβ42+saline (Figure 9C). The increase in Aβ42 levels was significant only at the initial time point of 2.5 minutes. However no significant increase was observed at 5 and 15 minutes. Overall the data showed that in the presence of ApoE4, compared to saline, latrepirdine reduced

the levels of intravenously injected Aβ42 in the plasma. This reduction in blood plasma corresponded with an accumulation in Aβ42 in the liver at an early time point, possibly indicating that latrepirdine mediates the rapid transport of Aβ42 from the plasma to the liver.

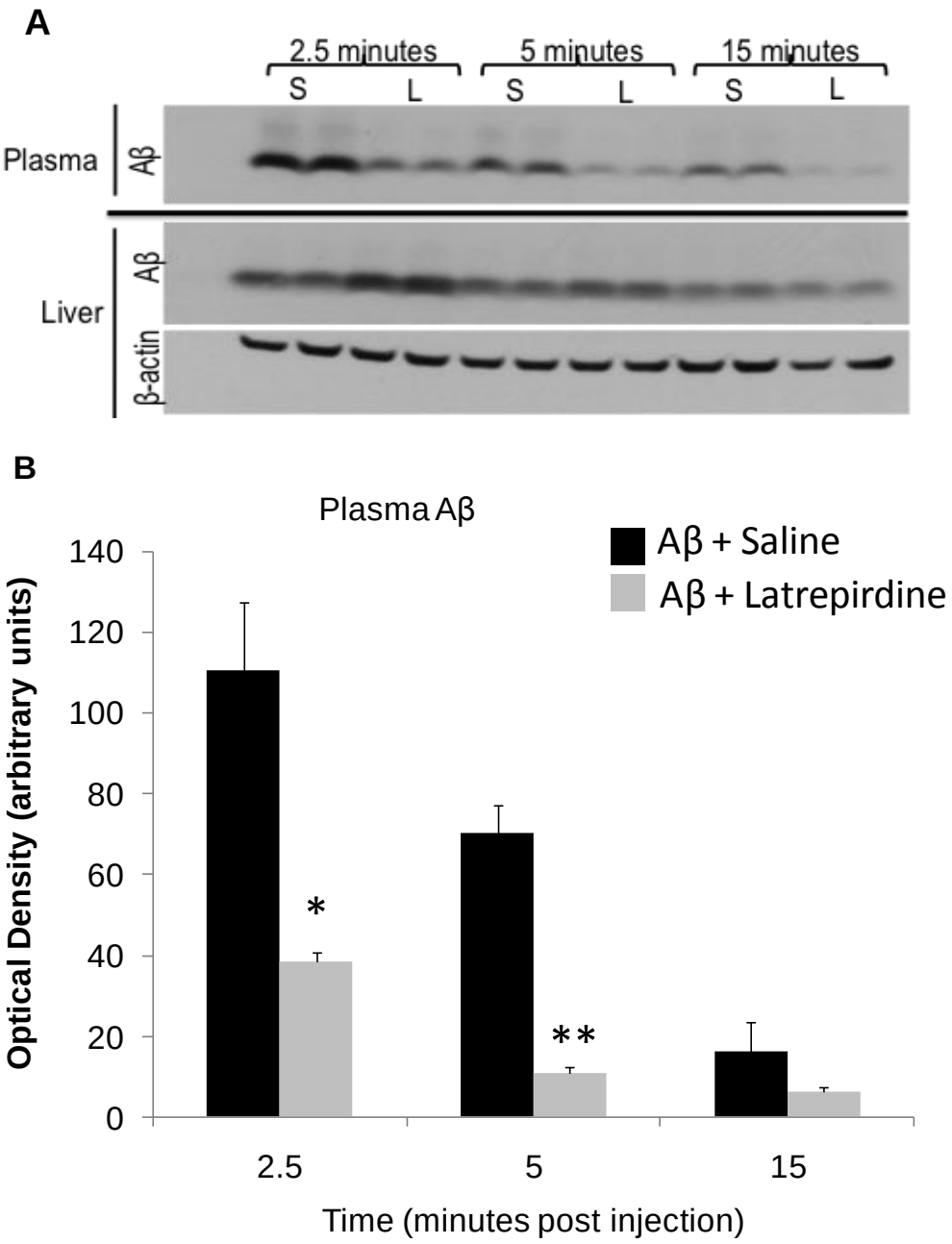

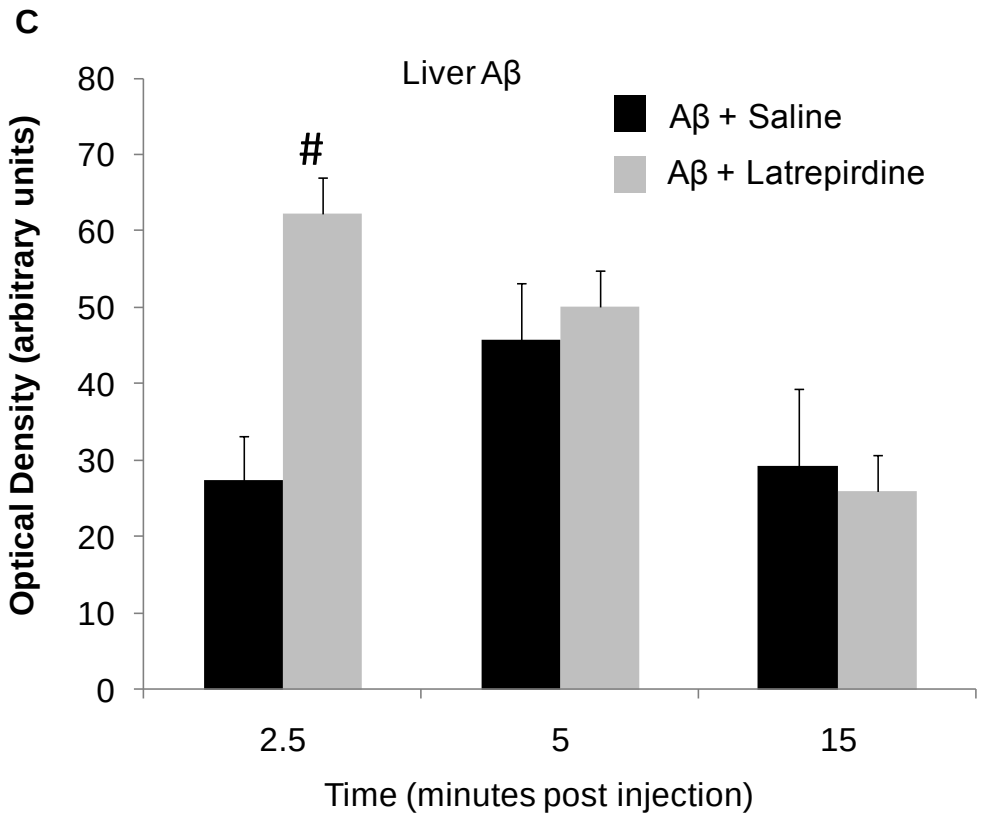

Figure 9: Peripheral Aβ42 Clearance in APOE KO mice administered ApoEε4 and Aβ42 in the presence or absence of latrepirdine.

Saline (S) or latrepirdine (L; 3.5mg/Kg) was co-incubated with Aβ42 (20μg) for 3h prior to combining with ApoEε4 lipid emulsion and injecting into the tail vein of APOE KO mice. Mice were sacrificed at 2.5, 5 and 15 min after injection and Aβ clearance assessed by immunoblotting plasma and liver homogenates **(A)**. In the presence of latrepirdine, more Aβ is cleared from the plasma **(B)**, particularly at 2.5 and 5 min, with a corresponding increased uptake by the liver at 2.5 min **(C)**. Data represents means ±SEM, n=4 in saline (S) group, n=5 in latrepirdine (L) group. Plasma Aβ levels are significantly reduced in mice injected with latrepirdine+Aβ42 compared to saline + Aβ42 injected ones (*, $p<0.05$; ** $p<0.01$). Liver Aβ levels was significantly increased in mice injected with latrepirdine+Aβ42 compared to saline + Aβ42 injected ones (#, $p<0.05$).

9.5 Discussion:

The ubiquitin-proteasome and autophagy-lysosome pathways are the main intracellular degradation pathways for protein and organelle clearance in eukaryotic cells. Dysfunction of these pathways resulting in the accumulation of aggregate prone and toxic proteins in cells contributes to the pathology of several neurodegenerative diseases including AD. Modulating these cellular degradation pathways to enhance clearance of protein aggregates is gaining interest as a therapeutic strategy. In chapter 8, I showed that the proteasome had a greater contribution to reducing intracellular Aβ42 levels in yeast than autophagy, particularly at early stages of cell growth. However, at late log phase of cell growth, autophagy was the major contributor to reducing Aβ42 as cells enter a nutrient starvation stage. It is suggested that enhancing the autophagy-lysosome pathway is a more favourable target to promote clearance of protein aggregates compared to the ubiquitin-proteasome system (Rubinsztein, 2006). One reason is the substrate limitations for proteasome mediated degradation. The proteasome degrades proteins that are ubiquitin tagged and only unfolded proteins which can enter the proteasomal core. By contrast, autophagy has the capacity to degrade folded proteins, large aggregates and even entire organelles. Upregulating autophagy is also considered to be safer and a more attractive alternative compared to enhancing the proteasomal activity as discussed previously in the introduction to this chapter (Section 9.1). Studies from a variety of models have shown that up-regulation of autophagy; both pharmacologically and physiologically can promote clearance of protein aggregates and attenuate neurodegeneration (Berger et al., 2006; Mizushima et al., 2008; Ravikumar et al., 2004; Sarkar et al., 2007b; Williams et al., 2008).

In chapters 7 and 8, the GFP-Aβ expressing yeast model was used to investigate intracellular Aβ accumulation and degradation pathways involved in clearance of Aβ. Disruption of both ubiquitin-proteasome and autophagy-lysosome pathway resulted in increased accumulation of GFP-Aβ42 compared to the wild type in the yeast cell. The use of this model to determine the effect of

rapamycin, a known activator of autophagy, in the clearance of GFP-Aβ42 in yeast cells has been presented here. Further, the ability of latrepirdine in activating autophagy, promoting clearance of GFP-Aβ42 and protecting cells from Aβ42 toxicity provides a novel mechanism of action for this promising drug for AD.

9.5.1 Rapamycin reduced intracellular GFP-Aβ42 levels in yeast

The typical pathway for modulating autophagy is via mTOR, a protein kinase that is central to nutrient-sensing signal transduction, regulation of translation and cell-cycle progression (Klionsky et al., 2005; Noda and Klionsky, 2008). mTOR can be inhibited by rapamycin and related molecules, which belongs to a family of lipophilic macrolide antibiotics that form a complex with the immunophilin FK506-binding protein 12 (FKBP12), which then binds to and inactivates mTOR, leading to an up-regulation of autophagy. Inhibition of mTOR by rapamycin has been widely reported to enhance clearance of aggregate-prone proteins (Berger et al., 2006; Ravikumar et al., 2004; Sarkar and Rubinsztein, 2008). In mammalian AD models, rapamycin induced activation of autophagy have been shown to be neuroprotective and confer cognitive benefits (Hung et al., 2009; Spilman et al., 2010).

Rapamycin treatment of GFP-Aβ42 expressing wild-type cells resulted in a reduction in GFP-Aβ42 levels (Figure 1). It is noted that rapamycin also led to a reduction in levels of GFP-Aβ42 expressed in atg8Δ mutant cells and the levels of the GFP-Aβ42 (19:34) expressed in wild-type cells. This may be due to rapamycin's action as a potent inhibitor of mTOR signalling, which is an important pathway for growth and cell cycle progression. Also rapamycin has been demonstrated to attenuate cell growth and inhibit protein synthesis in many cell lines (Hay and Sonenberg, 2004; Heitman et al., 1991). Results presented in Figure 1C show that cell viability was not significantly altered, however inhibition of protein synthesis cannot be ruled out which may have contributed to the decreased Aβ levels in atg8Δ cells. Moreover,

macroautophagy is largely a non-specific process which sequesters bulk cytoplasmic material for degradation in the vacuole (Nair and Klionsky, 2005) and thus, apart from aggregate proteins, soluble cytosolic proteins and organelles are also degraded which may account for the reduction in levels of the non-aggregated GFP-Aβ42 (19:34). Nevertheless, it was shown that rapamycin mediated reduction in intracellular Aβ42 levels were more pronounced in the wild type cells expressing GFP-Aβ42 (Figure 1) compared to those expressing GFP-Aβ42 (19:34) and atg8Δ mutant cells expressing GFP-Aβ42. The results suggest that rapamycin enhanced autophagy contributes to the removal of aggregated forms of Aβ. However, as is seen by the reduction in Aβ levels in cells that are unable to undergo autophagy, other non-autophagy related effects must be taken into consideration.

Its effects on mTOR signalling cell growth, proliferation and protein synthesis (Hay and Sonenberg, 2004) and its known immunosuppressant effects (Abraham, 1998) indicates that rapamycin can have multiple cellular targets, some undesirable. Synthetic small molecule derivatives of rapamycin have been shown to have benefits at reducing toxicity induced by Huntington protein aggregates whist minimising its adverse effects (Floto et al., 2007; Ravikumar et al., 2004). A recent study has also shown that small molecule enhancer of rapamycin (SMER28) decreased levels of Aβ and APP-CTF via Atg5 dependent autophagy in neuronal cells (Tian et al., 2011). Further, derivatives of known agents shown to have benefits in AD models, such as resveratrol, have been developed and shown to modulate mTOR signalling and facilitate autophagy and Aβ clearance (Vingtdeux et al., 2010).

Autophagy can also be induced by an mTOR-independent route by physiological stress, such as starvation or by 1) lowering myo-inositol-1,4,5-triphosphate (IP3) levels (lithium, sodium valproate and carbamezapine) 2) L-type Ca^{2+} channel antagonists (e.g. verapamil), 3) calpain inhibitors (e.g. calpastatin and calpeptin) and 4) Gsα inhibitors (such as NF449) (Zhang et al., 2007) (Fornai et al., 2008; Sarkar et al., 2005). Trehalose, an mTOR

independent autophagy activator has also shown to enhance clearance of protein aggregates in HD and PD models (Sarkar et al., 2007a). As discussed below, the results presented in this chapter provide evidence in support of latrepirdine's ability to induce autophagy and reduce intracellular Aβ levels, without exhibiting the non-autophagy related effects observed for rapamycin.

9.5.2 Latrepirdine induced autophagy and reduced intracellular levels of GFP-Aβ42

Latrepirdine (Dimebon™; dimebolin) is a neuroactive compound with antagonist activity at histaminergic, α-adrenergic, and serotonergic receptors (Wu et al., 2008). Latrepirdine is another small molecule that appears to mediate a number of activities associated with receptor inhibition (Grigorev et al., 2003), enhancing cognitive function (Lermontova et al., 2000), promoting neuronal survival (Bachurin et al., 2001; Zhang et al., 2010b), intracellular Ca^{+2} stabilisation (Lermontova et al., 2001), Aβ secretion and metabolism (Steele et al., 2009) and clearance of α-synuclein protein aggregates (Wu et al., 2008; Yamashita et al., 2009). Some recent studies have also reported latrepirdine's cognitive enhancing properties (Giorgetti et al., 2010; Vignisse et al., 2011). In the current study an additional function for latrepirdine in enhancing autophagy was demonstrated. Latrepirdine was shown to induce autophagy by three independent methods, including morphological detection of autophagic bodies using FM 4-64 staining, measuring the autophagic flux by determining Pho8 enzyme activity and by monitoring the vesicle delivery into the vacuole using a GFP-Atg8p expressing yeast (Figure 2, 3 and 4).

The FM 4-64 dye belongs to a group of cationic amphiphilic styryl dyes that fluoresce in the presence of a hydrophobic environment (Betz et al., 1992). Under normal conditions the FM 4-64 dye is associated with the biological membrane and with longer incubations they are internalized and concentrate onto the vacuolar membranes. During starvation conditions, autophagic bodies accumulate in the cell and are transported into the vacuole for degradation.

When the breakdown of the autophagic bodies in the vacuole is inhibited by protease inhibitor (PMSF), intravacuolar bodies are observed accumulating in the vacuole marked by intense FM 4-64 staining inside the vacuole (Takeshige et al., 1992). Known activators of autophagy like nitrogen starvation and rapamycin induced accumulation of autophagic bodies associated with strong intravacuolar staining of FM 4-64 in yeast (Figure 2B, C). Latrepirdine treatment induced a similar phenotype in yeast indicating an increased accumulation of autophagic bodies in the vacuole (Figure 2D). Latrepirdine treatment (1-2.5μM) induced intravacuolar FM 4-64 uptake in approximately 40% of cells compared to ~90% in N-starved and rapamycin treated. However in the atg8Δ cells, where autophagy is impaired, such morphology was absent with nitrogen starvation, rapamycin and latrepirdine treatment (Figure 2I-L).

Measurement of the activity of autophagy is referred to as autophagic flux. The Pho8 assay is a commonly used quantitative monitoring system of yeast autophagic flow based on the measurement of the enzyme activity during stimulation of autophagy (Noda and Klionsky, 2008). PHO8 is the gene encoding the sole vacuolar alkaline phosphatase in yeast. It is a type II transmembrane protein containing an N-terminal cytosolic tail with the active site and the C-terminus are located within the vacuolar lumen (Klionsky and Emr, 1989). During autophagy, the C terminal pro-peptide is cleaved off by vacuolar proteases resulting in the generation of the active form. Pho8 activity was measured using a specific substrate (α-naphthyl phosphate) using a fluorimetric assay. Latrepirdine increased the Pho8 activity in a dose dependent fashion at concentrations (0.25-5μM) (Figure 3). Similar to the FM 4-64 staining, latrepirdine treatment stimulation of Pho8 activity was markedly less than nitrogen starvation and rapamycin treatment. No increase in activity with latrepirdine, nitrogen starvation or rapamycin treatment was observed in atg8Δ cells, indicating that AV synthesis and Atg8p were essential for latrepirdine induced alkaline phosphatase activity.

The Atg8p molecule is an ubiquitin-like protein which conjugates to phosphatidylethanolamine (PE) and associates with the autophagosome/AV membrane during autophagy (Huang et al., 2000; Xie et al., 2008). After delivery to the vacuole, the Atg8p–PE complex is cleaved from the outer surface of the sequestering vesicle, but the GFP tag (in the GFP-Atg8p transformant) located on the inside of the vesicle remains trapped and was used as a functional marker for monitoring delivery of vesicles to the vacuole (Kim et al., 2001a). The released GFP moiety remains relatively stable from vacuolar hydrolysis, whereas Atg8p is rapidly degraded. Nitrogen starvation and rapamycin treatment induced a vacuolar GFP fluorescence phenotype in ~90% of cells, whereas latrepirdine treatment (2.5μM) induced a similar phenotype in ~25% (Figure 4).

Although not as efficient as rapamycin or N-starvation, latrepirdine promoted uptake of the vacuole stain FM 4-64, increased activity of the vacuolar alkaline phosphatase and up-regulation of GFP-Atg8p. Overall the data indicated that latrepirdine can promote autophagy in yeast cells. The lack of activation of autophagy in cells deficient in Atg8p may suggest that latrepirdine mediated autophagy in yeast was Atg8 dependent. However the exact mechanism of action is unclear. The concentrations needed to induce autophagy for latrepirdine in yeast is around 1-5μM, which is approximately 5-50 times (by molarity) more than rapamycin (0.1-0.2μM). This probably suggests that latrepirdine may be a weak inhibitor of TOR, targeting a downstream signalling molecule of mTOR pathway or even mTOR independent. Isolating yeast mutants resistant to latrepirdine stimulated autophagy can assist in the identification of the potential mechanism of latrepirdine induced autophagy. In addition, analysis of other mutants lacking particular genes in the autophagic pathway, such as *Atg1* (protein kinase required for vesicle formation) or *Atg5* (formation and transport of autophagosome) may provide further insight into potential targets for latrepirdine in the autophagic-vacuolar pathway in yeast.

Latrepirdine significantly reduced GFP-Aβ42 levels expressed in wild-type

yeast cells but not in atg8Δ mutant cells, indicating the involvement of autophagic-vacuolar pathways. Similar to the activity observed in the autophagic assays, latrepirdine mediated decrease in GFP-Aβ42 levels in yeast was significantly lower compared to rapamycin treatment [40% decrease with 5μM latrepirdine compared to ~95% with 0.2μM rapamycin (compare Figure 5 and 1)]. The decreased ability of latrepirdine to stimulate autophagy compared to rapamycin may account for this. Assessing GFP-Aβ42 clearance in yeast cells deficient in essential components involved in the initiation of the pathway (through inhibition of mTOR), autophagosome formation and transport or autophagosome-vacuolar fusion, will provide further insight into possible targets for latrepirdine. Once identified this would require further validation in mammalian neuronal cells.

9.5.3 Activation of autophagy protects yeast cells from Aβ42 toxicity

Activation of autophagy has been shown to be protective against a variety of stresses to cells (Levine and Kroemer, 2008; Mizushima et al., 2008). The pro-survival function of autophagy has been demonstrated in cells and animal models during nutrient and growth factor deprivation, endoplasmic reticulum stress, development, microbial infection, and diseases characterized by the accumulation and toxicity of protein aggregates (Lum et al., 2005; Yorimitsu and Klionsky, 2007).

Stimulation of autophagy by rapamycin and latrepirdine was shown to reduce the levels of GFP-Aβ42 aggregates in yeast cells (Section 9.5.1 and 9.5.2). Therefore, I further determined whether activation of autophagy reduced toxicity of oligomeric Aβ42 using the colony count viability assay in yeast (Bharadwaj et al., 2008). Wild type and autophagy deficient atg8Δ cells were pre-treated with rapamycin, latrepirdine or nitrogen starved followed by oligomer Aβ42 treatment (Figure 8). The data showed that activation of autophagy by rapamycin, latrepirdine and nitrogen starvation enhanced survival against Aβ42

toxicity. The increase in cell survival was evident only in wild type cells and was absent in the atg8Δ cells. This result indicated that stimulation of autophagy in wild type cells increased its resistance against Aβ42 toxicity, whereas due to the lack of autophagy atg8Δ cells did not show any increase in cell survival. The observations that atg8Δ cells do not respond to rapamycin, nitrogen starvation or latrepirdine treatment (Figure 3, 4 and 5) further supported the notion that activation of autophagy enhanced survival against oligomer Aβ42 toxicity.

Interestingly, under normal conditions (without any pre-treatment) atg8Δ cells displayed an increased resistance to Aβ42 toxicity compared to the wild type (compare Figure 8A with 8B). Ideally, the atg8Δ mutant would have expected to be more susceptible to oligomeric Aβ42 treatment due to its inability to undergo autophagy. However in the yeast Aβ42 toxicity assay, atg8Δ cells showed almost ~2 fold increase in cell survival comparing the wild type. Studies indicate that autophagic related (ATG) genes can act both in cellular protection and also in cell death (Levine and Kroemer, 2008; Mizushima et al., 2008). Notably, many examples of ATG-gene dependent death occur in mammalian cells (Levine and Yuan, 2005; Pattingre et al., 2005). Whether Aβ42 mediated cell death in yeast is associated with *Atg8* gene expression in cells is yet to be determined. Another likely possibility is that the knock-out of *Atg8* gene in yeast may be associated with effects beyond autophagy which may contribute to this phenomenon. It is therefore unclear whether the increased resistance of atg8Δ cells to oligomer Aβ42 toxicity is autophagy dependent or a result of a secondary effect of *Atg8* gene deletion. Investigation of oligomer Aβ42 toxicity in other ATG gene knock out mutants including *Atg1*, *Atg5*, *Atg8*, and *Atg9* can provide a better insight into this effect.

9.5.4 Latrepirdine promotes peripheral clearance of Aβ42 in the presence of ApoE4

In addition to intracellular degradation pathways like autophagy, one of the important mechanisms of action with respect to clearance of Aβ from the

brain is the “peripheral sink” hypothesis (DeMattos et al., 2001). The main basis of this hypothesis is that Aβ is transported out of the brain, into the periphery where proteins in the circulation can sequester Aβ and deliver it to peripheral tissues like liver and kidney for clearance. Plasma Aβ levels in the periphery are typically low (Gandy et al., 2001), indicating that metabolic process facilitates rapid clearance of this protein in the periphery. Earlier studies (DeMattos et al., 2001; DeMattos et al., 2002) have shown that Aβ can be cleared to the plasma from the brain by the use of anti-Aβ antibodies. In addition, work by Matsuoka et al. (Matsuoka et al., 2003) has showed that peripheral treatment with an agent having a high affinity for Aβ reduced brain levels of Aβ.

While the yeast studies clearly provide valuable insight into the mechanism of action of latrepirdine in clearing Aβ its clinical significance requires an *in vivo* model. Latrepirdine was therefore assessed for its ability to promote Aβ42 clearance in the periphery using APOE knockout mice injected with Aβ42+ lipidated ApoE4 (Figure 9). Substantial differences in the expression levels of total plasma ApoE has been observed in different APOE (ε2, ε3, and ε4) knock-in mice (APOE-targeted replacement (TR) mice) (Knouff et al., 1999; Sullivan et al., 1998). Therefore, to control for the differeing levels of plasma ApoE across genotypes, the peripheral clearance of Aβ42 was evaluated in the APOE knockout mouse model utilizing lipidated recombinant ApoE isoforms (Sharman et al., 2010). Regardless of the model used (APOE-TR mice or APOE KO mice +lipidated ApoE4), Sharman and colleagues showed that the presence of ApoE4 impaired the peripheral clearance of injected human Aβ42. The results presented in this chapter show that latrepirdine, compared to the saline control, can markedly improve the clearance of Aβ42 from the blood plasma and promote uptake by the liver, (Figure 9), in the presence of ApoE4. The reasons for these marked effects of latrepirdine on the peripheral clearance of Aβ42 are unclear. A possible explanation is that latrepirdine interacts with Aβ42; either preventing its further aggregation (thus promoting more effective clearance of Aβ monomers) or this interaction may promote its uptake (possibly

receptor mediated) and clearance/degradation by the liver. Steele et al., (2009) study reported increased Aβ levels in ISF of mice treated with latrepirdine. It is conceivable that as part of latrepirdine's overall effect, it enhances clearance of Aβ from the ISF and the CNS into the periphery where it is rapidly cleared.

The findings presented in this chapter have provided initial evidence for a novel mechanism of action for latrepirdine in promoting the clearance of Aβ, *in vivo*. Further investigation into whether latrepirdine could modulate the aggregation and degradation of Aβ in mammalian *in vitro* and *in vivo* systems would be required.

9.6 Summary

Overall the data presented in this chapter has established the use of the yeast model for screening compounds which can reduce intracellular accumulation of Aβ, by possibly enhancing its clearance. A novel mechanism of action has also been identified for the AD drug latrepirdine. Latrepirdine was shown to enhance autophagy and promote Aβ clearance in cells. Although latrepirdine has shown mixed results in AD clinical trials, more recent studies are reporting its cognitive benefits in animal models. The ability of latrepirdine to stimulate autophagy in the yeast model can be used to develop analogues with increased potency and lesser toxicity. While rapamycin is the most widely used autophagy stimulating drug, growing evidence has emphasized the need for more specific and potent agents/small molecules to replace this first generation autophagy promoting drug. The identification of novel compounds which can specifically inhibit particular elements of autophagy combined with genetic screens can be resourceful to understand the pathways and the proteins involved with the clearance of intracellular aggregates. Besides its ability to modulate autophagy, *in vivo* studies showed that latrepirdine can promote peripheral Aβ42 clearance and also increase uptake into liver. In general, the data presented in this chapter have suggested that latrepirdine may operate by

multiple mechanisms to promote Aβ clearance thereby reducing its accumulation and toxicity. How and which of these effects relate to drug-related changes in cognition and behaviour will need to be elucidated in order to selectively modify this promising drug candidate and thus develop more potent related molecules that are tailored to effectively treat AD.

Chapter 10

Conclusions and Future Directions

General Discussion: Cellular models are essential for studying the underlying pathology of a disease and designing novel techniques for drug discovery. Yeast has been used as a model for several neurological disorders characterized by protein misfolding and aggregation: reviewed in [(Braun et al., 2010; Winderickx et al., 2008)]. In addition to its conserved nature, yeast cells are robust and have better tractability and reduced complexity compared to other mammalian cells which makes it a resourceful model for studying disease pathways and drug mechanisms. The work presented in my thesis has primarily focussed on establishing yeast models for investigating the toxicity and intracellular clearance pathways of beta amyloid (Aβ), a peptide central to the pathogenesis of Alzheimer's disease (AD). In this thesis, I have also demonstrated the use of the yeast model in investigating novel agents which can attenuate Aβ toxicity or enhance its clearance.

10.1 Oligomer Aβ Toxicity

10.1.1 Membrane associated toxicity of Oligomeric Aβ42

AD is characterized by extensive neuronal loss associated with senile amyloid plaques in the brain. There is considerable evidence to clearly indicate that the soluble oligomeric forms of Aβ protein are the main toxic species which are responsible for the pathology of the disease. Aβ is an intramembrane cleavage product of APP and is largely secreted into the extracellular lumen. It can therefore have a major impact on neuronal functions and viability by interacting with cell surface membranes (Talaga and Quere, 2002; Verdier and Penke, 2004; Verdier et al., 2004). Due to its hydrophobic nature, Aβ has an inherent ability to associate with biological membranes. The ability to interact with membranes is therefore an important feature of oligomer Aβ mediated toxicity to cells.

In earlier work I had demonstrated that Aβ was shown to be toxic to yeast cells (Bharadwaj et al., 2008). I now show in chapter 3 of this thesis the significance of Aβ42 binding to the plasma membrane in causing cell death in

yeast. The uptake of the Aβ42 peptide by yeast and its localisation indicated that oligomeric Aβ42 mediated cell death was associated with binding to the plasma membrane. Taken together with previous reports in neuronal cells (Ciccotosto et al., 2004; Hung et al., 2008), the data supports the notion that reduced binding to the plasma membrane is associated with decreased toxicity.

In yeast, oligomeric Aβ42 was shown to alter the activity of the plasma membrane proton pump H^+ATPase (Section 3.4.5, Chapter 3), a functional homolog of the mammalian Na^+/K^+ ATPase. This data is consistent with previous reports from a non-yeast model which showed decreased Na^+/K^+ ATPase and Cl^--ATPase activity in plasma membranes isolated from Aβ42 peptide treated hippocampal cells (Bores et al., 1998; Mark et al., 1995; Xiao et al., 2002). This may be one mechanism by which oligomeric Aβ42 can impact cellular homeostasis and cause cell death. Further investigation is required to determine how oligomer Aβ42 inhibits the H^+ATPase and whether modulating the activity of H^+ATPase can rescue Aβ mediated cell death.

10.1.2 Suppression of Aβ42 Oligomerization prevented Toxicity

Preventing the formation or disrupting the specific toxic oligomer structures to reduce Aβ caused neuronal dysfunction in the brain has been proposed as a therapeutic strategy in AD (Klein, 2007; Kruzel et al., 2001). In my study, the effect of dairy peptides on Aβ oligomerization and toxicity was determined using the yeast model. Dairy peptides lowered the net β-sheet content and more specifically the anti-parallel β-sheet content in Aβ42 thereby inhibiting oligomerization. Studies indicating the essential role of anti-parallel β-sheets in the formation of Aβ oligomers further supported this data (Cerf et al., 2009). The concomitant reduction in the toxicity of the Aβ42 peptides with reduced oligomerization was clearly evident in both yeast and neuronal cells. The pattern of loss of high mass oligomers (Figure 5, Chapter 4) of Aβ42 and associated toxicity was very similar to that seen in the presence of curcumin (Yang et al., 2005). It appears that the high mass oligomers represent the main

toxic species involved in cell death. However, their exact structural nature is unclear and needs further investigation. Overall, a positive correlation between suppression of β-sheet content and oligomerization by dairy peptides (Figures 2-5, Chapter 4) and protection against Aβ42-mediated toxicity to both yeast and neuronal cells (Figure 6, Chapter 4) was observed. The results presented in this chapter 4 established the application of the yeast model for screening compounds which can affect Aβ oligomerization and toxicity. Comparing neuronal cell cultures, the use of yeast cells for screening such compounds can be cost effective and is more amenable to developing a rapid *in vitro* screening tool for agents targeting oligomeric Aβ mediated toxicity.

10.1.3 MBP-Aβ42 fusion protein: A model for oligomeric Aβ

The majority of the assays used for identifying compounds which bind Aβ or target oligomerization and toxicity are based on using synthetic Aβ preparations [derived from solid phase peptide synthesis (SPSS)]. As discussed in Chapter 5, the preparation of oligomeric Aβ peptide solutions from synthetic Aβ is expensive and can be unsuitable for large scale studies. As a result, an increasing number of studies are adopting methods for recombinant production of Aβ (Dobeli et al., 1995; Hortschansky et al., 2005; Lee et al., 2005; Li et al., 2009; Luhrs et al., 2005; Sharpe et al., 2005; Subramanian and Shree, 2007; Walsh et al., 2009; Wiesehan et al., 2007). The maltose binding protein tagged Aβ42 (MBP-Aβ42) fusion protein reported by Caine et al. (2007) is a recombinant protein which can be stably produced in large quantities, purified easily using affinity columns and also showed properties (binding to Cu and Zn) similar to Aβ peptide (Caine et al., 2007b). The work presented in this thesis investigated the structural properties and toxicity of MBP-Aβ fusion proteins in yeast and neuronal cells (Caine et al., 2011).

Overall the data provided clear evidence that MBP-Aβ42 formed oligomers in solution and was more toxic compared to the truncated MBP-Aβ16 (Chapter 5). However compared with the Aβ42 peptide, the MBP-Aβ42 fusion protein

showed reduced ability to form higher oligomeric structures (greater than hexamer) and also fibrillar forms. Consequently, the MBP-Aβ42 also showed decreased toxicity compared to Aβ42 peptide in yeast and neuronal cells [Chapter 3, (Bharadwaj et al., 2008)]. The reduced toxicity of the MBP-Aβ42 solutions could be attributed to the absence of higher oligomeric structures which are observed with Aβ42. The data supported the notion that oligomer Aβ42 mediated cell death is caused collectively by an array of soluble oligomeric Aβ species with neurotoxic properties (Haass and Selkoe, 2007). Further investigation using stable cross-linking analysis of the different MBP-Aβ42 species may provide greater insight into the individual contributions of the different isoforms to toxicity and cell death.

Although MBP-Aβ42 may not be a naturally occurring form, it can have multiple applications based on its structural and toxic properties demonstrated in this thesis. Due to its relatively cheap manufacturing costs and high stability, it is a well suited model for large unbiased screening methods for structural elucidation and physicochemical studies for identifying Aβ binding ligands and compounds which can affect Aβ oligomerization. Moreover, it provides the opportunity for developing assays for identifying potential inhibitors of Aβ peptide toxicity in yeast.

10.1.4 Cell cycle dependent effects of Aβ

In addition to its toxic effects, reports have also demonstrated neurotrophic properties of Aβ peptides (Chan et al., 1999; Koo et al., 1993; Luo et al., 1996a; Whitson et al., 1989; Yankner et al., 1990). Studies indicate that the neurotrophic effects of Aβ reflect its role in neuronal development. But why a certain population of neurons become susceptible to Aβ42 mediated neurodegeneration in the AD brain is uncertain. Data presented in this thesis provides evidence that Aβ42 mediated toxicity or growth effects is dependent on the cell cycle which may explain the selective vulnerability of neurons in AD.

The results showed that Aβ42 can promote proliferation only in cells that are in the stationary phase and induce cell death in exponentially growing cells (Chapter 6). The Aβ-induced growth and toxic effects within different cell cycles in yeast is comparable to the initial report showing that Aβ can enhance survival in freshly plated undifferentiated hippocampal cells (Yankner et al., 1990), but toxic in aged differentiated cultures. Studies showing Aβ42 mediated cell death in neurons expressing particular cell cycle-related elements (Giovanni et al., 1999; Liu et al., 2004), and in G1 cell cycle stage (Simakova and Arispe, 2007) further supported the notion that Aβ42 mediated toxicity or growth is dependent on the cell cycle. mTOR is one important eukaryotic cell signalling pathway associated with Aβ induced growth effects. It was shown that rapamycin; an mTOR inhibitor, suppressed Aβ42-induced cell division in stationary phase yeast cells. This data supported the previous reports showing that mTOR inhibitors block Aβ42 induced neuronal cell cycle events (Bhaskar et al., 2009; Frasca et al., 2004; Malik et al., 2008; Varvel et al., 2008; Wu et al., 2000).

However, the exact role of mTOR signalling in AD is contentious as some studies have shown increased levels of p-mTOR in the AD brain (Chang et al., 2002; Li et al., 2005; Li et al., 2004), whereas a significant decrease in p-mTOR levels has also been reported (Lafay-Chebassier et al., 2005). A recent study showed that long-term inhibition of mTOR by rapamycin reduced Aβ levels in the brain and prevented AD-like cognitive deficits (Spilman et al., 2010). In contrast, another recent study showed correlation between the inhibition of mTOR signalling and Aβ induced impairment of synaptic plasticity (Ma et al., 2010b). It is evident that Aβ42 and mTOR are closely associated in AD pathology and can regulate each other. However, further investigation is required to determine the exact role of mTOR signalling and its association with Aβ42 mediated neurodegeneration in AD.

Data presented in this work has suggested a significant role of Aβ42 in mediating both growth and toxicity which can be associated with essential signalling pathways in the cell like mTOR. The strong association of Aβ42 on

the yeast plasma membrane (Section 3.4.4) suggests that the peptide mediated effects could be a result of its interaction with cell surface receptors. The reduced toxicity in stationary phase cells compared to the actively growing cells and the levels required for Aβ42 induced toxicity (micromolar) and cell proliferation (nanomolar) suggests that diverse receptors or their varied expression levels depending on the cell cycle may influence the Aβ42 mediated effects (Section 6.5.1). Interestingly, Aβ42 induced growth effect was observed only in *Candida glabrata* and was absent in *Saccharomyces cerevisiae* cells (Section 4.4.4). This observation is particular intriguing and further investigation of other fungal species using mutational analysis would provide a greater understanding of the pathways and receptor molecules involved in Aβ mediated proliferation and cell cycle events.

10.2 Intracellular Aβ42 Accumulation

10.2.1 Aβ clearance pathways in the cell

Data presented in chapters 7 and 8 of this thesis employ a GFP tagged Aβ expressing yeast model (Caine et al., 2007a) for investigating intracellular clearance pathways involved in the degradation of Aβ42. Further in chapter 9, enhancing autophagy to promote clearance of intracellular Aβ42 was investigated.

GFP-Aβ42 was found localized into vesicles reminiscent of autophagic bodies or endosome like structures [(Caine et al., 2007a), Chapter 7]. Reports showing that Aβ accumulates in vesicular/lysosomal structures in neurons of a variety of AD mouse models (Oddo et al., 2006; Wirths, 2001), human AD brains (Gouras et al., 2000; Nixon et al., 2005) and in neuronal cells treated with extracellular Aβ42 (Hu et al., 2009) supports the idea that GFP-Aβ42 may accumulate in such vesicles. The reduced levels and the punctate staining of GFP-Aβ42 observed in yeast indicated that Aβ42 is sequestered into these vesicles and targeted for degradation (Chapter 7). The results suggested that expression of GFP-Aβ42 in the cell elicited a degradative response and that it

can be cleared via distinct pathways. Autophagy-lysosome and ubiquitin proteasome system (UPS) are the main protein degradative mechanisms in cells. Data presented in Chapter 8 provided evidence for Aβ clearance by both the UPS and autophagic pathways.

10.2.2 Lack of autophagic vesicle synthesis, vacuolar hydrolases and proteasomal activity elevates intracellular Aβ42 accumulation

The morphology of neurons and the plasticity of synapses impose unique challenges on the cellular machinery for both protein synthesis and degradation (Steward and Schuman, 2003). Therefore post-mitotic differentiated neurons in the adult brain are highly vulnerable to accumulation of protein aggregates which is a main feature in several neurodegenerative diseases including AD. Hence disruption of protein homeostasis or imbalance in synthesis/clearance can be a major contributing factor of neuronal dysfunction.

It was shown that disruption of autophagy (atg8Δ) or vacuolar hydrolase (pep4Δ, cvt1Δ) activity elevated total GFP-Aβ42 levels and accumulation of GFP-Aβ42 containing vesicles in the yeast cell especially during the starvation periods of growth (Chapter 8). Baseline levels of autophagy during the active growth phase also contributed to the clearance of GFP-Aβ42 in yeast. The accumulation of Aβ has been reported in the absence of other autophagy genes such as Atg5p, Beclin1 and Ulk1 (Pickford et al., 2008; Tian et al., 2011). Accumulation of autophagic vesicles with loss of cathepsins (hydrolases) has also been previously reported. (Felbor et al., 2002; Koike et al., 2000; Koike et al., 2005). Besides autophagy, the UPS also showed a significant contribution towards the degradation of GFP-Aβ42 especially during the active growth phase. Interestingly, autophagy was shown to partially compensate for Aβ clearance during the growth phase in the proteasomal mutant (pre1-2Δ) lacking chymotrypsin activity (Chapter 8). This indicates that Aβ accumulation in AD

brain may be a collective contribution of aberrant degradation mechanisms. The findings presented in the work showed that both autophagy and the proteasome are actively involved in regulating the levels of Aβ42 aggregates and disruption of these functions leads to increased Aβ42 accumulation in the cell. The study of these pathways in yeast as presented in this thesis has provided evidence for the use of this *in vitro* model to screen compounds which can reduce intracellular accumulation of Aβ.

10.2.3 Stimulating Autophagy and a novel mechanism of action for Latrepirdine in Enhancing Aβ42 Clearance

Although less potent compared to the known autophagy activator rapamycin, the findings presented in this thesis have provided, for the first time, a novel mechanism of action for latrepirdine on enhancing autophagy and promoting the clearance of GFP-Aβ42 in yeast cells. Notably, rapamycin mediated reduction of GFP-Aβ42 levels was associated with pleotropic effects including inhibition of protein synthesis in cells (Heitman et al., 1991). In contrast, latrepirdine did not show such effects and was found to be dependent on the activity of the *Atg8* gene, which is essential in the formation of autophagosomes which is a critical step prior to the fusion with the vacuole to release its contents for degradation. The ability of latrepirdine to stimulate autophagy in yeast model can be used to develop analogues with increased potency and lesser toxicity. Besides its ability to modulate autophagy, *in vivo* studies showed that latrepirdine can promote peripheral Aβ42 clearance and also increase its uptake into liver. Overall the data showed that latrepirdine may operate via multiple mechanisms both indirectly (via stimulation of intracellular degradation pathways) and directly (transport and clearance in the periphery) to promote Aβ clearance. It is also possible that latrepirdine modulates Aβ structure and aggregation to promote these effects. Further investigation is required to determine how these mechanisms explain the overall effects of latrepirdine on cognitive and memory function.

10.3 Future Directions

The work presented in this thesis has provided evidence for the use of yeast in studying pathological mechanisms underlying Aβ toxicity and clearance and its utilization as a model to screen novel agents which can attenuate toxicity or enhance Aβ clearance. One direction for future research is to identify pathways and putative receptors involved in Aβ42 mediated cell proliferation in yeast cells. The Aβ growth effect can be systematically designed to be tested in a wide range of selected yeast species with diverse genomic backgrounds to determine the various pathways and associated receptor protein complexes involved with this action of Aβ. Another important course for future research is to establish a mutation screen in yeast for dissecting the various autophagic genes involved in degradation of intracellular Aβ42. More than 30 ATG (autophagy related) genes have been identified in yeast. Expression of GFP-Aβ42 in each of the 30 ATG gene deletion mutants followed by quantitative Aβ immunoblotting assays and localization analysis can be done to identify the mechanism and the genes directly involved in the degradation process of Aβ aggregates. A similar screen can be used for identifying the mechanism of latrepirdine induced autophagy and Aβ clearance. It will also be useful to determine the global effects of latrepirdine in cells using DNA microarray analysis to assess the possible influence of other non-autophagic genes and regulatory proteins in the modulation of degradation pathways. However, it is important to demonstrate that the findings in yeast are replicated in neuronal cells.

10.4 Conclusion

This study has established and broadened the application of yeast models for investigating toxicity and intracellular clearance mechanisms of Aβ. Using the yeast model for oligomer Aβ toxicity, this work has identified protective functions for dairy derived peptides and established recombinant MBP-Aβ fusion proteins as a model for studying Aβ oligomers. Furthermore using the

GFP-Aβ expressing yeast, the degradation pathways involved in clearance of Aβ aggregates was investigated and a novel mechanism identified for a drug currently in clinical trials, latrepirdine, in enhancing autophagy and promoting clearance of intracellular Aβ.

References:

Abeliovich, H., and Klionsky, D.J. (2001). Autophagy in yeast: mechanistic insights and physiological function. Microbiol Mol Biol Rev *65*, 463-479, table of contents.

Abraham, R.T. (1998). Mammalian target of rapamycin: immunosuppressive drugs uncover a novel pathway of cytokine receptor signaling. Curr Opin Immunol *10*, 330-336.

Adlard, P.A., Cherny, R.A., Finkelstein, D.I., Gautier, E., Robb, E., Cortes, M., Volitakis, I., Liu, X., Smith, J.P., Perez, K.*, et al.* (2008). Rapid restoration of cognition in Alzheimer's transgenic mice with 8-hydroxy quinoline analogs is associated with decreased interstitial Abeta. Neuron *59*, 43-55.

Aerts, A.M., Zabrocki, P., Govaert, G., Mathys, J., Carmona-Gutierrez, D., Madeo, F., Winderickx, J., Cammue, B.P., and Thevissen, K. (2009). Mitochondrial dysfunction leads to reduced chronological lifespan and increased apoptosis in yeast. FEBS Lett *583*, 113-117.

Ahmed, M., Davis, J., Aucoin, D., Sato, T., Ahuja, S., Aimoto, S., Elliott, J.I., Van Nostrand, W.E., and Smith, S.O. (2010). Structural conversion of neurotoxic amyloid-beta(1-42) oligomers to fibrils. Nat Struct Mol Biol *17*, 561-567.

Aisen, P.S., Gauthier, S., Vellas, B., Briand, R., Saumier, D., Laurin, J., and Garceau, D. (2007). Alzhemed: a potential treatment for Alzheimer's disease. Curr Alzheimer Res *4*, 473-478.

Aleshkov, S., Abraham, C.R., and Zannis, V.I. (1997). Interaction of nascent ApoE2, ApoE3, and ApoE4 isoforms expressed in mammalian cells with amyloid peptide beta (1-40). Relevance to Alzheimer's disease. Biochemistry *36*, 10571-10580.

Allinson, T.M., Parkin, E.T., Turner, A.J., and Hooper, N.M. (2003). ADAMs family members as amyloid precursor protein alpha-secretases. J Neurosci Res *74*, 342-352.

Almeida, C.G., Takahashi, R.H., and Gouras, G.K. (2006). Beta-amyloid accumulation impairs multivesicular body sorting by inhibiting the ubiquitin-proteasome system. J Neurosci *26*, 4277-4288.

Amar, N., Lustig, G., Ichimura, Y., Ohsumi, Y., and Elazar, Z. (2006). Two newly identified sites in the ubiquitin-like protein Atg8 are essential for autophagy. EMBO Rep *7*, 635-642.

Ambesi, A., Miranda, M., Petrov, V.V., and Slayman, C.W. (2000). Biogenesis and function of the yeast plasma-membrane H(+)-ATPase. J Exp Biol *203*, 155-160.

Ames, A. (2000). CNS energy metabolism as related to function. Brain Res Brain Res Rev *34*, 42-68.

Amijee, H., Madine, J., Middleton, D.A., and Doig, A.J. (2009). Inhibitors of protein aggregation and toxicity. Biochem Soc Trans *37*, 692-696.

Ammerer, G., Hunter, C.P., Rothman, J.H., Saari, G.C., Valls, L.A., and Stevens, T.H. (1986). PEP4 gene of Saccharomyces cerevisiae encodes proteinase A, a vacuolar enzyme required for processing of vacuolar precursors. Mol Cell Biol *6*, 2490-2499.

Anandatheerthavarada, H.K., Biswas, G., Robin, M.A., and Avadhani, N.G. (2003). Mitochondrial targeting and a novel transmembrane arrest of Alzheimer's amyloid precursor protein impairs mitochondrial function in neuronal cells. J Cell Biol *161*, 41-54.

Anglade, P., Vyas, S., Javoy-Agid, F., Herrero, M.T., Michel, P.P., Marquez, J., Mouatt-Prigent, A., Ruberg, M., Hirsch, E.C., and Agid, Y. (1997). Apoptosis and autophagy in nigral neurons of patients with Parkinson's disease. Histol Histopathol *12*, 25-31.

Antony, H. (2008). Study of cellular responses and protein interactions of Aβ in yeast models. In School of Applied Sciences (Melbourne, Royal Melbourne Institute of Technology).

Area-Gomez, E., de Groof, A.J., Boldogh, I., Bird, T.D., Gibson, G.E., Koehler, C.M., Yu, W.H., Duff, K.E., Yaffe, M.P., Pon, L.A.*, et al.* (2009). Presenilins are enriched in endoplasmic reticulum membranes associated with mitochondria. Am J Pathol *175*, 1810-1816.

Arjona, A.A., Pooler, A.M., Lee, R.K., and Wurtman, R.J. (2002). Effect of a 5-HT(2C) serotonin agonist, dexnorfenfluramine, on amyloid precursor protein metabolism in guinea pigs. Brain Res *951*, 135-140.

Armakola, M., Hart, M.P., and Gitler, A.D. (2010). TDP-43 toxicity in yeast. Methods *53*, 238-245.

Aronson, M.K., Ooi, W.L., Geva, D.L., Masur, D., Blau, A., and Frishman, W. (1991). Dementia. Age-dependent incidence, prevalence, and mortality in the old old. Arch Intern Med *151*, 989-992.

Arriagada, P.V., Marzloff, K., and Hyman, B.T. (1992). Distribution of Alzheimer-type pathologic changes in nondemented elderly individuals matches the pattern in Alzheimer's disease. Neurology *42*, 1681-1688.

Atwood, C.S., Obrenovich, M.E., Liu, T., Chan, H., Perry, G., Smith, M.A., and Martins, R.N. (2003). Amyloid-beta: a chameleon walking in two worlds: a review of the trophic and toxic properties of amyloid-beta. Brain Res Brain Res Rev *43*, 1-16.

Atwood, C.S., Perry, G., Zeng, H., Kato, Y., Jones, W.D., Ling, K.Q., Huang, X., Moir, R.D., Wang, D., Sayre, L.M.*, et al.* (2004). Copper mediates dityrosine cross-linking of Alzheimer's amyloid-beta. Biochemistry *43*, 560-568.

Avila, J. (2006). Tau phosphorylation and aggregation in Alzheimer's disease pathology. FEBS Lett *580*, 2922-2927.

Bachurin, S., Bukatina, E., Lermontova, N., Tkachenko, S., Afanasiev, A., Grigoriev, V., Grigorieva, I., Ivanov, Y., Sablin, S., and Zefirov, N. (2001). Antihistamine agent Dimebon as a novel neuroprotector and a cognition enhancer. Ann N Y Acad Sci *939*, 425-435.

Bachurin, S.O., Ustyugov, A.A., Peters, O., Shelkovnikova, T.A., Buchman, V.L., and Ninkina, N.N. (2009). Hindering of proteinopathy-induced neurodegeneration as a new mechanism of action for neuroprotectors and cognition enhancing compounds. Dokl Biochem Biophys *428*, 235-238.

Bagriantsev, S., and Liebman, S. (2006). Modulation of Aβ42 low-n oligomerization using a novel yeast reporter system. BMC Biol *4*, 32.

Balch, W.E., Morimoto, R.I., Dillin, A., and Kelly, J.W. (2008). Adapting proteostasis for disease intervention. Science *319*, 916-919.

Baloyannis, S.J., Costa, V., and Michmizos, D. (2004). Mitochondrial alterations in Alzheimer's disease. Am J Alzheimers Dis Other Demen *19*, 89-93.

Barghorn, S., Nimmrich, V., Striebinger, A., Krantz, C., Keller, P., Janson, B., Bahr, M., Schmidt, M., Bitner, R.S., Harlan, J.*, et al.* (2005). Globular amyloid beta-peptide oligomer - a homogenous and stable neuropathological protein in Alzheimer's disease. J Neurochem *95*, 834-847.

Barnham, K.J., Ciccotosto, G.D., Tickler, A.K., Ali, F.E., Smith, D.G., Williamson, N.A., Lam, Y.H., Carrington, D., Tew, D., Kocak, G.*, et al.* (2003). Neurotoxic, redox-competent Alzheimer's beta-amyloid is released from lipid membrane by methionine oxidation. J Biol Chem *278*, 42959-42965.

Barnham, K.J., Haeffner, F., Ciccotosto, G.D., Curtain, C.C., Tew, D., Mavros, C., Beyreuther, K., Carrington, D., Masters, C.L., Cherny, R.A.*, et al.* (2004). Tyrosine gated electron transfer is key to the toxic mechanism of Alzheimer's disease beta-amyloid. FASEB J *18*, 1427-1429.

Bastianetto, S., Krantic, S., and Quirion, R. (2008). Polyphenols as potential inhibitors of amyloid aggregation and toxicity: possible significance to Alzheimer's disease. Mini Rev Med Chem *8*, 429-435.

Bates, K.A., Verdile, G., Li, Q.X., Ames, D., Hudson, P., Masters, C.L., and Martins, R.N. (2009). Clearance mechanisms of Alzheimer's amyloid-beta peptide: implications for therapeutic design and diagnostic tests. Mol Psychiatry *14*, 469-486.

Bednarski, E., Ribak, C.E., and Lynch, G. (1997). Suppression of cathepsins B and L causes a proliferation of lysosomes and the formation of meganeurites in hippocampus. J Neurosci *17*, 4006-4021.

Beffert, U., Aumont, N., Dea, D., Lussier-Cacan, S., Davignon, J., and Poirier, J. (1998). Beta-amyloid peptides increase the binding and internalization of apolipoprotein E to hippocampal neurons. J Neurochem *70*, 1458-1466.

Beffert, U., Aumont, N., Dea, D., Lussier-Cacan, S., Davignon, J., and Poirier, J. (1999a). Apolipoprotein E isoform-specific reduction of extracellular amyloid in neuronal cultures. Brain Res Mol Brain Res *68*, 181-185.

Beffert, U., Cohn, J.S., Petit-Turcotte, C., Tremblay, M., Aumont, N., Ramassamy, C., Davignon, J., and Poirier, J. (1999b). Apolipoprotein E and beta-amyloid levels in the hippocampus and frontal cortex of Alzheimer's disease subjects are disease-related and apolipoprotein E genotype dependent. Brain Res *843*, 87-94.

Behl, C., Davis, J.B., Lesley, R., and Schubert, D. (1994). Hydrogen peroxide mediates amyloid beta protein toxicity. Cell *77*, 817-827.

Behrends, C., Sowa, M.E., Gygi, S.P., and Harper, J.W. (2010). Network organization of the human autophagy system. Nature *466*, 68-76.

Beisiegel, U., Weber, W., Ihrke, G., Herz, J., and Stanley, K.K. (1989). The LDL-receptor-related protein, LRP, is an apolipoprotein E-binding protein. Nature *341*, 162-164.

Bell, R.D., Sagare, A.P., Friedman, A.E., Bedi, G.S., Holtzman, D.M., Deane, R., and Zlokovic, B.V. (2007). Transport pathways for clearance of human Alzheimer's amyloid beta-peptide and apolipoproteins E and J in the mouse central nervous system. J Cereb Blood Flow Metab *27*, 909-918.

Bennett, L., Williams, R., Ecroyd, H., Liu, Y.Q., Sudharmarajan, S., and Carver, J. (2009). Protective interactions of dairy peptides with fibril structures and relevance to Alzheimer's Disease. Aust J Dairy Technol *64*, 117-121.

Berger, Z., Ravikumar, B., Menzies, F.M., Oroz, L.G., Underwood, B.R., Pangalos, M.N., Schmitt, I., Wullner, U., Evert, B.O., O'Kane, C.J.*, et al.* (2006). Rapamycin alleviates toxicity of different aggregate-prone proteins. Hum Mol Genet *15*, 433-442.

Bernstein, S.L., Wyttenbach, T., Baumketner, A., Shea, J.E., Bitan, G., Teplow, D.B., and Bowers, M.T. (2005). Amyloid beta-protein: Monomer structure and early aggregation states of A beta 42 and its Pro(19) alloform. J Am Chem Soc *127*, 2075-2084.

Bertram, L., Hiltunen, M., Parkinson, M., Ingelsson, M., Lange, C., Ramasamy, K., Mullin, K., Menon, R., Sampson, A.J., Hsiao, M.Y.*, et al.* (2005). Family-based association between Alzheimer's disease and variants in UBQLN1. N Engl J Med *352*, 884-894.

Bertram, L., McQueen, M.B., Mullin, K., Blacker, D., and Tanzi, R.E. (2007). Systematic meta-analyses of Alzheimer disease genetic association studies: the AlzGene database. Nat Genet *39*, 17-23.

Betz, W.J., Mao, F., and Bewick, G.S. (1992). Activity-dependent fluorescent staining and destaining of living vertebrate motor nerve terminals. J Neurosci *12*, 363-375.

Bezprozvanny, I. (2010). The rise and fall of Dimebon. Drug News Perspect *23*, 518-523.

Bharadwaj, P., Martins, R., and Macreadie, I. (2010). Yeast as a model for studying Alzheimer's disease. FEMS Yeast Res.

Bharadwaj, P., Waddington, L., Varghese, J., and Macreadie, I.G. (2008). A new method to measure cellular toxicity of non-fibrillar and fibrillar Alzheimer's Aβ using yeast. J Alzheimers Dis *13*, 147-150.

Bharadwaj, P.R., Dubey, A.K., Masters, C.L., Martins, R.N., and Macreadie, I.G. (2009). Aβ aggregation and possible implications in Alzheimer's disease pathogenesis. J Cell Mol Med *13*, 412-421.

Bhaskar, K., Miller, M., Chludzinski, A., Herrup, K., Zagorski, M., and Lamb, B.T. (2009). The PI3K-Akt-mTOR pathway regulates Abeta oligomer induced neuronal cell cycle events. Mol Neurodegener *4*, 14.

Bibl, M., Mollenhauer, B., Esselmann, H., Lewczuk, P., Klafki, H.W., Sparbier, K., Smirnov, A., Cepek, L., Trenkwalder, C., Ruther, E.*, et al.* (2006). CSF amyloid-beta-peptides in Alzheimer's disease, dementia with Lewy bodies and Parkinson's disease dementia. Brain *129*, 1177-1187.

Biere, A.L., Ostaszewski, B., Zhao, H., Gillespie, S., Younkin, S.G., and Selkoe, D.J. (1995). Co-expression of beta-amyloid precursor protein (betaAPP) and apolipoprotein E in cell culture: analysis of betaAPP processing. Neurobiol Dis *2*, 177-187.

Bilikiewicz, A., and Gaus, W. (2004). Colostrinin (a naturally occurring, proline-rich, polypeptide mixture) in the treatment of Alzheimer's disease. J Alzheimers Dis *6*, 17-26.

Billack, B., Pietka-Ottlik, M., Santoro, M., Nicholson, S., Mlochowski, J., and Lau-Cam, C. (2010). Evaluation of the antifungal and plasma membrane H+-ATPase inhibitory action of ebselen and two ebselen analogs in S. cerevisiae cultures. J Enzyme Inhib Med Chem *25*, 312-317.

Biran, Y., Masters, C.L., Barnham, K.J., Bush, A.I., and Adlard, P.A. (2009). Pharmacotherapeutic targets in Alzheimer's disease. J Cell Mol Med *13*, 61-86.

Bissette, G., Smith, W.H., Dole, K.C., Crain, B., Ghanbari, H., Miller, B., and Nemeroff, C.B. (1991). Alterations in Alzheimer's disease-associated protein in Alzheimer's disease frontal and temporal cortex. Arch Gen Psychiatry *48*, 1009-1012.

Bitan, G., Kirkitadze, M.D., Lomakin, A., Vollers, S.S., Benedek, G.B., and Teplow, D.B. (2003). Amyloid beta -protein (Abeta) assembly: Abeta 40 and Abeta 42 oligomerize through distinct pathways. Proc Natl Acad Sci U S A *100*, 330-335.

Bitan, G., and Teplow, D.B. (2005). Preparation of aggregate-free, low molecular weight amyloid-beta for assembly and toxicity assays. Methods Mol Biol *299*, 3-9.

Bliss, T.V., and Collingridge, G.L. (1993). A synaptic model of memory: long-term potentiation in the hippocampus. Nature *361*, 31-39.

Boland, B., Kumar, A., Lee, S., Platt, F.M., Wegiel, J., Yu, W.H., and Nixon, R.A. (2008). Autophagy induction and autophagosome clearance in neurons: relationship to autophagic pathology in Alzheimer's disease. J Neurosci *28*, 6926-6937.

Boldogh, I., Aguilera-Aguirre, L., Bacsi, A., Choudhury, B.K., Saavedra-Molina, A., and Kruzel, M. (2008). Colostrinin decreases hypersensitivity and allergic responses to common allergens. Int Arch Allergy Immunol *146*, 298-306.

Boldogh, I., and Kruzel, M.L. (2008). Colostrinin: an oxidative stress modulator for prevention and treatment of age-related disorders. J Alzheimers Dis *13*, 303-321.

Bonda, D.J., Lee, H.P., Kudo, W., Zhu, X., Smith, M.A., and Lee, H.G. (2010). Pathological implications of cell cycle re-entry in Alzheimer disease. Expert Rev Mol Med *12*, e19.

Bores, G.M., Smith, C.P., Wirtz-Brugger, F., and Giovanni, A. (1998). Amyloid beta-peptides inhibit Na+/K+-ATPase: tissue slices versus primary cultures. Brain Res Bull *46*, 423-427.

Bowman, B.H., Taylor, J.W., and White, T.J. (1992). Molecular evolution of the fungi: human pathogens. Mol Biol Evol *9*, 893-904.

Bozulic, L.D., Dean, W.L., and Delamere, N.A. (2004). The influence of Lyn kinase on Na,K-ATPase in porcine lens epithelium. Am J Physiol Cell Physiol *286*, C90-96.

Braak, H., and Braak, E. (1991). Neuropathological stageing of Alzheimer-related changes. Acta Neuropathol *82*, 239-259.

Brandis, K.A., Holmes, I.F., England, S.J., Sharma, N., Kukreja, L., and DebBurman, S.K. (2006). alpha-Synuclein fission yeast model: concentration-dependent aggregation without plasma membrane localization or toxicity. J Mol Neurosci *28*, 179-191.

Braun, R.J., Buttner, S., Ring, J., Kroemer, G., and Madeo, F. (2010). Nervous yeast: modeling neurotoxic cell death. Trends Biochem Sci *35*, 135-144.

Brining, S.K. (1997). Predicting the in vitro toxicity of synthetic beta-amyloid (1-40). Neurobiol Aging *18*, 581-589.

Brion, J.P., Couck, A.M., Passareiro, E., and Flament-Durand, J. (1985). Neurofibrillary tangles of Alzheimer's disease: an immunohistochemical study. J Submicrosc Cytol *17*, 89-96.

Brookmeyer, R., Johnson, E., Ziegler-Graham, K., and Arrighi, H.M. (2007). Forecasting the global burden of Alzheimer's disease. Alzheimers Dement *3*, 186-191.

Brown, E.J., Albers, M.W., Shin, T.B., Ichikawa, K., Keith, C.T., Lane, W.S., and Schreiber, S.L. (1994). A mammalian protein targeted by G1-arresting rapamycin-receptor complex. Nature *369*, 756-758.

Bubber, P., Haroutunian, V., Fisch, G., Blass, J.P., and Gibson, G.E. (2005). Mitochondrial abnormalities in Alzheimer brain: mechanistic implications. Ann Neurol *57*, 695-703.

Burdick, D., Soreghan, B., Kwon, M., Kosmoski, J., Knauer, M., Henschen, A., Yates, J., Cotman, C., and Glabe, C. (1992). Assembly and Aggregation Properties of Synthetic Alzheimer's A4/β Amyloid Peptide Analogs. *J Biol Chem 267*, 546-554.

Burkoth, T.S., Benzinger, T.L.S., Urban, V., Morgan, D.M., Gregory, D.M., Thiyagarajan, P., Botto, R.E., Meredith, S.C., and Lynn, D.G. (2000). Structure of the beta-amyloid((10-35)) fibril. J Am Chem Soc *122*, 7883-7889.

Busciglio, J., Gabuzda, D.H., Matsudaira, P., and Yankner, B.A. (1993). Generation of beta-amyloid in the secretory pathway in neuronal and nonneuronal cells. Proc Natl Acad Sci U S A *90*, 2092-2096.

Busciglio, J., Lorenzo, A., and Yankner, B.A. (1992). Methodological variables in the assessment of beta amyloid neurotoxicity. Neurobiol Aging *13*, 609-612.

Butterfield, D.A., Castegna, A., Lauderback, C.M., and Drake, J. (2002). Evidence that amyloid beta-peptide-induced lipid peroxidation and its sequelae in Alzheimer's disease brain contribute to neuronal death. Neurobiol Aging *23*, 655-664.

Butterfield, D.A., Drake, J., Pocernich, C., and Castegna, A. (2001). Evidence of oxidative damage in Alzheimer's disease brain: central role for amyloid -peptide Trends in Molecular Medicine *7*, 548-554.

Buttner, S., Carmona-Gutierrez, D., Vitale, I., Castedo, M., Ruli, D., Eisenberg, T., Kroemer, G., and Madeo, F. (2007). Depletion of endonuclease G selectively kills polyploid cells. Cell Cycle *6*, 1072-1076.

Cabrejo, L., Guyant-Maréchal, L., Laquerrière, A., Vercelletto, M., De La Fournière, F., Thomas-Antérion, C., Verny, C., Letournel, F., Pasquier, F., Vital, A.*, et al.* (2006). Phenotype associated with APP duplication in five families. Brain *129*, 2966-2976.

Caine, J., Sankovich, S., Antony, H., Waddington, L., Macreadie, P., Varghese, J., and Macreadie, I. (2007a). Alzheimer's Aβ fused to green fluorescent protein induces growth stress and a heat shock response. FEMS Yeast Res *7*, 1230-1236.

Caine, J., Volitakis, I., Cherny, R., Varghese, J., and Macreadie, I. (2007b). Aβ produced as a fusion to maltose binding protein can be readily purified and stably associates with copper and zinc. Protein Pept Lett *14*, 83-86.

Caine, J.M., Bharadwaj, P.R., Sankovich, S.E., Ciccotosto, G.D., Streltsov, V.A., and Varghese, J. (2011). Oligomerization and toxicity of Abeta fusion proteins. Biochem Biophys Res Commun.

Cam, J.A., Zerbinatti, C.V., Knisely, J.M., Hecimovic, S., Li, Y., and Bu, G. (2004). The low density lipoprotein receptor related protein 1B retains ß amyloid precursor protein at the cell surface and reduces Amyloid-ß peptide production. J Biol Chem *279*, 29639-29646.

Cardenas, M.E., Cutler, N.S., Lorenz, M.C., Di Como, C.J., and Heitman, J. (1999). The TOR signaling cascade regulates gene expression in response to nutrients. Genes Dev *13*, 3271-3279.

Carrell, R.W., Mushunje, A., and Zhou, A. (2008). Serpins show structural basis for oligomer toxicity and amyloid ubiquity. FEBS Lett *582*, 2537-2541.

Caselli, R.J., Osborne, D., Reiman, E.M., Hentz, J.G., Barbieri, C.J., Saunders, A.M., Hardy, J., Graff-Radford, N.R., Hall, G.R., and Alexander, G.E. (2001). Preclinical cognitive decline in late middle-aged asymptomatic apolipoprotein E-e4/4 homozygotes: a replication study. J Neurol Sci *189*, 93-98.

Casley, C.S., Canevari, L., Land, J.M., Clark, J.B., and Sharpe, M.A. (2002). Beta-amyloid inhibits integrated mitochondrial respiration and key enzyme activities. J Neurochem *80*, 91-100.

Caspersen, C., Wang, N., Yao, J., Sosunov, A., Chen, X., Lustbader, J.W., Xu, H.W., Stern, D., McKhann, G., and Yan, S.D. (2005). Mitochondrial Abeta: a potential focal point for neuronal metabolic dysfunction in Alzheimer's disease. FASEB J *19*, 2040-2041.

Castano, E.M., Prelli, F., Pras, M., and Frangione, B. (1995). Apolipoprotein E carboxyl-terminal fragments are complexed to amyloids A and L. Implications for amyloidogenesis and Alzheimer's disease. J Biol Chem *270*, 17610-17615.

Castegna, A., Aksenov, M., Aksenova, M., Thongboonkerd, V., Klein, J.B., Pierce, W.M., Booze, R., Markesbery, W.R., and Butterfield, D.A. (2002). Proteomic identification of oxidatively modified proteins in Alzheimer's disease brain. Part I: creatine kinase BB, glutamine synthase, and ubiquitin carboxy-terminal hydrolase L-1. Free Radic Biol Med *33*, 562-571.

Cataldo, A.M., Barnett, J.L., Berman, S.A., Li, J., Quarless, S., Bursztajn, S., Lippa, C., and Nixon, R.A. (1995). Gene expression and cellular content of

cathepsin D in Alzheimer's disease brain: evidence for early up-regulation of the endosomal-lysosomal system. Neuron *14*, 671-680.

Cataldo, A.M., Barnett, J.L., Mann, D.M., and Nixon, R.A. (1996). Colocalization of lysosomal hydrolase and beta-amyloid in diffuse plaques of the cerebellum and striatum in Alzheimer's disease and Down's syndrome. J Neuropathol Exp Neurol *55*, 704-715.

Cataldo, A.M., Petanceska, S., Terio, N.B., Peterhoff, C.M., Durham, R., Mercken, M., Mehta, P.D., Buxbaum, J., Haroutunian, V., and Nixon, R.A. (2004). Abeta localization in abnormal endosomes: association with earliest Abeta elevations in AD and Down syndrome. Neurobiol Aging *25*, 1263-1272.

Cedazo-Minguez, A., and Cowburn, R.F. (2001). Apolipoprotein E: a major piece in the Alzheimer's disease puzzle. J Cell Mol Med *5*, 254-266.

Cedazo-Minguez, A., Wiehager, B., Winblad, B., Huttinger, M., and Cowburn, R.F. (2001). Effects of apolipoprotein E (apoE) isoforms, beta-amyloid (Abeta) and apoE/Abeta complexes on protein kinase C-alpha (PKC-alpha) translocation and amyloid precursor protein (APP) processing in human SH-SY5Y neuroblastoma cells and fibroblasts. Neurochem Int *38*, 615-625.

Cerf, E., Sarroukh, R., Tamamizu-Kato, S., Breydo, L., Derclaye, S., Dufrene, Y.F., Narayanaswami, V., Goormaghtigh, E., Ruysschaert, J.M., and Raussens, V. (2009). Antiparallel beta-sheet: a signature structure of the oligomeric amyloid beta-peptide. Biochem J *421*, 415-423.

Chagnon, P., Betard, C., Robitaille, Y., Cholette, A., and Gauvreau, D. (1995). Distribution of brain cytochrome oxidase activity in various neurodegenerative diseases. Neuroreport *6*, 711-715.

Chan, C.W., Dharmarajan, A., Atwood, C., S,, Huang, X., Tanzi, R.E., Bush, A.I., and Martins, R.N. (1999). Anti-apoptotic action of Alzheimer Ab. Alzheimer’s Reports *2*, 1-6.

Chang, R.C., Suen, K.C., Ma, C.H., Elyaman, W., Ng, H.K., and Hugon, J. (2002). Involvement of double-stranded RNA-dependent protein kinase and phosphorylation of eukaryotic initiation factor-2alpha in neuronal degeneration. J Neurochem *83*, 1215-1225.

Cheng, L., Yin, W.J., Zhang, J.F., and Qi, J.S. (2009). Amyloid beta-protein fragments 25-35 and 31-35 potentiate long-term depression in hippocampal CA1 region of rats in vivo. Synapse *63*, 206-214.

Cheong, H., and Klionsky, D.J. (2008). Biochemical methods to monitor autophagy-related processes in yeast. Methods Enzymol *451*, 1-26.

Cherny, R.A., Legg, J.T., McLean, C.A., Fairlie, D.P., Huang, X., Atwood, C.S., Beyreuther, K., Tanzi, R.E., Masters, C.L., and Bush, A.I. (1999). Aqueous dissolution of Alzheimer's disease Abeta amyloid deposits by biometal depletion. J Biol Chem *274*, 23223-23228.

Chevrier, M., Brakch, N., Lesueur, C., Genty, D., Ramdani, Y., Moll, S., Djavaheri-Mergny, M., Brasse-Lagnel, C., Laquerriere, A., Barbey, F.*, et al.* (2010). Autophagosome maturation is impaired in Fabry disease. Autophagy *6*.

Chishti, M.A., Yang, D.S., Janus, C., Phinney, A.L., Horne, P., Pearson, J., Strome, R., Zuker, N., Loukides, J., French, J.*, et al.* (2001). Early-onset amyloid deposition and cognitive deficits in transgenic mice expressing a double mutant form of amyloid precursor protein 695. J Biol Chem *276*, 21562-21570.

Christensen, D.Z., Schneider-Axmann, T., Lucassen, P.J., Bayer, T.A., and Wirths, O. (2010). Accumulation of intraneuronal Abeta correlates with ApoE4 genotype. Acta Neuropathol *119*, 555-566.

Ciccotosto, G.D., Tew, D., Curtain, C.C., Smith, D., Carrington, D., Masters, C.L., Bush, A.L., Cherny, R.A., Cappai, R., and Barnham, K.J. (2004). Enhanced Toxicity and Cellular Binding of a Modified Amyloid Peptide with a Methionine to Valine Substitution. J Biol Chem *279*, 42528-42534.

Cirrito, J.R., Yamada, K.A., Finn, M.B., Sloviter, R.S., Bales, K.R., May, P.C., Schoepp, D.D., Paul, S.M., Mennerick, S., and Holtzman, D.M. (2005). Synaptic activity regulates interstitial fluid amyloid-beta levels in vivo. Neuron *48*, 913-922.

Citron, M., Oltersdorf, T., Haass, C., McConlogue, L., Hung, A.Y., Seubert, P., Vigo-Pelfrey, C., Lieberburg, I., and Selkoe, D.J. (1992). Mutation of the beta-amyloid precursor protein in familial Alzheimer's disease increases beta-protein production. Nature *360*, 672-674.

Cleary, J.P., Walsh, D.M., Hofmeister, J.J., Shankar, G.M., Kuskowski, M.A., Selkoe, D.J., and Ashe, K.H. (2005). Natural oligomers of the amyloid-beta protein specifically disrupt cognitive function. Nat Neurosci *8*, 79-84.

Cohen, M.M., Leboucher, G.P., Livnat-Levanon, N., Glickman, M.H., and Weissman, A.M. (2008). Ubiquitin-proteasome-dependent degradation of a mitofusin, a critical regulator of mitochondrial fusion. Mol Biol Cell *19*, 2457-2464.

Cole, G.M., and Ard, M.D. (2000). Influence of lipoproteins on microglial degradation of Alzheimer's amyloid beta-protein. Microsc Res Tech *50*, 316-324.

Cooke, S.F., and Bliss, T.V. (2006). Plasticity in the human central nervous system. Brain *129*, 1659-1673.

Cooney, J.R., Hurlburt, J.L., Selig, D.K., Harris, K.M., and Fiala, J.C. (2002). Endosomal compartments serve multiple hippocampal dendritic spines from a widespread rather than a local store of recycling membrane. J Neurosci *22*, 2215-2224.

Cooper, A.A., Gitler, A.D., Cashikar, A., Haynes, C.M., Hill, K.J., Bhullar, B., Liu, K., Xu, K., Strathearn, K.E., Liu, F.*, et al.* (2006). Alpha-synuclein blocks ER-Golgi traffic and Rab1 rescues neuron loss in Parkinson's models. Science *313*, 324-328.

Cooper, A.J., and Kristal, B.S. (1997). Multiple roles of glutathione in the central nervous system. Biol Chem *378*, 793-802.

Corder, E.H., Saunders, A.M., Pericak-Vance, M.A., and Roses, A.D. (1995a). There is a pathologic relationship between ApoE-epsilon 4 and Alzheimer's disease. Arch Neurol *52*, 650-651.

Corder, E.H., Saunders, A.M., Strittmatter, W.J., Schmechel, D.E., Gaskell, P.C., Jr., Rimmler, J.B., Locke, P.A., Conneally, P.M., Schmader, K.E., Tanzi, R.E.*, et al.* (1995b). Apolipoprotein E, survival in Alzheimer's disease patients, and the competing risks of death and Alzheimer's disease. Neurology *45*, 1323-1328.

Corder, E.H., Saunders, A.M., Strittmatter, W.J., Schmechel, D.E., Gaskell, P.C., Small, G.W., Roses, A.D., Haines, J.L., and Pericak-Vance, M.A. (1993).

Gene dose of apolipoprotein E type 4 allele and the risk of Alzheimer's disease in late onset families. Science *261*, 921-923.

Corneveaux, J.J., Myers, A.J., Allen, A.N., Pruzin, J.J., Ramirez, M., Engel, A., Nalls, M.A., Chen, K., Lee, W., Chewning, K.*, et al.* (2010). Association of CR1, CLU and PICALM with Alzheimer's disease in a cohort of clinically characterized and neuropathologically verified individuals. Hum Mol Genet *19*, 3295-3301.

Cota, D., Proulx, K., Smith, K.A., Kozma, S.C., Thomas, G., Woods, S.C., and Seeley, R.J. (2006). Hypothalamic mTOR signaling regulates food intake. Science *312*, 927-930.

Crews, L., Spencer, B., Desplats, P., Patrick, C., Paulino, A., Rockenstein, E., Hansen, L., Adame, A., Galasko, D., and Masliah, E. (2010). Selective molecular alterations in the autophagy pathway in patients with Lewy body disease and in models of alpha-synucleinopathy. PLoS One *5*, e9313.

Crouch, P.J., Blake, R., Duce, J.A., Ciccotosto, G.D., Li, Q.X., Barnham, K.J., Curtain, C.C., Cherny, R.A., Cappai, R., Dyrks, T.*, et al.* (2005). Copper-dependent inhibition of human cytochrome c oxidase by a dimeric conformer of amyloid-beta1-42. J Neurosci *25*, 672-679.

Crouch, P.J., Harding, S.M., White, A.R., Camakaris, J., Bush, A.I., and Masters, C.L. (2008). Mechanisms of A beta mediated neurodegeneration in Alzheimer's disease. Int J Biochem Cell Biol *40*, 181-198.

Curtain, C.C., Ali, F., Volitakis, I., Cherny, R.A., Norton, R.S., Beyreuther, K., Barrow, C.J., Masters, C.L., Bush, A.I., and Barnham, K.J. (2001). Alzheimer's disease amyloid-beta binds copper and zinc to generate an allosterically ordered membrane-penetrating structure containing superoxide dismutase-like subunits. J Biol Chem *276*, 20466-20473.

Cutler, N.S., Heitman, J., and Cardenas, M.E. (1999). TOR kinase homologs function in a signal transduction pathway that is conserved from yeast to mammals. Mol Cell Endocrinol *155*, 135-142.

Dahlgren, K.N., Manelli, A.M., Stine Jr., W.B., Baker, L.K., Krafft, G.A., and LaDu, M.J. (2002). Oligomeric and Fibrillar Species of Amyloid- Peptides Differentially Affect Neuronal Viability. J Biol Chem *277*, 32046-32053.

David, D.C., Layfield, R., Serpell, L., Narain, Y., Goedert, M., and Spillantini, M.G. (2002). Proteasomal degradation of tau protein. J Neurochem *83*, 176-185.

Davies, C.A., Mann, D.M., Sumpter, P.Q., and Yates, P.O. (1987). A quantitative morphometric analysis of the neuronal and synaptic content of the frontal and temporal cortex in patients with Alzheimer's disease. J Neurol Sci *78*, 151-164.

De Fusco, M., Marconi, R., Silvestri, L., Atorino, L., Rampoldi, L., Morgante, L., Ballabio, A., Aridon, P., and G., C. (2003). Haploinsufficiency of ATP1A2 encoding the Na+/K+ pump alpha2 subunit associated with familial hemiplegic migraine type 2. Nat Genet *33*, 192-196.

De Strooper, B. (2007). Loss-of-function presenilin mutations in Alzheimer disease. Talking Point on the role of presenilin mutations in Alzheimer disease. EMBO Rep *8*, 141-146.

Deane, R., Sagare, A., Hamm, K., Parisi, M., Lane, S., Finn, M.B., Holtzman, D.M., and Zlokovic, B.V. (2008). apoE isoform-specific disruption of amyloid beta peptide clearance from mouse brain. J Clin Invest *118*, 4002-4013.

Deary, I.J., Whiteman, M.C., Pattie, A., Starr, J.M., Hayward, C., Wright, A.F., Carothers, A., and Whalley, L.J. (2002). Cognitive change and the APOE epsilon 4 allele. Nature *418*, 932.

Delacourte, A., and Defossez, A. (1986). Alzheimer's disease: Tau proteins, the promoting factors of microtubule assembly, are major components of paired helical filaments. J Neurol Sci *76*, 173-186.

DeMattos, R.B., Bales, K.R., Cummins, D.J., Dodart, J.C., Paul, S.M., and Holtzman, D.M. (2001). Peripheral anti-A beta antibody alters CNS and plasma A beta clearance and decreases brain A beta burden in a mouse model of Alzheimer's disease. Proc Natl Acad Sci U S A *98*, 8850-8855.

DeMattos, R.B., Bales, K.R., Cummins, D.J., Paul, S.M., and Holtzman, D.M. (2002). Brain to plasma amyloid-beta efflux: a measure of brain amyloid burden in a mouse model of Alzheimer's disease. Science *295*, 2264-2267.

Demuro, A., Mina, E., Kayed, R., Milton, S.C., Parker, I., and Glabe, C.G. (2005). Calcium dysregulation and membrane disruption as a ubiquitous

neurotoxic mechanism of soluble amyloid oligomers. J Biol Chem *280*, 17294-17300.

Demuro, A., Parker, I., and Stutzmann, G.E. (2010). Calcium signaling and amyloid toxicity in Alzheimer disease. J Biol Chem *285*, 12463-12468.

Devi, L., Prabhu, B.M., Galati, D.F., Avadhani, N.G., and Anandatheerthavarada, H.K. (2006). Accumulation of amyloid precursor protein in the mitochondrial import channels of human Alzheimer's disease brain is associated with mitochondrial dysfunction. J Neurosci *26*, 9057-9068.

Dickey, C.A., Gordon, M.N., Wilcock, D.M., Herber, D.L., Freeman, M.J., and Morgan, D. (2005). Dysregulation of Na+/K+ ATPase by amyloid in APP+PS1 transgenic mice. BMC Neurosci *6*, 1-11.

Dickey, C.A., Loring, J.F., Montgomery, J., Gordon, M.N., Eastman, P.S., and Morgan, D. (2003). Selectively reduced expression of synaptic plasticity-related genes in amyloid precursor protein + presenilin-1 transgenic mice. J Neurosci *23*, 5219-5226.

Dickson, D.W. (1997). Neuropathological diagnosis of Alzheimer's disease: a perspective from longitudinal clinicopathological studies. Neurobiol Aging *18*, S21-26.

Ding, X.L., Husseman, J., Tomashevski, A., Nochlin, D., Jin, L.W., and Vincent, I. (2000). The cell cycle Cdc25A tyrosine phosphatase is activated in degenerating postmitotic neurons in Alzheimer's disease. Am J Pathol *157*, 1983-1990.

Dobeli, H., Draeger, N., Huber, G., Jakob, P., Schmidt, D., Seilheimer, B., Stuber, D., Wipf, B., and Zulauf, M. (1995). A biotechnological method provides access to aggregation competent monomeric Alzheimer's 1-42 residue amyloid peptide. Biotechnology (N Y) *13*, 988-993.

Dong, J., Atwood, C.S., Anderson, V.E., Siedlak, S.L., Smith, M.A., Perry, G., and Carey, P.R. (2003). Metal binding and oxidation of amyloid-beta within isolated senile plaque cores: Raman microscopic evidence. Biochemistry *42*, 2768-2773.

Doody, R.S., Gavrilova, S.I., Sano, M., Thomas, R.G., Aisen, P.S., Bachurin, S.O., Seely, L., and Hung, D. (2008). Effect of dimebon on cognition, activities of daily living, behaviour, and global function in patients with mild-to-moderate

Alzheimer's disease: a randomised, double-blind, placebo-controlled study. Lancet *372*, 207-215.

Dreyer, R.N., Bausch, K.M., Fracasso, P., Hammond, L.J., Wunderlich, D., Wirak, D.O., Davis, G., Brini, C.M., Buckholz, T.M., Konig, G.*, et al.* (1994). Processing of the pre-beta-amyloid protein by cathepsin D is enhanced by a familial Alzheimer's disease mutation. Eur J Biochem *224*, 265-271.

Duara, R., Grady, C., Haxby, J., Sundaram, M., Cutler, N.R., Heston, L., Moore, A., Schlageter, N., Larson, S., and Rapoport, S.I. (1986). Positron emission tomography in Alzheimer's disease. Neurology *36*, 879-887.

Dubois, B., Feldman, H.H., Jacova, C., Dekosky, S.T., Barberger-Gateau, P., Cummings, J., Delacourte, A., Galasko, D., Gauthier, S., Jicha, G.*, et al.* (2007). Research criteria for the diagnosis of Alzheimer's disease: revising the NINCDS-ADRDA criteria. Lancet Neurol *6*, 734-746.

Duce, J.A., Tsatsanis, A., Cater, M.A., James, S.A., Robb, E., Wikhe, K., Leong, S.L., Perez, K., Johanssen, T., Greenough, M.A.*, et al.* (2010). Iron-export ferroxidase activity of beta-amyloid precursor protein is inhibited by zinc in Alzheimer's disease. Cell *142*, 857-867.

Duff, K., and Suleman, F. (2004). Transgenic mouse models of Alzheimer's disease: how useful have they been for therapeutic development? Brief Funct Genomic Proteomic *3*, 47-59.

Dumery, L., Bourdel, F., Soussan, Y., Fialkowsky, A., Viale, S., Nicolas, P., and Reboud-Ravaux, M. (2001). beta-amyloid protein aggregation: its implication in the physiopathology of Alzheimer's disease. Pathol Biol *49*, 72-85.

Duyckaerts, C., Potier, M.C., and Delatour, B. (2008). Alzheimer disease models and human neuropathology: similarities and differences. Acta Neuropathol *115*, 5-38.

Dyrks, T., Dyrks, E., Hartmann, T., Masters, C.L., and Beyreuther, K. (1992). Amyloidogenicity of bA4 and bA4-bearing APP fragments by metal catalysed oxidation. J Biol Chem *267*, 18210-18217.

Eckhardt, M. (2010). Pathology and current treatment of neurodegenerative sphingolipidoses. Neuromolecular Med *12*, 362-382.

Eckman, C.B., Mehta, N.D., Crook, R., Perez-tur, J., Prihar, G., Pfeiffer, E., Graff-Radford, N., Hinder, P., Yager, D., Zenk, B.*, et al.* (1997). A new pathogenic mutation in the APP gene (I716V) increases the relative proportion of A beta 42(43). Hum Mol Genet *6*, 2087-2089.

Edbauer, D., Kaether, C., Steiner, H., and Haass, C. (2004). Co-expression of nicastrin and presenilin rescues a loss of function mutant of APH-1. J Biol Chem *279*, 37311-37315.

Edbauer, D., Winkler, E., Haass, C., and Steiner, H. (2002). Presenilin and nicastrin regulate each other and determine amyloid beta-peptide production via complex formation. Proc Natl Acad Sci U S A *99*, 8666-8671.

Edbauer, D., Winkler, E., Regula, J.T., Pesold, B., Steiner, H., and Haass, C. (2003). Reconstitution of gamma-secretase activity. Nat Cell Biol *5*, 486-488.

Editorial (2010a). Learning from failure. Nat Rev Drug Discov *9*, 499.

Editorial (2010b). Mechanism matters. Nat Med *16*, 347.

Egner, R., Mahe, Y., Pandjaitan, R., and Kuchler, K. (1995). Endocytosis and vacuolar degradation of the plasma membrane-localized Pdr5 ATP-binding cassette multidrug transporter in Saccharomyces cerevisiae. Mol Cell Biol *15*, 5879-5887.

Ehehalt, R., Keller, P., Haass, C., Thiele, C., and Simons, K. (2003). Amyloidogenic processing of the Alzheimer beta-amyloid precursor protein depends on lipid rafts. J Cell Biol *160*, 113-123.

Einstein, G., Buranosky, R., and Crain, B.J. (1994). Dendritic pathology of granule cells in Alzheimer's disease is unrelated to neuritic plaques. J Neurosci *14*, 5077-5088.

Eisenberg, T., Buttner, S., Kroemer, G., and Madeo, F. (2007). The mitochondrial pathway in yeast apoptosis. Apoptosis *12*, 1011-1023.

Elgersma, R.C., Mulder, G.E., Kruijtzer, J.A.W., Posthuma, G., Rijkers, D.T.S., and Liskamp, R.M.J. (2007). Transformation of the amyloidogenic peptide amylin(20-29) into its corresponding peptoid and retropeptoid: Access to both an amyloid inhibitor and template for self-assembled supramolecular tapes. Bioorg Med Chem Lett *17*, 1837-1842.

Enya, M., Morishima-Kawashima, M., Yoshimura, M., Shinkai, Y., Kusui, K., Khan, K., Games, D., Schenk, D., Sugihara, S., Yamaguchi, H.*, et al.* (1999). Appearance of sodium dodecyl sulfate-stable amyloid beta-protein (Abeta) dimer in the cortex during aging. Am J Pathol *154*, 271-279.

Erecinska, M., Cherian, S., and Silver, I.A. (2004). Energy metabolism in mammalian brain during development. Prog Neurobiol *73*, 397-445.

Esselens, C., Oorschot, V., Baert, V., Raemaekers, T., Spittaels, K., Serneels, L., Zheng, H., Saftig, P., De Strooper, B., Klumperman, J.*, et al.* (2004). Presenilin 1 mediates the turnover of telencephalin in hippocampal neurons via an autophagic degradative pathway. J Cell Biol *166*, 1041-1054.

Estrada, L.D., and Soto, C. (2007). Disrupting beta-amyloid aggregation for Alzheimer disease treatment. Curr Top Med Chem *7*, 115-126.

Evin, G., Cappai, R., Li, Q.X., Culvenor, J.G., Small, D.H., Beyreuther, K., and Masters, C.L. (1995). Candidate gamma-secretases in the generation of the carboxyl terminus of the Alzheimer's disease beta A4 amyloid: possible involvement of cathepsin D. Biochemistry *34*, 14185-14192.

Falkevall, A., Alikhani, N., Bhushan, S., Pavlov, P.F., Busch, K., Johnson, K.A., Eneqvist, T., Tjernberg, L., Ankarcrona, M., and Glaser, E. (2006). Degradation of the amyloid beta-protein by the novel mitochondrial peptidasome, PreP. J Biol Chem *281*, 29096-29104.

Farrer, L.A., Cupples, L.A., Haines, J.L., Hyman, B., Kukull, W.A., Mayeux, R., Myers, R.H., Pericak-Vance, M.A., Risch, N., and van Duijn, C.M. (1997). Effects of age, sex, and ethnicity on the association between apolipoprotein E genotype and Alzheimer disease. A meta-analysis. APOE and Alzheimer Disease Meta Analysis Consortium. JAMA *278*, 1349-1356.

Feddersen, R.M., Ehlenfeldt, R., Yunis, W.S., Clark, H.B., and Orr, H.T. (1992). Disrupted cerebellar cortical development and progressive degeneration of Purkinje cells in SV40 T antigen transgenic mice. Neuron *9*, 955-966.

Felbor, U., Kessler, B., Mothes, W., Goebel, H.H., Ploegh, H.L., Bronson, R.T., and Olsen, B.R. (2002). Neuronal loss and brain atrophy in mice lacking cathepsins B and L. Proc Natl Acad Sci U S A *99*, 7883-7888.

Ferrandini, E., Castillo, M., Lopez, M.B., and Laencina, J. (2005). A review of the models for the structure of the casein micelle. J Anim Sci *83*, 143-143.

Ferreira, S.T., Vieira, M.N., and De Felice, F.G. (2007). Soluble protein oligomers as emerging toxins in Alzheimer's and other amyloid diseases. IUBMB Life *59*, 332-345.

Ferrer, I., and Gullotta, F. (1990). Down's syndrome and Alzheimer's disease: dendritic spine counts in the hippocampus. Acta Neuropathol *79*, 680-685.

Ferri, C.P., Prince, M., Brayne, C., Brodaty, H., Fratiglioni, L., Ganguli, M., Hall, K., Hasegawa, K., Hendrie, H., Huang, Y.*, et al.* (2005). Global prevalence of dementia: a Delphi consensus study. Lancet *366*, 2112-2117.

Fezoui, Y., Hartley, D.M., Harper, J.D., Khurana, R., Walsh, D.M., Condron, M.M., Selkoe, D.J., Lansbury, P.T., Jr., Fink, A.L., and Teplow, D.B. (2000). An improved method of preparing the amyloid beta-protein for fibrillogenesis and neurotoxicity experiments. Amyloid *7*, 166-178.

Findeis, M.A. (2002). Peptide inhibitors of beta amyloid aggregation. Curr Top Med Chem *2*, 417-423.

Finelli, A., Kelkar, A., Song, H.J., Yang, H., and Konsolaki, M. (2004). A model for studying Alzheimer's Abeta42-induced toxicity in Drosophila melanogaster. Mol Cell Neurosci *26*, 365-375.

Fischer-Parton, S., Parton, R.M., Hickey, P.C., Dijksterhuis, J., Atkinson, H.A., and Read, N.D. (2000). Confocal microscopy of FM4-64 as a tool for analysing endocytosis and vesicle trafficking in living fungal hyphae. J Microsc *198*, 246-259.

Fiskum, G., Murphy, A.N., and Beal, M.F. (1999). Mitochondria in neurodegeneration: acute ischemia and chronic neurodegenerative diseases. J Cereb Blood Flow Metab *19*, 351-369.

Flory, J.D., Manuck, S.B., Ferrell, R.E., Ryan, C.M., and Muldoon, M.F. (2000). Memory performance and the apolipoprotein E polymorphism in a community sample of middle-aged adults. Am J Med Genet *96*, 707-711.

Floto, R.A., Sarkar, S., Perlstein, E.O., Kampmann, B., Schreiber, S.L., and Rubinsztein, D.C. (2007). Small molecule enhancers of rapamycin-induced TOR inhibition promote autophagy, reduce toxicity in Huntington's disease models and enhance killing of mycobacteria by macrophages. Autophagy *3*, 620-622.

Flower, T.R., Chesnokova, L.S., Froelich, C.A., Dixon, C., and Witt, S.N. (2005). Heat shock prevents alpha-synuclein-induced apoptosis in a yeast model of Parkinson's disease. J Mol Biol *351*, 1081-1100.

Foguel, D., Robinson, C.R., Sousa Jr., P.C., Silva, J.L., and Robinson, A.S. (1999). Hydrostatic pressure rescues native protein from aggregates. Biotechnol Bioeng, 552-558.

Fonte, J., Miklossy, J., Atwood, C., and Martins, R. (2001). The severity of cortical Alzheimer's type changes is positively correlated with increased amyloid-beta Levels: Resolubilization of amyloid-beta with transition metal ion chelators. J Alzheimers Dis *3*, 209-219.

Fonte, V., Kapulkin, V., Taft, A., Fluet, A., Friedman, D., and Link, C.D. (2002). Interaction of intracellular beta amyloid peptide with chaperone proteins. Proc Natl Acad Sci U S A *99*, 9439-9444.

Fonte, V., Kipp, D.R., Yerg, J., Merin, D., Forrestal, M., Wagner, E., Roberts, C.M., and Link, C.D. (2008). Suppression of in vivo beta-amyloid peptide toxicity by overexpression of the HSP-16.2 small chaperone protein. J Biol Chem *283*, 784-791.

Fornai, F., Longone, P., Cafaro, L., Kastsiuchenka, O., Ferrucci, M., Manca, M.L., Lazzeri, G., Spalloni, A., Bellio, N., Lenzi, P.*, et al.* (2008). Lithium delays progression of amyotrophic lateral sclerosis. Proc Natl Acad Sci U S A *105*, 2052-2057.

Forsberg, H., Gilstring, C.F., Zargari, A., Martinez, P., and Ljungdahl, P.O. (2001). The role of the yeast plasma membrane SPS nutrient sensor in the metabolic response to extracellular amino acids. Mol Microbiol *42*, 215-228.

Forsberg, H., and Ljungdahl, P.O. (2001a). Genetic and biochemical analysis of the yeast plasma membrane Ssy1p-Ptr3p-Ssy5p sensor of extracellular amino acids. Mol Cell Biol *21*, 814-826.

Forsberg, H., and Ljungdahl, P.O. (2001b). Sensors of extracellular nutrients in Saccharomyces cerevisiae. Curr Genet *40*, 91-109.

Forstl, H., and Kurz, A. (1999). Clinical features of Alzheimer's disease. Eur Arch Psychiatry Clin Neurosci *249*, 288-290.

Foury, F. (1997). Human genetic diseases: a cross-talk between man and yeast. Gene *195*, 1-10.

Francis, R., McGrath, G., Zhang, J., Ruddy, D.A., Sym, M., Apfeld, J., Nicoll, M., Maxwell, M., Hai, B., Ellis, M.C.*, et al.* (2002). aph-1 and pen-2 are required for Notch pathway signaling, gamma-secretase cleavage of betaAPP, and presenilin protein accumulation. Dev Cell *3*, 85-97.

Franssens, V., Boelen, E., Anandhakumar, J., Vanhelmont, T., Buttner, S., and Winderickx, J. (2009). Yeast unfolds the road map toward alpha-synuclein-induced cell death. Cell Death Differ *17*, 746-753.

Frasca, G., Chiechio, S., Vancheri, C., Nicoletti, F., Copani, A., and Angela Sortino, M. (2004). Beta-amyloid-activated cell cycle in SH-SY5Y neuroblastoma cells: correlation with the MAP kinase pathway. J Mol Neurosci *22*, 231-236.

Fuentealba, R.A., Farias, G., Scheu, J., Bronfman, M., Marzolo, M.P., and Inestrosa, N.C. (2004). Signal transduction during amyloid-beta-peptide neurotoxicity: role in Alzheimer disease. Brain Res Brain Res Rev *47*, 275-289.

Fukuda, T., Roberts, A., Ahearn, M., Zaal, K., Ralston, E., Plotz, P.H., and Raben, N. (2006). Autophagy and lysosomes in Pompe disease. Autophagy *2*, 318-320.

Funato, H., Enya, M., Yoshimura, M., Morishima-Kawashima, M., and Ihara, Y. (1999). Presence of sodium dodecyl sulfate-stable amyloid beta-protein dimers in the hippocampus CA1 not exhibiting neurofibrillary tangle formation. Am J Pathol *155*, 23-28.

Furukawa, K., Sopher, B.L., Rydel, R.E., Begley, J.G., Pham, D.G., Martin, G.M., Fox, M., and Mattson, M.P. (1996). Increased activity-regulating and neuroprotective efficacy of alpha-secretase-derived secreted amyloid precursor protein conferred by a C-terminal heparin-binding domain. J Neurochem *67*, 1882-1896.

Futai, E., Yagishita, S., and Ishiura, S. (2009). Nicastrin is dispensable for gamma-secretase protease activity in the presence of specific presenilin mutations. J Biol Chem *284*, 13013-13022.

Gabbita, S.P., Lovell, M.A., and Markesbery, W.R. (1998). Increased nuclear DNA oxidation in the brain in Alzheimer's disease. J Neurochem *71*, 2034-2040.

Gandy, S., Almeida, O.P., Fonte, J., Lim, D., Waterrus, A., Spry, N., Flicker, L., and Martins, R.N. (2001). Chemical andropause and amyloid-beta peptide. JAMA *285*, 2195-2196.

Ganguly, A., Feldman, R.M., and Guo, M. (2008). ubiquilin antagonizes presenilin and promotes neurodegeneration in Drosophila. Hum Mol Genet *17*, 293-302.

Gasch, A.P., Spellman, P.T., Kao, C.M., Carmel-Harel, O., Eisen, M.B., Storz, G., Botstein, D., and Brown, P.O. (2000). Genomic expression programs in the response of yeast cells to environmental changes. Mol Biol Cell *11*, 4241-4257.

Gauthier, S., Aisen, P.S., Ferris, S.H., Saumier, D., Duong, A., Haine, D., Garceau, D., Suhy, J., Oh, J., Lau, W.*, et al.* (2009). Effect of tramiprosate in patients with mild-to-moderate Alzheimer's disease: exploratory analyses of the MRI sub-group of the Alphase study. J Nutr Health Aging *13*, 550-557.

Georgiades, J.A. (2004). Novel peptides isolated from colostrinin polypeptide, useful for treating viral and bacterial infections, disorders of immune system and central nervous system e.g., Alzheimer's disease, dementia, and as food additive (REGEN THERAPEUTICS PLC (REGE-Non-standard) GEORGIADES J A (GEOR-Individual)), pp. 1341816-A1341812:.

Geula, C., Wu, C.K., Saroff, D., Lorenzo, A., Yuan, M., and Yankner, B.A. (1998). Aging renders the brain vulnerable to amyloid beta-protein neurotoxicity. Nat Med *4*, 827-831.

Giaever, G., et al. (2002). Functional profiling of the Saccharomyces cerevisiae genome. Nature *418*, 387-391.

Gilman, S., Koller, M., Black, R.S., Jenkins, L., Griffith, S.G., Fox, N.C., Eisner, L., Kirby, L., Rovira, M.B., Forette, F.*, et al.* (2005). Clinical effects of Abeta immunization (AN1792) in patients with AD in an interrupted trial. Neurology *64*, 1553-1562.

Giorgetti, M., Gibbons, J.A., Bernales, S., Alfaro, I.E., Drieu La Rochelle, C., Cremers, T., Altar, C.A., Wronski, R., Hutter-Paier, B., and Protter, A.A. (2010). Cognition-enhancing properties of Dimebon in a rat novel object recognition task are unlikely to be associated with acetylcholinesterase inhibition or N-methyl-D-aspartate receptor antagonism. J Pharmacol Exp Ther *333*, 748-757.

Giovanni, A., Wirtz-Brugger, F., Keramaris, E., Slack, R., and Park, D.S. (1999). Involvement of cell cycle elements, cyclin-dependent kinases, pRb, and E2F x DP, in B-amyloid-induced neuronal death. J Biol Chem *274*, 19011-19016.

Giulian, D., Haverkamp, L.J., Yu, J.H., Karshin, W., Tom, D., Li, J., Kirkpatrick, J., Kuo, Y.M., and Roher, A.E. (1996). Specific domains of beta-amyloid from Alzheimer plaque elicit neuron killing in human microglia. J Neurosci 6021-6037

Glabe, C.G. (2006). Common mechanisms of amyloid oligomer pathogenesis in degenerative disease. Neurobiol Aging *27*, 570-575.

Glabe, C.G., and Kayed, R. (2006). Common structure and toxic function of amyloid oligomers implies a common mechanism of pathogenesis. Neurology *66*, S74-78.

Glenner, G.G., and Wong, C.W. (1984a). Alzheimer's disease: initial report of the purification and characterization of a novel cerebrovascular amyloid protein. Biochem Biophys Res Commun *120*, 885-890.

Glenner, G.G., and Wong, C.W. (1984b). Alzheimer's disease and Down's syndrome: sharing of a unique cerebrovascular amyloid fibril protein. Biochem Biophys Res Commun *122*, 1131-1135.

Goedert, M., and Spillantini, M.G. (2006). A century of Alzheimer's disease. Science *314*, 777-781.

Goedert, M., Spillantini, M.G., Jakes, R., Rutherford, D., and Crowther, R.A. (1989). Multiple isoforms of human microtubule-associated protein tau: sequences and localization in neurofibrillary tangles of Alzheimer's disease. Neuron *3*, 519-526.

Gokhale, K.C., Newnam, G.P., Sherman, M.Y., and Chernoff, Y.O. (2005). Modulation of prion-dependent polyglutamine aggregation and toxicity by chaperone proteins in the yeast model. J Biol Chem *280*, 22809-22818.

Golde, T.E., Estus, S., Younkin, L.H., Selkoe, D.J., and Younkin, S.G. (1992). Processing of the amyloid protein precursor to potentially amyloidogenic derivatives. Science *255*, 728-730.

Goldman, W.P., Price, J.L., Storandt, M., Grant, E.A., McKeel, D.W., Jr., Rubin, E.H., and Morris, J.C. (2001). Absence of cognitive impairment or decline in preclinical Alzheimer's disease. Neurology *56*, 361-367.

Gong, B., Cao, Z., Zheng, P., Vitolo, O.V., Liu, S., Staniszewski, A., Moolman, D., Zhang, H., Shelanski, M., and Arancio, O. (2006). Ubiquitin hydrolase Uch-L1 rescues beta-amyloid-induced decreases in synaptic function and contextual memory. Cell *126*, 775-788.

Gong, Y., Chang, L., Viola, K.L., Lacor, P.N., Lambert, M.P., Finch, C.E., Krafft, G.A., and Klein, W.L. (2003). Alzheimer's disease-affected brain: presence of oligomeric A beta ligands (ADDLs) suggests a molecular basis for reversible memory loss. Proc Natl Acad Sci U S A *100*, 10417-10422.

Goormaghtigh, E., Raussens, V., and Ruysschaert, J.M. (1999). Attenuated total reflection infrared spectroscopy of proteins and lipids in biological membranes. Biochim Biophys Acta-Rev Biomembr *1422*, 105-185.

Gordon, D.J., Tappe, R., and Meredith, S.C. (2002). Design and characterization of a membrane permeable N-methyl amino acid-containing peptide that inhibits A beta(1-40) fibrillogenesis. J Pept Res *60*, 37-55.

Gouras, G.K., Tsai, J., Naslund, J., Vincent, B., Edgar, M., Checler, F., Greenfield, J.P., Haroutunian, V., Buxbaum, J.D., Xu, H.*, et al.* (2000). Intraneuronal Abeta42 accumulation in human brain. Am J Pathol *156*, 15-20.

Grabowski, T.J., Cho, H.S., Vonsattel, J.P., Rebeck, G.W., and Greenberg, S.M. (2001). Novel amyloid precursor protein mutation in an Iowa family with dementia and severe cerebral amyloid angiopathy. Ann Neurol *49*, 697-705.

Gregori, L., Fuchs, C., Figueiredo-Pereira, M.E., Van Nostrand, W.E., and Goldgaber, D. (1995). Amyloid beta-protein inhibits ubiquitin-dependent protein degradation in vitro. J Biol Chem *270*, 19702-19708.

Gregori, L., Hainfeld, J.F., Simon, M.N., and Goldgaber, D. (1997). Binding of Amyloid b Protein to the 20 S Proteasome. J Biol Chem *272*, 58-62.

Griffin, W.S., Stanley, L.C., Ling, C., White, L., MacLeod, V., Perrot, L.J., White III, C.L., and Araoz, C. (1989). Brain interleukin 1 and S-100 immunoreactivity are elevated in Down syndrome and Alzheimer disease. Proc Natl Acad Sci USA *86*, 7611-7615.

Grigorev, V.V., Dranyi, O.A., and Bachurin, S.O. (2003). Comparative study of action mechanisms of dimebon and memantine on AMPA- and NMDA-subtypes glutamate receptors in rat cerebral neurons. Bull Exp Biol Med *136*, 474-477.

Guo, Q., Fu, W., Sopher, B.L., Miller, M.W., Ware, C.B., Martin, G.M., and Mattson, M.P. (1999). Increased vulnerability of hippocampal neurons to excitotoxic necrosis in presenilin-1 mutant knock-in mice. Nat Med *5*, 101-106.

Haass, C., Hung, A.Y., Schlossmacher, M.G., Teplow, D.B., and Selkoe, D.J. (1993). beta-Amyloid peptide and a 3-kDa fragment are derived by distinct cellular mechanisms. J Biol Chem *268*, 3021-3024.

Haass, C., Lemere, C.A., Capell, A., Citron, M., Seubert, P., Schenk, D., Lannfelt, L., and Selkoe, D.J. (1995). The Swedish mutation causes early-onset Alzheimer's disease by beta-secretase cleavage within the secretory pathway. Nat Med *1*, 1291-1296.

Haass, C., Schlossmacher, M.G., Hung, A.Y., Vigo-Pelfrey, C., Mellon, A., and Ostaszewski, B.L. (1992). Amyloid b-peptide is produced by cultured cells during normal metabolism. Nature *359*, 322-325.

Haass, C., and Selkoe, D.J. (2007). Soluble protein oligomers in neurodegeneration: lessons from the Alzheimer's amyloid beta-peptide. Nat Rev Mol Cell Biol *8*, 101-112.

Hansson, C.A., Frykman, S., Farmery, M.R., Tjernberg, L.O., Nilsberth, C., Pursglove, S.E., Ito, A., Winblad, B., Cowburn, R.F., Thyberg, J.*, et al.* (2004). Nicastrin, presenilin, APH-1, and PEN-2 form active gamma-secretase complexes in mitochondria. J Biol Chem *279*, 51654-51660.

Hara, T., Nakamura, K., Matsui, M., Yamamoto, A., Nakahara, Y., Suzuki-Migishima, R., Yokoyama, M., Mishima, K., Saito, I., Okano, H.*, et al.* (2006). Suppression of basal autophagy in neural cells causes neurodegenerative disease in mice. Nature *441*, 885-889.

Harkany, T., Abraham, I., Konya, C., Nyakas, C., Zarandi, M., Penke, B., and Luiten, P.G. (2000). Mechanisms of beta-amyloid neurotoxicity: perspectives of pharmacotherapy. Rev Neurosci *11*, 329-382.

Harold, D., Abraham, R., Hollingworth, P., Sims, R., Gerrish, A., Hamshere, M.L., Pahwa, J.S., Moskvina, V., Dowzell, K., Williams, A.*, et al.* (2009).

Genome-wide association study identifies variants at CLU and PICALM associated with Alzheimer's disease. Nat Genet *41*, 1088-1093.

Hartig, W., Stieler, J., Boerema, A.S., Wolf, J., Schmidt, U., Weissfuss, J., Bullmann, T., Strijkstra, A.M., and Arendt, T. (2007). Hibernation model of tau phosphorylation in hamsters: selective vulnerability of cholinergic basal forebrain neurons - implications for Alzheimer's disease. Eur J Neurosci *25*, 69-80.

Hartmann, H., Eckert, A., and Muller, W.E. (1994). Disturbances of the neuronal calcium homeostasis in the aging nervous system. Life Sci 2011-2018.

Hartwell, L. (2004a). Genetics. Robust interactions. Science *303*, 774-775.

Hartwell, L.H. (2004b). Yeast and cancer. Biosci Rep *24*, 523-544.

Hattori, N., Kitagawa, K., Higashida, T., Yagyu, K., Shimohama, S., Wataya, T., Perry, G., Smith, M.A., and Inagaki, C. (1998). CI-ATPase and Na+/K(+)-ATPase activities in Alzheimer's disease brains. Neurosci Lett *254*, 141-144.

Havel, R.J. (1998). Receptor and non-receptor mediated uptake of chylomicron remnants by the liver. Atherosclerosis *141 Suppl 1*, S1-7.

Haxby, J.V., Grady, C.L., Duara, R., Schlageter, N., Berg, G., and Rapoport, S.I. (1986). Neocortical metabolic abnormalities precede nonmemory cognitive defects in early Alzheimer's-type dementia. Arch Neurol *43*, 882-885.

Hay, N., and Sonenberg, N. (2004). Upstream and downstream of mTOR. Genes Dev *18*, 1926-1945.

Haynes, C.M., Titus, E.A., and Cooper, A.A. (2004). Degradation of misfolded proteins prevents ER-derived oxidative stress and cell death. Mol Cell *15*, 767-776.

He, C., and Klionsky, D.J. (2009). Regulation mechanisms and signaling pathways of autophagy. Annu Rev Genet *43*, 67-93.

Heinemeyer, W., Gruhler, A., Mohrle, V., Mahe, Y., and Wolf, D.H. (1993). PRE2, highly homologous to the human major histocompatibility complex-linked RING10 gene, codes for a yeast proteasome subunit necessary for

chrymotryptic activity and degradation of ubiquitinated proteins. J Biol Chem *268*, 5115-5120.

Heinemeyer, W., Kleinschmidt, J.A., Saidowsky, J., Escher, C., and Wolf, D.H. (1991). Proteinase yscE, the yeast proteasome/multicatalytic-multifunctional proteinase: mutants unravel its function in stress induced proteolysis and uncover its necessity for cell survival. EMBO J *10*, 555-562.

Heitman, J., Movva, N.R., and Hall, M.N. (1991). Targets for cell cycle arrest by the immunosuppressant rapamycin in yeast. Science *253*, 905-909.

Hemelaar, J., Lelyveld, V.S., Kessler, B.M., and Ploegh, H.L. (2003). A single protease, Apg4B, is specific for the autophagy-related ubiquitin-like proteins GATE-16, MAP1-LC3, GABARAP, and Apg8L. J Biol Chem *278*, 51841-51850.

Hendriks, L., van Duijn, C.M., Cras, P., Cruts, M., Van Hul, W., van Harskamp, F., Warren, A., McInnis, M.G., Antonarakis, S.E., and Martin, J.J. (1992). Presenile dementia and cerebral haemorrhage linked to a mutation at codon 692 of the beta-amyloid precursor protein gene. Nat Genet *1*, 218-221.

Herl, L., Thomas, A.V., Lill, C.M., Banks, M., Deng, A., Jones, P.B., Spoelgen, R., Hyman, B.T., and Berezovska, O. (2009). Mutations in amyloid precursor protein affect its interactions with presenilin/gamma-secretase. Mol Cell Neurosci *41*, 166-174.

Herman, P.K. (2002). Stationary phase in yeast. Curr Opin Microbiol *5*, 602-607.

Hershko, A., and Ciechanover, A. (1998). The ubiquitin system. Annu Rev Biochem *67*, 425-479.

Hilt, W., Heinemeyer, W., and Wolf, D.H. (1996). The proteasome and protein degradation in yeast. Adv Exp Med Biol *389*, 197-202.

Hilt, W., and Wolf, D.H. (1996). Proteasomes: destruction as a programme. Trends Biochem Sci *21*, 96-102.

Hirai, K., Aliev, G., Nunomura, A., Fujioka, H., Russell, R.L., Atwood, C.S., Johnson, A.B., Kress, Y., Vinters, H.V., Tabaton, M.*, et al.* (2001). Mitochondrial abnormalities in Alzheimer's disease. J Neurosci *21*, 3017-3023.

Hochstrasser, M. (1995). Ubiquitin, proteasomes, and the regulation of intracellular protein degradation. Curr Opin Cell Biol *7*, 215-223.

Hochstrasser, M. (1996). Protein degradation or regulation: Ub the judge. Cell *84*, 813-815.

Hof, P.R., and Morrison, J.H. (2004). The aging brain: morphomolecular senescence of cortical circuits. Trends Neurosci *27*, 607-613.

Hof, P.R., Vogt, B.A., Bouras, C., and Morrison, J.H. (1997). Atypical form of Alzheimer's disease with prominent posterior cortical atrophy: a review of lesion distribution and circuit disconnection in cortical visual pathways. Vision Res *37*, 3609-3625.

Hollingworth, P., Harold, D., Sims, R., Gerrish, A., Lambert, J.C., Carrasquillo, M.M., Abraham, R., Hamshere, M.L., Pahwa, J.S., Moskvina, V.*, et al.* (2011). Common variants at ABCA7, MS4A6A/MS4A4E, EPHA1, CD33 and CD2AP are associated with Alzheimer's disease. Nat Genet *43*, 429-435.

Holtzman, D.M. (2001). Role of apoE/Aβ interactions in the pathogenesis of Alzheimer's disease and cerebral amyloid angiopathy. J Mol Neurosci *17*, 147-155.

Holtzman, D.M., Pitas, R.E., Kilbridge, J., Nathan, B., Mahley, R.W., Bu, G., and Schwartz, A.L. (1995). Low density lipoprotein receptor-related protein mediates apolipoprotein E-dependent neurite outgrowth in a central nervous system-derived neuronal cell line. Proc Natl Acad Sci U S A *92*, 9480-9484.

Hone, E., Martins, I.J., Fonte, J., and Martins, R.N. (2003). Apolipoprotein E influences amyloid-beta clearance from the murine periphery. J Alzheimers Dis *5*, 1-8.

Hong, E., Davidson, A.R., and Kaiser, C.A. (1996). A pathway for targeting soluble misfolded proteins to the yeast vacuole. J Cell Biol *135*, 623-633.

Hortschansky, P., Schroeckh, V., Christopeit, T., Zandomeneghi, G., and Fandrich, M. (2005). The aggregation kinetics of Alzheimer's beta-amyloid peptide is controlled by stochastic nucleation. Protein Sci *14*, 1753-1759.

Howieson, D.B., Dame, A., Camicioli, R., Sexton, G., Payami, H., and Kaye, J.A. (1997). Cognitive markers preceding Alzheimer's dementia in the healthy oldest old. J Am Geriatr Soc *45*, 584-589.

Howlett, D.R., Jennings, K.H., Lee, D.C., Clark, M.S., Brown, F., Wetzel, R., Wood, S.J., Camilleri, P., and Roberts, G.W. (1995). Aggregation state and neurotoxic properties of Alzheimer beta-amyloid peptide. Neurodegeneration *4*, 23-32.

Hu, X., Crick, S.L., Bu, G., Frieden, C., Pappu, R.V., and Lee, J.M. (2009). Amyloid seeds formed by cellular uptake, concentration, and aggregation of the amyloid-beta peptide. Proc Natl Acad Sci U S A *106*, 20324-20329.

Huang, W.P., Scott, S.V., Kim, J., and Klionsky, D.J. (2000). The itinerary of a vesicle component, Aut7p/Cvt5p, terminates in the yeast vacuole via the autophagy/Cvt pathways. J Biol Chem *275*, 5845-5851.

Hughes, S.R., Goyal, S., Sun, J.E., Gonzalez-DeWhitt, P., Fortes, M.A., Riedel, N.G., and Sahasrabudhe, S.R. (1996). Two-hybrid system as a model to study the interaction of β-amyloid peptide monomers. Proc Natl Acad Sci *93*, 2065-2070.

Hughes, T.R. (2002). Yeast and drug discovery. Funct Integr Genomics *2*, 199-211.

Huh, W.K., Falvo, J.V., Gerke, L.C., Carroll, A.S., Howson, R.W., Weissman, J.S., and O'Shea, E.K. (2003). Global analysis of protein localization in budding yeast. Nature *425*, 686-691.

Hung, L.W., Ciccotosto, G.D., Giannakis, E., Tew, D.J., Perez, K., Masters, C.L., Cappai, R., Wade, J.D., and Barnham, K.J. (2008). Amyloid-beta peptide (Aβ) neurotoxicity is modulated by the rate of peptide aggregation: Aβ dimers and trimers correlate with neurotoxicity. J Neurosci *28*, 11950-11958.

Hung, S.Y., Huang, W.P., Liou, H.C., and Fu, W.M. (2009). Autophagy protects neuron from Abeta-induced cytotoxicity. Autophagy *5*, 502-510.

Hussain, I., Powell, D., Howlett, D.R., Tew, D.G., Meek, T.D., Chapman, C., Gloger, I.S., Murphy, K.E., Southan, C.D., Ryan, D.M.*, et al.* (1999). Identification of a novel aspartic protease (Asp 2) as beta-secretase. Mol Cell Neurosci *14*, 419-427.

Husseman, J.W., Nochlin, D., and Vincent, I. (2000). Mitotic activation: a convergent mechanism for a cohort of neurodegenerative diseases. Neurobiol Aging *21*, 815-828.

Hy, L.X., and Keller, D.M. (2000). Prevalence of AD among whites: a summary by levels of severity. Neurology *55*, 198-204.

Hyman, B.T., Van Hoesen, G.W., Damasio, A.R., and Barnes, C.L. (1984). Alzheimer's disease: cell-specific pathology isolates the hippocampal formation. Science *225*, 1168 -1170.

Ida, N., Masters, C.L., and Beyreuther, K. (1996). Rapid cellular uptake of Alzheimer amyloid betaA4 peptide by cultured human neuroblastoma cells. FEBS Lett *394*, 174-178.

Ihara, Y., Nukina, N., Miura, R., and Ogawara, M. (1986). Phosphorylated tau protein is integrated into paired helical filaments in Alzheimer's disease. J Biochem *99*, 1807-1810.

Iqbal, K., Grundke-Iqbal, I., Zaidi, T., Merz, P.A., Wen, G.Y., Shaikh, S.S., Wisniewski, H.M., Alafuzoff, I., and Winblad, B. (1986). Defective brain microtubule assembly in Alzheimer's disease. Lancet *2*, 421-426.

Irizarry, M.C., Deng, A., Lleo, A., Berezovska, O., Von Arnim, C.A., Martin-Rehrmann, M., Manelli, A., LaDu, M.J., Hyman, B.T., and Rebeck, G.W. (2004). Apolipoprotein E modulates gamma-secretase cleavage of the amyloid precursor protein. J Neurochem *90*, 1132-1143.

Ito, S., Ohtsuki, S., Kamiie, J., Nezu, Y., and Terasaki, T. (2007). Cerebral clearance of human amyloid-beta peptide (1-40) across the blood-brain barrier is reduced by self-aggregation and formation of low-density lipoprotein receptor-related protein-1 ligand complexes. J Neurochem *103*, 2482-2490.

Ito, T., Chiba, T., Ozawa, R., Yoshida, M., Hattori, M., and Sakaki, Y. (2001). A comprehensive two-hybrid analysis to explore the yeast protein interactome. Proc Natl Acad Sci U S A *98*, 4569-4574.

Ivy, G.O., Kitani, K., and Ihara, Y. (1989). Anomalous accumulation of tau and ubiquitin immunoreactivities in rat brain caused by protease inhibition and by normal aging: a clue to PHF pathogenesis? Brain Res *498*, 360-365.

Iwata, N., Tsubuki, S., Takaki, Y., Watanabe, K., Sekiguchi, M., Hosoki, E., Kawashima-Morishima, M., Lee, H.J., Hama, E., and Sekine-Aizawa, Y. (2000). Identification of the major Aβ1-42-degrading catabolic pathway in brain parenchyma: Suppression leads to biochemical and pathological deposition. Nat Med *6*, 143-150

Jacobs, D.M., Sano, M., Dooneief, G., Marder, K., Bell, K.L., and Stern, Y. (1995). Neuropsychological detection and characterization of preclinical Alzheimer's disease. Neurology *45*, 957-962.

Jaeger, S., and Pietrzik, C.U. (2008). Functional role of lipoprotein receptors in Alzheimer's disease. Curr Alzheimer Res *5*, 15-25.

Jan, A., Gokce, O., Luthi-Carter, R., and Lashuel, H.A. (2008). The ratio of monomeric to aggregated forms of A beta 40 and A beta 42 is an important determinant of amyloid-beta aggregation, fibrillogenesis, and toxicity. J Biol Chem *283*, 28176-28189.

Janciauskiene, S., Rubin, H., Lukacs, C.M., and Wright, H.T. (1998). Alzheimer's peptide A beta(1-42) binds to two beta-sheets of alpha(1)-antichymotrypsin and transforms it from inhibitor to substrate. J Biol Chem *273*, 28360-28364.

Jankowsky, J.L., Fadale, D.J., Anderson, J., Xu, G.M., Gonzales, V., Jenkins, N.A., Copeland, N.G., Lee, M.K., Younkin, L.H., Wagner, S.L.*, et al.* (2004). Mutant presenilins specifically elevate the levels of the 42 residue beta-amyloid peptide in vivo: evidence for augmentation of a 42-specific gamma secretase. Hum Mol Genet *13*, 159-170.

Jarrett, J.T., Berger, E.P., and Lansbury, P.T., Jr. (1993). The carboxy terminus of the beta amyloid protein is critical for the seeding of amyloid formation: implications for the pathogenesis of Alzheimer's disease. Biochemistry *32*, 4693-4697.

Jelic, V., Kivipelto, M., and Winblad, B. (2006). Clinical trials in mild cognitive impairment: lessons for the future. J Neurol Neurosurg Psychiatry *77*, 429-438.

Jentsch, S. (1992a). The ubiquitin-conjugation system. Annu Rev Genet *26*, 179-207.

Jentsch, S. (1992b). Ubiquitin-dependent protein degradation: a cellular perspective. Trends Cell Biol *2*, 98-103.

Jeyakumar, M., Dwek, R.A., Butters, T.D., and Platt, F.M. (2005). Storage solutions: treating lysosomal disorders of the brain. Nat Rev Neurosci *6*, 713-725.

Ji, Y., Permanne, B., Sigurdsson, E.M., Holtzman, D.M., and Wisniewski, T. (2001). Amyloid beta40/42 clearance across the blood-brain barrier following intra-ventricular injections in wild-type, apoE knock-out and human apoE3 or E4 expressing transgenic mice. J Alzheimers Dis *3*, 23-30.

Ji, Z.S., Brecht, W.J., Miranda, R.D., Hussain, M.M., Innerarity, T.L., and Mahley, R.W. (1993). Role of heparan sulfate proteoglycans in the binding and uptake of apolipoprotein E-enriched remnant lipoproteins by cultured cells. J Biol Chem *268*, 10160-10167.

Johnson, B.S., McCaffery, J.M., Lindquist, S., and Gitler, A.D. (2008). A yeast TDP-43 proteinopathy model: Exploring the molecular determinants of TDP-43 aggregation and cellular toxicity. Proc Natl Acad Sci U S A *105*, 6439-6444.

Jones, E.W., Zubenko, G.S., and Parker, R.R. (1982). PEP4 gene function is required for expression of several vacuolar hydrolases in Saccharomyces cerevisiae. Genetics *102*, 665-677.

Jones, R.W. (2010). Dimebon disappointment. Alzheimers Res Ther *2*, 25.

Jonghe, C.D., Esselens, C., Singh, S.K., Craessaerts, K., Serneels, S., Checler, F., Annaert, W., Van Broeckhoven, C., and Strooper, B.D. (2001). Pathogenic APP mutations near the γ-secretase cleavage site differentially affect Aß secretion and APP C-terminal fragment stability Human Molecular Genetics *10*, 1665-1671.

Journo, D., Winter, G., and Abeliovich, H. (2008). Monitoring autophagy in yeast using FM 4-64 fluorescence. Methods Enzymol *451*, 79-88.

Kabeya, Y., Mizushima, N., Ueno, T., Yamamoto, A., Kirisako, T., Noda, T., Kominami, E., Ohsumi, Y., and Yoshimori, T. (2000). LC3, a mammalian homologue of yeast Apg8p, is localized in autophagosome membranes after processing. EMBO J *19*, 5720-5728.

Kamenetz, F., Tomita, T., Hsieh, H., Seabrook, G., Borchelt, D., Iwatsubo, T., Sisodia, S., and Malinow, R. (2003). APP processing and synaptic function. Neuron *37*, 925-937.

Karow, D.S., McEvoy, L.K., Fennema-Notestine, C., Hagler, D.J., Jr., Jennings, R.G., Brewer, J.B., Hoh, C.K., and Dale, A.M. (2010). Relative capability of MR imaging and FDG PET to depict changes associated with prodromal and early Alzheimer disease. Radiology *256*, 932-942.

Kawarabayashi, T., Shoji, M., Younkin, L.H., Wen-Lang, L., Dickson, D.W., Murakami, T., Matsubara, E., Abe, K., Ashe, K.H., and Younkin, S.G. (2004). Dimeric amyloid beta protein rapidly accumulates in lipid rafts followed by apolipoprotein E and phosphorylated tau accumulation in the Tg2576 mouse model of Alzheimer's disease. J Neurosci *24*, 3801-3809.

Kayed, R., Sokolov, Y., Edmonds, B., McIntire, T.M., Milton, S.C., Hall, J.E., and Glabe, C.G. (2004). Permeabilization of lipid bilayers is a common conformation-dependent activity of soluble amyloid oligomers in protein misfolding diseases. J Biol Chem *279*, 46363-46366.

Kazee, A.M., and Johnson, E.M. (1998). Alzheimer's Disease Pathology in Non-Demented Elderly. J Alzheimers Dis *1*, 81-89.

Keck, S., Nitsch, R., Grune, T., and Ullrich, O. (2003). Proteasome inhibition by paired helical filament-tau in brains of patients with Alzheimer's disease. J Neurochem *85*, 115-122.

Keller, J.N., Hanni, K.B., and Markesbery, W.R. (2000). Impaired proteasome function in Alzheimer's disease. J Neurochem *75*, 436-439.

Kelly, J.W., and Balch, W.E. (2003). Amyloid as a natural product. J Cell Biol *161*, 461-462.

Khachaturian, Z.S. (1985). Diagnosis of Alzheimer's disease. Arch Neurol *42*, 1097-1105.

Kieburtz, K., McDermott, M.P., Voss, T.S., Corey-Bloom, J., Deuel, L.M., Dorsey, E.R., Factor, S., Geschwind, M.D., Hodgeman, K., Kayson, E.*, et al.* (2010). A randomized, placebo-controlled trial of latrepirdine in Huntington disease. Arch Neurol *67*, 154-160.

Kim, J., Basak, J.M., and Holtzman, D.M. (2009). The role of apolipoprotein E in Alzheimer's disease. Neuron *63*, 287-303.

Kim, J., Huang, W.P., and Klionsky, D.J. (2001a). Membrane recruitment of Aut7p in the autophagy and cytoplasm to vacuole targeting pathways requires Aut1p, Aut2p, and the autophagy conjugation complex. J Cell Biol *152*, 51-64.

Kim, J.H., Anwyl, R., Suh, Y.H., Djamgoz, M.B., and Rowan, M.J. (2001b). Use-dependent effects of amyloidogenic fragments of (beta)-amyloid precursor protein on synaptic plasticity in rat hippocampus in vivo. J Neurosci *21*, 1327-1333.

Kinoshita, A., Fukumoto, H., Shah, T., Whelan, C.M., Irizarry, M.C., and Hyman, B.T. (2003). Demonstration by FRET of BACE interaction with the amyloid precursor protein at the cell surface and in early endosomes. J Cell Sci *116*, 3339-3346.

Kirisako, T., Baba, M., Ishihara, N., Miyazawa, K., Ohsumi, M., Yoshimori, T., Noda, T., and Ohsumi, Y. (1999). Formation process of autophagosome is traced with Apg8/Aut7p in yeast. J Cell Biol *147*, 435-446.

Kirisako, T., Ichimura, Y., Okada, H., Kabeya, Y., Mizushima, N., Yoshimori, T., Ohsumi, M., Takao, T., Noda, T., and Ohsumi, Y. (2000). The reversible modification regulates the membrane-binding state of Apg8/Aut7 essential for autophagy and the cytoplasm to vacuole targeting pathway. J Cell Biol *151*, 263-276.

Klein, J. (2007). Phenserine. Expert Opin Investig Drugs *16*, 1087-1097.

Klionsky, D.J. (2010). An autophagy glossary. Autophagy *6*.

Klionsky, D.J., and Emr, S.D. (1989). Membrane protein sorting: biosynthesis, transport and processing of yeast vacuolar alkaline phosphatase. EMBO J *8*, 2241-2250.

Klionsky, D.J., and Emr, S.D. (2000). Autophagy as a regulated pathway of cellular degradation. Science *290*, 1717-1721.

Klionsky, D.J., Meijer, A.J., and Codogno, P. (2005). Autophagy and p70S6 kinase. Autophagy *1*, 59-60; discussion 60-51.

Klyubin, I., Walsh, D.M., Lemere, C.A., Cullen, W.K., Shankar, G.M., Betts, V., Spooner, E.T., Jiang, L., Anwyl, R., Selkoe, D.J.*, et al.* (2005). Amyloid beta

protein immunotherapy neutralizes Abeta oligomers that disrupt synaptic plasticity in vivo. Nat Med *11*, 556-561.

Knouff, C., Hinsdale, M.E., Mezdour, H., Altenburg, M.K., Watanabe, M., Quarfordt, S.H., Sullivan, P.M., and Maeda, N. (1999). Apo E structure determines VLDL clearance and atherosclerosis risk in mice. J Clin Invest *103*, 1579-1586.

Kobe, B., Center, R.J., Kemp, B.E., and Poumbourios, P. (1999). Crystal structure of human T cell leukemia virus type 1 gp21 ectodomain crystallized as a maltose-binding protein chimera reveals structural evolution of retroviral transmembrane proteins. Proc Natl Acad Sci U S A *96*, 4319-4324.

Koedam, E.L., Lauffer, V., van der Vlies, A.E., van der Flier, W.M., Scheltens, P., and Pijnenburg, Y.A. (2010). Early-versus late-onset Alzheimer's disease: more than age alone. J Alzheimers Dis *19*, 1401-1408.

Koedam, E.L., Pijnenburg, Y.A., Deeg, D.J., Baak, M.M., van der Vlies, A.E., Scheltens, P., and van der Flier, W.M. (2008). Early-onset dementia is associated with higher mortality. Dement Geriatr Cogn Disord *26*, 147-152.

Koike, M., Nakanishi, H., Saftig, P., Ezaki, J., Isahara, K., Ohsawa, Y., Schulz-Schaeffer, W., Watanabe, T., Waguri, S., Kametaka, S.*, et al.* (2000). Cathepsin D deficiency induces lysosomal storage with ceroid lipofuscin in mouse CNS neurons. J Neurosci *20*, 6898-6906.

Koike, M., Shibata, M., Waguri, S., Yoshimura, K., Tanida, I., Kominami, E., Gotow, T., Peters, C., von Figura, K., Mizushima, N.*, et al.* (2005). Participation of autophagy in storage of lysosomes in neurons from mouse models of neuronal ceroid-lipofuscinoses (Batten disease). Am J Pathol *167*, 1713-1728.

Koistinaho, M., Ort, M., Cimadevilla, J.M., Vondrous, R., Cordell, B., Koistinaho, J., Bures, J., and Higgins, L.S. (2001). Specific spatial learning deficits become severe with age in beta -amyloid precursor protein transgenic mice that harbor diffuse beta -amyloid deposits but do not form plaques. Proc Natl Acad Sci U S A *98*, 14675-14680.

Kojro, E., and Fahrenholz, F. (2005). The non-amyloidogenic pathway: structure and function of alpha-secretases. Subcell Biochem *38*, 105-127.

Kokkoni, N., Stott, K., Amijee, H., Mason, J.M., and Doig, A.J. (2006). N-methylated peptide inhibitors of beta-amyloid aggregation and toxicity. Optimization of the inhibitor structure. Biochemistry *45*, 9906-9918.

Komatsu, M., Waguri, S., Chiba, T., Murata, S., Iwata, J., Tanida, I., Ueno, T., Koike, M., Uchiyama, Y., Kominami, E.*, et al.* (2006). Loss of autophagy in the central nervous system causes neurodegeneration in mice. Nature *441*, 880-884.

Koo, E.H., Park, L., and Selkoe, D.J. (1993). Amyloid beta-protein as a substrate interacts with extracellular matrix to promote neurite outgrowth. Proc Natl Acad Sci U S A *90*, 4748-4752.

Koo, E.H., and Squazzo, S.L. (1994). Evidence that production and release of amyloid beta-protein involves the endocytic pathway. J Biol Chem *269*, 17386-17389.

Koutnikova, H., Campuzano, V., Foury, F., Dolle, P., Cazzalini, O., and Koenig, M. (1997). Studies of human, mouse and yeast homologues indicate a mitochondrial function for frataxin. Nat Genet *16*, 345-351.

Kragt, A., Voorn-Brouwer, T., van den Berg, M., and Distel, B. (2005). The Saccharomyces cerevisiae peroxisomal import receptor Pex5p is monoubiquitinated in wild type cells. J Biol Chem *280*, 7867-7874.

Krebs, M.R.H., Domike, K.R., Cannon, D., and Donald, A.M. (2008). Common motifs in protein self-assembly. Faraday Discuss *139*, 265-274.

Kremer, J.J., Pallitto, M.M., Sklansky, D.J., and Murphy, R.M. (2000). Correlation of beta-amyloid aggregate size and hydrophobicity with decreased bilayer fluidity of model membranes. Biochemistry *39*, 10309-10318.

Krishnaswamy, S., Verdile, G., Groth, D., Kanyenda, L., and Martins, R.N. (2009). The structure and function of Alzheimer's gamma secretase enzyme complex. Crit Rev Clin Lab Sci *46*, 282-301.

Krobitsch, S., and Lindquist, S. (2000). Aggregation of huntingtin in yeast varies with the length of the polyglutamine expansion and the expression of chaperone proteins. Proc Natl Acad Sci U S A *97*, 1589-1594.

Kruzel, M.L., Janusz, M., Lisowski, J., Fischleigh, R.V., and Georgiades, J.A. (2001). Towards an understanding of biological role of colostrinin peptides. J Mol Neurosci *17*, 379-389.

Kryndushkin, D., Wickner, R.B., and Shewmaker, F. (2011). FUS/TLS forms cytoplasmic aggregates, inhibits cell growth and interacts with TDP-43 in a yeast model of amyotrophic lateral sclerosis. Protein Cell *2*, 223-236.

Kulstad, J.J., McMillan, P.J., Leverenz, J.B., Cook, D.G., Green, P.S., Peskind, E.R., Wilkinson, C.W., Farris, W., Mehta, P.D., and Craft, S. (2005). Effects of chronic glucocorticoid administration on insulin-degrading enzyme and amyloid-beta peptide in the aged macaque. J Neuropathol Exp Neurol *64*, 139-146.

LaDu, M.J., Falduto, M.T., Manelli, A.M., Reardon, C.A., Getz, G.S., and Frail, D.E. (1994). Isoform-specific binding of apolipoprotein E to beta-amyloid. J Biol Chem *269*, 23403-23406.

Lafay-Chebassier, C., Paccalin, M., Page, G., Barc-Pain, S., Perault-Pochat, M.C., Gil, R., Pradier, L., and Hugon, J. (2005). mTOR/p70S6k signalling alteration by Abeta exposure as well as in APP-PS1 transgenic models and in patients with Alzheimer's disease. J Neurochem *94*, 215-225.

Lafay-Chebassier, C., Perault-Pochat, M.C., Page, G., Rioux Bilan, A., Damjanac, M., Pain, S., Houeto, J.L., Gil, R., and Hugon, J. (2006). The immunosuppressant rapamycin exacerbates neurotoxicity of Abeta peptide. J Neurosci Res *84*, 1323-1334.

LaFerla, F.M., Green, K.N., and Oddo, S. (2007). Intracellular amyloid-β in Alzheimer's disease. Nature Reviews Neuroscience *8*, 499-509

LaFerla, F.M., Troncoso, J.C., Strickland, D.K., Kawas, C.H., and Jay, G. (1997). Neuronal cell death in Alzheimer's disease correlates with apoE uptake and intracellular Abeta stabilization. J Clin Invest *100*, 310-320.

Lambert, J.C., and Amouyel, P. (2011). Genetics of Alzheimer's disease: new evidences for an old hypothesis? Curr Opin Genet Dev.

Lambert, J.C., Heath, S., Even, G., Campion, D., Sleegers, K., Hiltunen, M., Combarros, O., Zelenika, D., Bullido, M.J., Tavernier, B.*, et al.* (2009). Genome-wide association study identifies variants at CLU and CR1 associated with Alzheimer's disease. Nat Genet *41*, 1094-1099.

Lambert, M.P., Barlow, A.K., Chromy, B.A., Edwards, C., Freed, R., and Liosatos, M. (1998). Diffusible, nonfibrillar ligands derived from Ab1-42 are potent central nervous system neurotoxins. Proc Natl Acad Sci USA *95*, 6448-6453.

Lambert, M.P., Viola, K.L., Chromy, B.A., Chang, L., Morgan, T.E., Yu, J., Venton, D.L., Krafft, G.A., Finch, C.E., and Klein, W.L. (2001). Vaccination with soluble Abeta oligomers generates toxicity-neutralizing antibodies. J Neurochem *79*, 595-605.

Landreth, G., Jiang, Q., Mandrekar, S., and Heneka, M. (2008). PPARgamma agonists as therapeutics for the treatment of Alzheimer's disease. Neurotherapeutics *5*, 481-489.

Lansbury Jr, P.T. (1996). A Reductionist View of Alzheimer's Disease. Acc Chem Res *29*, 317-321.

Laws, S.M., Hone, E., Gandy, S., and Martins, R.N. (2003). Expanding the association between the APOE gene and the risk of Alzheimer's disease: possible roles for APOE promoter polymorphisms and alterations in APOE transcription. J Neurochem *84*, 1215-1236.

Le Brocque, D., Henry, A., Cappai, R., Li, Q.X., Tanner, J.E., Galatis, D., Gray, C., Holmes, S., Underwood, J.R., Beyreuther, K.*, et al.* (1998). Processing of the Alzheimer's disease amyloid precursor protein in Pichia pastoris: immunodetection of alpha-, beta-, and gamma-secretase products. Biochemistry *37*, 14958-14965.

Lee, E.K., Hwang, J.H., Shin, D.Y., Kim, D.I., and Yoo, Y.J. (2005). Production of recombinant amyloid-beta peptide 42 as an ubiquitin extension. Protein Expr Purif *40*, 183-189.

Lee, H.G., Casadesus, G., Zhu, X., Castellani, R.J., McShea, A., Perry, G., Petersen, R.B., Bajic, V., and Smith, M.A. (2009). Cell cycle re-entry mediated neurodegeneration and its treatment role in the pathogenesis of Alzheimer's disease. Neurochem Int *54*, 84-88.

Lee, I.H., Kim, H.Y., Kim, M., Hahn, J.S., and Paik, S.R. (2008). Dequalinium-induced cell death of yeast expressing alpha-synuclein-GFP fusion protein. Neurochem Res *33*, 1393-1400.

Lee, J.H., Cheng, R., Schupf, N., Manly, J., Lantigua, R., Stern, Y., Rogaeva, E., Wakutani, Y., Farrer, L., St George-Hyslop, P.*, et al.* (2007). The association between genetic variants in SORL1 and Alzheimer disease in an urban, multiethnic, community-based cohort. Arch Neurol *64*, 501-506.

Lee, J.H., Yu, W.H., Kumar, A., Lee, S., Mohan, P.S., Peterhoff, C.M., Wolfe, D.M., Martinez-Vicente, M., Massey, A.C., Sovak, G.*, et al.* (2010). Lysosomal proteolysis and autophagy require presenilin 1 and are disrupted by Alzheimer-related PS1 mutations. Cell *141*, 1146-1158.

Lee, S.J., Liyanage, U., Bickel, P.E., Xia, W., Lansbury, P.T., Jr., and Kosik, K.S. (1998). A detergent-insoluble membrane compartment contains A beta in vivo. Nat Med *4*, 730-734.

Lee, V.M., Goedert, M., and Trojanowski, J.Q. (2001). Neurodegenerative tauopathies. Annu Rev Neurosci *24*, 1121-1159.

Lelandais, G., Tanty, V., Geneix, C., Etchebest, C., Jacq, C., and Devaux, F. (2008). Genome adaptation to chemical stress: clues from comparative transcriptomics in Saccharomyces cerevisiae and Candida glabrata. Genome Biol *9*, R164.

Lermontova, N.N., Lukoyanov, N.V., Serkova, T.P., Lukoyanova, E.A., and Bachurin, S.O. (2000). Dimebon improves learning in animals with experimental Alzheimer's disease. Bull Exp Biol Med *129*, 544-546.

Lermontova, N.N., Redkozubov, A.E., Shevtsova, E.F., Serkova, T.P., Kireeva, E.G., and Bachurin, S.O. (2001). Dimebon and tacrine inhibit neurotoxic action of beta-amyloid in culture and block L-type Ca(2+) channels. Bull Exp Biol Med *132*, 1079-1083.

Lesne, S., Koh, T.M., Kotilinek, L., Kayed, R., Glabe, C.G., Yang, A., Gallagher, M., and Ashe, K.H. (2006). A specific amyloid-β protein assembly in the brain impairs memory. Nature *440*, 352-357.

Levine, B., and Kroemer, G. (2008). Autophagy in the pathogenesis of disease. Cell *132*, 27-42.

Levine, B., and Yuan, J. (2005). Autophagy in cell death: an innocent convict? J Clin Invest *115*, 2679-2688.

Levy-Lahad, E., Wasco, W., Poorkaj, P., Romano, D.M., Oshima, J., Pettingell, W.H., Yu, C.E., Jondro, P.D., Schmidt, S.D., and Wang, K. (1995). Candidate gene for the chromosome 1 familial Alzheimer's disease locus. Science *269*, 973-977.

Li, S., Hong, S., Shepardson, N.E., Walsh, D.M., Shankar, G.M., and Selkoe, D. (2009). Soluble oligomers of amyloid Beta protein facilitate hippocampal long-term depression by disrupting neuronal glutamate uptake. Neuron *62*, 788-801.

Li, X., Alafuzoff, I., Soininen, H., Winblad, B., and Pei, J.J. (2005). Levels of mTOR and its downstream targets 4E-BP1, eEF2, and eEF2 kinase in relationships with tau in Alzheimer's disease brain. FEBS J *272*, 4211-4220.

Li, X., An, W.L., Alafuzoff, I., Soininen, H., Winblad, B., and Pei, J.J. (2004). Phosphorylated eukaryotic translation factor 4E is elevated in Alzheimer brain. Neuroreport *15*, 2237-2240.

Liberski, P.P., Brown, D.R., Sikorska, B., Caughey, B., and Brown, P. (2008). Cell death and autophagy in prion diseases (transmissible spongiform encephalopathies). Folia Neuropathol *46*, 1-25.

Lillie, S.H., and Pringle, J.R. (1980). Reserve carbohydrate metabolism in Saccharomyces cerevisiae: responses to nutrient limitation. J Bacteriol *143*, 1384-1394.

Lindsten, K., de Vrij, F.M., Verhoef, L.G., Fischer, D.F., van Leeuwen, F.W., Hol, E.M., Masucci, M.G., and Dantuma, N.P. (2002). Mutant ubiquitin found in neurodegenerative disorders is a ubiquitin fusion degradation substrate that blocks proteasomal degradation. J Cell Biol *157*, 417-427.

Lingrel, J.B., Williams, M.T., Vorhees, C.V., and Moseley, A.E. (2007). Na,K-ATPase and the role of alpha isoforms in behavior. J Bioenerg Biomembr *39*, 385-389.

Link, C.D. (1995). Expression of human beta-amyloid peptide in transgenic Caenorhabditis elegans. Proc Natl Acad Sci U S A *92*, 9368-9372.

Linn, R.T., Wolf, P.A., Bachman, D.L., Knoefel, J.E., Cobb, J.L., Belanger, A.J., Kaplan, E.F., and D'Agostino, R.B. (1995). The 'preclinical phase' of probable Alzheimer's disease. A 13-year prospective study of the Framingham cohort. Arch Neurol *52*, 485-490.

Liu, T., Perry, G., Chan, H.W., Verdile, G., Martins, R.N., Smith, M.A., and Atwood, C.S. (2004). Amyloid-beta-induced toxicity of primary neurons is dependent upon differentiation-associated increases in tau and cyclin-dependent kinase 5 expression. J Neurochem *88*, 554-563.

Loayza, D., and Michaelis, S. (1998). Role for the ubiquitin-proteasome system in the vacuolar degradation of Ste6p, the a-factor transporter in Saccharomyces cerevisiae. Mol Cell Biol *18*, 779-789.

Lovell, M.A., Ehmann, W.D., Butler, S.M., and Markesbery, W.R. (1995). Elevated thiobarbituric acid-reactive substances and antioxidant enzyme activity in the brain in Alzheimer's disease. Neurology *45*, 1594-1601.

Lovell, M.A., Gabbita, S.P., and Markesbery, W.R. (1999). Increased DNA oxidation and decreased levels of repair products in Alzheimer's disease ventricular CSF. J Neurochem *72*, 771-776.

Lue, L.F., Kuo, Y.M., Roher, A.E., Brachova, L., Shen, Y., Sue, L., Beach, T., Kurth, J.H., Rydel, R.E., and Rogers, J. (1999). Soluble amyloid beta peptide concentration as a predictor of synaptic change in Alzheimer's disease. Am J Pathol *155*, 853-862.

Luhrs, T., Ritter, C., Adrian, M., Riek-Loher, D., Bohrmann, B., Dobeli, H., Schubert, D., and Riek, R. (2005). 3D structure of Alzheimer's amyloid-beta(1-42) fibrils. Proc Natl Acad Sci U S A *102*, 17342-17347.

Lum, J.J., DeBerardinis, R.J., and Thompson, C.B. (2005). Autophagy in metazoans: cell survival in the land of plenty. Nat Rev Mol Cell Biol *6*, 439-448.

Luo, Y., Sunderland, T., Roth, G.S., and Wolozin, B. (1996a). Physiological levels of beta-amyloid peptide promote PC12 cell proliferation. Neurosci Lett *217*, 125-128.

Luo, Y., Sunderland, T., and Wolozin, B. (1996b). Physiologic levels of beta-amyloid activate phosphatidylinositol 3-kinase with the involvement of tyrosine phosphorylation. J Neurochem *67*, 978-987.

Lustbader, J.W., Cirilli, M., Lin, C., Xu, H.W., Takuma, K., and Wang, N. (2004a). ABAD directly links Aβ to mitochondrial toxicity in Alzheimer’s disease. Science *304*, 448-452.

Lustbader, J.W., Cirilli, M., Lin, C., Xu, H.W., Takuma, K., Wang, N., Caspersen, C., Chen, X., Pollak, S., Chaney, M.*, et al.* (2004b). ABAD directly links Abeta to mitochondrial toxicity in Alzheimer's disease. Science *304*, 448-452.

Luthi, U., Schaerer-Brodbeck, C., Tanner, S., Middendorp, O., Edler, K., and Barberis, A. (2003). Human beta-secretase activity in yeast detected by a novel cellular growth selection system. Biochim Biophys Acta *1620* 167-178.

Ma, J., Meng, Y., Kwiatkowski, D.J., Chen, X., Peng, H., Sun, Q., Zha, X., Wang, F., Wang, Y., Jing, Y.*, et al.* (2010a). Mammalian target of rapamycin regulates murine and human cell differentiation through STAT3/p63/Jagged/Notch cascade. J Clin Invest *120*, 103-114.

Ma, T., Hoeffer, C.A., Capetillo-Zarate, E., Yu, F., Wong, H., Lin, M.T., Tampellini, D., Klann, E., Blitzer, R.D., and Gouras, G.K. (2010b). Dysregulation of the mTOR pathway mediates impairment of synaptic plasticity in a mouse model of Alzheimer's disease. PLoS One *5*.

Madeo, F., Carmona-Gutierrez, D., Ring, J., Buttner, S., Eisenberg, T., and Kroemer, G. (2009). Caspase-dependent and caspase-independent cell death pathways in yeast. Biochem Biophys Res Commun *382*, 227-231.

Madeo, F., Frohlich, E., and Frohlich, K.U. (1997). A yeast mutant showing diagnostic markers of early and late apoptosis. J Cell Biol *139*, 729-734.

Madeo, F., Frohlich, E., Ligr, M., Grey, M., Sigrist, S.J., Wolf, D.H., and Frohlich, K.U. (1999). Oxygen stress: a regulator of apoptosis in yeast. J Cell Biol *145*, 757-767.

Mager, W.H., and Winderickx, J. (2005). Yeast as a model for medical and medicinal research. Trends Pharmacol Sci *26*, 265-273.

Malik, B., Currais, A., and Soriano, S. (2008). Cell cycle-driven neuronal apoptosis specifically linked to amyloid peptide Abeta1-42 exposure is not exacerbated in a mouse model of presenilin-1 familial Alzheimer's disease. J Neurochem *106*, 912-916.

Manavathu, E.K., Dimmock, J.R., Vashishtha, S.C., and Chandrasekar, P.H. (1999). Proton-pumping-ATPase-targeted antifungal activity of a novel conjugated styryl ketone. Antimicrob Agents Chemother *43*, 2950-2959.

Manczak, M., Anekonda, T.S., Henson, E., Park, B.S., Quinn, J., and Reddy, P.H. (2006). Mitochondria are a direct site of A beta accumulation in Alzheimer's disease neurons: implications for free radical generation and oxidative damage in disease progression. Hum Mol Genet *15*, 1437-1449.

Mandel, S.A., Amit, T., Kalfon, L., Reznichenko, L., Weinreb, O., and Youdim, M.B. (2008). Cell signaling pathways and iron chelation in the neurorestorative activity of green tea polyphenols: special reference to epigallocatechin gallate (EGCG). J Alzheimers Dis *15*, 211-222.

Mangialasche, F., Solomon, A., Winblad, B., Mecocci, P., and Kivipelto, M. (2010). Alzheimer's disease: clinical trials and drug development. Lancet Neurol *9*, 702-716.

Manolio, T.A. (2010). Genomewide association studies and assessment of the risk of disease. N Engl J Med *363*, 166-176.

Marcade, M., Bourdin, J., Loiseau, N., Peillon, H., Rayer, A., Drouin, D., Schweighoffer, F., and Desire, L. (2008). Etazolate, a neuroprotective drug linking GABA(A) receptor pharmacology to amyloid precursor protein processing. J Neurochem *106*, 392-404.

Mark, R.J., Hensley, K., Butterfield, D.A., and Mattson, M.P. (1995). Amyloid beta-peptide impairs ion-motive ATPase activities: evidence for a role in loss of neuronal Ca2+ homeostasis and cell death. J Neurosci *15*, 6239-6249.

Markesbery, W.R., and Lovell, M.A. (1998). Four-hydroxynonenal, a product of lipid peroxidation, is increased in the brain in Alzheimer's disease. Neurobiol Aging *19*, 33-36.

Martin, B.L., Schrader-Fischer, G., Busciglio, J., Duke, M., Paganetti, P., and Yankner, B.A. (1995). Intracellular accumulation of beta-amyloid in cells expressing the Swedish mutant amyloid precursor protein. J Biol Chem *270*, 26727-26730.

Martinet, W., Agostinis, P., Vanhoecke, B., Dewaele, M., and De Meyer, G.R. (2009). Autophagy in disease: a double-edged sword with therapeutic potential. Clin Sci (Lond) *116*, 697-712.

Martins, R.N., Harper, C.G., Stokes, G.B., and Masters, C.L. (1986). Increased cerebral glucose-6-phosphate dehydrogenase activity in Alzheimer's disease may reflect oxidative stress. J Neurochem *46*, 1042-1045.

Masters, C.L., Multhaup, G., Simms, G., Pottgiesser, J., Martins, R.N., and Beyreuther, K. (1985a). Neuronal origin of a cerebral amyloid: neuro-fibrillary tangles of Alzheimer's disease contain the same protein as the amyloid of plaque cores and blood vessels. EMBO J *4*, 2757-2763.

Masters, C.L., Simms, G., Weinman, N.A., Multhaup, G., McDonald, B.L., and Beyreuther, K. (1985b). Amyloid plaque core protein in Alzheimer disease and Down syndrome. Proc Natl Acad Sci U S A *82*, 4245-4249.

Masur, D.M., Sliwinski, M., Lipton, R.B., Blau, A.D., and Crystal, H.A. (1994). Neuropsychological prediction of dementia and the absence of dementia in healthy elderly persons. Neurology *44*, 1427-1432.

Matsuoka, Y., Saito, M., LaFrancois, J., Gaynor, K., Olm, V., Wang, L., Casey, E., Lu, Y., Shiratori, C., Lemere, C.*, et al.* (2003). Novel therapeutic approach for the treatment of Alzheimer's disease by peripheral administration of agents with an affinity to beta-amyloid. J Neurosci *23*, 29-33.

Mattson, M.P., and Chan, S.L. (2003). Neuronal and glial calcium signaling in Alzheimer's disease. Cell Calcium *34*, 385-397.

Mattson, M.P., Tomaselli, K.J., and Rydel, R.E. (1993). Calcium-destablizing and neurodegenerative effect of aggregate beta-amyloid peptide are attenuated by basic FGF. Brain Res, 35-49.

Mawuenyega, K.G., Sigurdson, W., Ovod, V., Munsell, L., Kasten, T., Morris, J.C., Yarasheski, K.E., and Bateman, R.J. (2010). Decreased clearance of CNS beta-amyloid in Alzheimer's disease. Science *330*, 1774.

May, P.C., Gitter, B.D., Waters, D.C., Simmons, L.K., Becker, G.W., Small, J.S., and Robison, P.M. (1992). beta-Amyloid peptide in vitro toxicity: lot-to-lot variability. Neurobiol Aging *13*, 605-612.

McGeer, P.L., Akiyama, H., Itagaki, S., and McGeer, E.G. (1989). Activation of the classical complement pathway in brain tissue of Alzheimer patients. Neurosci Lett *107*, 341-346.

McGeer, P.L., Walker, D.G., Akiyama, H., Yasuhara, O., and McGeer, E.G. (1994). Involvement of microglia in Alzheimer's disease. . Neuropathol Appl Neurobiol *20*, 191-192.

McLaurin, J., Kierstead, M.E., Brown, M.E., Hawkes, C.A., Lambermon, M.H., Phinney, A.L., Darabie, A.A., Cousins, J.E., French, J.E., Lan, M.F.*, et al.* (2006). Cyclohexanehexol inhibitors of Abeta aggregation prevent and reverse Alzheimer phenotype in a mouse model. Nat Med *12*, 801-808.

McLean, C.A., Cherny, R.A., Fraser, F.W., Fuller, S.J., Smith, M.J., Beyreuther, K., Bush, A.I., and Masters, C.L. (1999). Soluble pool of Aβ amyloid as a determinant of severity of neurodegeneration in Alzheimer's disease. Ann Neurol *46*, 860-866.

McShea, A., Wahl, A.F., and Smith, M.A. (1999). Re-entry into the cell cycle: a mechanism for neurodegeneration in Alzheimer disease. Med Hypotheses *52*, 525-527.

Mecocci, P., MacGarvey, U., and Beal, M.F. (1994). Oxidative damage to mitochondrial DNA is increased in Alzheimer's disease. Ann Neurol *36*, 747-751.

Meriin, A.B., Zhang, X., He, X., Newnam, G.P., Chernoff, Y.O., and Sherman, M.Y. (2002). Huntington toxicity in yeast model depends on polyglutamine aggregation mediated by a prion-like protein Rnq1. J Cell Biol *157*, 997-1004.

Middendorp, O., Ortler, C., Neumann, U., Paganetti, P., Luthi, U., and Barberis, A. (2004). Yeast growth selection system for the identification of cell active inhibitors of beta-secretase. Biochim Biophys Acta *1674* 29-39.

Miller, B.C., Eckman, E.A., Sambamurti, K., Dobbs, N., Chow, K.M., Eckman, C.B., Hersh, L.B., and Thiele, D.L. (2003). Amyloid-beta peptide levels in brain are inversely correlated with insulysin activity levels in vivo. Proc Natl Acad Sci USA *100*, 6221-6226.

Miners, J.S., Baig, S., Palmer, J., Palmer, L.E., Kehoe, P.G., and Love, S. (2008). Abeta-degrading enzymes in Alzheimer's disease. Brain Pathol *18*, 240-252.

Mirra, S.S., Heyman, A., McKeel, D., Sumi, S.M., Crain, B.J., Brownlee, L.M., Vogel, F.S., Hughes, J.P., van Belle, G., and Berg, L. (1991). The Consortium to Establish a Registry for Alzheimer's Disease (CERAD). Part II. Standardization of the neuropathologic assessment of Alzheimer's disease. Neurology *41*, 479-486.

Mirza, S.P., Halligan, B.D., Greene, A.S., and Olivier, M. (2007). Improved method for the analysis of membrane proteins by mass spectrometry. Physiol Genomics *30*, 89-94.

Mizuguchi, M., Ikeda, K., and Kim, S.U. (1992). Differential distribution of cellular forms of β-amyloid precursor protein in murine glial cell cultures. Brain Res *584*, 219-225.

Mizushima, N., Levine, B., Cuervo, A.M., and Klionsky, D.J. (2008). Autophagy fights disease through cellular self-digestion. Nature *451*, 1069-1075.

Mizushima, N., Sugita, H., Yoshimori, T., and Ohsumi, Y. (1998). A new protein conjugation system in human. The counterpart of the yeast Apg12p conjugation system essential for autophagy. J Biol Chem *273*, 33889-33892.

Mizushima, N., Yamamoto, A., Hatano, M., Kobayashi, Y., Kabeya, Y., Suzuki, K., Tokuhisa, T., Ohsumi, Y., and Yoshimori, T. (2001). Dissection of autophagosome formation using Apg5-deficient mouse embryonic stem cells. J Cell Biol *152*, 657-668.

Monk, B.C., Kurtz, M.B., Marrinan, J.A., and Perlin, D.S. (1991). Cloning and characterization of the plasma membrane H(+)-ATPase from Candida albicans. J Bacteriol *173*, 6826-6836.

Moolman, D.L., Vitolo, O.V., Vonsattel, J.P., and Shelanski, M.L. (2004). Dendrite and dendritic spine alterations in Alzheimer models. J Neurocytol *33*, 377-387.

Mori, C. (2002). Intraneuronal Aß42 accumulation in Down syndrome brain Amyloid *9*, 88-102.

Mori, H., Kondo, J., and Ihara, Y. (1987). Ubiquitin is a component of paired helical filaments in Alzheimer's disease. Science *235*, 1641-1644.

Mori, K. (2009). Signalling pathways in the unfolded protein response: development from yeast to mammals. J Biochem *146*, 743-750.

Morishima-Kawashima, M., Hasegawa, M., Takio, K., Suzuki, M., Titani, K., and Ihara, Y. (1993). Ubiquitin is conjugated with amino-terminally processed tau in paired helical filaments. Neuron *10*, 1151-1160.

Morrison, J.H., and Hof, P.R. (2002). Selective vulnerability of corticocortical and hippocampal circuits in aging and Alzheimer's disease. Prog Brain Res *136*, 467-486.

Mortimer, R.K., and Johnston, J.R. (1959). Life span of individual yeast cells. Nature *183*, 1751-1752.

Moseley, A.E., Williams, M.T., Schaefer, T.L., Bohanan, C.S., Neumann, J.C., Behbehani, M.M., Vorhees, C.V., and Lingrel, J.B. (2007). Deficiency in Na,K-ATPase alpha isoform genes alters spatial learning, motor activity, and anxiety in mice. J Neurosci *27*, 616-626.

Mosmann, T. (1983). Rapid colorimetric assay for cellular growth and survival: application to proliferation and cytotoxicity assays. J Immunol Methods *65*, 55-63.

Müller, W.E., Kirsch, C., and Eckert, G.P. (2001). Membrane-disordering effects of b-amyloid peptides. Biochem Soc Trans, 617-623.

Muhs, A., Hickman, D.T., Pihlgren, M., Chuard, N., Giriens, V., Meerschman, C., van der Auwera, I., van Leuven, F., Sugawara, M., Weingertner, M.C.*, et al.* (2007). Liposomal vaccines with conformation-specific amyloid peptide antigens define immune response and efficacy in APP transgenic mice. Proc Natl Acad Sci U S A *104*, 9810-9815.

Mulholland, J., and Botstein, D. (2002). Immunoelectron microscopy of aldehyde-fixed yeast cells. Methods Enzymol *351*, 50-81.

Mumberg, D., Muller, R., and Funk, M. (1995). Yeast vectors for the controlled expression of heterologous proteins in different genetic backgrounds. Gene *156*, 119-122.

Murakami, K., Irie, K., Morimoto, A., Ohigashi, H., Shindo, M., Nagao, M., Shimizu, T., and Shirasawa, T. (2002). Synthesis, aggregation, neurotoxicity, and secondary structure of various A beta 1-42 mutants of familial Alzheimer's disease at positions 21-23. Biochem Biophys Res Commun *294*, 5-10.

Mutisya, E.M., Bowling, A.C., and Beal, M.F. (1994). Cortical cytochrome oxidase activity is reduced in Alzheimer's disease. J Neurochem *63*, 2179-2184.

Nagele, R.G., D'Andrea, M.R., Anderson, W.J., and Wang, H.Y. (2002). Intracellular accumulation of ß-amyloid1-42 in neurons is facilitated by the α7 nicotinic acetylcholine receptor in Alzheimer's disease. Neuroscience *110*, 199-211.

Nagerl, U.V., Eberhorn, N., Cambridge, S.B., and Bonhoeffer, T. (2004). Bidirectional activity-dependent morphological plasticity in hippocampal neurons. Neuron *44*, 759-767.

Nair, U., and Klionsky, D.J. (2005). Molecular mechanisms and regulation of specific and nonspecific autophagy pathways in yeast. J Biol Chem *280*, 41785-41788.

Namba, Y., Tomonaga, M., Kawasaki, H., Otomo, E., and Ikeda, K. (1991). Apolipoprotein E immunoreactivity in cerebral amyloid deposits and neurofibrillary tangles in Alzheimer.s disease and kuru plaque amyloid in Creutzfeldt-Jakob disease. Brain Res *541*, 163-166.

Necula, M., Kayed, R., Milton, S., and Glabe, C.G. (2007). Small molecule inhibitors of aggregation indicate that amyloid beta oligomerization and fibrillization pathways are independent and distinct. J Biol Chem *282*, 10311-10324.

Nedelsky, N.B., Todd, P.K., and Taylor, J.P. (2008). Autophagy and the ubiquitin-proteasome system: collaborators in neuroprotection. Biochim Biophys Acta *1782*, 691-699.

Nerelius, C., Johansson, J., and Sandegren, A. (2009). Amyloid beta-peptide aggregation. What does it result in and how can it be prevented? Front Biosci *14*, 1716-U3856.

Newman, M., Wilson, L., Camp, E., Verdile, G., Martins, R., and Lardelli, M. (2010). A zebrafish melanophore model of amyloid beta toxicity. Zebrafish *7*, 155-159.

Nicholls, D.G., and Budd, S.L. (2000). Mitochondria and neuronal survival. Physiol Rev Neurosci *80*, 315-360.

Nilsberth, C., Westlind-Danielsson, A., Eckman, C., Condron, M.M., Axelman, K., Forsell, C., Stenh, C., Luthman, J., Teplow, D.B., Younkin, S.G.*, et al.* (2001). The 'Arctic' APP mutation (E693G) causes Alzheimer's disease by enhanced Aβ protofibril formation. Nat Neurosci *4*, 887-893.

Nixon, R.A. (2007). Autophagy, amyloidogenesis and Alzheimer disease. J Cell Sci *120*, 4081-4091.

Nixon, R.A., and Cataldo, A.M. (1993). The lysosomal system in neuronal cell death: a review. Ann N Y Acad Sci *679*, 87-109.

Nixon, R.A., Wegiel, J., Kumar, A., Yu, W.H., Peterhoff, C., Cataldo, A., and Cuervo, A.M. (2005). Extensive involvement of autophagy in Alzheimer disease: an immuno-electron microscopy study. J Neuropathol Exp Neurol *64*, 113-122.

Nixon, R.A., and Yang, D.S. (2011). Autophagy failure in Alzheimer's disease-locating the primary defect. Neurobiol Dis.

Nixon, R.A., Yang, D.S., and Lee, J.H. (2008). Neurodegenerative lysosomal disorders: a continuum from development to late age. Autophagy *4*, 590-599.

Noda, T., and Klionsky, D.J. (2008). The quantitative Pho8Delta60 assay of nonspecific autophagy. Methods Enzymol *451*, 33-42.

Nurse, P., Masui, Y., and Hartwell, L. (1998). Understanding the cell cycle. Nat Med *4*, 1103-1106.

Oddo, S., Billings, L., Kesslak, J.P., Cribbs, D.H., and LaFerla, F.M. (2004). Abeta immunotherapy leads to clearance of early, but not late, hyperphosphorylated tau aggregates via the proteasome. Neuron *43*, 321-332.

Oddo, S., Caccamo, A., Smith, I.F., Green, K.N., and LaFerla, F.M. (2006). A dynamic relationship between intracellular and extracellular pools of Abeta. Am J Pathol *168*, 184-194.

Oh, S., Hong, H.S., Hwang, E., Sim, H.J., Lee, W., Shin, S.J., and Mook-Jung, I. (2005). Amyloid peptide attenuates the proteasome activity in neuronal cells. Mech Ageing Dev *126*, 1292-1299.

Ohsawa, I., Takamura, C., Morimoto, T., Ishiguro, M., and Kohsaka, S. (1999). Amino-terminal region of secreted form of amyloid precursor protein stimulates proliferation of neural stem cells. Eur J Neurosci *11*, 1907-1913.

Oien, D.B., Shinogle, H.E., Moore, D.S., and Moskovitz, J. (2009). Clearance and phosphorylation of alpha-synuclein are inhibited in methionine sulfoxide reductase a null yeast cells. J Mol Neurosci *39*, 323-332.

Omerovic, M., Teipel, S.J., and Hampel, T. (2007). [Dementia with Lewy bodies. Clinical improvement under treatment with an acetylcholinesterase inhibitor]. Nervenarzt *78*, 1052-1057.

Outeiro, T.F., and Lindquist, S. (2003). Yeast cells provide insight into alpha-synuclein biology and pathobiology. Science *302*, 1772-1775.

Palmblad, M., Westlind-Danielsson, A., and Bergquist, J. (2002). Oxidation of Methionine 35 Attenuates Formation of Amyloid -Peptide 1-40 Oligomers. J Biol Chem *277*, 19506-19510.

Park, D.S., Obeidat, A., Giovanni, A., and Greene, L.A. (2000). Cell cycle regulators in neuronal death evoked by excitotoxic stress: implications for neurodegeneration and its treatment. Neurobiol Aging *21*, 771-781.

Park, K.H., Hallows, J.L., Chakrabarty, P., Davies, P., and Vincent, I. (2007). Conditional neuronal simian virus 40 T antigen expression induces Alzheimer-like tau and amyloid pathology in mice. J Neurosci *27*, 2969-2978.

Pasinetti, G.M. (2001). Use of cDNA microarray in the search for molecular markers involved in the onset of Alzheimer's disease dementia. J Neurosci Res *65*, 471-476.

Pattingre, S., Tassa, A., Qu, X., Garuti, R., Liang, X.H., Mizushima, N., Packer, M., Schneider, M.D., and Levine, B. (2005). Bcl-2 antiapoptotic proteins inhibit Beclin 1-dependent autophagy. Cell *122*, 927-939.

Paz, I., and Choder, M. (2001). Eukaryotic translation initiation factor 4E-dependent translation is not essential for survival of starved yeast cells. J Bacteriol *183*, 4477-4483.

Pearson, T.A., and Manolio, T.A. (2008). How to interpret a genome-wide association study. JAMA *299*, 1335-1344.

Pei, J.J., and Hugon, J. (2008). mTOR-dependent signalling in Alzheimer's disease. J Cell Mol Med *12*, 2525-2532.

Peralvarez-Marin, A., Mateos, L., Zhang, C., Singh, S., Cedazo-Minguez, A., Visa, N., Morozova-Roche, L., Graslund, A., and Barth, A. (2009). Influence of Residue 22 on the Folding, Aggregation Profile, and Toxicity of the Alzheimer's Amyloid beta Peptide. Biophys J *97*, 277-285.

Pereira, C., Ferreiro, E., Cardoso, S.M., and de Oliveira, C.R. (2004). Cell degeneration induced by amyloid-beta peptides: implications for Alzheimer's disease. J Mol Neurosci *23*, 97-104.

Perez, R.G., Soriano, S., Hayes, J.D., Ostaszewski, B., Xia, W., Selkoe, D.J., Chen, X., Stokin, G.B., and Koo, E.H. (1999). Mutagenesis identifies new signals for beta-amyloid precursor protein endocytosis, turnover, and the generation of secreted fragments, including Abeta42. J Biol Chem *274*, 18851-18856.

Perry, G., Castellani, R.J., Smith, M.A., Harris, P.L., Kubat, Z., Ghanbari, K., Jones, P.K., Cordone, G., Tabaton, M., Wolozin, B.*, et al.* (2003). Oxidative damage in the olfactory system in Alzheimer's disease. Acta Neuropathol *106*, 552-556.

Perry, G., Friedman, R., Shaw, G., and Chau, V. (1987). Ubiquitin is detected in neurofibrillary tangles and senile plaque neurites of Alzheimer disease brains. Proc Natl Acad Sci U S A *84*, 3033-3036.

Pickford, F., Masliah, E., Britschgi, M., Lucin, K., Narasimhan, R., Jaeger, P.A., Small, S., Spencer, B., Rockenstein, E., Levine, B.*, et al.* (2008). The autophagy-related protein beclin 1 shows reduced expression in early Alzheimer disease and regulates amyloid beta accumulation in mice. J Clin Invest *118*, 2190-2199.

Pieper, A.A., Xie, S., Capota, E., Estill, S.J., Zhong, J., Long, J.M., Becker, G.L., Huntington, P., Goldman, S.E., Shen, C.H.*, et al.* (2010). Discovery of a proneurogenic, neuroprotective chemical. Cell *142*, 39-51.

Pike, C.J., Walencewicz-Wasserman, A.J., Kosmoski, J., Cribbs, D.H., Glabe, C.G., and Cotman, C.W. (1995). Structure-activity analyses of beta-amyloid peptides: contributions of the beta 25-35 region to aggregation and neurotoxicity. J Neurochem *64*, 253-265.

Pike, C.J., Walencewicz, A.J., Glabe, C.G., and Cotman, C.W. (1991a). Aggregation-related toxicity of synthetic beta-amyloid protein in hippocampal cultures. Eur J Pharmacol *207*, 367-368.

Pike, C.J., Walencewicz, A.J., Glabe, C.G., and Cotman, C.W. (1991b). In vitro aging of beta-amyloid protein causes peptide aggregation and neurotoxicity. Brain Res *563*, 311-314.

Pitas, R.E., Boyles, J.K., Lee, S.H., Hui, D., and Weisgraber, K.H. (1987). Lipoproteins and their receptors in the central nervous system. Characterization of the lipoproteins in cerebrospinal fluid and identification of apolipoprotein B,E(LDL) receptors in the brain. J Biol Chem *262*, 14352-14360.

Podlisny, M.B., Ostaszewski, B.L., Squazzo, S.L., Koo, E.H., Rydell, R.E., Teplow, D.B., and Selkoe, D.J. (1995). Aggregation of secreted amyloid beta-protein into sodium dodecyl sulfate-stable oligomers in cell culture. J Biol Chem *270*, 9564-9570.

Popik, P., Bobula, B., Janusz, M., Lisowski, J., and Vetulani, J. (1999). Colostrinin, a polypeptide isolated from early milk, facilitates learning and memory in rats. Pharmacol Biochem Behav *64*, 183-189.

Porat, Y., Stepensky, A., Ding, F.X., Naider, F., and Gazit, E. (2003). Completely different amyloidogenic potential of nearly identical peptide fragments. Biopolymers *69*, 161-164.

Portelius, E., Bogdanovic, N., Gustavsson, M.K., Volkmann, I., Brinkmalm, G., Zetterberg, H., Winblad, B., and Blennow, K. (2010). Mass spectrometric characterization of brain amyloid beta isoform signatures in familial and sporadic Alzheimer's disease. Acta Neuropathol *120*, 185-193.

Portelius, E., Brinkmalm, G., Tran, A., Andreasson, U., Zetterberg, H., Westman-Brinkmalm, A., Blennow, K., and Ohrfelt, A. (2009). Identification of novel N-terminal fragments of amyloid precursor protein in cerebrospinal fluid. Exp Neurol *223*, 351-358.

Powers, E.T., Morimoto, R.I., Dillin, A., Kelly, J.W., and Balch, W.E. (2009). Biological and chemical approaches to diseases of proteostasis deficiency. Annu Rev Biochem *78*, 959-991.

Prescott, M., Lourbakos, A., Bateson, M., Boyle, G., Nagley, P., and Devenish, R.J. (1997). A novel fluorescent marker for assembled mitochondria ATP synthase of yeast. OSCP subunit fused to green fluorescent protein is assembled into the complex in vivo. FEBS Lett *411*, 97-101.

Price, J.L., Davis, P.B., Morris, J.C., and White, D.L. (1991). The distribution of tangles, plaques and related immunohistochemical markers in healthy aging and Alzheimer's disease. Neurobiol Aging *12*, 295-312.

Priller, C., Bauer, T., Mitteregger, G., Krebs, B., Kretzschmar, H.A., and Herms, J. (2006). Synapse formation and function is modulated by the amyloid precursor protein. J Neurosci *26*, 7212-7221.

Quillin, M.L., and Matthews, B.W. (2000). Accurate calculation of the density of proteins. Acta Crystallogr D Biol Crystallogr *56*, 791-794.

Quiocho, F.A., Spurlino, J.C., and Rodseth, L.E. (1997). Extensive features of tight oligosaccharide binding revealed in high-resolution structures of the maltodextrin transport/chemosensory receptor. Structure *5*, 997-1015.

Rall, S.C., Jr., Weisgraber, K.H., and Mahley, R.W. (1982). Human apolipoprotein E. The complete amino acid sequence. J Biol Chem *257*, 4171-4178.

Raman, B., Ban, T., Sakai, M., Pasta, S.Y., Ramakrishna, T., Naiki, H., Goto, Y., and Rao, C.M. (2005). alpha B-crystallin, a small heat-shock protein, prevents the amyloid fibril growth of an amyloid beta-peptide and beta 2-microglobulin. Biochem J *392*, 573-581.

Raschetti, R., Albanese, E., Vanacore, N., and Maggini, M. (2007). Cholinesterase inhibitors in mild cognitive impairment: a systematic review of randomised trials. PLoS Med *4*, e338.

Ravikumar, B., Stewart, A., Kita, H., Kato, K., Duden, R., and Rubinsztein, D.C. (2003). Raised intracellular glucose concentrations reduce aggregation and cell death caused by mutant huntingtin exon 1 by decreasing mTOR phosphorylation and inducing autophagy. Hum Mol Genet *12*, 985-994.

Ravikumar, B., Vacher, C., Berger, Z., Davies, J.E., Luo, S., Oroz, L.G., Scaravilli, F., Easton, D.F., Duden, R., O'Kane, C.J.*, et al.* (2004). Inhibition of mTOR induces autophagy and reduces toxicity of polyglutamine expansions in fly and mouse models of Huntington disease. Nat Genet *36*, 585-595.

Raymond, C.R., Ireland, D.R., and Abraham, W.C. (2003). NMDA receptor regulation by amyloid-beta does not account for its inhibition of LTP in rat hippocampus. Brain Res *968*, 263-272.

Reisberg, B., Borenstein, J., Salob, S.P., Ferris, S.H., Franssen, E., and Georgotas, A. (1987). Behavioral symptoms in Alzheimer's disease: phenomenology and treatment. J Clin Psychiatry *48 Suppl*, 9-15.

Riddell, D.R., Christie, G., Hussain, I., and Dingwall, C. (2001). Compartmentalization of beta-secretase (Asp2) into low-buoyant density, noncaveolar lipid rafts. Curr Biol *11*, 1288-1293.

Robert, R., Dolezal, O., Waddington, L., Hattarki, M.K., Cappai, R., Masters, C.L., Hudson, P.J., and Wark, K.L. (2009). Engineered antibody intervention strategies for Alzheimer's disease and related dementias by targeting amyloid and toxic oligomers. Protein Eng Des Sel *22*, 199-208.

Rogaev, E.I., Sherrington, R., Rogaeva, E.A., Levesque, G., Ikeda, M., Liang, Y., Chi, H., Lin, C., Holman, K., and Tsuda, T. (1995). Familial Alzheimer's disease in kindreds with missense mutations in a gene on chromosome 1 related to the Alzheimer's disease type 3 gene. Nature *376*, 775-778.

Roheim, P.S., Carey, M., Forte, T., and Vega, G.L. (1979). Apolipoproteins in human cerebrospinal fluid. Proc Natl Acad Sci U S A *76*, 4646-4649.

Roher, A.E., Chaney, M.O., Kuo, Y.M., Webster, S.D., Stine, W.B., Haverkamp, L.J., Woods, A.S., Cotter, R.J., Tuohy, J.M., Krafft, G.A.*, et al.* (1996). Morphology and toxicity of Abeta-(1-42) dimer derived from neuritic and vascular amyloid deposits of Alzheimer's disease. J Biol Chem *271*, 20631-20635.

Roses, A.D. (1996). Apolipoprotein E alleles as risk factors in Alzheimer's disease. Annu Rev Med *47*, 387-400.

Rovelet-Lecrux, A., Hannequin, D., Raux, G., Le Meur, N., Laquerrière, A., Vital, A., Dumanchin, C., Feuillette, S., Brice, A., Vercelletto, M.*, et al.* (2006). APP locus duplication causes autosomal dominant early-onset Alzheimer disease with cerebral amyloid angiopathy. Nature Genet *38*, 24-26.

Rubinsztein, D.C. (2006). The roles of intracellular protein-degradation pathways in neurodegeneration. Nature *443*, 780-786.

Rubinsztein, D.C. (2007). Autophagy induction rescues toxicity mediated by proteasome inhibition. Neuron *54*, 854-856.

Rubinsztein, D.C., Gestwicki, J.E., Murphy, L.O., and Klionsky, D.J. (2007). Potential therapeutic applications of autophagy. Nat Rev Drug Discov *6*, 304-312.

Rudnicki, D.D., Pletnikova, O., Vonsattel, J.P., Ross, C.A., and Margolis, R.L. (2008). A comparison of huntington disease and huntington disease-like 2 neuropathology. J Neuropathol Exp Neurol *67*, 366-374.

Salloway, S., Sperling, R., Gilman, S., Fox, N.C., Blennow, K., Raskind, M., Sabbagh, M., Honig, L.S., Doody, R., van Dyck, C.H.*, et al.* (2009). A phase 2 multiple ascending dose trial of bapineuzumab in mild to moderate Alzheimer disease. Neurology *73*, 2061-2070.

Santhoshkumar, P., and Sharma, K.K. (2004). Inhibition of amyloid fibrillogenesis and toxicity by a peptide chaperone. Mol Cell Biochem *267*, 147-155.

Sarkar, S., Davies, J.E., Huang, Z., Tunnacliffe, A., and Rubinsztein, D.C. (2007a). Trehalose, a novel mTOR-independent autophagy enhancer, accelerates the clearance of mutant huntingtin and alpha-synuclein. J Biol Chem *282*, 5641-5652.

Sarkar, S., Floto, R.A., Berger, Z., Imarisio, S., Cordenier, A., Pasco, M., Cook, L.J., and Rubinsztein, D.C. (2005). Lithium induces autophagy by inhibiting inositol monophosphatase. J Cell Biol *170*, 1101-1111.

Sarkar, S., Perlstein, E.O., Imarisio, S., Pineau, S., Cordenier, A., Maglathlin, R.L., Webster, J.A., Lewis, T.A., O'Kane, C.J., Schreiber, S.L.*, et al.* (2007b). Small molecules enhance autophagy and reduce toxicity in Huntington's disease models. Nat Chem Biol *3*, 331-338.

Sarkar, S., and Rubinsztein, D.C. (2008). Small molecule enhancers of autophagy for neurodegenerative diseases. Mol Biosyst *4*, 895-901.

Sarroukh, R., Cerf, E., Derclaye, S., Dufrene, Y.F., Goormaghtigh, E., Ruysschaert, J.M., and Raussens, V. (2010). Transformation of amyloid b(1-40) oligomers into fibrils is characterized by a major change in secondary structure. Cellular and Molecular Life Sciences.

Sastre, M., Steiner, H., Fuchs, K., Capell, A., Multhaup, G., Condron, M.M., Teplow, D.B., and Haass, C. (2001). Presenilin-dependent gamma-secretase processing of beta-amyloid precursor protein at a site corresponding to the S3 cleavage of Notch. EMBO Rep *2*, 835-841.

Saunders, A.M. (2000). Apolipoprotein E and Alzheimer disease: an update on genetic and functional analyses. J Neuropathol Exp Neurol *59*, 751-758.

Saunders, A.M., Strittmatter, W.J., Schmechel, D., George-Hyslop, P.H., Pericak-Vance, M.A., Joo, S.H., Rosi, B.L., Gusella, J.F., Crapper-MacLachlan, D.R., Alberts, M.J*., et al.* (1993). Association of apolipoprotein E allele epsilon 4 with late-onset familial and sporadic Alzheimer's disease. Neurology *43*, 1467-1472.

Sayre, L.M., Zelasko, D.A., Harris, P.L., Perry, G., Salomon, R.G., and Smith, M.A. (1997). 4-Hydroxynonenal-derived advanced lipid peroxidation end products are increased in Alzheimer's disease. J Neurochem *68*, 2092-2097.

Schmittgen, T.D., and Livak, K.J. (2008). Analyzing real-time PCR data by the comparative C(T) method. Nat Protoc *3*, 1101-1108.

Schneeberger, A., Mandler, M., Otawa, O., Zauner, W., Mattner, F., and Schmidt, W. (2009). Development of AFFITOPE vaccines for Alzheimer's disease (AD)--from concept to clinical testing. J Nutr Health Aging *13*, 264-267.

Schuster, D., Rajendran, A., Hui, S.W., Nicotera, T., Srikrishnan, T., and Kruzel, M.L. (2005). Protective effect of colostrinin on neuroblastoma cell survival is due to reduced aggregation of beta-amyloid. Neuropeptides *39*, 419-426.

Seeger, G., Gartner, U., Ueberham, U., Rohn, S., and Arendt, T. (2009). FAD-mutation of APP is associated with a loss of its synaptotrophic activity. Neurobiol Dis *35*, 258-263.

Seshadri, S., Fitzpatrick, A.L., Ikram, M.A., DeStefano, A.L., Gudnason, V., Boada, M., Bis, J.C., Smith, A.V., Carassquillo, M.M., Lambert, J.C*., et al.* (2010). Genome-wide analysis of genetic loci associated with Alzheimer disease. JAMA *303*, 1832-1840.

Sethuraman, A., and Belfort, G. (2005). Protein structural perturbation and aggregation on homogeneous surfaces. Biophys J *88*, 1322-1333.

Settembre, C., Fraldi, A., Rubinsztein, D.C., and Ballabio, A. (2008). Lysosomal storage diseases as disorders of autophagy. Autophagy *4*, 113-114.

Shankar, G.M., Bloodgood, B.L., Townsend, M., Walsh, D.M., Selkoe, D.J., and Sabatini, B.L. (2007). Natural Oligomers of the Alzheimer Amyloid-β Protein Induce Reversible Synapse Loss by Modulating an NMDA-Type Glutamate Receptor-Dependent Signaling Pathway. J Neurosci *27*, 2866-2875.

Shankar, G.M., Li, S., Mehta, T.H., Garcia-Munoz, A., Shepardson, N.E., Smith, I., Brett, F.M., Farrell, M.A., Rowan, M.J., Lemere, C.A.*, et al.* (2008). Amyloid-β protein dimers isolated directly from Alzheimer's brains impair synaptic plasticity and memory. Nature Medicine *14* 837-842.

Sharma, N., Brandis, K.A., Herrera, S.K., Johnson, B.E., Vaidya, T., Shrestha, R., and Debburman, S.K. (2006). alpha-Synuclein budding yeast model: toxicity enhanced by impaired proteasome and oxidative stress. J Mol Neurosci *28*, 161-178.

Sharman, M.J., Morici, M., Hone, E., Berger, T., Taddei, K., Martins, I.J., Lim, W.L., Singh, S., Wenk, M.R., Ghiso, J.*, et al.* (2010). APOE genotype results in differential effects on the peripheral clearance of amyloid-beta42 in APOE knock-in and knock-out mice. J Alzheimers Dis *21*, 403-409.

Sharpe, S., Yau, W.M., and Tycko, R. (2005). Expression and purification of a recombinant peptide from the Alzheimer's beta-amyloid protein for solid-state NMR. Protein Expr Purif *42*, 200-210.

Sherrington, R., Rogaev, E.I., Liang, Y., Rogaeva, E.A., Levesque, G., Ikeda, M., Chi, H., Lin, C., Li, G., and Holman, K. (1995). Cloning of a gene bearing missense mutations in early-onset familial Alzheimer's disease. Nature *375*, 754-760.

Silver, I., and Erecinska, M. (1998). Oxygen and ion concentrations in normoxic and hypoxic brain cells. Adv Exp Med Biol *454*, 7-16.

Simakova, O., and Arispe, N.J. (2007). The cell-selective neurotoxicity of the Alzheimer's Abeta peptide is determined by surface phosphatidylserine and cytosolic ATP levels. Membrane binding is required for Abeta toxicity. J Neurosci *27*, 13719-13729.

Simmons, L.K., May, P.C., Tomaselli, K.J., Rydel, R.E., Fuson, K.S., Brigham, E.F., Wright, S., Lieberburg, I., Becker, G.W., Brems, D.N.*, et al.* (1994). Secondary structure of amyloid beta peptide correlates with neurotoxic activity in vitro. Mol Pharmacol *45*, 373-379.

Simon, J.A., and Bedalov, A. (2004). Yeast as a model system for anticancer drug discovery. Nat Rev Cancer *4*, 481-492.

Singh, S.K., Julliamsa, A., Nuydensk, R., Ceuterick, C., Labeur, C., Serneels, S., Vennekens, K., van Osta, P., Geerts, H., de Strooper, B.*, et al.* (2002). In

Vitro Studies of Flemish, Dutch, and Wild-Type β-Amyloid Provide Evidence for Two-Staged Neurotoxicity Neurobiology of Disease *11*, 330-340.

Sinha, S., Anderson, J.P., Barbour, R., Basi, G.S., Caccavello, R., Davis, D., Doan, M., Dovey, H.F., Frigon, N., Hong, J.*, et al.* (1999). Purification and cloning of amyloid precursor protein beta-secretase from human brain. Nature *402*, 537-540.

Skou, J.C. (1982). The (Na+ + K+)-ATPase: coupling of the reaction with ATP to the reaction with Na+ and K+. Ann N Y Acad Sci *402*, 169-184.

Skovronsky, D.M., Doms, R.W., and Lee, V.M. (1998). Detection of a novel intraneuronal pool of insoluble amyloid beta protein that accumulates with time in culture. J Cell Biol *141*, 1031-1039.

Small, D.H., Mok, S.S., and Bornstein, J.C. (2001). Alzheimer's disease and Aß toxicity: from top to bottom. Nature Rev Neurosci *2*, 595-598.

Smith, A.D., Jobst, K.A., Navaratnam, D.S., Shen, Z.X., Priddle, J.D., McDonald, B., King, E., and Esiri, M.M. (1991). Anomalous acetylcholinesterase in lumbar CSF in Alzheimer's disease. Lancet *338*, 1538.

Snyder, E.M., Nong, Y., Almeida, C.G., Paul, S., Moran, T., Choi, E.Y., Nairn, A.C., Salter, M.W., Lombroso, P.J., Gouras, G.K.*, et al.* (2005). Regulation of NMDA receptor trafficking by amyloid-beta. Nat Neurosci *8*, 1051-1058.

Sokolov, S., Pozniakovsky, A., Bocharova, N., Knorre, D., and Severin, F. (2006). Expression of an expanded polyglutamine domain in yeast causes death with apoptotic markers. Biochim Biophys Acta *1757*, 660-666.

Sokolowska, A., Bednarz, R., Pacewicz, M., Georgiades, J.A., Wilusz, T., and Polanowski, A. (2008). Colostrum from different mammalian species - A rich source of colostrinin. Int Dairy J *18*, 204-209.

Song, S., Kim, S.Y., Hong, Y.M., Jo, D.G., Lee, J.Y., Shim, S.M., Chung, C.W., Seo, S.J., Yoo, Y.J., Koh, J.Y.*, et al.* (2003). Essential role of E2-25K/Hip-2 in mediating amyloid-beta neurotoxicity. Mol Cell *12*, 553-563.

Soper, J.H., Roy, S., Stieber, A., Lee, E., Wilson, R.B., Trojanowski, J.Q., Burd, C.G., and Lee, V.M. (2008). Alpha-synuclein-induced aggregation of cytoplasmic vesicles in Saccharomyces cerevisiae. Mol Biol Cell *19*, 1093-1103.

Soto, C., Castano, E.M., Frangione, B., and Inestrosa, N.C. (1995a). The alpha-helical to beta-strand transition in the amino-terminal fragment of the amyloid beta-peptide modulates amyloid formation. J Biol Chem *270*, 3063-3067.

Soto, C., Castano, E.M., Kumar, R.A., Beavis, R.C., and Frangione, B. (1995b). Fibrillogenesis of synthetic amyloid-beta peptides is dependent on their initial secondary structure. Neurosci Lett *200*, 105-108.

Sparvero, L.J., Patz, S., Brodsky, J.L., and Coughlan, C.M. (2007). Proteomic analysis of the amyloid precursor protein fragment C99: expression in yeast. Anal Biochem *370* 162-170.

Spilman, P., Podlutskaya, N., Hart, M.J., Debnath, J., Gorostiza, O., Bredesen, D., Richardson, A., Strong, R., and Galvan, V. (2010). Inhibition of mTOR by rapamycin abolishes cognitive deficits and reduces amyloid-beta levels in a mouse model of Alzheimer's disease. PLoS One *5*, e9979.

Stahl, A., Moberg, P., Ytterberg, J., Panfilov, O., Brockenhuus Von Lowenhielm, H., Nilsson, F., and Glaser, E. (2002). Isolation and identification of a novel mitochondrial metalloprotease (PreP) that degrades targeting presequences in plants. J Biol Chem *277*, 41931-41939.

Steele, J.W., Kim, S.H., Cirrito, J.R., Verges, D.K., Restivo, J.L., Westaway, D., Fraser, P., Hyslop, P.S., Sano, M., Bezprozvanny, I.*, et al.* (2009). Acute dosing of latrepirdine (Dimebon), a possible Alzheimer therapeutic, elevates extracellular amyloid-beta levels in vitro and in vivo. Mol Neurodegener *4*, 51.

Stefani, M. (2007). Generic cell dysfunction in neurodegenerative disorders: role of surfaces in early protein misfolding, aggregation, and aggregate cytotoxicity. Neuroscientist *13*, 519-531.

Steiner, H., Winkler, E., Edbauer, D., Prokop, S., Basset, G., Yamasaki, A., Kostka, M., and Haass, C. (2002). PEN-2 is an integral component of the gamma-secretase complex required for coordinated expression of presenilin and nicastrin. J Biol Chem *277*, 39062-39065.

Steinerman, J.R., Irizarry, M., Scarmeas, N., Raju, S., Brandt, J., Albert, M., Blacker, D., Hyman, B., and Stern, Y. (2008). Distinct Pools of β-Amyloid in Alzheimer Disease-Affected Brain: A Clinicopathologic Study. Arch Neurol *65*, 906-912.

Steward, O., and Schuman, E.M. (2003). Compartmentalized synthesis and degradation of proteins in neurons. Neuron *40*, 347-359.

Stine, W.B., Dahlgren, K.N., Krafft, G.A., and LaDu, M.J. (2003). In Vitro Characterization of Conditions for Amyloid-β Peptide Oligomerization and Fibrillogenesis. J Biol Chem *278*, 11612-11622.

Stine, W.B., Jungbauer, L., Yu, C., and LaDu, M.J. (2010). Preparing synthetic Abeta in different aggregation states. Methods Mol Biol *670*, 13-32.

Storandt, M., Grant, E.A., Miller, J.P., and Morris, J.C. (2006). Longitudinal course and neuropathologic outcomes in original vs revised MCI and in pre-MCI. Neurology *67*, 467-473.

Strauss, S., Bauer, J., Ganter, U., Jonas, U., Berger, M., and Volk, B. (1992). Detection of interleukin-6 and alpha 2-macroglobulin immunoreactivity in cortex and hippocampus of Alzheimer.s disease patients. Lab Invest *66*, 223-230.

Subramanian, S., and Shree, A.N. (2007). Expression, purification and characterization of a synthetic gene encoding human amyloid beta (Abeta1-42) in Escherichia coli. Indian J Biochem Biophys *44*, 71-75.

Suen, K.C., Yu, M.S., So, K.F., Chang, R.C., and Hugon, J. (2003). Upstream signaling pathways leading to the activation of double-stranded RNA-dependent serine/threonine protein kinase in beta-amyloid peptide neurotoxicity. J Biol Chem *278*, 49819-49827.

Sullivan, P.M., Mezdour, H., Quarfordt, S.H., and Maeda, N. (1998). Type III hyperlipoproteinemia and spontaneous atherosclerosis in mice resulting from gene replacement of mouse Apoe with human Apoe*2. J Clin Invest *102*, 130-135.

Suzuki, K., Kirisako, T., Kamada, Y., Mizushima, N., Noda, T., and Ohsumi, Y. (2001). The pre-autophagosomal structure organized by concerted functions of APG genes is essential for autophagosome formation. EMBO J *20*, 5971-5981.

Tabaton, M., Cammarata, S., Mancardi, G., Manetto, V., Autilio-Gambetti, L., Perry, G., and Gambetti, P. (1991). Ultrastructural localization of beta-amyloid, tau, and ubiquitin epitopes in extracellular neurofibrillary tangles. Proc Natl Acad Sci U S A *88*, 2098-2102.

Tagawa, K., Kunishita, T., Maruyama, K., Yoshikawa, K., Kominami, E., Tsuchiya, T., Suzuki, K., Tabira, T., Sugita, H., and Ishiura, S. (1991). Alzheimer's disease amyloid beta-clipping enzyme (APP secretase): identification, purification, and characterization of the enzyme. Biochem Biophys Res Commun *177*, 377-387.

Tagliavini, F., Rossi, G., Padovani, A., Magoni, M., Andora, G., Sgarzi, M., Bizzi, A., Savoiardo, M., Carella, F., Morbin, M.*, et al.* (1999). A new BPP mutation related to hereditary cerebral hemorrhage. Alzheimer's Rep *S28*.

Takahashi, R.H., Almeida, C.G., Kearney, P.F., Yu, F., Lin, M.T., Milner, T.A., and Gouras, G.K. (2004). Oligomerization of Alzheimer's beta-amyloid within processes and synapses of cultured neurons and brain. J Neurosci *24*, 3592-3599.

Takahashi, R.H., Nam, E.E., Edgar, M., and Gouras, G.K. (2002). Alzheimer beta-amyloid peptides: normal and abnormal localization. Histol Histopathol *17*, 239-246.

Takeshige, K., Baba, M., Tsuboi, S., Noda, T., and Ohsumi, Y. (1992). Autophagy in yeast demonstrated with proteinase-deficient mutants and conditions for its induction. J Cell Biol *119*, 301-311.

Takeuchi, I.K., and Takeuchi, Y.K. (2001). Transient accumulation of Gallyas-Braak-positive and phosphorylated tau-immunopositive substances in neuronal lipofuscin granules in the amygdala, hippocampus and entorhinal cortex of rats during long-term chloroquine intoxication. Acta Neuropathol *102*, 191-194.

Talaga, P., and Quere, L. (2002). The plasma membrane: a target and hurdle for the development of anti-Abeta drugs? Curr Drug Targets CNS Neurol Disord *1*, 567-574.

Tariot, P.N. (2006). Contemporary issues in the treatment of Alzheimer's disease: tangible benefits of current therapies. J Clin Psychiatry *67 Suppl 3*, 15-22; quiz 23.

Tatar, M., Khazaeli, A.A., and Curtsinger, J.W. (1997). Chaperoning extended life. Nature *390*, 30.

Teichert, U., Mechler, B., Muller, H., and Wolf, D.H. (1989). Lysosomal (vacuolar) proteinases of yeast are essential catalysts for protein degradation, differentiation, and cell survival. J Biol Chem *264*, 16037-16045.

Tekirian, T.L. (2001). Commentary: Abeta N- Terminal Isoforms: Critical contributors in the course of AD pathophysiology. J Alzheimers Dis *3*, 241-248.

Teplow, D.B. (2006). Preparation of amyloid beta-protein for structural and functional studies. Methods Enzymol *413*, 20-33.

Terry, R.D. (2006). Alzheimer's disease and the aging brain. J Geriatr Psychiatry Neurol *19*, 125-128.

Terry, R.D., Hansen, L.A., DeTeresa, R., Davies, P., Tobias, H., and Katzman, R. (1987). Senile dementia of the Alzheimer type without neocortical neurofibrillary tangles. J Neuropathol Exp Neurol *46*, 262-268.

Terry, R.D., Masliah, E., Salmon, D.P., Butters, N., DeTeresa, R., Hill, R., Hansen, L.A., and Katzman, R. (1991). Physical basis of cognitive alterations in Alzheimer disease: Synapse loss is the major correlate of cognitive impairment. . Annals of Neurology *30*, 572-580.

Terry, R.D., Peck, A., DeTeresa, R., Schechter, R., and Horoupian, D.S. (1981). Some morphometric aspects of the brain in senile dementia of the Alzheimer type. Ann Neurol *10*, 184-192.

Thal, D.R., Schober, R., and Birkenmeier, G. (1997). The subunits of alpha2-macroglobulin receptor/low density lipoprotein receptor-related protein, native and transformed alpha2-macroglobulin and interleukin 6 in Alzheimer.s disease. Brain Res *777*, 223-227

Thorn, D.C., Ecroyd, H., Sunde, M., Poon, S., and Carver, J.A. (2008). Amyloid fibril formation by bovine milk alpha(s2)-casein occurs under physiological conditions yet is prevented by its natural counterpart, alpha(s1)-casein. Biochemistry *47*, 3926-3936.

Thorn, D.C., Meehan, S., Sunde, M., Rekas, A., Gras, S.L., MacPhee, C.E., Dobson, C.M., Wilson, M.R., and Carver, J.A. (2005a). Amyloid fibril formation by bovine milk kappa-casein and its inhibition by the molecular chaperones alpha(s-) and beta-casein. Biochemistry *44*, 17027-17036.

Thorn, D.C., Meehan, S., Sunde, M., Rekas, A., Gras, S.L., MacPhee, C.E., Dobson, C.M., Wilson, M.R., and Carver, J.A. (2005b). Amyloid fibril formation by bovine milk kappa-casein and its inhibition by the molecular chaperones alphaS- and beta-casein. Biochemistry *44*, 17027-17036.

Tian, Y., Bustos, V., Flajolet, M., and Greengard, P. (2011). A small-molecule enhancer of autophagy decreases levels of A{beta} and APP-CTF via Atg5-dependent autophagy pathway. FASEB J.

Tierney, M.C., Yao, C., Kiss, A., and McDowell, I. (2005). Neuropsychological tests accurately predict incident Alzheimer disease after 5 and 10 years. Neurology *64*, 1853-1859.

Tokuda, T., Calero, M., Matsubara, E., Vidal, R., Kumar, A., Permanne, B., Zlokovic, B., Smith, J.D., Ladu, M.J., Rostagno, A.*, et al.* (2000). Lipidation of apolipoprotein E influences its isoform-specific interaction with Alzheimer's amyloid beta peptides. Biochem J *348 Pt 2*, 359-365.

Tomita, T. (2009). Secretase inhibitors and modulators for Alzheimer's disease treatment. Expert Rev Neurother *9*, 661-679.

Tomiyama, T., Nagata, T., Shimada, H., Teraoka, R., Fukushima, A., Kanemitsu, H., Takuma, H., Kuwano, R., Imagawa, M., Ataka, S.*, et al.* (2008). A new amyloid mu variant favoring oligomerization in Alzheimer's-type dementia. Ann Neurol *63*, 377-387.

Tong, A.H., Evangelista, M., Parsons, A.B., Xu, H., Bader, G.D., Page, N., Robinson, M., Raghibizadeh, S., Hogue, C.W., Bussey, H.*, et al.* (2001). Systematic genetic analysis with ordered arrays of yeast deletion mutants. Science *294*, 2364-2368.

Townsend, M., Shankar, G.M., Mehta, T., Walsh, D.M., and Selkoe, D.J. (2006). Effects of secreted oligomers of amyloid beta-protein on hippocampal synaptic plasticity: a potent role for trimers. J Physiol *572*, 477-492.

Tseng, B.P., Green, K.N., Chan, J.L., Blurton-Jones, M., and LaFerla, F.M. (2008). Abeta inhibits the proteasome and enhances amyloid and tau accumulation. Neurobiol Aging *29*, 1607-1618.

Turner, P.R., O'Connor, K., Tate, W.P., and Abraham, W.C. (2003). Roles of amyloid precursor protein and its fragments in regulating neural activity, plasticity and memory. Prog Neurobiol *70*, 1-32.

Tycko, R. (2003). Insights into the Amyloid Folding Problem from Solid -State NMR. Biochemistry *42*, 3151-3159.

Tyynela, J., Sohar, I., Sleat, D.E., Gin, R.M., Donnelly, R.J., Baumann, M., Haltia, M., and Lobel, P. (2000). A mutation in the ovine cathepsin D gene causes a congenital lysosomal storage disease with profound neurodegeneration. EMBO J *19*, 2786-2792.

Tzur, A., Moore, J.K., Jorgensen, P., Shapiro, H.M., and Kirschner, M.W. (2011). Optimizing optical flow cytometry for cell volume-based sorting and analysis. PLoS One *6*, e16053.

Vagin, A., and Teplyakov, A. (1997). MOLREP: an automated program for molecular replacement. Journal of Applied Crystallography *30*, 1022-1025.

Vandebroek, T., Terwel, D., Vanhelmont, T., Gysemans, M., Van Haesendonck, C., Engelborghs, Y., Winderickx, J., and Van Leuven, F. (2006). Microtubule binding and clustering of human Tau-4R and Tau-P301L proteins isolated from yeast deficient in orthologues of glycogen synthase kinase-3beta or cdk5. J Biol Chem *281* 25388-25397.

Vandebroek, T., Vanhelmont, T., Terwel, D., Borghgraef, P., Lemaire, K., Snauwaert, J., Wera, S., Van Leuven, F., and Winderickx, J. (2005). Identification and isolation of a hyperphosphorylated, conformationally changed intermediate of human protein tau expressed in yeast. Biochemistry *44* 11466-11475.

Vanhelmont, T., Vandebroek, T., De Vos, A., Terwel, D., Lemaire, K., Anandhakumar, J., Franssens, V., Swinnen, E., Van Leuven, F., and Winderickx, J. (2010). Serine-409 phosphorylation and oxidative damage define aggregation of human protein tau in yeast. FEMS Yeast Res *10*, 992-1005.

Varvel, N.H., Bhaskar, K., Patil, A.R., Pimplikar, S.W., Herrup, K., and Lamb, B.T. (2008). Abeta oligomers induce neuronal cell cycle events in Alzheimer's disease. J Neurosci *28*, 10786-10793.

Vassar, R., Bennett, B.D., Babu-Khan, S., Kahn, S., Mendiaz, E.A., Denis, P., Teplow, D.B., Ross, S., Amarante, P., Loeloff, R.*, et al.* (1999). Beta-secretase cleavage of Alzheimer's amyloid precursor protein by the transmembrane aspartic protease BACE. Science *286*, 735-741.

Verdier, Y., and Penke, B. (2004). Binding sites of amyloid β-peptide in cell plasma membrane and implications for Alzheimer's disease. Curr Protein Pept Sci *5*, 19-31.

Verdier, Y., Zarandi, M., and Penke, B. (2004). Amyloid beta-peptide interactions with neuronal and glial cell plasma membrane: binding sites and implications for Alzheimer's disease. J Pept Sci *10*, 229-248.

Verghese, P.B., Castellano, J.M., and Holtzman, D.M. (2011). Apolipoprotein E in Alzheimer's disease and other neurological disorders. Lancet Neurol *10*, 241-252.

Vetrivel, K.S., Cheng, H., Kim, S.H., Chen, Y., Barnes, N.Y., Parent, A.T., Sisodia, S.S., and Thinakaran, G. (2005). Spatial segregation of gamma-secretase and substrates in distinct membrane domains. J Biol Chem *280*, 25892-25900.

Vignisse, J., Steinbusch, H.W., Bolkunov, A., Nunes, J., Santos, A.I., Grandfils, C., Bachurin, S., and Strekalova, T. (2011). Dimebon enhances hippocampus-dependent learning in both appetitive and inhibitory memory tasks in mice. Prog Neuropsychopharmacol Biol Psychiatry *35*, 510-522.

Vigo-Pelfrey, C., Lee, D., Keim, P., Lieberburg, I., and Schenk, D.B. (1993). Characterization of beta-amyloid peptide from human cerebrospinal fluid. J Neurochem *61*, 1965-1968.

Vincent, I., Bu, B., Hudson, K., Husseman, J., Nochlin, D., and Jin, L. (2001). Constitutive Cdc25B tyrosine phosphatase activity in adult brain neurons with M phase-type alterations in Alzheimer's disease. Neuroscience *105*, 639-650.

Vingtdeux, V., Giliberto, L., Zhao, H., Chandakkar, P., Wu, Q., Simon, J.E., Janle, E.M., Lobo, J., Ferruzzi, M.G., Davies, P.*, et al.* (2010). AMP-activated protein kinase signaling activation by resveratrol modulates amyloid-beta peptide metabolism. J Biol Chem *285*, 9100-9113.

Voisine, C., Pedersen, J.S., and Morimoto, R.I. (2010). Chaperone networks: Tipping the balance in protein folding diseases. Neurobiol Dis *40*, 12-20.

von der Haar, T., Josse, L., Wright, P., Zenthon, J., and Tuite, M.F. (2007). Development of a novel yeast cell-based system for studying the aggregation of Alzheimer's disease-associated Aβ peptides in vivo. Neurodegener Dis *4*, 136-147.

Walkley, S.U. (1998). Cellular pathology of lysosomal storage disorders. Brain Pathol *8*, 175-193.

Walkley, S.U. (2009). Pathogenic cascades in lysosomal disease-Why so complex? J Inherit Metab Dis *32*, 181-189.

Walsh, D.M., Klyubin, I., Fadeeva, J.V., Cullen, W.K., Anwyl, R., Wolfe, M.S., Rowan, M.J., and Selkoe, D.J. (2002a). Naturally secreted oligomers of amyloid beta protein potently inhibit hippocampal long-term potentiation in vivo. Nature *416*, 535-539.

Walsh, D.M., Lomakin, A., Benedek, G.B., Condron, M.M., and Teplow, D.B. (1997). Amyloid beta-protein fibrillogenesis. Detection of a protofibrillar intermediate. J BiolChem *272*, 22364-22372.

Walsh, D.M., Thulin, E., Minogue, A.M., Gustavsson, N., Pang, E., Teplow, D.B., and Linse, S. (2009). A facile method for expression and purification of the Alzheimer's disease-associated amyloid beta-peptide. FEBS J *276*, 1266-1281.

Walsh, D.M., Tseng, B.P., Rydel, R.E., Podlisny, M.B., and Selkoe, D.J. (2000). The oligomerization of amyloid beta-protein begins intracellularly in cells derived from human brain. Biochemistry *39*, 10831-10839.

Walsh, D.W., Wolfe, K.H., and Butler, G. (2002b). Genomic differences between Candida glabrata and Saccharomyces cerevisiae around the MRPL28 and GCN3 loci. Yeast *19*, 991-994.

Wang, C.Y., Finstad, C.L., Walfield, A.M., Sia, C., Sokoll, K.K., Chang, T.Y., Fang, X.D., Hung, C.H., Hutter-Paier, B., and Windisch, M. (2007). Site-specific UBITh amyloid-beta vaccine for immunotherapy of Alzheimer's disease. Vaccine *25*, 3041-3052.

Wang, Q., Rowan, M.J., and Anwyl, R. (2004). Beta-amyloid-mediated inhibition of NMDA receptor-dependent long-term potentiation induction involves activation of microglia and stimulation of inducible nitric oxide synthase and superoxide. J Neurosci *24*, 6049-6056.

Ward, R.V., Jennings, K.H., Jepras, R., Neville, W., Owen, D.E., Hawkins, J., Christie, G., Davis, J.B., George, A., Karran, E.H.*, et al.* (2000). Fractionation and characterization of oligomeric, protofibrillar and fibrillar forms of beta-amyloid peptide. Biochem J *348 Pt 1*, 137-144.

Webb, J.L., Ravikumar, B., Atkins, J., Skepper, J.N., and Rubinsztein, D.C. (2003). Alpha-Synuclein is degraded by both autophagy and the proteasome. J Biol Chem *278*, 25009-25013.

Wei, W., Norton, D.D., Wang, X., and Kusiak, J.W. (2002). Aβ 17-42 in Alzheimer's disease activates JNK and caspase-8 leading to neuronal apoptosis. Brain *125*, 2036-2043.

Weller, R.O., Massey, A., Newman, T.A., Hutchings, M., Kuo, Y.M., and Roher, A.E. (1998). Cerebral amyloid angiopathy: Amyloid beta accumulates in putative interstitial fluid drainage pathways in Alzheimer's disease. Am J Pathol *153*, 725-733.

Werner-Washburne, M., Braun, E., Johnston, G.C., and Singer, R.A. (1993). Stationary phase in the yeast Saccharomyces cerevisiae. Microbiol Rev *57*, 383-401.

Werner-Washburne, M., Braun, E.L., Crawford, M.E., and Peck, V.M. (1996). Stationary phase in Saccharomyces cerevisiae. Mol Microbiol *19*, 1159-1166.

Werner, E.D., Brodsky, J.L., and McCracken, A.A. (1996). Proteasome-dependent endoplasmic reticulum-associated protein degradation: an unconventional route to a familiar fate. Proc Natl Acad Sci U S A *93*, 13797-13801.

West, M.J., Coleman, P.D., Flood, D.G., and Troncoso, J.C. (1994). Differences in the pattern of hippocampal neuronal loss in normal ageing and Alzheimer's disease. Lancet *344*, 769-772.

West, M.J., Kawas, C.H., Stewart, W.F., Rudow, G.L., and Troncoso, J.C. (2004). Hippocampal neurons in pre-clinical Alzheimer's disease. Neurobiol Aging *25*, 1205-1212.

White, A.R., Multhaup, G., Maher, F., Bellingham, S., Camakaris, J., Zheng, H., Bush, A.I., Beyreuther, K., Masters, C.L., and Cappai, R. (1999). The Alzheimer's disease amyloid precursor protein modulates copper-induced toxicity and oxidative stress in primary neuronal cultures. J Neurosci *19*, 9170-9179.

Whitehouse, P.J., Price, D.L., Struble, R.G., Clark, A.W., Coyle, J.T., Delon, M.R., and Whitehouse, P.J. (1982). Alzheimer's disease and senile dementia: loss of neurons in the basal forebrain. Science *215*, 1237-1242.

Whitson, J.S., Selkoe, D.J., and Cotman, C.W. (1989). Amyloid beta protein enhances the survival of hippocampal neurons in vitro. Science *243*, 1488-1490.

Wiesehan, K., Funke, S.A., Fries, M., and Willbold, D. (2007). Purification of recombinantly expressed and cytotoxic human amyloid-beta peptide 1-42. J Chromatogr B Analyt Technol Biomed Life Sci *856*, 229-233.

Wilcock, D.M., and Colton, C.A. (2008). Anti-amyloid-beta immunotherapy in Alzheimer's disease: relevance of transgenic mouse studies to clinical trials. J Alzheimers Dis *15*, 555-569.

Wild-Bode, C., Yamazaki, T., Capell, A., Leimer, U., Steiner, H., Ihara, Y., and Haass, C. (1997). Intracellular generation and accumulation of amyloid beta-peptide terminating at amino acid 42. J Biol Chem *272*, 16085-16088.

Wilkins, D.K., Grimshaw, S.B., Receveur, V., Dobson, C.M., Jones, J.A., and Smith, L.J. (1999). Hydrodynamic Radii of Native and Denatured Proteins Measured by Pulse Field Gradient NMR Techniquesâ€ Biochemistry *38*, 16424-16431.

Williams, A., Sarkar, S., Cuddon, P., Ttofi, E.K., Saiki, S., Siddiqi, F.H., Jahreiss, L., Fleming, A., Pask, D., Goldsmith, P.*, et al.* (2008). Novel targets for Huntington's disease in an mTOR-independent autophagy pathway. Nat Chem Biol *4*, 295-305.

Willingham, S., Outeiro, T.F., DeVit, M.J., Lindquist, S.L., and Muchowski, P.J. (2003). Yeast genes that enhance the toxicity of a mutant huntingtin fragment or alpha-synuclein. Science *302*, 1769-1772.

Wilson, C.A., Murphy, D.D., Giasson, B.I., Zhang, B., Trojanowski, J.Q., and Lee, V.M. (2004). Degradative organelles containing mislocalized alpha-and beta-synuclein proliferate in presenilin-1 null neurons. J Cell Biol *165*, 335-346.

Winderickx, J., Delay, C., De Vos, A., Klinger, H., Pellens, K., Vanhelmont, T., Van Leuven, F., and Zabrocki, P. (2008). Protein folding diseases and neurodegeneration: lessons learned from yeast. Biochim Biophys Acta *1783*, 1381-1395.

Winzeler, E.A., et al. (1999). Functional characterization of the Saccharomyces cerevisiae genome by gene deletion and parallel analysis. Science, 901-906.

Wirths, O. (2001). Intraneuronal Aß42 accumulation precedes plaque formation in ß-amyloid precursor protein and presenilin-1 double transgenic mice. Neuroscience Lett *306*, 116-120.

Wisniewski, T., Castano, E.M., Golabek, A., Vogel, T., and Frangione, B. (1994). Acceleration of Alzheimer's fibril formation by apolipoprotein E in vitro. Am J Pathol *145*, 1030-1035.

Wolfe, M.S., De Los Angeles, J., Miller, D.D., Xia, W., and Selkoe, D.J. (1999a). Are presenilins intramembrane-cleaving proteases? Implications for the molecular mechanism of Alzheimer's disease. Biochemistry *38*, 11223-11230.

Wolfe, M.S., Xia, W., Ostaszewski, B.L., Diehl, T.S., Kimberly, W.T., and Selkoe, D.J. (1999b). Two transmembrane aspartates in presenilin-1 required for presenilin endoproteolysis and gamma-secretase activity. Nature *398*, 513-517.

Woodruff-Pak, D.S., Agelan, A., and Del Valle, L. (2007). A rabbit model of Alzheimer's disease: valid at neuropathological, cognitive, and therapeutic levels. J Alzheimers Dis *11*, 371-383.

Wright, R. (2000). Transmission electron microscopy of yeast. Microsc Res Tech *51*, 496-510.

Wu, J., Li, Q., and Bezprozvanny, I. (2008). Evaluation of Dimebon in cellular model of Huntington's disease. Mol Neurodegener *3*, 15.

Wu, Q., Combs, C., Cannady, S.B., Geldmacher, D.S., and Herrup, K. (2000). Beta-amyloid activated microglia induce cell cycling and cell death in cultured cortical neurons. Neurobiol Aging *21*, 797-806.

Wurth, C., Guimard, N.K., and Hecht, M.H. (2002). Mutations that reduce aggregation of the Alzheimer's Aβ42 peptide: an unbiased search for the sequence determinants of Aβ amyloidogenesis. J Mol Biol *319*, 1279-1290.

Xiao, A.Y., Wang, X.Q., Yang, A., and Yu, S.P. (2002). Slight impairment of Na+,K+-ATPase synergistically aggravates ceramide- and beta-amyloid-induced apoptosis in cortical neurons. Brain Res *955*, 253-259.

Xie, Z., Nair, U., and Klionsky, D.J. (2008). Atg8 controls phagophore expansion during autophagosome formation. Mol Biol Cell *19*, 3290-3298.

Xu, H., Greengard, P., and Gandy, S. (1995). Regulated formation of Golgi secretory vesicles containing Alzheimer β- amyloid precursor protein. J Biol Chem *270*, 23243-23245.

Yaar, M., Zhai, S., Pilch, P.F., Doyle, S.M., Eisenhauer, P.B., Fine, R.E., and Gilchrest, B.A. (1997). Binding of beta-amyloid to the p75 neurotrophin receptor induces apoptosis. A possible mechanism for Alzheimer's disease. J Clin Invest *100*, 2333-2340.

Yadav, A.K., and Bachhawat, A.K. CgCYN1, a plasma membrane cystine-specific transporter of Candida glabrata with orthologues prevalent amongst pathogenic yeasts and fungi. J Biol Chem.

Yagishita, S., Futai, E., and Ishiura, S. (2008). In vitro reconstitution of gamma-secretase activity using yeast microsomes. Biochem Biophys Res Commun *377*, 141-145.

Yagyu, K., Kitagawa, K., Irie, T., Wu, B., Zeng, X.T., Hattori, N., and Inagaki, C. (2001). Amyloid beta proteins inhibit Cl(-)-ATPase activity in cultured rat hippocampal neurons. J Neurochem *78*, 569-576.

Yamashita, M., Nonaka, T., Arai, T., Kametani, F., Buchman, V.L., Ninkina, N., Bachurin, S.O., Akiyama, H., Goedert, M., and Hasegawa, M. (2009). Methylene blue and dimebon inhibit aggregation of TDP-43 in cellular models. FEBS Lett *583*, 2419-2424.

Yamauchi, K., Tozuka, M., Hidaka, H., Nakabayashi, T., Sugano, M., and Katsuyama, T. (2002). Isoform-specific effect of apolipoprotein E on endocytosis of beta-amyloid in cultures of neuroblastoma cells. Ann Clin Lab Sci *32*, 65-74.

Yamauchi, K., Tozuka, M., Hidaka, H., Nakabayashi, T., Sugano, M., Kondo, Y., Nakagawara, A., and Katsuyama, T. (2000). Effect of apolipoprotein AII on the interaction of apolipoprotein E with beta-amyloid: some apo(E-AII) complexes inhibit the internalization of beta-amyloid in cultures of neuroblastoma cells. J Neurosci Res *62*, 608-614.

Yan, S.D. (1996). RAGE and amyloid-b peptide neurotoxicity in Alzheimer's disease. Nature *382*, 685-691.

Yang, D., Yip, C.M., Huang, T.H.J., Chakrabartty, V., and Fraser, P.E. (1999a). Manipulating the Amyloid- Aggregation Pathway with Chemical Chaperones. J Biol Chem *274*, 32970-32974.

Yang, D.S., Kumar, A., Stavrides, P., Peterson, J., Peterhoff, C.M., Pawlik, M., Levy, E., Cataldo, A.M., and Nixon, R.A. (2008). Neuronal apoptosis and

autophagy cross talk in aging PS/APP mice, a model of Alzheimer's disease. Am J Pathol *173*, 665-681.

Yang, D.S., Small, D.H., Seydel, U., Smith, J.D., Hallmayer, J., Gandy, S.E., and Martins, R.N. (1999b). Apolipoprotein E promotes the binding and uptake of beta-amyloid into Chinese hamster ovary cells in an isoform-specific manner. Neuroscience *90*, 1217-1226.

Yang, D.S., Smith, J.D., Zhou, Z., Gandy, S.E., and Martins, R.N. (1997). Characterization of the binding of amyloid-beta peptide to cell culture-derived native apolipoprotein E2, E3, and E4 isoforms and to isoforms from human plasma. J Neurochem *68*, 721-725.

Yang, D.S., Stavrides, P., Mohan, P.S., Kaushik, S., Kumar, A., Ohno, M., Schmidt, S.D., Wesson, D., Bandyopadhyay, U., Jiang, Y.*, et al.* (2011). Reversal of autophagy dysfunction in the TgCRND8 mouse model of Alzheimer's disease ameliorates amyloid pathologies and memory deficits. Brain *134*, 258-277.

Yang, F., Lim, G.P., Begum, A.N., Ubeda, O.J., Simmons, M.R., Ambegaokar, S.S., Chen, P.P., Kayed, R., Glabe, C.G., Frautschy, S.A.*, et al.* (2005). Curcumin inhibits formation of amyloid beta oligomers and fibrils, binds plaques, and reduces amyloid in vivo. J Biol Chem *280*, 5892-5901.

Yang, Y., Mufson, E.J., and Herrup, K. (2003). Neuronal cell death is preceded by cell cycle events at all stages of Alzheimer's disease. J Neurosci *23*, 2557-2563.

Yang, Z., and Klionsky, D.J. (2009). An overview of the molecular mechanism of autophagy. Curr Top Microbiol Immunol *335*, 1-32.

Yankner, B.A., Duffy, L.K., and Kirschner, D.A. (1990). Neurotrophic and neurotoxic effects of amyloid beta protein: reversal by tachykinin neuropeptides. Science *250*, 279-282.

Yasuhara, O., Kawamata, T., Aimi, Y., McGeer, E.G., and McGeer, P.L. (1994). Two types of dystrophic neurites in senile plaques of Alzheimer disease and elderly non-demented cases. Neurosci Lett *171*, 73-76.

Yazawa, H. (2001). ß Amyloid peptide (Aß42) is internalized via the G-protein coupled receptor FPRL1 and forms fibrillar aggregates in macrophages. FASEB J *15*, 2454-2462.

Yen, W.L., Legakis, J.E., Nair, U., and Klionsky, D.J. (2007). Atg27 is required for autophagy-dependent cycling of Atg9. Mol Biol Cell *18*, 581-593.

Yorimitsu, T., and Klionsky, D.J. (2007). Eating the endoplasmic reticulum: quality control by autophagy. Trends Cell Biol *17*, 279-285.

Younkin, S.G. (1998). The role of A beta 42 in Alzheimer's disease. J Physiol Paris *92*, 289-292.

Yu, W.H., Cuervo, A.M., Kumar, A., Peterhoff, C.M., Schmidt, S.D., Lee, J.H., Mohan, P.S., Mercken, M., Farmery, M.R., Tjernberg, L.O*., et al.* (2005). Macroautophagy--a novel Beta-amyloid peptide-generating pathway activated in Alzheimer's disease. J Cell Biol *171*, 87-98.

Yu, W.H., Kumar, A., Peterhoff, C., Shapiro Kulnane, L., Uchiyama, Y., Lamb, B.T., Cuervo, A.M., and Nixon, R.A. (2004). Autophagic vacuoles are enriched in amyloid precursor protein-secretase activities: implications for beta-amyloid peptide over-production and localization in Alzheimer's disease. Int J Biochem Cell Biol *36*, 2531-2540.

Yue, Z., Horton, A., Bravin, M., DeJager, P.L., Selimi, F., and Heintz, N. (2002). A novel protein complex linking the delta 2 glutamate receptor and autophagy: implications for neurodegeneration in lurcher mice. Neuron *35*, 921-933.

Zabrocki, P., Bastiaens, I., Delay, C., Bammens, T., Ghillebert, R., Pellens, K., De Virgilio, C., Van Leuven, F., and Winderickx, J. (2008). Phosphorylation, lipid raft interaction and traffic of alpha-synuclein in a yeast model for Parkinson. Biochim Biophys Acta *1783*, 1767-1780.

Zabrocki, P., Pellens, K., Vanhelmont, T., Vandebroek, T., Griffioen, G., Wera, S., Van Leuven, F., and Winderickx, J. (2005). Characterization of alpha-synuclein aggregation and synergistic toxicity with protein tau in yeast. FEBS J *272*, 1386-1400.

Zagorski, M.G., Yang, J., Shao, H., Ma, K., Zeng, H., and Hong, A. (1999). Methodological and chemical factors affecting amyloid beta peptide amyloidogenicity. Methods Enzymol *309*, 189-204.

Zannis, V.I., and Breslow, J.L. (1982). Apolipoprotein E. Mol Cell Biochem *42*, 3-20.

Zerbinatti, C.V., Wahrle, S.E., Kim, H., Cam, J.A., Bales, K., Paul, S.M., Holtzman, D.M., and Bu, G. (2006). Apolipoprotein E and low density lipoprotein receptor-related protein facilitate intraneuronal Aß42 accumulation in Amyloid model mice. J Biol Chem *281*, 36180-36186.

Zhang, H., Komano, H., Fuller, R.S., Gandy, S.E., and Frail, D.E. (1994). Proteolytic processing and secretion of human beta-amyloid precursor protein in yeast. Evidence for a yeast secretase activity. J Biol Chem *269* 27799-27802.

Zhang, L., Yu, H., Zhao, X., Lin, X., Tan, C., Cao, G., and Wang, Z. (2010a). Neuroprotective effects of salidroside against beta-amyloid-induced oxidative stress in SH-SY5Y human neuroblastoma cells. Neurochem Int *57*, 547-555.

Zhang, L., Yu, H.X., Song, C.C., Lin, X.F., Chen, B., Tan, C., Cao, G.X., and Wang, Z.W. (2009). Expression, purification, and characterization of recombinant human beta-amyloid42 peptide in Escherichia coli. Protein Expr Purif *64*, 55-62.

Zhang, L., Yu, J., Pan, H., Hu, P., Hao, Y., Cai, W., Zhu, H., Yu, A.D., Xie, X., Ma, D.*, et al.* (2007). Small molecule regulators of autophagy identified by an image-based high-throughput screen. Proc Natl Acad Sci U S A *104*, 19023-19028.

Zhang, S., Hedskog, L., Petersen, C.A., Winblad, B., and Ankarcrona, M. (2010b). Dimebon (latrepirdine) enhances mitochondrial function and protects neuronal cells from death. J Alzheimers Dis *21*, 389-402.

Zhang, W., Espinoza, D., Hines, V., Innis, M., Mehta, P., and Miller, D.L. (1997). Characterization of beta-amyloid peptide precursor processing by the yeast Yap3 andMkc7 proteases. Biochim Biophys Acta *1359* 110-122.

Zhang, Y.W., Thompson, R., Zhang, H., and Xu, H. (2011). APP processing in Alzheimer's disease. Mol Brain *4*, 3.

Zhao, G., Mao, G., Tan, J., Dong, Y., Cui, M.Z., Kim, S.H., and Xu, X. (2004). Identification of a new presenilin-dependent zeta-cleavage site within the transmembrane domain of amyloid precursor protein. J Biol Chem *279*, 50647-50650.

Zhou, H., Li, S.H., and Li, X.J. (2001). Chaperone suppression of cellular toxicity of huntingtin is independent of polyglutamine aggregation. J Biol Chem *276*, 48417-48424.

Zhou, L., Miller, B.L., McDaniel, C.H., Kelly, L., Kim, O.J., and Miller, C.A. (1998). Frontotemporal dementia: neuropil spheroids and presynaptic terminal degeneration. Ann Neurol *44*, 99-109.

Zhou, Q., Homma, K.J., and Poo, M.M. (2004). Shrinkage of dendritic spines associated with long-term depression of hippocampal synapses. Neuron *44*, 749-757.

Zhu, X., Siedlak, S.L., Wang, Y., Perry, G., Castellani, R.J., Cohen, M.L., and Smith, M.A. (2008). Neuronal binucleation in Alzheimer disease hippocampus. Neuropathol Appl Neurobiol *34*, 457-465.

Ziegler-Graham, K., Brookmeyer, R., Johnson, E., and Arrighi, H.M. (2008). Worldwide variation in the doubling time of Alzheimer's disease incidence rates. Alzheimers Dement *4*, 316-323.

Zimecki, M. (2008). A proline-rich polypeptide from ovine colostrum: colostrinin with immunomodulatory activity. Adv Exp Med Biol *606*, 241-250.